THE DEVELOPMENT OF NEW CLASSES OF ENANTIOSELECTIVE HYDROGEN BOND DONOR CATALYSTS FOR ORGANIC SYNTHESIS BASED UPON WERNER COMPLEXES

A Dissertation

by

SUBRATA KUMAR GHOSH

Submitted to the Office of Graduate and Professional Studies of
Texas A&M University
in partial fulfillment of the requirements for the degree of

DOCTOR OF PHILOSOPHY

Chair of Committee,	John A. Gladysz
Committee Members,	Daniel A. Singleton
	Donald J. Darensbourg
	Aaron M. Tarone
Head of Department,	Simon North

December 2017

Major Subject: Chemistry

ABSTRACT

In this dissertation, the development of highly effective, chiral monofunctional and bifunctional hydrogen bond donor catalysts based on cobalt(III) Werner complexes and their applications in enantioselective catalysis have been described. Furthermore, a protocol was developed to extend this chemistry into the fluorous media.

Section 1 provides an overview of the hydrogen bond mediated organocatalysis and the scope of Werner complexes as hydrogen bond donors.

Section 2 describes the fundamental stereochemical features of the trication $[Co(en)_3]^{3+}$ (en = ethylenediamine). Interactions between the trication, counter anions, and solvates are analyzed and a systematic nomenclature is developed.

Section 3 provides highly diastereoselective syntheses of variety of diastereopure salts Λ- and Δ-$[Co((S,S)\text{-}NH_2CHArCHArNH_2)_3]^{3+}$ $2X^-X'^-$ (Ar = C_6H_5, 4-C_6H_4*n*-Bu, 4-C_6H_4Cl, 4-$C_6H_4CF_3$, 4-$C_6H_4OCH_3$, α-naphthyl, ß-naphthyl, 2-C_6H_4OBn; X/X' = Cl/BAr_f (BAr_f = B(3,5-$C_6H_3(CF_3)_2)_4$), PF_6/BAr_f, BF_4/BAr_f, $PhBF_3/BAr_f$, Cl/BAr_{f20} (BAr_{f20} = $B(C_6F_5)_4$), BAr_f/BAr_f, BAr_{f20}/BAr_{f20}, BF_4/BF_4, PF_6/PF_6) and probes their properties.

Sections 4 and 5 provide detail applications of the lipophilic salts of Λ- or Δ-$[Co((S,S)\text{-dpen})_3]^{3+}$ ((*S*,*S*)-dpen = (*S*,*S*)-1,2-diphenylethylenediamine) in enantioselective addition reactions. Under optimized conditions, Λ-$[Co((S,S)\text{-dpen})_3]^{3+}$ $3BF_4^-$ catalyzes the Michael addition of dialkyl malonate to nitroalkenes in the presence of Et_3N, affording adducts in up to 98% yields and 96% ee. Interestingly, Δ-$[Co((S,S)\text{-dpen})_3]^{3+}$ $2Cl^-BAr_{f20}^-$ is superior for the additions of cyclic ß-ketoesters to azodicarboylate diesters (up to 99% yields and >99% ee).

Section 6 describes efficient syntheses of tris(hydrochloric acid) salts of chiral triamines $H_2NCH((CH_2)_nNMe_2)CH_2NH_2$ (n = 1-4) from commercial starting materials in overall yields of 38-18%.

Section 7 highlights syntheses of bifunctional catalysts and their applications in additions of dialkyl malonates to nitroalkenes. Racemic $[Co(en)_2O_2CO]^+$ Cl^- and enantiopure (*S*)-$[H_3NCH((CH_2)_nNHMe_2)CH_2NH_3]^{3+}$ $3Cl^-$ (n = 1-4) are combined (water/charcoal/100 °C) to give $[Co(en)_2((S)\text{-}H_2NCH((CH_2)_nNMe_2H)CH_2NH_2)]^{4+}$ $4Cl^-$. The cobalt diastereomers (Λ/Δ) are separated via chiral Sephadex columns. Reactions with NaOH and Na^+ BAr_f^- give the catalysts Λ- or Δ-$[Co(en)_2((S)\text{-}H_2NCH((CH_2)_nNMe_2)CH_2NH_2)]^{3+}$ $3BAr_f^-$. Under optimized condition, Λ-$[Co(en)_2((S)\text{-}H_2NCH((CH_2)_3NMe_2)CH_2NH_2)]^{3+}$ $3BAr_f^-$ gives addition products up to 98% yield and 99% ee.

Section 8 describes an optimized procedure for the synthesis of highly fluorous Na^+ $B(3,5\text{-}C_6H_3((CF_2)_5CF_3)_2)_4^-$ and its application in transporting polycations into fluorous media.

DEDICATION

This dissertation is dedicated to my grandparents Subal Chandra Ghosh and Shefali Ghosh, parents Prabhat Ghosh and Namita Ghosh, and wife Swagata Ghosh. All of them have played an immense role in my life and throughout this entire process.

ACKNOWLEDGEMENTS

First and foremost, I would like to thank my research advisor, Dr. John A. Gladysz for providing me the opportunity to work in his lab and explore new chemistry. He always allowed me to pursue my research with intellectual freedom and let me steer my project in my own direction. These were most rewarding for an young scientist like me. For years, he has put much effort towards my research and recently much time and effort on this dissertation. I have learned a lot from him. I would also like to thank my committee members, Dr. Daniel A. Singleton, Dr. Donald J. Darensbourg, and Dr. Aaron M. Tarone for taking their time to review this dissertation. Thanks to Dr. Nattamai Bhuvanesh for his crystallographic studies.

The entire Gladysz group has also been immensely helpful. I want to thank everyone for your friendships and chemical discussions, but there are a few that I would like to acknowledge specifically. I would like to thank Dr. Kyle G. Lewis for the helpful discussions about our related chemistry projects. Additionally, a special thank to Dr. Tobias Fiedler for his help during writing the papers.

To my grandparents and parents, I have no words to describe what your support has meant to me in my educational career. You have never lost faith in me and you encouraged me to always do my best even if I wasn't the best. You taught me that there was always a lesson to learn in everything that I did. That drive to learn has brought me to where I am today. A special thanks to my wife, Swagata, for her patience and love. She has been my number one support through years of late nights and weekends at the lab. Thanks to my uncle Partha Sarathi Ghosh, brother Debabrata Ghosh, and father-in-law Netai Chandra Ghosh for their encouragement.

CONTRIBUTORS AND FUNDING SOURCES

Contributors

Part 1, faculty committee recognition

This work was supervised by a dissertation committee consisting of Dr. John A. Gladysz, Dr. Daniel A. Singleton, and Dr. Donald J. Darensbourg of the Department of Chemistry and Dr. Aaron M. Tarone of the Department of Entomology.

Part 2, student/collaborator contributions

The work of section 2 of dissertation was completed by the student, in collaboration with Andreas Ehnbom and Dr. Kyle G. Lewis of the Department of Chemistry.

The work of section 3 of dissertation was completed by the student, in collaboration with Dr. Kyle G. Lewis and Dr. Anil Kumar of the Department of Chemistry.

The work of section 4 of dissertation was completed by the student, in collaboration with Dr. Kyle G. Lewis of the Department of Chemistry.

The work of section 5 of dissertation was completed by the student, in collaboration with Dr. Anil Kumar of the Department of Chemistry.

The work of section 6 of dissertation was completed by the student, in collaboration with Dr. Carola Ganzmann of the Institut für Organische Chemie and Interdisciplinary Center for Molecular Materials, Friedrich-Alexander-Universität Erlangen-Nürnberg, Henkestraße 42, 91054 Erlangen (Germany).

The work of section 7 of dissertation was completed by the student, in collaboration with Dr. Carola Ganzmann of the Institut für Organische Chemie and

Interdisciplinary Center for Molecular Materials, Friedrich-Alexander-Universität Erlangen-Nürnberg, Henkestraße 42, 91054 Erlangen (Germany).

The work of section 8 of dissertation was completed by the student, in collaboration with Ann Sullivan Ojeda and Dr. Juan Guerrero-Leal of the Department of Chemistry.

All crystal structures were determined by crystallographer Dr. Nattamai Bhuvanesh, although all crystallographic data were interpreted by the student.

All other work conducted for the dissertation was completed by the student independently.

Funding Sources

This work was made possible in part by Welch Foundation under Grant Number A-1656 and Pathways to the Doctorate fellowship from Texas A&M University.

NOMENCLATURE

δ	chemical shift
ε	molar extinction coefficient
ν	stretching mode (IR)
$\{^1H\}$	proton decoupled
Å	Angstrom
Anal.	analysis
Ar	aryl
aq	aqueous
Bn	benzyl
br	broad
Bz	benzoyl
Bu	butyl
Calcd.	calculated
CD	circular dichroism
chxn	1,2-cyclohexanediamine
d	doublet (NMR), days
dec	decomposition
DMAP	dimethylamino pyridine
dr	diastereomer ratio
DMSO	dimethylsulfoxide
dnen	dinaphthyl ethylenediamine
dpen	1,2-diphenyl ethylenediamine
ee	enantiomeric excess
en	ethylenediamine
Et	ethyl
Et_3N	triethylamine

EtOAc	ethyl acetate
equiv	equivalent
fac	facial
h	hour
HPLC	high pressure liquid chromatography
Hz	hertz
i	*ipso*, iso
$^{i}J_{jk}$	scalar coupling constant for coupling of nucleus j with nucleus k through i bonds
IR	infrared
kcal	kilocalorie
lel	parallel to the C_3 axis
M	mol/Liter
m	multiplet (NMR), medium (IR)
m	*meta*
Me	methyl
MeOH	methanol
mer	meridional
mg	milligram
min	minutes
mol	mole
mmol	millimole
mp	melting point
NMM	N-methyl morpholine
NMR	nuclear magnetic resonance
o	*ortho*
OAc	acetate
ob	oblique to the C_3 axis
OTf	triflate

p	*para*
Ph	phenyl
ppm	parts per million
Pr	propyl
q	quartet
R	organic group
rac	racemic
rt	room temperature
s	singlet (NMR), strong (IR)
t	triplet
t	tertiary
temp	temperature
TLC	thin layer chromatography
UV	ultraviolet
v/v	volume/volume
vis	visible
vs	very strong
w	weak

TABLE OF CONTENTS

Page

ABSTRACT ii

DEDICATION iv

ACKNOWLEDGEMENTS v

CONTRIBUTORS AND FUNDING SOURCES vi

NOMENCLATURE viii

TABLE OF CONTENTS xi

LIST OF FIGURES xiv

LIST OF SCHEMES xxi

LIST OF TABLES xxiv

1. INTRODUCTION 1

    1.1 Hydrogen bond mediated organocatalysis 1
    1.2 Werner complexes as hydrogen bond donors 3
    1.3 References 6

2. HYDROGEN BONDING MOTIFS IN STRUCTURALLY CHARACTERIZED SALTS OF THE TRIS(ETHYLENEDIAMINE) COBALT TRICATION, $[Co(en)_3]^{3+}$ 8

    2.1 Introduction 8
    2.2 Ethylenediamine ligand conformations 13
    2.3 A syntax for hydrogen bonding to the trication $[Co(en)_3]^{3+}$. 17
    2.4 Overview of crystallographically characterized salts of the trication $[Co(en)_3]^{3+}$ 24
    2.5 Additional structural information and generalizations. 56
    2.6 Conclusion 60
    2.7 References 61

3. SYNTHESES OF FAMILIES OF ENANTIOPURE AND DIASTEREOPURE COBALT CATALYSTS DERIVED FROM TRICATIONS OF THE FORMULA $[Co(NH_2CHArCHArNH_2)_3]^{3+}$ 67

3.1 Introduction 67
3.2 Results 71
3.3 Discussion 83
3.4 Summary 88
3.5 Experimental section 89
3.6 References 119

4. COBALT(III) WERNER COMPLEXES WITH 1,2-DIPHENYLETHYLENE-DIAMINE LIGANDS: READILY AVAILABLE, INEXPENSIVE, AND MODULAR CHIRAL HYDROGEN BOND DONOR CATALYSTS FOR ENANTIOSELECTIVE MICHAEL REACTIONS 125

4.1 Introduction 125
4.2 Results 127
4.3 Discussion 138
4.4 Experimental section 141
4.5 Crystallography 154
4.6 References 157

5. TRIS(1,2-DIPHENYLETHYLENEDIAMINE) COBALT(III) COMPLEXES: CHIRAL HYDROGEN BOND DONOR CATALYSTS FOR ENANTIO-SELECTIVE α-AMINATIONS OF 1,3-DICARBONYL COMPOUNDS..... 161

5.1 Introduction 161
5.2 Results 163
5.3 Discussion 167
5.4 Experimental section 170
5.5 References 176

6. SYNTHESIS OF A SERIES OF ω-DIMETHYLAMINOALKYL SUBSTITU-TED ETHYLENEDIAMINE LIGANDS FOR USE IN ENANTIOSELECT-IVE CATALYSIS 179

6.1 Introduction 179

6.2 Results 180
6.3 Discussion 186
6.4 Experimental section 188
6.5 References 203

7. WERNER COMPLEXES WITH ω-DIMETHYLAMINOALKYL SUBSTITUTED ETHYLENEDIAMINE LIGANDS: BIFUNCTIONAL HYDROGEN BOND DONOR CATALYSTS FOR HIGHLY ENANTIOSELECTIVE MICHAEL ADDITIONS 206

7.1 Introduction 206
7.2 Results 209
7.3 Discussion 219
7.4 Experimental section 222
7.5 Crystallography 241
7.6 References 243

8. NEW MEDIA FOR CLASSICAL COORDINATION CHEMISTRY: PHASE TRANSFER OF WERNER AND RELATED POLYCATIONS INTO HIGHLY NONPOLAR FLUOROUS SOLVENTS 249

8.1 Introduction 249
8.2 Results 251
8.3 Discussion 262
8.4 Summary 266
8.5 Experimental section 267
8.6 Crystallography 273
8.7 References 275

9. SUMMARY AND CONCLUSIONS 281

APPENDIX A 284

APPENDIX B 344

LIST OF FIGURES

FIGURE		Page
1.1	Representative hydrogen bond donors	2
1.2	First and second generation Werner cation catalysts.	5
2.1	Representations of the enantiomeric Λ- and Δ-$[Co(en)_3]^{3+}$ trications.....	10
2.2	Chelate conformations of ethylenediamine..	14
2.3	Accommodation of ethylenediamine ligands with three λ or three δ conformations in the coordination sphere of an octahedral cobalt atom with a Δ configuration..	15
2.4	All possible stereoisomers of the $[Co(en)_3]^{3+}$ trications.....	16
2.5	Representations of the C_2 and C_3 binding sites of the Δ–*λλλ*-$[Co(en)_3]^{3+}$ trication, and a general nomenclature system for hydrogen bonding to a given anion	21
2.6	Anion binding modes involving hydrogen bonding to both the C_2 and C_3 sites of the Δ–*λλλ*-$[Co(en)_3]^{3+}$ trication.....	23
2.7	Representative hydrogen bonding motifs for the Δ–*λλλ*-$[Co(en)_3]^{3+}$ trication (*lel*$_3$, D_3) and the nitrate anion..	25
2.8	Hydrogen bonding interactions in Λ–*δδδ*-$[Co(en)_3]^{3+}$ $3Cl^-\cdot 2.8H_2O$ (*lel*$_3$) viewed along the C_3 axis (left) and a C_2 axis (right)..	27
2.9	Hydrogen bonding interactions in Λ–*δδδ*-$[Co(en)_3]^{3+}$ $3Cl^-$ (*lel*$_3$) viewed along the C_3 axis (left) and a C_2 axis (right)..	28
2.10	Hydrogen bonding interactions in Λ–*δδδ*-$[Co(en)_3]^{3+}$ $3Br^-\cdot H_2O$ (*lel*$_3$) viewed along the C_3 axis (left) and a C_2 axis (right)..	29
2.11	Hydrogen bonding interactions in Λ–*λδδ*-$[Co(en)_3]^{3+}$ $3I^-\cdot H_2O$ (*oblel*$_2$) viewed along the pseudo C_3 axis (left) and a C_2 axis (right)..	30

2.12 Hydrogen bonding interactions in Λ–*λδδ*-$[Co(en)_3]^{3+}$ $3ReO_4^-$ (*oblel*$_2$) viewed along the pseudo C_3 axis (left) and a C_2 axis (right). Non-interacting oxygen atoms of the ReO_4^- anions have been omitted for clarity..... 32

2.13 Hydrogen bonding interactions in Λ–*δδδ*-$[Co(en)_3]^{3+}$ $Cl^-2I^-\cdot H_2O$ (*lel*$_3$) viewed along the pseudo C_3 axis (left) and a C_2 axis (right).. 33

2.14 Hydrogen bonding interactions in Λ–*λδδ*-$[Co(en)_3]^{3+}$ $B_5O_6(OH)^{4-}$ $B_8O_{10}(OH)_6^{2-}\cdot 5H_2O$ (*oblel*$_2$) viewed along the pseudo C_3 axis (left) and the C_2 axis (right). The larger borate dianion is colored orange and the smaller borate monoanion is colored light green. In both cases, some non-interacting atoms have been omitted for clarity..... 35

2.15 Hydrogen bonding interactions in Λ–*λδδ*-$[Co(en)_3]^{3+}$ $1.5C_4O_4^{2-}$ $\cdot 4.5H_2O$ (*oblel*$_2$) viewed along the pseudo C_3 axis (left) and the C_2 axis (right). Several non-interacting atoms of the squarate anions have been omitted for clarity. 36

2.16 Hydrogen bonding interactions in Λ–*δλλ*-$[Co(en)_3]^{3+}\cdot 1.5C_5O_5^{2-}\cdot 3H_2O$ (*lelob*$_2$) viewed along the pseudo C_3 axis (left) and the C_2 axis (right). Several atoms of the $C_5O_5^{2-}$ dianions have been omitted for clarity..... 37

2.17 Hydrogen bonding interactions in Λ–*δδδ*-$[Co(en)_3]^{3+}$ Cl^-(*R*,*R*)-$tart^{2-}$ $\cdot 5H_2O$ (*lel*$_3$) viewed along the C_3 axis (left) and the C_2 axis (right). Most non-interacting atoms of the tartrate dianions have been omitted for clarity..... 39

2.18 Hydrogen bonding interactions in the two independent trications of Δ–*λλλ*-$[Co(en)_3]^{3+}$ 1.5(*R*,*R*)-$tart^{2-}\cdot 5.75H_2O$ (*lel*$_3$) viewed along the C_3 axis (left middle, left bottom) and a C_2 axis (right middle, right bottom), or as linked together (top). In the middle and bottom representations, most non-interacting atoms of the tartrate dianions have been omitted for clarity..... 41

2.19 Hydrogen bonding interactions in the two independent trications of Λ–*δδδ*-$[Co(en)_3]^{3+}$ 1.5(*R*,*R*)-$tart^{2-}\cdot 9.5H_2O$ (*lel*$_3$) viewed along the C_3 axis (left) and a C_2 axis (right). Most non-interacting atoms of the tartrate dianions have been omitted for clarity.... 43

2.20 Hydrogen bonding interactions in Λ–*δδδ*-$[Co(en)_3]^{3+}$ $AsO_4^{3-}\cdot 3H_2O$ (*lel*$_3$) viewed along the C_3 axis (left) and a C_2 axis (right). Non-interacting oxygen atoms of the arsenate trianion have been omitted for clarity..... 45

2.21 Hydrogen bonding interactions in Λ–*λδδ*-$[Co(en)_3]^{3+}$ AsS_4^{3-} (*oblel*$_2$) viewed along the pseudo C_3 axis (left) and the C_2 axis (right). Non-interacting sulfur atoms of the tetrathioarsenate trianion have been omitted for clarity..... 47

2.22 Hydrogen bonding interactions in Λ–*δδδ*-$[Co(en)_3]^{3+}$ GaF_6^{3-} viewed along the C_3 axis (left) and a C_2 axis (right). Non-interacting fluorine atoms of the hexafluorogallate trianion have been omitted for clarity... ... 48

2.23 Hydrogen bonding interactions in Λ–*λδδ*-$[Co(en)_3]^{3+}$ $Co(CN)_6^{3-}\cdot 5H_2O$ (*oblel*$_2$) viewed along the pseudo C_3 axis (left) and the C_2 axis (right). Except for the interacting CN units, the $Co(CN)_6^{3-}$ trianions have been omitted for clarity. Disordered H_2O molecules are denoted with an X.... 49

2.24 Hydrogen bonding interactions in Λ–*δδδ*-$[Co(en)_3]^{3+}$ Λ-$Rh(C_2O_4)_3^{3-}$ (*lel*$_3$) viewed along the C_3 axis (left) and a C_2 axis (right). Non interacting atoms of the trianion have been omitted for clarity..... 51

2.25 Hydrogen bonding interactions in Λ–*δδδ*-$[Co(en)_3]^{3+}$ Δ-$Rh(C_2O_4)_3^{3-}$ (*lel*$_3$) viewed along the C_3 axis (left) and a C_2 axis (right). Non interacting atoms of the trianion have been omitted for clarity..... 52

2.26 Hydrogen bonding interactions in Λ–*λδδ*-$[Co(en)_3]^{3+}$ $C_6H_3(CO_2)_3^{3-}\cdot 5.55H_2O$ (*oblel*$_2$) viewed along the pseudo C_3 axis (left) and the C_2 axis (right). Non-interacting atoms of the trianion have been omitted for clarity..... 53

2.27 Hydrogen bonding interactions in Λ–*δδδ*-$[Co(en)_3]^{3+}$ $P_3O_9^{3-}\cdot 2H_2O$ (*lel*$_3$) viewed along the C_3 axis (left) and a C_2 axis (right). Most non-interacting atoms of the trianion have been omitted for clarity..... 54

2.28 Hydrogen bonding interactions in Λ–*δδδ*-$[Co(en)_3]^{3+}$ $P_3O_9^{3-}\cdot 2H_2O$ (*lel*$_3$) viewed along the C_3 axis (left) and a C_2 axis (right). Most non-interacting atoms of the trianion have been omitted for clarity..... 55

3.1 Thermal ellipsoid diagram (50% probability level) of the trication of Λ-(*S*,*S*)-**1**$^{3+}$ 3Cl^{-}·2H$_2$O·2CH$_3$OH: **A**, view down the idealized C_3 axis; **B**, view down one of the three C_2 axes..... 68

3.2 ^{1}H NMR spectra (CD_2Cl_2) of (a) Λ-(*S*,*S*)-**1**$^{3+}$ 2Cl^{-}BAr$_f^{-}$, (b) Λ-(*S*,*S*)-**1**$^{3+}$ 2BF$_4^{-}$BAr$_f^{-}$, (c) Λ-(*S*,*S*)-**1**$^{3+}$ 2PF$_6^{-}$BAr$_f^{-}$, and (d) Λ-(*S*,*S*)-**1**$^{3+}$ 3BAr$_f^{-}$..... 81

3.3 Dependence of the chemical shifts of the diastereotopic NHH' protons of (a) Λ-(*S*,*S*)-**1**$^{3+}$ 2Cl^{-}BAr$_f^{-}$, (b) Λ-(*S*,*S*)-**1**$^{3+}$ 2BF$_4^{-}$BAr$_f^{-}$, and (c) Λ-(*S*,*S*)-**1**$^{3+}$ 3BAr$_f^{-}$ upon concentration (CD_2Cl_2, ambient probe temperature)..... 83

3.4 Proposed ion pairing equilibria for the two chloride ions of Λ-(*S*,*S*)-**1**$^{3+}$ 2Cl^{-}X'$^{-}$; **C**, most stable; **D**, intermediate; **E**, least stable..... 84

3.5 Chelate conformations of dpen and all possible trications [Co(dpen)$_3$]$^{3+}$ with pseudoequatorial phenyl substituents..... 87

3.6 (a) Components of the gas circulating flask; (b) The assembled flask..... . 123

4.1 Thermal ellipsoid diagram (50% probability level) of Λ-(*S*,*S*)-**1**$^{3+}$ 3Cl^{-} •2H$_2$O•2CH$_3$OH with solvent molecules removed for clarity. Upper left and right, views down the idealized C_3 and C_2 axes with chloride ions omitted; lower left and right, analogous views with chloride ions..... 130

4.2 Thermal ellipsoid diagram (50% probability level) of Δ-(*S*,*S*)-**1**$^{3+}$ 3Cl^{-} •12.5H$_2$O with solvent molecules removed for clarity. Upper left and right, views down the idealized C_3 and C_2 axes with chloride ions omitted; lower left and right, analogous views with chloride ions..... 130

4.3 Thermal ellipsoid diagram (50% probability level) of Δ-(*R*,*R*)-**1**$^{3+}$ 3Cl^{-} •H$_2$O•3CH$_3$OH with solvent molecules removed for clarity. Upper left and right, views down the idealized C_3 and C_2 axes with chloride ions omitted; lower left and right, analogous views with chloride ions..... 131

4.4 Rate profiles for additions of dimethyl malonate (**22c**) to *trans*-4-methoxy-ß-nitrostyrene (**21d**) catalyzed by lipophilic Werner salts. Conditions: 2 mol% catalyst, 0.35 equiv Et_3N, CD_2Cl_2, rt..... 134

4.5 ^{1}H NMR spectra: titration of a 0.017 M CD_2Cl_2 solution of Λ-(*S*,*S*)-**1**$^{3+}$ 2Cl$^-$BAr$_f^-$ with *trans*-ß-nitrostyrene (**21a**). Data (equiv of **21a**/NH signals, δ in ppm): 0.250/4.010 and 8.127; 0.500/4.053 and 8.134; 0.750/4.094 and 8.141; 1.00/4.129 and 8.131; 1.25/4.165 and 8.155; 1.50/4.195 and 8.158; 1.75/4.204 and 8.162; 2.00/4.241 and 8.169; 2.50/4.28 and 8.179; 2.75/4.296 and 8.183; 3.00/4.31 and 8.178; 4.00/4.342 and 8.184; 5.00/4.368 and 8.196; 6.00/4.387 and 8.227; 7.00/4.405 and 8.236; 8.00/4.418 and 8.234; 9.00/4.432 and 8.249..... 135

4.6 Catalytic systems with active sites having C_3 symmetry..... 138

4.7 Metal catalysts with hydrogen bond donors *remote* from coordinating atoms..... 139

6.1 Target ligands and complexes..... 180

7.1 Monofunctional and bifunctional thiourea catalysts and their possible activation modes..... 207

7.2 Separation of the tetracation **27c**·H^{4+} 4Cl$^-$ from redistribution products..... 210

7.3 Separation of the diastereomers of **27c**·H^{4+} 4Cl$^-$ and structure of SP-Sephadex..... 211

7.4 Circular dichroism spectra of (a) Δ- and Λ-[Co(en)$_3$]$^{3+}$ 3I$^-$, (b) Δ- and Λ-**27a**·H^{4+} 4Cl$^-$, and (c) Δ- and Λ-**27b-d**·H^{4+} 4Cl$^-$..... 213

7.5 The crystal structure of the tetracation of Δ-**27a**·H^{4+} 4Cl$^-$·3H$_2$O with thermal ellipsoids at the 50% probability level (the anions and water molecules are not shown). Key bond lengths (Å) and angles (°): Co-N1 1.9692(18), Co-N2 1.9703(19), Co-N3 1.9634(18), Co-N4 1.9627(18), Co-N5 1.9685(19), Co-N6 1.9710(18), C1-N1 1.489(3), C2-N2 1.488(3), C3-N3 1.489(3), C4-N4 1.494(3), C5-N5 1.495(3), C6-N6 1.483(3), C7-N7 1.488(3), C8-N7 1.490(3), C9-N7 1.492(3), C1-C2 1.504(3), C3-C4 1.510(3), C5-C6 1.517(3), C6-C7 1.532(3), N1-Co-N2 85.06(8), N1-Co-N3 91.57(8), N4-Co-N1 175.52(8), N1-Co-N5 90.82(8), N1-Co-N6 92.60(8), N3-Co-N6 175.39(8), N5-Co-N2 173.98(7), N4-Co-N3 84.58(8), N4-Co-N6 91.33(8), N4-Co-N5 91.70(8), N4-Co-N2 92.71(8)..... 214

7.6 Rates of reaction of *trans*-ß-nitrostyrene (**21a**) and dimethyl malonate (**22c**, 1.2 equiv) in CD_2Cl_2 in the presence of an internal standard and catalyst (2 mol%; see experimental section): (■) Λ-$[Co(en)_3]^{3+}$ $3BAr_f/Et_3N$, (♦) Λ-**27c**$^{3+}$ $3BAr_f^-$, (▲) Δ-**27c**$^{3+}$ $3BAr_f^-$, Λ-$[Co(en)_3]^{3+}$ $3BAr_f^-$..... 218

7.7 Hydrogen bond donor catalysts that have been reported to give high ee values for some of the products in Scheme 7.4..... 220

8.1 Two views of the molecular structure of **29** with thermal ellipsoids at the 50% probability level. Key bond lengths (Å) and angles (°): C1-Br 1.899(2), C1-C2 1.385(3), C2-C3 1.391(3), C4-C5 1.394(3), C5-C6 1.391(3), C6-C1 1.383(3), C3-C7 1.507(3), C5-C13 1.506(3), average of ten CF-CF 1.544(5), Br-C1-C2 119.14(17), C1-C2-C3 118.7(2), C2-C3-C4 120.7(2), C3-C4-C5 119.3(2), C4-C5-C6 120.8(2), C5-C6-C1 118.5(2), C6-C1-C2 121.9(2), C6-C1-Br 118.93(17), C2-C3-C7 120.3(2), C4-C3-C7 119.0(2), C4-C5-C13 119.2(2), C6-C5-C13 120.0(2), average of eight CF-CF-CF 115.0(8)..... 253

8.2 (a) 2.1×10^{-3} M aqueous solution of $[Co(en)_3]^{3+}$ $3Cl^-$ (10 mL). (b) 6.3×10^{-3} M Na^+ BAr_{f6}^- solution in PFMC (10 mL). (c) Biphasic mixture after gentle addition of (b) to (a). (d) The sample from (c) was stirred (10 min). (e) The sample from (d) after stirring was halted..... 257

8.3 (a) 2.1×10^{-3} M aqueous solution of $[Co(R,R\text{-chxn})_3]^{3+}$ $3Cl^-$ (10 mL). (b) 6.3×10^{-3} M Na^+ BAr_{f6}^- solution in PFMC (10 mL). (c) Biphasic mixture after gentle addition of (b) to (a). (d) The sample from (c) was stirred (10 min). (e) The sample from (d) after stirring was halted..... 257

8.4 (a) 2.1×10^{-3} M aqueous solution of $[Ru(bipy)_3]^{2+}$ $2Cl^- \cdot 6H_2O$ (10 mL). (b) 4.20×10^{-3} M Na^+ BAr_{f6}^- solution in PFMC (10 mL). (c) Biphasic mixture after gentle addition of (b) to (a). (d) The sample from (c) was stirred (10 min). (e) The sample from (d) after stirring was halted..... 258

8.5 (a) Biphasic mixture after gentle addition of a 1.74×10^{-3} M CH_2Cl_2 solution of $[Co(en)_3]^{3+}$ $3BAr_f^-$ (10 mL, upper layer) to a 5.22×10^{-3} M PFMC solution of Na^+ BAr_{f6}^- (10 mL, bottom layer). (b) The sample from (a) after stirring was halted. (c) Biphasic mixture after gentle addition of a 1.74×10^{-3} M CH_2Cl_2 solution of $[Co(en)_3]^{3+}$ $3BAr_f^-$ (10

mL, upper layer) to a 6.96×10^{-3} M PFMC solution of Na^+ BAr_{f6}^- (10 mL, bottom layer). (d) The sample from (c) after stirring was halted..... . 261

8.6 A fluorophilic salt of $[Ru(bipy)_3]^{2+}$ prepared by Vincent..... 263

8.7 Packing of **29** in the unit cell (Z = 8). Top: ball and stick representation; bottom: space filling representation..... 265

9.1 Chiral-at-metal hydrogen bond donor catalysts based on cobalt(III) Werner complexes..... 281

LIST OF SCHEMES

SCHEME		Page
1.1	Claisen rearrangement in the presence of diarylurea **Ia**.....	2
1.2	Michael reaction catalyzed by chiral bifunctional thiourea **IIa** and two possible transition states for the reaction.....	3
1.3	Enantioselective Michael addition catalyzed by a chiral Werner type complex.....	4
2.1	Resolution of the enantiomeric Λ and Δ-$[Co(en)_3]^{3+}$ trications.....	11
3.1	Syntheses of substituted dpen ligands and related species.....	70
3.2	Syntheses of salts of the formula $[Co((S,S)\text{-dpen})_3]^{3+}$ $3X^-$ ((*S*,*S*)-$\mathbf{1}^{3+}$ 3X; X = Cl, ClO_4); kinetic and thermodynamic Λ/Δ diastereoselectivities.....	72
3.3	Syntheses of lipophilic Werner salts (yields: 83-96%). The procedures for Δ diastereomers are analogous.....	74
3.4	Thermal epimerization of Λ-(*S*,*S*)-$\mathbf{1}^{3+}$ $2X^-BAr_f^-$ to Δ-(*S*,*S*)-$\mathbf{1}^{3+}$ $2X^-$ BAr_f^-.....	76
3.5	Syntheses of catalysts from substituted (*S*,*S*)-dpen ligands.....	78
3.6	Syntheses of catalysts from a tetrakis(trifluoromethyl) substituted (*S*,*S*)-dpen ligands.....	79
3.7	Comproportionation of two salts to give a mixed salt.....	82
4.1	Syntheses of salts of the formula $[Co((S,S)\text{-dpen})_3]^{3+}$ $3X^-$ ((*S*,*S*)-$\mathbf{1}^{3+}$ 3X; X = Cl, ClO_4); kinetic and thermodynamic Λ/Δ diastereoselectivities.....	128
4.2	Syntheses of lipophilic Werner salts (yields: 83-96%).The procedures for Δ diastereomers are analogous.....	129

4.3 Initial screening reactions: Data for additions of dialkyl malonates (**22**) to *trans*-β-nitrostyrene (**21a**) catalyzed by Λ- and Δ-(*S*,*S*)-$\mathbf{1}^{3+}$ $2Cl^{-}BAr_f^{-}$ in CD_2Cl_2 at room temperature (entries 1-6), and additions catalyzed by other salts of Λ-(*S*,*S*)-$\mathbf{1}^{3+}$ in acetone-d_6 at 0 °C (entries 7-11) 132

4.4 Substrate scope. Data for additions of dimethyl malonate (**22c**) to nitroalkenes catalyzed by Λ-(*S*,*S*)-$\mathbf{1}^{3+}$ $2Cl^{-}BAr_f^{-}$, Λ-(*S*,*S*)-$\mathbf{1}^{3+}$ $2BF_4^{-}$ BAr_f^{-}, and Λ-(*S*,*S*)-$\mathbf{1}^{3+}$ $3BF_4^{-}$..... 137

5.1 A chiral cobalt(III) trication originally separated into enantiomers by Werner (top); general catalyst family (middle); reaction to be investigated (bottom)..... 162

5.2 Optimization of catalysts and conditions..... 164

5.3 Substrate scope under optimized conditions..... 166

5.4 Views of the C_3 and C_2 faces of the trication of Λ-(*S*,*S*)-$\mathbf{1}^{3+}$ $3Cl^{-}$ (top), A possible transition state Assembly (middle), Other chiral hydrogen bond donor catalysts employed for the title reaction (bottom)..... 168

6.1 Synthesis of the tris(hydrochloric acid) salt of (*S*)-**L1**..... 181

6.2 Synthesis of the tris(hydrochloric acid) salt of (*S*)-**L2**..... 183

6.3 Synthesis of the tris(hydrochloric acid) salt of (*S*)-**L3**..... 184

6.4 Synthesis of the tris(hydrochloric acid) salt of (*S*)-**L4**..... 185

7.1 Design of families of cobalt(III) hydrogen bond donor catalysts..... 208

7.2 Syntheses of bifunctional catalysts **27a-d**$^{3+}$ $3BAr_f^{-}$ from (*S*)-**L*n***·$(HCl)_3$ (*n* = 1-4)..... 209

7.3 Optimization of conditions for catalysis..... 215

7.4 Scope of additions under optimum conditions..... 217

8.1 Enantiomers of the trication of $[Co(en)_3]^{3+}$ $3Cl^{-}$..... 249

8.2 Modified syntheses of Na^+ BAr_{f6}^- (**28**)..... 251

8.3 Syntheses of fluorous BAr_{f6} salts of Werner trications..... 256

8.4 Synthesis of a fluorous BAr_{f6} salt of the dication $[Ru(bipy)_3]^{2+}$..... 258

8.5 Partitioning of $[Co(en)_3]^{3+}$ between a CH_2Cl_2 solution of $3BAr_f^-$ and a PFMC solution of $xBAr_{f6}^-$ in the presence of xNa^+ (x = 3, 4) as determined by ^1H NMR and UV-vis spectroscopy (unbracketed and bracketed values)..... 260

LIST OF TABLES

TABLE		Page
2.1	Syntax for hydrogen bonding interactions between the $[Co(en)_3]^{3+}$ trication and anions or solvent molecules.....	19
3.1	Selected ^1H NMR and hydration data for isolated cobalt(III) salts	77
7.1	Crystallographic data for Δ-**27a**·H^{4+} $4Cl^-$·$3H_2O$	242
8.1	Crystallographic data for **29**	254
8.2	Solubility data (24 °C).....	255
8.3	Partition coefficients measured by ^{19}F NMR (24 °C).....	259

1. INTRODUCTION

1.1. Hydrogen bond mediated organocatalysis

In the last twenty years, the field of organocatalysis has exploded from a few isolated reactions in the literature to a thriving new field of chemical research encompassing a broad range of useful transformations and unprecedented reactivities.[1] Organocatalysis is the process of acceleration of a chemical reaction with an organic compound that does not contain a metal atom in its active center[2] or its "primary" catalytic cycle — the bond forming and breaking steps of the reaction. This type of catalysis is complementary with the metal-complex mediated biocatalytic transformations. Preparative advantages of organocatalysts are notable: they are readily available from simple chiral feedstocks. Furthermore, the organocatalytic reactions can usually be performed under an aerobic atmosphere, with wet solvents, and in many cases protection of functional groups is not required.[1]

Hydrogen bonding acts as a ubiquitous glue to sustain the intricate architecture and functionality of proteins, nucleic acids, and many supramolecular assemblies, and thus is responsible for the structure of much of the world around us.[3] The enormous potential of hydrogen bonding for activating an intermediate has been recognized only recently. For example, catalysis by urea and thiourea derivatives through hydrogen bonding found momentum after the pioneering work of Curran who discovered that substoichiometic amounts of diarylurea (**Ia**) accelerated the Claisen rearrangement of 6-methoxyallyl vinyl ether compared to the uncatalyzed reaction (Scheme 1.1).[4] Soon thereafter asymmetric variants came into play. Besides urea (**I**) and thiourea (**II**), additional new hydrogen bond donor motifs like guanidine (**III**),[5] squaramide (**IV**),[6] TADDOL (**V**),[7] BINOL (**VI**),[8] silanediols (**VII**)[9] etc were also developed (Figure 1.1).

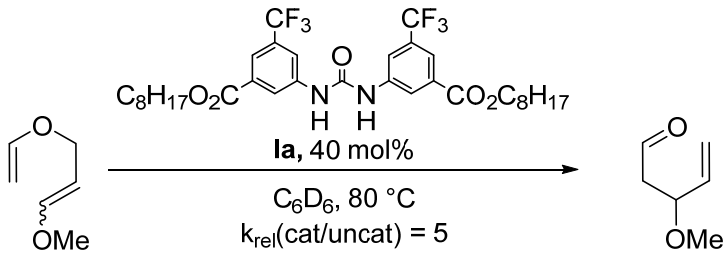

Scheme 1.1. Claisen rearrangement in the presence of diarylurea **Ia.**

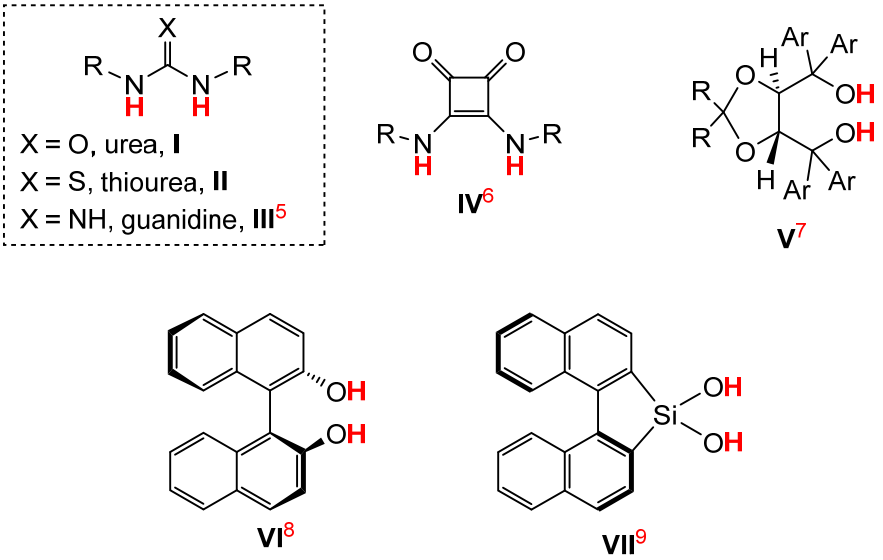

Figure 1.1. Representative hydrogen bond donors

The scope of applications for thiourea catalysts was considerably broadened by the introduction of an additional basic group. Takemoto et al. developed such a bifunctional organocatalyst which combined the quasi-Lewis acidic thiourea and a Brønsted basic tertiary amine. These two functionalities operate in a single chiral environment to generate a highly efficient catalyst that promotes the Michael addition of malonates to nitroolefins to afford products with high enantioselectivities (Scheme 1.2).[10] The authors also investigated the mechanism of this reaction and proposed a bifunctional mode of activation (TSa) of both the substrates by the catalyst. Later, another group suggested the alternative TSb (Scheme 1.2).[11]

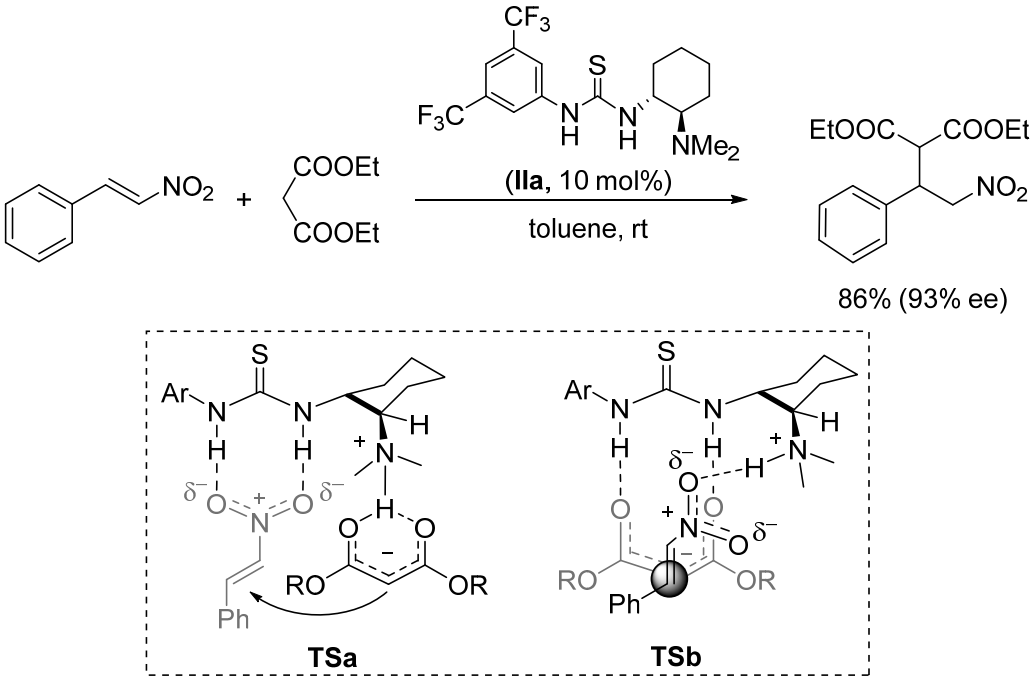

Scheme 1.2. Michael reaction catalyzed by chiral bifunctional thiourea **IIa** and two possible transition states for the reaction.

1.2. Werner complexes as hydrogen bond donors

There is currently much interest in chiral hydrogen bond donors as enantioselective catalysts for organic reactions.[12] A variety of literature data suggest that many Werner cations with amine ligands are exceptional hydrogen bond donors to the anions and small molecules such as water (see Section 2).[13] This hydrogen bonding pattern is conceptually similar to those of catalysts having thiourea backbones. Since octahedral cobalt(III) Werner cations are substitution inert and do not readily exchange ligands, activation and asymmetric induction must take place via the second-coordination sphere involving hydrogen bonding to the NH_2 moieties of the amine ligands. Thus, cobalt(III) Werner complexes were considered as possible metal-containing hydrogen bond donor catalysts. The role of central metal cobalt(III) is

altering the electronic properties of the ligand and fixing them in a defined position without being involved in any bond forming and breaking steps.

When octahedral cobalt(III) Werner cations feature at least two chelating ligands, they are chiral, often termed "chiral-at-metal". Accordingly, in 2008 the Gladysz group reported that the classical Werner complexes of the type $[Co(en)_3]^{3+}$ (en = ethylenediamine), and related species provide a novel architecture for asymmetric hydrogen bond mediated catalysis.[14] The Michael addition of dimethyl malonate to 2-cyclopenten-1-one with a stoichiometric amount of Et_3N was performed in the presence of 9 mol% Δ-$[Co(en)_3]^{3+}$ $3BAr_f^- \cdot 14H_2O$ (BAr_f = $B(3,5\text{-}C_6H_3(CF_3)_2)_4$) in CH_2Cl_2 to give the addition product in 78% yield and 33% ee (Scheme 1.3).

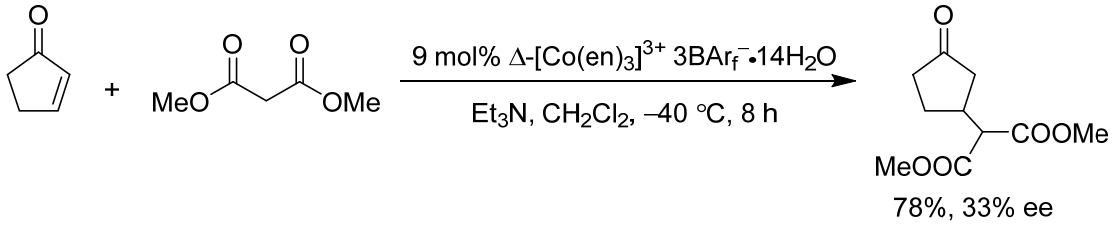

Scheme 1.3. Enantioselective Michael addition catalyzed by a chiral Werner type complex.

Despite extensive optimization of reactions and screening of substrates, reactions with higher enantioselectivities could not be achieved. Thus, the first generation catalytic moiety $[Co(en)_3]^{3+}$ was modified to (1) the bulkier hexa(aryl) Werner cations of the formula $[Co((S,S)\text{-}NH_2CHArCHArNH_2)_3]^{3+}$ (Figure 1.2) and (2) bifunctional Werner cations $[Co(en)_2((S)\text{-}H_2NCH((CH_2)_nNMe_2)CH_2NH_2)]^{3+}$ in which one chelating diamine incorporates a pendant basic moiety $(CH_2)_nNMe_2$ (Figure 1.2). It was thought

that the fixed basic functionality might lead to a higher enantioselectivity as the reaction may occur through a highly organized transition state.

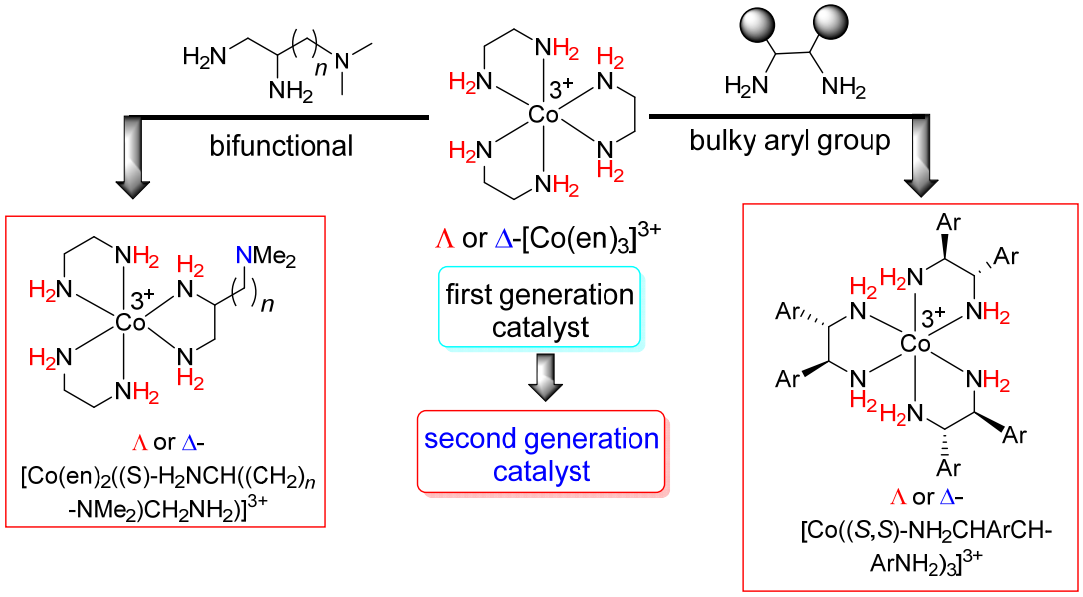

Figure 1.2. First and second generation Werner cation catalysts.

The syntheses of these types of second generation Werner complexes and their applications are described in the next sections.

1.3. References

(1) *Asymmetric Organocatalysis*, Berkessel, A., Gröger, H., Eds.; Wiley-VCH: Weinheim, **2005**.

(2) Cozzi, F. *Adv. Synth. Catal.* **2006**, *348*, 1367-1390.

(3) *The Organic Chemistry of Enzyme-Catalyzed Reactions*, Silverman, R. B. Academic Press, San Diego, CA, **2002**.

(4) Curran, D. P.; Kuo, L. H. *Tetrahedron Lett.* **1995**, *36*, 6647-6650.

(5) (a) Corey, E. J.; Grogan, M. J. *Org. Lett.* **1999**, *1*, 157-160. (b) Kita, T.; Georgieva, A.; Hashimoto, Y.; Nakata, T.; Nagasawa, K. *Angew. Chem., Int. Ed.* **2002**, *41*, 2832-2834; *Angew. Chem.* **2002**, *114*, 2956-2958. (c) Terada, M.; Ube, H.; Yaguchi, Y. *J. Am. Chem. Soc.* **2006**, *128*, 1454-1455. (d) Terada, M.; Nakano. M.; Ube, H. *J. Am. Chem. Soc.* **2006**, *128*, 16044-16045. (e) Yu, Z.; Liu, X.; Zhou, L.; Lin, L.; Feng, X. *Angew. Chem., Int. Ed.* **2009**, *48*, 5195-5198; *Angew. Chem.* **2009**, *121*, 5297-5300. (f) Misaki, T.; Takimoto, G.; Sugimura, T. *J. Am. Chem. Soc.* **2010**, *132*, 6286-6287. (g) Dong, S. X.; Liu, X. H.; Chen, X. H.; Mei, F.; Zhang, Y. L.; Gao, B.; Lin, L. L.; Feng, X. M. *J. Am. Chem. Soc.* **2010**, *132*, 10650-10651. (h) Sohtome, Y.; Shin, B.; Horitsugi, N.; Takagi, R.; Noguchi, K.; Nagasawa, K. *Angew. Chem., Int. Ed.* **2010**, *49*, 7299-7303; *Angew. Chem.* **2010**, *122*, 7457-7461. (i) Sohtome, Y.; Tanaka, S.; Takada, K.; Yamaguchi, T.; Nagasawa, K. *Angew. Chem., Int. Ed.* **2010**, *49*, 9254-9257; *Angew. Chem.* **2010**, *122*, 9440-9443.

(6) (a) Yang, W.; Du, D.-M. *Org. Lett.* **2010**, *12*, 5450-5453. (b) Dai, L.; Wang, S.-X.; Chen, F.-E. *Adv. Synth. Catal.* **2010**, *352*, 2137-2141. (c) Xu, D.-Q.; Wang, Y.-F.; Zhang, W.; Luo, S.-P.; Zhong, A.-G.; Xia, A.-B.; Xu, Z.-Y. *Chem. Eur. J.* **2010**, *16*, 4177-4180. (d) Lee, J. W.; Ryu, T. H.; Oh, J. S.; Bae, H. Y.; Jang, H. B.; Song, C. E. *Chem. Commun.* **2009**, 7224-7226.

(7) (a) Huang, Y.; Unni, A. K.; Thadani, A. N.; Rawal, V. H. *Nature* **2003**, *424*, 146. (b) Thadani, A. N.; Stankovic, A. R.; Rawal, V. H. *Proc. Natl. Acad. Sci.* **2004**, *101*, 5846-5850. (c) Du, H.; Zhao, D.; Ding, K. *Chem. Eur. J.* **2004**, *10*, 5964-5970. (d) McGilvra, J. D.; Unni, A. K.; Modi, K.; Rawal, V. H. *Angew. Chem., Int. Ed.* **2006**, *45*, 6130-6133; *Angew. Chem.* **2006**, *118*, 6276-6279. (e) Unni, A. K.; Takenaka, N.; Yamamoto, H.; Rawal, V. H. *J. Am. Chem. Soc.* **2005**, *127*, 1336-1337.

(8) (a) McDougal, N. T.; Schaus, S. E. *J. Am. Chem. Soc.* **2003**, *125*, 12094-12095. (b). McDougal, N. T.; Trevellini, W. L.; Rodgen, S. A.; Kliman, L. T.; Schaus, S. E. *Adv. Synth. Catal.* **2004**, *346*, 1231-1240. (c) Matsui, K.; Takizawa, S.; Sasai, H. *J. Am. Chem. Soc.* **2005**, *127*, 3680-3681. (d) Wang, J.; Li, H.; Yu, X.; Zu, L.; Wang, W. *Org. Lett.* **2005**, *19*, 4293-4296. (e) Tillman, A. L.; Dixon, D. *Org. Biomol. Chem.* **2007**, *5*, 606-609.

(9) Schafer, A. G.; Wieting, J. M.; Mattson, A. E. *Org. Lett.* **2011**, *13*, 5228-5231.

(10) (a) Okino, T.; Hoashi, Y.; Takemoto, Y. *J. Am. Chem. Soc.* **2003**, *125*, 12672-12673. (b) Okino, T.; Hoashi, Y.; Furukawa, T.; Xu, X.; Takemoto, Y. *J. Am. Chem. Soc.* **2005**, *127*, 119-125.

(11) Hamza, A.; Schubert, G.; Soós, T.; Pápai, I. *J. Am. Chem. Soc.* **2006**, *128*, 13151-13160.

(12) (a) Taylor, M. S.; Jacobsen, E. N. *Angew. Chem., Int. Ed.* **2006**, *45*, 1520-1543; *Angew. Chem.* **2006**, *118*, 1550-1573. (b) Doyle, A. G.; Jacobsen, E. N. *Chem. Rev.* **2007**, *107*, 5713-5743.

(13) Ghosh, S. K.; Ehnbom, A.; Lewis, K. G.; Gladysz, J. A. *Coord. Chem. Rev.* **2017**, in press. DOI: 10.1016/j.ccr.2017.04.002.

(14) Ganzmann, C.; Gladysz, J. A. *Chem. Eur. J.* **2008**, *14*, 5397-5400.

2. HYDROGEN BONDING MOTIFS IN STRUCTURALLY CHARACTERIZED SALTS OF THE TRIS(ETHYLENEDIAMINE) COBALT TRICATION, $[Co(en)_3]^{3+}$†

2.1. Introduction

The title complexes, Werner salts of the trication $[Co(en)_3]^{3+}$ (en = ethylene-diamine), have always been a classroom favorite.[1,2] However, until recently the emphasis has been on illustrating well understood physical phenomena that were established long ago. For example, the trication is chiral, as can easily be appreciated when the non-superimposable mirror images are represented in a "Star of David" motif as shown in Figure 2.1-**A**.[3] The descriptors Λ and Δ are used to specify the cobalt configuration. The former indicates a left handed helix, consistent with the counterclockwise direction that the chelates must take in connecting the front and rear triangles in the left structure (Figure 2.1-**A**). The latter indicates a right handed helix, with the chelates taking a clockwise direction when connecting the front and rear triangles (right structure). The hydrogen atoms on each NH_2 group are diastereotopic, and are sometimes distinguished as NHH'.

Salts of the types $[Co(en)_3]^{3+}\ yX^{z-}$, $[Co(en)_2(A—A)]^{n+}\ yX^{z-}$, and $[Co(en)_2(A—B)]^{n+}\ yX^{z-}$ were the first inorganic compounds to be resolved into enantiomers, as detailed by Werner in a series of five papers in 1911-1912.[3] Several recipes have been applied to the trication $[Co(en)_3]^{3+}$.[3e,4] The original procedure of Werner began with an aqueous solution of silver (*R*,*R*)-tartrate ($2Ag^+$ (*R*,*R*)-$tart^{2-}$), as shown in Scheme 2.1.[3e]

†Reproduced with permission from Ghosh, S. K.; Ehnbom, A.; Lewis, K. G.; Gladysz, J. A. *Coord. Chem. Rev.* **2017**, in press, doi: 10.1016/j.ccr.2017.04.002.

This led to the diastereomeric mixed chloride/tartrate salts Λ- and Δ-$[Co(en)_3]^{3+}$ Cl^- (*R*,*R*)-$tart^{2-}$. The former crystallized as a pentahydrate, and the latter remained in solution. Chloride ion exchange then provided the resolved enantiomers Λ- and Δ-$[Co(en)_3]^{3+}$ $3Cl^-$. Later, Broomhead replaced silver (*R*,*R*)-tartrate with the less expensive and more stable barium salt (Ba^{2+} (*R*,*R*)-$tart^{2-}$).[4a] He also treated the intermediate chloride/tartrate salts with iodide ion, leading to Λ- and Δ-$[Co(en)_3]^{3+}$ $3I^-$. Additional variants, such as with antimony tartrate, have also been described.[4b] These procedures are so simple and forgiving that they are often used as undergraduate laboratory experiments.

Despite the chirality of the trication $[Co(en)_3]^{3+}$, symmetry elements are present. For example, there is a principal C_3 axis that runs perpendicular to the plane of the paper and through the centers of the triangles in Figure 2.1-**A**. This axis is also easily visualized in the wire-frame representations in Figure 2.1-**C**, or the space filling analogs in Figure 2.1-**D**. There are furthermore three C_2 axes in a perpendicular plane, parallel to that of the paper. One C_2 axis is redirected perpendicular to the plane of the paper in Figures 2.1-**E** and 2.1-**F**. Together, the C_3 and three C_2 axes code for the chiral point group D_3. Importantly, this symmetry requires that the three chelates either (1) be planar (which is not the case for ethylenediamine, but would be applicable to bipy, 1,10-phenanthroline, and related ligands), or (2) have identical non-planar conformations. These issues are parsed in more detail elsewhere,[5] and the non-planar conformations are analyzed further below.

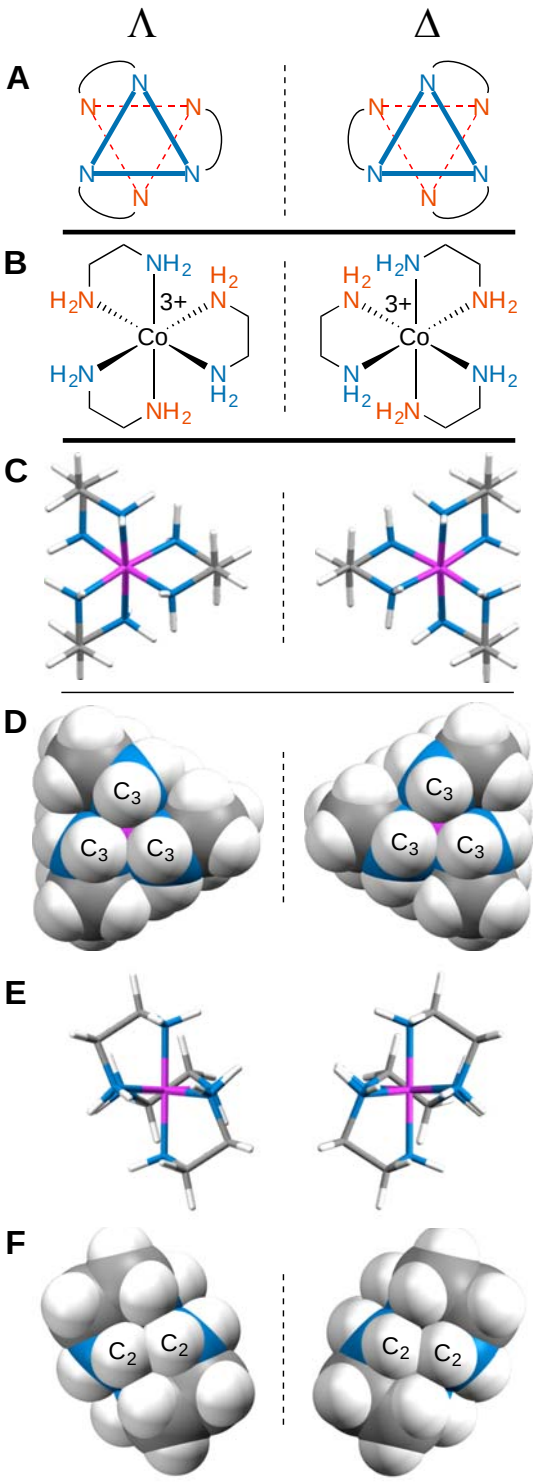

Figure 2.1. Representations of the enantiomeric Λ- and Δ-$[Co(en)_3]^{3+}$ trications.

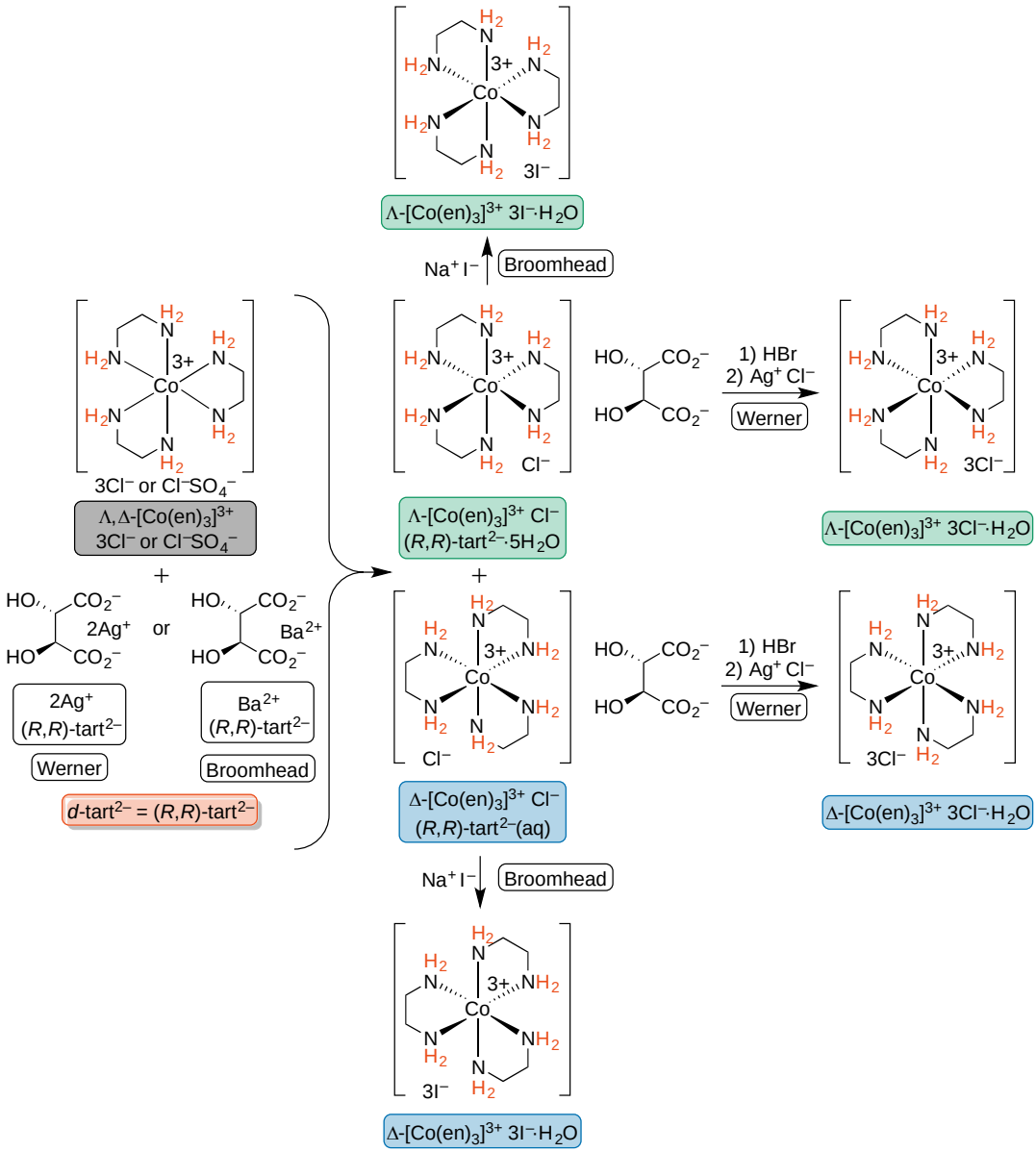

Scheme 2.1. Resolution of the enantiomeric Λ and Δ-$[Co(en)_3]^{3+}$ trications.[3e,4a]

Several recent developments have prompted renewed interest in salts of the trication $[Co(en)_3]^{3+}$ and related complexes. One has been the realization that the NH bonds associated with coordinated amines are capable of functioning as hydrogen bond donors towards Lewis basic organic substrates.[6,7] Over the last 20 years, a number of

chiral organic hydrogen bond donors have been found to be effective catalysts for a multitude of enantioselective transformations.[8] Due to my work, the same is proving to be true for Werner complexes and related species.[7,9-11]

These results were to some extent foreshadowed by the resolution of enantiomers in Scheme 2.1. It is thought that the relative solubilities of the diastereomeric salts are primarily controlled by the strengths of the trication/tartrate hydrogen bonding interactions (stronger interaction = lower aqueous solubility). Thus, the resolution reflects the thermodynamic binding preference of a given cobalt configuration for a specific tartrate configuration. It has been established crystallographically that for diastereomeric tartrate salts of the tris(*trans*-1,2-cyclohexanediamine) cobalt trication, Λ- and Δ-$[Co(S,S\text{-chxn})_3]^{3+}$ $Cl^-(R,R)\text{-tart}^{2-}\cdot 2H_2O$, the more soluble diastereomer exhibits longer NH···O contacts and an unfavorable tartrate conformation.[12,13]

These investigators also conclude, in line with earlier analyses,[14] that a similar scenario applies with tartrate salts of the tris(ethylenediamine) trication $[Co(en)_3]^{3+}$, where there is much crystallographic data.[15] However, here comparisons must be made between diastereomers with different hydration levels and/or counteranions that accompany tartrate, per the mixed chloride and iodide salts in Scheme 2.1 (as well as crystals that contain more than one independent trication).[15e] Furthermore, some of these analyses involve crystal structures that have never been deposited in publically accessible databases (apparently not an editorial requirement for early papers in *Chem. Lett.*).[16] Hence, certain published conclusions are difficult to independently assess.

Given the increasing numbers of enantioselective reactions catalyzed by tris(1,2-diamine) cobalt(III) species,[7] I sought to better understand the nature of hydrogen bonding to the $[Co(en)_3]^{3+}$ trication. In contrast to the many organic hydrogen bond donors applied in catalysis, which commonly feature one or two binding sites,

$[Co(en)_3]^{3+}$ contains twelve NH groups. As can be inferred from Figure 2.1, at least three of these, and more likely four or five, can be simultaneously accessed in transition state assemblies. As one approach to systematizing the possibilities, I, together with my collaborator for most of this section, decided to examine hydrogen bonding in crystalline salts of the formula $[Co(en)_3]^{3+}\ yX^{z-}$ (y/z = 3/1, 1/3, 1.5/2), and analogous species with mixed anions. We wondered whether there might be recurring or "conserved" motifs – or rare and presumably disfavored motifs – that could provide guidance.

Indeed, over one hundred fifty crystal structures of such salts have been reported in the literature, and everyone, including those with anions that are poor hydrogen bond acceptors, show extensive hydrogen bonding in the solid state. An exhaustive list of structures is given in Table A-1 (Appendix), and several dozen representative complexes are examined in detail in sections 2.4.2-2.4.8 below. Nomenclature for classifying the various modes of hydrogen bonding is developed.

2.2. Ethylenediamine ligand conformations

In order to thoroughly analyze the hydrogen bonding motifs, certain stereochemical features of ethylenediamine ligands must be briefly reviewed.[5] With respect to the CH_2CH_2 backbone, a gauche orientation of the two NH_2 groups (torsion angle 60°) would be expected to be much more stable than an eclipsed orientation (torsion angle ca. 0°). Thus, as illustrated by **I** and **II** in Figure 2.2, nonplanar chelate rings would be anticipated.

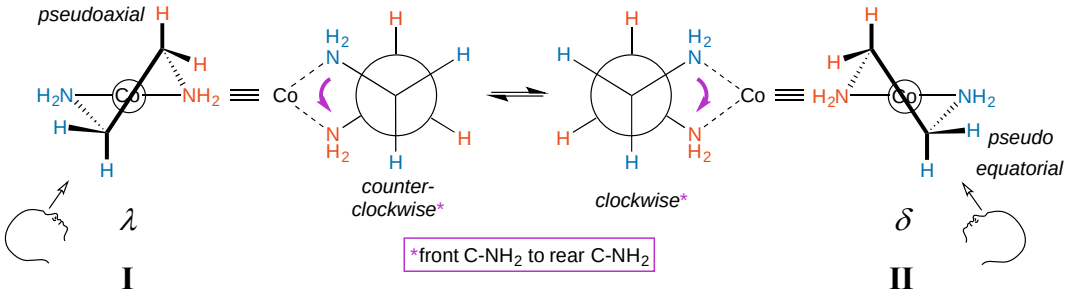

Figure 2.2. Chelate conformations of ethylenediamine.

For each Co(en) moiety, two nonsuperimposable mirror images are possible. These are commonly designated with the lower case Greek letters λ and δ and correspond to left handed and right handed helices, respectively.[5,17] The counterclockwise and clockwise senses are illustrated with purple arrows in Figure 2.2. Each NH_2 and CH_2 group features one hydrogen atom that is pseudoaxial, and one that is pseudoequatorial. The axial and equatorial atoms rapidly exchange via "ring flips". Thus, the λ and δ conformers will readily equilibrate. However, in the absence of disorder, each chelate will crystallize in one conformation or the other.

Importantly, the conformation of the chelate affects the relative orientations of the CH_2–CH_2 bonds and the symmetry of the $[Co(en)_3]^{3+}$ trication. First, consider the "docking" of three λ ethylenediamine units to give a trication with a Δ configuration at cobalt. The initial step is shown in Figure 2.3-**A**, and when all three chelates are in place, the structure represented as Δ–$\lambda\lambda\lambda$ results. Next, consider the docking of three δ ethylenediamine units to give a trication with the *same* Δ configuration at cobalt (i.e., an identical spatial orientation of chelating cobalt-nitrogen bonds). The initial step is shown in Figure 2.3-**B**. In order for the cobalt-nitrogen bond locations to "match up", the δ ethylenediamine must first be rotated by 90°. When all three chelates have been similarly put in place, a Δ–$\delta\delta\delta$ structure results.

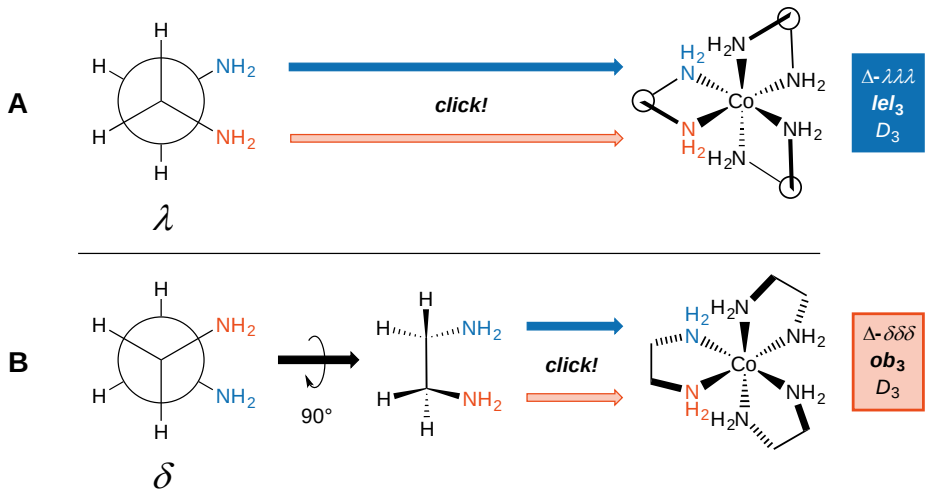

Figure 2.3. Accommodation of ethylenediamine ligands with three λ or three δ conformations in the coordination sphere of an octahedral cobalt atom with a Δ configuration.

In the first or Δ–$\lambda\lambda\lambda$ structure (Figure 2.3-**A**), the λ chelates are said to adopt *lel* orientations, so named because the three CH_2–CH_2 bonds are paral*lel* to the C_3 symmetry axis.[5,17] These linkages are often incorporated into Newman type projections, as indicated by hollow circles. In the second or Δ–$\delta\delta\delta$ structure (Figure 2.3-**B**), the δ chelates are said to adopt *ob* orientations, so named because the three CH_2–CH_2 bonds are *ob*lique to the C_3 axis. The designations Δ–$\lambda\lambda\lambda$ and Δ-*lel*$_3$ (Figure 2.3-**A**) are both found in the literature, and can be used interchangeably. The same holds for Δ–$\delta\delta\delta$ and Δ-*ob*$_3$. However, an important caveat follows below.

When the $[Co(en)_3]^{3+}$ trication has a Λ configuration at cobalt, these relationships are reversed. A λ chelate leads to an *ob* orientation while a δ chelate results in a *lel* orientation. Furthermore, each of the three ethylenediamine ligands can independently adopt either an *ob* or *lel* orientation. Therefore, for a complex with a given cobalt configuration, four diastereomers exist. All possibilities are depicted in Figure 2.4. In contrast, in Figure 2.1 only the *lel*$_3$ orientations of Λ- and Δ-$[Co(en)_3]^{3+}$ were depicted.

One motivation was to keep the number of structural variables to a minimum in the introduction; another was that, as will be seen below, *lel* chelate orientations dominate in the crystal structures. Indeed, a number of studies point to the lel_3 form of each enantiomer being more stable than the ob_3 form.[17,18] Figure 2.4 also illustrates a "trap" or potential error in identifying enantiomers. Just like the descriptors *R*/*S* always identify enantiomers of compounds with a single tetrahedral carbon stereocenter, so will the

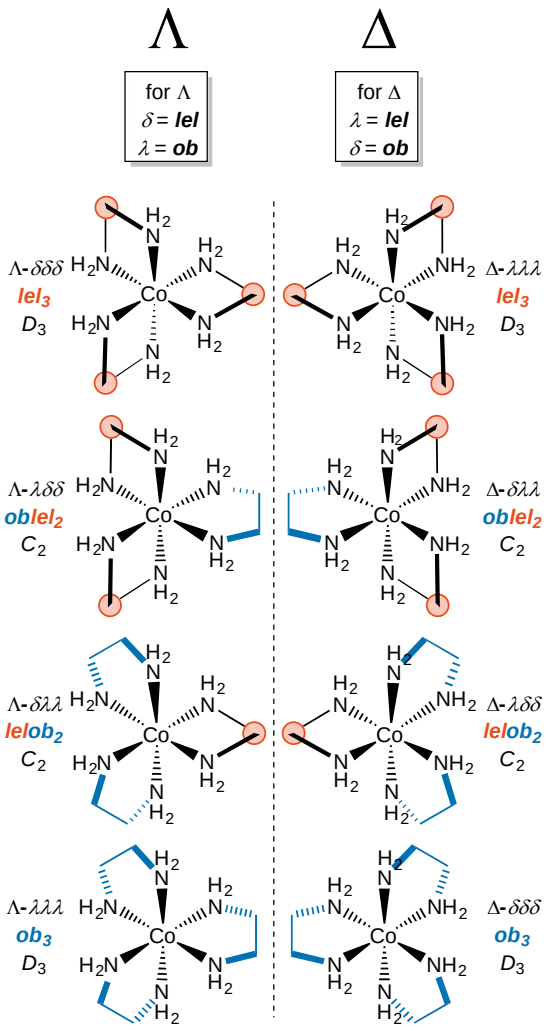

Figure 2.4. All possible stereoisomers of the $[Co(en)_3]^{3+}$ trication.

family of descriptors consisting of upper/ lower case delta/lambda identify mirror image components of the $[Co(en)_3]^{3+}$ trication. In other words, Λ–$\lambda\lambda\lambda$ and Δ–$\delta\delta\delta$ stereoisomers can automatically be regarded as enantiomers.

However, this is *not* the case with *lel*/*ob*. Instead, Λ-lel_3 and Δ-ob_3 stereoisomers are *diastereomers*, as is easily seen in the upper left and lower right structures in Figure 2.4. Rather, Λ-lel_3 and Δ-lel_3 would designate enantiomers. Another way to view this is as follows: if the C_3 axis is perpendicular to the plane of the paper, and one enantiomer is reflected in the plane of the paper to give the other, a "parallel" (*lel*) orientation of the CH_2–CH_2 bond with respect to the C_3 axis must be preserved. For these reasons, I generally refer to *lel*/*ob* as "orientations" or "perspectives".

In practice, the conformations of the ethylenediamine chelate rings rapidly interconvert in solution, and therefore the diastereomeric trications in Figure 2.4 will usually not be distinguishable. However, crystal structures will normally exhibit fixed motifs. Importantly, since the mixed *lel*/*ob* stereoisomers in Figure 2.4 have C_2 symmetry, they lack a formal C_3 axis. Nonetheless, a comparable pseudo-C_3 reference axis is available. This runs perpendicular to the two unique Star of David triangles that are comprised of one NH_2 group from each of the three chelate rings.

2.3. A syntax for hydrogen bonding to the trication $[Co(en)_3]^{3+}$

Certain views provide instructive starting points for the hydrogen bond classifications that follow. Some are illustrated in Figure 2.5 for $[Co(en)_3]^{3+}$ with a Δ–$\lambda\lambda\lambda$ configuration (lel_3, D_3 symmetry). In Figure 2.5-**B** (middle row), the C_3 symmetry axis is (as usual) perpendicular to the plane of the paper and highlighted with two blue spheres above and below the plane. Three synperiplanar nitrogen-hydrogen bonds, one from each chelate and together defining a C_3 binding site, point in the direction of the blue spheres. These N**H**H' units are also readily visualized in Figures

2.1-**C**,**D**; the Δ enantiomer of the former, a wire-frame representation, is repeated in Figure 2.5-**B** (right). The three orange spheres in Figure 2.5-**B** "hover" above the C_2 binding sites, each comprised of two nitrogen-hydrogen bonds from different chelates. These NH**H'** units are also readily visualized in Figures 2.1-**E**,**F**.

In Figure 2.5-**A** (top row), the structures in 1.5-**B** are rotated 90° about a vertical axis to bring the C_3 axis into the plane of the paper. The second blue sphere associated with the C_3 binding sites is now better visible, but in the interest of clarity all the atoms and bonds have been omitted. The wire-frame structures in Figures 2.5-**B** and 2.5-**A** provide alternative points of reference. Figure 2.5-**C** (bottom row) depicts a different 90° rotation of 2.5-**B**, now involving a horizontal axis. This nicely highlights each C_3 binding site with three vertically directed synperiplanar nitrogen-hydrogen bonds. The hydrogen atoms associated with the C_2 binding sites are color coded; the symmetry relationship between the two depicted in red is particularly clear.

Various types of hydrogen bonding motifs for individual anions (or cocrystallized molecules) are summarized in Table 2.1, and "named" using the general formula $[C_W{}^X][YZ]$ in Figure 2.5 (bottom). The terms comprising the formula are defined as follows: (a) C_W denotes the origin of the NH hydrogen bond donor, the C_3 site or C_2 site; (b) X denotes the number of acceptor atoms of the anion that are engaged by the NH hydrogen bond donor (default = 1); (c) Y denotes the number of acceptor atoms of the anion engaged by the NH hydrogen bond donor; (d) Z denotes the type of atom that is accepting the hydrogen bond, which is only included in cases of potential ambiguity, such as with ambident anions. For a given salt, there will be a set of such formulae, as illustrated in the examples that follow.

Table 2.1. Syntax for hydrogen bonding interactions between the $[Co(en)_3]^{3+}$ trication and anions or solvent molecules.

Hydrogen bond motif	C_2 N-H	C_3 N-H	Interligand C_2,C_3 N-H	Intraligand (C_2/C_3) N-H[a]	Intraligand (C_2//C_3) N-H[b]
one N-H unit binds to anion at a single atom	$[C_2][1]$	$[C_3][1]$	---	---	---
two N-H units bind to anion at a single atom	$[C_2,C_2][1]$	$[C_3,C_3][1]$	$[C_3,C_2][1]$	$[(C_3/C_2)][1]$	$[(C_3//C_2)][1]$
three N-H units bind to anion at a single atom	---	$[C_3,C_3,C_3][1]$	$[C_3,C_3,C_2][1]$[c] or $[C_3,C_2,C_2][1]$[c]	$[C_3,(C_3/C_2)][1]$[c] or $[(C_3/C_2),C_2][1]$[c]	$[C_3,(C_3//C_2)][1]$[c] or $[(C_3//C_2),C_2][1]$[c]
one N-H unit bind to anion at two different atoms	$[C_2^2][2]$	$[C_3^2][2]$	---	---	---
two N-H units bind to anion at two different atoms	$[C_2,C_2][2]$	$[C_3,C_3][2]$	$[C_3,C_2][2]$	$[(C_3/C_2)][2]$	$[(C_3//C_2)][2]$
three N-H units bind to anion at two different atoms	---	$[C_3,C_3,C_3][2]$	$[C_3,C_3,C_2][2]$ or $[C_3,C_2,C_2][2]$	$[C_3,(C_3/C_2)][2]$ or $[(C_3/C_2),C_2][2]$	$[C_3,(C_3//C_2)][2]$ or $[(C_3//C_2),C_2][2]$
one N-H unit binds to anion at three different atoms	$[C_2^3][3]$	$[C_3^3][3]$	---	---	---
two N-H units bind to anion at three different atoms	$[C_2^2,C_2][3]$	$[C_3^2,C_3][3]$	$[C_3,C_2^2][3]$ or $[C_3^2,C_2][3]$	$[(C_3^2/C_2)][3]$ or $[(C_3/C_2^2)][3]$	$[(C_3^2//C_2)][3]$ or $[(C_3//C_2^2)][3]$
three N-H units bind to anion at three different atoms	---	$[C_3,C_3,C_3][3]$	$[C_3,C_3,C_2][3]$ or $[C_3,C_2,C_2][3]$	$[C_3,(C_3/C_2)][3]$ or $[(C_3/C_2),C_2][3]$	$[C_3,(C_3//C_2)][3]$ or $[(C_3//C_2),C_2][3]$
Miscellaneous motifs from Section 2.4					
three N-H units bind to anion at two different atoms with each atom of the anion making two hydrogen bonds		$[C_3^2,C_3,C_3][2,2:2]$			

Table 2.1. Continued. Syntax for hydrogen bonding interactions between the $[Co(en)_3]^{3+}$ trication and anions or solvent molecules.

Hydrogen bond motif	C_2 N-H	C_3 N-H	Interligand C_2,C_3 N-H	Intraligand (C_2/C_3) N-H[a]	Intraligand (C_2//C_3) N-H[b]
three N-H units bind to anion at two different atoms, with one atom making two hydrogen bonds and the other making one.		$[C_3^2,C_3,C_3][1,3:2]$			

[a] The N-H bonds are geminal (NH_2; see Figure 2.6). [b] The N-H bonds involve different nitrogen atoms on the same ligand (see Figure 2.6). [c] Considering the substantial distance at which the third N-H unit will be from the other two, this will be a rare motif.

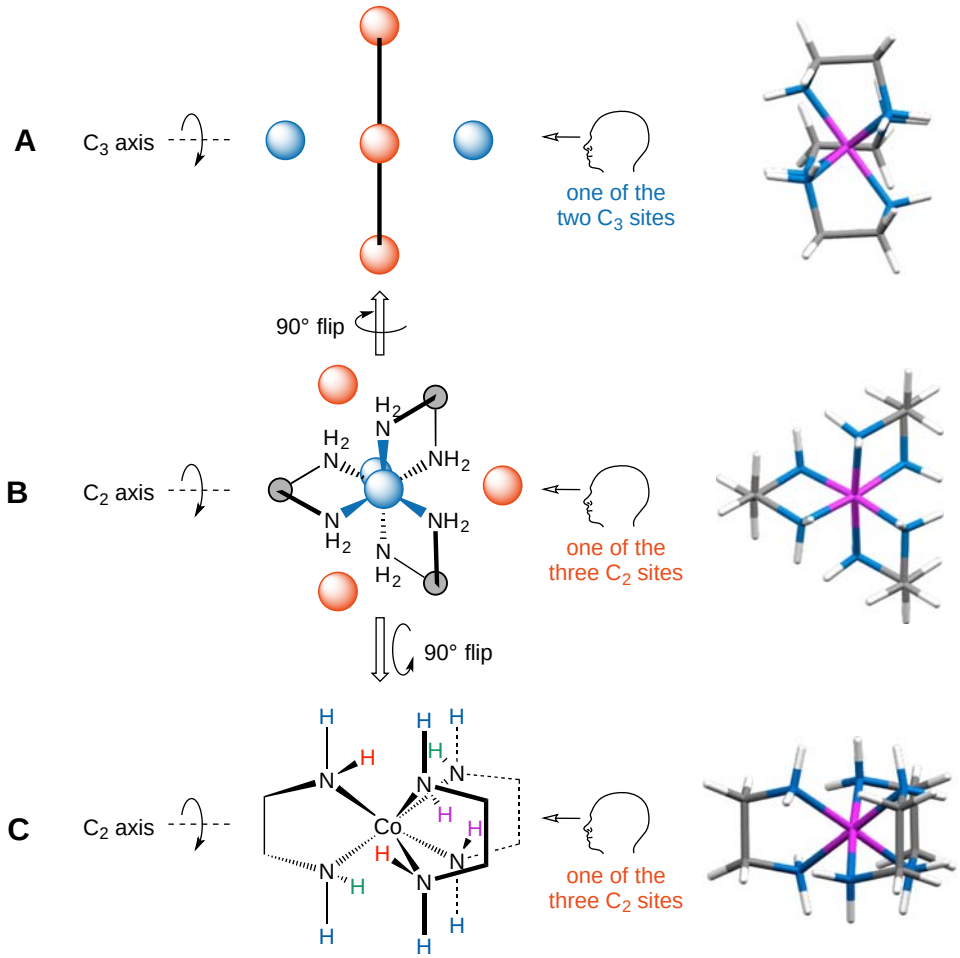

$[C_W^X][YZ]$

W = symmetry label of the N-H hydrogen bond donor (W = 2 or 3)
X = number of H-bond accepting atoms engaged by a single N-H hydrogen bond donor (default = 1)
Y = total number of H-bond accepting atoms engaged
Z = type of atom that is accepting a hydrogen bond (only included if ambiguous)

Figure 2.5. Representations of the C_2 and C_3 binding sites of the Δ–$\lambda\lambda\lambda$-$[Co(en)_3]^{3+}$ trication, and a general nomenclature system for hydrogen bonding to a given anion.

Thus, when one N-H unit of a C_2 site binds to an anion X^- at a single acceptor atom, the representation $[C_2][1]$ is employed. For a corresponding interaction at a C_3 site, the representation $[C_3][1]$ is employed. When the same anion binds two or more N-

H units via a single atom, representations such as $[C_2,C_2][1]$, $[C_3,C_3][1]$, and $[C_3,C_3,C_3][1]$ are employed. When such binding involves two distinct but *like* atoms of the anion, representations such as $[C_2,C_2][2]$ and $[C_3,C_3][2]$ may apply. When binding involves three distinct but *like* atoms of the anion, the representation $[C_3,C_3,C_3][3]$ may apply.

Of course, each like atom of an anion could make more than one hydrogen bond. Thus, there are additional manifolds of motifs along the lines of $[C_2^2,C_2][2]$ (three hydrogen bonds between two N-H units of a C_2 site and two like atoms of anion) or $[C_3^2,C_3^2,C_3][2]$ (five hydrogen bonds between three N-H units of a C_3 site and two like atoms of an anion). A reader who would like to see these relationships developed in a more systematic as opposed to intuitive way should consult Tables A-1 and A-2 (Appendix). The latter includes graphical representations.

It should also be possible for anions to hydrogen bond to both C_2 and C_3 sites. Complementary views of the three most likely motifs are depicted in Figure 2.6. First, the C_2 and C_3 N-H units can be on the same ethylenediamine ligand. The most easily conceptualized possibility involves the same NH_2 group, as shown in Figure 2.6-**A**. In structures with crystallographic D_3 symmetry (vide infra), this H···H distance is typically 1.46 Å.[19] Alternatively, hydrogen bonding could involve a pseudoequatorial C_3 N-H unit of one NH_2 group, and a pseudoaxial C_2 N-H unit of the other (Figure 2.6-**B**). In structures with crystallographic D_3 symmetry, this H···H distance is typically 3.73 Å.[19b] This is much longer than in the preceding example, but the atoms can easily be bridged by delocalized multidentate anions.

As shown in Figure 2.6-**C**, the C_2 and C_3 N-H units can also be on different ethylenediamine ligands. In structures with crystallographic D_3 symmetry, this H···H distance is typically 2.95 Å.[19b] With regard to nomenclature, these motifs are designated

as summarized in Figure 2.6. The binding sites are separated by commas for the interligand case ([C_3,C_2]), and one or two slashes for the intraligand cases ([C_3/C_2] for the shorter contact in Figure 2.6-**A**; [C_3//C_2] for the longer contact in Figure 2.6-**B**).[20]

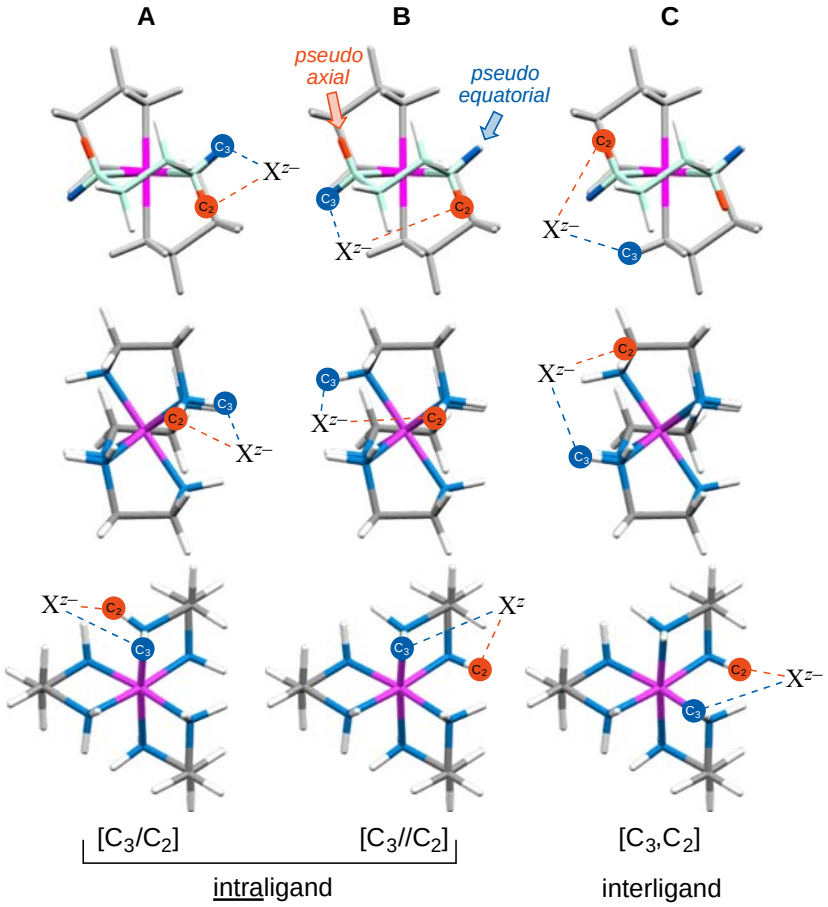

Figure 2.6. Anion binding modes involving hydrogen bonding to both the C_2 and C_3 sites of the Δ–$\lambda\lambda\lambda$-$[Co(en)_3]^{3+}$ trication.

Some illustrative examples are presented in Figure 2.7 using the enantiomer of a nitrate salt analyzed below. In Figures 2.6-**A**-**C**, the nitrate anion occupies a position near the blue sphere in Figure 2.5-**B** – i.e., in the vicinity of the C_3 site, but not symmetrically arrayed. In Figure 2.7-**A**, one oxygen atom of the nitrate anion is bound to

one N-H unit of the C_3 site, and is thus designated $[C_3][1]$. In Figure 2.7-**B**, one oxygen atom binds to the same N-H unit of the C_3 site, and the same oxygen atom as well as a second one binds to a different N-H unit of the C_3 site. This motif is designated $[C_3^2,C_3][2]$.

In Figure 2.7-**C**, one oxygen atom is bound to all three N-H units of the C_3 site. A second oxygen atom binds to one. This might have been designated $[C_3^2,C_3,C_3][2]$. However, this would also be consistent with an alternative motif in which the two oxygen atoms each make two hydrogen bonds. Therefore it is designated $[C_3^2,C_3,C_3][1,3:2]$, with the alternative motif then being $[C_3^2,C_3,C_3][2,2:2]$. The first two integers in the second square bracket represent the numbers of hydrogen bonds to each oxygen atom.

Figures 2.6-**D** and 2.6-**E** involve nitrate anion binding to the C_2 site. In the first, one oxygen atom is bound to one N-H unit of the C_2 site, and the other to both N-H units. This motif is designated $[C_2^2,C_2][2]$. In the second, both oxygen atoms bind to both N-H units. This is designated $[C_2^2,C_2^2][2]$.

2.4. Overview of crystallographically characterized salts of the trication $[Co(en)_3]^{3+}$

2.4.1. General procedures and comments

Table A-1 (Appendix) summarizes the 150 unique crystal structures containing the trication $[Co(en)_3]^{3+}$ that have been deposited in the Cambridge Structural Database (CSD). There are furthermore nineteen duplicate crystal structures, as listed in Table A-2 (Appendix). Of the 150, six are lacking atomic coordinates, and in two the trication is severely disordered. Hence, 142 $[Co(en)_3]^{3+}$ salts are amenable to detailed analyses, and a few more to partial analyses. The 21 structures in the following sections 2.4.2-2.4.8 are representative. They are arranged in order of increasing charge and/or complexity of the counter anions.

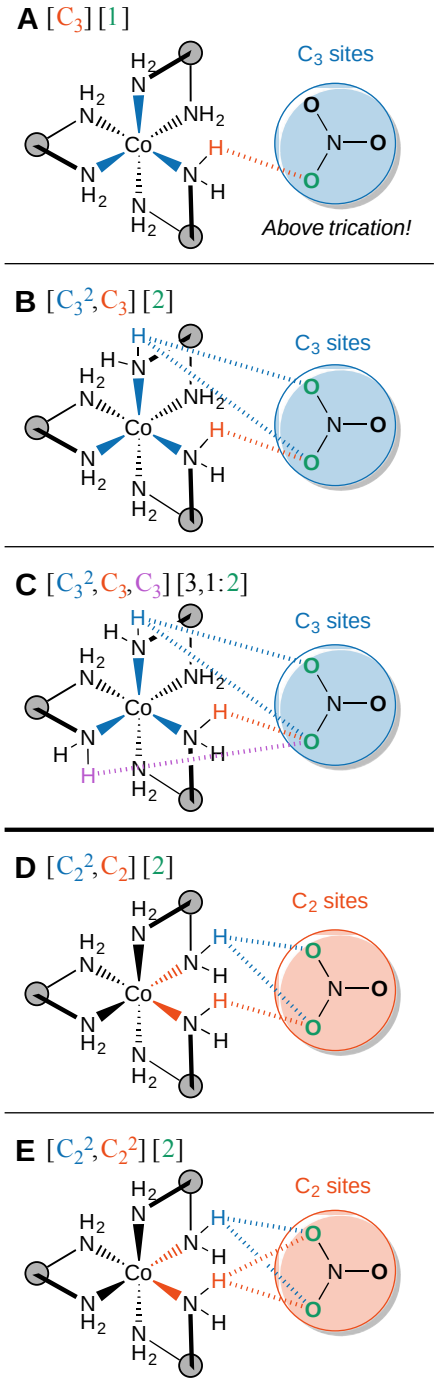

Figure 2.7. Representative hydrogen bonding motifs for the Δ–$\lambda\lambda\lambda$-$[Co(en)_3]^{3+}$ trication (lel_3, D_3) and the nitrate anion.

All anions as well as cocrystallized water molecules that hydrogen bond to a given trication are considered. In many cases, these species also hydrogen bond to adjacent trications. However, these are not enumerated. Rather, the priority is to visualize all second coordination sphere interactions about a single trication.

For determining the presence or absence of hydrogen bonds, the default parameters in the program Mercury[21] have been employed. These take into account the van der Waals radius of the acceptor atom, so different atoms have different cutoff distances. Since hydrogen bonding is not an "all or nothing" property, the cutoff distances in the structures in sections 2.4.2-2.4.8 were increased by 5%. No additional hydrogen bonds were revealed.

Some of the crystal structures in sections 2.4.2-2.4.8 were determined using enantiopure Λ-$[Co(en)_3]^{3+}$ salts, and others using racemates. In the latter cases, only the Λ enantiomers have been depicted. Crystal structures of enantiopure Δ-$[Co(en)_3]^{3+}$ salts have also been determined, but these are less common (reflecting the manner that the resolution in Scheme 2.1 is most commonly applied). Only one example is presented in the text (2.4.7.2), and the Λ/Δ ratio in Table A-1 (Appendix) is 32:12 (21%/8%).

For all structures, two views are given. One is always labeled as along the C_3 axis, even though the idealized C_3 axes evident in Figures 2.1-**A**-**D** translate in only a few cases to crystallographic C_3 axes (for mixed *lel*/*ob* systems, this is denoted as a pseudo C_3 axis; *vide supra*). The other is a view down one of the three C_2 axes (or for mixed *lel*/*ob* systems, the only C_2 axis). Again, in only a few cases do these correspond to crystallographic C_2 axes.

2.4.2. Salts with three monoanions (point charge)

Note that for cases in which the anion can be approximated as a point charge, the generalized hydrogen bonding nomenclature $[C_W^X][YZ]$ (Figure 2.5) will reduce to $[C_W^X][1]$.

2.4.2.1. Λ–δδδ-[Co(en)$_3$]$^{3+}$ 3Cl$^-$·2.8H$_2$O (lel$_3$)

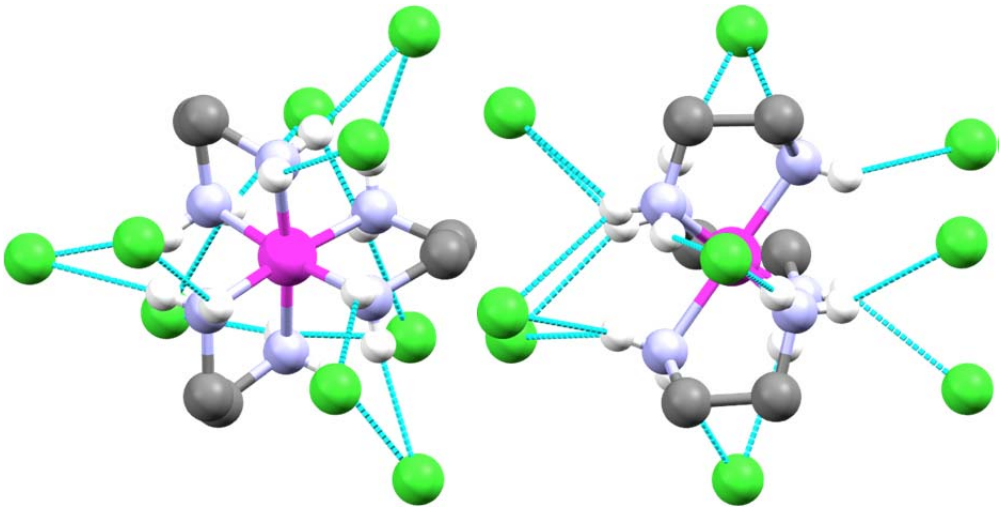

H-bond acceptor	type of H-bond	number of similar interactions
Cl^-	$[C_3][1]$	3
Cl^-	$[C_2,C_2][1]$	3
Cl^-	$[C_3,C_3][1]$	3

Figure 2.8. Hydrogen bonding interactions in Λ–δδδ-[Co(en)$_3$]$^{3+}$ 3Cl$^-$·2.8H$_2$O (*lel*$_3$) viewed along the C_3 axis (left) and a C_2 axis (right).

The structure and hydrogen bonding interactions of the polyhydrated trichloride salt Λ–δδδ-[Co(en)$_3$]$^{3+}$ 3Cl$^-$·2.8H$_2$O (*lel*$_3$) are shown in Figure 2.8.[22] This represents one of the two enantiomers in the crystallographically characterized racemate. There is a

crystallographic C_3 axis corresponding to the idealized C_3 axis of the trication, and three crystallographic C_2 axes that do *not* pass through a trication. All twelve N-H units engage in hydrogen bonding to nine Cl^- anions. The two N-H units of all three C_2 sites exhibit a single hydrogen bond to a chelating Cl^- anion. Each N-H unit of one C_3 site exhibits a single hydrogen bond to a non-chelating Cl^- anion, and each N-H unit of the other C_3 site exhibits two hydrogen bonds to two chelating Cl^- anions.

2.4.2.2. Λ–δδδ-[Co(en)$_3$]$^{3+}$ 3Cl$^-$ (lel$_3$)

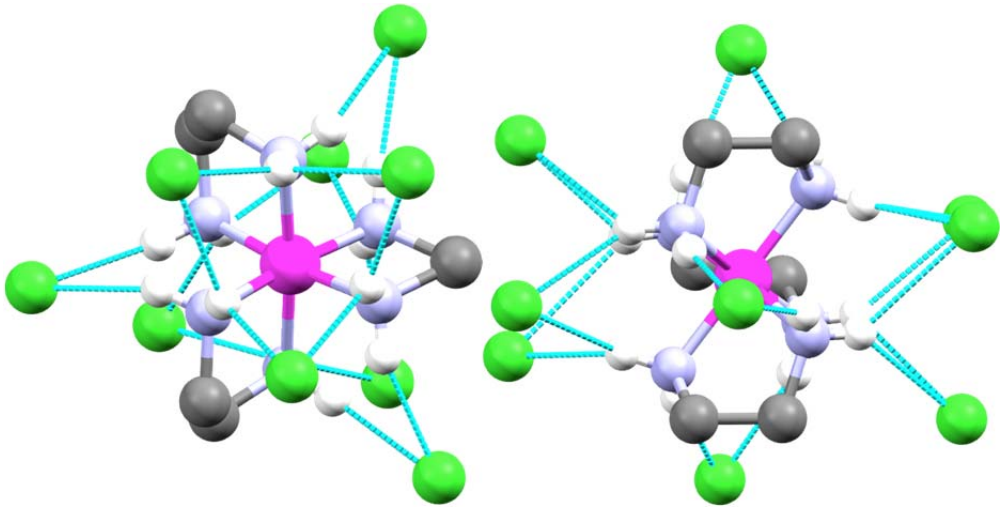

H-bond acceptor	type of H-bond	number of similar interactions
Cl^-	$[C_2,C_2][1]$	3
Cl^-	$[C_3,C_3][1]$	6

Figure 2.9. Hydrogen bonding interactions in Λ–δδδ-$[Co(en)_3]^{3+}$ 3Cl^- (*lel*$_3$) viewed along the C_3 axis (left) and a C_2 axis (right).

The structure and hydrogen bonding interactions of Λ–δδδ-$[Co(en)_3]^{3+}$ 3Cl^- (*lel*$_3$) are shown in Figure 2.9.[23] This represents one of the two enantiomers in the crystallographically characterized racemate. There is a crystallographic C_3 axis corresp-

onding to the idealized C_3 axis of the trication, and three crystallographic C_2 axes that do *not* pass through a trication. All twelve N-H units are engaged in hydrogen bonding with nine Cl^- anions. The pattern is quite close to that of the previous structure (a polyhydrate), except that now each N-H unit of *both* C_3 sites exhibits two hydrogen bonds to two chelating Cl^- anions.

2.4.2.3. Λ–δδδ-[Co(en)$_3$]$^{3+}$ 3Br$^-$·H$_2$O (lel$_3$)

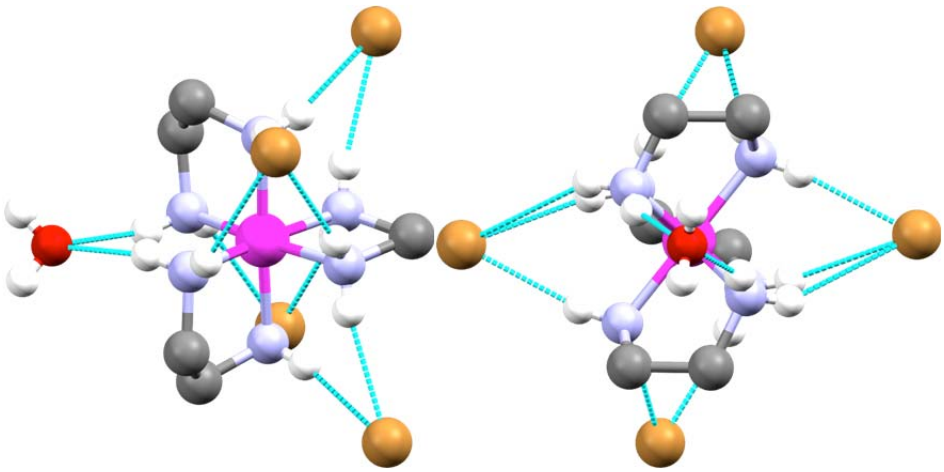

H-bond acceptor	type of H-bond	number of similar interactions
Br^-	$[C_2,C_2][1]$	2
Br^-	$[C_3,C_3,C_3][1]$	2
H_2O	$[C_2,C_2][1]$	1

Figure 2.10. Hydrogen bonding interactions in Λ–δδδ-[Co(en)$_3$]$^{3+}$ 3Br$^-$·H$_2$O (*lel*$_3$) viewed along the C_3 axis (left) and a C_2 axis (right).

The structure and hydrogen bonding interactions of the enantiopure monohydrated bromide salt, Λ–δδδ-[Co(en)$_3$]$^{3+}$ 3Br$^-$·H$_2$O (*lel*$_3$), are shown in Figure 2.10.[24] All

twelve N-H units engage in hydrogen bonding to four Br^- anions and one H_2O molecule. There is a crystallographic C_2 axis corresponding to one idealized C_2 axis of the trication (right view). The three N-H units of each C_3 site form a single hydrogen bond to a triply bridging Br^- anion. The two N-H units of two C_2 sites exhibit a single hydrogen bond to a chelating Br^- anion. Those of the third C_2 site exhibit a single hydrogen bond to a chelating H_2O molecule.

2.4.2.4. Λ–λδδ-[Co(en)$_3$]$^{3+}$ 3I$^-$·H$_2$O (oblel$_2$)

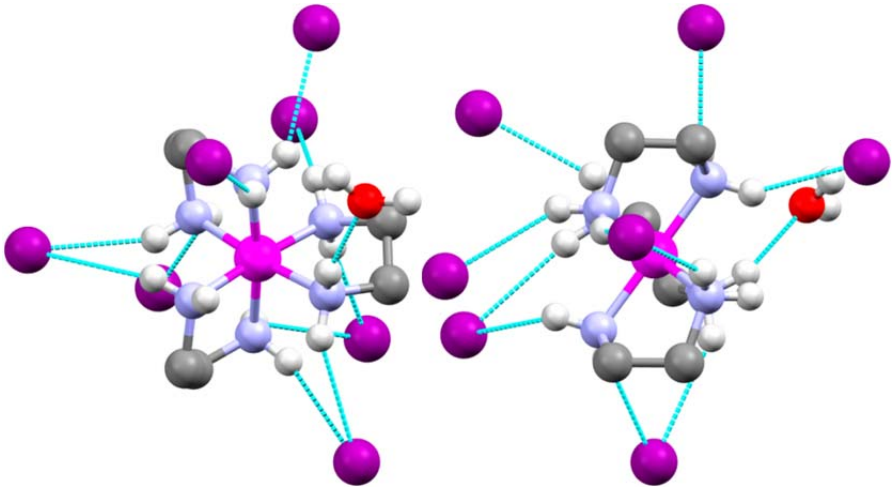

H-bond acceptor	type of H-bond	number of similar interactions
I^-	[C_2][1]	2
I^-	[C_2,C_2][1]	2
I^-	[C_3][1]	2
I^-	[C_3,C_3][1]	1
H_2O	[C_3][1]	1

Figure 2.11. Hydrogen bonding interactions in Λ–λδδ-[Co(en)$_3$]$^{3+}$ 3I$^-$·H$_2$O (*oblel$_2$*) viewed along the pseudo C_3 axis (left) and the C_2 axis (right).

The structure and hydrogen bonding interactions of the enantiopure monohydrated iodide salt, Λ–$\lambda\delta\delta$-$[Co(en)_3]^{3+}$ $3I^-\cdot H_2O$ (*oblel*$_2$), are shown in Figure 2.11.[25] Although one might have thought that this complex would be isostructural with the preceding tribromide salt, it crystallizes instead in an *oblel*$_2$ orientation – i.e., with one chelate in an *ob* as opposed to a *lel* conformation. Despite the lower symmetry, a pseudo C_3 reference axis remains (*vide supra*).

The trication forms hydrogen bonds to seven I^- anions and one H_2O molecule. In contrast to the preceding halide salts, only eleven N-H units are engaged in hydrogen bonding; one C_3 N-H unit remains free. Some of the I^- anions are singly hydrogen bonded, and others doubly; no pattern is apparent. The H_2O molecule is engaged by one C_3 N-H unit.

2.4.3. Salts with three monoanions (delocalized)

Now possibilities for the hydrogen bonding nomenclature $[C_W^X][YZ]$ (Figure 2.5) include $[C_W^X][1Z]$ and $[C_W^X][2Z]$ (and potentially but also much less frequently higher values of Y).

2.4.3.1. Λ–λδδ-[Co(en)$_3$]$^{3+}$ 3ReO$_4^-$ (oblel$_2$)

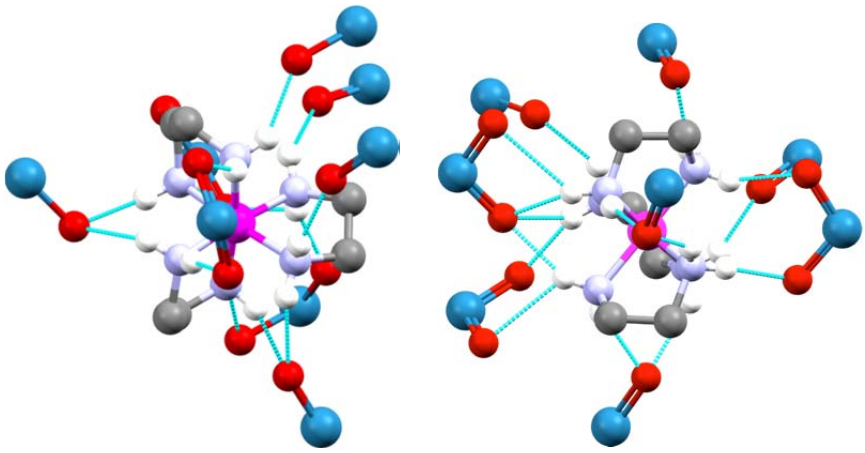

H-bond acceptor	type of H-bond	number of similar interactions
ReO_4^-	$[C_2][1]$	2
ReO_4^-	$[C_2,C_2][1]$	2
ReO_4^-	$[C_3][1]$	1
ReO_4^-	$[C_3,C_3][2]$	2
ReO_4^-	$[C_3^2,C_3,C_3][3,1:2]$	1

Figure 2.12. Hydrogen bonding interactions in the Λ–λδδ-[Co(en)$_3$]$_3^{3+}$ 3ReO$_4^-$ (*oblel$_2$*) viewed along the pseudo C$_3$ axis (left) and the C$_2$ axis (right). Non-interacting oxygen atoms of the ReO$_4^-$ anions have been omitted for clarity.

The structure and hydrogen bonding interactions of the enantiopure perrhenate salt, Λ–λδδ-[Co(en)$_3$]$^{3+}$ 3ReO$_4^-$ (*oblel$_2$*), are shown in Figure 2.12.[26] As with 2.4.2.4, the complex crystallizes in an *oblel$_2$* orientation. All twelve N-H units are engaged in hydrogen bonding to eight ReO$_4^-$ anions. The six C$_2$ N-H units are singly hydrogen bonded to the oxygen atoms of four ReO$_4^-$ anions (two chelating, two non chelating). Each C$_3$ site interacts with two ReO$_4^-$ anions, one of which chelates two N-H units via a

O-Re-O linkage. The remaining ReO_4^- anion is either singly hydrogen bonded to the third N-H unit, or quadruply hydrogen bonded to all three N-H units via a O-Re-O linkage.

2.4.4. Salts with three monoanions (two types)

2.4.4.1. Λ–δδδ-[Co(en)$_3$]$^{3+}$ Cl$^-$2I$^-$·H$_2$O (lel$_3$)

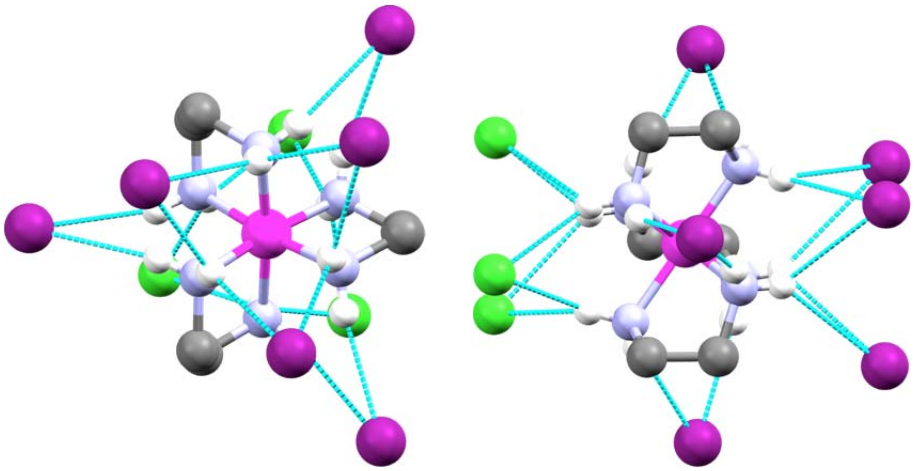

H-bond acceptor	type of H-bond	number of similar interactions
I^-	$[C_2,C_2][1]$	3
I^-	$[C_3,C_3][1]$	3
Cl^-	$[C_3,C_3][1]$	3

Figure 2.13. Hydrogen bonding interactions in Λ–δδδ-[Co(en)$_3$]$^{3+}$ Cl$^-$2I$^-$·H$_2$O (*lel*$_3$) viewed along the C_3 axis (left) and a C_2 axis (right).

The structure and hydrogen bonding interactions of the mixed chloride/diiodide salt, Λ–δδδ-[Co(en)$_3$]$^{3+}$ Cl$^-$2I$^-$·H$_2$O (*lel*$_3$) are shown in Figure 2.13.[27] This represents one of the two enantiomers in the crystallographically characterized racemate. All twelve N-H units are engaged in hydrogen bonding to six I^- anions and three Cl^- anions. At one C_3 site, all three N-H units are doubly hydrogen bonded to one of three Cl^-

anions. On the opposite C_3 site, all three N-H units are doubly hydrogen bonded to one of three I^- anions. The former motif was seen in the trichloride salts in 2.4.2.1 and 2.4.2.2, but the latter was not seen in the triiodide salt in 2.4.2.4. The two N-H units of each C_2 site chelate to a single I^- anion.

2.4.5. Salts with two anions (one monoanion and one dianion)

2.4.5.1. Λ–λδδ-[Co(en)$_3$]$^{3+}$ B$_5$O$_6$(OH)$_4^-$B$_8$O$_{10}$(OH)$_6^{2-}$·5H$_2$O (oblel$_2$). The structure and hydrogen bonding interactions of the pentahydrated bis(borate) salt, Λ–λδδ-[Co(en)$_3$]$^{3+}$ B$_5$O$_6$(OH)$_4^-$B$_8$O$_{10}$(OH)$_6^{2-}$·5H$_2$O (*oblel*$_2$) are shown in Figure 2.14.[28] This represents one of the two enantiomers in the crystallographically characterized racemate. As with 2.4.2.4, the complex crystallizes in an *oblel*$_2$ orientation. All twelve N-H units are engaged in hydrogen bonding to two octaboron *di*anions and three pentaboron *mono*anions.

All three C_2 sites exhibit different hydrogen bonding motifs. The two N-H units of one make separate hydrogen bonds to a H_2O molecule and a $B_5O_6(OH)_4^-$ monoanion. The two N-H units of another make a total of three hydrogen bonds to a $B_5O_6(OH)_4^-$ monoanion. The two N-H units of the third chelate a H_2O molecule, and make a third hydrogen bond to a $B_8O_{10}(OH)_6^{2-}$ dianion. This initiates a very unique motif, as this dianion further hydrogen bonds to two N-H units of a C_3 site; one involves a O-B-O chelate interaction with the same ethylenediamine ligand (see Figure 2.6-**A**), and the other a B-O-H interaction with a different ethylenediamine ligand (see Figure 2.6-**C**). This may provide a model for the interactions of Lewis basic substrates with an extended catalytic site, or the binding of a multifunctional product. Two N-H units on this site also chelate to an oxygen atom of a $B_5O_6(OH)_4^-$ monoanion. The three N-H units of the remaining C_3 site make a total of three hydrogen bonds to two oxygen atoms of another $B_8O_{10}(OH)_6^{2-}$ dianion.

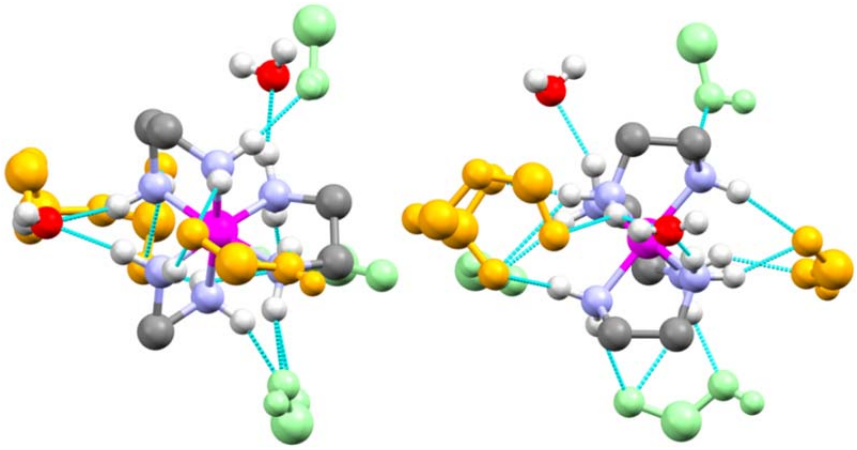

H-bond acceptor	type of H-bond	number of similar interactions
$B_5\underline{O}_6(OH)_4^-$	$[C_2][1]$	1
$B_5\underline{O}_6(\underline{O}H)_4^-$ [a]	$[C_2^2,C_2][2]$	1
$B_5O_6(\underline{O}H)_4^-$	$[C_3,C_3][1]$	1
$B_8\underline{O}_{10}(\underline{O}H)_6^{2-}$ [a]	$[C_3,C_3,C_3][2]$	1
$B_8\underline{O}_{10}(\underline{O}H)_6^{2-}$ [b]	$[(C_3^2/C_2),C_3][3]$	1
H_2O	$[C_2][1]$	1
H_2O	$[C_2,C_2][1]$	1

[a] Two of the hydrogen bonds involve BOB linkages, and one a BOH linkage. [b] Two of the hydrogen bonds involve BOB linkages, and two BOH linkages.

Figure 2.14. Hydrogen bonding interactions in Λ–$\lambda\delta\delta$-$[Co(en)_3]^{3+}$ $B_5O_6(OH)_4^-$ $B_8O_{10}(OH)_6^{2-}\cdot 5H_2O$ (*oblel*$_2$) viewed along the pseudo C_3 axis (left) and the C_2 axis (right). The larger borate dianion is colored orange and the smaller borate monoanion is colored light green. In both cases, some non-interacting atoms have been omitted for clarity.

2.4.6. Salts with achiral dianions

2.4.6.1. Λ–$\delta\delta\delta$-$[Co(en)_3]^{3+}$ $1.5C_4O_4^{2-}\cdot 4.5H_2O$ (oblel$_2$). The structure and hydrogen bonding interactions of the polyhydrated squarate salt, Λ–$\lambda\delta\delta$-$[Co(en)_3]^{3+}$ $1.5C_4O_4^{2-}\cdot 4.5H_2O$ (*oblel*$_2$), are shown in Figure 2.15.[29] This represents one of the two enantiomers in the crystallographically characterized racemate. As with 2.4.2.4, 2.4.3.1,

and 2.4.5.1, the complex crystallizes in an *oblel*$_2$ orientation. All twelve N-H units are engaged in hydrogen bonding to five $C_4O_4^{2-}$ dianions and two H_2O molecules. One C_3 site is occupied by one $C_4O_4^{2-}$ dianion, two oxygen atoms of which each make two hydrogen bonds (two to one N-H unit, one to two N-H units). The other C_3 site is occupied by two $C_4O_4^{2-}$ dianions; two oxygen atoms of one dianion chelate two N-H units, and one oxygen atom of the other bonds to the remaining N-H unit. For two C_2 sites, both N-H units chelate to two oxygen atoms of a $C_4O_4^{2-}$ dianion. For the third, each N-H unit is singly hydrogen bonded to separate H_2O molecules.

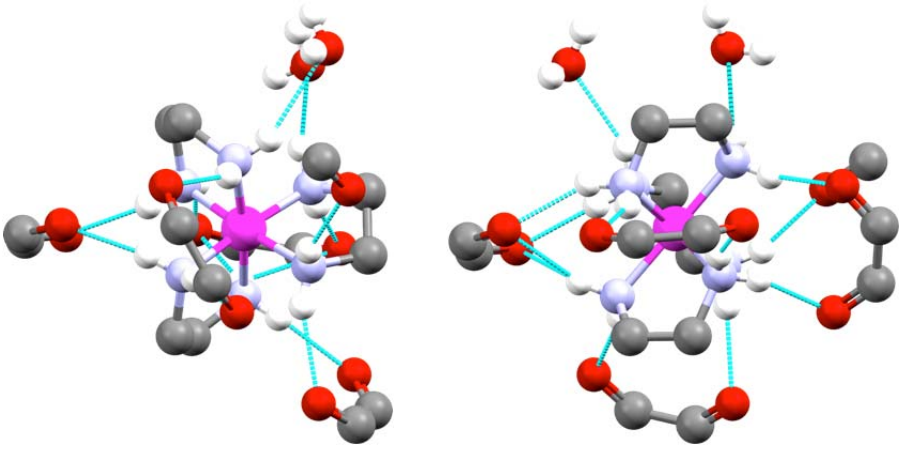

H-bond acceptor	type of H-bond	number of similar interactions
$C_4O_4^{2-}$	$[C_2,C_2][2]$	2
$C_4O_4^{2-}$	$[C_3][1]$	1
$C_4O_4^{2-}$	$[C_3,C_3][2]$	1
$C_4O_4^{2-}$	$[C_3^2,C_3,C_3][2,2:2]$	1
H_2O	$[C_2][1]$	2

Figure 2.15. Hydrogen bonding interactions in Λ–$\lambda\delta\delta$-$[Co(en)_3]^{3+}$ $1.5C_4O_4^{2-}\cdot 4.5H_2O$ (*oblel*$_2$) viewed along the pseudo C_3 axis (left) and the C_2 axis (right). Several non-interacting atoms of the squarate anions have been omitted for clarity.

2.4.6.2. Λ–δλλ-[Co(en)$_3$]$^{3+}$·1.5C$_5$O$_5^{2-}$·3H$_2$O (lelob$_2$)

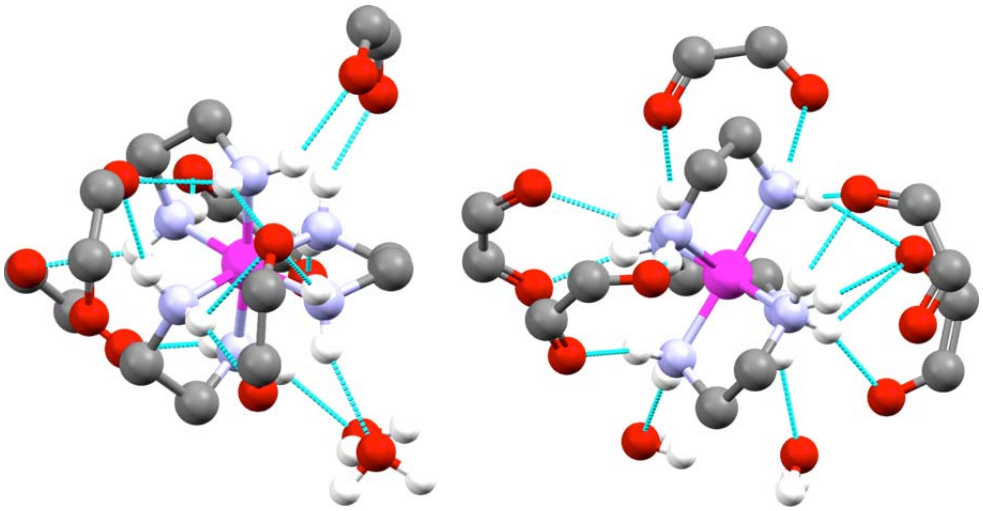

H-bond acceptor	type of H-bond	number of similar interactions
$C_5O_5^{2-}$	$[C_3,C_2][1]$	1
$C_5O_5^{2-}$	$[C_2,C_2][2]$	1
$C_5O_5^{2-}$	$[C_3,C_2][2]$	1
$C_5O_5^{2-}$	$[C_3,C_3][2]$	1
$C_5O_5^{2-}$	$[C_3^2,C_3,C_3][3,1:2]$	1
H_2O	$[C_2][1]$	2

Figure 2.16. Hydrogen bonding interactions in Λ–δλλ-[Co(en)$_3$]$^{3+}$·1.5C$_5$O$_5^{2-}$·3H$_2$O (*lelob*$_2$) viewed along the pseudo C$_3$ axis (left) and the C$_2$ axis (right). Several atoms of the C$_5$O$_5^{2-}$ dianions have been omitted for clarity.

The structure and hydrogen bonding interactions of the trihydrated croconate salt, Λ–δλλ-[Co(en)$_3$]$^{3+}$·1.5C$_5$O$_5^{2-}$·3H$_2$O (*lelob*$_2$), are shown in Figure 2.16.[30] The cyclic croconate dianion is the next higher homolog of squarate. Figure 2.16 shows one of the two enantiomers in the crystallographically characterized racemate. This is the only salt

presented in the text in which the trication $[Co(en)_3]^{3+}$ crystallizes in a *lelob*$_2$ orientation.

All twelve N-H units are engaged in hydrogen bonding to five $C_5O_5^{2-}$ dianions and two H_2O molecules. The two N-H units of one C_2 site each hydrogen bond to separate H_2O molecules. The N-H units of another C_2 site chelate a O-C-C-O linkage of a $C_5O_5^{2-}$ dianion. The N-H units of the third C_2 site each hydrogen bond to a single oxygen atom of separate $C_5O_5^{2-}$ dianions. However, in a rare motif, one of these oxygen atoms further hydrogen bonds to a N-H unit of a C_3 site. This involves two different ethylenediamine ligands, per Figure 2.6-**C**. With the other $C_5O_5^{2-}$ dianion, a second oxygen atom hydrogen bonds to a N-H unit of the opposite C_3 site. This also involves two different ethylenediamine ligands, but now the N-H units are spanned by four atoms as opposed to one. An additional $C_5O_5^{2-}$ dianion completes the hydrogen bonding at each C_3 site (one uses two oxygen atoms to chelate two N-H units, and the other uses two oxygen atoms to make four hydrogen bonds involving all three N-H units).

2.4.7. Salts with chiral tartrate dianions

As noted above, there is a series of papers in which the relative ability of a given enantiomer of the trication $[Co(en)_3]^{3+}$ or substituted derivatives to hydrogen bond to a given enantiomer of the tartrate dianion is critiqued.[12-15] The analyses that follow are restricted to the modes of hydrogen bonding.

2.4.7.1. Λ–δδδ-[Co(en)$_3$]$^{3+}$ Cl$^-$(R,R)-tart^{2-}·5H$_2$O (lel$_3$)

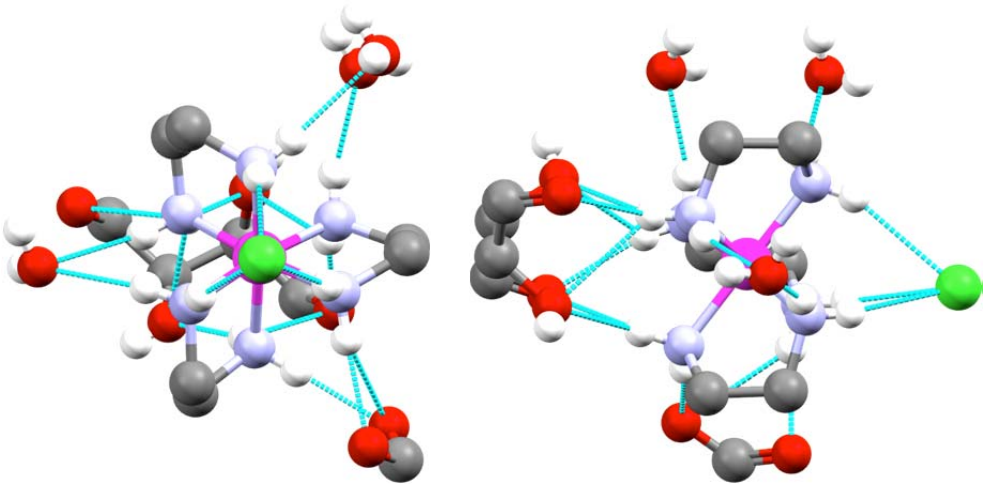

H-bond acceptor	type of H-bond	number of similar interactions
(*R*,*R*)-tart^{2-}	[C_2^2,C_2][2]	1
(*R*,*R*)-tart^{2-}	[C_3^3,C_3^2,C_3^2][2,2,2,1:4]	1
Cl$^-$	[C_3,C_3,C_3][1]	1
H_2O	[C_2][1]	2
H_2O	[C_2,C_2][1]	1

Figure 2.17. Hydrogen bonding interactions in Λ–δδδ-[Co(en)$_3$]$^{3+}$ Cl$^-$(*R*,*R*)-tart^{2-}·5H$_2$O (*lel$_3$*) viewed along the C_3 axis (left) and a C_2 axis (right). Most non-interacting atoms of the tartrate dianions have been omitted for clarity.

The structure and hydrogen bonding interactions of the enantiopure pentahydrated mixed chloride/tartrate salt, Λ–$\delta\delta\delta$-$[Co(en)_3]^{3+}$ Cl^-(*R*,*R*)-$tart^{2-}\cdot 5H_2O$ (*lel*$_3$), are shown in Figure 2.17.[15a] All twelve N-H units are engaged in hydrogen bonding to two (*R*,*R*)-$tart^{2-}$ dianions, one Cl^- anion, and two H_2O molecules. At one C_3 site, all three N-H units hydrogen bond to a single chloride ion, a motif seen in 2.4.2.3 above. At the other, the three N-H units bind to four oxygen atoms of a single (*R*,*R*)-$tart^{2-}$ dianion (O=C-CHOH-CHOH-C=O) via a total of seven hydrogen bonds. At one C_2 site, the two N-H units make three hydrogen bonds to the two oxygen atoms of a carboxylate group. At the other C_2 sites, there is hydrogen bonding either to one (chelating) or two (non-chelating) H_2O molecules.

2.4.7.2. Δ–$\lambda\lambda\lambda$-$[Co(en)_3]^{3+}$ 1.5(R,R)-$tart^{2-}\cdot 5.75H_2O$ (lel$_3$). The structure and hydrogen bonding interactions of the enantiopure polyhydrated tartrate salt, Δ–$\lambda\lambda\lambda$–$[Co(en)_3]^{3+}$ 1.5(*R*,*R*)-$tart^{2-}\cdot 5.75H_2O$, are shown in Figure 2.18.[15e] This complex lacks the chloride anion found in the previous example 2.4.7.1. There are two independent trications in the unit cell, which are linked as shown at the top of Figure 2.18, and separately depicted in the middle and bottom. Of the N-H units, ten and twelve are engaged in hydrogen bonding, respectively.

With the first trication (middle), all three C_2 sites are different. In one, the two N-H units chelate a H_2O molecule. In another, the N-H units make three hydrogen bonds to two oxygen atoms of a carboxylate group. In the third, there is no hydrogen bonding, which is unique to all the structures surveyed. Each of the C_3 sites is occupied by a single tartrate dianion. In one, the three N-H units make a total of six hydrogen bonds to three oxygen atoms (O=C-CHOH-CHOH). In the other, the three N-H units make five hydrogen bonds to the two oxygen atoms of a carboxylate group.

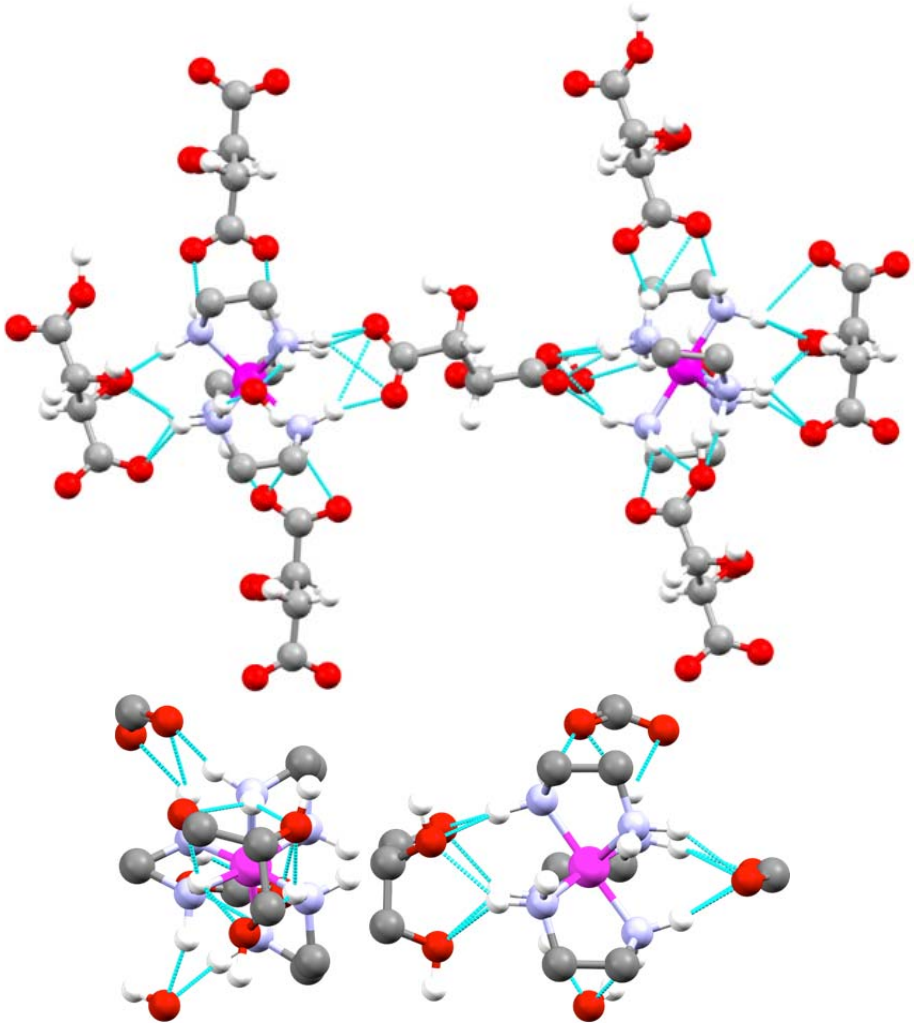

H-bond acceptor	type of H-bond	number of similar interactions
(*R*,*R*)-tart^{2-}	[C_2^2,C_2][2]	1
(*R*,*R*)-tart^{2-}	[C_3^2,C_3^2,C_3][3,2:2]	1
(*R*,*R*)-tart^{2-}	[C_3^2,C_3^2,C_3^2][2,2,2:3]	1
H_2O	[C_2,C_2][1]	1

Figure 2.18. Hydrogen bonding interactions in the two independent trications of Δ–*λλλ*-[Co(en)$_3$]$^{3+}$ 1.5(*R*,*R*)-tart^{2-}·5.75H_2O (*lel*$_3$) viewed along the C_3 axis (left middle, left bottom) and a C_2 axis (right middle, right bottom), or as linked together (top). In the middle and bottom representations, most non-interacting atoms of the tartrate dianions have been omitted for clarity.

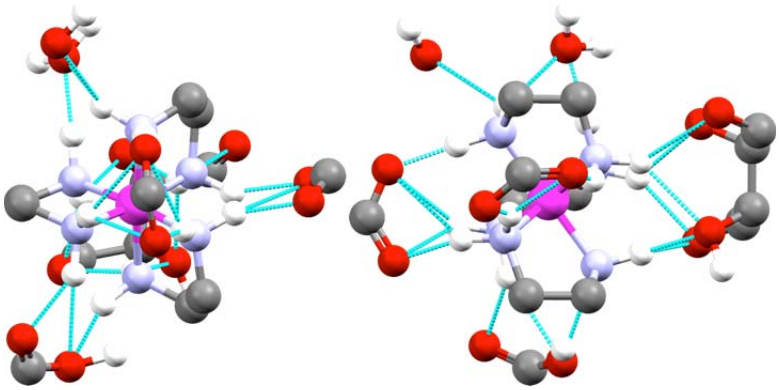

H-bond acceptor	type of H-bond	number of similar interactions
(*R*,*R*)-tart^{2-}	$[C_2^2,C_2][2]$	2
(*R*,*R*)-tart^{2-}	$[C_3^2,C_3^2,C_3][3,2:2]$	1
(*R*,*R*)-tart^{2-}	$[C_3^3,C_3^2,C_3^2][2,2,2,1:4]$	1
H_2O	$[C_2][1]$	1
H_2O	$[C_2,C_2][1]$	1

Figure 2.18 Continued.

With the second trication (bottom), the two N-H units of two C_2 sites each make three hydrogen bonds to two oxygen atoms of a carboxylate group.[31] The N-H units of the remaining C_2 site make three hydrogen bonds to two H_2O molecules (one chelating, one not). Each of the C_3 sites is again occupied by a single tartrate dianion. In one, the three N-H units make a total seven hydrogen bonds to four oxygen atoms (O=C-CHOH-CHOH-C=O); an identical motif was observed in 2.4.7.1. In the other (as in the independent trication), the three N-H units make five hydrogen bonds to the two oxygen atoms of a carboxylate group.

2.4.7.3. Λ–δδδ-[Co(en)$_3$]$^{3+}$ 1.5(R,R)-tart^{2-}·9.5H$_2$O (lel$_3$). The structure and hydrogen bonding interactions of the enantiopure polyhydrated tartrate salt, Λ–*δδδ*-[Co(en)$_3$]$^{3+}$ 1.5(*R*,*R*)-tart^{2-}·9.5H$_2$O (*lel*$_3$), are shown in Figure 2.19.[15e] This is simply a different hydrate – sometimes called a pseudopolymorph[32] – of the salt in 2.4.7.2. As with 2.4.7.3, there are two independent trications in the unit cell, which are depicted in the top and bottom of Figure 2.19. The hydrogen bonding motifs do not break any new ground vis-à-vis the previous structure. Of the N-H units, eleven and twelve are engaged in hydrogen bonding, respectively.

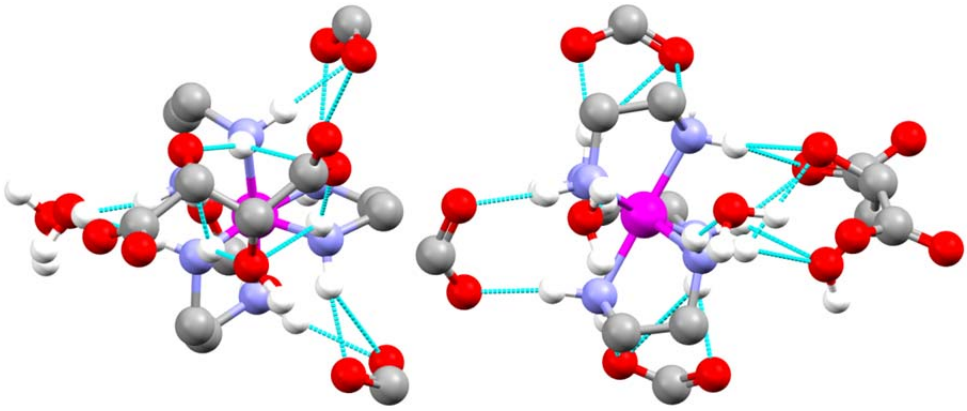

H-bond acceptor	type of H-bond	number of similar interactions
H$_2$O	[C$_2$][1]	2
H$_2$O	[C$_2$,C$_2$][1]	1
(*R*,*R*)-tart^{2-}	[C$_2^2$,C$_2$][2]	2
(*R*,*R*)-tart^{2-}	[C$_3$,C$_3$][2]	1
(*R*,*R*)-tart^{2-}	[C$_3^2$,C$_3^2$,C$_3^2$][2,2,2:3]	1

Figure 2.19. Hydrogen bonding interactions in the two independent trications of Λ–*δδδ*-[Co(en)$_3$]$^{3+}$ 1.5(*R*,*R*)-tart^{2-}·9.5H$_2$O (*lel*$_3$) viewed along the C$_3$ axis (left) and a C$_2$ axis (right). Most non-interacting atoms of the tartrate dianions have been omitted for clarity.

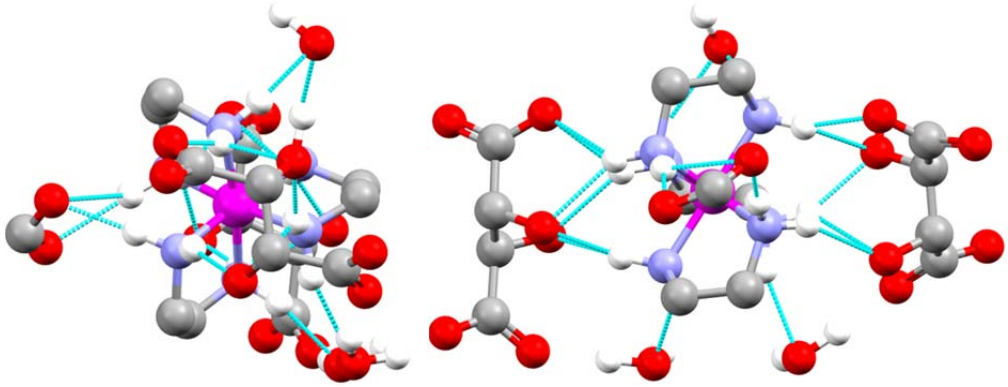

H-bond acceptor	type of H-bond	number of similar interactions
H_2O	$[C_2][1]$	2
H_2O	$[C_2,C_2][1]$	1
(*R*,*R*)-$tart^{2-}$	$[C_2^2,C_2][2]$	1
(*R*,*R*)-$tart^{2-}$	$[C_3^2,C_3^2,C_3][2,2,1:3]$	1
(*R*,*R*)-$tart^{2-}$	$[C_3^2,C_3^2,C_3^2][2,2,2:3]$	1

Figure 2.19 Continued.

For the first independent cation (top), two N-H units of one C_3 site chelate the O-C-O linkage of a carboxylate group; the third N-H unit exhibits no hydrogen bonding. The three N-H units of the other C_3 site make a total of six hydrogen bonds to three oxygen atoms of a tartrate dianion (O=C-CHOH-CHOH). The two N-H units of two C_2 sites each make three hydrogen bonds to the two oxygen atoms of separate carboxylate groups. In the third C_2 site, each N-H unit hydrogen bonds to an oxygen atom of a separate H_2O molecule.

For the second independent trication (bottom), three N-H units of one C_3 site make (as in the other trication) a total of six hydrogen bonds to three different oxygen

atoms of a tartrate dianion (O=C-CHOH-CHOH). The three N-H units of the other C_3 site make five hydrogen bonds to the same three oxygen atoms of a second tartrate dianion. The two N-H units of one C_2 site make a total three hydrogen bonds to the two oxygen atoms of a carboxylate. In another C_2 site, the N-H units chelate an oxygen atom of a disordered H_2O molecule. In the third C_2 site, each N-H unit hydrogen bonds to an oxygen atom of a separate H_2O molecule.

2.4.8. Salts with one trianion

2.4.8.1. Λ–δδδ-$[Co(en)_3]^{3+}$ $AsO_4^{3-}\cdot 3H_2O$ (lel_3)

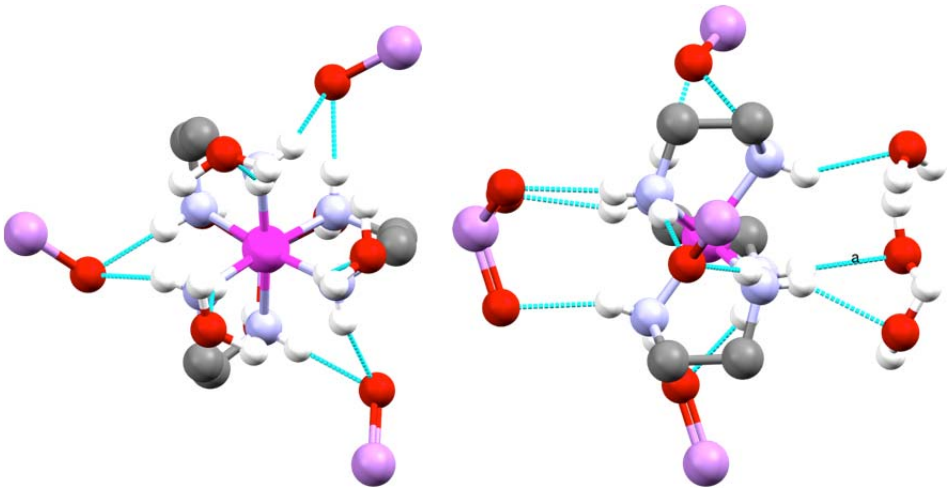

H-bond acceptor	type of H-bond	number of similar interactions
AsO_4^{3-}	$[C_3,C_3,C_3][3]$	1
AsO_4^{3-}	$[C_2,C_2][1]$	3
H_2O	$[C_3][1]$	3

Figure 2.20. Hydrogen bonding interactions in Λ–δδδ-$[Co(en)_3]^{3+}$ $AsO_4^{3-}\cdot 3H_2O$ (lel_3) viewed along the C_3 axis (left) and a C_2 axis (right). Non-interacting oxygen atoms of the arsenate trianion have been omitted for clarity.

The structure and hydrogen bonding interactions of the trihydrated arsenate salt, Λ–*δδδ*-$[Co(en)_3]^{3+}$ $AsO_4^{3-}\cdot 3H_2O$ (*lel*$_3$) are shown in Figure 2.20.[33] This represents one of the two enantiomers in the crystallographically characterized racemate. There is a crystallographic C_3 axis corresponding to the idealized C_3 axis of the trication. All twelve N-H units engage in hydrogen bonding to four arsenate anions and three H_2O molecules. The AsO_4^{3-} trianions exhibit only two hydrogen bonding motifs. The two N-H units of all three C_2 sites chelate to an AsO_4^{3-} oxygen atom. The three N-H units of one C_3 site each hydrogen bond to a different oxygen atom of the AsO_4^{3-} anion. In the other C_3 site, each N-H unit hydrogen bonds to the oxygen atom of a separate H_2O molecule.

2.4.8.2. Λ–λδδ-$[Co(en)_3]^{3+}$ AsS_4^{3-} (oblel$_2$). The structure and hydrogen bonding interactions of the tetrathioarsenate(V) salt, Λ–*λδδ*-$[Co(en)_3]^{3+}$ AsS_4^{3-} (*oblel*$_2$) are shown in Figure 2.21.[34] This represents one of the two enantiomers in the crystallographically characterized racemate. As with 2.4.2.4, 2.4.3.1, 2.4.5.1, and 2.4.6.1 above, the complex crystallizes in an *oblel*$_2$ orientation. There is a crystallographic C_2 axis, but it does not correspond to the idealized C_2 axis of the trication. All twelve N-H units engage in hydrogen bonding to five AsS_4^{3-} trianions. Each of the three N-H units of each C_3 site hydrogen bond to one of two sulfur atoms of a AsS_4^{3-} trianion. The two N-H units of each C_2 site hydrogen bond either to two sulfur atoms of a AsS_4^{3-} trianion, or the same sulfur atom.

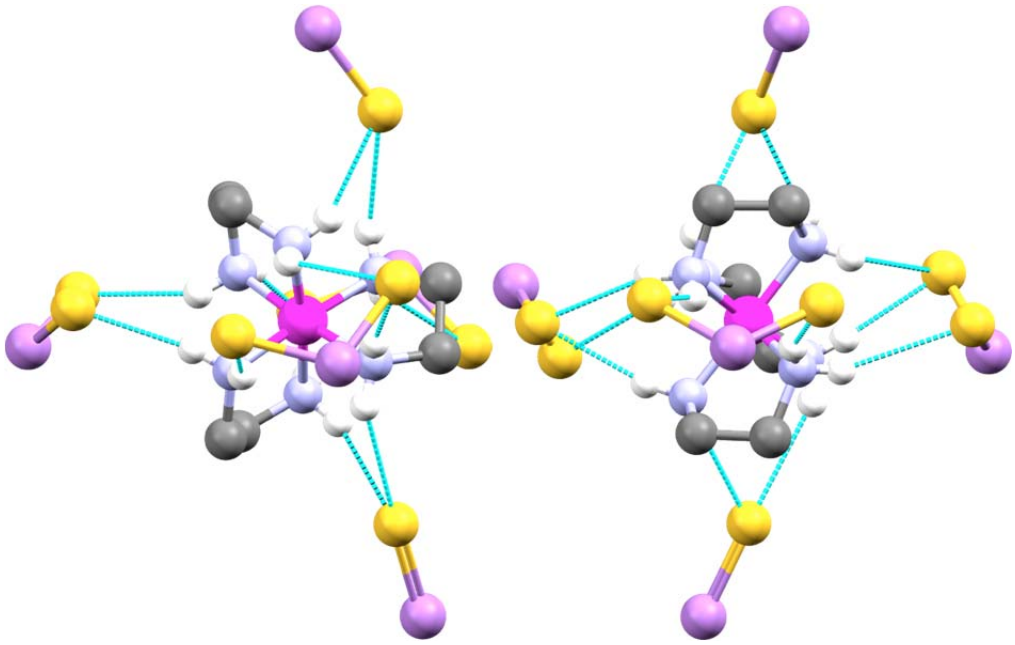

H-bond acceptor	type of H-bond	number of similar interactions
AsS_4^{3-}	$[C_2,C_2][1]$	2
AsS_4^{3-}	$[C_2,C_2][2]$	1
AsS_4^{3-}	$[C_3,C_3,C_3][2]$	2

Figure 2.21. Hydrogen bonding interactions in Λ–$\lambda\delta\delta$-$[Co(en)_3]^{3+}$ AsS_4^{3-} (*oblel*$_2$) viewed along the pseudo C_3 axis (left) and the C_2 axis (right). Non-interacting sulfur atoms of the tetrathioarsenate trianion have been omitted for clarity.

2.4.8.3. Λ–δδδ-[Co(en)$_3$]$^{3+}$ GaF$_6^{3-}$ (lel$_3$)

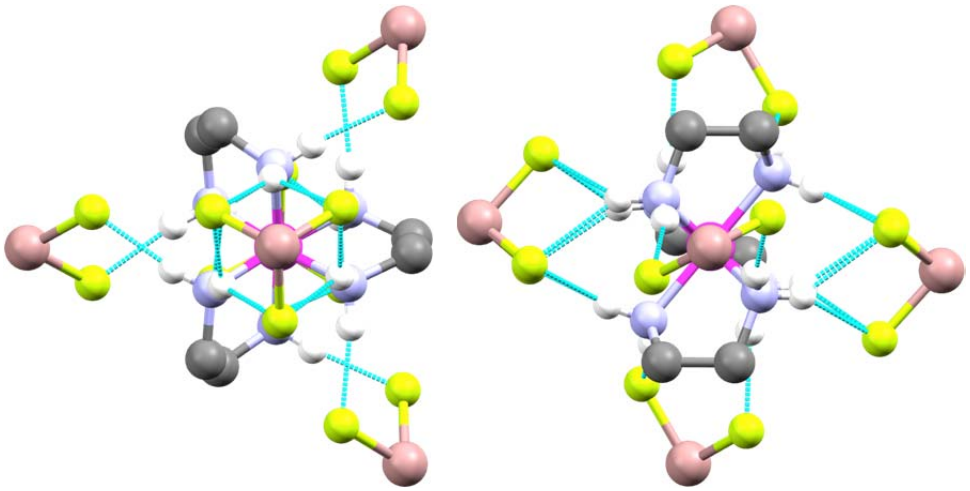

H-bond acceptor	type of H-bond	number of similar interactions
GaF_6^{3-}	$[C_2,C_2][2]$	3
GaF_6^{3-}	$[C_3^2,C_3^2,C_3^2][2,2,2:3]$	2

Figure 2.22. Hydrogen bonding interactions in Λ–*δδδ*-[Co(en)$_3$]$^{3+}$ GaF$_6^{3-}$ viewed along the C_3 axis (left) and a C_2 axis (right). Non-interacting fluorine atoms of the hexafluorogallate trianion have been omitted for clarity.

The structure and hydrogen bonding interactions of the enantiopure hexafluorogallate salt, Λ–*δδδ*-[Co(en)$_3$]$^{3+}$ GaF$_6^{3-}$ (*lel*$_3$), are shown in Figure 2.22.[35] There are crystallographic C_3 and C_2 axes corresponding to the idealized C_3 and C_2 axes of the trication. All twelve N-H units engage in hydrogen bonding to five GaF$_6^{3-}$ trianions. The three N-H units of each C_3 site each bind to two of three *fac* oriented fluoride ions of a single GaF$_6^{3-}$ trianion. The two N-H units of each C_2 site each bind to two (*cis*) fluoride ions of a single GaF$_6^{3-}$ trianion.

2.4.8.4. Λ–λδδ-[Co(en)$_3$]$^{3+}$ Co(CN)$_6^{3-}$·5H$_2$O (oblel$_2$)

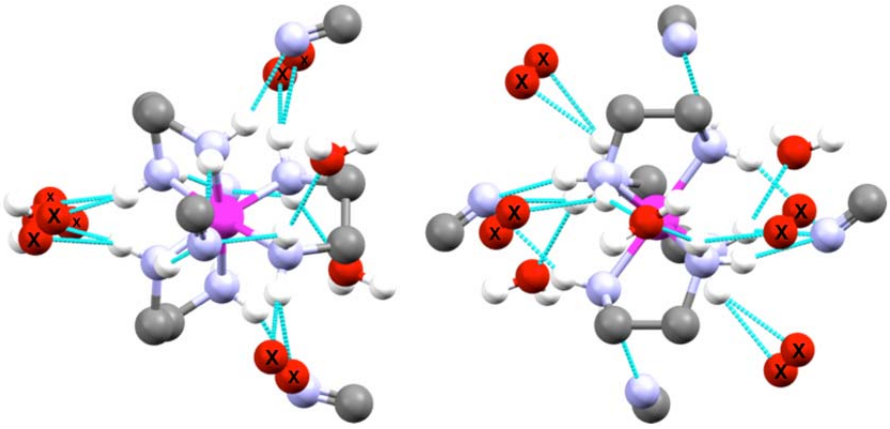

H-bond acceptor	type of H-bond	number of similar interactions
H_2O[a]	$[C_2][1]$	4
H_2O	$[C_3][1]$	2
H_2O	$[C_2,C_2][1]$	1
$Co(CN)_6^{3-}$	$[C_2][1N]$	2
$Co(CN)_6^{3-}$	$[C_3,C_3,C_3][1N]$	2

[a] Although this salt has a stoichiometry of five H_2O molecules per trication, there are seven H_2O molecules in the second coordination sphere, four of which are shared with neighboring trications and disordered over two positions (each highlighted with an "X").

Figure 2.23. Hydrogen bonding interactions in Λ–λδδ-[Co(en)$_3$]$^{3+}$ Co(CN)$_6^{3-}$·5H$_2$O (*oblel$_2$*) viewed along the pseudo C_3 axis (left) and the C_2 axis (right). Except for the interacting CN units, the Co(CN)$_6^{3-}$ trianions have been omitted for clarity. Disordered H_2O molecules are denoted with an X.

The structure and hydrogen bonding interactions of the pentahydrated hexacyanocobaltate salt, Λ–λδδ-[Co(en)$_3$]$^{3+}$ Co(CN)$_6^{3-}$·5H$_2$O (*oblel$_2$*) are shown in Figure 2.23.[36] This represents one of the two enantiomers in the crystallographically characterized racemate. As with 2.4.2.4, 2.4.3.1, 2.4.5.1, 2.4.6.1, and 2.4.8.2, the complex crystallizes in an *oblel$_2$* orientation. Although some disorder is apparent as

described in the following paragraph, there is a crystallographic C_2 axis corresponding to the idealized C_2 axis of the trication (right view).

The three N-H units of each C_3 site are hydrogen bonded to the same nitrogen atom of a cyanide ligand. In addition, one N-H unit of each C_3 site also hydrogen bonds to the oxygen atom of a H_2O molecule. The two N-H units of two C_2 sites are separately hydrogen bonded to a H_2O molecule and the nitrogen atom of a cyanide ligand. The N-H units of the third C_2 site bind three H_2O molecules (one chelating, two not). The four non-chelating H_2O molecules associated with the C_2 sites (labeled with "X" in Figure 2.23) are disordered over two positions, and furthermore engage in hydrogen bonding with the N-H units of neighboring trications.

2.4.8.5. Λ–δδδ-[Co(en)$_3$]$^{3+}$ Λ-Rh(C$_2$O$_4$)$_3^{3-}$ (lel$_3$). The structure and hydrogen bonding interactions of the enantiopure Λ-tris(oxalate)rhodate(III) salt, Λ–*δδδ*-[Co(en)$_3$]$^{3+}$ Λ-Rh(C$_2$O$_4$)$_3^{3-}$ (*lel*$_3$), are shown in Figure 2.24.[37] Note that the tris(chelate) trianion now also has helical (Λ/Δ) chirality. The crystal structure bears a number of similarities to that of the arsenate salt in 2.4.8.1. There is a crystallographic C_3 axis corresponding to the idealized C_3 axis of the trication (which also contains the C_3 axis of the trianion). All twelve N-H units are engaged in hydrogen bonding to five trianions in one of two motifs. The two N-H units of all three C_2 sites chelate to a carbonyl oxygen atom of an oxalate ligand. The three N-H units of each C_3 site each bind to two of three *fac* oriented Rh-O linkages.

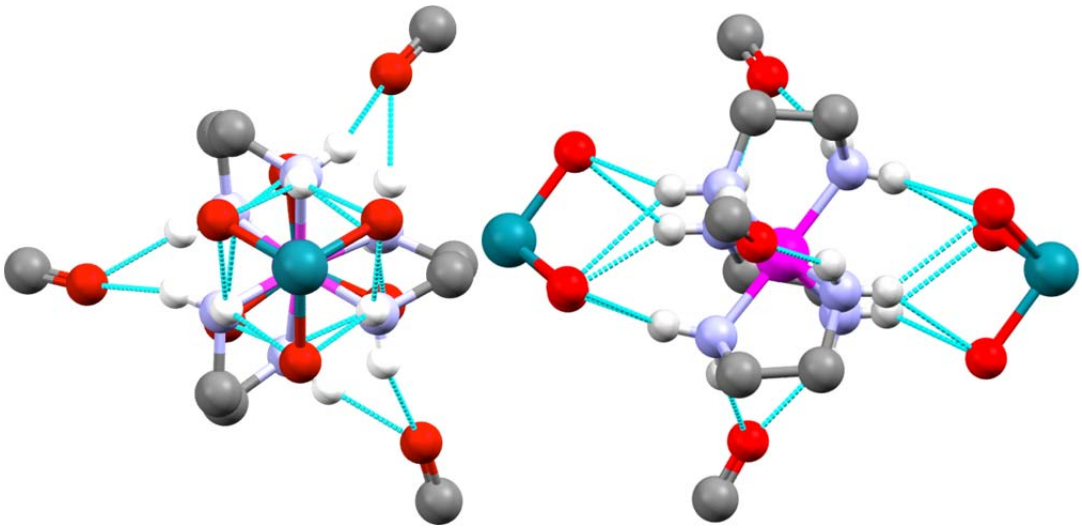

H-bond acceptor	type of H-bond	number of similar interactions
Λ-$Rh(C_2O_4)_3^{3-}$	$[C_2,C_2][1]$	3
Λ-$Rh(C_2O_4)_3^{3-}$	$[C_3^2,C_3^2,C_3^2][2,2,2:3]$	2

Figure 2.24. Hydrogen bonding interactions in Λ–*δδδ*-$[Co(en)_3]^{3+}$ Λ-$Rh(C_2O_4)_3^{3-}$ (*lel*$_3$) viewed along the C_3 axis (left) and a C_2 axis (right). Non interacting atoms of the trianion have been omitted for clarity.

2.4.8.6. Λ–δδδ-[Co(en)$_3$]$^{3+}$Δ-Rh(C$_2$O$_4$)$_3^{3-}$ (lel$_3$). The structure and hydrogen bonding interactions of the enantiopure Δ-tris(oxalate)rhodate(III) salt, Λ–*δδδ*-$[Co(en)_3]^{3+}$ Δ-$Rh(C_2O_4)_3^{3-}$ (*lel*$_3$), are shown in Figure 2.25.[37] This complex is diastereomeric with that in 2.4.8.5 (opposite $Rh(C_2O_4)_3^{3-}$ chirality), and has an identical degree of hydration. As is easily seen with a quick glance at the "type of H-bond" entries in Figures 2.24 and 2.25, the second coordination spheres markedly differ, with only one type of hydrogen bond (a single $[C_2,C_2][1]$ linkage) common to each.

All twelve N-H units are engaged in hydrogen bonding to six trianions. The three C_2 sites exhibit different motifs. In one, the two N-H units chelate a carbonyl oxygen atom of an oxalate ligand. In another, the two N-H units make a total of three hydrogen

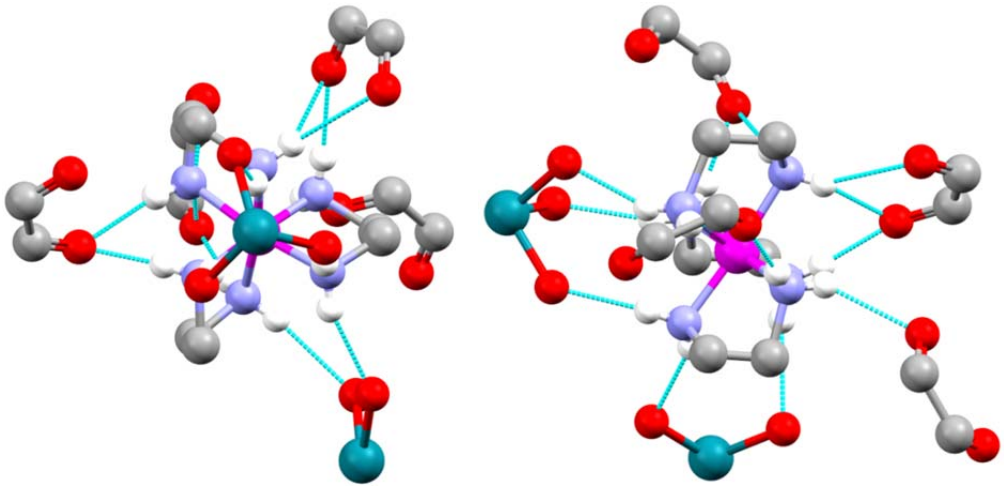

H-bond acceptor	type of H-bond[a]	number of similar interactions
Δ-$Rh(C_2O_4)_3^{3-}$	$[C_3][1]$	1
Δ-$Rh(C_2O_4)_3^{3-}$	$[C_2,C_2][1]$	1
Δ-$Rh(C_2O_4)_3^{3-}$	$[C_2,C_2][2]$	1
Δ-$Rh(C_2O_4)_3^{3-}$	$[C_2^2,C_2][2]$	1
Δ-$Rh(C_2O_4)_3^{3-}$	$[C_3^2,C_3][2]$	1
Δ-$Rh(C_2O_4)_3^{3-}$	$[C_3,C_3,C_3][3]$	1

[a] The CIF file for this molecule did not indicate any hydrogen atoms. Hence, they were introduced in idealized positions using the program Olex2.[38]

Figure 2.25. Hydrogen bonding interactions in Λ–*δδδ*-$[Co(en)_3]^{3+}$ Δ-$Rh(C_2O_4)_3^{3-}$ (*lel*$_3$) viewed along the C_3 axis (left) and a C_2 axis (right). Non interacting atoms of the trianion have been omitted for clarity.

bonds to the two oxygen atoms of a O=C-C=O moiety. In the third, the N-H units bind a separate oxygen atom of a O-Rh-O linkage. At one C_3 site, each N-H unit makes one hydrogen bond to a different oxygen atom of three facially directed Rh-O linkages. At the other, one N-H unit makes a single hydrogen bond to a carbonyl oxygen atom of an oxalate ligand. The other two N-H units make a total of three hydrogen bonds to the two

oxygen atoms of a O=C-C=O moiety.

2.4.8.7. Λ–λδδ-[Co(en)$_3$]$^{3+}$ C$_6$H$_3$(CO$_2$)$_3^{3-}$·5.55H$_2$O (oblel$_2$). The structure and hydrogen bonding interactions of the polyhydrated benzene-1,3,5-tricarboxylate (trimesate) salt, Λ–λδδ-[Co(en)$_3$]$^{3+}$ C$_6$H$_3$(CO$_2$)$_3^{3-}$·5.55H$_2$O (*oblel$_2$*), are shown in Figure 2.26.[34] This represents one of the two enantiomers in the crystallographically characterized racemate. The H$_2$O molecules about the Δ enantiomer (but not the Λ enantiomer) are disordered. As with 2.4.2.4, 2.4.3.1, 2.4.5.1, 2.4.6.1, 2.4.8.2, and 2.4.8.4, the complex crystallizes in an *oblel$_2$* orientation.

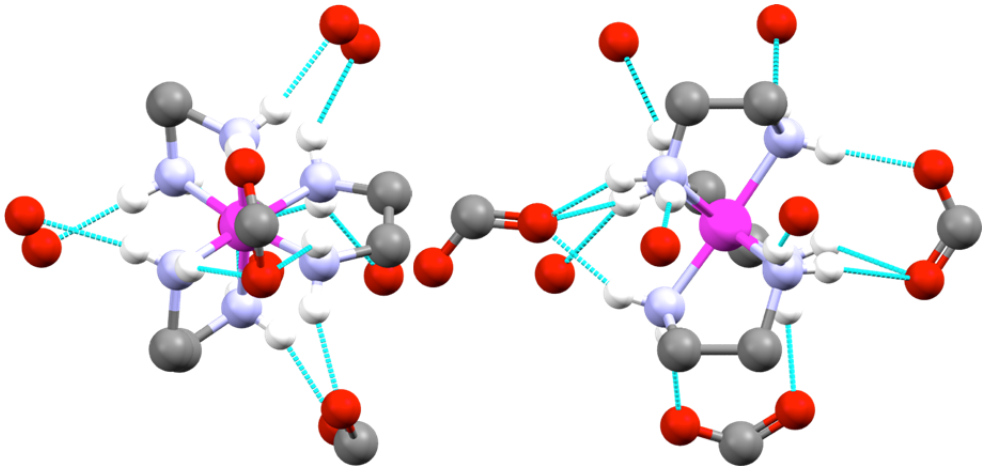

H-bond acceptor	type of H-bond	number of similar interactions
H$_2$O	[C$_2$][1]	4
H$_2$O	[C$_3$][1]	1
C$_6$H$_3$(CO$_2$)$_3^{3-}$	[C$_2$,C$_2$][2]	1
C$_6$H$_3$(CO$_2$)$_3^{3-}$	[C$_3$,C$_3$,C$_3$][2]	1
C$_6$H$_3$(CO$_2$)$_3^{3-}$	[C$_3$,C$_3$,C$_3$][1]	1

Figure 2.26. Hydrogen bonding interactions in Λ–λδδ-[Co(en)$_3$]$^{3+}$ C$_6$H$_3$(CO$_2$)$_3^{3-}$ ·5.55H$_2$O (*oblel$_2$*) viewed along the pseudo C$_3$ axis (left) and the C$_2$ axis (right). Non-interacting atoms of the trianion have been omitted for clarity.

All twelve N-H units engage in hydrogen bonding to three tris(carboxylate) trianions and five H_2O molecules. At two C_2 sites, each N-H unit hydrogen bonds to the oxygen atom of a separate H_2O molecule. At the third, the N-H units chelate the O-C-O linkage of a carboxylate group. At one C_3 site, the three N-H units interact with both oxygen atoms of a carboxylate group via three hydrogen bonds. At the other C_3 site, each N-H unit hydrogen bonds to the same oxygen atom of a carboxylate group, and one N-H unit makes an additional hydrogen bond with the oxygen atom of a H_2O molecule.

2.4.8.8. Λ–δδδ-[Co(en)$_3$]$^{3+}$ P$_3$O$_9$$^{3–}$·2H$_2$O (lel$_3$) (from racemic salt)

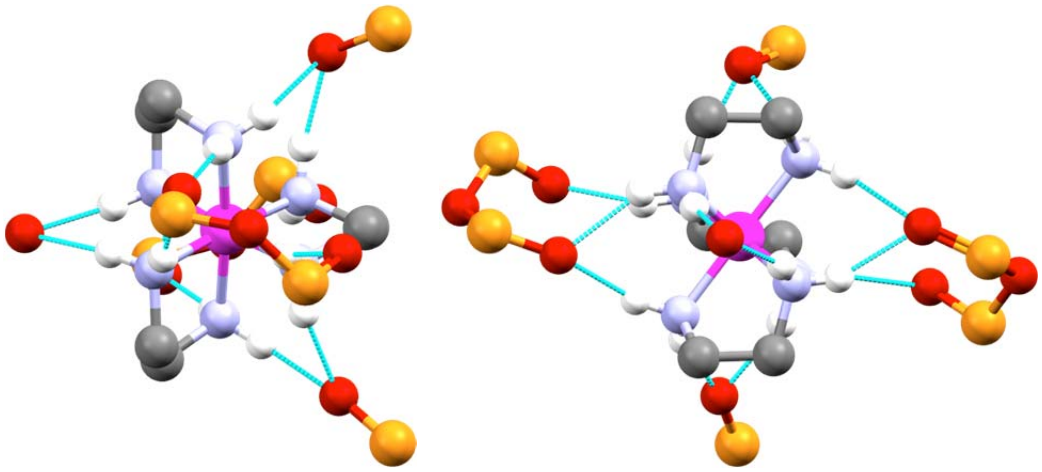

H-bond acceptor	type of H-bond	number of similar interactions
$P_3O_9^{3-}$	$[C_2,C_2][1]$	2
H_2O	$[C_2,C_2][1]$	1
$P_3O_9^{3-}$	$[C_3,C_3,C_3][2]$	2

Figure 2.27. Hydrogen bonding interactions in Λ–*δδδ*-$[Co(en)_3]^{3+}$ $P_3O_9^{3-}\cdot 2H_2O$ (*lel*$_3$) viewed along the C_3 axis (left) and a C_2 axis (right). Most non-interacting atoms of the trianion have been omitted for clarity.

The structure and hydrogen bonding interactions of the dihydrated cyclotriphosphate salt, Λ–$\delta\delta\delta$-$[Co(en)_3]^{3+}$ $P_3O_9^{3-}\cdot 2H_2O$ (*lel*$_3$) are shown in Figure 2.27.[39] This represents one of the two enantiomers in the crystallographically characterized racemate. All twelve N-H units are engaged in hydrogen bonding to four $P_3O_9^{3-}$ trianions and one H_2O molecule. The three N-H units of both C_3 sites hydrogen bond to two different oxygen atoms of a $P_3O_9^{3-}$ trianion (1,5-relationship). The two N-H units of two C_2 sites chelate to a single oxygen atom of a $P_3O_9^{3-}$ trianion. The N-H units of the third C_2 site chelate the oxygen atom of a H_2O molecule.

2.4.8.9. Λ–$\delta\delta\delta$-$[Co(en)_3]^{3+}$ $P_3O_9^{3-}\cdot 2H_2O$ (lel$_3$) (from enantiopure salt)

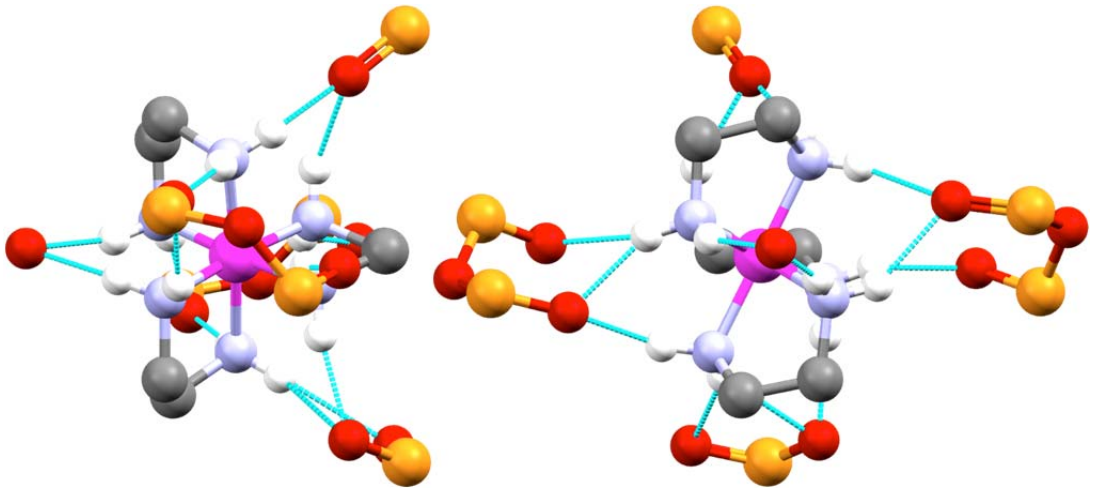

H-bond acceptor	type of H-bond	number of similar interactions
H_2O	$[C_2,C_2][1]$	1
$P_3O_9^{3-}$	$[C_2,C_2][1]$	1
$P_3O_9^{3-}$	$[C_2^2,C_2][2]$	1
$P_3O_9^{3-}$	$[C_3,C_3,C_3][2]$	2

Figure 2.28. Hydrogen bond interactions in Λ–$\delta\delta\delta$-$[Co(en)_3]^{3+}$ $P_3O_9^{3-}\cdot 2H_2O$ (*lel*$_3$) viewed along the C_3 axis (left) and a C_2 axis (right). Most non-interacting atoms of the trianion have been omitted for clarity.

The structure and hydrogen bonding interactions of the enantiopure dihydrated cobalt cyclotriphosphate salt, Λ–*δδδ*-$[Co(en)_3]^{3+}$ $P_3O_9^{3-}\cdot 2H_2O$ (*lel*$_3$), are depicted in Figure 2.28.[39] The bonding motifs are very similar to those of the racemate in 2.4.8.8, which is also a dihydrate. All twelve N-H units are engaged in hydrogen bonding to four $P_3O_9^{3-}$ trianions and one H_2O molecule. The C_3 sites exhibit the same interactions as with the racemate. However, the two N-H units of one C_2 site no longer chelate to a single oxygen atom of a $P_3O_9^{3-}$ trianion. Rather, they form three hydrogen bonds to two oxygen atoms with a 1,3-relationship.

2.5. Additional structural information and generalizations

2.5.1. General and scope of hydrogen bonding

As noted above, Table A-1 summarizes the 150 unique crystal structures containing the trication $[Co(en)_3]^{3+}$, and 142 of these are amenable to detailed analyses (a few more to partial analyses). The anions or other features in about one third of these can be regarded (at least from an organic chemist's perspective) as *mondo bizzarro* (e.g., $Zn_6P_8O_{32}H_8^{3-}$,[40] $V_3P_3BO_{19}^{5-}$ $H_2PO_4^-$,[41] $[(Co^{(II)}O_6)Mo^{(VI)}{}_6O_{18}(As^{(III)}{}_3O_3)_2]^{4-}$,[42] $[Ru_2(C_2H_4O_7P_2)_2Cl_2]^{5-}$,[43] *trans*-$CdBr_4Cl_2^{4-}$,[44] $Zr_4F_{22}O_2^{10-}$,[45] $SiMo_8V_4O_{40}(VO)_2^{6-}$,[46] $In_3(H_2PO_4)_6(HPO_4)_3^{3-}$).[47] Eight different small molecule clathrates of $[Co(en)_3]^{3+}$ $3Cl^-$ have been structurally characterized.[48] These types of exotic species were generally excluded from sections 2.4.2-2.4.8, but not from further analyses below.

An important initial remark is that the N-H units of the $[Co(en)_3]^{3+}$ trications of all 150 structures are extensively hydrogen bonded. Indeed, in sections 2.4.2-2.4.8 it was rather unusual to find cases in which all twelve of the N-H units were *not* so engaged. The N-H donor strengths must be substantial, as they interact with a variety of weak hydrogen bond acceptors. Although the hydrogen bond accepting strengths of many anions have been quantified,[49] relatively few of those in Table A-1 (Appendix) have

been ranked. Some of the extensively delocalized anions in the previous paragraph, as well as GaF_6^{3-} (2.4.8.3) or $AuCl_4^-$ and SiF_6^{2-} (Table A-1 in Appendix), are likely among the weakest.

Four crystal structures with perchlorate anions – a very feeble hydrogen bond acceptor[49] – can be found in Table A-1 (Appendix). One is of the mixed oxalate/perchlorate salt $[Co(en)_3]^{3+}$ $C_2O_4^{2-}ClO_4^-$ (entry 70).[50] Although carboxylate anions are good hydrogen bond acceptors,[49] the perchlorate anion competes, binding in a $[C_3,C_3][1]$ mode with N-H···O distances of 2.596 and 2.707 Å. Two others involve cocrystals of $[Co(en)_3]^{3+}$ $3ClO_4^-$ and a neutral palladium penicillimate complex.[51] One lattice (entry 65) features two independent trications, many N-H units of which interact with donor atoms of the penicillin moiety. However two perchlorate anions hydrogen bond to one trication ($[C_3][1]$, N-H···O 2.169 Å; $[C_3,C_2][2]$, N-H···O 2.197, 2.536 Å), and one to the other ($[C_2,C_2][2]$, N-H···O 2.144, 2.340 Å). Hydrogen bonding to perchlorate is evident in another structure (entry 77), but severe disorder precludes further analyses.

2.5.2. Types of hydrogen bonding

In the salts in sections 2.4.2-2.4.8, a number of very common hydrogen bonding motifs are apparent. For example, many anions and H_2O molecules interact with two N-H units of the same C_2 binding site, or multiple N-H units from the same C_3 binding site. However, taking the opposite perspective, H_2O molecules never interact with multiple N-H units originating from *both* C_2 and C_3 binding sites. Anions only do so in a few special cases involving larger species with multiple acceptor sites.

The most likely modes by which anions might interact with two N-H units from different C_2 and C_3 binding sites have been summarized in Figure 2.6. The first, denoted $[C_3/C_2]$, entails anion binding to the N-H units of the same NH_2 group. This motif is

unequivocally absent in the 27 salts in sections 2.4.2-2.4.8, and no examples have been found in the remaining structures (Table A-1 in Appendix). I have also examined the crystal structures of all 6259 primary and secondary organoammonium halides, $[RNH_3]^+$ X^- and $[RR'NH_2]^+$ X^-, in the Cambridge Structural Database. Interestingly, none showed hydrogen bonding of the halide anion to two geminal N-H units. Hence, this motif appears to be intrinsically disfavored, presumably due to stereoelectronic reasons and/or the larger H-X-H angle required.

Although rare, it is possible to bridge the geminal N-H units of organoammonium halides with unusual larger anions that feature multiple acceptor sites.[52,53] Interestingly, a more complicated variant, $[(C_3^2/C_2),C_3][3]$, occurs in 2.4.5.1 (Figure 2.14). Here a large borate dianion, $B_8O_{10}(OH)_6^{2-}$, bridges the C_3 and C_2 sites. The C_3 N-H unit is chelated by two oxygen atoms of the dianion, and the dianion makes an additional hydrogen bond with another C_3 N-H unit.

The second type of hydrogen bonding in Figure 2.6, involving an anion and non-geminal N-H units from the same ligand $[C_3//C_2]$, is not found in any of the salts in sections 2.4.2-2.4.8 or Table A-1 (see Appendix). The distance between the N-H units is much too great to be bridged by a single atom. However, hydrogen bonding to a structurally extended anion, like the borate in the previous example, should in principle be feasible. The third type of hydrogen bonding in Figure 2.6, involving an anion and C_3 and C_2 sites on different ligands $[C_3,C_2]$, is seen in 2.4.6.2 (Figure 2.16). Here the cyclic croconate dianion, $C_5O_5^{2-}$, provides two variants: one in which a single oxygen atom binds to the two N-H units ($[C_3,C_2][1]$), and another in which two different oxygen atoms bind to the two N-H units ($[C_3,C_2][2]$).

2.5.3. Possible connections to catalysis

The ensemble of second coordination sphere binding motifs embodied in the

preceding $[Co(en)_3]^{3+}$ salts do not directly bear on the mechanisms of any catalytic reactions. However, they certainly point to the viability of coordinating two reactive substrates to a single C_2 site, or to a single C_3 site. They are also entirely consistent with the initial binding of one substrate to a C_2 site and the other to a C_3 site. However, this might lead to a transition state or product that spans C_2 and C_3 sites. While there do not seem to be any steric or electronic impediments to such as assembly, this has much less precedent among the crystal structures.

Interestingly, sixteen of the 27 structures in sections 2.4.2-2.4.8 are hydrates. The conspicuous lack of other molecules of crystallization simply reflects the fact that all of these salts are prepared under aqueous conditions. With the recent syntheses of many lipophilic salts,[6,54] the stage is now set to attempt the cocrystallization of guest molecules that are also substrates for catalysis. Strong interactions with substrates are evident by NMR in solution.[7a] Their binding modes are likely to provide better starting points for the development of mechanistic models, including rationales for the observed enantioselection.

2.5.4. Other stereochemical issues

Consider the relative frequencies of the various *lel*/*ob* orientations outlined in Figure 2.4. Well over half the $[Co(en)_3]^{3+}$ salts crystallize in lel_3 orientations, per the following distribution: lel_3, 81; $oblel_2$, 35; $lelob_2$, 14; ob_3, 4 (134 total). There are an additional seven salts that crystallize with two independent trications, one with a lel_3 orientation and the other with an $oblel_2$ orientation. There are also an additional three salts that crystallize with two independent cations, one with a lel_3 orientation and the other with a $lelob_2$ orientation. Taking all of the independent trications in this series of 144 compounds, the overall distribution becomes lel_3, 99; $oblel_2$, 48; $lelob_2$, 18; ob_3, 4 (169 total).

Although it is by no means a proof, this distribution suggests that *lel*$_3$ orientations have the greatest thermodynamic stabilities, and *ob*$_3$ orientations the lowest thermodynamic stabilities. This is in agreement with available experimental and computational literature.[17,55] Finally, I note that the salts in which larger anions span C_3 and C_2 binding sites (2.4.5.1, Figure 2.14; 2.4.6.2, Figure 2.16) possess *oblel*$_2$ and *lelob*$_2$ orientations. Perhaps in these lower symmetry structures, the distances between the hydrogen atoms of the N-H units, or other geometric features, are more conducive to this motif (the analysis in Figure 2.6 is for *lel*$_3$ orientations).

2.6. Conclusion

The $[Co(en)_3]^{3+}$ trication is a hydrogen bond donor extraordinaire. Adducts readily form with counter anions and H_2O molecules in the solid state. These usually engage all twelve N-H units, even when the anions include very poor hydrogen bond acceptors. These properties presumably extend to many other cationic metal complexes of primary and secondary amines. There is good NMR evidence that most of these interactions remain extant in solution.[54]

In the preceding sections, some generalizations could be offered about relatively common or less common hydrogen bonding motifs. However, the main take-home lesson of this review is the *diversity* of hydrogen bonding motifs. Insight regarding the energetics of various binding modes is currently being sought through computational studies.[56] Perhaps the situation is not too different from that in nuclei acid chemistry, where Watson-Crick, Hoogsteen, and reverse Hoogsten base pairs – as well as other hydrogen bonding arrangements – can all be encountered and serve as determinants of biological function, depending upon circumstances.[57] In any case, an essential analytical step has been taken in the quest for insight as to how $[Co(en)_3]^{3+}$ and related cations might bind and activate organic substrates in catalysis.

2.7. References

(1) (a) Miessler G. L.; Tarr, D. A. *Inorganic Chemistry*, 3rd ed.; Pearson Prentice Hall: Upper Saddle River, New Jersey, **2004**, pp. 299-321. (b) De, A. K. *Inorganic Chemistry*, 9th ed.; New Age International Publishers: New Delhi, **2003**, pp. 88-108.

(2) (a) Borer, L. L.; Russell, J. G.; Settlage, R. E. *J. Chem. Educ.* **2002**, *79*, 494-497. (b) Ernst, K-H.; Wild, F. R. W. P.; Blacque, O.; Berke, H. *Angew. Chem. Int. Ed.* **2011**, *50*, 10780-10787; *Angew. Chem.* **2011**, *123*, 10970-10977.

(3) (a) Werner, A. *Chem. Ber.* **1911**, *44*, 1887-1898. V. L. King is listed as an author for the experimental section. (b) Werner, A. *Chem. Ber.* **1911**, *44*, 2445-2455. (c) Werner, A. *Chem. Ber.* **1911**, *44*, 3272-3278. (d) Werner, A. *Chem. Ber.* **1911**, *44*, 3279-3284. (e) Werner, A. *Chem. Ber.* **1912**, *45*, 121-130.

(4) (a) Broomhead, J. A.; Dwyer, F. P.; Hogarth, J. W. *Inorg. Synth.* **1960**, *6*, 183-186. (b) Nakazawa, H.; Yoneda H. *J. Chromatogr*. **1978**, *160*, 89-99.

(5) Ehnbom, A.; Ghosh, S. K.; Lewis, K. G.; Gladysz, J. A. *Chem*. *Soc*. *Rev*. **2016**, *45*, 6799-6811.

(6) Ganzmann, C.; Gladysz, J. A. *Chem. Eur*. *J*. **2008**, *14*, 5397-5400.

(7) (a) Lewis, K. G.; Ghosh, S. K.; Bhuvanesh, N.; Gladysz, J. A. *ACS Cent*. *Sci*. **2015**, *1*, 50-56. (b) Ghosh, S. K.; Ganzmann, C.; Bhuvanesh, N.; Gladysz, J. A. *Angew*. *Chem*., *Int*. *Ed*. **2016**, *55*, 4356-4360; *Angew*. *Chem*. **2016**, *128*, 4429-4433. (c) Kumar, A.; Ghosh, S. K.; Gladysz, J. A. *Org*. *Lett*. **2016**, *18*, 760-763. (d) Joshi, H.; Ghosh, S. K.; Gladysz, J. A. *Synthesis* **2017** (in press).

(8) (a) Taylor, M. S.; Jacobsen, E. N. *Angew. Chem., Int. Ed.* **2006**, *45*, 1520-1543; *Angew*. *Chem*. **2006**, *118*, 1550-1573. (b) Doyle, A. G.; Jacobsen, E. N. *Chem. Rev.* **2007**, *107*, 5713-5743. (c) Yu, X.; Wang, W. *Chem. Asian J.* **2008**, *3*, 516-532.

(9) See also (a) Thomas, C.; Gladysz, J. A. *ACS Catalysis* **2014**, *4*, 1134-1138.

(b) Scherer, A.; Mukherjee, T.; Hampel, F.; Gladysz, J. A. *Organometallics* **2014**, *33*, 6709-6722. (c) Mukherjee, T.; Ganzmann, C.; Bhuvanesh, N.; Gladysz, J. A. *Organometallics* **2014**, *33*, 6723-6737.

(10) (a) Chen, L.-A.; Xu, W.; Huang, B.; Ma, J.; Wang, L.; Xi, J.; Harms, K.; Meggers, E. *J. Am. Chem. Soc*. **2013**, *135*, 10598-10601. (b) Chen, L.-A.; Tang, X.; Xi, J.; Xu, W.; Gong, L.; Meggers, E. *Angew. Chem., Int. Ed*. **2013**, *52*, 14021-14025; *Angew. Chem*. **2013**, 12*5*, 14271-14275. (c) Ma, J.; Ding, X.; Hu, Y.; Huang, Y.; Gong, L.; Meggers, E. *Nat. Commun*. **2014**, *5*:4531 (d) Huo, H.; Fu, C.; Wang, C.; Harms, K.; Meggers, E. *Chem. Commun*. **2014**, *50*, 10409-10411. (e) Liu, J.; Gong, L.; Meggers, E. *Tetrahedron Lett*. **2015**, *56*, 4653-4656. (f) Hu, Y.; Zhou, Z.; Gong, L.; Meggers, E. *Org. Chem. Front.* **2015**, *2*, 968-972. (g) Xu, W.; Shen, X.; Ma, Q.; Gong, L.; Meggers, E. *ACS Catal.* **2016**, *6*, 7641-7646. (h) Xu, W.; Arieno, M.; Löw, H.; Huang, K.; Xie, X.; Cruchter, T.; Ma, Q.; Xi, J.; Huang, B.; Wiest, O.; Gong, L.; Meggers, E. *J. Am. Chem. Soc.* **2016**, *138*, 8774-8780.

(11) Maleev, V. I.; North, M.; Larionov, V. A.; Fedyanin, I. V.; Savel´yeva, T. F.; Moscalenko, M. A.; Smolyakov, A. F.; Belokon, Y. N. *Adv. Synth. Catal.* **2014**, *356*, 1803-1810.

(12) Mizuta, T.; Toshitani, K.; Miyoshi, K.; Yoneda, H. *Inorg. Chem.* **1990**, *29*, 3020-3026.

(13) See also (a) Ogino, K.; Saito, U. *Bull. Chem. Soc. Jpn.* **1967**, *40*, 826-829. (b) Yoneda, H.; Taura, T. *Chem. Lett.* **1977**, 63-66.

(14) Yoneda, H. *J. Chromatogr.* **1984**, *313*, 59-91.

(15) (a) Templeton, D. H.; Zalkin, A.; Ruben H. W.; Templeton, L. K. *Acta Cryst*. **1979**, *35*, 1608-1613. (b) Magill, L. S.; Korp, J. D.; Bernal, I. *Inorg. Chem*. **1981**, *20*, 1187-1192. (c) Tada, T.; Kushi, Y.; Yoneda, H. *Chem. Lett*. **1977**, 379-382. (d)

Kushi, Y.; Kuramoto, M.; Yoneda, H. *Chem*. *Lett*. **1976**, 135-136. (e) Mizuta, T.; Tada, T.; Kushi, Y.; Yoneda, H. *Inorg*. *Chem*. **1988**, *27*, 3836-3841.

(16) To the best of my knowledge, atomic coordinates or related data are not available for Λ-$[Co(en)_3]^{3+}\cdot H_3O^+$ 2(*R*,*R*)-$tart^{2-}\cdot 2H_2O$ reported in reference 15c and Λ-$[Co(en)_3]^{3+}$ Br^-(*R*,*R*)-$tart^{2-}\cdot 5H_2O$ reported in reference 15d.

(17) Corey, E. J.; Bailar, J. C. Jr. *J. Am. Chem. Soc.* **1959**, *81*, 2620-2628.

(18) Jorge F. E.; Autschbach, J.; Ziegler, T. *J. Am. Chem. Soc.* **2005**, *127*, 975-985.

(19) (a) There would be a range of values in structures of lower symmetry. (b) The C-H and N-H bond lengths in crystal structures are commonly underestimated (ca. 10%); therefore, this distance, which is taken from structures with N-H bond lengths of 0.90 Å (vs. $\geq$1.00 Å as typically determined by other methods), must be slightly lower than the true distance.

(20) In the interest of uniformity, some additional conventions are followed: (a) The N-H units of the higher symmetry binding site are specified first, giving any "tie" to the N-H unit that bonds to the greatest number of anion atoms. For example, $[C_3^2,C_3,C_2][2]$ is written in preference to $[C_3,C_2,C_3^2][2]$, even though either representation is unambiguous. (b) In a list, $[C_2,C_2][1]$ takes priority over $[C_3][1]$ because the latter has only one N-H unit engaged in hydrogen bonding. Similarly, $[C_3][1]$ takes precedence over $[C_2^3][1]$ (value for W weighted over that of X), and $[C_2][2]$ takes precedence over $[C_2][1]$ (higher Y value used as tiebreaker). Thus, a illustrative descending order of hierarchy would be $[C_3^2,C_3^2][2]$, $[C_3^2,C_3^2][1]$, $[C_3^2,C_3][1]$, $[C_3,C_2][1]$, $[C_2,C_2][1]$, $[C_3^2][1]$, $[C_3][1]$, $[C_2^3][1]$, $[C_2^2][2]$, $[C_2^2][1]$, $[C_2][1]$.

(21) Macrae, C. F.; Bruno, I. J.; Chisholm, J. A.; Edgington, P. R.; McCabe, P.;

Pidcock, E.; Rodriguez-Monge, L.; Taylor, R.; van de Streek, J.; Wood, P. A. *J. Appl. Cryst.* **2008**, *41*, 466-470.

(22) Whuler, A.; Brouty, C.; Spinat, P.; Herpin, P. *Acta Cryst.* **1975**, *B31*, 2069-2076.

(23) Ueda, T.; Bernard, G. M.; McDonald, R.; Wasylishen. R. E. *Solid State Nucl. Magn. Reson*. **2003**, *24*, 163-183.

(24) Nakatsu, K.; *Bull. Chem. Soc. Jpn.* **1962**, *35*, 832-834.

(25) Matsuki, R.; Shiro, M.; Asahi, T.; Asai, H.; *Acta Cryst.* **2001**, *57*, 448-450.

(26) Baidina, I. A.; Filatov, E. Y.; Makotchenko, E. V.; Smolentsev, A. I. *J. Struct. Chem.* **2012**, *53*, 112-118.

(27) Zhang, Z. -J.; Zheng, F. -K.; Fu, M. L.; Guo, G. -C.; Huang, J. -S. *Acta Cryst*. **2005**. *E61*, 89-91.

(28) Altahan, M. A.; Beckett, M. A.; Coles, S. J.; Horton, P. N. *Inorg. Chem*. **2015**, *54*, 412-414.

(29) Yeşilel, O. Z.; Ölmez, H.; Soylu, S. *Trans. Met. Chem*. **2006**, *31*, 396-404.

(30) Wang, C.-C.; Yeh, C.-T.; Cheng, Y.-T.; Chen, I.-H.; Lee, G.-H.; Shih, W.-J.; Sheu, H.-S.; Fedorov, V. E.; *CrystEngComm*, **2012**, *14*, 4637-4643.

(31) One of these carboxylates appears to be protonated in the CIF file, but this is believed to be an artifact of the refinement (similarly, what would logically be a H_2O molecule in the lattice is missing a hydrogen atom).

(32) Nangia, A. *Cryst. Growth Des.* **2006**, *6*, 2-4.

(33) Rius, J.; Gali, S. *Cryst. Struct. Commun.* **1982**, *11*, 829-831.

(34) Hu, Z.; Dang, L,-Q.; Bao, D,-H.; An, Y,-L. *Acta Cryst*. **2006**, *E62*, m2756-m2757.

(35) Loiseau, T.; Serpaggi, F.; Ferey, G. *Z. Kristallogr. New Cryst. St*. **2004**, *219*,

469-470.

(36) Serada, O.; Stoeckli-Evans, H. *Private Communication to the Cambridge Structural Database (CSD)*. **2008**. See (a) http://webcsd.ccdc.cam.ac.uk/display_csd _entry.php?identifier=WOQDUC (b) http://webcsd.ccdc.cam.ac.uk/display_csd_entry .php?identifier=WOQFAK.

(37) Kuroda, R. *Inorg. Chem*. **1991**, *30*, 4954-4959.

(38) Dolomanov, O. V.; Bourhis, L. J.; Gildea, R. J.; Howard, J. A. K.; Puschmann, H. *J. Appl. Cryst.* **2009**, *42*, 339-341.

(39) Nakashima, T.; Mishiro, J.; Ito, M.; Kura, G.; Ikuta, Y.; Matsumoto, N.; Nakajima, K.; Kojima, M. *Inorg. Chem*. **2003**, *42*, 2323-2330.

(40) (a) Yu, J. H.; Wang, Y.; Shi, Z.; Xu, R. R. *Chem. Mater.* **2001**, *13*, 2972-2978.

(41) Wang, Y.; Yu, J. H.; Pan, Q. H.; Du, Y.; Zou, Y. C.; Xu, R. R. *Inorg. Chem.* **2004**, *43*, 559-565.

(42) He, Q. L.; Wang, E. B. *Inorg. Chim. Acta.* **1999**, *295*, 244-247.

(43) Peng, Y.; Li, Y. Z.; Bao, S. S.; Zheng, L. M. *Acta Crystallogr. Sect. C: Cryst. Struct. Commun.* **2004**, *60*, M302-M304.

(44) Sharma, R. P.; Shashni, R.; Singh, A.; Venugopalan, P.; Yu, J.; Guo, Y. A.; Ferretti, V. *J. Mol. Struct.* **2011**, *1006*, 121-127.

(45) Du, Y.; Yu, J. H.; Chen, Y.; Yang, Y. H. *Dalton Trans.* **2009**, 6736-6740.

(46) Lu, Y. K.; Tian, M. M.; Xu, S. G.; Lu, R. Q.; Liu, Y. Q. *Acta Crystallogr. Sect. E: Struct. Rep. Online.* **2011**, *67*, M1776-U1523.

(47) Du, Y.; Yu, J. H.; Wang, Y.; Pan, Q. H.; Zou, Y. C.; Xu, R. R. *J. Solid State Chem.* **2004**, *177*, 3032-3037.

(48) Takamizawa, S.; Akatsuka, T.; Ueda, T. *Angew. Chem. Int. Ed.* **2008**, *47*,

1689-1692; *Angew. Chem.* **2008**, *120*, 1713-1716.

(49) (a) Lungwitz, R.; Spange, S. A. *New. J. Chem*. **2008**, *32*, 392-394. (b) Cláudio, A. F. M.; Swift, L.; Hallett, J. P.; Welton, T.; Coutinho, J. A. P.; Freire, M. G. *Phys*. *Chem*. *Chem*. *Phys*. **2014,** *16*, 6593-6601.

(50) Cai, J. W.; Zhang, Y. F.; Hu, X. P.; Feng, X. L. *Acta Crystallogr. Sect. C: Cryst. Struct. Commun.* **2000**, *56*, 661-663.

(51) Hirai, Y.; Nagao, Y.; Igashira-Kamiyama, A.; Konno, T. *Inorg. Chem.* **2011**, *50*, 2040-2042.

(52) (a) Zarychta, B.; Bujak, M.; Zaleski, J. *Z. Naturforsch. B*. **2004**, *59*, 1029-1034. (b) Tacke, R.; Burschka, C.; Richter, I.; Wagner, B.; Willeke, R. *J. Am. Chem. Soc*. **2000**, *122*, 8480-8485.

(53) (a) Jiang, W.; Sattler, D.; Rissanen, K.; Schalley, C. A. *Org. Lett.* **2011**, *13*, 4502-4505. (b) Bu, X. H.; Feng, P. Y.; Stucky, G. D. *Chem. Mater.* **2000**, *12*, 1505-1507.

(54) Ghosh, S. K.; Lewis, K. G.; Kumar, A.; Gladysz, J. A. *Inorg. Chem.* **2017**, 56, 2304-2320.

(55) Jorge, F. E.; Autschbach, J.; Ziegler, T. *J. Am. Chem. Soc.* **2005**, *127*, 975-985.

(56) Ehnbom, A. work in progress, Texas A&M University.

(57) Sessler, J. L.; Lawrence, C. M.; Jayawickramarajah, J. *Chem. Soc. Rev.* **2007**, *36*, 314-325.

3. SYNTHESES OF FAMILIES OF ENANTIOPURE AND DIASTEREOPURE COBALT CATALYSTS DERIVED FROM TRICATIONS OF THE FORMULA $[Co(NH_2CHArCHArNH_2)_3]^{3+}$†

3.1. Introduction

The rational development of enantioselective catalysis requires well characterized catalyst precursors, a thorough understanding of configurational and conformational equilibria, and in increasing numbers of cases data regarding second coordination sphere phenomena[1] and/or special roles of anions.[2] In recent papers as well as some of the upcoming sections, I and my collaborators have exploited salts of the enantiopure chiral tris(1,2-diamine) cobalt trications $[Co(en)_3]^{3+}$ (en = ethylenediamine),[3,4] $[Co(dpen)_3]^{3+}$ (**1**$^{3+}$; dpen = 1,2-diphenylethylenediamine),[5] and $[Co(en)_2(NH_2CH_2CH((CH_2)_nN(CH_3)_2)NH_2)]^{3+}$ (n = 1-4)[6] as catalysts for enantioselective organic transformations[5,6] or polymerizations.[7] All three families feature cobalt stereocenters, the configurations of which are traditionally designated Λ/Δ.[8] The last two also feature carbon stereocenters (*R*/*S*) in the chelate backbones.

The last two families have proven to be highly successful enantioselective catalysts. The NH units in these systems form strong hydrogen bonds to Lewis basic organic functional groups, which can activate them towards addition reactions.[5] The metal centers, like other octahedral cobalt(III) low spin complexes with nitrogen or oxygen donor ligands, are substitution inert under normal conditions.[9] Hence, none of these transformations involve direct substrate coordination or activation by the metal, as

†Reproduced in part with the permission from Ghosh, S. K.; Lewis, K. G.; Kumar, A.; Gladysz, J. A. *Inorg. Chem.* **2017**, *56*, 2304-2320.

found with so many other transition metal catalysts. Other types of metal containing chiral hydrogen bond donor catalysts are seeing study in other groups, in some cases with outstanding results.[10-12]

In the course of optimizing the catalytic reactions, it became apparent that there were profound counter anion effects. Definitive evidence could be obtained for hydrogen bonding of the NH units to anions both in solution (NMR) and the solid state (crystallography).[5a] In this context, the symmetries of the trications merit note. Both $[Co(en)_3]^{3+}$ and $[Co((S,S)\text{-dpen})_3]^{3+}$ ((*S*, *S*)-**1**$^{3+}$) have formal D_3 symmetry, as illustrated for the latter in Figure 3.1. This entails a C_3 axis, which gives rise to two "C_3 faces" consisting of three synperiplanar NH groups (one from each chelate) on opposite sides of the trication. There are furthermore three C_2 axes in a perpendicular plane, which in turn give rise to three "C_2 faces" comprised of two NH groups (from different chelates). Both types of faces are apparent in Figure 3.1.

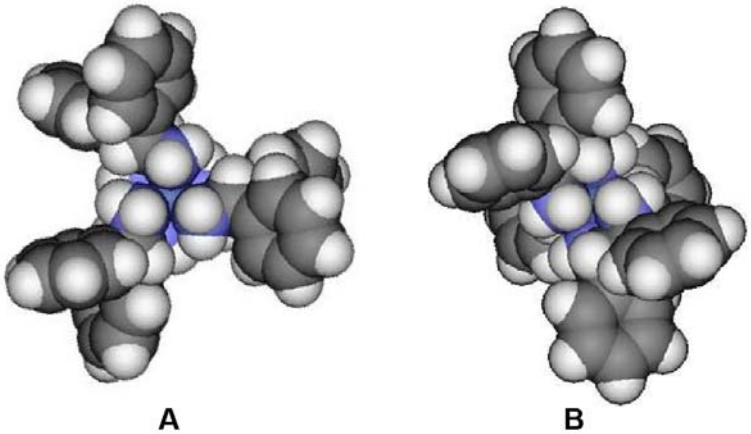

Figure 3.1. Thermal ellipsoid diagram (50% probability level) of the trication of Λ-(*S*,*S*)-**1**$^{3+}$ $3Cl^{-}\cdot 2H_2O\cdot 2CH_3OH$: **A**, view down the idealized C_3 axis; **B**, view down one of the three C_2 axes.[5a]

Hydrogen bonding to counter anions would be expected to be stronger at the C_3 faces, in accord with the greater number of NH groups available.[5a] However, both the C_2 and C_3 faces are competent for substrate binding. As detailed in the following section current evidence suggests that a C_3 face provides the active site for at least some catalytic reactions.[5a] In the examples investigated, a hydrogen bonded anion must first dissociate. One of several open questions is whether anion binding is maintained at the opposite C_3 face.

Unlike many chiral ligands, both enantiomers of dpen are available at modest prices ((*S*,*S*)-dpen, \$408/100 g; (*R*,*R*)-dpen, \$420/100 g).[13] Hence, it is an attractive building block for enantioselective catalysts. However, an obvious strategy for catalyst optimization would involve replacement of the phenyl groups by other aryl moieties. This would allow both electronic and steric properties of the diamine to be fine tuned. For example, electron withdrawing groups normally enhance Brønsted acidities, and should therefore render the NH groups stronger hydrogen bond donors.

In this context, a simple and elegant route to diaryl analogs of dpen has been developed in industry, as outlined in Scheme 3.1.[14] It begins with (*R*,*R*)-bis(*o*-hydroxy)dpen ((*R*,*R*)-**2**), which is relatively inexpensive (\$329/10 g).[15] This is condensed with aromatic aldehydes to yield the di-Schiff bases (*R*,*R*)-**3**. Due to a combination of factors, subsequent [3.3] sigmatropic rearrangements are exothermic, giving (via chair transition states that formally invert configurations) new di-Schiff bases (*S*,*S*)-**4**. Workups then afford the target ligands. As shown in Scheme 3.1 (bottom), the 1,2-diaryldiamines (*S*,*S*)-**5** through (*S*,*S*)-**12** were so prepared. Whereas (*S*,*S*)-**6-9** have been previously synthesized by this protocol,[14] (*S*,*S*)-**5,10-12** are new compounds that are described in the experimental section.

Against this backdrop, I and my collaborators have prepared a variety of salts of

(*S*,*S*)-**1**$^{3+}$ and analogs with the 1,2-diaryldiamine ligands shown in Scheme 3.1. These include "mixed salts" comprised of two different counter anions (2:1) that are of an exceptionally well defined nature. As an alternative to the incremental disclosure of these catalysts over a series of papers, we have combined them into one resource describing all relevant protocols and the most distinctive spectroscopic properties. This furthermore facilitates analysis of the unusual kinetic and thermodynamic diastereoselectivities often encountered in these syntheses – i.e., the dominant cobalt configuration (Λ/Δ) obtained from a given dpen configuration and counter anion set.

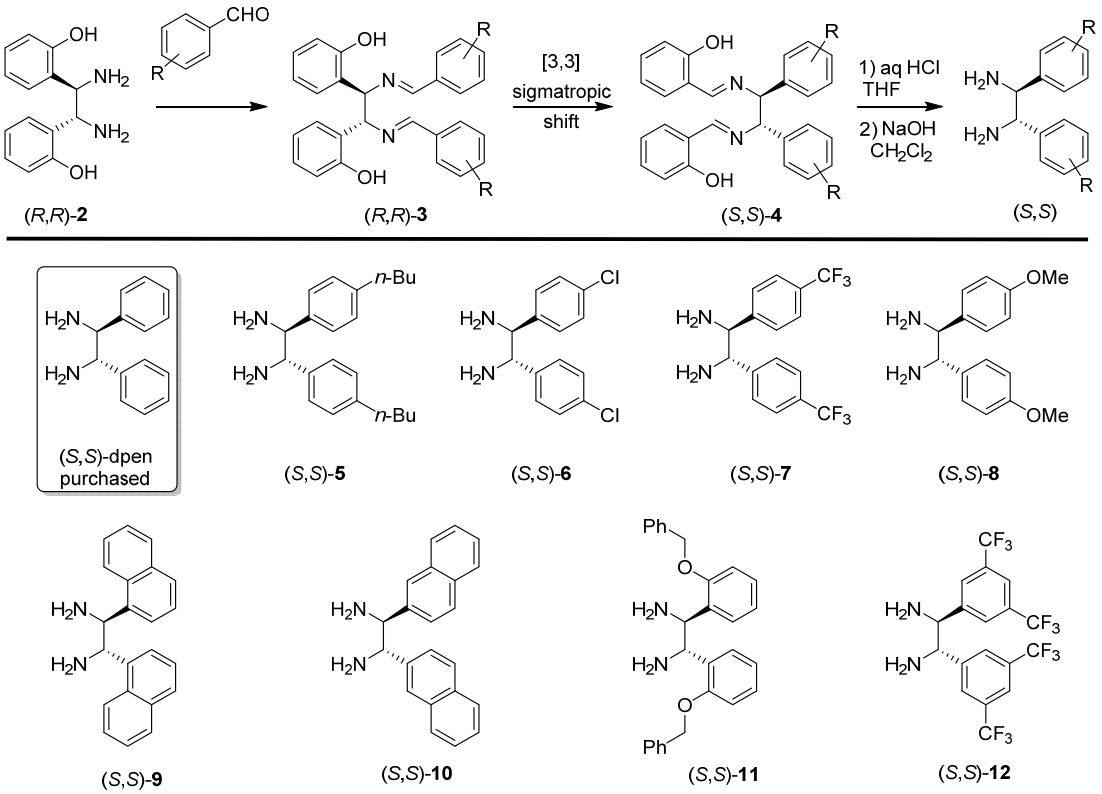

Scheme 3.1. Syntheses of substituted dpen ligands and related species.

3.2. Results

3.2.1. Lipophobic Salts of $[Co((S,S)\text{-dpen})_3]^{3+}$ ((S,S)-$\mathbf{1}^{3+}$).

The first objective was to access salts of the diastereomeric trications Λ- and Δ-(S,S)-$\mathbf{1}^{3+}$ from simple cobalt precursors and (S,S)-dpen.[13] One diastereomer would logically give more enantioselective catalysts than the other. Towards this end, earlier procedures of Bosnich,[16] Mason,[17] and others[18,19] were adapted. These feature substitution labile cobalt(II) educts, aerobic conditions to generate cobalt(III), and charcoal, which promotes the isomerization of cobalt(III) stereocenters.[20] Some of these papers contain incorrect stereochemical assignments,[16,18] which are treated in the discussion section in the interest of aiding readers who may consult these earlier works.

As shown in Scheme 3.2 (step **I**), the acetate complex $Co(OAc)_2 \cdot 4H_2O$ or chloride complex $CoCl_2 \cdot 6H_2O$ and (S,S)-dpen (3.4 equiv) were combined in CH_3OH. The solution was purged with air, and excess HCl was added. This gave a 67/10/23 mixture of the orange trichloride salt Λ-(S,S)-$\mathbf{1}^{3+}$ $3Cl^-$,[16,17] the diastereomer Δ-(S,S)-$\mathbf{1}^{3+}$ $3Cl^-$, and the green bis(dpen) complex *trans*-$[Co((S,S)\text{-dpen})_2(Cl)_2]^+$ Cl^-,[21] as assayed from their easily distinguished **C**HPh ^{13}C NMR signals (δ 63.5/66.1/66.7 ppm, CD_3OD).[22] Workup afforded diastereomerically pure Λ-(S,S)-$\mathbf{1}^{3+}$ $3Cl^-$ in 65% yield.[23]

An analogous procedure was carried out with the perchlorate complex $Co(ClO_4)_2 \cdot 6H_2O$ (Scheme 3.2, step **II**). Now, NMR analysis showed predominantly the opposite diastereomer of the tris(perchlorate) salt, Δ-(S,S)-$\mathbf{1}^{3+}$ $3ClO_4^-$ (8:92 Λ/Δ). Workup afforded a 17:83 Λ/Δ mixture in 60% yield.[24] The minor diastereomer, Λ-(S,S)-$\mathbf{1}^{3+}$ $3ClO_4^-$, could be independently prepared in 64% yield by a room temperature anion metathesis of the trichloride salt Λ-(S,S)-$\mathbf{1}^{3+}$ $3Cl^-$ (step **III**).[22]

When Λ-(S,S)-$\mathbf{1}^{3+}$ $3ClO_4^-$ was heated at 70 °C in CH_3OH in the presence of charcoal (150 h), equilibration to <4:>96 Λ/Δ mixtures gradually occurred (step **IV**),

together with a minor amount of decomposition to an unidentified but easily separable species (16%). Under similar conditions, the 17:83 Λ/Δ mixture gave a <4:>96 Λ/Δ mixture in 99-95% yields (triplicate run). This salt or the 17:83 Λ/Δ mixture could be converted to the trichloride salt Δ-(*S*,*S*)-**1**$^{3+}$ 3Cl^{-} or a 17:83 Λ/Δ mixture in 82-93%

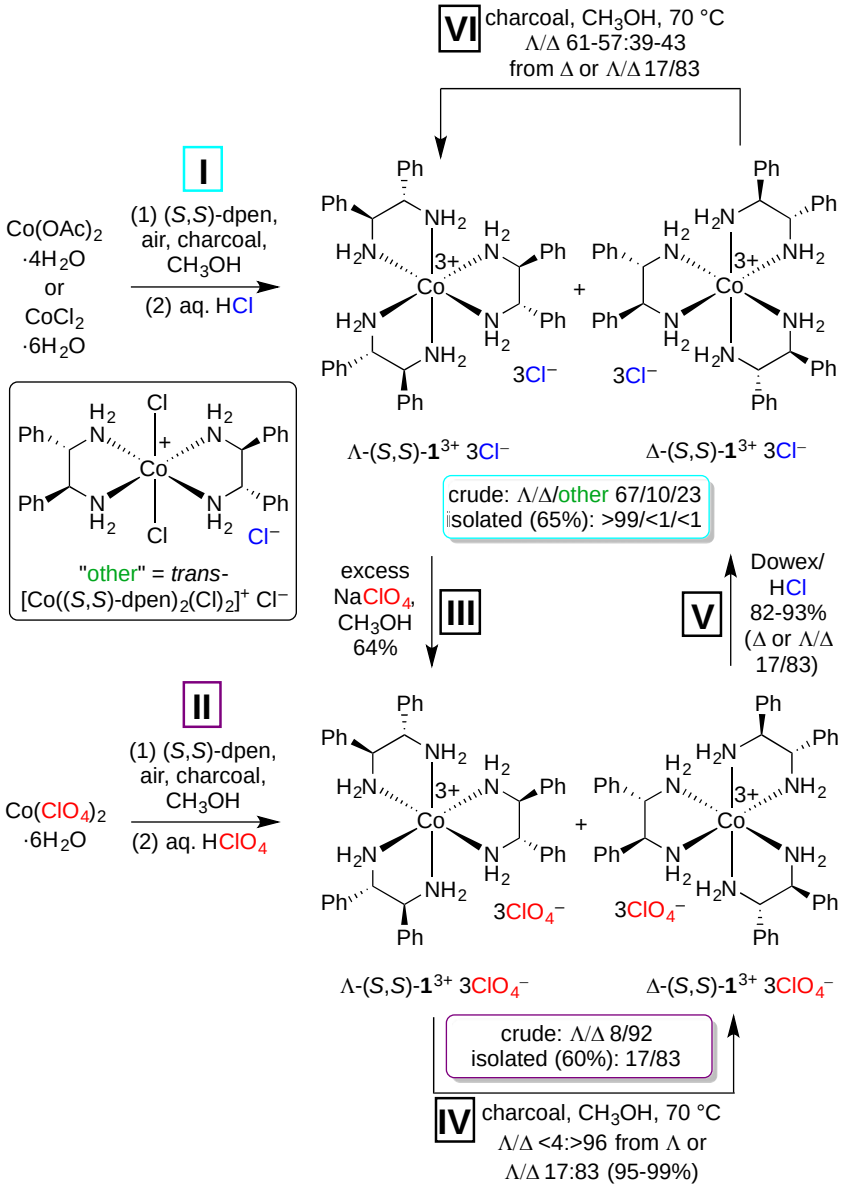

Scheme 3.2. Syntheses of salts of the formula [Co((*S*,*S*)-dpen)$_3$]$^{3+}$ 3X^{-} ((*S*,*S*)-**1**$^{3+}$ 3X^{-}; X = Cl, ClO4); kinetic and thermodynamic Λ/Δ diastereoselectivities.

yields by room temperature anion metatheses (step **V**). When these samples were heated at 70 °C in CH_3OH in the presence of charcoal (step **VI**), equilibration to mixtures enriched in the opposite diastereomer, Λ-(*S*,*S*)-**1**$^{3+}$ 3Cl$^-$, occurred (61:39 to 57: 43). Steps **IV** and **VI** show that the trichloride and tris(perchlorate) salts of (*S*,*S*)-**1**$^{3+}$ exhibit divergent Λ/Δ thermodynamic diastereoselectivities, paralleling the kinetic diastereoselectivities in steps **I** and **II**. This is analyzed further in the discussion section. For now, note that perchlorate is a very poor hydrogen bond acceptor, whereas chloride and acetate (the counter anion prior to anion metathesis when $Co(OAc)_2$ is employed in step **I**) are strong hydrogen bond acceptors.[25] As described elsewhere,[5a] the crystal structures of both trichloride salts Λ- and Δ-(*S*,*S*)-**1**$^{3+}$ 3Cl$^-$ could be determined, and verified the configurations assigned earlier.[17]

The trichloride salts were soluble in polar organic solvents such as DMSO and CH_3OH but insoluble in less polar solvents such as CH_2Cl_2. Unlike the trichloride salts of the tris(ethylenediamine) trication $[Co(en)_3]^{3+}$, they were not soluble in water. As with other new salts described below, they were characterized by NMR (^{1}H, ^{13}C{^{1}H}) and microanalyses, as summarized in the experimental section. The protons of each NH_2 group are diastereotopic, and separate signals were observed as listed in Table 3.1. Some samples underwent slow NH/ND exchange in certain deuterated solvents, so occasionally the integrals were less than the theoretical values.

3.2.2. Lipophilic Salts of (*S*,*S*)-1^{3+}

Less polar complexes were sought to improve solubilities and facilitate catalytic applications in organic media. These were accessed as exemplified for the Λ diastereomers shown in Scheme 3.3. Thus, Λ-(*S*,*S*)-**1**$^{3+}$ 3Cl$^-$ was suspended in CH_2Cl_2 and 1.0-1.2 equiv of the lipophilic tetraarylborate salt Na^+ BAr_f^- was added (BAr_f = $B(3,5\text{-}C_6H_3(CF_3)_2)_4$). The mixture was sonicated, and the solids dissolved as the solvent

turned bright orange. The resulting NaCl precipitated.

Interestingly, the new salt was sufficiently nonpolar to be chromatographed on silica gel (CH_2Cl_2/CH_3OH gradient, 100:0 to 98:2 v/v). This gave the mixed salt Λ-(*S*,*S*)-**1**$^{3+}$ 2Cl$^-$BAr$_f^-$ in 93% yield as an orange solid.[23] Analogous procedures afforded the diastereomer Δ-(*S*,*S*)-**1**$^{3+}$ 2Cl$^-$BAr$_f^-$ (76%) and (using Δ-(*R*,*R*)-**1**$^{3+}$ 3Cl$^-$ or Λ-(*R*,*R*)-**1**$^{3+}$ 3Cl$^-$) the enantiomers Δ-(*R*,*R*)-**1**$^{3+}$ 2Cl$^-$BAr$_f^-$ and Λ-(*R*,*R*)-**1**$^{3+}$ 2Cl$^-$BAr$_f^-$. Mixed salts sometimes have checkered reputations, as they can be confused (in this case for

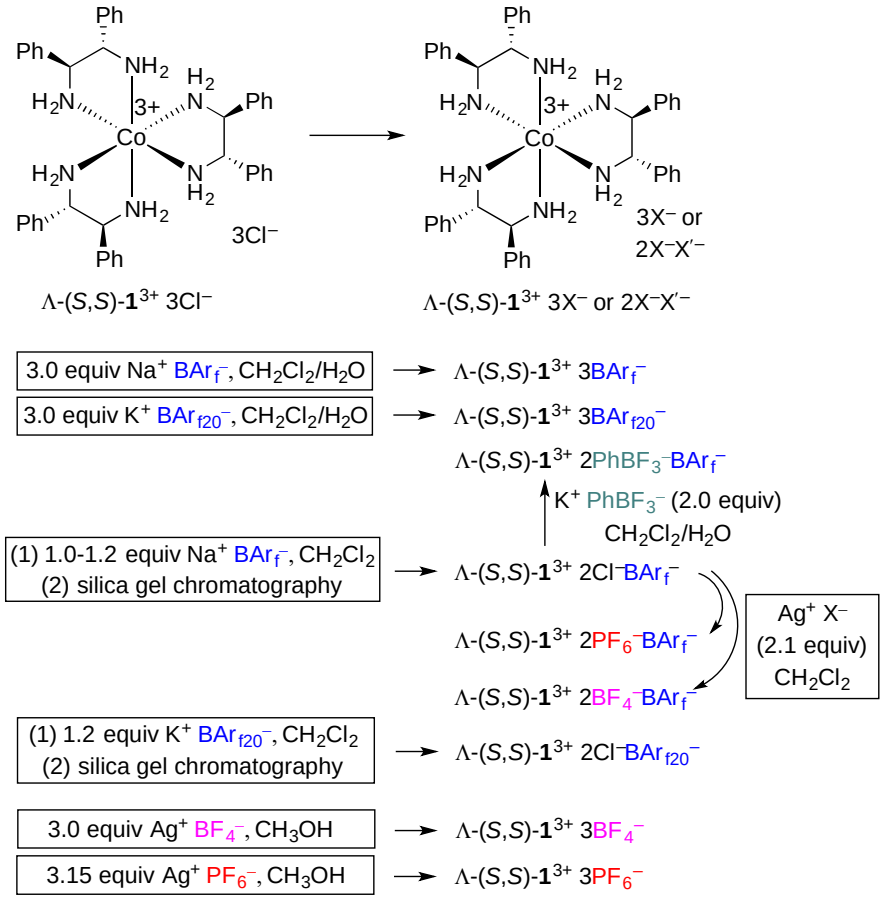

Scheme 3.3. Syntheses of lipophilic Werner salts (yields: 83-96%). The procedures for Δ diastereomers are analogous.

example) with a 2:1 mixture of two *non* mixed salts. In support of my formulation, ^{1}H NMR spectra always exhibited identical integral ratios for the CH protons associated with the trication and the single BAr_f^- anion (6:12).

As shown in Scheme 3.3, a similar procedure was carried out with Λ-(*S*,*S*)-**1**$^{3+}$ 3Cl$^-$ and the slightly less lipophilic tetrakis(pentafluorophenyl)borate salt K^+ $B(C_6F_5)_4^-$ (K^+ BAr_{f20}^-). Chromatography gave the analogous mixed salt Λ-(*S*,*S*)-**1**$^{3+}$ 2Cl$^-$$BAr_{f20}^-$ in 87% yield. In order to expand the range of salts with a single tetraarylborate anion, CH_2Cl_2 solutions of Λ-(*S*,*S*)-**1**$^{3+}$ 2Cl$^-$$BAr_f^-$ were treated with the silver salts Ag^+ BF_4^- and Ag^+ PF_6^-. The silver chloride byproduct was removed by filtration, and workups gave the mixed tetrafluoroborate and hexafluorophosphate salts Λ-(*S*,*S*)-**1**$^{3+}$ 2$BF_4^-$$BAr_f^-$ and Λ-(*S*,*S*)-**1**$^{3+}$ 2$PF_6^-$$BAr_f^-$ in 95-83% yields. Finally, Λ-(*S*,*S*)-**1**$^{3+}$ 2Cl$^-$$BAr_f^-$ was treated with the trifluorophenylborate salt K^+ $PhBF_3^-$ (2.0 equiv) in a biphasic CH_2Cl_2/ H_2O mixture. Workup of the CH_2Cl_2 layer gave the mixed tris(organoborate) salt Λ-(*S*,*S*)-**1**$^{3+}$ 2$PhBF_3^-$$BAr_f^-$ in 96% yield.

Related non-mixed salts were also sought. Thus, as shown in Scheme 3.3, Λ-(*S*,*S*)-**1**$^{3+}$ 3Cl$^-$ was treated with 3.0 equiv of Na^+ BAr_f^- in CH_2Cl_2/H_2O. Workup of the CH_2Cl_2 layer gave the anion exchanged salt Λ-(*S*,*S*)-**1**$^{3+}$ 3BAr_f^- in 94% yield. The pentafluorophenylborate analog Λ-(*S*,*S*)-**1**$^{3+}$ 3BAr_{f20}^- was similarly prepared in 92% yield. Next, Λ-(*S*,*S*)-**1**$^{3+}$ 3Cl$^-$ was treated with 3.0-3.5 equiv of Ag^+ BF_4^- or Ag^+ PF_6^- in CH_3OH. Workups gave Λ-(*S*,*S*)-**1**$^{3+}$ 3BF_4^- or Λ-(*S*,*S*)-**1**$^{3+}$ 3PF_6^- in 93-87% yields. These last two salts were less lipophilic than the others; they remained soluble in acetone, but were only sparingly soluble in CH_2Cl_2.

The Δ diastereomers were similarly synthesized. All of these complexes were orange solids. The ^{1}H NMR chemical shifts of the diastereotopic NHH' protons are summarized in Table 3.1, and the trends interpreted below. The UV-visible spectra of

the representative complexes Λ-(*S*,*S*)-**1**$^{3+}$ 2X^{-}BAr$_f^{-}$ (X = Cl, BF_4, PF_6) and Δ-(*S*,*S*)-**1**$^{3+}$ 2Cl^{-}BAr$_f^{-}$ were determined, and exhibited weak bands at 447-462 nm (λ_{max}, CH_2Cl_2; ε 157-302 M^{-1} cm^{-1}; see experimental section). The data agreed well with earlier reports for Λ- and Δ-(*S*,*S*)-**1**$^{3+}$ 3Cl^{-} (460 nm, CH_3OH; ε 120-125 M^{-1} cm^{-1}).[16]

I sought to probe whether other salts of Δ-(*S*,*S*)-**1**$^{3+}$ with poor hydrogen bond accepting counter anions might, like the tris(perchlorate) salt Δ-(*S*,*S*)-**1**$^{3+}$ 3ClO_4^{-}, be more stable than the corresponding Λ diastereomers. Thus, a sample of Λ-(*S*,*S*)-**1**$^{3+}$ 2BF_4^{-}BAr$_f^{-}$ was kept in DMSO-d_6 at 80 °C and periodically monitored by $^{13}C\{^1H\}$ NMR. As shown in Scheme 3.4, after 1 d a ca. 80:20 mixture of Λ/Δ diastereomers was apparent (δ 61.4/63.2 ppm). After 30 d, epimerization to Δ-(*S*,*S*)-**1**$^{3+}$ 2BF_4^{-}BAr$_f^{-}$ was 88% complete. An analogous experiment conducted in the presence of charcoal gave a 0.2:99.8 Λ/Δ mixture after only 10 h.

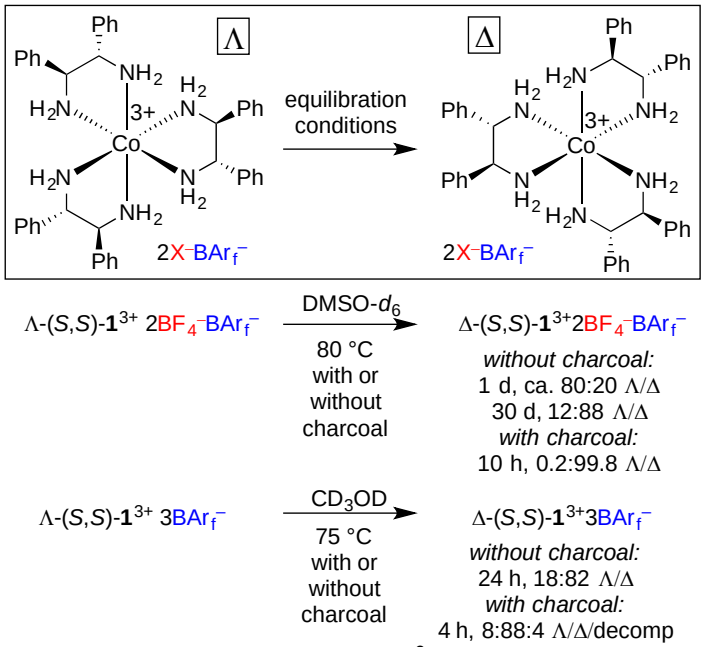

Scheme 3.4. Thermal epimerization of Λ-(*S*,*S*)-**1**$^{3+}$ 2X^{-}BAr$_f^{-}$ to Δ-(*S*,*S*)-**1**$^{3+}$ 2X^{-}BAr$_f^{-}$.

Table 3.1. Selected ^{1}H NMR and hydration data for isolated cobalt(III) salts.

complex	solvent	δ NH/C_3 (ppm)[a]	δ NH'/C_2 (ppm)[a]	number H_2O molecules[b]
Λ-(*S*,*S*)-**1**$^{3+}$ 3Cl$^-$	DMSO-d_6/CD_3OD	6.86	5.31	3/5[c]
Λ-(*S*,*S*)-**1**$^{3+}$ 3ClO_4^-	CD_3OD	-[d]	-[d]	4[e]/12[c]
Δ-(*S*,*S*)-**1**$^{3+}$ 3Cl$^-$	CD_3OD	6.41[f]	5.94	2/6[c]
Δ-(*S*,*S*)-**1**$^{3+}$ 3ClO_4^-	CD_3OD	-[d]	-[d]	[g]/13[c]
Λ-(*S*,*S*)-**1**$^{3+}$ 2Cl$^-$$BAr_f^-$[h]	CD_2Cl_2	8.17	3.86	2/3.5
Λ-(*S*,*S*)-**1**$^{3+}$ 2Cl$^-$$BAr_f^-$[h]	CD_2Cl_2	7.90	4.07	2/3.5
Λ-(*S*,*S*)-**1**$^{3+}$ 2Cl$^-$$BAr_{f20}^-$	acetone-d_6	8.27	5.21	3/3
Λ-(*S*,*S*)-**1**$^{3+}$ 2$BF_4^-$$BAr_f^-$	CD_2Cl_2	6.04	4.17	3/4
Λ-(*S*,*S*)-**1**$^{3+}$ 2$PhBF_3^-$$BAr_f^-$	acetone-d_6	6.33	5.79	2/2
Λ-(*S*,*S*)-**1**$^{3+}$ 2$PF_6^-$$BAr_f^-$	CD_2Cl_2	5.77	4.10	1/1.5
Λ-(*S*,*S*)-**1**$^{3+}$ 3BAr_f^-	acetone-d_6	6.38	6.22	8/12
Λ-(*S*,*S*)-**1**$^{3+}$ 3BAr_f^-	CD_2Cl_2	5.54	4.68	8/11
Λ-(*S*,*S*)-**1**$^{3+}$ 3BAr_{f20}^-	acetone-d_6	6.39	6.20	11/11
Λ-(*S*,*S*)-**1**$^{3+}$ 3BF_4^-	acetone-d_6	5.83 (11 H)[i]		2/3.5
Λ-(*S*,*S*)-**1**$^{3+}$ 3PF_6^-	DMSO-d_6	5.64	5.34	6/6.5
Δ-(*S*,*S*)-**1**$^{3+}$ 2Cl$^-$$BAr_f^-$	acetone-d_6	7.13	6.16[f]	1/4
Δ-(*S*,*S*)-**1**$^{3+}$ 2Cl$^-$$BAr_f^-$	CD_2Cl_2/CH_3OH	6.58	5.35	1[j]
Δ-(*S*,*S*)-**1**$^{3+}$ 2Cl$^-$$BAr_{f20}^-$	CD_2Cl_2/acetone-d_6	6.92	6.01-5.82[k]	3/3
Δ-(*S*,*S*)-**1**$^{3+}$ 2$BF_4^-$$BAr_f^-$	acetone-d_6	6.41	5.90	3/3
Δ-(*S*,*S*)-**1**$^{3+}$ 2$PF_6^-$$BAr_f^-$	acetone-d_6	6.53	5.92	2/8.5
Δ-(*S*,*S*)-**1**$^{3+}$ 3BAr_f^-	acetone-d_6	6.87-6.70[k]	5.93	9/10
Λ-(*S*,*S*)-**13**$^{3+}$ 2Cl$^-$$BAr_f^-$	acetone-d_6	8.16	5.10	1/3.5
Λ-(*S*,*S*)-**14**$^{3+}$ 2Cl$^-$$BAr_f^-$	acetone-d_6	8.25	5.53	2/3.5
Λ-(*S*,*S*)-**14**$^{3+}$ 2$BF_4^-$$BAr_f^-$	acetone-d_6	5.92	3.21	[g]/1
Λ-(*S*,*S*)-**15**$^{3+}$ 2Cl$^-$$BAr_f^-$	acetone-d_6	8.38	5.94	1/3
Λ-(*S*,*S*)-**16**$^{3+}$ 2Cl$^-$$BAr_f^-$	CD_2Cl_2	7.67	4.16	3/5.5
Δ-(*S*,*S*)-**16**$^{3+}$ 2Cl$^-$$BAr_f^-$	CD_2Cl_2/CD_3OD	5.82 (2H)[i]	5.67 (2H)[i]	2/6.5[c]
Δ-(*S*,*S*)-**17**$^{3+}$ 2Cl$^-$$BAr_f^-$	acetone-d_6	9.27	5.70	4/4
Λ-(*S*,*S*)-**17**$^{3+}$ 2Cl$^-$$BAr_f^-$	CD_2Cl_2	9.72	3.65	2/1.5
Λ-(*S*,*S*)-**17**$^{3+}$ 2$BF_4^-$$BAr_f^-$	CD_2Cl_2	6.32	4.04	3/2
Λ-(*S*,*S*)-**18**$^{3+}$ 2Cl$^-$$BAr_f^-$	acetone-d_6	8.60	5.62-5.41[i,l]	4/4
Λ-(*S*,*S*)-**19**$^{3+}$ 2Cl$^-$$BAr_f^-$	acetone-d_6	8.56	5.15	1/3.5
Λ-(*S*,*S*)-**20**$^{3+}$ Cl$^-$2BAr_f^-	acetone-d_6	6.64-6.52[k]	5.86-5.74[k]	3/2.5

[a]All signals are broad singlets unless noted. [b]The number of H_2O molecules based upon fitting of the microanalysis data/^{1}H NMR integration of the OH signal (δ 4.89-1.85 as given in the experimental section). [c]The integration of this ^{1}H NMR signal reflects a combination of CD_3O**H** ("impurity" in the NMR solvent CD_3O**D**) and $\mathbf{H_2O}$. [d]No signal was observed due to NH/ND exchange with the solvent CD_3OD. [e]This value is taken from the preparation of this salt in reference 16. [f]Apparent doublet. [g]Not determined. [h]Two samples; see text and Figure 3.3 for concentration dependences of the N**HH'** chemical shifts. [i]The signal intensity was reduced due to NH/ND exchange with the solvent. [j]The O**H** integration is not meaningful in the presence of the CH_3OH cosolvent. [k]Apparent multiplet. [l]This signal overlaps with the C**H**NHH' signal.

A sample of the tris(tetraarylborate) salt Λ-(*S*,*S*)-**1**$^{3+}$ 3BAr$_f^-$ was kept in CD_3OD at 75 °C. This complex can be viewed as having the least coordinating set of counter anions among the lipophilic salts. Epimerization was somewhat faster, with a 18:82 Λ/Δ mixture after 24 h in the absence of charcoal (δ 64.6/66.5 ppm). However, some decomposition occurred in the presence of charcoal, with a 8:88:4 Λ/Δ/byproduct mixture after 4 h. In any case, the diastereomer stabilities for both salts in Scheme 3.4 – and probably all those in Scheme 3.3 that do not involve chloride anions – parallel those of the tris(perchlorate) salt (*S*,*S*)-**1**$^{3+}$ 3ClO_4^- (Δ > Λ, see experimental section).

3.2.3. Lipophilic Salts of [Co((*S*,*S*)-$NH_2CHArCHArNH_2$)$_3$]$^{3+}$ (Ar ≠ Ph)

As shown in Scheme 3.5, $Co(OAc)_2{\cdot}4H_2O$ or $CoCl_2{\cdot}6H_2O$ and the 1,2-diaryldiamines (*S*,*S*)-**5-11** (see Scheme 3.1) were reacted under conditions similar to those used for (*S*,*S*)-dpen in Scheme 3.2. The resulting crude trichloride salts, (*S*,*S*)-**13-19**$^{3+}$ 3Cl^-, were treated with 1.0-1.2 equiv of Na^+ BAr$_f^-$. Silica gel column chromatography gave the diastereomerically pure mixed salts Λ-(*S*,*S*)-**13-19**$^{3+}$ 2Cl^- BAr$_f^-$ in 39-23% yields.[23] In all of these syntheses, the main objective was to obtain

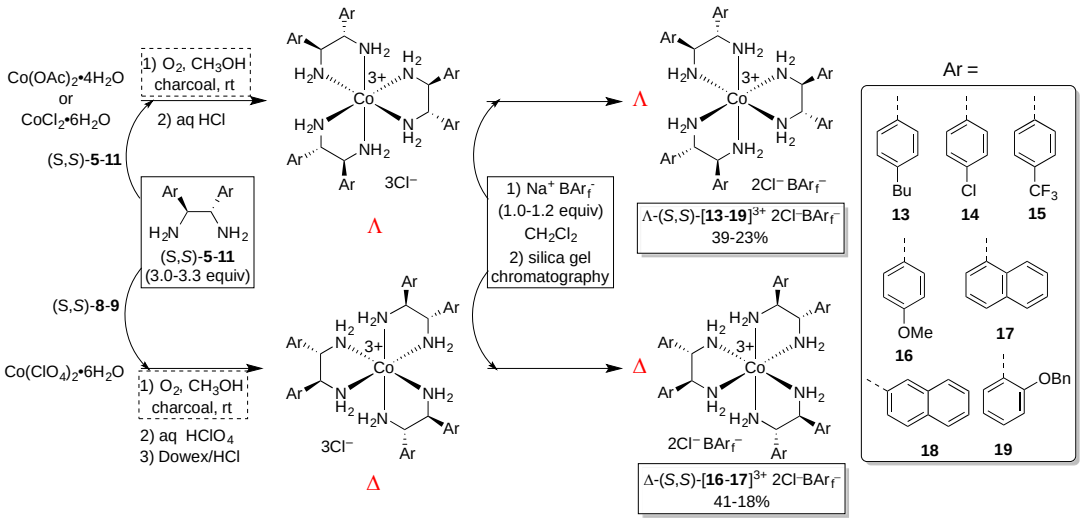

Scheme 3.5. Syntheses of catalysts from substituted (*S*,*S*)-dpen ligands.

samples that could be evaluated as enantioselective catalysts, as opposed to optimizing yields as done in Scheme 3.2. However, the kinetic diastereoselectivities were high (>90:<10 Λ/Δ as assayed by $^{13}C\{^1H\}$ NMR of the trichloride salts).

Reactions of $Co(ClO_4)_2{\cdot}6H_2O$ and (*S*,*S*)-**8**-**9** were conducted under conditions analogous to those of $Co(OAc)_2{\cdot}4H_2O$ or $CoCl_2{\cdot}6H_2O$, followed by anion exchange to give the crude trichloride salts (*S*,*S*)-**16**-**17**$^{3+}$ 3Cl$^-$ (Scheme 3.5). These were treated with 1.0-1.2 equiv of Na^+ BAr_f^-, and silica gel chromatography gave the diastereomerically pure mixed salts Δ-(*S*,*S*)-**16**$^{3+}$ 2Cl$^-$$BAr_f^-$ and Δ-(*S*,*S*)-**17**$^{3+}$ 2Cl$^-$$BAr_f^-$ in 41-18% yields. Again, the kinetic diastereoselectivities were high (>85:<15 Δ/Λ), as assayed by $^{13}C\{^1H\}$ NMR of the trichloride salts.

As shown in Scheme 3.6, the bis(3,5-trifluoromethyl)phenyl substituted diamine (*S*,*S*)-**12** and $Co(OAc)_2{\cdot}4H_2O$ were similarly reacted, and the intermediate trichloride salt was treated with Na^+ BAr_f^- (1.0 equiv). However, a green complex was obtained upon silica gel chromatography, and efforts to purify the trichloride salt gave several products. Apparently the reduced nucleophilicity or basicity of (*S*,*S*)-**12** affects the

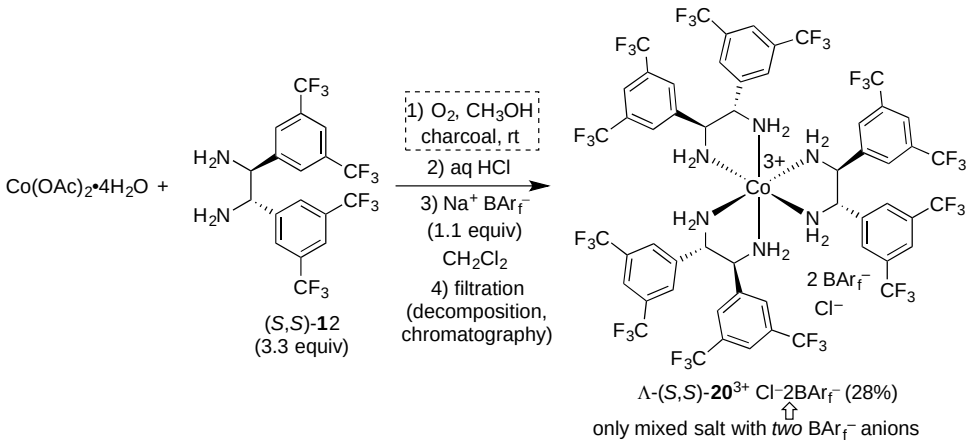

Scheme 3.6. Syntheses of catalysts from a tetrakis(trifluoromethyl) substituted (*S*,*S*)-dpen ligands.

efficiency of the synthesis and/or the product stability. Interestingly, a non-chromatographic workup gave the target trication, but as a different type of mixed salt, with one chloride and *two* tetraarylborate anions, Λ-(*S*,*S*)-**20**$^{3+}$ $Cl^{-}2BAr_f^{-}$ (28%). The trication/BAr_f^{-} ratio was assigned on the basis of the ^{1}H NMR spectrum and micro-analysis.

Most of the salts in Schemes 3.5 and 3.6 were orange, but *p*-methoxyphenyl substituted Λ- and Δ-(*S*,*S*)-**16**$^{3+}$ $2Cl^{-}BAr_f^{-}$ were bright yellow. In procedures analogous to one in Scheme 3.3, Λ-(*S*,*S*)-**14**$^{3+}$ $2Cl^{-}BAr_f^{-}$ and Λ-(*S*,*S*)-**17**$^{3+}$ $2Cl^{-}BAr_f^{-}$ were treated with Ag^{+} BF_4^{-} (2.1-2.2 equiv). Workups gave the mixed bis(tetrafluoroborate)/ tetraarylborate salts Λ-(*S*,*S*)-**14**$^{3+}$ $2BF_4^{-}BAr_f^{-}$ and Λ-(*S*,*S*)-**17**$^{3+}$ $2BF_4^{-}BAr_f^{-}$ in 92-91% yields. The former exhibited the usual orange color, but the latter α-naphthyl substituted salt was red.

3.2.4. Key Properties

As noted above, the NHH' protons in the preceding complexes are diastereotopic, and with a single exception exhibited separate ^{1}H NMR signals, indicative of slow exchange. As summarized in Table 3.1, the Δδ values ranged from 0.20 to greater than 4.00 ppm. This large variance is illustrated by the four spectra in Figure 3.2, all of which were recorded at ambient probe temperature in CD_2Cl_2 with salts of the formula Λ-(*S*,*S*)-**1**$^{3+}$ $2X^{-}BAr_f^{-}$. Due to solubility and other issues, it was necessary to use a range of solvents in Table 3.1.

In Figure 3.2, the anions of the salts are varied from $2Cl^{-}/BAr_f^{-}$ (top spectrum) to $2BF_4^{-}/BAr_f^{-}$ to $2PF_6^{-}/BAr_f^{-}$ to $2BAr_f^{-}/BAr_f^{-}$ ($3BAr_f^{-}$; bottom spectrum). The two chloride ions – which are strong hydrogen bond acceptors – are replaced by progressively weaker and finally extremely poor (BAr_f^{-}) hydrogen bond acceptors.[25] In all cases, the six upfield NH' protons fall into a relatively narrow chemical shift range (δ

3.86-4.68 ppm). In Λ-(*S*,*S*)-**1**$^{3+}$ 2Cl^{-}BAr$_f^{-}$, the other six NH protons are far downfield (δ 8.17 ppm, or Δδ 4.31 ppm). In the other three salts, these shift monotonically upfield (δ 6.04/5.77/5.54 ppm), with the chemical shift difference vs. the other NH protons (NH') progressively narrowing (Δδ 1.87/1.67/0.86 ppm).

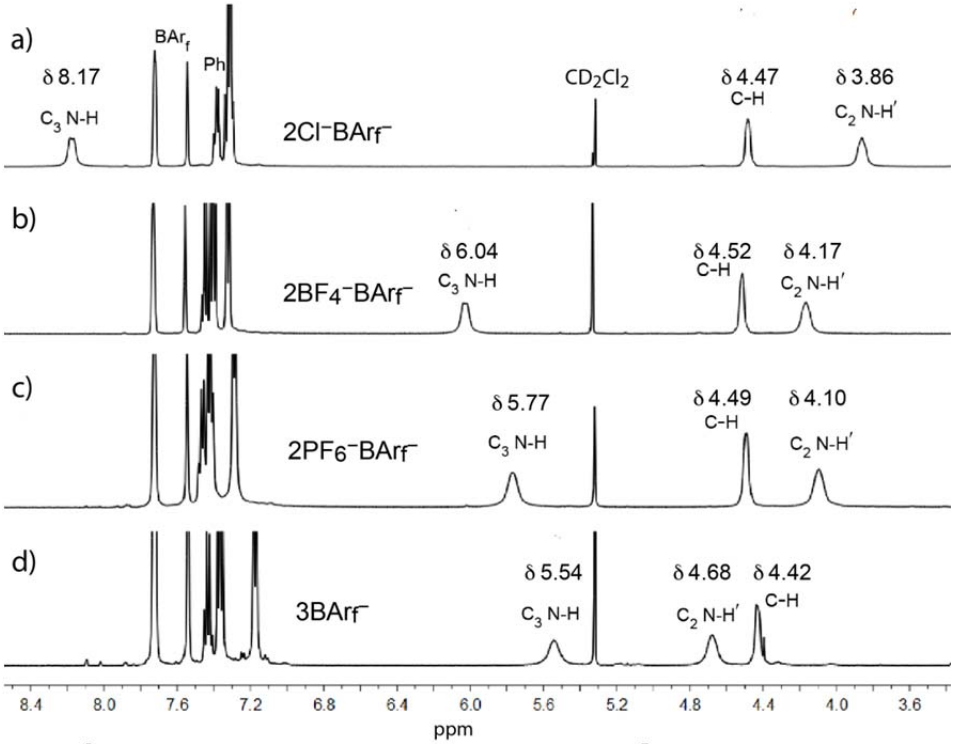

Figure 3.2. ^{1}H NMR spectra (CD_2Cl_2) of (a) Λ-(*S*,*S*)-**1**$^{3+}$ 2Cl^{-}BAr$_f^{-}$, (b) Λ-(*S*,*S*)-**1**$^{3+}$ 2BF$_4^{-}$BAr$_f^{-}$, (c) Λ-(*S*,*S*)-**1**$^{3+}$ 2PF$_6^{-}$BAr$_f^{-}$, and (d) Λ-(*S*,*S*)-**1**$^{3+}$ 3BAr$_f^{-}$.

These data suggest that six of the twelve NH protons are much more predisposed towards hydrogen bonding, and give enthalpically stronger interactions. A model is proposed in the discussion section. Among the other mixed 2Cl^{-}BAr$_f^{-}$ salts in Table 3.1, only the α-naphthyl substituted Λ-(*S*,*S*)-**17**$^{3+}$ 2Cl^{-}BAr$_f^{-}$ showed a distinctly higher Δδ value (6.07 ppm), perhaps due to additional influences arising from the magnetic

anisotropies of the naphthyl moieties. The Δ diastereomers consistently gave much lower Δδ values than the Λ diastereomers. Finally, all of the non-mixed salts, in which all anions have equal hydrogen bond acceptor strengths, gave still lower Δδ values.

The discrete natures of the mixed salts were supported by comproportionation experiments, as exemplified in Scheme 3.7. Here two parts of the trichloride salt Λ-(*S*,*S*)-**1**$^{3+}$ 3Cl^{-} were mixed with one part of the tris(tetraarylborate) salt Λ-(*S*,*S*)-**1**$^{3+}$ 3BAr$_f^{-}$ in CD_2Cl_2 or CH_2Cl_2. The diastereotopic NHH' protons exhibited chemical shifts in good agreement with those of the isolated mixed salt Λ-(*S*,*S*)-**1**$^{3+}$ 2Cl^{-}BAr$_f^{-}$ in Table 3.1 (δ 8.07-7.83/3.95-4.14 ppm vs. 8.17-7.90/ 3.86-4.07).

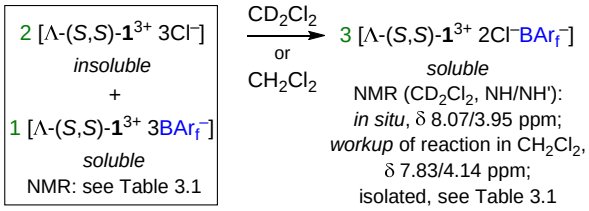

Scheme 3.7. Comproportionation of two salts to give a mixed salt.

The moderate variance of the chemical shifts for the two samples of Λ-(*S*,*S*)-**1**$^{3+}$ 3BAr$_f^{-}$ in Scheme 3.7 and Table 3.1 prompted us to test for a concentration dependence. Accordingly, the ^{1}H NMR spectra of samples that were 0.0043 M, 0.0086 M, 0.017 M, 0.026 M, 0.034 M, 0.043 M, and 0.051 M in CD_2Cl_2 were recorded. The chemical shifts varied linearly but in opposite directions, from δ 8.34 to 7.72 ppm and δ 3.77 to 4.15 ppm as illustrated in Figure 3.3 (see also, Table A-3 in Appendix). Thus, the chemical shift data in Table 3.1 – which simply reflect spectra taken to characterize reaction products without attention to exact concentrations – are likely subject to some variance (although most samples would be 0.02-0.03 M for purposes of recording ^{13}C{^{1}H} NMR

spectra on convenient time scales).[26]

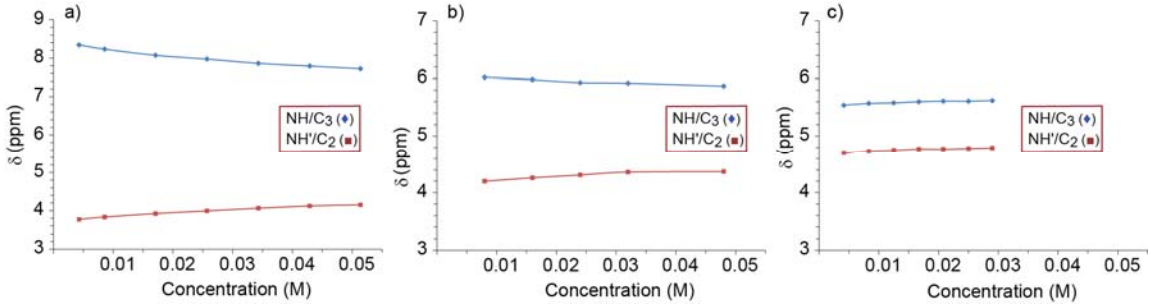

Figure 3.3. Dependence of the chemical shifts of the diastereotopic NHH' protons of (a) Λ-(*S*,*S*)-**1**$^{3+}$ 2Cl^{-}BAr$_f^{-}$, (b) Λ-(*S*,*S*)-**1**$^{3+}$ 2BF$_4^{-}$BAr$_f^{-}$, and (c) Λ-(*S*,*S*)-**1**$^{3+}$ 3BAr$_f^{-}$ upon concentration (CD_2Cl_2, ambient probe temperature).

The hydration levels of the preceding complexes are also summarized in Table 3.1.[23] This represents a nuisance with regard to the precise characterization of these salts, but is a logical consequence of the hydrogen bond donor properties. In any case, reproducibility is quite good. All efforts to date to exhaustively dry any salt (elevated temperatures, high vacuum) have given decomposition. In general, there are fewer water molecules than found with salts of the more polar trication $[Co(en)_3]^{3+}$.[3,6] Within Table 3.1, certain tetraarylborate salts seem to give higher degrees of hydration. It is noted in passing that Na^+ BAr$_f^{-}$ itself is isolated as a hydrate with 2.5-3.0 water molecules.[27]

3.3. Discussion

3.3.1. Hydrogen Bonding

As noted above, a number of properties of the title complexes $[Co(NH_2CHArCHArNH_2)_3]^{3+}$ 2X^{-}X'$^{-}$ appear to be functions of the hydrogen bond acceptor strengths of the counter anions. It is widely appreciated that chloride and acetate anions are excellent hydrogen bond acceptors, and that perchlorate and BAr$_f^{-}$ are

two of the poorest.[25] The trend BF_4^- > PF_6^- is also well established, although both are considered weak acceptors.

The ^{1}H NMR data in Figure 3.2 and Table 3.1 make a persuasive case for strong chloride ion association with six of the twelve NHH' protons in Λ-(*S*,*S*)-**1**$^{3+}$ 2Cl$^-$BAr$_f^-$. As noted in connection with Figure 3.1, every trication Λ-(*S*,*S*)-**1**$^{3+}$ can be viewed as having five general hydrogen bonding sites: two C_3 sites involving three synperiplanar NH groups each, and three C_2 sites involving two NH groups each. One would logically expect the enthalpy of hydrogen bonding to be greater with the three fold donor C_3 sites than the two fold donor C_2 sites. Hence, it is proposed that the two chloride ions preferentially hydrogen bond as shown in **C** in Figure 3.4. This is currently being probed in a detailed computational study.[28]

There are of course alternative motifs. Both chloride ions could hydrogen bond to C_2 sites as shown in **E** (Figure 3.4), but this is likely much less stable. Intermediate would be **D**, with one chloride ion bound to each type of site. Both **D** and **E** would be less likely to give ^{1}H NMR spectra with six downfield NH protons. This model is supported by the crystal structure of the *tri*chloride salt Λ-(*S*,*S*)-**1**$^{3+}$ 3Cl$^-$, which shows

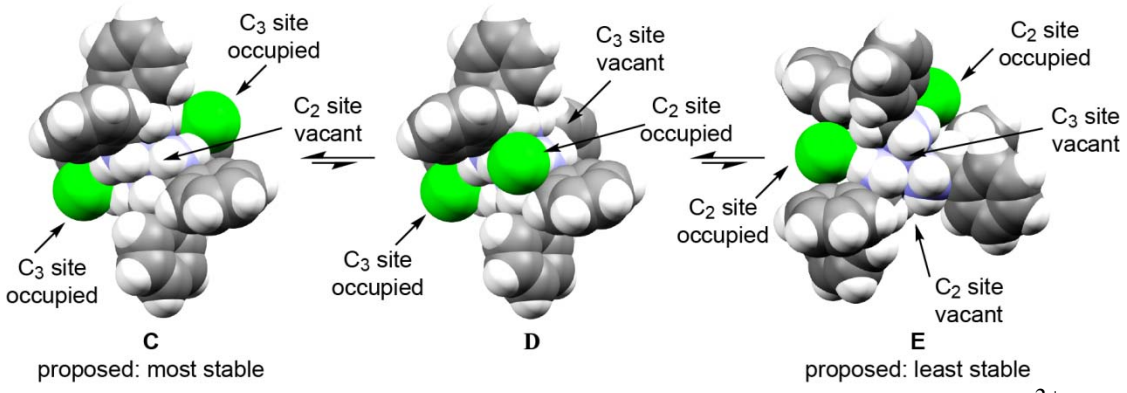

Figure 3.4. Proposed ion pairing equilibria for the two chloride ions of Λ-(*S*,*S*)-**1**$^{3+}$ 2Cl$^-$ X^{t-}; **C**, most stable; **D**, intermediate; **E**, least stable.

hydrogen bonding of the *three* anions to two C_3 sites and one C_2 site (as opposed, for example, to three C_2 sites).[5a] Presumably it is the weaker association of the chloride anion to the C_2 site that facilitates a single anion exchange to give the mixed salts Λ-(*S*,*S*)-**1**$^{3+}$ 2Cl^{-}BAr$_4^{-}$ in Scheme 3.3.

Although it is premature to extrapolate much further, there are other suggestive trends in Table 3.1. For example, the lower δΔ values for the NHH' ^{1}H NMR signals of the opposite diastereomers, Δ-(*S*,*S*)-**1**$^{3+}$ 2X^{-}BAr$_4^{-}$, suggest a lower differential between the hydrogen bonding donor strengths of the C_3 and C_2 sites. This is in accord with the crystal structure of the *tri*chloride salt Δ-(*S*,*S*)-**1**$^{3+}$ 3Cl^{-}, which exhibits a less convergent array of NH bonds at the two C_3 sites.[5a]

3.3.2 Diastereoselectivities

The data in Schemes 3.2-3.5 define a number of diastereoselectivity trends, which may be summarized as follows: (1) $Co(ClO_4)_2$ gives the tris(1,2-diarylethylenediamine) complexes Δ-(*S*,*S*)-**1**$^{3+}$ 3ClO$_4^{-}$ or Δ-[Co((*S*,*S*)-NH$_2$CHArCHArNH$_2$)$_3$]$^{3+}$ 3ClO$_4^{-}$ with high kinetic selectivities; (2) $CoCl_2$ or $Co(OAc)_2$ (after chloride ion metathesis) give the tris(1,2-diarylethylenediamine) complexes Λ-(*S*,*S*)-**1**$^{3+}$ 3Cl^{-} or Λ-[Co((*S*,*S*)-NH$_2$CHArCHArNH$_2$)$_3$]$^{3+}$ 3Cl^{-} with high kinetic selectivities; (3) The thermodynamic Λ/Δ selectivities parallel the kinetic selectivities found in (1) and (2); (4) The thermodynamic stability order established for the tris(perchlorate) salts holds for other salts with three poor hydrogen bond accepting anions (Scheme 3.4).

Since perchlorate is such a feeble hydrogen bond acceptor, my current model is that the stability trend Δ-(*S*,*S*)-**1**$^{3+}$ 3ClO$_4^{-}$ > Λ-(*S*,*S*)-**1**$^{3+}$ 3ClO$_4^{-}$ reflects the intrinsic thermodynamic preference of the trication in the gas phase. This would presumably have some type of stereoelectronic basis. The reversed stability trends with the trichloride or dichloride salts, Λ-(*S*,*S*)-**1**$^{3+}$ 3Cl^{-} > Δ-(*S*,*S*)-**1**$^{3+}$ 3Cl^{-} or Λ-(*S*,*S*)-**1**$^{3+}$ 2Cl^{-}BAr$_f^{-}$ > Δ-

(*S*,*S*)-**1**$^{3+}$ 2Cl^{-}BAr$_f^{-}$ (see experimental section), presumably reflect a greater enthalpy of hydrogen bonding in the Λ diastereomers. Both of these hypotheses are currently being probed computationally.[28]

3.3.3. Earlier Work Relevant to Scheme 3.2

Salts of the trication [Co(dpen)$_3$]$^{3+}$ were first described in 1959 with racemic ligands[19] and then in 1965 with enantiopure ligands.[18a] Subsequently, the latter were more extensively studied by Bosnich[16] and Mason.[17,18b] As noted above, Bosnich reported a synthesis of Δ-[Co((*S*,*S*)-dpen)$_3$]$^{3+}$ 3ClO$_4^{-}$, which he designated (–)-[Co((–)-stien)$_3$]$^{3+}$ 3ClO$_4^{-}$,[21b] similar to that in Scheme 3.2. He also showed the Λ diastereomer, which he designated (+)-[Co((–)-stien)$_3$]$^{3+}$ 3ClO$_4^{-}$,[21b] to be less stable. In both cases, Bosnich correctly assigned the cobalt configurations according to well established circular dichroism relationships, specifying the levorotatory complex as Δ and the dextrorotatory complex as Λ. However, the carbon configurations of the dpen ligands were misassigned.

The misstep involved two structural features common to octahedral complexes of chelate ligands of the formula H$_2$NCHRCHRNH$_2$. First, as more fully analyzed in a recent review,[8] the five membered chelate rings adopt chiral conformations, commonly denoted λ (left handed helix) and δ (right handed helix) as depicted in Figure 3.5. For a given CHR configuration, the conformation that maximizes the occupancy of pseudoequatorial vs. pseudoaxial positions will be favored (**G** >> **F** and **H** >> **I**, Figure 3.5). From these conformations, there are only limited numbers of ways to "build up" octahedral complexes. If all three chelate conformations are identical, there are four possibilities, given by Λ-$\delta\delta\delta$-[Co((*S*,*S*)-dpen)$_3$]$^{3+}$ (**J**), Δ-$\delta\delta\delta$-[Co((*S*,*S*)-dpen)$_3$]$^{3+}$ (**K**), Δ-$\lambda\lambda\lambda$-[Co((*R*,*R*)-dpen)$_3$]$^{3+}$ (**L**), and Λ-$\lambda\lambda\lambda$-[Co((*R*,*R*)-dpen)$_3$]$^{3+}$ (**M**).

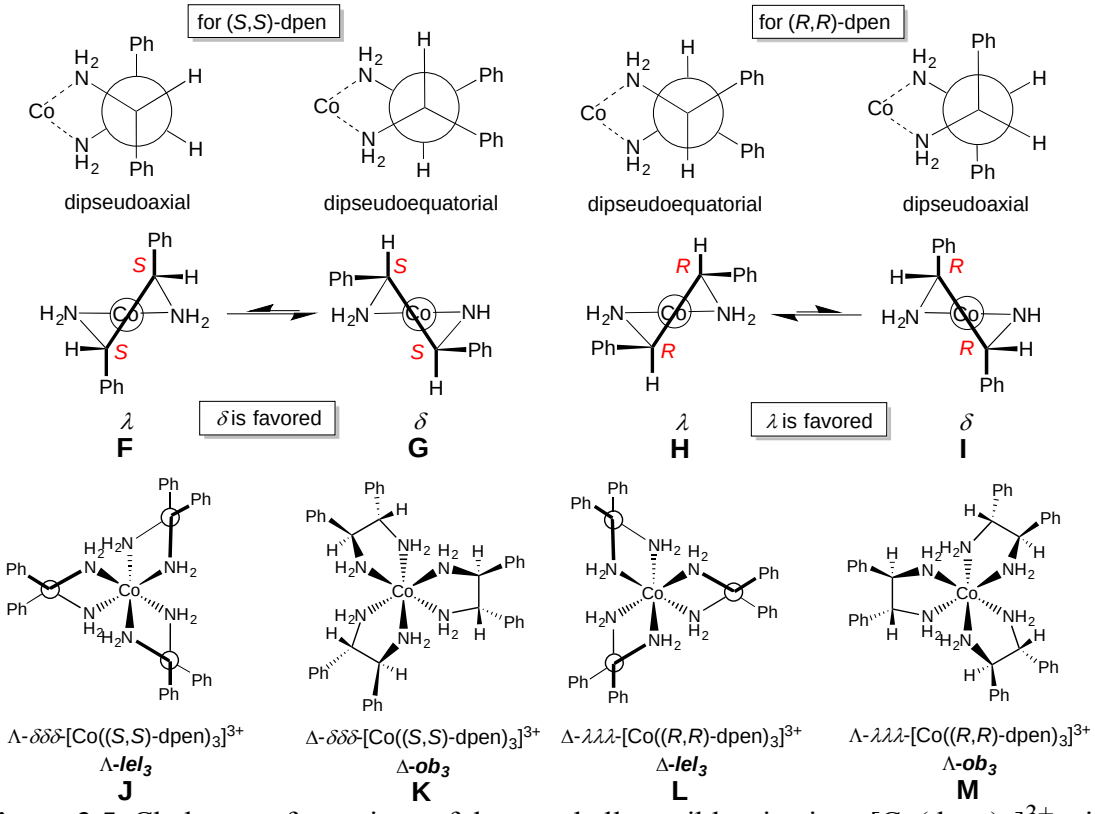

Figure 3.5. Chelate conformations of dpen and all possible trications $[Co(dpen)_3]^{3+}$ with pseudoequatorial phenyl substituents.

In **J** and **L**, the three CHPh-CHPh bonds are parallel to the C_3 axis, which runs perpendicular to the plane of the paper. Such species are said to have "lel_3" orientations. In **K** and **M**, the three CHPh-CHPh bonds are oblique to the C_3 axis. Such species are said to have "ob_3" orientations. For the trications $[Co(en)_3]^{3+}$ and $[Co(trans\text{-chxn})_3]^{3+}$ (chxn = 1,2-cyclohexanediamine), lel_3 orientations were known to be more stable than ob_3 orientations.[29,30] Citing these examples, Bosnich assumed that the (–)-dpen ligands of the more stable Δ diastereomer (–)-$[Co((–)\text{-stien})_3]^{3+}$ $3ClO_4^-$ should also adopt lel_3 orientations. Thus, he paired the Δ diastereomer with an (*R*,*R*)-dpen configuration as in **L**, or Δ-λλλ-$[Co((R,R)\text{-dpen})_3]^{3+}$.

This issue was put to rest when Mason determined the crystal structure and

absolute configuration of (+)-$[Co((–)\text{-dpen})_3]^{3+}$ $3NO_3^-\cdot H_2O$.[17] His data confirmed that the dextrorotatory diastereomer possessed a Λ cobalt configuration (and the levorotatory diastereomer a Δ configuration), and established an *S*,*S* configuration for (–)-dpen (opposite to Bosnich's assignment). Each chelate adopted a *δ* conformation and a *lel* orientation, corresponding to **J**. The trication in Bosnich's complex (–)-$[Co((–)\text{-stien})_3]^{3+}$ $3ClO_4^-$ would then correspond to **K** as opposed to **L**.

3.4. Summary

This study has established efficient and highly diastereoselective syntheses of a variety of enantiopure salts of the title trications, $[Co(NH_2CHArCHArNH_2)_3]^{3+}$. The salts are effective hydrogen bond donors, and are easily rendered lipophobic or lipophilic. Lipophilic salts are usually preferable for catalysis, as reactions can be conducted in solvents such as CH_2Cl_2 or acetonitrile, allowing the organic substrates to interact with the hydrogen bond donor sites without competition from polar, hydrogen bond accepting solvents such as alcohols.

Different aromatic residues can be introduced on the 1,2-diarylethylenediamine ligands essentially "at will" (Scheme 3.1), although multiple electronegative substituents can lead to spurious synthetic results (Scheme 3.6). In future reports from the Gladysz group, salts with chiral anions will be disclosed,[31] and driving forces associated with various equilibria further clarified.[28] In conclusion, an especially broad family of tunable catalysts applicable to a variety of enantioselective organic reactions[5-7] has been developed and stands ready for further empirical or systematic[32] optimization.

3.5. Experimental section

General Data. NMR spectra were recorded on a 500 MHz spectrometer at ambient probe temperature and referenced as follows (δ, ppm): ^{1}H, residual internal $CHCl_3$ (7.26), DMSO-d_5 (2.49), CHD_2OD (3.30), $CDHCl_2$ (5.32), or acetone-d_5 (2.05); ^{13}C, $CDCl_3$, (77.0); DMSO-d_6, (39.5), CD_3OD (49.0), CD_2Cl_2 (54.0), or acetone-d_6 (29.8). IR spectra were recorded on a Shimadzu IRAffinity-1 spectrometer (Pike MIRacle ATR system, diamond/ZnSe crystal). UV-visible spectra were recorded on a Shimadzu UV-1800 UV spectrometer. Melting points were determined using an OptiMelt MPA 100 instrument. Microanalyses were conducted by Atlantic Microlab.

NMR solvents (DMSO-d_6, $CDCl_3$, CD_2Cl_2, acetone-d_6, CD_3OD; Cambridge Isotopes) were stored over molecular sieves. DMSO (Fischer, ACS grade), CH_2Cl_2 (EMD Chemicals, ACS grade), diethyl ether (Fischer, ACS grade), CH_3OH (EMD, anhydrous, 99.8%), THF (EMD Chemicals, ACS grade), and acetone (BDH, ACS grade) were used as received.

(*S*,*S*)-dpen (dpen = 1,2-diphenylethylenediamine, Combi-blocks, 95%), (*R*,*R*)-dpen (Oakwood, 95%), (*R*,*R*)-bis(*o*-hydroxy)dpen ((*R*,*R*)-**2**); Aldrich, 95%), Co(O-Ac)$_2$·4H_2O (Alfa Aesar, 98%) $CoCl_2$·6H_2O (Alfa Aesar, 99.9%), $Co(ClO_4)_2$·6H_2O (Alfa Aesar, reagent grade), HCl (Macron, ACS grade), $HClO_4$ (35%, Macron, ACS grade), NaOH (Macron, ACS grade), Et_3N (Alfa Aesar, 98%), Na^+ BAr_f^- (BAr_f^- = $B(3,5\text{-}C_6H_3(CF_3)_2)_4^-$, Ark Pharm, Inc., 95%), K^+ BAr_{f20}^- (BAr_{f20}^- = $B(C_6F_5)_4^-$, Boulder Scientific Company, 97%), Ag^+ BF_4^- (Aldrich, 98%), Ag^+ PF_6^- (Strem, 99%), K^+ $PhBF_3^-$ (Aldrich, 95%), 4-butylbenzaldehyde (Aldrich, 90%), β-naphthaldehyde (Aldrich, 98%), 2-benzyloxybenzaldehyde (Aldrich, 98%), 3,5-bis(trifluoromethyl)benzaldehyde (TCI, 95%), activated charcoal (Acros, Norit SX 4), DOWEX 50WX2 (200-400 mesh, Aldrich), silica gel (Silicycle SiliaFlash® F60), and Celite 545 (Aldrich) were

used as received.

(*S*,*S*)-H_2NCH(4-C_6H_4*n*-Bu)CH(4-C_6H_4*n*-Bu)NH_2 ((*S*,*S*)-5). A round bottom flask was charged with (*R*,*R*)-**2** (2.42 g, 10.0 mmol) and DMSO (50 mL). Then 4-*n*-butylbenzaldehyde (4.20 mL; 4.05 g, 25.0 mmol) was added with stirring. After 24 h, the mixture was poured into H_2O (100 mL), which was extracted with diethyl ether (3 × 100 mL). The combined extracts were washed with H_2O and dried (Na_2SO_4). The solvent was removed by rotary evaporation and then oil pump vacuum (6 h). The yellow solid was dissolved in CH_3OH (50 mL), and aqueous HCl (3.0 mL, 12.0 M) was added with stirring. After 14 h, the solvent was removed by rotary evaporation, and H_2O (70 mL) was added. Then aqueous NaOH (3.0 M) was added with stirring until the pH reached 11-12. The mixture was extracted with diethyl ether (3 × 80 mL) and the combined extracts were dried (Na_2SO_4). The solvent was removed by rotary evaporation and the residue chromatographed on a silica gel column (4 × 17 cm, 100:0 to 90:10 v/v CH_2Cl_2/ CH_3OH). The solvent was removed from the product containing fractions by rotary evaporation and then oil pump vacuum (12 h) to give **(***S*,*S***)-5** as an off white solid (2.22 g, 6.84 mmol, 68%), mp 46-49 °C (open capillary).

NMR ($CDCl_3$, δ in ppm):[33] ^{1}H (500 MHz) 7.19 (d, $^3J_{HH}$ = 8.5 Hz, 4H, Ar), 7.09 (d, $^3J_{HH}$ = 8.5 Hz, 4H, Ar), 4.08 (s, 2H, C**H**NH_2), 2.57 (t, $^3J_{HH}$ = 8.5 Hz, 4H, ArC**H**$_2$), 1.73 (br s, 4H, N**H**$_2$), 1.61-1.53 and 1.38-1.29 (2 × m, 4H each, $ArCH_2C\mathbf{H}_2C\mathbf{H}_2$), 0.92 (t, $^3J_{HH}$ = 7.4 Hz, 6H, $ArCH_2CH_2CH_2C\mathbf{H}_3$); $^{13}C\{^1H\}$ (125 MHz) 141.6, 140.5, 128.2, 126.7 (4 × s, Ar), 61.4 (s, **C**HNH_2), 35.2, 33.6, 22.3, 13.9 (4 × s, $Ar\mathbf{C}H_2\mathbf{C}H_2\mathbf{C}H_2\mathbf{C}H_3$).

(*S*,*S*)-H_2NCH(β-naphthyl)CH(β-naphthyl)NH_2 ((*S*,*S*)-10). A round bottom flask was charged with (*R*,*R*)-**2** (0.749 g, 3.07 mmol) and DMSO (17 mL). Then β-naphthaldehyde (1.29 g, 8.28 mmol) was added with stirring. After 18 h, the mixture was poured into H_2O (100 mL), which was extracted with diethyl ether (2 × 100 mL). The

combined extracts were washed with H_2O and dried (Na_2SO_4). The solvent was removed by rotary evaporation and then oil pump vacuum (6 h). The yellow solid was dissolved in THF (30 mL), and aqueous HCl (3.0 mL, 12.0 M) was added with stirring. After 1 h, a white precipitate had formed, which was isolated by filtration and washed with diethyl ether. Then H_2O (50 mL) was added, and the sample was washed with CH_2Cl_2. Then aqueous NaOH (3.0 M) was added with stirring until the pH reached 11-12. The mixture was extracted with CH_2Cl_2 (3 × 100 mL) and the combined extracts were dried (Na_2SO_4). The solvent was removed by rotary evaporation and then oil pump vacuum (12 h) to give (*S*,*S*)-**10** as a yellow solid (0.566 g, 1.78 mmol, 58%), mp 139-145 °C (open capillary).

NMR ($CDCl_3$, δ in ppm): ^{1}H (500 MHz) 7.85 (br s, 2H), 7.84-7.79 (m, 5H), 7.78 (s, 1H), 7.50-7.42 (m, 6H), 4.43 (s, 2H, C**H**NH_2), 1.64 (br s, 4H, N**H**$_2$); ^{13}C{^{1}H} (125 MHz) 140.7, 133.3, 132.7, 127.93, 127.87, 127.6, 126.0, 125.6, 125.4, 125.3 (10 × s, **C**$_{10}H_7$), 61.5 (s, **C**HNH_2).

(*S*,*S*)-H_2NCH(2-C_6H_4OBn)CH(2-C_6H_4OBn)NH_2 ((*S*,*S*)-11). A round bottom flask was charged with (*R*,*R*)-**2** (1.73 g, 7.09 mmol) and DMSO (50 mL). Then 2-benzyloxybenzaldehyde (2.69 mL; 3.61 g, 17.02 mmol) was added with stirring. After 18 h, the mixture was poured into H_2O (100 mL), which was extracted with diethyl ether (3 × 70 mL). The combined extracts were washed with H_2O and dried (Na_2SO_4). The solvent was removed by rotary evaporation and then oil pump vacuum (6 h). The yellow solid was dissolved in THF (80 mL) and aqueous HCl (3.0 mL, 12.0 M) was added with stirring. After 12 h, the solvent was removed by rotary evaporation, and H_2O (70 mL) was added. Then aqueous NaOH (3.0 M) was added with stirring until the pH reached 11-12. The mixture was extracted with diethyl ether (2 × 80 mL) and CH_2Cl_2 (80 mL). The combined extracts were dried (Na_2SO_4). The solvent was removed by rotary

evaporation and then oil pump vacuum (12 h) to give (*S*,*S*)-**11** as a sticky yellow solid (1.69 g, 3.99 mmol, 56%).

NMR ($CDCl_3$, δ in ppm): ^1H (500 MHz) 7.37-7.27 (m, 10 H), 7.23 (d, $^3J_{HH}$ = 7.5 Hz, 2H), 7.11-7.05 (m, 2H), 6.81 (t, $^3J_{HH}$ = 7.5 Hz, 2H), 6.75 (d, $^3J_{HH}$ = 7.5 Hz, 2H), 4.88 (d, $^2J_{HH}$ = 7.0 Hz, 2H, 2 × OC**H**H'Ph), 4.80 (d, $^2J_{HH}$ = 7.0 Hz, 2H, 2 × OCH**H**'Ph), 4.57 (s, 2H, C**H**NH_2), 1.83 (br s, 4H, N**H**$_2$); $^{13}C\{^1H\}$ (125 MHz) 155.9, 137.2, 132.2, 128.5, 128.3, 127.7, 127.5, 127.2, 120.5, 111.5 (10 × s, Ar), 69.7 (s, O**C**H_2), 55.7 (s, **C**HNH_2).

(*S*,*S*)-H_2NCH(3,5-$C_6H_3(CF_3)_2$)CH(3,5-$C_6H_3(CF_3)_2$)NH_2 ((*S*,*S*)-12). A round bottom flask was charged with (*R*,*R*)-**2** (2.44 g, 10.0 mmol) and DMSO (50 mL). Then 3,5-bis(trifluoromethyl)benzaldehyde (3.95 mL; 5.81 g, 24.0 mmol) was added with stirring. After 48 h, the mixture was poured into H_2O (100 mL), which was extracted with diethyl ether (3 × 100 mL). The combined extracts were washed with H_2O and dried (Na_2SO_4). The solvent was removed by rotary evaporation and then oil pump vacuum (8 h). The yellow solid was dissolved in THF (80 mL) and aqueous HCl (5.0 mL, 12.0 M) was added with stirring. After 24 h, the solvent was removed by rotary evaporation, and H_2O (100 mL) was added. Then aqueous NaOH (3.0 M) was added with stirring until the pH reached 11-12. The mixture was extracted with diethyl ether (3 × 100 mL). The combined extracts were dried (Na_2SO_4). The solvent was removed by rotary evaporation and the residue chromatographed on a silica gel column (4 × 17 cm, 100:0 to 96:4 v/v CH_2Cl_2/CH_3OH). The solvent was removed from the product containing fractions by rotary evaporation and then oil pump vacuum (12 h) to give **(***S*,*S***)-12** as a brown oil (3.41 g, 7.04 mmol, 70%).

NMR (DMSO-d_6, δ in ppm):[33] ^1H (500 MHz) 7.80 (s, 2H, *p*-Ar), 7.76 (s, 4H, *o*-Ar), 4.19 (s, 2H, C**H**NH_2), 2.25 (br s, 4H, N**H**$_2$); $^{13}C\{^1H\}$ (125 MHz) 147.3 (s, *i*-Ar),

129.2 (q, $^2J_{CF}$ = 32.3 Hz, *m*-Ar), 128.2 (s, *o*-Ar), 123.4 (q, $^1J_{CF}$ = 271.1 Hz, **C**F_3), 119.9 (s, *p*), 61.0 (s, **C**HNH_2).

Λ-[Co((*S*,*S*)-H_2NCH(C_6H_5)CH(C_6H_5)NH_2)$_3$] 3Cl$^-$ (Λ-(*S*,*S*)-1^{3+} 3Cl$^-$). A gas circulating flask[34] was charged with a solution of $Co(OAc)_2{\cdot}4H_2O$ (0.296 g, 1.19 mmol) in CH_3OH (50 mL). Activated charcoal (0.1 g) and (*S*,*S*)-dpen (0.849 g, 4.00 mmol, 3.4 equiv) were added with vigorous stirring. After 17 h, the mixture was filtered through Celite and aqueous HCl (1.5 mL, 12.0 M) was added. The solvent was removed by rotary evaporation to give an orange solid. A portion was dissolved in CD_3OD ($^{13}C\{^1H\}$ NMR: **C**HPh at δ 63.5/66.1/66.7 ppm (67/10/23); Λ-(*S*,*S*)-**1**$^{3+}$ 3Cl$^-$, Δ-(*S*,*S*)-**1**$^{3+}$ 3Cl$^-$, and *trans*-[Co((*S*,*S*)-dpen)$_2$(Cl)$_2$]$^+$ Cl$^-$).[21,35] Then H_2O (100 mL) was added. The suspension was filtered. The filter cake was washed with H_2O (100 mL) and dissolved in CH_3OH. The solvent was removed by rotary evaporation and oil pump vacuum (14 h) to give Λ-(*S*,*S*)-**1**$^{3+}$ 3Cl$^-{\cdot}3H_2O$ as an orange solid (0.662 g, 0.773 mmol, 65%), mp 220-230 °C dec (green liquid; open capillary). The $^{13}C\{^1H\}$ spectrum showed only one **C**HPh signal, indicative of the Λ diastereomer, as confirmed crystallographically.[3a] Anal. Calcd. for $C_{42}H_{48}Cl_3CoN_6{\cdot}3H_2O$ (856.21): C 58.92, H 6.36, N 9.82; found C 58.95, H 6.46, N 9.68.

NMR (10:1 v/v DMSO-d_6/CD_3OD, δ in ppm):[33] ^1H (500 MHz) 7.65-7.42 (m, 12H, Ph), 7.41-7.15 (m, 18H, Ph), 6.86 (br s, 6H, N**H**H'), 5.31 (br s, 6H, NH**H'**), 4.97 (s, 6H, C**H**NH_2), 4.06 (br s, 10H, CD_3O**H**/**H**$_2O$); $^{13}C\{^1H\}$ (125 MHz) 137.3 (s, *i*-Ph), 128.9 and 128.8 (2 s, *o*/*m*-Ph), 128.6 (s, *p*-Ph), 61.8 (s, **C**HNH_2).

Δ-(*S*,*S*)-1^{3+} 3ClO_4^-. *This and the following procedure involve perchlorate salts that are potentially explosive.*[36] *Although they have been carried out repeatedly without mishap, special care and protection are always required when working with perchlorate salts or $HClO_4$ solutions.* A gas circulating flask[34] was charged with a solution of

$Co(ClO_4)_2 \cdot 6H_2O$ (0.261 g, 0.711 mmol) in CH_3OH (50 mL). Activated charcoal (0.1 g) and (*S*,*S*)-dpen (0.505 g, 2.38 mmol, 3.3 equiv) were added with vigorous stirring. After 17 h, the mixture was filtered through Celite, and $HClO_4$ (2.0 mL, 35% in H_2O) was added. The solvent was removed by rotary evaporation to give an orange solid. A portion was dissolved in DMSO-d_6 ($^{13}C\{^1H\}$ NMR: **C**HPh at δ 63.0/61.2 ppm (92/8); Δ- and Λ-(*S*,*S*)-$\mathbf{1}^{3+}$ $3ClO_4^-$). The solid was washed with water and dissolved in CH_3OH. The solvent was removed by rotary evaporation to give crude (*S*,*S*)-$\mathbf{1}^{3+}$ $3ClO_4^-$ as an orange powder (0.422 g, 0.425 mmol, 60%) and an 83:17 Δ/Λ mixture, as assayed by $^{13}C\{^1H\}$ NMR (δ, DMSO-d_6, 63.2/61.4 ppm).[23b,24]

NMR (CD_3OD, δ in ppm; after equilibration to a >96:<4 Δ/Λ mixture as described below): ^1H (500 MHz) 7.41-7.37 (m, 12H, Ph), 7.34-7.30 (m, 18H, Ph), 4.89 (br s, 26H, $CD_3O\mathbf{H}/\mathbf{H}_2O$), 4.52 (s, 6H, C**H**$NH_2$);[37] $^{13}C\{^1H\}$ (125 MHz): 136.5 (s, *i*-Ph), 130.4 (s, *p*-Ph), 130.0 and 129.0 (2 s, *o*/*m*-Ph), 66.5 (s, **C**HNH_2).

Λ-(*S*,*S*)-$\mathbf{1}^{3+}$ $\mathbf{3ClO_4^-}$. A beaker was charged with Λ-(*S*,*S*)-$\mathbf{1}^{3+}$ $3Cl^- \cdot 3H_2O$ (0.502 g, 0.0.586 mmol) and boiling CH_3OH (200 mL). Then $NaClO_4$ (ca. 0.765 g, 6.25 mmol) was added with stirring, followed by warm water (400 mL). The solution was kept at 0 °C. After 7 h, the yellow precipitate was collected, washed with water, dried by oil pump vacuum, and dissolved in a minimum of hot acetone. Ten volumes of ethanol were added. Ether was slowly added, initiating precipitation. More ether was added, and the mixture was kept at 0 °C. After 14 h, the orange solid was collected by filtration and dried by oil pump vacuum to give Λ-(*S*,*S*)-$\mathbf{1}^{3+}$ $3ClO_4^- \cdot 4H_2O$ (0.401 g, 0.376 mmol, 64%).[39]

NMR (CD_3OD, δ in ppm):[33] ^1H (500 MHz) 7.41 (br s, 12H, Ph), 7.35 (br s, 18H, Ph), 4.88 (br s, 24H, $CD_3O\mathbf{H}/\mathbf{H}_2O$), 4.81 (s, 6H, C**H**$NH_2$);[37] $^{13}C\{^1H\}$ (125 MHz) 136.4 (s, *i*-Ph), 130.5 (s, *p*-Ph), 130.3 and 129.7 (2 s, *o*/*m*-Ph), 63.7 (s, **C**HNH_2).

Δ-(*S*,*S*)-$\mathbf{1}^{3+}$ 3Cl⁻. A (*Scheme 3.2, step V with diastereomer mixture*)**.** A beaker was charged with the 83:17 mixture of Δ- and Λ-(*S*,*S*)-$\mathbf{1}^{3+}$ $3ClO_4^-$ obtained above (0.302 g, 0.304 mmol) and CH_3OH (50 mL). The solution was sorbed onto a Dowex cation exchange column (3.0 × 12 cm), which was washed with H_2O/CH_3OH (1:1 v/v, 100 mL) and eluted with increasing concentrations of 12.0 M aqueous HCl in CH_3OH (CH_3OH/HCl 9:1 v/v (100 mL), 8:2 v/v (100 mL), 7:3 v/v (100 mL), 6:4 v/v until product elution). An orange band was collected and the solvents were removed by rotary evaporation (45 °C bath; base trap to scavenge HCl). This gave (*S*,*S*)-$\mathbf{1}^{3+}$ $3Cl^-$ (0.227 g, 0.283 mmol, 93%) as a bright orange solid and a 83:17 Δ/Λ mixture, as assayed by $^{13}C\{^1H\}$ NMR (δ, 63.7/62.0 ppm).[23b] **B** (*Scheme 3.2, step V with Δ diastereomer*)**.** A beaker was charged with Δ-(*S*,*S*)-$\mathbf{1}^{3+}$ $3ClO_4^-$ (0.200 g, 0.202 mmol; see below) and CH_3OH (50 mL). The solution was sorbed onto a Dowex cation exchange column. A workup identical to that in **A** gave Δ-(*S*,*S*)-$\mathbf{1}^{3+}$ $3Cl^-\cdot 2H_2O$ (0.0.139 g, 0.0.166 mmol, 82%) as a bright orange solid, mp 193-197 °C dec (green liquid; open capillary). Anal. Calcd. for $C_{42}H_{48}Cl_3CoN_6\cdot 2H_2O$ (838.19): C 60.18, H 6.25, N 10.03; found C 60.23, H 6.24, N 9.90.

Δ-(*S*,*S*)-$\mathbf{1}^{3+}$ 3Cl⁻. NMR (3:1 v/v DMSO-d_6/CD_3OD, δ in ppm, from route **A**): ^1H (500 MHz) 7.54-7.49 (m, 0.17·12H, Ph), 7.48-7.43 (m, 0.83·12H, Ph), 7.34-7.22 (m, 0.17·18H and 0.83·18H, Ph), 6.77 (br s, 0.17·6H, N**H**H'), 6.53 (d, $^3J_{HH}$ = 11 Hz, 0.83·6H, N**H**H'), 5.43 (br s, 0.83·6H, N**H**H'), 5.32 (br s, 0.17·6H, N**H**H'), 4.96 (s, 0.17·6H, C**H**NH_2), 4.77-4.62 (m, 0.83·6H, C**H**NH_2), 4.06 (br s, 20H, CD_3O**H**/**H**$_2O$); $^{13}C\{^1H\}$ (125 MHz) 137.6 (s, *i*-Ph), 129.2 (s, Ph),[s3] 129.0 (s, Ph), 128.9 (s, Ph), 128.6 (s, Ph), 63.7 (s, **C**HNH_2, 83%), 62.0 (s, **C**HNH_2, 17%).

NMR (CD_3OD, δ in ppm, from **B**):[33] ^1H (500 MHz) 7.46-7.44 (m, 12H, Ph), 7.30 (br s, 18H, Ph), 6.41 (d, 6H, $^3J_{HH}$ = 10 Hz, N**H**H'), 5.94 (bs s, 6H, NH**H'**), 4.88 (br

s, 13H, $CD_3O\mathbf{H}/\mathbf{H}_2O$), 4.58 (d, 6H, $^3J_{HH}$ = 10 Hz, C**H**NH_2); $^{13}C\{^1H\}$ (125 MHz) 137.3 (s, *i*-Ph), 130.2 (s, *p*-Ph), 130.0 and 129.1 (2 s, *o*/*m*-Ph), 66.7 (s, **C**HNH_2).

Epimerization of (*S*,*S*)-$\mathbf{1}^{3+}$ $3X^-$ (Scheme 3.2). A (*Scheme 3.2, step IV with Λ diastereomer*)**.**[40] A 5 mm NMR tube was charged with Λ-(*S*,*S*)-$\mathbf{1}^{3+}$ $3ClO_4^-\cdot 4H_2O$ (0.027 g, 0.025 mmol), activated charcoal (0.005 g), CD_3OD (0.5 mL), and a stir bar, and kept at 70 °C with stirring. The sample was monitored by $^{13}C\{^1H\}$ NMR (stir bar removed prior to each spectrum), which showed the isomerization to Δ-(*S*,*S*)-$\mathbf{1}^{3+}$ $3ClO_4^-$ (δ 63.6 ppm to 66.6 ppm), with a minor byproduct (δ 71.9 ppm) becoming increasingly visible after 24 h. Data (time, ratios): 4 h, 25/75/-, 22 h, 14/86/-, 68 h, 10/76/14, 150 h, 3/81/16). No other signals were evident. **B** (*Scheme 3.2, step IV with Δ diastereomer dominant*)**.** A round bottom flask was charged with (*S*,*S*)-$\mathbf{1}^{3+}$ $3ClO_4^-$ (0.118 g, 0.119 mmol; 83:17 Δ/Λ, see above), CH_3OH (10 mL), and activated charcoal (0.051 g), and fitted with a condenser. The mixture was kept at 70 °C for 48 h, and then filtered through Celite. The solvent was removed by rotary evaporation and dried by oil pump vacuum to give Δ-(*S*,*S*)-$\mathbf{1}^{3+}$ $3ClO_4^-$ (0.114 g, 0.115 mmol, 97% (95-99%, triplicate runs); <4% Λ)[24b] as an orange solid, NMR data for which are given above. **C** (*Scheme 3.2, step VI with diastereomer mixture*)**.** A 5 mm NMR tube was charged with (*S*,*S*)-$\mathbf{1}^{3+}$ $3Cl^-$ (0.030 g, 0.0373 mmol; 17:83 Λ/Δ), activated charcoal (0.0063 g), CD_3OD (0.5 mL), and a stir bar, and kept at 70 °C with stirring. The sample was monitored by $^{13}C\{^1H\}$ NMR as in **A**. This showed gradual isomerization (δ 66.6 ppm to 63.5 ppm). Data (time, Λ/Δ ratios): 18 h, 58/42, 37 h, 61/39). No other signals were evident. **D** (*Scheme 3.2, step VI with Δ diastereomer*)**.** A 5 mm NMR tube was charged with Δ-(*S*,*S*)-$\mathbf{1}^{3+}$ $3Cl^-$ (0.025 g, 0.0311 mmol), activated charcoal (0.0010 g), CD_3OD (0.5 mL), and a stir bar, and kept at 70 °C with stirring. The sample was monitored by $^{13}C\{^1H\}$ NMR as in **A**. This showed gradual isomerization (δ 66.6 ppm to 63.5 ppm). Data (time, Λ/Δ ratios: 24 h, 54/46; 50 h,

57/43). No other signals were evident.

Λ-(*S*,*S*)-1^{3+} 2Cl^{-}BAr$_f^{-}$. A round bottom flask was charged with Λ-(*S*,*S*)-**1**$^{3+}$ 3Cl^{-}·3H$_2$O (0.320 g, 0.374 mmol), CH_2Cl_2 (15 mL) and Na^{+} BAr$_f^{-}$ (0.382 g, 0.431 mmol, 1.2 equiv). The mixture was sonicated (5 min)[41] and filtered. The filtrate was loaded onto a silica gel column (1.9 × 15 cm), which was eluted with CH_2Cl_2/CH_3OH (100:0 to 98:2 v/v). The solvent was removed from the main orange band by rotary evaporation and then oil pump vacuum (14 h) to give Λ-(*S*,*S*)-**1**$^{3+}$ 2Cl^{-}BAr$_f^{-}$·2H$_2$O as an orange solid (0.5802 g, 0.3478 mmol, 93%), mp 116-119 °C dec (open capillary). Anal. Calcd. for $C_{74}H_{60}BCl_2CoF_{24}N_6$·2H$_2$O (1665.95): C 53.35, H 3.87, N 5.04, Cl 4.26; found C 53.50, H 3.82, N 4.84, Cl 3.94. IR (powder film, cm^{-1}): 3039 (m, ν_{NH}), 1609 (m, δ_{NH}), 1354 (s, $\nu_{Ar\text{-}CF_3}$), 1275 (vs, ν_{CF}), 1119 (vs, δ_{CCN}). UV-visible (nm, 1.66 × 10^{-3} M in CH_2Cl_2 (ε, M^{-1} cm^{-1})): 455 (157).

NMR (CD_2Cl_2, δ in ppm):[33] ^{1}H (500 MHz) BAr$_f^{-}$ at 7.73 (s, 8H, *o*), 7.54 (s, 4H, *p*); (*S*,*S*)-dpen ligand at 8.17 (br s, 6H, N**H**H'), 7.40-7.37 (m, 6H, *p*-Ph), 7.34-7.30 (m, 24H, *o*/*m*-Ph), 4.48 (s, 6H, C**H**NH$_2$), 3.86 (br s, 6H, NH**H'**), 2.14 (br s, 7H, **H**$_2$O); ^{13}C{^{1}H} (125 MHz) BAr$_f^{-}$ at 162.3 (q, $^1J_{BC}$ = 49.4 Hz, *i*), 135.4 (s, *o*), 129.4 (q, $^2J_{CF}$ = 31.3 Hz, *m*), 125.2 (q, $^1J_{CF}$ = 271.0 Hz, **C**F$_3$), 118.1 (s, *p*); (*S*,*S*)-dpen ligand at 134.8 (s, *i*-Ph), 131.1 (s, *p*-Ph), 130.6 (s, *o*-Ph), 128.0 (s, *m*-Ph),[38] 63.6 (s, **C**HNH$_2$). See Figure 3.3 for the concentration dependence of the N**HH'** signals.

Λ-(*S*,*S*)-1^{3+} 2Cl^{-}BAr$_{f20}^{-}$. A round bottom flask was charged with Λ-(*S*,*S*)-**1**$^{3+}$ 3Cl^{-}·3H$_2$O (0.602 g, 0.703 mmol), CH_2Cl_2, (25 mL), and K^{+} BAr$_{f20}^{-}$ (0.606 g, 0.843 mmol, 1.2 equiv). The mixture was sonicated (10 min)[41] and filtered. The filtrate was loaded onto a silica gel column (3 × 14 cm), which was eluted with CH_2Cl_2/CH_3OH (100:0 to 97:3 v/v). The solvent was removed from the main orange band by rotary evaporation and then oil pump vacuum (14 h) to give Λ-(*S*,*S*)-**1**$^{3+}$ 2Cl^{-}BAr$_{f20}^{-}$·3H$_2$O as

an orange solid (0.918 g, 0.611 mmol, 87%), mp 138-141 °C dec (open capillary). Anal. Calcd. for $C_{66}H_{48}BCl_2CoF_{20}N_6 \cdot 3H_2O$ (1499.79): C 52.85, H 3.63, N 5.60; found C 52.87, H 3.58, N 5.35.

NMR (acetone-d_6, δ in ppm):[33] ^{1}H (500 MHz) 8.27 (br s, 6H, N**H**H'), 7.54-7.44 (m, 12H, Ph), 7.38-7.25 (m, 18H, Ph), 5.21 (br s, 6H, NH**H'**), 5.14-5.05 (m, 6H, C**H**NH_2), 2.87 (br s, 6H, **H**$_2$O); ^{13}C{^{1}H,^{19}F} (125 MHz) BAr_{f20}^- at 149.0 (s), 139.0 (s), 137.1 (s), 125.0 (q, $^1J_{BC}$ = 50.0 Hz, *i*); (*S*,*S*)-dpen ligand at 137.3 (s, *i*-Ph), 130.01 (s, *p*-Ph), 129.95 and 129.5 (2 s, *o/m*-Ph), 63.5 (s, **C**HNH_2).

Λ-(*S*,*S*)-1^{3+} 2BF$_4^-$BAr$_f^-$. A round bottom flask was charged with a solution of Λ-(*S*,*S*)-**1**$^{3+}$ 2Cl$^-$BAr$_f^-\cdot$2H$_2$O (0.9985 g, 0.599 mmol) in CH_2Cl_2 (4 mL), and Ag^+ BF_4^- (0.2412 g, 1.24 mmol, 2.1 equiv) was added with stirring. The mixture was sonicated (10 min) and filtered through Celite. The solvent was removed from the filtrate by rotary evaporation and then oil pump vacuum (14 h) to give Λ-(*S*,*S*)-**1**$^{3+}$ 2BF$_4^-$BAr$_f^-\cdot$3H$_2$O as a bright orange solid (1.019 g, 0.570 mmol, 95%), mp 140-147 °C dec (open capillary). Anal. Calcd. for $C_{74}H_{60}B_3CoF_{32}N_6 \cdot 3H_2O$ (1786.67): C 49.75, H 3.72, N 4.70; found C 49.94, H 3.69, N 4.52. IR (powder film, cm^{-1}): 3254 (m, ν_{NH}), 1608 (m, δ_{NH}), 1354 (s, $\nu_{Ar\text{-}CF_3}$), 1277 (vs, ν_{CF}), 1121 (vs, δ_{CCN}). UV-visible (nm, 1.67 × 10^{-3} M in CH_2Cl_2 (ε, M^{-1} cm^{-1})): 451 (sh, 231).

NMR (CD_2Cl_2, δ in ppm):[33] ^{1}H (500 MHz) BAr$_f^-$ at 7.73 (s, 8H, *o*), 7.56 (s, 4H, *p*); (*S*,*S*)-dpen ligand at 7.45 (t, $^3J_{HH}$ = 7.0 Hz, 6H, *p*-Ph), 7.40 (t, $^3J_{HH}$ = 7.0 Hz, 12H, *m*-Ph), 7.32 (d, $^3J_{HH}$ = 7.0 Hz, 12H, *o*-Ph), 6.04 (br s, 6H, N**H**H'), 4.52 (s, 6H, C**H**NH_2), 4.17 (br s, 6H, NH**H'**), 2.01 (s, 8H, **H**$_2$O); ^{13}C{^{1}H} (125 MHz) BAr$_f^-$ at 162.2 (q, $^1J_{BC}$ = 48.8 Hz, *i*), 135.3 (s, *o*), 129.4 (q, $^2J_{CF}$ = 27.5 Hz, *m*), 125.1 (q, $^1J_{CF}$ = 271.3 Hz, **C**F_3), 118.1 (s, *p*); (*S*,*S*)-dpen ligand at 133.6 and 131.4 (2 s, *i/p*-Ph), 130.7, (s, *o*-Ph), 127.8 (s, *m*-Ph),[38] 64.5 (s, **C**HNH_2).

Λ-(*S*,*S*)-$\mathbf{1}^{3+}$ $\mathbf{2PF_6^-BAr_f^-}$. A round bottom flask was charged with a solution of Λ-(*S*,*S*)-$\mathbf{1}^{3+}$ $2Cl^-BAr_f^-\cdot 2H_2O$ (0.1200 g, 0.072 mmol) in CH_2Cl_2 (2 mL). A solution of Ag^+ PF_6^- (0.0373 g, 0.148 mmol, 2.1 equiv) in CH_2Cl_2 (2 mL) was added with stirring. A white precipitate immediately formed. The sample was sonicated (1 min) and filtered through Celite. The filtrate was washed with H_2O (2 × 1 mL) and the solvent was removed by rotary evaporation and then oil pump vacuum (5 h) to give Λ-(*S*,*S*)-$\mathbf{1}^{3+}$ $2PF_6^-BAr_f^-\cdot H_2O$ as a bright orange solid (0.1121 g, 0.060 mmol, 83%), which when warmed (open capillary) continually darkened and then liquefied at 160 °C. Anal. Calcd. for $C_{74}H_{60}BCoF_{36}N_6P_2\cdot H_2O$ (1866.96): C 47.61, H 3.35, N 4.50; found C 47.86, 3.49, 4.62. IR (powder film, cm^{-1}): 3287 (m, ν_{NH}), 1609 (m, δ_{NH}), 1354 (s, $\nu_{Ar\text{-}CF_3}$), 1276 (vs, ν_{CF}), 1122 (vs, δ_{CCN}). UV-visible (nm, 1.67×10^{-3} M in CH_2Cl_2 (ε, M^{-1} cm^{-1})): 449 (302).

NMR (CD_2Cl_2, δ in ppm):[33] ^1H (500 MHz) BAr_f^- at 7.73 (s, 8H, *o*), 7.55 (s, 4H, *p*); (*S*,*S*)-dpen ligand at 7.47 (t, $^3J_{HH}$ = 7.0 Hz, 6H, *p*-Ph), 7.42 (t, $^3J_{HH}$ = 7.5 Hz, 12H, *m*-Ph), 7.29 (d, $^3J_{HH}$ = 7.0 Hz, 12H, *o*-Ph), 5.77 (br s, 6H, N**H**H'), 4.49 (s, 6H, C**H**NH_2), 4.10 (br s, 6H, NH**H'**), 2.16 (br s, 3H, $\mathbf{H}_2O$); $^{13}C\{^1H\}$ (125 MHz) BAr_f^- at 162.2 (q, $^1J_{BC}$ = 48.8 Hz, *i*), 135.3 (s, *o*), 129.4 (q, $^2J_{CF}$ = 33.8 Hz, *m*), 125.1 (q, $^1J_{CF}$ = 271.2 Hz, **C**CF_3), 118.1 (s, *p*); (*S*,*S*)-dpen ligand at 133.0 (s, *i*-Ph), 131.9 (s, *p*-Ph), 131.0 (s, *o*-Ph), 127.8 (s, *m*-Ph),[38] 64.0 (s, **C**HNH_2).

Λ-(*S*,*S*)-$\mathbf{1}^{3+}$ $\mathbf{2PhBF_3^-BAr_f^-}$. A beaker was charged with Λ-(*S*,*S*)-$\mathbf{1}^{3+}$ $2Cl^-BAr_f^-\cdot 2H_2O$ (0.166 g, 0.0996 mmol), K^+ $PhBF_3^-$ (0.0367 g, 0.199 mmol, 2.0 equiv), CH_2Cl_2 (15 mL), and H_2O (15 mL). The biphasic mixture was vigorously stirred (10 min) and then allowed to stand. The lower orange CH_2Cl_2 phase was separated. The solvent was removed by rotary evaporation to give Λ-(*S*,*S*)-$\mathbf{1}^{3+}$ $2PhBF_3^-BAr_f^-\cdot 2H_2O$ as a bright orange solid (0.181 g, 0.0960 mmol, 96%), mp 120-134 °C dec (open capillary). Anal.

Calcd. for $C_{86}H_{70}B_3CoF_{30}N_6 \cdot 2H_2O$ (1884.86): C 54.80, H 3.96, N 4.46; found C 55.00, H 4.02, N 4.12.

NMR (acetone-d_6, δ in ppm):[33] ^{1}H (500 MHz) BAr_f^- at 7.80 (s, 24H, *o*), 7.68 (s, 12H, *p*); $PhBF_3^-$ at 7.49-7.44 (m, 4H, Ph), 7.24-7.15 (s, 6H, Ph); (*S*,*S*)-dpen ligand at 7.61-7.51 (m, 12H, Ph), 7.37-7.28 (m, 18H, Ph), 6.33 (br s, 6H, N**H**H'), 5.79 (br s, 6H, NH**H'**), 5.25 (br s, 6H, C**H**NH_2), 2.87 (br s, 4H, $\mathbf{H}_2O$); $^{13}C\{^1H\}$ (125 MHz) BAr_f^- at 162.5 (q, $^1J_{BC}$ = 49.6 Hz, *i*), 135.5 (s, *o*), 130.1 (m, *m*), 125.3 (q, $^1J_{CF}$ = 270.0 Hz, **C**F_3), 118.4 (m, *p*); $PhBF_3^-$ and (*S*,*S*)-dpen ligand at 136.3 (br s), 134.9 (s), 132.1 (s), 130.2 (s), 129.9 (s), 129.7 (s), 127.6 (s), 127.2 (s), 63.9 (s, **C**HNH_2).

Λ-(*S*,*S*)-$\mathbf{1}^{3+}$ 3$\mathbf{BAr_f^-}$. **A**. A beaker was charged with Λ-(*S*,*S*)-$\mathbf{1}^{3+}$ 2$Cl^-BAr_f^-$ $\cdot 2H_2O$ (0.170 g, 0.102 mmol), CH_2Cl_2 (15 mL), Na^+ BAr_f^- (0.188 g, 0.204 mmol, 2.0 equiv), and H_2O (15 mL). The biphasic mixture was vigorously stirred (10 min) and then allowed to stand. The lower orange CH_2Cl_2 phase was separated and the solvent allowed to evaporate in a hood to give Λ-(*S*,*S*)-$\mathbf{1}^{3+}$ 3$BAr_f^-$$\cdot 8H_2O$ as an orange solid (0.336 g, 0.0979 mmol, 96%). **B**. The salt Λ-(*S*,*S*)-$\mathbf{1}^{3+}$ 3$Cl^-$$\cdot 3H_2O$ (0.170 g, 0.199 mmol), CH_2Cl_2 (15 mL), Na^+ BAr_f^- (0.532 g, 0.60 mmol, 3.0 equiv), and H_2O (15 mL) were combined in a procedure analogous to that in **A**. An identical workup gave Λ-(*S*,*S*)-$\mathbf{1}^{3+}$ 3BAr_f^- $\cdot 8H_2O$ as an orange solid (0.644 g, 0.188 mmol, 94%), dec pt 68-98 °C (no melting), which liquefied at 106 °C (open capillary). Anal. Calcd. for $C_{138}H_{84}B_3CoF_{72}N_6 \cdot 8H_2O$ (3429.55): C 48.33, H 2.94, N 2.45; found C 48.16, H 2.90, N 2.40.

NMR (acetone-d_6, δ in ppm):[33] ^{1}H (500 MHz) BAr_f^- at 7.79 (s, 24H, *o*), 7.67 (s, 12H, *p*); (*S*,*S*)-dpen ligand at 7.40-7.37 (m, 6H, *p*-Ph), 7.34-7.30 (m, 24H, *o*/*m*-Ph), 6.38 (br s, 6H, N**H**H'), 6.22 (br s, 6H, NH**H'**), 5.30 (s, 6H, C**H**NH_2), 2.95 (br s, 24H, $\mathbf{H}_2O$); $^{13}C\{^1H\}$ (125 MHz) BAr_f^- at 162.6 (q, $^1J_{BC}$ = 50.0 Hz, *i*), 135.5 (s, *o*), 130.0 (q, $^2J_{CF}$ = 32.5 Hz, *m*), 125.3 (q, $^1J_{CF}$ = 270.0 Hz, **C**F_3), 118.4 (m, *p*); (*S*,*S*)-dpen ligand at 135.5

(s, *i*-Ph), 130.8 (s, *p*-Ph), 130.3 and 129.4 (2 s, *o/m*-Ph), 64.1 (s, **C**HNH$_2$).

^{1}H NMR (500 MHz, CD_2Cl_2, δ in ppm):[33] BAr_f^- at 7.72 (s, 24H, *o*), 7.54 (s, 12H, *p*); (*S*,*S*)-dpen ligand at 7.44 (t, $^3J_{HH}$ = 7.5 Hz, 6H, *p*-Ph), 7.37 and 7.17 (t and d, $^3J_{HH}$ = 7.5 and 7.5 Hz, 12H and 12H, *o*/*m*-Ph), 5.54 (br s, 6H, N**H**H'), 4.68 (br s, 6H, NH**H'**), 4.44 (s, 6H, C**H**NH$_2$), 2.82 (br s, 22H, **H**$_2$O).

Λ-(*S*,*S*)-1^{3+} 3BAr$_{f20}^-$. The salt Λ-(*S*,*S*)-**1**$^{3+}$ 3Cl$^-$·3H$_2$O (0.171 g, 0.199 mmol), CH_2Cl_2 (15 mL), K^+ BAr_{f20}^- (0.431 g, 0.60 mmol, 3.0 equiv), and H_2O (15 mL) were combined in a procedure analogous to those given for Λ-(*S*,*S*)-**1**$^{3+}$ 3BAr_f^-. An identical workup gave Λ-(*S*,*S*)-**1**$^{3+}$ 3BAr_{f20}^-·11H_2O as an orange solid (0.549 g, 0.184 mmol, 92%), mp 84-130 °C (open capillary). Anal. Calcd. for $C_{114}H_{48}B_3CoF_{60}N_6$·11$H_2O$ (2732.91): C 46.71.1, H 2.41, N 2.87; found C 46.80, H 2.35, N 2.72.

NMR (acetone-d_6, δ in ppm):[33] ^{1}H (500 MHz) 7.57-7.44 (m, 12H, Ph), 7.42-7.28 (m, 18H, Ph), 6.39 (br s, 6H, N**H**H'), 6.20 (br s, 6H, NH**H'**), 5.29 (s, 6H, C**H**NH$_2$), 3.08 (br s, 22H, **H**$_2$O); $^{13}C\{^1H,^{19}F\}$ (125 MHz) BAr_{f20}^- at 149.0 (s), 140.0 (m), 138.0 (m), 136.2 (s), 125.0 (q, $^1J_{BC}$ = 50.0 Hz, *i*);[42] (*S*,*S*)-dpen ligand at 135.8 (s, *i*-Ph), 130.8 (s, *p*-Ph), 130.3 (s, *o*-Ph), 129.3 (s, *m*-Ph),[38] 64.2 (s, **C**HNH$_2$).

Λ-(*S*,*S*)-1^{3+} 3BF_4^-. A round bottom flask was charged with a solution of Λ-(*S*,*S*)-**1**$^{3+}$ 3Cl$^-$·3H_2O (0.173 g, 0.202 mmol) in CH_3OH (15 mL) and Ag^+ BF_4^- (0.118 g, 0.606 mmol, 3.0 equiv). The mixture was sonicated (10 min) and filtered through Celite. The solvent was removed from the filtrate by rotary evaporation and then oil pump vacuum (14 h) to give Λ-(*S*,*S*)-**1**$^{3+}$ 3BF_4^-·2H_2O as a bright orange solid (0.185 g, 0.187 mmol, 93%), mp 198-202 °C dec (open capillary). Anal. Calcd. for $C_{42}H_{48}B_3CoF_{12}N_6$·2$H_2O$ (992.24): C 50.84, H 5.28, N 8.47; found C 51.16, H 5.42, N 8.47.

NMR (δ in ppm):[33] ^{1}H (500 MHz, acetone-d_6) 7.57-7.43 (m, 12H, Ph), 7.42-7.23

(m, 18H, Ph), 5.83 (br s, 11H, N**HH'**),[37] 5.18 (s, 6H, C**H**NH_2), 2.87 (s, 7H, $\mathbf{H}_2O$); $^{13}C\{^1H\}$ (125 MHz, CD_3OD): 136.1 (s, *i*-Ph), 130.5 (s, *p*-Ph), 130.2 and 129.6 (2 s, *o/m*-Ph), 63.7 (s, **C**HNH_2).

Λ-(*S*,*S*)-$\mathbf{1}^{3+}$ $\mathbf{3PF_6^-}$. A solution of Λ-(*S*,*S*)-$\mathbf{1}^{3+}$ $3Cl^-\cdot 3H_2O$ (0.255 g, 0.298 mmol) in CH_3OH (15 mL) and Ag^+ PF_6^- (0.237 g, 0.939 mmol, 3.2 equiv) were combined in a procedure analogous to that for Λ-(*S*,*S*)-$\mathbf{1}^{3+}$ $3BF_4^-$. An identical workup gave Λ-(*S*,*S*)-$\mathbf{1}^{3+}$ $3PF_6^-\cdot 6H_2O$ as a bright orange solid (0.321 g, 0.259 mmol, 87%), mp 219-226 °C dec (open capillary). Anal. Calcd. for $C_{42}H_{48}P_3CoF_{18}N_6\cdot 6H_2O$ (1238.77): C 40.72, H 4.88, N 6.78; found C 40.51, H 4.51, N 6.56.

NMR (δ in ppm):[33] ^1H (500 MHz, DMSO-d_6) 7.46 (d, $^3J_{CH}$ = 7.5 Hz, 12H, *o*-Ph), 7.38 (t, $^3J_{CH}$ = 7.5 Hz, 12H, *m*-Ph), 7.32 (t, $^3J_{CH}$ = 7.5 Hz, 6H, *p*-Ph), 5.64 (br s, 6H, N**H**H'), 5.34 (br s, 6H, NH**H'**), 4.82 (s, 6H, C**H**NH_2), 3.33 (s, 13H, $\mathbf{H}_2O$); $^{13}C\{^1H\}$ (125 MHz, 10:1 v/v DMSO-d_6/CH_3OH): 136.7 (s, *i*-Ph), 128.9, 128.8, and 128.6 (3 s, *o/m/p*-Ph), 61.4 (s, **C**HNH_2).

Δ-(*S*,*S*)-$\mathbf{1}^{3+}$ $\mathbf{2Cl^-BAr_f^-}$. A round bottom flask was charged with (*S*,*S*)-$\mathbf{1}^{3+}$ $3Cl^-$ (0.188 g, 0.234 mmol; 83:17 Δ/Λ), CH_2Cl_2 (10 mL), Na^+ BAr_f^- (0.240 g, 0.270 mmol), and CH_3OH (0.10 mL). The mixture was sonicated (5 min)[41] and filtered. The filtrate was loaded onto a silica gel column (1.9 × 14 cm), which was eluted with CH_2Cl_2/CH_3OH (100:0 to 97:3 v/v). Aliquots of the main orange band were collected. These were analyzed by TLC, and combined accordingly. The solvents were removed by rotary evaporation and then oil pump vacuum to give Λ-(*S*,*S*)-$\mathbf{1}^{3+}$ $2Cl^-BAr_f^-\cdot 2H_2O$ (0.0586 g, 0.0352 mmol, 15% (higher R_f); see data above) and Δ-(*S*,*S*)-$\mathbf{1}^{3+}$ $2Cl^-BAr_f^-\cdot H_2O$ as an orange solid (0.2932 g, 0.1779 mmol, 76% (lower R_f)), which when warmed continually darkened and liquefied at 110 °C. Anal. Calcd. for $C_{74}H_{60}BCl_2CoF_{24}N_6\cdot H_2O$ (1647.94): C 53.93, H 3.79, N 5.10, Cl 4.30; found C 53.96, H 4.02, N 4.98,

Cl 4.20. IR (powder film, cm^{-1}): 3068 (m, ν_{NH}), 1608 (m, δ_{NH}), 1574 (m, δ_{NH}), 1354 (s, $\nu_{Ar\text{-}CF_3}$), 1275 (vs, ν_{CF}), 1119 (vs, δ_{CCN}). UV-visible (nm, 1.66×10^{-3} M in CH_2Cl_2 (ε, M^{-1} cm^{-1})): 462 (191).

NMR (0.40:0.001 mL v/v CD_2Cl_2/CH_3OH, δ in ppm):[33] ^1H (500 MHz) BAr_f^- at 7.73 (s, 8H, *o*), 7.55 (s, 4H, *p*); (*S*,*S*)-dpen ligand at 7.30-7.27 (m, 18H, Ph), 7.22-7.19 (t, $^3J_{HH}$ = 7.5 Hz, 12H, Ph), 6.58 (br s, 6H, N**H**H'), 5.35 (br s, 6H, NH**H'**), 4.25 (s, 6H, C**H**NH_2), 2.53 (br s, 14H, CH_3O**H**/$\mathbf{H}_2O$); $^{13}C\{^1H\}$ (125 MHz) BAr_f^- at 162.3 (q, $^1J_{BC}$ = 49.6 Hz, *i*), 135.4 (s, *o*), 129.4 (q, $^2J_{CF}$ = 31.4 Hz, *m*), 125.2 (q, $^1J_{CF}$ = 271.0 Hz, **C**F_3), 118.0 (s, *p*); (*S*,*S*)-dpen ligand at 134.3 (s, *i*-Ph), 130.6 (s, *p*-Ph), 129.9 (s, *o*-Ph), 128.0 (s, *m*-Ph),[38] 66.7 (s, **C**HNH_2).

Δ-(*S*,*S*)-$\mathbf{1}^{3+}$ $\mathbf{2Cl^-BAr_{f20}^-}$. The salt (*S*,*S*)-$\mathbf{1}^{3+}$ $3Cl^-$ (0.510 g, 0.635 mmol; 83:17 Δ/Λ), CH_2Cl_2 (20 mL), K^+ BAr_{f20}^- (0.548 g, 0.762 mmol, 1.2 equiv), and CH_3OH (0.20 mL) were combined in a procedure analogous to that for Λ-(*S*,*S*)-$\mathbf{1}^{3+}$ $2Cl^-BAr_f^-$. An identical workup gave Δ-(*S*,*S*)-$\mathbf{1}^{3+}$ $2Cl^-BAr_{f20}^-\cdot 3H_2O$ (0.664 g, 0.443 mmol, 58% or 84% of theory) as an orange solid, mp 120-123 °C dec (open capillary). Anal. Calcd. for $C_{66}H_{48}BCl_2CoF_{20}N_6\cdot 3H_2O$ (1499.79): C 52.85, H 3.63, N 5.60; found C 53.02, H 3.63, N 5.60.

NMR (δ in ppm):[33] ^1H (500 MHz, 9:1 v/v CD_2Cl_2/acetone-d_6) 7.35-7.24 (m, 18H, Ph), 7.23-7.13 (m, 12H, Ph), 6.92 (br s, 6H, N**H**H'), 6.01-5.82 (m, 6H, NH**H'**), 4.84-4.68 (m, 6H, C**H**NH_2), 2.34 (br s, 6H, $\mathbf{H}_2O$); $^{13}C\{^1H,^{19}F\}$ (125 MHz, 9:1 v/v CD_2Cl_2/CD_3OD) BAr_{f20}^- at 149.1 (d, $^1J_{CF}$ = 133.0 Hz),[42] 137.7 (s), 135.1 (s), 124.4 (q, $^1J_{BC}$ = 50.0 Hz, *i*); (*S*,*S*)-dpen ligand at 135.7 (s, *i*-Ph), 130.1 (s, *p*-Ph), 129.6 (s, *o*-Ph), 127.7 (s, *m*-Ph),[38] 66.5 (s, **C**HNH_2).

Δ-(*S*,*S*)-$\mathbf{1}^{3+}$ $\mathbf{2BF_4^-BAr_f^-}$. A round bottom flask was charged with a solution of Δ-(*S*,*S*)-$\mathbf{1}^{3+}$ $2Cl^-BAr_f^-\cdot 2H_2O$ (0.2400 g, 0.144 mmol) in CH_2Cl_2 (6 mL), and Ag^+ BF_4^-

(0.0589 g, 0.3024 mmol, 2.1 equiv) was added with stirring. The mixture was sonicated (10 min) and filtered through Celite. The solvent was removed from the filtrate by rotary evaporation and then oil pump vacuum (12 h) to give Δ-(*S*,*S*)-$\mathbf{1}^{3+}$ $2BF_4^-BAr_f^-\cdot 3H_2O$ as an orange solid (0.2344 g, 0.133 mmol, 94%), mp 121-124 °C dec (open capillary). Anal. Calcd. for $C_{74}H_{60}B_3CoF_{32}N_6\cdot 3H_2O$ (1786.66): C 49.75, H 3.72, N 4.70; found C 49.99, H 3.71, N 4.39.

NMR (acetone-d_6, δ in ppm):[33] ^{1}H (500 MHz) BAr_f^- at 7.81 (m, 8H, *o*), 7.68 (s, 4H, *p*); (*S*,*S*)-dpen ligand at 7.42 (m, 12H, Ph), 7.32 (m, 18H, Ph), 6.41 (br s, 6H, N**H**H'), 5.90 (br s, 6H, NH**H'**), 5.21 (s, 6H, C**H**NH_2), 3.14 (s, 6H, $\mathbf{H}_2O$); $^{13}C\{^1H\}$ (125 MHz) BAr_f^- at 162.6 (q, $^1J_{BC}$ = 49.6 Hz, *i*), 135.5 (s, *o*), 130.1 (m, *m*), 125.3 (q, $^1J_{CF}$ = 271 Hz, **C**F_3), 118.4 (s, *p*); (*S*,*S*)-dpen ligand at 136.6 (s, *i*-Ph), 130.2 (s, *p*-Ph), 129.9 (s, *o*-Ph), 128.8 (s, *m*-Ph),[38] 65.8 (s, **C**HNH_2).

Δ-(*S*,*S*)-$\mathbf{1}^{3+}$ $\mathbf{2PF_6^-BAr_f^-}$. A solution of Δ-(*S*,*S*)-$\mathbf{1}^{3+}$ $2Cl^-BAr_f^-\cdot 2H_2O$ (0.120 g, 0.072 mmol) in CH_2Cl_2 (4 mL) and a solution of Ag^+ PF_6^- (0.0373 g, 0.148 mmol, 2.1 equiv) in CH_2Cl_2 (2 mL) were combined in a procedure analogous to that for Δ-(*S*,*S*)-$\mathbf{1}^{3+}$ $2BF_4^-BAr_f^-$. An identical workup gave Δ-(*S*,*S*)-$\mathbf{1}^{3+}$ $2PF_6^-BAr_f^-\cdot 2H_2O$ as a bright orange solid (0.1084 g, 0.5356 mmol, 81%), mp 58 °C dec (open capillary). Anal. Calcd. for $C_{74}H_{60}BCoF_{36}N_6P_2\cdot 2H_2O$ (1884.97): C 47.15, H 3.42, N 4.46; found C 47.43, H 3.20, N 4.05.

NMR (acetone-d_6, δ in ppm):[33] ^{1}H (500 MHz) BAr_f^- at 7.79 (m, 8H, *o*), 7.67 (s, 4H, *p*); (*S*,*S*)-dpen ligand at 7.44 (m, 12H, Ph), 7.33 (m, 18H, Ph), 6.53 (br s, 6H, N**H**H'), 5.92 (br s, 6H, NH**H'**), 5.19 (s, 6H, C**H**NH_2), 2.93 (17H, $\mathbf{H}_2O$); $^{13}C\{^1H\}$ (125 MHz) BAr_f^- at 162.6 (q, $^1J_{BC}$ = 49.8 Hz, *i*), 135.6 (s, *o*), 128.9 (m, *m*), 125.4 (q, $^1J_{CF}$ = 271.2 Hz, **C**F_3), 117.5 (m, *p*); (*S*,*S*)-dpen ligand at 136.4 (s, *i*-Ph), 130.4, 130.2, and 130.1 (3s, *o*/*m*/*p*-Ph), 66.0 (s, **C**HNH_2).

Δ-(*S*,*S*)-$\mathbf{1}^{3+}$ 3$\mathbf{BAr_f^-}$. A beaker was charged with Δ-(*S*,*S*)-$\mathbf{1}^{3+}$ 2$Cl^-BAr_f^-\cdot H_2O$ (0.0824 g, 0.050 mmol), Na^+ BAr_f^- (0.0923 g, 0.100 mmol, 2.0 equiv), CH_2Cl_2 (10 mL), and H_2O (10 mL). The biphasic mixture was vigorously stirred (10 min) and then allowed to stand. The lower orange CH_2Cl_2 phase was separated. The solvent allowed to evaporate in a hood to give Δ-(*S*,*S*)-$\mathbf{1}^{3+}$ 3$BAr_f^-\cdot 9H_2O$ as an orange solid (0.158 g, 0.0458 mmol, 92%), which when warmed (open capillary) continually darkened and then liquefied at 90 °C. Anal. Calcd. for $C_{138}H_{84}B_3CoF_{72}N_6\cdot 9H_2O$ (3447.57): C 48.08, H 2.98, N 2.44; found C 48.04, H 2.78, N 2.46.

NMR (acetone-d_6, δ in ppm):[33] ^{1}H (500 MHz) BAr_f^- at 7.80 (s, 24H, *o*), 7.67 (s, 12H, *p*); (*S*,*S*)-dpen ligand at 7.51-7.45 (m, 12H, Ph), 7.43-7.31 (m, 18H, Ph), 6.87-6.70 (m, 6H, N**H**H'), 5.93 (br s, 6H, NH**H'**), 5.31-5.21 (m, 6H, C**H**NH_2), 3.01 (br s, 20H, $\mathbf{H}_2O$); $^{13}C\{^1H\}$ (125 MHz) BAr_f^- at 162.6 (q, $^1J_{BC}$ = 50.0 Hz, *i*), 135.5 (s, *o*), 130.0 (m, *m*), 125.3 (q, $^1J_{CF}$ = 270.0 Hz, $\mathbf{C}F_3$), 118.4 (m, *p*); (*S*,*S*)-dpen ligand at 135.8 (s, *i*-Ph), 130.9 (s, *p*-Ph), 130.3 (s, *o*-Ph), 128.6 (s, *m*-Ph),[38] 65.9 (s, **C**HNH_2).

Comproportionation, Λ-[Co((*S*,*S*)-$\mathbf{1}^{3+}$ 3$\mathbf{BAr_f^-}$ and Λ-[Co((*S*,*S*)-$\mathbf{1}^{3+}$ 3$\mathbf{Cl^-}$ (Scheme 3.7). A. A round bottom flask was charged with a solution of Λ-(*S*,*S*)-$\mathbf{1}^{3+}$ 3$BAr_f^-\cdot 8H_2O$ (0.035 g, 0.0102 mmol) in CD_2Cl_2 (1.0 mL), and Λ-(*S*,*S*)-$\mathbf{1}^{3+}$ 3$Cl^-\cdot 3H_2O$ (0.0175 g, 0.0204 mmol, 2.0 equiv) was added. The heterogeneous mixture was sonicated (2 h). A ^{1}H NMR spectrum of the homogeneous solution showed only Λ-(*S*,*S*)-$\mathbf{1}^{3+}$ 2$Cl^-BAr_f^-$ (CD_2Cl_2, δ in ppm, 500 MHz, key data): 7.83 (d, $^3J_{HH}$ = 5.0 Hz, 6H, N**H**H'), 4.50 (s, 6H, C**H**NH_2), 4.14 (br s, 6H, NH**H'**). **B.** An analogous experiment was conducted with Λ-(*S*,*S*)-$\mathbf{1}^{3+}$ 3$BAr_f^-\cdot 8H_2O$ (0.035 g, 0.0102 mmol), CH_2Cl_2 (8 mL), and Λ-(*S*,*S*)-$\mathbf{1}^{3+}$ 3$Cl^-\cdot 3H_2O$ (0.0175 g, 0.0204 mmol, 2.0 equiv). The solvent was removed by rotary evaporation and oil pump vacuum (8 h) to give Λ-(*S*,*S*)-$\mathbf{1}^{3+}$ 2Cl^- $BAr_f^-\cdot 2H_2O$ as an orange solid (0.048 g, 0.029 mmol, 95%). ^{1}H NMR (CD_2Cl_2, δ in

ppm, 500 MHz, key data): 8.07 (br s, 6H, N**H**H'), 4.46 (s, 6H, C**H**NH_2), 3.95 (br s, 6H, NH**H'**); $^{13}C\{^1H\}$ (CD_2Cl_2, δ in ppm, 125 MHz, key data): 63.3 (s, **C**HNH_2).

Epimerizations (Scheme 3.4). A. A 5 mm NMR tube was charged with Λ-(*S*,*S*)-**1**$^{3+}$ 2$BF_4^-BAr_f^-$ (0.025 g, 0.014 mmol) and DMSO-d_6 (0.5 mL) and kept at 80 °C. The isomerization to Δ-(*S*,*S*)-**1**$^{3+}$ 2$BF_4^-BAr_f^-$ was monitored by $^{13}C\{^1H\}$ NMR (Λ/Δ δ 61.4/63.2 ppm). Data (time, ratios): 1 d, 80/20, 30 d, 12/88. No other signals were evident. **B**. A mixture of Λ-(*S*,*S*)-**1**$^{3+}$ 2$BF_4^-BAr_f^-$ (0.030 g, 0.017 mmol), activated charcoal (0.020 g), and DMSO-d_6 (0.5 mL) was similarly kept at 80 °C. After 10 h, conversion to Δ-(*S*,*S*)-**1**$^{3+}$ 2$BF_4^-BAr_f^-$ was 99.8% complete. No other signals were evident. **C.** A mixture of Λ-(*S*,*S*)-**1**$^{3+}$ 3BAr_{f24}^- (0.034 g, 0.0099 mmol) and CD_3OD (0.5 mL) was similarly kept at 75 °C. After 24 h, a 18:82 Λ/Δ mixture was present ($^{13}C\{^1H\}$ NMR, δ 64.4/66.5 ppm). No other signals were evident. **D**. A mixture of Λ-(*S*,*S*)-**1**$^{3+}$ 3BAr_f^- (0.034 g, 0.0099 mmol), activated charcoal (0.018 g), and CD_3OD (0.5 mL) was similarly kept at 75 °C. After 4 h, a 8:88:4 Λ/Δ/byproduct mixture was present ($^{13}C\{^1H\}$ NMR, δ 64.6/66.5/71.6 ppm). No other signals were evident. **E**. A 5 mm NMR tube was charged with Δ-(*S*,*S*)-**1**$^{3+}$ 2$Cl^-BAr_f^-$ (0.031 g, 0.018 mmol), activated charcoal (0.015 g), and acetone-d_6 (0.7 mL), and kept at 60 °C. The isomerization to Λ-(*S*,*S*)-**1**$^{3+}$ 2Cl^- BAr_f^- was monitored by $^{13}C\{^1H\}$ NMR (Δ/Λ δ 66.0/63.1 ppm). After 12 h, a 24:76 Δ/Λ mixture was present. No other signals were evident. **F**. A mixture of Δ-(*S*,*S*)-**1**$^{3+}$ 2Cl^- BAr_f^- (0.030 g, 0.018 mmol) and acetone-d_6 (0.7 mL) was similarly kept at 60 °C. After 40 h, no detectable isomerization had occurred. **G**. A mixture of Δ-(*S*,*S*)-**1**$^{3+}$ 2$Cl^-BAr_f^-$ (0.030 g, 0.018 mmol), activated charcoal (0.014 g), and CD_3OD (0.7 mL) was similarly kept at 70 °C. After 12 h, a 34:66 Δ/Λ mixture was present ($^{13}C\{^1H\}$ NMR, δ 66.6/63.4 ppm). No other signals were evident. **H.** A mixture of Δ-(*S*,*S*)-**1**$^{3+}$ 2$Cl^-BAr_f^-$ (0.022 g, 0.013 mmol) and DMSO-d_6 (0.5 mL) was similarly kept at 80 °C. No reaction was

observed over 24 h. The mixture was then kept at 110 °C. After 7 h, a 88:9:3 Λ/Δ/by-product mixture was present ($^{13}C\{^1H\}$ NMR, δ 63.2/61.5/60.2 ppm). After 19 h, several additional byproduct peaks appeared (δ 60-65 ppm), and the solution had turned green. **I.** A mixture of Δ-(*S*,*S*)-**1**$^{3+}$ 2Cl$^-$BAr$_f^-$ (0.030 g, 0.018 mmol), activated charcoal (0.015 g), and DMSO-d_6 (0.5 mL) was similarly kept at 85 °C. No reaction was observed over 4 h. The mixture was then kept at 100 °C. After 12 h, several byproduct peaks appeared (δ 61-80 ppm), and the solution had turned green.

Λ-[Co((*S*,*S*)-H$_2$NCH(4-C$_6$H$_4$*n*-Bu)CH(4-C$_6$H$_4$*n*-Bu)NH$_2$)$_3$]$^{3+}$ 2Cl$^-$BAr$_f^-$ (Λ-(*S*,*S*)-13^{3+} 2Cl$^-$BAr$_f^-$). A gas circulating flask[34] was charged with a solution of Co(OAc)$_2$·4H$_2$O (0.179 g, 0.721 mmol) in CH$_3$OH (50 mL). Activated charcoal (0.11 g) and (*S*,*S*)-**5** (0.748 g, 2.31 mmol, 3.2 equiv) were added with vigorous stirring. After 16 h, the mixture was filtered through Celite, and aqueous HCl (2.0 mL, 12.0 M) was added. The solvent was removed by rotary evaporation and H$_2$O/CH$_3$OH (100 mL, 9:1 v/v) was added. The suspension was filtered. The filter cake was washed with H$_2$O (100 mL) and dissolved in CH$_3$OH. The solvent was removed by rotary evaporation and oil pump vacuum (6 h) to give crude Λ-(*S*,*S*)-**13**$^{3+}$ 3Cl$^-$ as an orange solid (0.665 g, 0.585 mmol assuming a pure sample). Then CH$_2$Cl$_2$ (15 mL) and Na$^+$ BAr$_f^-$ (0.622 g, 0.702 mmol, 1.2 equiv) were added. The mixture was sonicated (10 min)[41] and filtered. The filtrate was loaded onto a silica gel column (3.0 × 12 cm), which was eluted with CH$_2$Cl$_2$/CH$_3$OH (100:0 to 98:2 v/v). The solvent was removed from the main orange band by rotary evaporation and oil pump vacuum (14 h) to give Λ-(*S*,*S*)-**13**$^{3+}$ 2Cl$^-$BAr$_f^-$ ·H$_2$O as an orange solid (0.488 g, 0.246 mmol, 34%), mp 125-131 °C dec (open capillary). Anal. Calcd. for C$_{98}$H$_{108}$BCl$_2$CoF$_{24}$N$_6$·H$_2$O (1984.57): C 59.31, H 5.59, N 4.23; found C 59.36, H 5.60, N 4.13.

NMR (acetone-d_6, δ in ppm):[33] ^{1}H (500 MHz) BAr$_f^-$ at 7.79 (s, 8H, *o*), 7.68 (s,

4H, *p*); (*S*,*S*)-**5** ligand at 8.16 (br s, 6H, N**H**H'), 7.38 (d, $^3J_{CH}$ = 8.0 Hz, 12H, Ar), 7.15 (d, $^3J_{CH}$ = 8.5 Hz, 12H, Ar), 5.10 (br s, 6H, NH**H'**), 5.03 (s, 6H, C**H**NH_2), 2.54 (t, $^3J_{HH}$ = 7.5 Hz, 12H, ArC**H**$_2$), 1.58-1.48 and 1.35-1.27 (2 × m, 12H each, $ArCH_2C\mathbf{H}_2C\mathbf{H}_2$), 0.89 (t, $^3J_{HH}$ = 7.5 Hz, 18H, $ArCH_2CH_2CH_2C\mathbf{H}_3$), 2.88 (br s, 7H, $\mathbf{H}_2O$); $^{13}C\{^1H\}$ (125 MHz) BAr_f^- at 162.5 (q, $^1J_{BC}$ = 50 Hz, *i*), 135.5 (s, *o*), 129.9 (m, *m*), 125.3 (q, $^1J_{CF}$ = 270.0 Hz, **C**F_3), 118.4 (m, *p*); (*S*,*S*)-**5** ligand at 144.7 (s, *i*-Ar), 134.8 (s, Ar), 129.8 (s, Ar), 129.4 (s, Ar), 63.2 (s, **C**HNH_2), 35.8, 34.2, 23.0 (3 × s, Ar**C**H_2**C**H_2**C**H_2CH_3), 14.1 (s, $ArCH_2CH_2CH_2\mathbf{C}H_3$).

Λ-[Co((*S*,*S*)-H_2NCH(4-C_6H_4Cl)CH(4-C_6H_4Cl)NH_2)$_3$]$^{3+}$ 2Cl$^-$$BAr_f^-$ (Λ-(*S*,*S*)-14^{3+} 2Cl$^-$$BAr_f^-$). A gas circulating flask[34] was charged with a solution of $Co(OAc)_2{\cdot}4H_2O$ (0.273 g, 1.09 mmol) in CH_3OH (50 mL). Activated charcoal (0.10 g) and (*S*,*S*)-H_2NCH(4-C_6H_4Cl)CH(4-C_6H_4Cl)NH_2 ((*S*,*S*)-**6**;[14] 1.015 g, 3.612 mmol, 3.3 equiv) were added with vigorous stirring. After 16 h, the mixture was filtered through Celite and aqueous HCl (3.0 mL, 12.0 M) was added. The solvent was removed by rotary evaporation, and H_2O (100 mL) was added. The suspension was filtered. The filter cake was washed with H_2O (100 mL) and dissolved in CH_3OH. The solvent was removed by rotary evaporation and oil pump vacuum (12 h) to give crude Λ-(*S*,*S*)-**14**$^{3+}$ 3Cl$^-$ as an orange solid (0.805 g, 0.799 mmol assuming a pure sample). Then CH_2Cl_2 (15 mL) and Na^+ BAr_f^- (0.958 g, 1.04 mmol, 1.3 equiv) were added. The mixture was sonicated (5 min)[41] and filtered. The filtrate was loaded onto a silica gel column (3.0 × 15 cm), which was eluted with CH_2Cl_2/CH_3OH (100:0 to 98:2 v/v). The solvent was removed from the main orange band by rotary evaporation and oil pump vacuum (12 h) to give Λ-(*S*,*S*)-**14**$^{3+}$ 2Cl$^-$$BAr_f^-{\cdot}4H_2O$ as an orange solid (0.795 g, 0.425 mmol, 39%), mp 119-124 °C dec (open capillary). Anal. Calcd. for $C_{74}H_{54}BCl_8CoF_{24}N_6{\cdot}$ $2H_2O$ (1872.62): C 47.46, H 3.12, N 4.49; found C 47.43, H 3.36, N 5.04.

NMR (acetone-d_6, δ in ppm):[33] ^{1}H (500 MHz) BAr_f^- at 7.80 (s, 8H, *o*), 7.68 (s, 4H, *p*); (*S*,*S*)-**6** ligand at 8.25 (br s, 6H, N**H**H'), 7.50 (d, $^3J_{CH}$ = 8 Hz, 12H, Ar), 7.38 (d, $^3J_{CH}$ = 8 Hz, 12H, Ar), 5.53 (br s, 6H, NH**H'**), 5.11 (s, 6H, C**H**NH_2), 3.00 (br s, 7H, $\mathbf{H}_2O$); $^{13}C\{^1H\}$ (125 MHz) BAr_f^- at 162.5 (q, $^1J_{BC}$ = 50 Hz, *i*), 135.5 (s, *o*), 129.8 (q, $^2J_{CF}$ = 25.0 Hz, *m*), 125.3 (q, $^1J_{CF}$ = 270.0 Hz, **C**F_3), 118.4 (m, *p*); (*S*,*S*)-**6** ligand at 135.5 (s, *i*-Ar), 131.3 (s, Ar), 130.2 (s, Ar), 130.02 (s, Ar), 62.7 (s, **C**HNH_2).

Λ-[Co((*S*,*S*)-H_2NCH(4-C_6H_4Cl)CH(4-C_6H_4Cl)NH_2)$_3$]$^{3+}$ 2$BF_4^-$$BAr_f^-$ (Λ-(*S*,*S*)-14^{3+} 2$BF_4^-$$BAr_f^-$). A round bottom flask was charged with a solution of Λ-(*S*,*S*)-**14**$^{3+}$ 2$Cl^-$$BAr_f^-$·2$H_2O$ (0.086 g, 0.046 mmol) in CH_2Cl_2 (8 mL), and Ag^+ BF_4^- (0.0194 g, 0.0997 mmol, 2.2 equiv) was added with stirring. The mixture was sonicated (10 min) and filtered through Celite. The solvent was removed by rotary evaporation and oil pump vacuum (12 h) to give Λ-(*S*,*S*)-**14**$^{3+}$ 2$BF_4^-$$BAr_f^-$·$H_2O$ as a bright orange solid (0.0835 g, 0.0426 mmol, 92%), dec. at 96-128 °C (no melting), liquefies at 132 °C.

NMR (acetone-d_6, δ in ppm):[33] ^{1}H (500 MHz) BAr_f^- at 7.79 (s, 8H, *o*), 7.67 (s, 4H, *p*); (*S*,*S*)-**6** ligand at 7.50 (d, $^3J_{CH}$ = 8 Hz, 12H, Ar), 7.39 (d, $^3J_{CH}$ = 8 Hz, 12H, Ar), 5.92 (br s, 6H, NH**H'**); 5.18 (s, 6H, C**H**NH_2), 3.21 (br s, 8H, N**H**H', $\mathbf{H}_2O$); $^{13}C\{^1H\}$ (125 MHz) BAr_f^- at 162.6 (q, $^1J_{BC}$ = 50 Hz, *i*), 135.2 (s, *o*), 130.1 (s, *m*), 125.4 (q, $^1J_{CF}$ = 270.0 Hz, **C**F_3), 118.4 (m, *p*); (*S*,*S*)-**6** ligand at 135.7 (s, *i*-Ar), 135.5 (s, Ar), 131.4 (s, Ar), 130.1 (s, Ar), 62.8 (s, **C**HNH_2).

Λ-[Co((*S*,*S*)-H_2NCH(4-$C_6H_4CF_3$)CH(4-$C_6H_4CF_3$)NH_2)$_3$]$^{3+}$ 2$Cl^-$$BAr_f^-$ (Λ-(*S*,*S*)-15^{3+} 2$Cl^-$$BAr_f^-$). A gas circulating flask[34] was charged with a solution of $Co(OAc)_2$·4H_2O (0.933 g, 3.75 mmol) in CH_3OH (50 mL). Activated charcoal (0.150 g) and (*S*,*S*)-H_2NCH(4-$C_6H_4CF_3$)CH(4-$C_6H_4CF_3$)NH_2 ((*S*,*S*)-**7**;[14] 4.308 g, 12.38 mmol, 3.3 equiv) were added with vigorous stirring. After 24 h, the mixture was filtered through Celite, and aqueous HCl (5.0 mL, 12.0 M) was added. The solvent was removed

by rotary evaporation, and H_2O/CH_3OH (100 mL, 85:15 v/v) was added. The suspension was filtered. The filter cake was washed with H_2O/CH_3OH (100 mL, 80:20 v/v) and dissolved in CH_3OH. The solvent was removed by rotary evaporation and oil pump vacuum (12 h) to give crude Λ-(*S*,*S*)-**15**$^{3+}$ 3Cl$^-$ (2.158 g, 1.78 mmol assuming a pure sample) as a dark brown solid (NMR data: see SI). A portion (0.638 g, 0.527 mmol) was suspended in CH_2Cl_2 (20 mL) and Na^+ BAr_f^- (0.518 g, 0.582 mmol, 1.1 equiv) was added. The mixture was sonicated (10 min)[41] and filtered. The filtrate was loaded onto a silica gel column (1.9 × 15 cm), which was eluted with CH_2Cl_2/CH_3OH (100:0 to 98:2 v/v). The solvent was removed from the main orange band by rotary evaporation and oil pump vacuum (14 h) to give Λ-(*S*,*S*)-**15**$^{3+}$ 2Cl$^-$$BAr_f^-$·$H_2O$ as an orange solid (0.953 g, 0.464 mmol, 42%), mp 100-104 °C dec (open capillary). Anal. Calcd. for $C_{80}H_{54}BCl_2CoF_{42}N_6 \cdot H_2O$ (2055.92): C 46.74, H 2.75, N 4.09; found C 46.93, H 2.87, N 4.30.

NMR (acetone-d_6, δ in ppm):[33] ^{1}H (500 MHz) 8.38 (br s, 6H, N**H**H'), 7.82-7.65 (m, 12H BAr_f^- and 24H C_6H_4), 5.94 (br s, 6H, NH**H**'), 5.36 (s, 6H, C**H**NH_2), 3.07 (br s, 6H, **H**$_2$O); ^{13}C{^{1}H} (125 MHz) BAr_f^- at 162.5 (q, $^1J_{BC}$ = 50 Hz, *i*), 135.5 (s, *o*), 130.0 (m, *m*), 125.3 (q, $^1J_{CF}$ = 270.0 Hz, **C**F_3), 118.4 (m, *p*); (*S*,*S*)-**7** ligand at 140.8 (s, *i*-Ar), 131.6 (q, $^2J_{CF}$ = 32.5 Hz, Ar), 130.5 (s, Ar), 127.0 (s, Ar), 124.8 (q, $^1J_{CF}$ = 270.9 Hz, **C**F_3), 62.7 (s, **C**HNH_2).

Λ-[Co((*S*,*S*)-H_2NCH(4-$C_6H_4OCH_3$)CH(4-$C_6H_4OCH_3$)NH_2)$_3$]$^{3+}$ 2Cl$^-$$BAr_f^-$ (Λ-(*S*,*S*)-16^{3+} 2Cl$^-$$BAr_f^-$). A gas circulating flask[34] was charged with a solution of $Co(OAc)_2 \cdot 4H_2O$ (0.166 g, 0.666 mmol) in CH_3OH (50 mL). Activated charcoal (0.10 g) and (*S*,*S*)-H_2NCH(4-$C_6H_4OCH_3$)CH(4-$C_6H_4OCH_3$)NH_2 ((*S*,*S*)-**8**;[14] 0.570 g, 2.09 mmol, 3.1 equiv) were added with vigorous stirring. After 16 h, the mixture was filtered through Celite and aqueous HCl (2.0 mL, 12.0 M) was added. The solvent was removed

by rotary evaporation and H_2O/CH_3OH (10 mL, 7:3 v/v) was added. The suspension was filtered. The filter cake was washed with acetone (2 × 10 mL) and dried by oil pump vacuum (12 h) to give crude Λ-(*S*,*S*)-**16**$^{3+}$ 3Cl$^-$ (0.226 g, 0.231 mmol assuming a pure product). This was suspended in CH_2Cl_2 (5 mL), and Na^+ BAr_f^- (0.209 g, 0.236 mmol, 1.0 equiv) was added. The mixture was sonicated (1 min)[41] and filtered. The filtrate was loaded onto a silica gel column (1.9 × 12 cm), which was eluted with CH_2Cl_2/CH_3OH (100:0 to 97.5:2.5 v/v). The solvent was removed from the main orange band by rotary evaporation and oil pump vacuum (12 h) to give Λ-(*S*,*S*)-**16**$^{3+}$ $2Cl^-BAr_f^-{\cdot}3H_2O$ as a bright yellow solid (0.289 g, 0.155 mmol, 23%), mp 128-132 °C dec (open capillary). Anal. Calcd. for $C_{80}H_{72}BCl_2CoF_{24}N_6O_6{\cdot}3H_2O$ (1862.42): C 51.54, H 4.22, N 4.51, Cl 3.80; found C 51.58, H 4.12, N 4.57, Cl 3.73. IR (powder film, cm^{-1}): 3065 (m, ν_{NH}), 1611 (m, δ_{NH}), 1354 (s, $\nu_{Ar\text{-}CF_3}$), 1275 (vs, ν_{CF}), 1121 (vs, δ_{CCN}).

NMR (CD_2Cl_2, δ in ppm):[33] ^{1}H (500 MHz) BAr_f^- at 7.71 (s, 8H, *o*), 7.54 (s, 4H, *p*); (*S*,*S*)-**8** ligand at 7.67 (br s, 6H, N**H**H'), 7.17 (d, $^3J_{HH}$ = 9.0 Hz, 12H, Ar), 6.73 (d, $^3J_{HH}$ = 8.5 Hz, 12H, Ar), 4.34 (s, 6H, C**H**NH_2), 4.16 (br s, 6H, NH**H'**), 3.66 (s, 18H, OC**H**$_3$), 2.15 (br s, 11H, **H**$_2$O); $^{13}C\{^1H\}$ (125 MHz) BAr_f^- at 162.3 (q, $^1J_{BC}$ = 49.5 Hz, *i*), 135.3 (s, *o*), 129.4 (q, $^2J_{CF}$ = 34.5 Hz, *m*), 125.1 (q, $^1J_{CF}$ = 271.1 Hz, **C**F_3), 118.0 (s, *p*); (*S*,*S*)-**8** ligand at 161.2 (s, *i*-Ar), 129.8 (s, Ar), 126.8 (s, Ar), 115.6 (s, Ar), 62.9 (s, **C**HNH_2), 56.1 (s, O**C**H$_3$).

Δ-[Co((*S*,*S*)-H_2NCH(4-$C_6H_4OCH_3$)CH(4-$C_6H_4OCH_3$)NH_2)$_3$]$^{3+}$ 2Cl$^-$BAr$_f^-$ (Δ-(*S*,*S*)-16^{3+} 2Cl$^-$BAr$_f^-$). *The procedure involves perchlorate salts that are potentially explosive*.[36] A gas circulating flask[34] was charged with a solution of $Co(ClO_4)_2{\cdot}6H_2O$ (0.136 g, 0.372 mmol) in CH_3OH (50 mL). Activated charcoal (0.10 g) and (*S*,*S*)-**8**[14] (0.335 g, 1.22 mmol, 3.3 equiv) were added with vigorous stirring. After 16 h, the mixture was filtered through Celite, and $HClO_4$ (2.0 mL, 35% in H_2O) was added. The

solution was sorbed onto a Dowex cation exchange column (3.0 × 12 cm), which was washed with H_2O/CH_3OH (1:1 v/v, 100 mL) and eluted with increasing proportions of 12.0 M aqueous HCl in CH_3OH (CH_3OH/HCl 9:1 v/v (100 mL), 8:2 v/v (100 mL), 7:3 v/v (100 mL), 6:4 v/v until product elution). An orange band was collected and the solvents were removed by rotary evaporation (60 °C bath; base trap to scavenge HCl) to give crude Δ-(*S*,*S*)-**16**$^{3+}$ 3Cl$^-$ (0.103 g; 0.105 mmol assuming a pure product). This was suspended in CH_2Cl_2 (5.0 mL), and Na^+ BAr_f^- (0.0935 g, 0.105 mmol, 1.0 equiv) was added. The mixture was sonicated (5 min)[41] and filtered. The filtrate was loaded onto a silica gel column (1.9 × 10 cm), which was eluted with CH_2Cl_2/CH_3OH (100:0 to 97.5:2.5 v/v). The solvent was removed from the main orange band by rotary evaporation and oil pump vacuum (12 h) to give Δ-(*S*,*S*)-**16**$^{3+}$ 2Cl$^-$$BAr_f^-$·2$H_2O$ as a bright yellow solid (0.125 g, 0.0678 mmol, 18%), mp 130-135 °C dec (open capillary). Anal. Calcd. for $C_{80}H_{72}BCl_2CoF_{24}N_6O_6$· 2$H_2O$ (1846.11): C 52.05, H 4.15, N 4.55, Cl 3.84; found C 52.43, H 4.49, N 4.59, Cl 3.44. IR (powder film, cm^{-1}): 1572 (m, $\nu_{Ar\text{-}CC}$), 1510 (m, $\nu_{Ar\text{-}CC}$), 1354 (s, $\nu_{Ar\text{-}CF_3}$), 1275 (vs, ν_{CF}), 1119 (vs, δ_{CCN}).

NMR (40:0.1 v/v CD_2Cl_2/CD_3OD, δ in ppm):[33] ^{1}H (500 MHz) BAr_f^- at 7.73 (s, 8H, *o*), 7.57 (s, 4H, *p*); (*S*,*S*)-**8** ligand at 7.25 (d, $^3J_{HH}$ = 8.5 Hz, 12H, Ar), 6.81 (d, $^3J_{HH}$ = 8.5 Hz, 12H, Ar), 5.82 (br s, 2H, N**H**H'),[37] 5.67 (br s, 2H, NH**H'**),[37] 4.27 (s, 6H, C**H**NH_2), 3.74 (s, 18H, OC**H**$_3$), 1.85 (br s, 13H, CD_3O**H**/**H**$_2$O); ^{13}C{^{1}H} (125 MHz) BAr_f^- at 162.3 (q, $^1J_{BC}$ = 49.6 Hz, *i*), 135.3 (s, *o*), 129.4 (q, $^2J_{CF}$ = 34.3 Hz, *m*), 125.1 (q, $^1J_{CF}$ = 270.6 Hz, **C**F_3), 118.0 (s, *p*); (*S*,*S*)-**8** ligand at 160.8 (s, *i*-Ar), 129.3 (s, Ar), 127.6 (s, Ar), 114.9 (s, Ar), 64.9 (s, **C**HNH_2), 55.8 (s, O**C**H_3).

Λ-[Co((*S*,*S*)-H_2NCH(α-naphthyl)CH(α-naphthyl)NH_2)$_3$]$^{3+}$ 2Cl$^-$$BAr_f^-$ (Λ-(*S*,*S*)-17^{3+} 2Cl$^-$$BAr_f^-$). A gas circulating flask[34] was charged with a solution of $Co(OAc)_2$·4H_2O (0.4002 g, 1.61 mmol) in CH_3OH (50 mL). Activated charcoal (0.10 g)

and (*S*,*S*)-$H_2NCH(\alpha\text{-naphthyl})CH(\alpha\text{-naphthyl})NH_2$ ((*S*,*S*)-**9**;[14] 1.64 g, 5.24 mmol, 3.3 equiv) were added with vigorous stirring. After 16 h, the mixture was filtered through Celite, and aqueous HCl (3.0 mL, 12.0 M) was added. The yellow precipitate was collected by filtration. The filtrate was concentrated to ca. 20 mL by rotary evaporation, and H_2O was added (100 mL). The yellow precipitate was collected by filtration. The combined precipitates were washed with H_2O/CH_3OH (100 mL, 9:1 v/v). The filter cake was dissolved in CH_3OH. The solvent was removed by rotary evaporation and oil pump vacuum (1 h) to give Λ-(*S*,*S*)-$\mathbf{17}^{3+}$ $3Cl^-$ (1.36 g, 1.23 mmol assuming pure product). This was suspended in CH_2Cl_2 (25 mL), and Na^+ BAr_f^- (1.09 g, 1.23 mmol, 1.0 equiv) was added. The mixture was sonicated (10 min)[41] and filtered. The filtrate was loaded onto a silica gel column (3.0 × 12 cm), which was eluted with CH_2Cl_2/CH_3OH (100:0 to 98:2 v/v). The solvent was removed from the main orange band by rotary evaporation and oil pump vacuum (12 h) to give Λ-(*S*,*S*)-$\mathbf{17}^{3+}$ $2Cl^-$ BAr_f^- $\cdot 2H_2O$ as an orange solid (1.415 g, 0.720 mmol, 45%), mp 131-135 °C dec. (open capillary). Anal. Calcd. for $C_{98}H_{72}BCl_2CoF_{24}N_6\cdot 2H_2O$ (1966.30): C 59.86, H 3.90, N 4.27, Cl 3.61; found C 59.90, H 4.07, N 4.31, Cl 3.40. IR (powder film, cm^{-1}): 3053 (m, ν_{NH}), 1604 (m, δ_{NH}), 1354 (s, $\nu_{Ar\text{-}CF_3}$), 1275 (vs, ν_{CF}), 1121 (vs, δ_{CCN}).

NMR (CD_2Cl_2, δ in ppm):[33] ^1H (500 MHz) BAr_f^- at 7.73 (s, 8H, *o*), 7.55 (s, 4H, *p*); (*S*,*S*)-**9** ligand at 9.72 (br s, 6H, N**H**H'), 8.51 (s, 6H, $C_{10}\mathbf{H}_7$), 8.02-7.95 (m, 24H, $C_{10}\mathbf{H}_7$), 7.18 (s, 12H, $C_{10}\mathbf{H}_7$), 5.61 (s, 6H, C**H**NH_2), 3.65 (br s, 6H, NH**H'**), 2.16 (br s, 3H, $\mathbf{H}_2O$); $^{13}C\{^1H\}$ (125 MHz) BAr_f^- at 162.3 (q, $^1J_{BC}$ = 48.9 Hz, *i*), 135.4 (s, *o*), 129.4 (q, $^2J_{CF}$ = 31.6 Hz, *m*), 125.2 (q, $^1J_{CF}$ = 271.0 Hz, **C**F_3), 118.0 (s, *p*); (*S*,*S*)-**9** ligand at 134.8, 131.9, 131.1 130.3, 128.8, 127.8, 125.52, 125.48, 124.5, 122.8 (10 × s, $\mathbf{C}_{10}H_7$), 59.7 (s, **C**HNH_2).

Λ-[Co((*S*,*S*)-H_2NCH((α-naphthyl)CH((α-naphthyl)NH_2)$_3$]$^{3+}$ 2$BF_4^-$$BAr_f^-$ (Λ-(*S*,*S*)-17^{3+} 2$BF_4^-$$BAr_f^-$). A round bottom flask was charged with a solution of Λ-(*S*,*S*)-**17**$^{3+}$ 2$Cl^-BAr_f^-$·2H_2O (0.405 g, 0.206 mmol) in CH_2Cl_2 (10 mL), and Ag^+ BF_4^- (0.0851 g, 0.44 mmol, 2.1 equiv) was added with stirring. The mixture was sonicated (10 min) and filtered through Celite. The solvent was removed by rotary evaporation and oil pump vacuum (1 h) to give Λ-(*S*,*S*)-**17**$^{3+}$ 2$BF_4^-$$BAr_f^-$·(3.5±0.5)$H_2O$ as a red solid (0.393 g, 0.188 mmol, 91%), mp 161-167 °C dec. (open capillary). Anal. Calcd. For $C_{98}H_{72}B_3CoF_{32}N_6$·3$H_2O$/$C_{98}H_{72}B_3CoF_{32}N_6$·4$H_2O$ (2087.05/ 2104.53): C 56.40/55.90, H 3.77/3.83, N 4.03/3.99; found C 55.97, H 3.41, N 3.85. IR (powder film, cm^{-1}): 3251 (m, ν_{NH}), 1602 (m, δ_{NH}), 1354 (s, $\nu_{Ar\text{-}CF_3}$), 1275 (vs, ν_{CF}), 1119 (vs, δ_{CCN}).

NMR (CD_2Cl_2, δ in ppm):[33] ^{1}H (500 MHz) BAr_f^- at 7.74 (s, 8H, *o*), 7.56 (s, 4H, *p*); (*S*,*S*)-**9** ligand at 8.07 (d, $^3J_{HH}$ = 8.0 Hz, 6H, $C_{10}\mathbf{H}_7$), 7.92 (d, $^3J_{HH}$ = 8.0 Hz, 6H, $C_{10}\mathbf{H}_7$), 7.71-7.64 (m, 18H, $C_{10}\mathbf{H}_7$), 7.04 (t, $^3J_{HH}$ = 7.5 Hz, 6H, $C_{10}\mathbf{H}_7$), 6.92 (s, 6H, $C_{10}\mathbf{H}_7$), 6.32 (s, 6H, N**H**H'), 5.40 (s, 6H, C**H**NH_2), 4.04 (s, 6H, NH**H'**), 1.96 (s, 4H, $\mathbf{H}_2O$); $^{13}C\{^1H\}$ (125 MHz) BAr_f^- at 162.2 (q, $^1J_{BC}$ = 62.5 Hz, *i*), 135.3 (s, *o*), 129.4 (q, $^2J_{CF}$ = 32.4 Hz, *m*), 125.2 (q, $^1J_{CF}$ = 271.3 Hz, **C**F_3), 118.2 (s, *p*); (*S*,*S*)-**9** ligand at 134.9, 132.5, 130.8, 130.0, 129.4, 128.6, 128.2, 125.7, 124.1, 121.3 (10 × s, $\mathbf{C}_{10}H_7$), 59.4 (s, **C**HNH_2).

Δ-[Co((*S*,*S*)-H_2NCH(α-naphthyl)CH(α-naphthyl)NH_2)$_3$]$^{3+}$ 2$Cl^-BAr_f^-$ (Δ-(*S*,*S*)-17^{3+} 2$Cl^-BAr_f^-$). *The procedure involves perchlorate salts that are potentially explosive*.[36] A gas circulating flask[34] was charged with a solution of $Co(ClO_4)_2$·6H_2O (0.352 g, 0.961 mmol) in CH_3OH (50 mL). Activated charcoal (0.13 g) and (*S*,*S*)-**9**[14] (0.989 g, 3.17 mmol, 3.3 equiv) were added with vigorous stirring. After 18 h, the mixture was filtered through Celite, and $HClO_4$ (4.0 mL, 35% in H_2O) was added. The

solution was sorbed onto a Dowex cation exchange column (3.0 × 12 cm), which was washed with H_2O/CH_3OH (1:1 v/v, 100 mL) and eluted with increasing concentrations of 12.0 M aqueous HCl in CH_3OH (CH_3OH/HCl 9:1 v/v (100 mL), 8:2 v/v (100 mL), 7:3 v/v (100 mL), 6:4 v/v until product elution). An orange band was collected. The solvents were removed by rotary evaporation (60 °C bath; base trap to scavenge HCl) to give crude Δ-(*S*,*S*)-**17**$^{3+}$ 3Cl$^-$ (0.518 g; 0.471 mmol assuming a pure product). This was suspended in CH_2Cl_2 (15 mL), and Na^+ BAr_f^- (0.461 g, 0.518 mmol, 1.1 equiv) was added. The mixture was sonicated (10 min)[41] and filtered. The filtrate was loaded onto a silica gel column (2.4 × 12 cm), which was eluted with CH_2Cl_2/CH_3OH (100:0 to 98:2 v/v). The solvent was removed from the main orange band by rotary evaporation and oil pump vacuum (12 h) to give Δ-(*S*,*S*)-**17**$^{3+}$ 2Cl$^-$BAr$_f^-$·4H_2O as an orange solid (0.781 g, 0.390 mmol, 41%), mp 124-128 °C dec. (open capillary). Anal. Calcd. for $C_{98}H_{72}BCl_2CoF_{24}N_6$· 4$H_2O$ (2002.33): C 58.78, H 4.03, N 4.20; found C 58.96, H 3.73, N 4.11.

NMR (acetone-d_6, δ in ppm):[33] ^{1}H (500 MHz) BAr_f^- at 7.80 (s, 8H, *o*), 7.68 (s, 4H, *p*); (*S*,*S*)-**9** ligand at 9.27 (br s, 6H, N**H**H'), 8.67 (d, $^3J_{CH}$ = 7.5 Hz, 6H, $C_{10}\mathbf{H}_7$), 7.97 (d, $^3J_{CH}$ = 8.0 Hz, 6H, $C_{10}\mathbf{H}_7$), 7.87 (d, $^3J_{CH}$ = 8.5 Hz, 6H, $C_{10}\mathbf{H}_7$), 7.65-7.39 (m, 18H, $C_{10}\mathbf{H}_7$), 7.16 (t, $^3J_{CH}$ = 7.5.0 Hz, 6H, $C_{10}\mathbf{H}_7$), 6.30 (s, 6H, C**H**NH_2), 5.70 (br s, 6H, NH**H'**), 2.86 (br s, 8H, $\mathbf{H}_2O$); $^{13}C\{^1H\}$ (125 MHz) BAr_f^- at 162.5 (q, $^1J_{BC}$ = 50 Hz, *i*), 135.5 (s, *o*), 129.9 (m, *m*), 125.3 (q, $^1J_{CF}$ = 271.0 Hz, **C**F_3), 118.4 (s, *p*); (*S*,*S*)-**9** ligand at 135.0, 133.1, 132.1 130.6, 129.5, 128.1, 127.4, 126.0, 125.9, 125.1 (10 × s, $\mathbf{C}_{10}H_7$), 59.0 (s, **C**HNH_2).

Λ-[Co((*S*,*S*)-$\mathbf{H_2}$NCH((β-naphthyl)CH((β-naphthyl)$\mathbf{NH_2)_3}$]$^{3+}$ 2Cl$^-$BAr$_f^-$ (Λ-(*S*,*S*)-18^{3+} 2Cl$^-$BAr$_f^-$). A gas circulating flask[34] was charged with a solution of $CoCl_2$·6H_2O (0.033 g, 0.138 mmol) in CH_3OH (50 mL). Activated charcoal (0.10 g) and

(*S*,*S*)-**10** (0.139 g, 0.445 mmol, 3.2 equiv) were added with vigorous stirring. After 16 h, the mixture was filtered through Celite, and aqueous HCl (2.0 mL, 12.0 M) was added. The filtrate was concentrated to a moist paste by rotary evaporation, and H_2O (100 mL) was added. The suspension was filtered. The filter cake was washed with H_2O (50 mL) and dissolved in CH_3OH. The solvent was removed by rotary evaporation and oil pump vacuum (1 h) to give crude Λ-(*S*,*S*)-**18**$^{3+}$ 3Cl$^-$ (0.127 g, 0.115 mmol, assuming a pure product). A portion (0.115 g, 0.105 mmol) was suspended in CH_2Cl_2 (25 mL), and Na^+ BAr_f^- (0.094 g, 0.106 mmol, 1.0 equiv) was added. The mixture was sonicated (5 min)[41] and filtered. The filtrate was loaded onto a silica gel column (1.9 × 15 cm), which was eluted with CH_2Cl_2/CH_3OH (100:0 to 99:1 v/v). The solvent was removed from the main orange band by rotary evaporation and oil pump vacuum (12 h) to give Λ-(*S*,*S*)-**18**$^{3+}$ 2Cl$^-$ BAr_f^- (0.085 g, 0.042 mmol, 34%), mp 126-130 °C dec. (open capillary). Anal. Calcd. for $C_{98}H_{72}BCl_2CoF_{24}N_6 \cdot 4H_2O$ (2002.33): C 58.78, H 4.03, N 4.20; found C 58.55, H 3.98, N 3.99.

NMR (acetone-d_6, δ in ppm):[33] ^{1}H (500 MHz) BAr_f^- at 7.79 (m, 8H, *o*), 7.68 (s, 4H, *p*); (*S*,*S*)-**10** ligand at 8.60 (br s, 6H, N**H**H'), 8.08 (s, 6H, $C_{10}\mathbf{H}_7$), 7.89 (d, $^3J_{HH}$ = 10.0 Hz, 6H, $C_{10}\mathbf{H}_7$), 7.85 (d, $^3J_{HH}$ = 10.0 Hz, 6H, $C_{10}\mathbf{H}_7$), 7.77-7.69 (m, 12H, $C_{10}\mathbf{H}_7$), 7.53-7.43 (m, 12H, $C_{10}\mathbf{H}_7$), 5.62-5.41 (br m, 12H, C**H**NH_2, NH**H'**), 2.85 (s, 8H, $\mathbf{H}_2O$); $^{13}C\{^1H\}$ (125 MHz) BAr_f^- at 162.5 (q, $^1J_{BC}$ = 50 Hz, *i*), 135.5 (s, *o*), 129.7 (m, *m*), 125.3 (q, $^1J_{CF}$ = 270 Hz, **C**F_3), 118.4 (m, *p*); (*S*,*S*)-**10** ligand at 134.7, 134.2, 134.0, 129.8 128.9, 128.8, 128.5, 127.8, 127.6, 126.7 (10 × s, $\mathbf{C}_{10}H_7$), 63.7 (s, **C**HNH_2).

Λ-[Co((*S*,*S*)-H_2NCH(2-C_6H_4OBn)CH(2-C_6H_4OBn)NH_2)$_3$]$^{3+}$ 2Cl$^-$$BAr_f^-$.(Λ-(*S*,*S*)-19^{3+} 2Cl$^-$$BAr_f^-$). A gas circulating flask[34] was charged with a solution of $Co(OAc)_2 \cdot 4H_2O$ (0.23 g, 0.93 mmol) in CH_3OH (50 mL). Activated charcoal (0.10 g) and (*S*,*S*)-**11** (1.31 g, 3.08 mmol, 3.3 equiv) were added with vigorous stirring. After 16

h, the mixture was filtered through Celite, and aqueous HCl (3.0 mL, 12.0 M) was added. The solvent was removed by rotary evaporation, and H_2O (100 mL) was added. The suspension was filtered. The filter cake was washed with H_2O (100 mL) and dissolved in CH_3OH. The solvent was removed by rotary evaporation and oil pump vacuum (12 h) to give crude Λ-(*S*,*S*)-**19**$^{3+}$ 3Cl$^-$ (1.288 g, 0.888 mmol assuming a pure product). This was suspended in CH_2Cl_2 (20 mL), and Na^+ BAr_f^- (0.993 g, 1.08 mmol, 1.2 equiv) was added. The mixture was sonicated (5 min)[41] and filtered. The filtrate was loaded onto a silica gel column (3.0 × 16 cm), which was eluted with CH_2Cl_2/CH_3OH (100:0 to 98:2 v/v). The solvent was removed from the main orange band by rotary evaporation and oil pump vacuum (12 h) to give Λ-(*S*,*S*)-**19**$^{3+}$ 2Cl$^-$ $BAr_f^-\cdot H_2O$ as a deep yellow solid (0.834 g, 0.365 mmol, 39%), mp 122-132 °C dec (open capillary). Anal. Calcd. for $C_{116}H_{96}BCl_2CoF_{24}N_6O_6\cdot H_2O$ (2284.66): C 60.98, H 4.32, N 3.68; found C 60.95, H 4.27, N 3.56.

NMR (acetone-d_6, δ in ppm):[33] ^{1}H (500 MHz) BAr_f^- at 7.80 (s, 8H, *o*), 7.62 (s, 4H, *p*); (*S*,*S*)-**11** ligand at 8.56 (br s, 6 H, N**H**H'), 7.62 (br s, 12H), 7.27 (t, $^3J_{HH}$ = 7.5 Hz, 6H), 7.20-7.08 (m, 30H), 6.73 (t, $^3J_{HH}$ = 7.5 Hz, 6H), 5.53 (d, $^2J_{HH}$ = 13 Hz, 6H, OC**H**H'Ph), 5.37 (s, 6H, C**H**NH_2), 5.28 (d, $^2J_{HH}$ = 13 Hz, 6H, OCH**H**'Ph), 5.15 (br s, 6H, NH**H**'), 2.89 (br s, 7H, **H**$_2$O); ^{13}C{^{1}H} (125 MHz) BAr_f^- at 162.6 (q, $^1J_{BC}$ = 50 Hz, *i*), 135.5 (s, *o*), 130.0 (q, $^2J_{CF}$ = 31.25 Hz, *m*), 125.3 (q, $^1J_{CF}$ = 270.0 Hz, **C**F_3), 118.4 (m, *p*); (*S*,*S*)-**11** ligand at 157.5, 138.3, 131.2, 129.3, 128.7, 128.4, 128.2, 125.5, 122.1, 114.1 (10 × s), 71.0 (s, O**C**H_2), 57.0 (s, **C**HNH_2).

Λ-[Co((*S*,*S*)-H_2NCH(3,5-$C_6H_3(CF_3)_2$)CH(3,5-$C_6H_3(CF_3)_2$)$NH_2)_3$]$^{3+}$ Cl$^-$ 2BAr_f^- (Λ-(*S*,*S*)-20^{3+} Cl$^-$2BAr_f^-). A gas circulating flask[34] was charged with a solution of $Co(OAc)_2\cdot 4H_2O$ (0.714 g, 2.87 mmol) in CH_3OH (50 mL). Activated charcoal (0.20 g) and (*S*,*S*)-**12** (4.60 g, 9.50 mmol, 3.3 equiv) were added with vigorous

stirring. After 72 h, the mixture was filtered through Celite, and aqueous HCl (3.0 mL, 12.0 M) was added. The solvent was removed by rotary evaporation, and H_2O/CH_3OH (100 mL, 70:30 v/v) was added. The suspension was filtered. The filter cake was washed with H_2O/CH_3OH (100 mL, 70:30 v/v) and dissolved in CH_3OH. The solvent was removed by rotary evaporation and oil pump vacuum (12 h) to give crude Λ-(*S*,*S*)-**20**$^{3+}$ 3Cl^- (2.54 g, 2.52 mmol assuming a pure product). A portion (1.52 g, 0.939 mmol) was suspended in CH_2Cl_2 (30 mL), and Na^+ BAr_f^- (0.917 g, 1.03 mmol, 1.1 equiv) was added. The mixture was sonicated (15 min)[41] and filtered. The solvent was removed by rotary evaporation and oil pump vacuum (12 h) to give Λ-(*S*,*S*)-**20**$^{3+}$ $Cl^-2BAr_f^-$ as an deep brown solid (1.594 g, 0.479 mmol, 28%), mp 55-69 °C dec (open capillary).[43] Anal. Calcd. for $C_{118}H_{60}B_2ClCoF_{84}N_6 \cdot 3H_2O$ (3327.70): C 42.59, H 2.00, N 2.53; found C 42.36, H 2.12, N 2.90.

NMR (acetone-d_6, δ in ppm): [33] ^{1}H (500 MHz) BAr_f^- at 7.80 (s, 16H, *o*), 7.67 (s, 8H, *p*); (*S*,*S*)-**12** ligand at 8.31 (s, 12H, Ar), 8.05 (s, 6H, Ar), 6.64-6.52 (br m, 6H, N**H**H'), 5.86-5.74 (br m, 6H, NH**H'**), 5.54-5.43 (m, 6H, C**H**NH_2), 3.31 (br s, 5H, **H**$_2$O);[43] ^{13}C{^{1}H} (125 MHz) BAr_f^- at 162.6 (q, $^1J_{BC}$ = 50 Hz, *i*), 135.6 (s, *o*), 130.0 (m, *m*), 125.4 (q, $^1J_{CF}$ = 270.0 Hz, **C**F_3), 118.4 (m, *p*); (*S*,*S*)-**12** ligand at 140.3 (s, *i*-Ar), 132.9 (q, $^2J_{CF}$ = 33.5 Hz, Ar), 130.1 (s, Ar), 124.02 (q, $^1J_{CF}$ = 270.9 Hz, **C**F_3), 124.00 (s, Ar), 65.0 (s, **C**HNH_2).

3.6. References

(1) (a) Zhao, M.; Wang, H.-B.; Ji, L.-N.; Mao, Z.-W. *Chem. Soc. Rev.* **2013**, *42*, 8360-8375. (b) García-Simón, C.; Gramage-Doria, R.; Raoufmoghaddam, S.; Parella, T.; Costas, M.; Ribas, X; Reek, J. N. H. *J. Am. Chem Soc.* **2015**, *137*, 2680-2687. (c) Chatterjee, A.; Mallin, H.; Klehr, J.; Vallapurackal, J.; Finke, A. D.; Vera, L.; Marsh, M.; Ward, T. R. *Chem. Sci.* **2016**, *7*, 673-677.

(2) Brak, K.; Jacobsen, E. N. *Angew. Chem. Int. Ed.* **2013**, *52*, 534-561; *Angew. Chem.* **2013**, *125*, 558-588.

(3) Ganzmann, C.; Gladysz, J. A. *Chem*. *Eur*. *J*. **2008**, *14*, 5397-5400.

(4) Ghosh, S. K.; Ehnbom, A.; Lewis, K. G.; Gladysz, J. A. *Coord. Chem. Rev.* **2017**, in press, doi: 10.1016/j.ccr.2017.04.002.

(5) (a) Lewis, K. G.; Ghosh, S. K.; Bhuvanesh, N.; Gladysz, J. A. *ACS Cent*. *Sci*. **2015**, *1*, 50-56. (b) Kumar, A.; Ghosh, S. K.; Gladysz, J. A. *Org*. *Lett*. **2016**, *18*, 760-763. (c) Joshi, H.; Ghosh, S. K.; Gladysz, J. A. *Synthesis* **2017** (in press).

(6) Ghosh, S. K.; Ganzmann, C.; Bhuvanesh, N.; Gladysz, J. A. *Angew*. *Chem*., *Int*. *Ed*. **2016**, *55*, 4356-4360; *Angew*. *Chem*. **2016**, *128*, 4429-4433.

(7) Thomas, C.; Gladysz, J. A. *ACS Catal.* **2014**, *4*, 1134-1138.

(8) Review of stereochemical properties: Ehnbom, A.; Ghosh, S. K.; Lewis, K. G.; Gladysz, J. A. *Chem. Soc. Rev.* **2016**, *45*, 6799-6811.

(9) (a) Taube, H. *Chem. Rev*. **1952**, *50*, 69-126. (b) Data for $[Co(en)_3]^{3+}$: Friend, J. A.; Nunn, E. K. *J. Chem. Soc.* **1958**, 1567-1571.

(10) Relevant papers from the Meggers group since 2014: (a) Ma, J.; Ding, X.; Hu, Y.; Huang, Y.; Gong, L.; Meggers, E. *Nat. Commun*. **2014**, *5*:4531 (b) Huo, H.; Fu, C.; Wang, C.; Harms, K.; Meggers, E. *Chem. Commun*. **2014**, *50*, 10409-10411. (c) Liu, J.; Gong, L.; Meggers, E. *Tetrahedron Lett*. **2015**, *56*, 4653-4656. (d) Hu, Y.; Zhou, Z.;

Gong, L.; Meggers, E. *Org. Chem. Front.* **2015**, *2*, 968-972. (e) Xu, W.; Shen, X.; Ma, Q.; Gong, L.; Meggers, E. *ACS Catal.* **2016**, *6*, 7641-7646. (f) Xu, W.; Arieno, M.; Löw, H.; Huang, K.; Xie, X.; Cruchter, T.; Ma, Q.; Xi, J.; Huang, B.; Wiest, O.; Gong, L.; Meggers, E. *J. Am. Chem. Soc.* **2016**, *138*, 8774-8780.

(11) Maleev, V. I.; North, M.; Larionov, V. A.; Fedyanin, I. V.; Savel´yeva, T. F.; Moscalenko, M. A.; Smolyakov, A. F.; Belokon, Y. N. *Adv. Synth. Catal.* **2014**, *356*, 1803-1810.

(12) (a) Scherer, A.; Mukherjee, T.; Hampel, F.; Gladysz, J. A. *Organometallics* **2014**, *33*, 6709-6722. (b) Mukherjee, T.; Ganzmann, C.; Bhuvanesh, N.; Gladysz, J. A. *Organometallics* **2014**, *33*, 6723-6737.

(13) This compound was available from many vendors. The best price in effect as of the submission date of the dissertation is from Aris Pharmaceuticals (http://www.arispharma.com).

(14) Kim, H.; Nguyen, Y.; Yen, C. P.-H.; Chagal, L.; Lough, A. J.; Kim, B. M.; Chin, J. *J. Am. Chem. Soc.* **2008**, *130*, 12184-12191.

(15) This compound was available from many vendors. The best price in effect as of the submission date of the dissertation is from Sigma-Aldrich (https://www.sigmaaldrich.com).

(16) Bosnich, B.; Harrowfield, J. MacB. *J. Am. Chem. Soc.* **1972**, *94*, 3425-3437.

(17) Kuroda, R.; Mason, S. F. *J. Chem. Soc., Dalton Trans.* **1977**, *10*, 1016-1020.

(18) (a) Gillard, R. D. *Tetrahedron* **1965**, *21*, 503-506. In this work, the carbon configurations were correctly assigned, but using salts with unspecified anions. There were no assignments of cobalt configurations. (b) Fereday, P. L.; Mason, S. F. *Chem. Commun.* **1971**, 1314-1315. In this work, the cobalt configurations were correctly assigned, but the carbon configurations misassigned, using CD spectra of salts with

unspecified anions.

(19) (a) Williams, O. F.; Bailar, Jr. J. C. *J. Am. Chem. Soc.* **1959**, *81*, 4464-4469. (b) The only tris(1,2-diamine) complex reported in this paper, $[Co(\textit{rac}\text{-dpen})_3]^{3+}$ $3Cl^-$, is derived from racemic dpen.

(20) Charcoal is believed to function as a redox catalyst, generating small quantities of substitution labile cobalt(II) salts: (a) Douglas, B. E. *J. Am. Chem. Soc.* **1954**, *76*, 1020-1021. (b) Sen, D.; Fernelius, W. C. *J. Inorg. Nucl. Chem.* **1959**, *10*, 269-274. (c) Bianchi, A, Bencini, A. Synthesis and Spectroscopy of Transition Metal Complexes. In *Inorganic and Bio-Inorganic Chemistry*, vol. II, part of Encyclopedia of Life Support Systems (EOLSS), Bertini, I., Ed.; EOLSS Publishers Co. Ltd., Oxford, 2009, pp 150-256.

(21) (a) In reference 19a, the synthesis and microanalysis of the analogous complex of racemic dpen, "*trans*-[Co(active-stien)$_2$Cl$_2$]Cl", is described. A similar synthesis of a complex of enantiopure dpen, "[Co(*l*-stien)$_2$Cl$_2$]Cl", is claimed, but no details are provided. Hence, to confirm the identity of the *trans*-$[Co((S,S)\text{-dpen})_2(Cl)_2]^+$ Cl^- produced in step **I** of Scheme 3.2, this synthesis was repeated and the product characterized by NMR, as described in the Appendix B. (b) In the older literature, "stien" is often used as a synonym for dpen. The "sti" refers to the stilbene backbone of the 1,2-diamine.

(22) For all trications $[Co((S,S)\text{-}NH_2CHArCHArNH_2)_3]^{3+}$ in this study (except Ar = α-naphthyl ((*S*,*S*)-**17**$^{3+}$), for which different solvents were employed), the ^{13}C NMR **C**HPh signal of the Δ diastereomer was downfield of that of the Λ diastereomer.

(23) (a) The title complexes were isolated as hydrates, consistent with the appreciable hydrogen bond donor strengths of the ligating NH_2 groups. To aid readability, these are not specified in the main text or graphics, but are taken into

account in the stoichiometries and yield calculations, as detailed in the experimental section. The hydration levels were assigned based upon ^{1}H NMR integrations and microanalyses, as summarized in Table 3.1. When these differed, the microanalytical values were given precedence, as the NMR integrations can be enhanced by protic impurities or NH/ND exchange. (b) No attempts were made to characterize the degree of hydration of salts that were mixtures of diastereomers (for which variable compositions would be expected).

(24) (a) This procedure was reported to give exclusively Δ-(*S*,*S*)-**1**$^{3+}$ 3ClO_4^- in reference 16, but a yield was not quoted. In my hands, I always obtained 15-18% of the Λ diastereomer (eight independent syntheses). (b) In reference 16, Δ-(*S*,*S*)-**1**$^{3+}$ 3ClO_4^- was also isolated as a non-hydrated crystalline byproduct from the synthesis of the diastereomer Λ-(*S*,*S*)-**1**$^{3+}$ 3ClO_4^-, and characterized by microanalysis and CD spectroscopy.

(25) (a) Lungwitz, R.; Spange, S. *New. J. Chem.* **2008**, *32*, 392-394. (b) Cláudio, A. F. M.; Swift, L.; Hallett, J. P.; Welton, T.; Coutinho, J. A. P.; Freire, M. G. *Phys. Chem. Chem. Phys.* **2014**, *16*, 6593-6601.

(26) The chemical shifts of the diastereotopic NHH' protons are also temperature dependent. These data, which remain to be interpreted, are given in Figure A-1 and Table A-4 (Appendix).

(27) (a) Yakelis, N. A.; Bergman, R. G. *Organometallics* **2005**, *24*, 3579-3581. (b) Nishida, H.; Takada, N.; Yoshimura, M.; Sonoda, T.; Kobayashi, H. *Bull. Chem. Soc. Jpn.* **1984**, *57*, 2600-2604.

(28) Ehnbom, A. work in progress, Texas A&M University

(29) Corey, E. J.; Bailar, Jr., J. C. *J. Am. Chem. Soc.* **1959**, *81*, 2620-2629.

(30) Harnung, S. E.; Sørensen, B. S.; Creaser, I.; Maegaard, H.; Pfenninger, U.;

Schäffer, C. E. *Inorg. Chem.* **1976**, *15*, 2123-2126.

(31) Ghosh, S. K.; Kumar, A.; Lewis, K. G.; Ehnbom, A.; Gladysz, J. A. work in progress, Texas A&M University.

(32) (a) Sigman, M. S.; Harper, K. C.; Bess, E. N.; Milo, A. *Acc. Chem. Res.*, **2016**, *49*, 1292-1301. (b) Santiago, C. B.; Milo, A; Sigman, M. S. *J. Am. Chem. Soc.* **2016**, *138*, 13424-13430. (c) Eiji, Y.; Hilton, M. J.; Orlandi, M.; Saini, V.; Toste, F. D.; Sigman, M. S. *J. Am. Chem. Soc.* **2016**, *138*, 15877-15880.

(33) For aryl groups with more than one substituent, the designations *i*/*o*/*m*/*p* are with respect to the boron or $CHNH_2$ moieties.

(34) **Gas circulating flask.** A three neck flask and hollow glass stopper is configured to hold a horizontal hollow glass rod that reaches from the bottom of the flask to the apex of the stopper (see below). The hollow rod has a hole at the top and a short perpendicular T-segment with two holes at the bottom. The T-segment must be beneath the surface of solvent. A magnetic stir bar is embedded in the rod immediately below the T-segment. When rotation is driven by a magnetic stirrer, an aspirator effect draws the ambient atmosphere down the rod and into the solution, producing a vigorous stream of bubbles out of the T-segment.

Figure 3.6. (a) Components of the gas circulating flask; (b) The assembled flask.

(35) Another **C**HPh signal was observed at δ 58.6 ppm, corresponding to the bis(HCl) adduct derived from the excess (*S*,*S*)-dpen. The intensity of this signal was disproportionate to the concentration (ca. × 2), as verified by spectra of independently prepared mixtures.

(36) Robinson, W. R. *J. Chem. Ed.* **1985**, *62*, 1001.

(37) The NH and/or NH' signal was not observed or was of reduced intensity due to H/D exchange.

(38) The $^{13}C\{^{1}H\}$ signal with the chemical shift closest to benzene was assigned to the *meta* carbon atom: Mann, B. E. *J. Chem. Soc. Perkin Trans. 2*, **1972**, 30-34.

(39) This compound was similarly prepared in reference 16 and characterized by microanalysis and CD spectroscopy. The degree of hydration was presumed to be identical.

(40) A similar experiment was mentioned in reference 16, but without any quantitative details. The conversion is represented as 100% in the experimental section, and "at least 90%" in the text.

(41) During this time, the solvent became bright orange and a white precipitate (NaCl or KCl) formed.

(42) The settings used for the $^{13}C\{^{1}H,^{19}F\}$ experiments gave complete decoupling of all of the ^{13}C signals of Λ-(*S*,*S*)-**1**$^{3+}$ 2Cl^{-}BAr$_{f20}^{-}$, but with Δ-(*S*,*S*)-**1**$^{3+}$ 2Cl^{-}BAr$_{f20}^{-}$ and Λ-(*S*,*S*)-**1**$^{3+}$ 3BAr$_{f20}^{-}$ one or more signals exhibited some residual ^{19}F coupling.

(43) The ^{1}H NMR spectrum showed very minor impurities in the aromatic region.

4. COBALT(III) WERNER COMPLEXES WITH 1,2-DIPHENYLETHYLENEDIAMINE LIGANDS: READILY AVAILABLE, INEXPENSIVE, AND MODULAR CHIRAL HYDROGEN BOND DONOR CATALYSTS FOR ENANTIOSELECTIVE MICHAEL REACTIONS†

4.1. Introduction

The pervasive role of hydrogen bonding in enzymatic catalysis has been recognized for more than a half century,[1] and recently numerous small molecule hydrogen bond donor catalysts have been developed,[2] in parallel with the growth of "organocatalysis".[3] Due to the desirability of single enantiomer pharmaceuticals and agrichemicals, enantiopure chiral donors have received particular focus.[2] However, from the standpoint of innovative new paradigms, much of the "chiral pool"[4] applicable to catalysis has been quite thoroughly picked over, especially with regard to inexpensive, readily available building blocks.

In this context, my attention was drawn to Werner complexes featuring the chiral tris(ethylenediamine) substituted trication $[Co(en)_3]^{3+}$, and related octahedral systems.

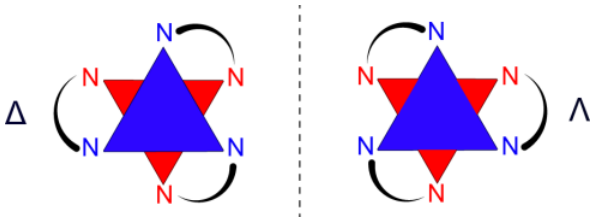

†Reproduced in part with the permission from Lewis, K. G.; Ghosh, S. K.; Bhuvanesh, N.; Gladysz, J. A. *ACS Cent. Sci.* **2015**, *1*, 50-56.

These were the first inorganic compounds resolved into enantiomers some 103 years ago,[5] with the configurations of the helically chiral mirror images later denoted as Λ and Δ. Cobalt is an earth abundant metal, but none of these salts has ever been applied in any type of enantioselective organic reaction, despite facile resolution procedures. Given the mechanisms of most transition metal catalysts, many would presume the necessity of a metal based vacant coordination site to bind and activate a substrate. However, such d^6 cobalt(III) systems are "substitution inert",[6,7] especially at temperatures lower than 100 °C.

I and my collaborator wondered about the possibility of an alternative binding/activation mode, in which the ligating NH_2 groups would function as hydrogen bond donors, leading to what could be termed "second coordination sphere promoted catalysis". Thus, nearly 150 crystal structures of salts of the formula $[Co(en)_3]^{3+}$ yX^{z-} (y/z = 3/1, 1.5/2, 1/3) were surveyed as detailed in section 2.[8] Every one showed significant NH···X hydrogen bonding, even when the anions were poor acceptors. Furthermore, data for related cobalt(III) complexes suggested pK_a values of 13-14,[9] or acidities greater than other hydrogen bond donors that are effective organocatalysts.[2]

Cobalt(III) has an extensive aqueous chemistry, but water would be expected to compete with substrates for hydrogen bond donor sites, suppressing rates. Accordingly, past researchers in the Gladysz group have shown that salts of the lipophilic BAr_f^- anion (BAr_f = $B(3,5\text{-}C_6H_3(CF_3)_2)_4$), such as Δ-$[Co(en)_3]^{3+}$ $3BAr_f^-$ and *trans*-1,2-cyclohexanediamine analogs, are soluble in a variety of organic solvents.[10,11] However, enantioselectivities in screening reactions were disappointing. I now report that similar adducts of (*S*,*S*)-1,2-diphenylethylenediamine ((*S*,*S*)-dpen),[12,13] which is commercially available as either enantiomer,[14] afford high enantioselectivities in a benchmark carbon-carbon bond forming reaction, the addition of malonate esters to nitroalkenes,[15] as well

as others. Together with recent studies involving metal catalysts with hydrogen bond donors *remote* from coordinating atoms,[16-19] this work firmly establishes the viability of highly enantioselective second coordination sphere promoted catalysis, and presages a "gold rush" on widely available NH-containing coordination compounds that have heretofore unrecognized potential as catalysts. Some of these reactions were carried out by Dr. Kyle G. Lewis.

4.2. Results

First, (*S*,*S*)-dpen was elaborated into a series of diastereomeric complexes Λ- and Δ-[Co((*S*,*S*)-dpen)$_3$]$^{3+}$ 3X$^-$ (Λ- and Δ-(*S*,*S*)-**1**$^{3+}$ 3X$^-$, X = Cl$^-$, ClO_4^- differing in the cobalt chirality, by adapting earlier procedures of Bosnich,[12] Mason,[13] and others as shown in Scheme 4.1. These efforts were detailed in section 3.[21]

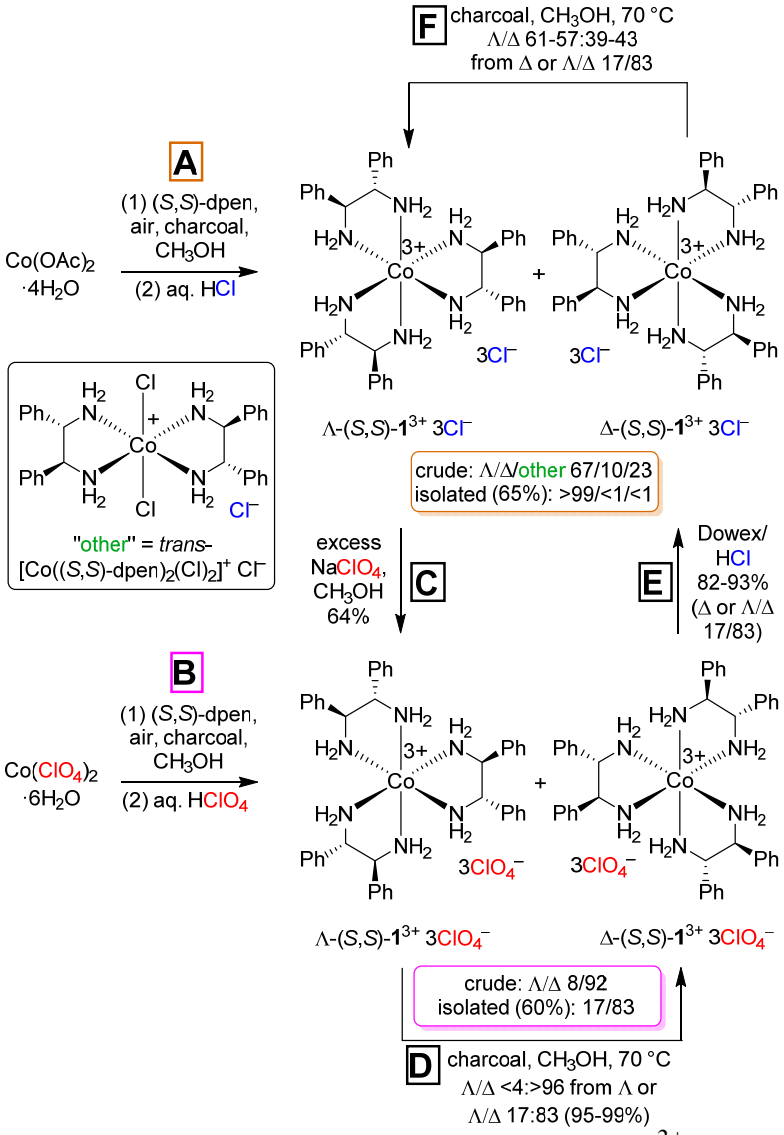

Scheme 4.1. Syntheses of salts of the formula $[Co((S,S)\text{-dpen})_3]^{3+}$ $3X^-$ ((S,S)-$\mathbf{1}^{3+}$ $3X^-$; X = Cl, ClO_4); kinetic and thermodynamic Λ/Δ diastereoselectivities.

Next, lipophilic salts were prepared as exemplified for the Λ diastereomers in Scheme 4.2 (see also section 3).[21] It has not yet been possible to obtain a crystal structure of one of the lipophilic salts. However, crystal structures of Λ-, Δ-(S,S)-$\mathbf{1}^{3+}$ $3Cl^-$, and Δ-(R,R)-$\mathbf{1}^{3+}$ $3Cl^-$ could be determined, as described in the experimental section. Views of the structures are presented in Figures 4.1-4.3.

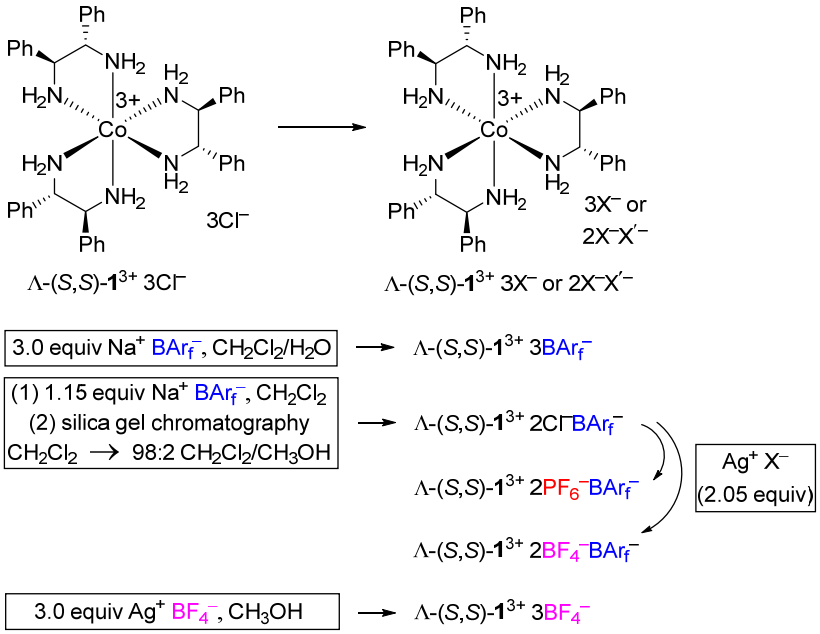

Scheme 4.2. Syntheses of lipophilic Werner salts (yields: 83-96%).The procedures for Δ diastereomers are analogous.

As expected, the trication in Λ-(*S*,*S*)-**1**$^{3+}$ 3Cl^{-} (Figure 4.1), exhibits a nearly idealized D_3 geometry, with a principal C_3 symmetry axis and three C_2 symmetry axes that define a plane perpendicular to the principal axis. The three NH protons on each of the two "C_3 faces" are oriented in a convergent manner that should afford particularly strong hydrogen bonds. The two protons on each of three "C_2 faces" are also effectively aligned for hydrogen bonding, but the enthaplic interactions should be lower, consistent with the more facile exchange of the first chloride ion by BAr$_f^-$ (Scheme 4.2).

A similar motif is found with the opposite diastereomer Δ-(*S*,*S*)-**1**$^{3+}$ 3Cl^{-} (Figure 4.2), but the protons on the C_3 faces are oriented in a divergent manner, and the C_2 faces are much more congested, precluding simultaneous bonding of chloride to both NH protons (Figure 4.2). In any event, for both diastereomers of the mixed salts (*S*,*S*)-**1**$^{3+}$ 2X$^-$BAr$_f^-$, the dominant hydrogen bonding interactions should involve X$^-$ and the C_3 faces.

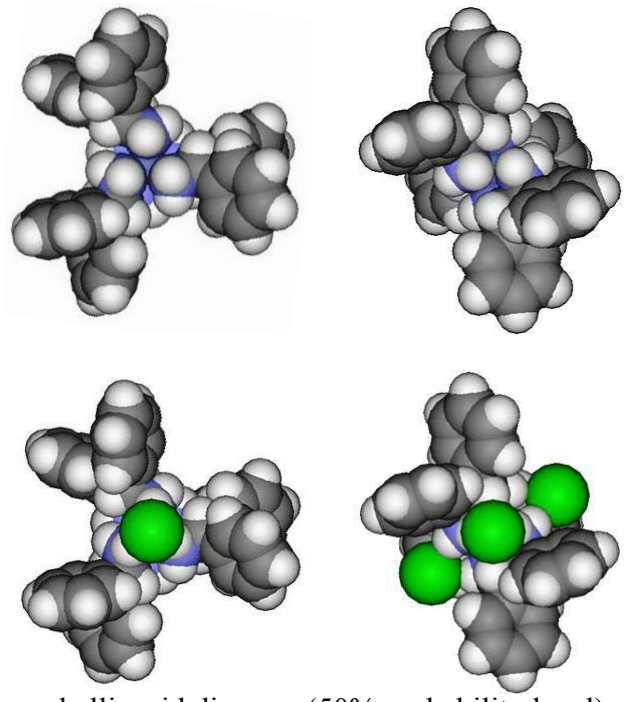

Figure 4.1. Thermal ellipsoid diagram (50% probability level) of Λ-(*S*,*S*)-$\mathbf{1}^{3+}$ $3Cl^-$ $\cdot 2H_2O \cdot 2CH_3OH$ with solvent molecules removed for clarity. Upper left and right, views down the idealized C_3 and C_2 axes with chloride ions omitted; lower left and right, analogous views with chloride ions.

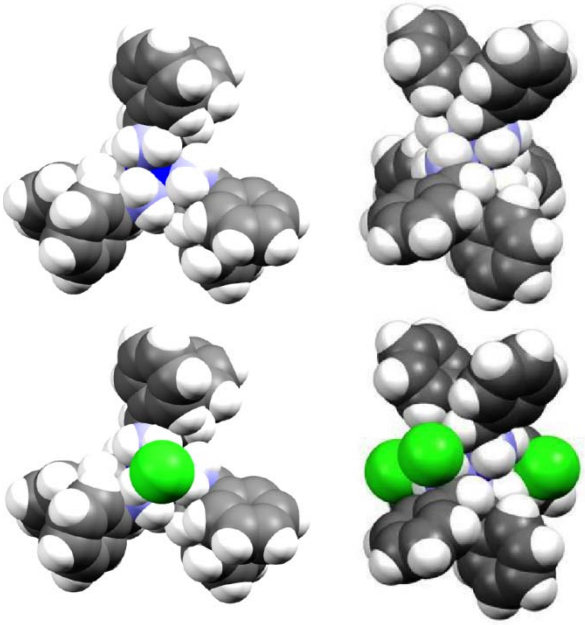

Figure 4.2. Thermal ellipsoid diagram (50% probability level) of Δ-(*S*,*S*)-$\mathbf{1}^{3+}$ $3Cl^-$ $\cdot 12.5H_2O$ with solvent molecules removed for clarity. Upper left and right, views down the idealized C_3 and C_2 axes with chloride ions omitted; lower left and right, analogous views with chloride ions.

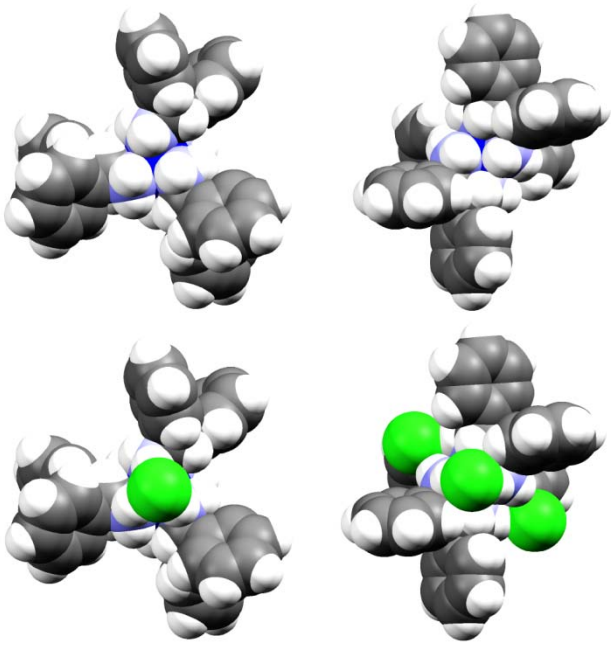

Figure 4.3. Thermal ellipsoid diagram (50% probability level) of Δ-(*R*,*R*)-**1**$^{3+}$ 3Cl^{-} ·H_2O·3CH_3OH with solvent molecules removed for clarity. Upper left and right, views down the idealized C_3 and C_2 axes with chloride ions omitted; lower left and right, analogous views with chloride ions.

The crystal structure of Δ-(*R*,*R*)-**1**$^{3+}$ 3Cl^{-} is shown in Figure 4.3. Though, this complex is the enantiomer of Λ-(*S*,*S*)-**1**$^{3+}$ 3Cl^{-}, a different solvate was obtained because of different crystallization conditions. There were one H_2O and three MeOH molecules within the asymmetric unit. Both of the enantiomers Λ-(*S*,*S*)-**1**$^{3+}$ 3Cl^{-} and Δ-(*R*,*R*)-**1**$^{3+}$ 3Cl^{-} have very similar trication geometries (Table A-6). The difference is that in Λ-(*S*,*S*)-**1**$^{3+}$ 3Cl^{-}, the chelating ligand (*S*,*S*-dpen) adopts a δ conformation, whereas in Δ-(*R*,*R*)-**1**$^{3+}$ 3Cl^{-}, the chelating ligand (*R*,*R*-dpen) adopts a λ conformation. Overall, both of the enantiomers have *lel*$_3$ conformations.

The complexes in Scheme 4.2 were screened as catalysts for additions of malonate esters to *trans*-ß-nitrostyrene (**21a**),[15] as summarized in Scheme 4.3. As shown in entries 1 and 2, di(isopropyl) malonate (**22a**) and **21a** were combined in the presence of Et_3N (1.0 equiv) and Λ- or Δ-(*S*,*S*)-**1**$^{3+}$ 2Cl^{-}BAr$_f^{-}$ (10 mol%) under an ambient air

atmosphere in CD_2Cl_2 at room temperature. Conversions were monitored by ^1H NMR in the presence of an internal standard. Over the course of 2 h, the enantiomeric addition products (*R*)- or (*S*)-**23aa** formed in 88 and >99% yields and 80% ee and 76% ee, respectively, as assayed by chiral HPLC. These impressive lead results also established

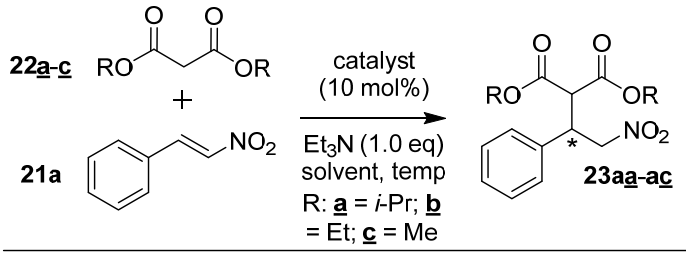

entry	malonate ester	catalyst	conversion (%) (time)[a]	ee (%) (config)[b]
A. CD_2Cl_2, rt[c]				
1	**22a**	Λ-(*S*,*S*)-**1**$^{3+}$ 2Cl$^-$BAr$_f^-$	88 (2 h)	80 (*R*)
2	**22a**	Δ-(*S*,*S*)-**1**$^{3+}$ 2Cl$^-$BAr$_f^-$	>99 (2 h)	76 (*S*)
3	**22b**	Λ-(*S*,*S*)-**1**$^{3+}$ 2Cl$^-$BAr$_f^-$	94 (3 h)	79 (*R*)
4	**22b**	Δ-(*S*,*S*)-**1**$^{3+}$ 2Cl$^-$BAr$_f^-$	99 (1 h)	59 (*S*)
5	**22c**	Λ-(*S*,*S*)-**1**$^{3+}$ 2Cl$^-$BAr$_f^-$	>99 (2 h)	82 (*R*)
6	**22c**	Δ-(*S*,*S*)-**1**$^{3+}$ 2Cl$^-$BAr$_f^-$	>99 (1 h)	40 (*S*)
B. acetone-d_6, 0 °C[c]				
7	**22c**	Λ-(*S*,*S*)-**1**$^{3+}$ 2Cl$^-$BAr$_f^-$	93 (24 h)	87 (*R*)
8	**22c**	Λ-(*S*,*S*)-**1**$^{3+}$ 2BF$_4^-$BAr$_f^-$	94 (10 h)	90 (*R*)
9	**22c**	Λ-(*S*,*S*)-**1**$^{3+}$ 2PF$_6^-$BAr$_f^-$	>99 (4 h)	85 (*R*)
10	**22c**	Λ-(*S*,*S*)-**1**$^{3+}$ 3BAr$_f^-$	>99 (1 h)	80 (*R*)
11	**22c**	Λ-(*S*,*S*)-**1**$^{3+}$ 3BF$_4^-$	>99 (6 h)	93 (*R*)

[a]The conversion was determined by ^1H NMR integration of the *p*-C_6H_5 signal of **21a** versus the internal standard Ph_2SiMe_2. [b]Enantioselectivities were determined by chiral HPLC analyses. [c]Reactions were conducted under ambient air atmospheres.

Scheme 4.3. Initial screening reactions: Data for additions of dialkyl malonates (**22**) to *trans*-β-nitrostyrene (**21a**) catalyzed by Λ- and Δ-(*S*,*S*)-**1**$^{3+}$ 2Cl$^-$BAr$_f^-$ in CD_2Cl_2 at room temperature (entries 1-6), and additions catalyzed by other salts of Λ-(*S*,*S*)-**1**$^{3+}$ in acetone-d_6 at 0 °C (entries 7-11).

that the cobalt configurations control the product configuration. However, when diethyl and dimethyl malonate (**22b**,**c**) were investigated, it became clear that Λ-(*S*,*S*)-$\mathbf{1}^{3+}$ $2Cl^-$ BAr_f^- was a more enantioselective catalyst (**23ab**, 79% (*R*) or 59% (*S*) ee; **23ac**, 82% (*R*) or 40% (*S*) ee). In optimization experiments, acetone was found to be a somewhat better solvent, especially at lower temperatures, and CH_3CN gave in many cases comparable data. Other bases were examined, but none gave better results than Et_3N.

Other salts were investigated, now at 0 °C in acetone-d_6 with **22c**, as summarized in entries 7-12 of Scheme 4.3. With Λ-(*S*,*S*)-$\mathbf{1}^{3+}$ $2Cl^-BAr_f^-$, the ee value of the resulting **23ac** increased to 87%. The other mixed salts Λ-(*S*,*S*)-$\mathbf{1}^{3+}$ $2BF_4^-BAr_f^-$ and Λ-(*S*,*S*)-$\mathbf{1}^{3+}$ $2PF_6^-BAr_f^-$ were comparably effective (90%, 85% ee). The slightly higher enantioselectivity with the former was reproducible, prompting Λ-(*S*,*S*)-$\mathbf{1}^{3+}$ $3BF_4^-$ to be synthesized (above) and tested. Interestingly, this catalyst gave the highest ee value of all (93%). In contrast, the tris(BAr_f) salt Λ-(*S*,*S*)-$\mathbf{1}^{3+}$ $3BAr_f^-$ was the least enantioselective catalyst, with an ee value of 80%.

The catalysts exhibited significant reactivity differences, as signaled by the reaction times in Scheme 4.3. Hence, rate profiles were measured in CD_2Cl_2, but using a lower catalyst loading (2 mol%), a less reactive Michael acceptor (*trans*-4-methoxy-β-nitrostyrene, **21d**), and a lower Et_3N charge (0.35 equiv) to enhance differentiation. As shown in Figure 4.4, the less enantioselective diastereomer, Δ-(*S*,*S*)-$\mathbf{1}^{3+}$ $2Cl^-BAr_f^-$ (■), was significantly more reactive than the more enantioselective diastereomer Λ-(*S*,*S*)-$\mathbf{1}^{3+}$ $2Cl^-BAr_f^-$ (◆). Among the Λ diastereomers, rates increased as the chloride anions in Λ-(*S*,*S*)-$\mathbf{1}^{3+}$ $2Cl^-BAr_f^-$ were replaced by progressively more weakly hydrogen bonding anions ($2Cl^- < 2BF_4^- < 2PF_6^- < 2BAr_f^-$).

These data are interpreted as indicative of substrate activation at the more strongly hydrogen bonding C_3 trication sites, subsequent to initial anion dissociation. In

the mixed salts, the C_2 sites should be unencumbered, or very weakly interacting with BAr_f^-; if these were responsible for catalysis, comparable rates would be expected as the other anions are varied.

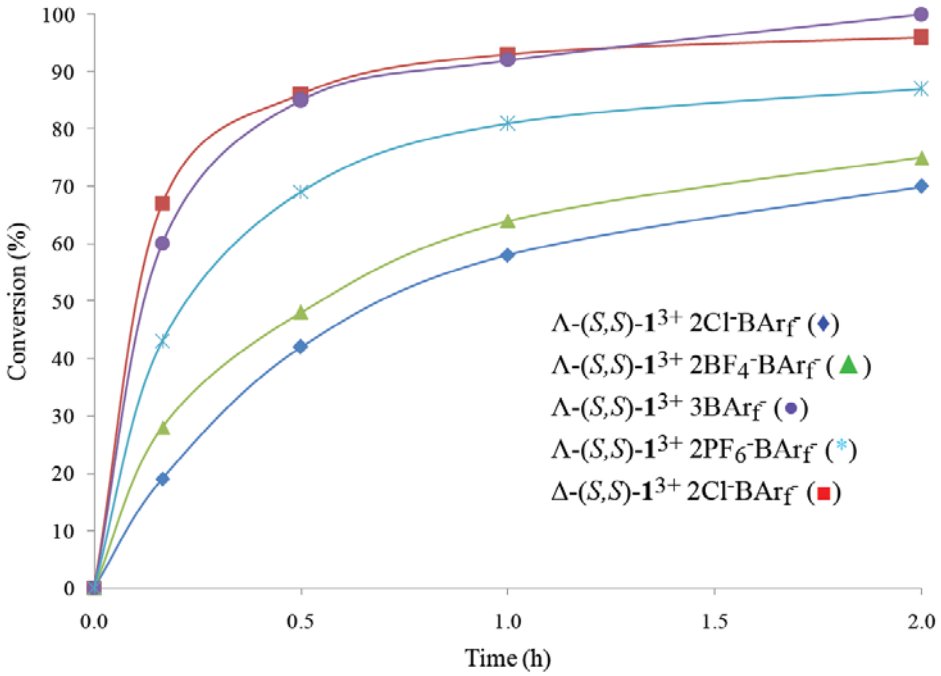

Figure 4.4. Rate profiles for additions of dimethyl malonate (**22c**) to *trans*-4-methoxy-ß-nitrostyrene (**21d**) catalyzed by lipophilic Werner salts. Conditions: 2 mol% catalyst, 0.35 equiv Et_3N, CD_2Cl_2, rt.

In this context, a CD_2Cl_2 solution of Λ-(*S*,*S*)-$\mathbf{1}^{3+}$ $2Cl^-BAr_f^-$ has been titrated with substrates such as *trans*-ß-nitrostyrene (**21a**) and dimethyl malonate (**22c**). Progressive downfield shifts of the upfield (non-hydrogen bonded) NH protons are observed, whereas the downfield (hydrogen bonded) NH protons are essentially unchanged. A series of spectra for a representative titration with **21a** is provided in Figure 4.5.

These experiments show that the C_2 sites are capable of binding substrates, but of course do not establish a reaction pathway. Faster catalysis with the diastereomer Δ-(*S*,*S*)-**1**$^{3+}$ 2Cl^{-}BAr$_f^{-}$ logically follows from the enthalpically weaker interactions of the Δ trication with chloride ion. The lower enantioselectivities would then be ascribed to less favorable architectural factors. With Λ-(*S*,*S*)-**1**$^{3+}$ 2X^{-}BAr$_f^{-}$, the moderate dependence of enantioselectivities upon the anion X^{-} might reflect the continued association of X^{-} with one of the two C_3 sites.

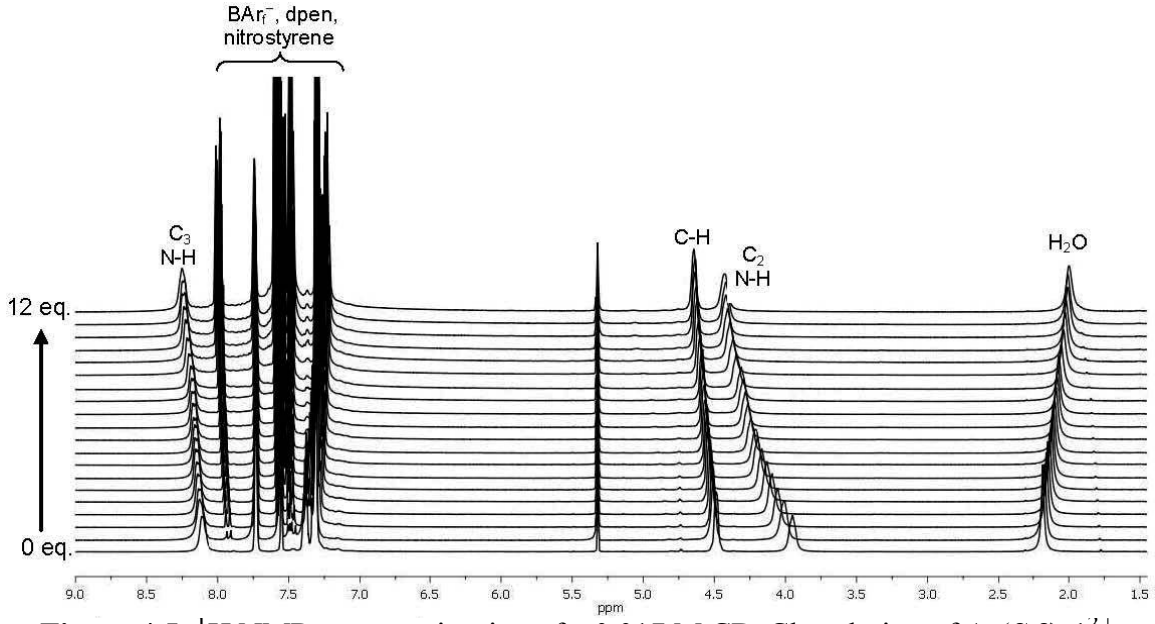

Figure 4.5. ^{1}H NMR spectra: titration of a 0.017 M CD_2Cl_2 solution of Λ-(*S*,*S*)-**1**$^{3+}$ 2Cl^{-}BAr$_f^{-}$ with *trans*-ß-nitrostyrene (**21a**). Data (equiv of **21a**/NH signals, δ in ppm): 0.250/4.010 and 8.127; 0.500/4.053 and 8.134; 0.750/4.094 and 8.141; 1.00/4.129 and 8.131; 1.25/4.165 and 8.155; 1.50/4.195 and 8.158; 1.75/4.204 and 8.162; 2.00/4.241 and 8.169; 2.50/4.28 and 8.179; 2.75/4.296 and 8.183; 3.00/4.31 and 8.178; 4.00/4.342 and 8.184; 5.00/4.368 and 8.196; 6.00/4.387 and 8.227; 7.00/4.405 and 8.236; 8.00/4.418 and 8.234; 9.00/4.432 and 8.249.

Despite any oversimplifications in the preceding models, the enantioselectivity trends in Scheme 4.3 generally hold for a variety of nitroalkene substrates, as

summarized in Scheme 4.4. Reactions were conducted in acetone at 0 °C, with the rates and yields determined by ^{1}H NMR (Λ-(*S*,*S*)-**1**$^{3+}$ 2Cl$^-$BAr$_f^-$) or isolation following chromatography (Λ-(*S*,*S*)-**1**$^{3+}$ 2BF$_4^-$BAr$_f^-$, Λ-(*S*,*S*)-**1**$^{3+}$ 3BF$_4^-$). In eight out of ten cases, the second catalyst afforded higher enantioselectivities than the first; the third tris(tetrafluoroborate) catalyst was superior in all cases, delivering an average of 94% ee for the aryl-substituted nitroalkenes. A good ee value was also obtained with an alkyl-substituted nitroalkene (**21l**, 86% ee).[20] Although these enantioselectivities have been matched or slightly exceeded by organic hydrogen bond donor catalysts,[15,20] these were in all cases bifunctional, incorporating the amine base. Thus, Scheme 4.4 represents an impressive debut for a new catalyst family at an early stage of development. Furthermore, Λ-(*S*,*S*)-**1**$^{3+}$ 2Cl$^-$BAr$_f^-$ is easily recovered in near quantitative yields chromatographically (experimental section).

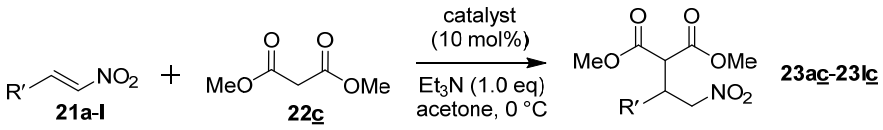

entry	R′	alkene/ product	Λ-(*S*,*S*)-**1**$^{3+}$ 2Cl^{-}BAr$_f^{-}$ time (h)	yield (%)[a]	ee (%)[b]	Λ-(*S*,*S*)-**1**$^{3+}$ 2BF$_4^{-}$BAr$_f^{-}$ time (h)	yield (%)[c]	ee (%)[b]	Λ-(*S*,*S*)-**1**$^{3+}$ 3BF$_4^{-}$ time (h)	yield (%)[c]	ee (%)[b]
1		**21a/23ac**	15	94	87 *R*	12	97	90 *R*	6	97	93 *R*
2	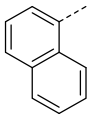	**21b/23bc**	20	>99	92 *R*	12	98	93 *R*	12	98	95 *R*
3	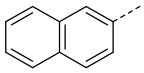	**21c/23cc**	20	95	88 *R*	12	92	83 *R*	12	96	93 *R*
4	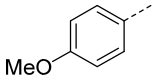	**21d/23dc**	20	95	82 *R*	18	87	78 *R*	12	95	85 *R*
5	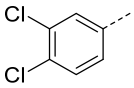	**21e/23ec**	20	>99	80 *R*	12	94	90 *R*	12	93	93 *R*
6		**21f/23fc**	24	98	81 *R*	12	86	86 *R*	-	-	-
7	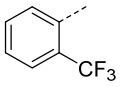	**21g/23gc**	20	>99	90 *R*	12	98	93 *R*	12	97	95 *R*
8	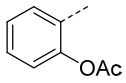	**21h/23hc**	21	98	84 *R*	12	96	94 *R*	12	97	96 *R*
9	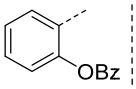	**21i/23ic**	48	94	92 *R*	18	86	93 *R*	12	95	96 *R*
10	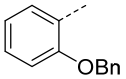	**21j/23jc**	22	98	94 *R*	12	95	96 *R*	12	98	98 *R*
11		**21k/23kc**	-	-	-	12	91	91 *S*	12	96	92 *S*
12		**21l/23lc**	-	-	-	12	83	80 *S*	18	93	86 *S*

[a]Yields were determined by ^{1}H NMR integration of a nitroolefin and/or product signal versus the internal standard Ph_2SiMe_2.
[b]Enantioselectivities were determined by chiral HPLC analyses. [c]Isolated yield after column chromatography.

Scheme 4.4. Substrate scope. Data for additions of dimethyl malonate (**22c**) to nitroalkenes catalyzed by Λ-(*S*,*S*)-**1**$^{3+}$ 2Cl^{-}BAr$_f^{-}$, Λ-(*S*,*S*)-**1**$^{3+}$ 2BF$_4^{-}$BAr$_f^{-}$, and Λ-(*S*,*S*)-**1**$^{3+}$ 3BF$_4^{-}$.

4.3. Discussion

Several additional themes merit emphasis. First, as established by chemists at Diaminopharm Inc. analogs of dpen with substituted aryl groups are readily available.[21] New families of catalysts in which the phenyl group has been replaced by other aromatic groups have been discussed in section 3. Chiral counter anions are easily introduced by extending Scheme 4.2. Thus, it should be possible to further optimize catalysis by exploiting these diversity elements, and by synthesizing bifunctional tertiary amine containing analogs.[22] Some of the systems described in section 7 may give improved results.

Second, many chiral ligands with a C_3 symmetry axis are known, but metal containing catalysts in which the active sites have C_3 symmetry (i.e., devoid of symmetry lowering ancillary ligands) are much less common, especially with transition metals.[23] Some transition metal based catalytic systems considered to have C_3 symmetric active sites are shown in Figure 4.6.[23b] The catalytic system in Figure 4.6-**A** was highly effective in asymmetric allylic oxidations. The Cu^{2+} is proposed to complex with the C_3 symmetric ligand N(CH_2-ox) *in situ* to give a highly enantioselective catalyst (up to 84% ee).

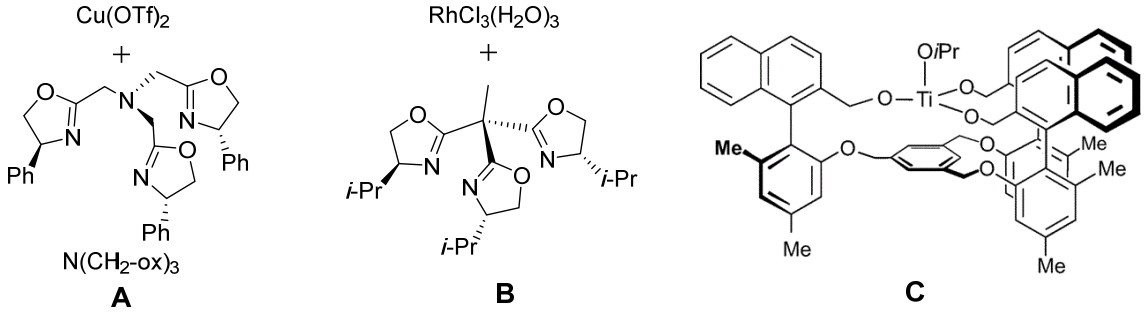

Figure 4.6. Catalytic systems with active sites having C_3 symmetry.

Similarly, in the catalytic system Figure 4.6-**B** rhodium(III) reacts with C_3 symmetric ligand tris(oxazoline) to give tris(oxazoline)rhodium complex, which catalyzes the asymmetric cyclopropanation of styrene with *tert*-butyl and ethyl diazoacetate with high stereoselectivity (up to 56% de and 67% ee). The rigid, C_3-symmetric titanium complex in Figure 4.6-**C** was formed *in situ* and catalyzed the ethylation of benzaldehyde with enantioselectivities of up to 98%.

Third, note that most other hydrogen bond donor catalysts feature two donor groups (e.g., thioureas). Since, per the crystallographic data[8] and other evidence, the title complexes are capable of 3-5 or more simultaneous NH interactions, they can potentially give rise to new chemistries, i.e. transformations that cannot be realized with established catalysts. Efforts involving all of these themes are in progress and will be reported in due course.

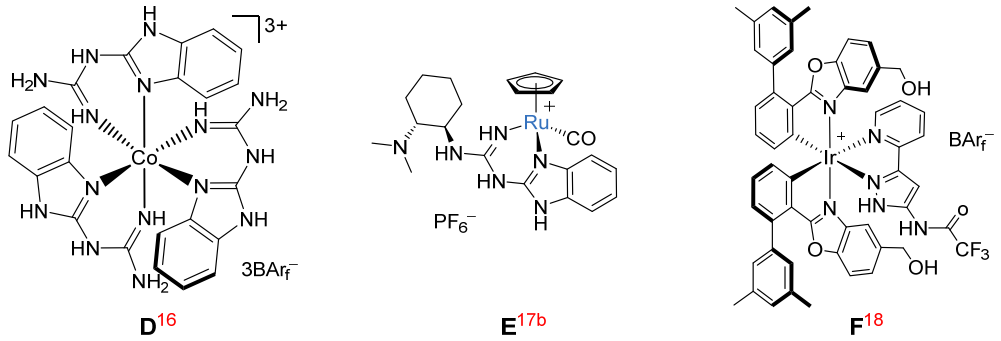

D[16] **E**[17b] **F**[18]

Figure 4.7. Metal catalysts with hydrogen bond donors *remote* from coordinating atoms.

Finally, there are other recently published metal catalysts with hydrogen bond donors *remote* from coordinating atoms, some of them are shown in Figure 4.7.[16-18] This study underscores the rich possibilities associated with enantioselective second coordination sphere promoted catalysis. This may presage a revival of interest in classical

NH coordination compounds, many of which feature inexpensive metals and ligands, can be utilized under an air atmosphere as in the above reactions, and can (when chiral) easily be obtained in enantiopure form. Such systems promise, in both conceptual and practical senses, to be transformational new additions to the chiral pool.

4.4. Experimental section

General Data. NMR spectra were recorded on a Varian NMRS 500 MHz spectrometer at ambient probe temperatures. Chemical shifts (δ in ppm) were referenced to residual solvent signals (^{1}H: $CHCl_3$, 7.26; 2.50; $CDHCl_2$, 5.32; acetone-d_5, 2.05; ^{13}C: $CDCl_3$, 77.2; CD_2Cl_2, 54.0; acetone-d_6, 29.8). IR spectra were recorded on a Shimadzu IRAffinity-1 spectrometer (Pike MIRacle ATR system, diamond/ZnSe crystal). Melting points were determined using an OptiMelt MPA 100 instrument. Microanalyses were conducted by Atlantic Microlab. HPLC analyses were carried out with a Shimadzu instrument package (pump/autosampler/detector LC-20AD/SIL-20A/SPD-M20A).

NMR solvents (Cambridge Isotopes) were treated as follows: $CDCl_3$, CD_2Cl_2, and acetone-d_6, stored over molecular sieves. HPLC solvents (hexanes, Fischer; isopropanol, JT Baker; both HPLC Grade) were degassed before use. CH_2Cl_2 (EMD Chemicals, ACS grade), CH_3OH (EMD, anhydrous, 99.8%), hexanes (Macron, ACS grade), EtOAc (Macron, ACS grade), and acetone (BDH, ACS grade), used as received unless noted.

Reactions were conducted under air unless noted. The syntheses and the equilibrium studies of the salts of (*S*,*S*)-**1**$^{3+}$ are described in the section 3. Chemicals were treated as follows. The *trans*-β-nitrostyrene (**21a**, Alfa Aesar, 98%) was column chromatographed (silica gel, 9:1 v/v hexanes/EtOAc). The *trans*-4-methoxy-β-nitrostyrene (**21d**), 3,4-dichloro-β-nitrostyrene (**21e**), and 1-(2-furyl)-2-nitroethylene (**21k**) were used as received from Alfa Aesar (NMR showed **21e,k** to be >98% *trans*). Other previously reported nitroolefins (**21b-c**, **21f-g**, **21j**, **21l**; see Scheme 4.4) were prepared by Henry reactions of nitromethane and the corresponding aldehydes.[24] Dimethyl malonate (**22c**, Alfa Aesar, 98%), diethyl malonate (**22b**, Alfa Aesar, 99%), diisopropyl malonate (**22a**, TCI, 99%), *trans*-2-(2-nitrovinyl)phenol (Aldrich, 97%), acetyl chloride

(Aldrich, 98%), benzoyl chloride (Aldrich, 99%), Et_3N (Alfa Aesar, 98%), silica gel (Silicycle SiliaFlash® F60), and Na_2SO_4 (EMD) were used as received.

Representative ^{1}H NMR titration. A 5 mm NMR tube was charged with Λ-(*S*,*S*)-**1**$^{3+}$ $2Cl^-BAr_f^-\cdot 2H_2O$ (0.0141 g, 0.00848 mmol) and CD_2Cl_2 (0.5 mL). A solution of **21a** (2.1 M in CD_2Cl_2) was added in increments of 0.001 mL (0.25 equiv) and ^{1}H NMR spectra were recorded. Selected peaks shifted, as shown by the spectra in Figure 4.5 (see text).

Syntheses of previously unreported nitroolefins. A (*trans*-2-acetoxy-β-nitrostyrene; 21h). A Schlenk flask was charged with *trans*-2-(2-nitrovinyl)phenol (0.5871 g, 3.54 mmol),[24a] Et_3N (0.500 mL, 3.58 mmol, 1.01 equiv), and CH_2Cl_2 (10 mL, dried and degassed using a Glass Contour solvent purification system) under N_2. The solution was cooled to 0 °C and acetyl chloride (0.375 mL, 5.28 mmol, 1.49 equiv) was added dropwise by syringe with stirring. The cold bath was removed. After 12 h, CH_2Cl_2 (50 mL) was added. The mixture was washed with H_2O (50 mL), 1.0 M HCl, (50 mL), and brine (50 mL). The organic layer was dried (Na_2SO_4) and the solvent was removed by rotary evaporation. The residue was chromatographed on a silica gel column (80:20 v/v hexanes/EtOAc). The solvent was removed from the combined product fractions by rotary evaporation. The residue was dried by oil pump vacuum at room temperature to give **21h** as a pale yellow solid (0.473 g, 2.28 mmol, 65%), which became a wax at 69-71 °C and liquefied at 74-76 °C (open capillary). Anal. Calcd. for $C_{10}H_9NO_4$ (207.18): C 57.97, H 4.38, N 6.76; found C 58.13, H 4.40, N 6.73. **B. (*trans*-2-benzoyloxy-β-nitrostyrene; 21i).** *trans*-2-(2-nitrovinyl)phenol (0.5943 g, 3.60 mmol),[24a] Et_3N (0.630 mL, 4.52 mmol, 1.26 equiv), CH_2Cl_2 (10 mL, dried and degassed using a Glass Contour solvent purification system), and benzoyl chloride (0.790 mL, 6.81 mmol, 1.89 equiv) were combined in a procedure analogous to A. An

identical workup gave **21i** as a pale yellow solid (0.6629 g, 2.46 mmol, 69%), which became a wax at 78-82 °C and liquefied at 87-89 °C (open capillary). Anal. Calcd. for $C_{15}H_{11}NO_4$ (269.25): C 66.91, H 4.12, N 5.20; found C 67.04, H 4.20, N 5.01.

Data for **21h**. NMR ($CDCl_3$, δ in ppm): ^{1}H (500 MHz) 8.06 (d, $^3J_{HH}$ = 13.5 Hz, 1H, C**H**NO_2), 7.61-7.58 (m, 2H, C**H**=$CHNO_2$ and 1H of C_6**H**$_4$), 7.52 (t, $^3J_{HH}$ = 8.5 Hz, 1H of C_6**H**$_4$), 7.32 (t, $^3J_{HH}$ = 7.5 Hz, 1H of C_6**H**$_4$), 7.23 (d, $^3J_{HH}$ = 8.5 Hz, 1H of C_6**H**$_4$), 2.43 (s, 3H, C**H**$_3$); ^{13}C{^{1}H} (125 MHz): 168.8 (s, **C**(O)Me), 150.2, 138.7, 133.2, 133.1, 129.1, 126.8, 123.8, 123.0 (8 × s, **C**$_6$H$_4$, **C**H=**C**HNO_2), 21.2 (s, **C**H$_3$). IR (powder film, cm^{-1}): 3115 (w), 1753 (s), 1638 (m), 1510 (s), 1339 (vs), 1194 (vs), 963 (s), 758 (s).

Data for **21i**. NMR ($CDCl_3$, δ in ppm): ^{1}H (500 MHz) 8.24 (m, 2H, C**H**NO_2 and 1 H of C_6**H**$_5$/C_6**H**$_4$), 8.13 (d, $^3J_{HH}$ = 13.5 Hz, 1H, C**H**=$CHNO_2$), 7.70 (t, $^3J_{HH}$ = 7.5 Hz, 1H of C_6**H**$_5$/ C_6**H**$_4$), 7.66-7.56 (m, 5H of C_6**H**$_5$/C_6**H**$_4$), 7.38-7.33 (m, 2H of C_6**H**$_5$/C_6**H**$_4$); ^{13}C{^{1}H} (125 MHz) 164.7 (s, **C**(O)Ph), 150.6 138.7, 134.5, 133.2, 133.2, 130.5, 129.2, 129.1, 128.5, 126.9, 124.0, 123.4 (12 × s, **C**H=**C**HNO_2, **C**$_6$H$_4$, **C**$_6$H$_5$). IR (powder film, cm^{-1}): 3105 (w), 1742 (s), 1340 (s), 1209 (vs), 1057 (vs), 700 (vs).

Rate profiles, Figure 4.4. A 5 mm NMR tube was charged with a solution of **21d** (0.0180 g, 0.101 mmol), dimethyl malonate (**22c**, 0.0127 mL, 0.111 mmol, 1.10 equiv), catalyst (0.0020 mmol, 0.020 equiv), and Ph_2SiMe_2 (0.0020 mL, internal standard) in CD_2Cl_2 (1.0 mL). A ^{1}H NMR spectrum was recorded to measure the initial ratio of **21d** to the standard. Then Et_3N (0.0050 mL, 0.036 mmol, 0.36 equiv) was added and the conversion to **23ac** was periodically measured by ^{1}H NMR. After 2 h, the mixture was loaded directly onto a plug of silica gel. The **23ac** was eluted with hexanes/EtOAc (1:1 v/v, 50 mL). The solvent was removed by rotary evaporation. The ee was assayed by chiral HPLC.[26]

Reactions, Scheme 4.3. A (entries 1-6). A 5 mm NMR tube was charged with a

solution of **21a** (0.0054 g, 0.036 mmol, 1.0 equiv), dialkyl malonate (**22**, 0.039 mmol, 1.1 equiv), catalyst (0.0036 mmol, 0.10 equiv), and Ph_2SiMe_2 (0.0020 mL, internal standard) in CD_2Cl_2 (0.40 mL). A ^1H NMR spectrum was recorded to measure the initial ratio of the nitroolefin to the standard. Then Et_3N (0.0050 mL, 0.0036 g, 0.036 mmol, 1.0 equiv) was added. The conversion was monitored by ^1H NMR. After the specified time (Scheme 4.3), the mixture was loaded onto a plug of silica gel. The organic product (**23a<u>a</u>-a<u>c</u>**) was eluted with hexanes/EtOAc (1:1 v/v, 50 mL). The solvent was removed by rotary evaporation. The product ee was assayed by chiral HPLC.[26] **B (entries 7-11).** A 5 mm NMR tube was charged with a solution of **21a** (0.0149 g, 0.10 mmol, 1.0 equiv), **22<u>c</u>**, (0.0138 mL, 0.0158 g, 0.120 mmol, 1.2 equiv), catalyst (0.010 mmol, 0.10 equiv), and Ph_2SiMe_2 (0.0020 mL, internal standard) in acetone-d_6 (0.7 mL). A ^1H NMR spectrum was recorded to measure the initial ratio of the nitroolefin to the standard. The sample was cooled to 0 °C, and Et_3N (0.0140 mL, 0.0101 g, 0.10 mmol, 1.0 equiv) was added. The conversion to **23a<u>c</u>** was monitored by ^1H NMR. After the specified time (Scheme 4.3), the mixture was loaded directly onto a plug of silica gel. The **23a<u>c</u>** was eluted with hexanes/EtOAc (7:3 v/v, 50 mL). The solvent was removed by rotary evaporation. The ee was assayed by chiral HPLC.[26]

Reactions, Scheme 4.4. A (with Λ-(*S*,*S*)-$\mathbf{1}^{3+}$ 2Cl$^-$BAr$_f^-$). A 5 mm NMR tube was charged with a solution of nitroolefin (0.036 mmol, 1.0 equiv), Λ-(*S*,*S*)-$\mathbf{1}^{3+}$ 2Cl$^-$ BAr$_f^-$·2H$_2$O (0.0059 g, 0.0036 mmol, 0.10 equiv), **22<u>c</u>** (0.0045 mL, 0.0052 g, 0.039 mmol, 1.1 equiv), and Ph_2SiMe_2 (0.0020 mL, internal standard) in acetone-d_6 (0.40 mL). A ^1H NMR spectrum was recorded to measure the initial ratio of the nitroolefin to the standard. The sample was cooled to 0 °C, and Et_3N (0.0050 mL, 0.0036 g, 0.036 mmol, 1.0 equiv) was added. The conversion was monitored by ^1H NMR. After the specified time (Scheme 4.4), the mixture loaded onto a plug of silica gel. The organic

product (**23a<u>c</u>-j<u>c</u>**) was eluted with hexanes/EtOAc (1:1 v/v). The solvent was removed by rotary evaporation. The product was dried by oil pump vacuum at room temperature and the ee assayed by chiral HPLC (Figures A-2 to A-15).[26] **B (with Λ-(*S*,*S*)-1^{3+} 2BF$_4^-$ BAr$_f^-$).** A round bottom flask was charged with a solution of nitroolefin (0.355 mmol, 1.0 equiv), Λ-(*S*,*S*)-**1**$^{3+}$ 2BF$_4^-$BAr$_f^-$·3H$_2$O (0.0634 g, 0.0355 mmol, 0.10 equiv), and **22<u>c</u>** (0.0458 mL, 0.0529 g, 1.13 equiv) in acetone (3.3 mL), and cooled to 0 °C. Then Et$_3$N (0.0495 mL, 0.0359 g, 0.355 mmol, 1.0 equiv) was added. The reaction was monitored by TLC. After the specified time (Scheme 4.4), the solvent was removed by rotary evaporation and the residue was dissolved in CH$_2$Cl$_2$ (2 mL). The orange solution was chromatographed on a silica gel column (1.9 × 14 cm, 9:1 v/v hexanes/ EtOAc). The solvent was removed from the product containing fractions by rotary evaporation. The product was dried by oil pump vacuum at room temperature (yields: Scheme 4.4) and the ee assayed by chiral HPLC (Figures A-2 to A-15 in appendix).[26] **C (with Λ-(*S*,*S*)-1^{3+} 3BF$_4^-$).** A 5 mL vial was charged with a solution of nitroolefin (0.10 mmol, 1.0 equiv), Λ-(*S*,*S*)-**1**$^{3+}$ 3BF$_4^-$·2H$_2$O (0.0099 g, 0.010 mmol, 0.1 equiv), **22<u>c</u>** (0.0138 mL, 0.0158 g, 0.120 mmol, 1.2 equiv), and Ph$_2$SiMe$_2$ (0.0020 mL, internal standard) in acetone-d_6 (0.70 mL). A ^{1}H NMR spectrum was recorded to measure the initial ratio of the nitroolefin to the standard. The sample was cooled to 0 °C, and Et$_3$N (0.0140 mL, 0.0101 g, 0.10 mmol, 1.0 equiv) was added. The reaction was monitored by ^{1}H NMR and TLC. After the specified time (Scheme 4.4), the mixture was worked up as described in B.

Catalyst recycling, Λ-(*S*,*S*)-1^{3+} 2Cl$^-$BAr$_f^-$. A round bottom flask was charged with a solution of **21a** (0.0529 g, 0.355 mmol, 1.0 equiv), Λ-(*S*,*S*)-**1**$^{3+}$ 2Cl$^-$BAr$_f^-$·2H$_2$O (0.0543 g, 0.0326 mmol, 0.0918 equiv), and **22<u>c</u>** (0.0460 mL, 0.401 mmol, 1.13 equiv) in acetone (3.3 mL), and cooled to 0 °C. Then Et$_3$N (0.0460 mL, 0.0333 g, 0.330 mmol,

0.93 equiv) was added. The reaction was monitored by TLC. After 15 h, the solvent was removed by rotary evaporation and the residue was dissolved in CH_2Cl_2 (2 mL). The orange solution was washed with 3.0 M HCl (1 mL) and H_2O (2 × 1 mL) and chromatographed on a silica gel column (1.9 × 14 cm, 9:1 v/v hexanes/EtOAc). The solvent was removed from the organic product containing fractions by rotary evaporation and oil pump vacuum to give **23a<u>c</u>** as a white solid (0.0940 g, 0.334 mmol, 94%), which was analyzed by HPLC and ^{1}H and $^{13}C\{^1H\}$ NMR as described below. The column was then washed with CH_2Cl_2 and the orange catalyst band was eluted with CH_2Cl_2/CH_3OH (98:2 v/v). The solvent was removed by rotary evaporation and oil pump vacuum at room temperature to recover Λ-(*S*,*S*)-$\mathbf{1}^{3+}$ $2Cl^-BAr_f^-\cdot H_2O$ (0.0526 g, 0.0319 mmol, 98%). Anal. Calcd. for $C_{74}H_{60}BCl_2CoF_{24}N_6\cdot H_2O$ (1647.94): C 53.91, H 3.79, N 5.10; found C 53.84, H 4.08, N 4.96.

Diisopropyl 2-(2-nitro-1-phenylethyl)malonate (23a<u>a</u>).[27] This known compound was obtained as a spectroscopically pure colorless oil per the general procedures for Scheme 4.3. NMR ($CDCl_3$, δ in ppm):[28] ^{1}H (500 MHz) 7.32-7.22 (m, 5H, $C_6\mathbf{H}_5$), 5.08 (sept, $^3J_{HH}$ = 6.0 Hz, 1H, C**H**$(CH_3)_2$), 4.92 (dd, $^2J_{HH}$ = 13.0 Hz, $^3J_{HH}$ = 4.5 Hz, 1H, C**H**H'NO_2), 4.86-4.60 (m, 2H, C'**H**$(C'H_3)_2$ and CH**H**'NO_2), 4.20 (td, $^3J_{HH}$ = 8.5 Hz, $^3J_{HH}$ = 5.0 Hz, 1H, C**H**=CH_2NO_2), 3.75 (d, $^3J_{HH}$ = 9.5 Hz, 1H, C**H**$(CO_2i\text{Pr})_2$), 1.24 (d, $^3J_{HH}$ = 6.5 Hz, 6H, CH$(C\mathbf{H}_3)_2$), 1.07 (d, $^3J_{HH}$ = 6.0 Hz, 3H, C'H$((C\mathbf{H}_3)(C'H_3))$), 1.01 (d, $^3J_{HH}$ = 6.5 Hz, 3H, C'H$((CH_3)(C'\mathbf{H}_3))$); $^{13}C\{^1H\}$ (125 MHz): 167.2 (s, **C**O_2iPr), 166.5 (s, **C**'O_2iPr), 136.4 (s, *i*), 129.0 (s, *o*), 128.4 (s, *p*), 128.3 (s, *m*),[25] 78.1 (s, **C**H_2NO_2), 70.1 (s, **C**$H(CH_3)_2$), 69.7 (s, **C**'$H(C'H_3)_2$), 55.3 (s, **C**$H(CO_2i\text{Pr})_2$), 43.1 (s, **C**H=CH_2NO_2), 21.7, 21.6, 21.41, 21.39 (4 × s, 4 × **C**H_3).

Enantiomeric excesses were determined by HPLC (see Figure A-2) with a Chiralcel OD column (95:05 v/v hexane/isopropanol, 0.75 mL/min, λ = 220 nm); for Λ-

(*S*,*S*)-**1**$^{3+}$ 2Cl^{-}BAr$_f^{-}$, t_R = 10.8 min (major), 13.3 min (minor); for Δ-(*S*,*S*)-**1**$^{3+}$ 2Cl^{-} BAr$_f^{-}$, similar but with major/minor reversed.[26]

Diethyl 2-(2-nitro-1-phenylethyl)malonate (23a<u>b</u>).[27] This known compound was obtained as a spectroscopically pure colorless oil per the general procedures for Scheme 4.3. NMR ($CDCl_3$, δ in ppm):[28] ^{1}H (500 MHz) 7.33-7.22 (m, 5H, $C_6\mathbf{H}_5$), 4.92 (dd, $^2J_{HH}$ = 13.5 Hz, $^3J_{HH}$ = 5.0 Hz, 1H, C**H**H'NO_2), 4.86 (dd, $^2J_{HH}$ = 13.0 Hz, $^3J_{HH}$ = 9.0 Hz, 1H, CH**H**'NO_2), 4.26-4.19 (m, 3H, C**H**$_2$C'H$_3$ and C**H**=C'H$_2$NO$_2$), 4.00 (q, $^3J_{HH}$ = 7.5 Hz, 2H, C'**H**$_2$C'H$_3$), 3.81 (d, $^3J_{HH}$ = 9.5 Hz, 1H, C**H**(C'O$_2$Et)$_2$), 1.26 (t, $^3J_{HH}$ = 7.0 Hz, 3H, CH$_2$C**H**$_3$), 1.04 (t, $^3J_{HH}$ = 7.0 Hz, 3H, C'H$_2$C'**H**$_3$); $^{13}C\{^1H\}$ (125 MHz): 167.6 (s, **C**O$_2$Et), 166.9 (s, **C**'O$_2$Et), 136.3 (s, *i*), 129.1 (s, o), 128.5 (s, *p*) 128.1 (s, *m*),[25] 77.8 (s, **C**H$_2$NO$_2$), 62.3 (s, **C**H$_2$CH$_3$), 62.0 (s, **C**'H$_2$C'H$_3$), 55.1 (s, **C**H(C'O$_2$Et)$_2$), 43.1 (s, **C**H=CH$_2$NO$_2$), 14.1 (s, **C**H$_3$), 13.9 (s, **C**'H$_3$).

Enantiomeric excesses were determined by HPLC (see Figure A-3) with a Chiralpak AS-H column (90:10 v/v hexane/isopropanol, 1.0 mL/min, λ = 220 nm); for Λ-(*S*,*S*)-**1**$^{3+}$ 2Cl^{-}BAr$_f^{-}$, t_R = 12.7 min (minor), 14.3 min (major); for Δ-(*S*,*S*)-**1**$^{3+}$ 2Cl^{-} BAr$_f^{-}$, similar but with major/minor reversed.[26]

Dimethyl 2-(2-nitro-1-phenylethyl)malonate (23a<u>c</u>).[27] This known compound was isolated as a white solid per the general procedures for Scheme 4.4. NMR ($CDCl_3$, δ in ppm):[28] ^{1}H (500 MHz) 7.33-7.21 (m, 5H, $C_6\mathbf{H}_5$), 4.93 (dd, $^2J_{HH}$ = 13.0 Hz, $^3J_{HH}$ = 5.0 Hz, 1H, C**H**H'NO_2), 4.87 (dd, $^2J_{HH}$ = 13.0 Hz, $^3J_{HH}$ = 9.0 Hz, 1H, CH**H**'NO_2), 4.24 (td, $^3J_{HH}$ = 9.0 Hz, $^3J_{HH}$ = 5.0 Hz, 1H, C**H**=C'H$_2$NO$_2$), 3.86 (d, $^3J_{HH}$ = 9.0 Hz, 1H, C**H**(C'O$_2$Me)$_2$), 3.75 (s, 3H, C**H**$_3$), 3.54 (s, 3H, C'**H**$_3$); $^{13}C\{^1H\}$ (125 MHz) 167.9 (s, **C**O$_2$Me), 167.3 (s, **C**'O$_2$Me), 136.2 (s, *i*), 129.1 (s, *o*) 128.4 (s, *p*), 128.0 (s, *m*), 77.5 (s, **C**H$_2$NO$_2$), 54.8 (s, **C**H(C'O$_2$Me)$_2$), 53.1 (s, **C**H$_3$), 52.9 (s, **C**'H$_3$), 43.0 (s, **C**H=CH$_2$NO$_2$).

Enantiomeric excesses were determined by HPLC (see Figure A-4) with a Chiralpak AD column (98:02 v/v hexane/isopropanol, 1.0 mL/min, λ = 220 nm); for Λ-(*S*,*S*)-**1**$^{3+}$ 2$BF_4^-$$BAr_f^-$ (Λ-(*S*,*S*)-**1**$^{3+}$ 2$Cl^-$$BAr_f^-$ similar), t_R = 32.4 min (major), 42.3 min (minor); for Λ-(*S*,*S*)-**1**$^{3+}$ 3BF_4^-, t_R = 33.3 min (major), 43.4 min (minor); for Δ-(*S*,*S*)-**1**$^{3+}$ 2$Cl^-$$BAr_f^-$, similar but with major/minor reversed.[26]

Dimethyl 2-(2-nitro-1-α-naphthylethyl)malonate (23bc).[15a,b] This known compound was isolated as a colorless oil per the general procedures for Scheme 4. NMR ($CDCl_3$, δ in ppm):[28] ^{1}H (500 MHz) 8.18 (d, $^3J_{HH}$ = 8.5 Hz, 1H of $C_{10}\mathbf{H}_7$), 7.87 (d, $^3J_{HH}$ = 8.0 Hz, 1H of $C_{10}\mathbf{H}_7$), 7.80 (d, $^3J_{HH}$ = 8.0 Hz, 1H of $C_{10}\mathbf{H}_7$), 7.62 (t, $^3J_{HH}$ = 8.5 Hz, 1H of $C_{10}\mathbf{H}_7$), 7.53 (t, $^3J_{HH}$ = 8.0 Hz, 1H of $C_{10}\mathbf{H}_7$), 7.44-7.38 (m, 2H of $C_{10}\mathbf{H}_7$), 5.25-5.16 (m, 2H, C**H**H′NO_2 and C**H**=CH_2NO_2), 5.07 (dd, $^2J_{HH}$ = 13.5 Hz, $^3J_{HH}$ = 4.5 Hz, 1H, CH**H**'NO_2), 4.12 (d, $^3J_{HH}$ = 7.5 Hz, 1H, C**H**$(CO_2Me)_2$), 3.72 (s, C$\mathbf{H}_3$), 3.54 (s, C'$\mathbf{H}_3$); $^{13}C\{^1H\}$ (125 MHz) 168.1 (s, **C**O_2Me), 167.6 (s, **C**'O_2Me), 134.3, 132.3, 131.1, 129.4, 129.2, 127.2, 126.2, 125.2, 124.1, 122.3 (10 × s, $\mathbf{C}_{10}H_7$), 76.7 (s, **C**H_2NO_2), 54.6 (s, **C**H$(CO_2Me)_2$), 53.1 (s, **C**H_3), 53.0 (s, **C**'H_3), 36.9 (s, **C**H=CH_2NO_2).

Enantiomeric excesses were determined by HPLC (see Figure A-5) with a Chiralpak AD column (90:10 v/v hexane/isopropanol, 1.0 mL/min, λ = 254 nm); for all catalysts t_R = 13.5-14.1 min (major), 18.9-19.6 min (minor).[26]

Dimethyl 2-(2-nitro-1-β-naphthylethyl)malonate (23cc).[15b,c] This known compound was isolated as a yellow solid per the general procedures for Scheme 4.4. NMR ($CDCl_3$, δ in ppm):[28] ^{1}H (500 MHz) 7.83-7.79 (m, 3H of $C_{10}\mathbf{H}_7$), 7.70 (s, 1H of $C_{10}\mathbf{H}_7$), 7.50-7.48 (m, 2H of $C_{10}\mathbf{H}_7$), 7.34 (d, $^3J_{HH}$ = 8.5 Hz, 1H of $C_{10}\mathbf{H}_7$), 5.01 (d, $^3J_{HH}$ = 8.0 Hz, 2H, C$\mathbf{H}_2NO_2$), 4.43 (q, $^3J_{HH}$ = 7.0 Hz, 1H, C**H**=CH_2NO_2), 3.98 (d, $^3J_{HH}$ = 9.0 Hz, 1H, C**H**$(CO_2Me)_2$), 3.77 (s, 3H, C$\mathbf{H}_3$), 3.54 (s, 3H, C'$\mathbf{H}_3$); $^{13}C\{^1H\}$ (125 MHz) 166.0 (s, **C**O_2Me), 167.4 (s, **C**'O_2Me), 133.7, 133.4, 133.2, 129.1, 128.1, 127.8,

127.5, 126.7, 126.6, 125.3 (10 × s, $\mathbf{C}_{10}H_7$), 77.5 (s, $\mathbf{C}H_2NO_2$), 54.9 (s, $\mathbf{C}H(CO_2Me)_2$), 53.2 (s, $\mathbf{C}H_3$), 53.0 (s, $\mathbf{C}'H_3$), 43.2 ($\mathbf{C}H{=}CH_2NO_2$).

Enantiomeric excesses were determined by HPLC (see Figure A-6) with a Chiralcel OD column (70:30 v/v hexane/isopropanol, 1.0 mL/min, λ = 254 nm); for Λ-(*S*,*S*)-$\mathbf{1}^{3+}$ $2BF_4^-BAr_f^-$, t_R = 14.4 min (major), 39.2 min (minor); for Λ-(*S*,*S*)-$\mathbf{1}^{3+}$ $3BF_4^-$ (older column), t_R = 12.5 min (major), 37.0 min (minor).[26]

Dimethyl 2-(2-nitro-1-(4-methoxyphenyl)ethyl)malonate (23dc).[15b,c] This known compound was isolated as a colorless oil per the general procedures for Scheme 4.4. NMR ($CDCl_3$, δ in ppm):[28] ^{1}H (500 MHz) 7.14 (d, $^3J_{HH}$ = 8.5 Hz, 2H, *m* to CH), 6.83 (d, $^3J_{HH}$ = 8.5 Hz, 2H, *o* to CH), 4.89 (dd, $^2J_{HH}$ = 13.0 Hz, $^3J_{HH}$ = 5.0 Hz, 1H, C**H**H'NO_2), 4.82 (dd, $^2J_{HH}$ = 13.5 Hz, $^3J_{HH}$ = 9.5 Hz, 1H, CH**H**'NO_2), 4.19 (td, $^3J_{HH}$ = 9.0 Hz, $^3J_{HH}$ = 5.0 Hz, 1H, C**H**=CH_2NO_2), 3.82 (d, $^3J_{HH}$ = 9.5 Hz, 1H, C**H**$(CO_2Me)_2$), 3.77 (s, 3H, $CO_2C\mathbf{H}_3$), 3.76 (s, 3H, $C'O_2C'\mathbf{H}_3$), 3.57 (s, 3H, $ArOC\mathbf{H}_3$); $^{13}C\{^1H\}$[29] (125 MHz) 168.0 (s, $\mathbf{C}O_2Me$), 167.4 (s, $\mathbf{C}'O_2Me$), 159.6 (s, *p* to CH), 129.1 (s, *o* to CH), 128.0 (s, *i* to CH), 114.5 (s, *m* to CH), 77.8 (s, $\mathbf{C}H_2NO_2$), 55.3 (s, $ArO\mathbf{C}H_3$), 55.0 ($\mathbf{C}H(CO_2Me)_2$), 53.1 (s, $CO_2\mathbf{C}H_3$), 53.0 (s, $C'O_2\mathbf{C}'H_3$), 42.4 (s, $\mathbf{C}H{=}CH_2NO_2$).

Enantiomeric excesses were determined by HPLC (see Figure A-7) with a Chiralpak AD column (80:20 v/v hexane/isopropanol, 1.0 mL/min, λ = 220 nm); for all catalysts t_R = 11.5-11.7 min (major), 17.5-18.2 min (minor).[26]

Dimethyl 2-(2-nitro-1-(3,4-dichlorophenyl)ethyl)malonate (23ec). This new compound was isolated as a white solid per the general procedures for Scheme 4.4. NMR ($CDCl_3$, δ in ppm):[28] ^{1}H (500 MHz) 7.40 (d, $^3J_{HH}$ = 9.0 Hz, 1H of $C_6\mathbf{H}_3$), 7.35 (s, 1H of $C_6\mathbf{H}_3$), 7.10 (d, $^3J_{HH}$ = 8.5 Hz, 1H of $C_6\mathbf{H}_3$), 4.90 (dd, $^2J_{HH}$ = 13.5 Hz, $^3J_{HH}$ = 5.0 Hz, 1H, C**H**H'NO_2), 4.85 (dd, $^2J_{HH}$ = 13.5 Hz, $^3J_{HH}$ = 9.5 Hz, 1H, CH**H**'NO_2), 4.20 (td, $^3J_{HH}$ = 9.0 Hz, $^3J_{HH}$ = 5.0 Hz, 1H, C**H**=CH_2NO_2), 3.82 (d, $^3J_{HH}$ = 9.5 Hz, 1H,

C**H**($CO_2Me)_2$), 3.77 (s, 3H, C**H$_3$**), 3.62 (s, 3H, C'**H**$_3$); $^{13}C\{^1H\}$ (125 MHz) 167.5 (s, **C**O_2Me), 167.0 (s, **C**'O_2Me), 136.5, 133.3, 132.9, 131.1, 130.2, 127.4 (6 × s, **C**$_6H_3$), 76.9 (s, **C**H_2NO_2), 54.4 (s, **C**H($CO_2Me)_2$) , 53.3 (**C**H_3), 53.2 (**C**'H_3), 42.1 (**C**H=CH_2NO_2). IR (powder film, cm^{-1}): 1744 (s), 1715 (s), 1549 (vs), 1265 (s), 1611 (s). mp 78-81 °C (open capillary). Anal. Calcd. for $C_{13}H_{13}Cl_2NO_6$ (350.15): C 44.59, H 3.74, N 4.00; found C 44.82, H 3.82, N 4.02.

Enantiomeric excesses were determined by HPLC (see Figure A-8) with a Chiralpak AS-H column (90:10 v/v hexane/isopropanol, 1.0 mL/min, λ = 220 nm); for all catalysts t_R = 20.4-21.3 min (minor), 22.7-23.5 min (major).[26]

Dimethyl 2-(2-nitro-1-(pyridine-3-yl)ethyl)malonate (23fc).[15a] This known compound was isolated as an off white solid per the general procedures for Scheme 4.4. NMR ($CDCl_3$, δ in ppm):[28] ^1H (500 MHz) 8.55-8.52 (m, 2H of C_5**H**$_4$N), 7.59 (dt, $^3J_{HH}$ = 8.0 Hz, J_{HH} = 2.0 Hz, 1H of C_5**H**$_4$N), 7.27-7.25 (m, 1H of C_5**H**$_4$N), 4.94 (dd, $^2J_{HH}$ = 13.5 Hz, $^3J_{HH}$ = 8.5 Hz, C**H**H'NO_2), 4.89 (dd, $^2J_{HH}$ = 13.5 Hz, $^3J_{HH}$ = 9.5 Hz, 1H, CH**H**'NO_2), 4.26 (td, $^3J_{HH}$ = 8.5 Hz, $^3J_{HH}$ = 5.0 Hz, C**H**=CH_2NO_2), 3.86 (d, $^3J_{HH}$ = 8.5 Hz, 1H, C**H**($CO_2Me)_2$), 3.76 (s, C**H$_3$**), 3.58 (s, C'**H**$_3$); $^{13}C\{^1H\}$ (125 MHz) 167.6 (s, **C**O_2Me), 167.0 (s, **C**'O_2Me), 149.9, 149.7, 135.5, 132.1, 123.8 (5 × s, **C**$_5H_4$N), 76.9 (s, **C**H_2NO_2), 54.3 (s, **C**H($CO_2Me)_2$), 53.3 (s, **C**H_3), 53.2 (s, **C**'H_3), 40.7 (s, **C**H=CH_2NO_2).

Enantiomeric excesses were determined by HPLC (see Figure A-9) with a Chiralpak AD column (60:40 v/v hexane/isopropanol, 1.0 mL/min, λ = 220 nm); for Λ-(*S*,*S*)-**1**$^{3+}$ 2$BF_4^-$$BAr_f^-$ (Λ-(*S*,*S*)-**1**$^{3+}$ 2$Cl^-$$BAr_f^-$ similar), t_R = 6.8 min (major), 9.2 min (minor).[26]

Dimethyl 2-(2-nitro-1-(2-trifluoromethylphenyl)ethyl)malonate (23gc). This new compound was isolated as a white solid per the general procedures for Scheme 4.4.

NMR ($CDCl_3$, δ in ppm):[28] ^1H (500 MHz) 7.72 (d, $^3J_{HH}$ = 7.5 Hz, 1H of $C_6\mathbf{H}_4$), 7.53 (t, $^3J_{HH}$ = 7.5 Hz, 1H of $C_6\mathbf{H}_4$), 7.43 (t, $^3J_{HH}$ = 8.0 Hz, 1H of $C_6\mathbf{H}_4$), 7.37 (d, $^3J_{HH}$ = 8.0 Hz, 1H of $C_6\mathbf{H}_4$), 5.16 (dd, $^2J_{HH}$ = 13.5 Hz, $^3J_{HH}$ = 7.5 Hz, 1H, C**H**H'NO_2), 4.94 (dd, $^2J_{HH}$ = 13.5 Hz, $^3J_{HH}$ = 4.5 Hz, 1H, CH**H**'NO_2), 4.65 (td, $^3J_{HH}$ = 7.5 Hz, $^3J_{HH}$ = 4.5 Hz, 1H, C**H**=CH_2NO_2), 4.11 (d, $^3J_{HH}$ = 7.5 Hz, 1H, C**H**$(CO_2Me)_2$), 3.75 (s, 3H, C$\mathbf{H}_3$), 3.64 (s, 3H, C'$\mathbf{H}_3$); ^{13}C (125 MHz) 168.0 (s, **C**O_2Me), 167.3 (s, **C**'O_2Me), 135.1, 132.5 (2 × s, $\mathbf{C}_6H_4$), 129.0 (q, $^2J_{CF}$ = 29.8 Hz, **C**CF_3), 128.6, 128.0 (2 × s, $\mathbf{C}_6H_4$), 127.3 (q, $^3J_{CF}$ = 5.9 Hz, **C**HCCF_3), 124.2 (q, $^1J_{CF}$ = 272.6 Hz, **C**F_3), 76.6 (s, **C**H_2NO_2), 54.0 (s, **C**H$(CO_2Me)_2$), 53.2 (**C**H_3), 53.1 (**C**'H_3), 38.1 (s, **C**H=CH_2NO_2). IR (powder film, cm^{-1}): 2957 (w), 1751 (s), 1734 (s), 1549 (s), 1126 (vs), 777 (s). mp 76-79 °C (open capillary). Anal. Calcd. for $C_{14}H_{14}F_3NO_6$ (349.26): C 48.14, H 4.04, N 4.01; found C 47.91, H 3.93, N 3.91.

Enantiomeric excesses were determined by HPLC (see Figure A-10) with a Chiralcel OD column (95:05 v/v hexane/isopropanol, 1.0 mL/min, λ = 220 nm); for all catalysts t_R = 12.7 min (minor), 26.6-28.6 min (major).[26]

Dimethyl 2-(2-nitro-1-(2-acetoxyphenyl)ethyl)malonate (23hc). This new compound was isolated as a colorless oil per the general procedures for Scheme 4.4. NMR ($CDCl_3$, δ in ppm):[28] ^1H (500 MHz) 7.32 (t, $^3J_{HH}$ = 7.0 Hz, 1H of $C_6\mathbf{H}_4$), 7.27-7.25 (m, 1H of $C_6\mathbf{H}_4$), 7.20 (t, $^3J_{HH}$ = 7.5 Hz, 1H of $C_6\mathbf{H}_4$), 7.15 (d, $^3J_{HH}$ = 8.0 Hz, 1H of $C_6\mathbf{H}_4$), 4.94-4.86 (m, 2H, C$\mathbf{H}_2NO_2$), 4.50 (q, $^3J_{HH}$ = 7.0 Hz, 1H, C**H**=CH_2NO_2), 3.92 (d, $^3J_{HH}$ = 8.5 Hz, 1H, C**H**$(CO_2Me)_2$), 3.74 (s, 3H, OC$\mathbf{H}_3$), 3.59 (s, 3H, OC'$\mathbf{H}_3$), 2.39 (s, 3H, C$\mathbf{H}_3$); $^{13}C\{^1H\}$ (125 MHz) 169.2, 168.0, 167.4 (3 × s, **C**O_2Me, **C**'O_2Me, **C**(O)Me), 148.7, 129.4, 128.5, 128.2, 126.5, 123.5 (6 × s, $\mathbf{C}_6H_4$), 76.7 (s, **C**H_2NO_2), 53.8 (s, **C**H$(CO_2Me)_2$), 53.1 (s, O**C**H_3, O**C**'H_3), 36.7 (s, **C**H=CH_2NO_2), 21.2 (s, **C**H_3), IR (neat oil, cm^{-1}): 2957 (w), 1734 (vs), 1555 (s), 1192 (s), 1171 (s). Anal. Calcd. for

$C_{15}H_{17}NO_8$ (339.30): C 53.10, H 5.05, N 4.13; found C 53.39, H 5.11, N 4.11.

Enantiomeric excesses were determined by HPLC (see Figure A-11) with a Chiralcel OD column (90:10 v/v hexane/isopropanol, 1.0 mL/min, λ = 220 nm); for Λ-(*S*,*S*)-**1**$^{3+}$ 2$BF_4^-$$BAr_f^-$ (Λ-(*S*,*S*)-**1**$^{3+}$ 2$Cl^-$$BAr_f^-$ similar), t_R = 18.9 min (minor), 28.5 min (major)); for Λ-(*S*,*S*)-**1**$^{3+}$ 3BF_4^- (older column), t_R = 19.7 min (minor), 31.3 min (major).[26]

Dimethyl 2-(2-nitro-1-(2-benzoyloxyphenyl)ethyl)malonate (23ic). This new compound was isolated as a pale yellow oil per the general procedures for Scheme 4.4. NMR ($CDCl_3$, δ in ppm):[28] ^{1}H (500 MHz) 8.27 (d, $^3J_{HH}$ = 7.0 Hz, 2H of $C_6\mathbf{H}_5$/$C_6\mathbf{H}_4$), 7.69 (t, $^3J_{HH}$ = 7.0 Hz, 1H of $C_6\mathbf{H}_5$/$C_6\mathbf{H}_4$), 7.57 (t. $^3J_{HH}$ = 8.0 Hz, 2H of $C_6\mathbf{H}_5$/$C_6\mathbf{H}_4$), 7.39-7.33 (m, 2H of $C_6\mathbf{H}_5$/$C_6\mathbf{H}_4$), 7.28-7.25 (m, 2H of $C_6\mathbf{H}_5$/$C_6\mathbf{H}_4$), 4.98 (dd, $^2J_{HH}$ = 13.5 Hz, $^3J_{HH}$ = 8.5 Hz, 1H, C**H**H'NO_2), 4.91 (dd, $^2J_{HH}$ = 13.5 Hz, $^3J_{HH}$ = 5.0 Hz, 1H, CH**H**'NO_2), 4.60 (td, $^3J_{HH}$ = 8.5 Hz, $^3J_{HH}$ = 5.0 Hz, 1H, C**H**=CH_2NO_2), 3.96 (d, $^2J_{HH}$ = 8.5 Hz, 1H, C**H**$(CO_2Me)_2$), 3.72 (s, 3H, C$\mathbf{H}_3$), 3.53 (s, 3H, C'$\mathbf{H}_3$); $^{13}C\{^1H\}$ (125 MHz) 167.9 (s, **C**O_2Me), 167.4 (s, **C**'O_2Me), 164.9 (s, **C**(O)Ph), 149.0, 134.1, 130.5, 129.6, 129.1, 129.0, 128.7, 128.3, 126.6, 123.6 (10 × s, $\mathbf{C}_6H_5$/$\mathbf{C}_6H_4$), 76.6 (s, **C**H_2NO_2), 53.8 (s, **C**H$(CO_2Me)_2$), 53.1 (s, **C**O_2Me), 53.1 (s, **C**'O_2Me), 36.7 (s, **C**H=CH_2NO_2). IR (neat oil, cm^{-1}): 2955 (w), 1732 (vs), 1555 (s), 1213 (s), 708 (vs). Anal. Calcd. for $C_{20}H_{19}NO_8$ (401.37): C 59.85, H 4.77, N 3.49; found C 59.59, H 4.80, N 3.40.

Enantiomeric excesses were determined by HPLC (see Figure A-12) with a Chiralpak AD column (90:10 v/v hexane/isopropanol, 1.0 mL/min, λ = 220 nm); for all catalysts t_R = 15.5-15.7 min (major), 26.0-26.3 min (minor).[26]

Dimethyl 2-(2-nitro-1-(2-benzyloxyphenyl)ethyl)malonate (23jc). This new compound was isolated as a colorless oil per the general procedures for Scheme 4.4. NMR ($CDCl_3$, δ in ppm):[28] ^{1}H (500 MHz) 7.47 (d, J = 7.5 Hz, 2H of $C_6\mathbf{H}_5$/$C_6\mathbf{H}_4$), 7.42

(t, 7.5 Hz, 2H of $C_6\mathbf{H}_5$/ $C_6\mathbf{H}_4$), 7.36 (t, J = 7.5 Hz, 1H of $C_6\mathbf{H}_5$/$C_6\mathbf{H}_4$), 7.24 (t, J = 7.5 Hz, 1H of $C_6\mathbf{H}_5$/$C_6\mathbf{H}_4$), 7.17 (d, J = 7.5 Hz, 1H of $C_6\mathbf{H}_5$/ $C_6\mathbf{H}_4$), 6.93 (d, J = 8.5 Hz, 1H of $C_6\mathbf{H}_5$/$C_6\mathbf{H}_4$), 6.89 (t, J = 7.5 Hz, 1H of $C_6\mathbf{H}_5$/$C_6\mathbf{H}_4$); 5.13 (d, $^3J_{HH}$ = 2.5 Hz, 2H, C$\mathbf{H}_2$Ph), 5.05 (dd, J = 13.0 Hz, J = 4.5 Hz, 1H, C**H**H'NO_2), 4.84 (dd, J = 13.0 Hz, J = 4.5 Hz, 1H, CH**H**'NO_2), 4.44 (td, $^3J_{HH}$ = 9.5 Hz, $^3J_{HH}$ = 4.5 Hz, 1H, C**H**=CH_2NO_2), 4.17 (d, $^3J_{HH}$ = 9.5 Hz, 1H, C**H**$(CO_2Me)_2$), 3.72 (s, 3H, C$\mathbf{H}_3$), 3.50 (s, 3H, C'$\mathbf{H}_3$); ^{13}C (125 MHz) 168.3, (s, **C**CO_2Me), 167.7 (s, **C**'O_2Me), 156.7, 136.5, 130.9, 129.8, 128.9, 128.3, 127.7, 123.9, 121.2, 112.4 (10 × s, $\mathbf{C}_6H_4$/$\mathbf{C}_6H_5$), 76.0 (s, **C**CH_2NO_2), 70.6 (**C**H_2Ph), 53.0 (s, **C**H$(CO_2Me)_2$), 52.7 (s, **C**H_3), 52.6 (s, **C**'H_3), 40.5 (s, **C**H=CH_2NO_2). IR (neat oil, cm^{-1}): 3034 (w), 2955 (w), 2886 (w), 1732 (vs), 1553 (vs), 1238 (vs), 752 (s), 696 (m). Anal. Calcd. for $C_{20}H_{21}NO_7$ (387.38): C 62.01, H 5.46, N 3.62; found C 62.25, H 5.46, N 3.57.

Enantiomeric excesses were determined by HPLC (see Figure A-13) with a Chiralcel OD column (90:10 v/v hexane/isopropanol, 1.0 mL/min, λ = 220 nm); for all catalysts t_R = 12.2-12.4 min (minor), 23.7-24.0 min (major).[26]

Dimethyl 2-(2-nitro-1-furylethyl)malonate (23k<u>c</u>).[15b,c] This known compound was isolated as a yellowish oil per the general procedures for Scheme 4.4. NMR ($CDCl_3$, δ in ppm):[28] ^{1}H (500 MHz) 7.33 (m, 1H of $C_4\mathbf{H}_3O$), 6.28 (m, 1H of $C_4\mathbf{H}_3O$), 6.21 (d, $^3J_{HH}$ = 3.5 Hz, 1H of $C_4\mathbf{H}_3O$), 4.89 (m, 2H, C$\mathbf{H}_2NO_2$), 4.39 (td, $^3J_{HH}$ = 17.5 Hz, $^3J_{HH}$ = 12.5 Hz, 1H, C**H**=CH_2NO_2), 3.93 (d, $^3J_{HH}$ = 8.0 Hz, 1H, C**H**$(CO_2Me)_2$), 3.75 (s, 3H, C$\mathbf{H}_3$), 3.68 (s, 3H, C'$\mathbf{H}_3$); ^{13}C{^{1}H} (125 MHz) 167.6 (s, **C**CO_2Me), 167.3 (s, **C**'O_2Me), 149.5, 143.0, 110.7, 106.5 (4 × s, $\mathbf{C}_4H_3O$), 75.4 (s, **C**CH_2NO_2), 53.2 (s, **C**H_3), 53.1 (s, **C**'H_3), 52.8 (s, **C**H$(CO_2Me)_2$), 36.9 (s, **C**H=CH_2NO_2).

Enantiomeric excesses were determined by HPLC (see Figure A-14) with a Chiralcel OD column (90:10 v/v hexane/isopropanol, 1.0 mL/min, λ = 220 nm); for all

catalysts t_R = 11.8-12.0 min (minor), 28.7-29.0 min (major).[26]

Dimethyl 2-(2-nitro-1-propylethyl)malonate (23l<u>c</u>).[20a] This known compound was isolated as a colorless oil per the general procedures for Scheme 4.4. NMR ($CDCl_3$, δ in ppm):[28] ^{1}H (500 MHz) 4.69 (dd, $^2J_{HH}$ = 13.5 Hz, $^3J_{HH}$ = 8.5 Hz, 1H, C**H**H'NO_2), 4.52 (dd, $^2J_{HH}$ = 13.5 Hz, $^3J_{HH}$ = 6.5 Hz, 1H, CH**H**'NO_2), 3.762 (s, 3H, OC**H**$_3$), 3.756 (s, 3H, OC'**H**$_3$), 3.66 (d, $^3J_{HH}$ = 6.0 Hz, 1H, C**H**$(CO_2Me)_2$), 2.90 (sext, $^3J_{HH}$ = 6.5 Hz, 1H, C**H**=CH_2NO_2), 1.46-1.34 (m, 4H, C**H**$_2$C**H**$_2$), 0.92 (t, $^3J_{HH}$ = 7.5 Hz, 3H, C**H**$_3$); ^{13}C{^{1}H} (125 MHz) 168.5 (s, **C**O_2Me), 168.3 (s, **C**'O_2Me), 76.7 (s, **C**H_2NO_2), 53.0 (s, O**C**H_3), 52.9 (s, O**C**'H_3), 52.4 (s, **C**H$(CO_2Me)_2$), 36.9 (s, **C**H=CH_2NO_2), 32.3 (s, **C**$H_2CH_2CH_3$), 20.0 (s, CH_2**C**H_2CH_3), 13.9 (s, **C**H_3).

Enantiomeric excesses were determined by HPLC (see Figure A-15) with a Chiralcel OD column (97.5:2.5 v/v hexane/isopropanol, 1.0 mL/min, λ = 220 nm); for (*S*,*S*)-**1**$^{3+}$ $2BF_4^-BAr_f^-$ (newer column), t_R = 12.4 min (minor), 20.3 min (major); for Λ-(*S*,*S*)-**1**$^{3+}$ $3BF_4^-$ (older column), t_R = 9.7 min (minor), 18.8 min (major).[26]

4.5. Crystallography.

A (Λ-(*S*,*S*)-1^{3+} 3Cl$^-$·2H$_2$O·2CH$_3$OH). A solution of Λ-(*S*,*S*)-**1**$^{3+}$ $3Cl^-$ in CH_3OH/H_2O (2:1 v/v) was allowed to slowly concentrate at room temperature. After 3 d, orange rods were collected. Data were obtained as noted in Table A-5. Cell parameters were determined from 60 data frames taken at 0.5° widths. Integrated intensity information for each reflection was obtained by reduction of the data frames with the program APEX2.[30] Data were corrected for Lorentz, polarization, and crystal decay effects. The program SADABS[31] was used to correct for absorption effects. The structure was solved by direct methods using SHELXTL (XS).[32] For each cobalt atom, two molecules of both H_2O and CH_3OH were located. Hydrogen atoms were placed in idealized positions and refined using a riding model. Non-hydrogen atoms were refined

with anisotropic thermal parameters. The thermal ellipsoids of the carbon atoms of two phenyl rings showed significant elongation, indicating disorder. This was successfully modeled (C2B/C, C3B/C, C4B/C, C5B/C, C6B/C, C7B/C, 61:39 occupancy ratio; C9A/E, C10A/E, C11A/E, C12A/E, C13A/E, and C14A/E, 53:47 occupancy ratio). The parameters were refined by weighted least squares refinement on F^2 to convergence.[32,33] The absolute stereochemistry was confirmed (absolute structure parameter = 0.000(12); Table A-5).[34] **B (Δ-(*R*,*R*)-1^{3+} 3Cl·H$_2$O·3CH$_3$OH).** A solution of Δ-(*R*,*R*)-**1**$^{3+}$ 3Cl$^-$ in CH_3OH was allowed to slowly concentrate at room temperature. After 5 d, orange rods were collected. Data were obtained as noted in Table A-5. Cell parameters were determined from 180 data frames taken at 0.5° widths. Integrated intensity information for each reflection was obtained by reduction of the data frames with the program APEX2.[30] Data were corrected for Lorentz, polarization, and crystal decay effects. The program SADABS[31] was used to correct for absorption effects. The structure was solved by direct methods using SHELXTL (XS).[32] For each cobalt atom, one molecule of water and ca. three molecules of CH_3OH were located. The thermal ellipsoids associated with one CH_3OH molecule indicated partial occupancy, which refined to 0.88; this value was fixed for the final refinement. Hydrogen atoms were placed in idealized positions and refined using a riding model. Non-hydrogen atoms were refined with anisotropic thermal parameters. The thermal ellipsoids of the carbon atoms of one phenyl ring indicated disorder. This refined to a 76:24 occupancy ratio (C30/30A, C31/31A, C32/32A, C33/33A, C34/34A, C35/35A). The ellipsoids of the disordered atoms were constrained. The parameters were refined by weighted least squares refinement on F^2 to convergence.[32,33] The absolute stereochemistry was confirmed (absolute structure parameter = 0.012 (4); Table A-5).[34] **C (Δ-(*S*,*S*)-1^{3+} 3Cl$^-$ ·12.5H$_2$O).** A solution of crude Δ-(*S*,*S*)-**1**$^{3+}$ 3Cl$^-$ (obtained from the Dowex column and

containing some Λ diastereomer) in hot H_2O was allowed to slowly concentrate at room temperature. After 7 d, orange blocks were collected. Data were obtained as noted in Table A-5. Cell parameters were determined from 180 data frames taken at 0.5° widths. Integrated intensity information for each reflection was obtained by reduction of the data frames with the program APEX2.[30] Data were corrected for Lorentz, polarization, and crystal decay effects. The program SADABS[31] was used to correct for absorption effects, and the structure was solved using SHELXTL (XS).[32] The asymmetric unit contained two unique Δ-(*S*,*S*)-$\mathbf{1}^{3+}$ moieties (Z = 4; Z′ = 2) and 25 molecules of water. Hydrogen atoms were placed in idealized positions and refined using a riding model. All non-hydrogen atoms were refined with anisotropic thermal parameters. Several atoms yielded non-positive definite matrices and some exhibited elongated thermal ellipsoids. Strong constraints (listed in the Validation Response Form of the CHECKCIF file) were placed to keep the thermal ellipsoids meaningful. The parameters were refined by weighted least squares refinement on F^2 to convergence.[32,33] Platon[35] was used to verify the absence of additional symmetry and voids. The absolute stereochemistry was confirmed (absolute structure parameter = 0.069(4); Table A-5).[34]

4.6. References

(1) (a) Simón, L.; Goodman, J. M. *J. Org. Chem*. **2010**, *75*, 1831-1840. (b) Cleland, W. W.; Frey, P. A.; Gerlt, J. A. *J. Biol. Chem.* **1998**, *273*, 25529-25532.

(2) (a) Takemoto, Y. *Org. Biomol. Chem.* **2005**, *3*, 4299-4306. (b) Doyle, A. G.; Jacobsen, E. N. *Chem. Rev*. **2007**, *107*, 5713-5743. (c) Taylor, M. S.; Jacobsen, E. N. *Angew. Chem., Int. Ed.* **2006**, *45*, 1520-1543; *Angew*. *Chem*. **2006**, *118*, 1550-1573. (d) Yu, X.; Wang, W. *Chem. Asian J*. **2008**, *3*, 516-532.

(3) MacMillan, D. W. C. *Nature* **2008**, *455*, 304-308.

(4) Blaser, H.-U. *Chem. Rev.* **1992**, *92*, 935-952.

(5) (a) Werner, A. *Chem. Ber.* **1912**, *45*, 121-130. (b) Werner, A. *Chem. Ber.* **1911**, *44*, 3279-3284. (c) Werner, A. *Chem. Ber.* **1911**, *44*, 3272-3278. (d) Werner, A. *Chem. Ber.* **1911**, *44*, 2445-2455. (e) Werner, A. *Chem. Ber.* **1911**, *44*, 1887-1898. V. L. King is listed as an author for the experimental section.

(6) Taube, H. *Chem. Rev*. **1952**, *50*, 69-126.

(7) Data for $[Co(en)_3]^{3+}$: Friend, J. A.; Nunn, E. K. *J. Chem. Soc.* **1958**, 1567-1571.

(8) Ghosh, S. K.; Ehnbom, A.; Lewis, K. G.; Gladysz, J. A. *Coord. Chem. Rev.***2017**, in press.DOI: 10.1016/j.ccr.2017.04.002.

(9) (a) Clarkson, A. J.; Buckingham, D. A.; Rogers, A. J.; Blackman, A. G.; Clark, C. R. *Inorg. Chem.* **2000**, *39*, 4769-4775. (b) Pearson, R. G.; Basolo, F. *J. Am. Chem. Soc.* **1956**, *78*, 4878-4883.

(10) Ganzmann, C.; Gladysz, J. A. *Chem*. *Eur*. *J*. **2008**, *14*, 5397-5400.

(11) See also Ghosh, S. K.; Ojeda, A. S.; Guerrero-Leal, J.; Bhuvanesh, N.; Gladysz, J. A. *Inorg. Chem.* **2013**, *52*, 9369-9378.

(12) Bosnich, B.; Harrowfield, J. MacB. *J. Am. Chem. Soc.* **1972**, *94*, 3425-3437.

(13) Kuroda, R.; Mason, S. F. *J. Chem. Soc., Dalton Trans.* **1977**, *10*, 1016-1020.

(14) These compounds are available from many vendors. The best prices in effect as of the submission date of the dissertation is from Ark Pharm (http://www.arkpharminc.com) for *R*,*R*-dpen ($420/100 g) and Aris Pharmaceuticals (http://www.arispharma.com) for *S*,*S*-dpen($408/100 g).

(15) (a) Okino, T.; Hoashi, Y.; Takemoto, Y. *J. Am. Chem. Soc.* **2003**, *125*, 12672-12673. (b) Li, H.; Wang, Y.; Tang, L.; Deng, L. *J. Am. Chem. Soc.* **2004**, *126*, 9906-9907. (c) Ye, J.; Dixon, D. J.; Hynes, P. S. *Chem. Commun.* **2005**, 4481-4483. (d) Andrés, J. M.; Manzano, R.; Pedrosa, R. *Chem. Eur. J.* **2008**, *14*, 5116-5119. (e) Almaşi, D.; Alfonso, D. A.; Gómez-Bengoa, E.; Nájera, C. *J. Org. Chem.* **2009**, *74*, 6163-6168.

(16) Thomas, C.; Gladysz, J. A. *ACS Catal*. **2014**, *4*, 1134-1138.

(17) (a) Scherer, A.; Mukherjee, T.; Hampel, F.; Gladysz, J. A. *Organometallics* **2014**, *33*, 6709-6722. (b) Mukherjee, T.; Ganzmann, C.; Bhuvanesh, N.; Gladysz, J. A. *Organometallics* **2014**, *33*, 6713-6737.

(18) (a) Liang-An, C.; Xu, W.; Huang, B.; Ma, J.; Wang, L.; Xi, J.; Harms, K.; Gong, L.; Meggers, E. *J. Am. Chem. Soc*. **2013**, *135*, 10598-10601. (b) Chen, L.-A.; Tang, X.; Xi, J.; Xu, W.; Gong, L.; Meggers, E. *Angew. Chem., Int. Ed*. **2013**, *52*, 14021-14025; *Angew. Chem*. **2013**, *125*, 14271-14275.

(19) (a) Maleev, V. I.; North, M.; Larionov, V. A.; Fedyanin, I. V.; Savel´yeva, T. F.; Moscalenko, M. A.; Smolyakov, A. F.; Belokon, Y. N. *Adv. Synth. Catal.* **2014**, *356*, 1803-1810. (b) Carmona, D.; Lamata, M. P.; Pardo, P.; Rodríguez, R.; Lahoz, F. J.; García-Orduña, P.; Alkorta, I.; Elguero, J.; Oro, L. A. *Organometallics* **2014**, *33*, 616-619.

(20) Li, X.-J.; Liu, K.; Ma, H.; Nie, J.; Ma, J.-A. *Synlett* **2008**, *20*, 3242-3246.

(21) Kim, H.; Nguyen, Y.; Yen, C. P.-H.; Chagal, L.; Lough, A. J.; Kim, B. M.;

Chin, J. *J. Am. Chem. Soc.* **2008**, *130*, 12184-12191.

(22) Ghosh, S. K.; Ganzmann, C.; Bhuvanesh, N.; Gladysz, J. A. *Angew. Chem., Int. Ed.* **2016**, *55*, 4356-4360; *Angew. Chem.***2016**, *128*, 4429-4433.

(23) (a) Moberg, C. *Angew. Chem. Int. Ed.* **1998**, *37*, 248-268; *Angew. Chem.* **1998**, *110*, 260-281. (b) Gibson, S. E.; Castaldi, M. P. *Chem. Commun*. **2006**, 3045-3062.

(24) (a) Xia, X.-F.; Shu, X.-Z.; Ji, K.-G.; Yag, Y.-F.; Shaukat, A.; Liu, X.-Y.; Liang, Y.-M. *J. Org. Chem.* **2010**, *75*, 2893-2902. (b) Lucet, D.; Sabelle, S.; Kostelitz, O.; Gall, T. L.; Mioskowski, C. *Eur. J. Org. Chem.* **1999**, 2583-2591.

(25) The $^{13}C\{^{1}H\}$ signal with the chemical shift closest to benzene was assigned to the *meta* carbon atom: Mann, B. E. *J. Chem. Soc. Perkin Trans. 2* **1972**, 30-34.

(26) The absolute configurations of **23aa-ac** were assigned by HPLC using conditions similar to those in the literature (see references 15d,e). Catalysts with Λ-(*S*,*S*) configurations gave predominantly *R* enantiomers. The dominant configurations of **23bc-23lc** were assigned assuming analogous relative retention times.

(27) Evans, D. A.; Mito, S.; Seidel, D. *J. Am. Chem. Soc.* **2007**, *129*, 11583-11592.

(28) The NMR signals of all addition products were assigned by analogy to those of **23ac**: see reference 15e.

(29) The aromatic NMR signals were assigned by analogy to those of $C_6H_5OCH_3$. Silverstein, R. M.; Webster, F. X.; Kiemle, D. J. *Spectrometric Identification of Organic Compounds*, 7th ed.; John Wiley & Sons: Hoboken, NJ, 2005; p 225.

(30) APEX2 "Program for Data Collection on Area Detectors" BRUKER AXS Inc., 5465 East Cheryl Parkway, Madison, WI 53711-5373 USA.

(31) Sheldrick, G. M. "SADABS (version 2008/1): Program for Absorption

Correction of Area Detector Frames", BRUKER AXS Inc., 5465 East Cheryl Parkway, Madison, WI 53711-5373 USA.

(32) Sheldrick, G. M. *Acta Cryst. A* **2008**, *64*, 112-122.

(33) Dolomanov, O. V.; Bourhis, L. J.; Gildea, R. J.; Howard, J. A. K.; Puschmann, H. *J. Appl. Cryst.* **2009***, 42*, 339-341.

(34) Flack, H. D. *Acta Cryst. A* **1983**, *39*, 876-881.

(35) Spek, A. L. *J. Appl. Cryst.* **2003**, *36*, 7-13.

5. TRIS(1,2-DIPHENYLETHYLENEDIAMINE) COBALT(III) COMPLEXES: CHIRAL HYDROGEN BOND DONOR CATALYSTS FOR ENANTIOSELECTIVE α-AMINATIONS OF 1,3-DICARBONYL COMPOUNDS†

5.1. Introduction

The last 15 years have witnessed an extensive development of small molecule hydrogen bond donor catalysts for enantioselective organic synthesis.[1] During this period, many types of catalyst based stereogenic elements have been evaluated. I and my collaborators have sought to (1) expand the chiral pool to include inorganic or organometallic molecules that exhibit chirality motifs not commonly encountered in organic systems,[2] and (2) explore the utility of NH hydrogen bond donor groups that are either ligated to the metal[3] or positioned at remote sites.[4,5] Related themes have been of interest in the Meggers group.[5,6]

In particular, our attention has been attracted to helically chiral Werner complexes, for which the D_3 symmetric trication $[Co(en)_3)]^{3+}$ (en = 1,2-ethylenediamine) is the prototype.[3] As noted in previous sections in this dissertation, the mirror images of $[Co(en)_3)]^{3+}$, depicted in Scheme 5.1 (top), have commonly been designated Λ and Δ. Salts of these trications were among the first inorganic compounds separated into enantiomers.[7] However, the solubilities of such species are generally restricted to water or other protic media, which can inhibit the binding of substrates to NH donor sites.

†Reproduced with permission from Kumar, A.; Ghosh, S. K.; Gladysz, J. A. *Org. Lett*. **2016**, *18*, 760-763. Copyright 2016 American Chemical Society.

In earlier work, I synthesized a series of salts of a related trication with (*S*,*S*)-1,2-diphenylethylenediamine ligands ((*S*,*S*)-dpen) as shown in Scheme 5.1 (middle).[3b] The starting trichloride $[Co((S,S)\text{-dpen})_3]^{3+}$ $3Cl^-$ ((*S*,*S*)-**1**$^{3+}$ $3Cl^-$) was easily obtained as the Λ or Δ diastereomer, and the exchange of one chloride for the lipophilic anion BAr_f^- ($B(3,5\text{-}C_6H_3(CF_3)_2)_4^-$) gave salts with high solubilities in aprotic media. This in turn facilitated the formation of a number of mixed salts of the formula Λ- or Δ-(*S*,*S*)-**1**$^{3+}$ $2X^-$ X'^- as well as analogs with three lipophilic anions (Λ- or Δ-(*S*,*S*)-**1**$^{3+}$ $3X''^-$, see section 3). Many of these gave high levels of enantioselection as catalysts for Michael additions of malonate esters to nitroalkenes (see section 4).[3b]

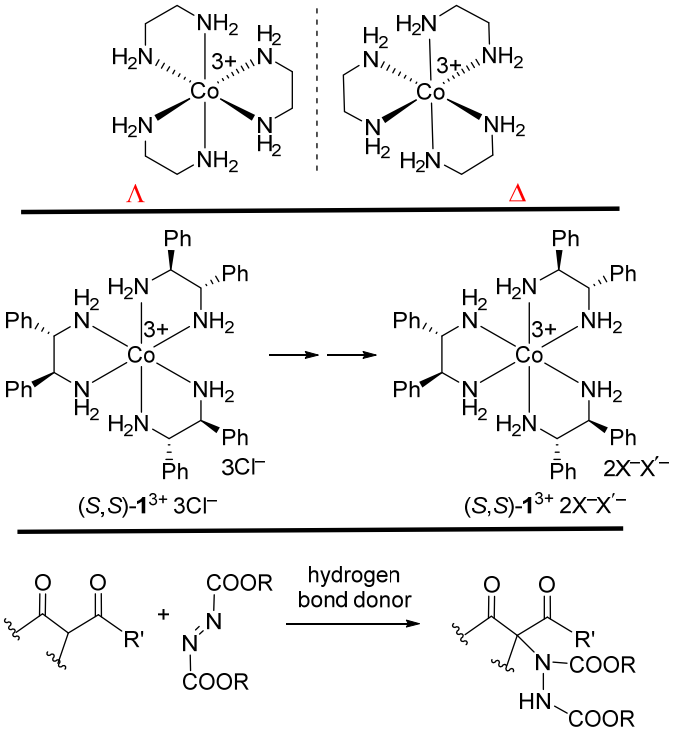

Scheme 5.1. A chiral cobalt(III) trication originally separated into enantiomers by Werner (top); general catalyst family (middle); reaction to be investigated (bottom).

In order to demonstrate the applicability of such catalysts to a broader palette of transformations, we began to investigate additions of 1,3-dicarbonyl and related compounds to azo linkages, a reaction type shown in Scheme 5.1 (bottom). Such additions, often termed aminations, have been demonstrated with other hydrogen bond donor catalysts,[8] and yield nitrogen functionalized systems that can be elaborated to α-amino acids.[9] In this section, I report that salts derived from the trication (*S*,*S*)-**1**$^{3+}$ also effect additions of activated methylene compounds to azo species in very high enantioselectivities. Some of these reactions were carried out by Dr. Anil Kumar.

5.2. Results

As shown in Scheme 5.2, catalysts were screened at 5 mol % loadings using the ß-keto ester **24a** and di-*t*-butyl azodicarboxylate (**25**). The first experiments used the base N-methylmorpholine and were carried out in CD_2Cl_2 in NMR tubes at room temperature. Entries 1 and 2, which involve the previously reported diastereomeric mixed bis(chloride) salts Λ- and Δ-(*S*,*S*)-**1**$^{3+}$ 2Cl$^-$BAr$_f^-$, gave opposite enantiomers of the addition product **26a** in 76% and 79% ee, respectively, roughly on same time scale. Hence, the cobalt configuration is the main determinant of the product configuration. The corresponding bis(tetrafluoroborate) and bis(hexafluorophosphate) salts gave diminished enantioselectivities (entries 3-6, 70-56% ee). However, the perfluorotetraphenylborate salts Δ- and Λ-(*S*,*S*)-**1**$^{3+}$ 2Cl$^-$ BAr$_{f20}^-$ gave equal or better results (entries 7, 8), with the improvement more pronounced in the Δ series (84% ee). Hence, this catalyst was selected for solvent, temperature, and base optimization.

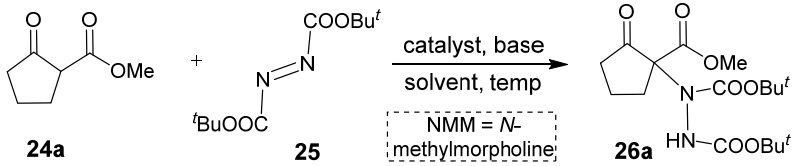

Entry[a]	catalyst	solvent	base (1 equiv)	temp (°C)	conversion (%) (time)[b]	ee (%) (config)[c]
1	Λ-(*S*,*S*)-**1**$^{3+}$ 2Cl$^-$BAr$_f^-$ (5)	CD_2Cl_2	NMM	rt	99 (20 min)	76 (*S*)
2	Δ-(*S*,*S*)-**1**$^{3+}$ 2Cl$^-$BAr$_f^-$ (5)	CD_2Cl_2	NMM	rt	99 (20 min)	79 (*R*)
3	Λ-(*S*,*S*)-**1**$^{3+}$ 2BF$_4^-$BAr$_f^-$ (5)	CD_2Cl_2	NMM	rt	99 (20 min)	70 (*S*)
4	Δ-(*S*,*S*)-**1**$^{3+}$ 2BF$_4^-$BAr$_f^-$ (5)	CD_2Cl_2	NMM	rt	99 (20 min)	56 (*R*)
5	Λ-(*S*,*S*)-**1**$^{3+}$ 2PF$_6^-$BAr$_f^-$ (5)	CD_2Cl_2	NMM	rt	99 (20 min)	60 (*S*)
6	Δ-(*S*,*S*)-**1**$^{3+}$ 2 PF$_6^-$BAr$_f^-$ (5)	CD_2Cl_2	NMM	rt	99 (20 min)	68 (*R*)
7	Λ-(*S*,*S*)-**1**$^{3+}$ 2Cl$^-$BAr$_{f20}^-$ (5)	CD_2Cl_2	NMM	rt	99 (20 min)	77 (*S*)
8	Δ-(*S*,*S*)-**1**$^{3+}$ 2Cl$^-$BAr$_{f20}^-$ (5)	CD_2Cl_2	NMM	rt	99 (20 min)	84 (*R*)
9	Δ-(*S*,*S*)-**1**$^{3+}$ 2Cl$^-$BAr$_{f20}^-$ (5)	acetone-d_6	NMM	rt	99 (20 min)	87 (*R*)
10	Δ-(*S*,*S*)-**1**$^{3+}$ 2Cl$^-$BAr$_{f20}^-$ (5)	CD_3CN	NMM	rt	99 (20 min)	89 (*R*)
11	Δ-(*S*,*S*)-**1**$^{3+}$ 2Cl$^-$BAr$_{f20}^-$ (5)	CD_3CN	NMM	0	99 (20 min)	91 (*R*)
12	Δ-(*S*,*S*)-**1**$^{3+}$ 2Cl$^-$BAr$_{f20}^-$ (5)	CD_3CN	NMM	–35	99 (20 min)	84 (*R*)
13	Δ-(*S*,*S*)-**1**$^{3+}$ 2Cl$^-$BAr$_{f20}^-$ (5)	CD_3CN	Et_3N	0	99 (20 min)	81 (*R*)
14	Δ-(*S*,*S*)-**1**$^{3+}$ 2Cl$^-$BAr$_{f20}^-$ (5)	CD_3CN	DABCO	0	99 (20 min)	77 (*R*)
15	Δ-(*S*,*S*)-**1**$^{3+}$ 2Cl$^-$BAr$_{f20}^-$ (5)	CD_3CN	DBU	0	99 (20 min)	80 (*R*)
16	Δ-(*S*,*S*)-**1**$^{3+}$ 2Cl$^-$BAr$_{f20}^-$ (5)	CD_3CN	DMAP	0	99 (20 min)	80 (*R*)
17	Δ-(*S*,*S*)-**1**$^{3+}$ 2Cl$^-$BAr$_{f20}^-$ (1)	CD_3CN	NMM	0	99 (8 h)	70 (*R*)
18	Δ-(*S*,*S*)-**1**$^{3+}$ 2Cl$^-$BAr$_{f20}^-$ (2)	CD_3CN	NMM	0	99 (4 h)	84 (*R*)
19	Δ-(*S*,*S*)-**1**$^{3+}$ 2Cl$^-$BAr$_{f20}^-$ (10)	CD_3CN	NMM	0	99 (20 min)	91 (*R*)
20	Δ-(*S*,*S*)-**1**$^{3+}$ 2Cl$^-$BAr$_{f20}^-$ (5)	CD_3CN	NMM[d]	0	99 (35 min)	91 (*R*)
21	Δ-(*S*,*S*)-**1**$^{3+}$ 2Cl$^-$BAr$_{f20}^-$ (5)	CD_3CN	NMM[e]	0	99 (6 h)	91 (*R*)

[a]Reactions were carried out with 0.050 mmol of **24a** and 0.050 mmol of **25** in 0.50 mL of solvent. [b]The conversion was determined by ^{1}H NMR integration of the C**H**CO$_2$Me proton of **24a** versus the internal standard Ph_2SiMe_2. [c]Enantioselectivities were determined by chiral HPLC analyses. [d]0.50 equiv base . [e]0.10 equiv base.

Scheme 5.2. Optimization of catalysts and conditions

For Δ-(*S*,*S*)-**1**$^{3+}$ 2Cl^{-}BAr$_{f20}^{-}$, enantioselectivities increased slightly in acetone-d_6 (87% ee, entry 9) and still more in CD_3CN (89% ee, entry 10). Next, reactions were conducted in CD_3CN at lower temperatures (entries 11-12). Interestingly, the ee values first increased (91% ee, 0 °C), but diminished with further cooling (84%, –35 °C). Thus, four additional bases were evaluated at 0 °C (Et_3N, DABCO, DBU, DMAP), but the ee values decreased to 81-77% ee (entries 13-16). Next, the catalyst charge was varied. At 1 and 2 mol% loadings (entries 17-18), enantioselectivities decreased (70% and 84% ee), presumably due to increased competition from background reaction or catalysis. However, 10% loadings gave no improvement (entry 19). Finally the amount of base was decreased from 1.0 equiv to 0.50-0.10 equiv (entry 20-21). Reactions times increased, but enantioselectivities were maintained.

Next, the optimal conditions from Scheme 5.2 were applied to additional substrates, giving the results summarized in Scheme 5.3. Five different cyclic ß-ketoesters were examined, providing products **26a-d**,**h** in 88-97% yields. The carboethyoxy cyclohexanone **26c** formed somewhat more slowly than the others, whereas the carbomethoxy cyclopentanone **26a** formed somewhat faster. Within this group, the ee values were excellent for the five and six membered ring keto esters (**26a-d**; >99-91% ee). However, the seven membered ring keto ester formed with lower enantioselectivity (5 h; 72% ee, Scheme 5.3).

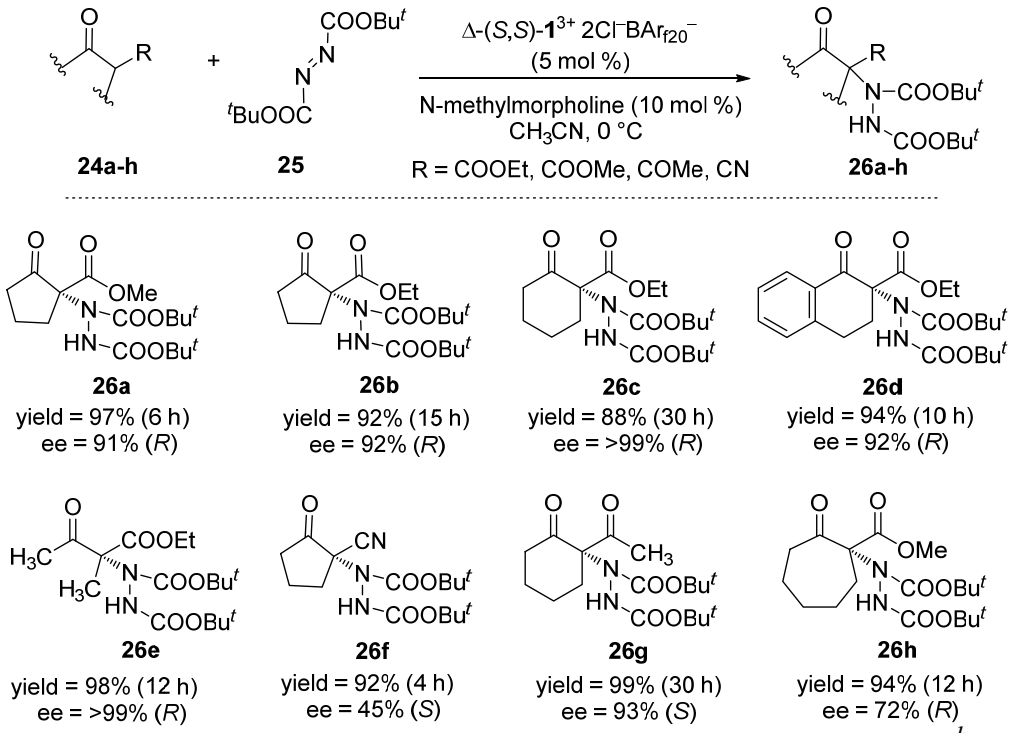

[a]All reactions were carried out with 0.1 mmol of **24** and 0.1 mmol of **25** in 1.0 mL of CH_3CN. [b]Yields are for isolated products. [c]Enantioselectivities were determined by chiral HPLC analyses.

Scheme 5.3. Substrate scope under optimized conditions.[a-c]

An acyclic ß-keto ester also underwent amination in high yield (98%) and enantioselectivity (>99% ee) to give **26e**. A cyclic 1,3 diketone was also efficiently derivatized to give **26g** in 99% yield and 93% ee. Finally, when α-cyanocyclopentanone was employed, **26f** was obtained in 92% yield, but the ee value dropped to 45%. Importantly, the dominant product configurations were, in a relative sense, the same in each case.

Naturally, it is by no means assured that the screening results in Scheme 5.2 reflect the optimum conditions for all of the substrates in Scheme 5.3. Thus, for the reactions yielding **26e** and **26g**, additional catalysts were investigated, as summarized in Table 5.1.

Table 5.1. Variation of the catalyst used for **26e** and **26g** under optimized conditions.[a]

entry	product	catalyst	time (h)	yield (%)	ee (%) (config)
1	**26e**	Δ-(*S*,*S*)-**1**$^{3+}$ 2Cl^{-}BAr$_{f20}^{-}$	12	94	>99 (*R*)
2	**26e**	Λ-(*S*,*S*)-**1**$^{3+}$ 2Cl^{-}BAr$_{f20}^{-}$	15	97	84 (*S*)
3	**26e**	Δ-(*S*,*S*)-**1**$^{3+}$ 2Cl^{-}BAr$_{f}^{-}$	13	93	84 (*R*)
4	**26g**	Δ-(*S*,*S*)-**1**$^{3+}$ 2Cl^{-}BAr$_{f20}^{-}$	30	98	93 (*R*)
5	**26g**	Λ-(*S*,*S*)-**1**$^{3+}$ 2Cl^{-}BAr$_{f20}^{-}$	28	97	92 (*S*)
6	**26g**	Δ-(*S*,*S*)-**1**$^{3+}$ 2Cl^{-}BAr$_{f}^{-}$	32	94	70 (*R*)

[a]All reactions were carried out with 0.10 mmol each of **24** and **25** in 1.0 mL of CH_3CN at 0 °C in the presence of N-methylmorpholine (0.10 equiv.).

These data confirm that the best overall catalyst is Δ-(*S*,*S*)-**1**$^{3+}$ 2Cl^{-}BAr$_{f20}^{-}$. For the acyclic substrate yielding **26e**, the Δ diastereomer gives significantly higher enantioselectivity than the Λ diastereomer (entries 1 vs. 2, >99% vs. 84% ee). However, for the diketone **26g**, these two catalysts give comparable enantioselectivities (entries 4 vs. 5, 93-92% ee). It is noted in passing that these would be excellent test systems for multivariate reaction parameter analyses.[10]

5.3. Discussion.

As summarized in Scheme 5.2, this study shows that all of the cobalt(III) salts prepared catalyze the title reaction with appreciable enantioselectivities. Curiously, the Δ diastereomers always afford slightly greater enantioselectivities. This is in stark contrast to the malonate/nitroalkene additions,[3b] for which the Λ diastereomers are distinctly superior; current evidence suggests that these proceed via a C_3 face of the trication, where three NH bonds are directed in a roughly synperiplanar fashion. As shown in Scheme 5.4 (top), the three NH protons on each C_3 face of the trichloride salt Δ-(*S*,*S*)-**1**$^{3+}$ 3Cl^{-} are directed in a more divergent fashion than those of Λ-(*S*,*S*)-**1**$^{3+}$ 3Cl^{-}, and the C_2 face is much more congested.[3b] While it borders on pure speculation to propose

transition state assemblies for the reactions in Schemes 5.2 and 5.3, the model **I** (Scheme 5.4, middle) can be offered as a starting point. Note the possibility that the educts may also simultaneously bind to one or more NH units associated with a C_2 face.

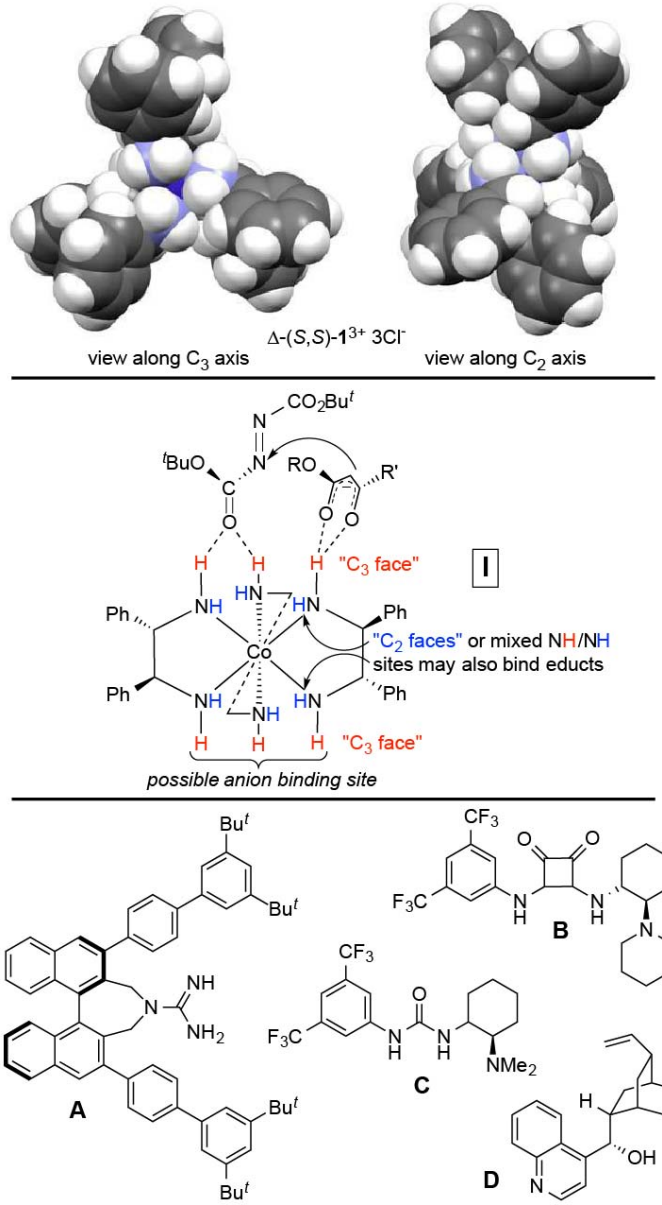

Scheme 5.4. Views of the C_3 and C_2 faces of the trication of Λ-(*S*,*S*)-**1**$^{3+}$ 3Cl$^-$ (top),[3b] A possible transition state Assembly (middle), Other chiral hydrogen bond donor catalysts employed for the title reaction (bottom).

Although it is difficult to quantitatively compare the effectiveness of different families of enantioselective catalysts, the ee values in Scheme 5.3 usually rank with the best in the literature. For products **26a**,**b**,**d**, the current "records" are 96% ee (vs. 91%),[8g] 98% ee (vs. 92%),[8e] and 97% ee (vs. 92%),[8e] respectively. For **26c**,**e**,**g**, our data are superior (>99% ee vs. 98%;[8e] >99% ee vs. 85%;[8e] 93% vs. no previous reports). With the products **26f**,**h**, our data are inferior (45% ee vs. 90%;[8g] 72% ee vs. 94%[8g]). The catalysts that feature in these comparisons are depicted in Scheme 5.4 (**A**, **B**; bottom), together with other representative examples (**C**, **D**). Importantly, **A** and **B** were effective at somewhat lower loadings than (*S*,*S*)-**1**$^{3+}$ 2Cl^{-}BAr$_{f20}^{-}$ (2-0.5 vs. 5 mol %). This may be due, at least in part, to their bifunctional nature, obviating the need for an external base.

In summary, this study has expanded the applicability of chiral Werner complexes based upon ethylenediamine chelates as hydrogen bond donor catalysts for enantioselective organic reactions. The anion effects evident in Scheme 5.2 furthermore raise the possibility of additional types of controlling interactions. These will be probed in future efforts, together with bifunctional catalysts that incorporate tertiary amines (section 7)[11] and transformations that cannot be effected with existing hydrogen bond donor catalysts.

5.4. Experimental section

General Data. Reactions were conducted under air. NMR spectra were recorded on a Varian NMRS 500 MHz spectrometer at ambient probe temperatures. Chemical shifts (δ in ppm) were referenced to residual solvent signals (^{1}H: $CDCl_3$, 7.26; CD_2Cl_2, 5.32; acetone-d_6, 2.05; CD_3CN, 1.94; ^{13}C: $CDCl_3$, 77.2; CD_2Cl_2, 54.0; acetone-d_6, 29.9). Melting points were determined using an OptiMelt MPA 100 instrument. Microanalyses were conducted by Atlantic Microlab. HPLC analyses were carried out with a Shimadzu instrument package (pump/autosampler/detector LC-20AD/SIL-20A/SPD-M20A).

NMR solvents (Cambridge Isotopes; $CDCl_3$, CD_2Cl_2, acetone-d_6, CD_3CN) were stored over molecular sieves. HPLC solvents (hexanes, Fischer; isopropanol, JT Baker; both HPLC Grade) were degassed before use. Other solvents (CH_2Cl_2 (EMD, ACS grade), hexanes (Macron, ACS grade), EtOAc (Macron, ACS grade), acetone (BDH, ACS grade), CH_3CN (BDH, ACS grade)) were used as received.

The following chemicals were used as received: di-*t*-butyl azodicarboxylate (**25**, Aldrich, 98%), methylcyclopentanone-2-carboxylate (**24a**, TCI, >97%), ethyl 2-oxocyclopentanecarboxylate and ethyl 2-oxocyclohexanecarboxylate (**24b**,**c**, Aldrich, 95%), ethyl-1-oxo-1,2,3,4-tetrahydronaphthalene-2-carboxylate, (**24d**, Oxchem, 95%), ethyl-2-methylacetoacetate (**24e**, Alfa Aesar, 95%), cyclopentanone-2-carbonitrile (**24f**, Oxchem, 95%), 2-acetylcyclopentanone (**24g**, Alfa Aesar, 98%), methyl 2-oxo-1-cycloheptanecarboxylate (**24h**, Aldrich, >99%), Et_3N (Alfa Aesar, 98%), *N*-methyl morpholine (Alfa Aesar, 99%), DBU (Acros Organics), DMAP (Aldrich, > 99%), DABCO (Aldrich, >99%), silica gel (Silicycle SiliaFlash® F60).

Reactions, Scheme 5.3. A 5 mm NMR tube was charged with a solution of β-ketoester or related compound (**24**; 0.10 mmol, 1.0 equiv), azodicarboxylate **25** (0.023 g, 0.10 mmol, 1.0 equiv) and catalyst (0.0050 mmol, 0.05 equiv) in CH_3CN (1.0 mL), and cooled to 0 °C. Then N-methylmorpholine (0.0011 mL, 0.010 mmol, 0.10 equiv) was added. The reaction was monitored by TLC. After the specified time (Scheme 5.3), the mixture was loaded onto a plug of silica gel. The organic product (**26**) was eluted with hexane/EtOAc (80:20 to 70:30 v/v). The solvent was removed by rotary evaporation. The product was dried by oil pump vacuum at room temperature and the ee assayed by chiral HPLC (Figure A-16 to Figure A-23 in appendix).

***N,N'*-Bis(*t*-butoxycarbonyl)-1-hydrazino-2-oxocyclopentanecarboxylic acid methyl ester (26a).**[8a] This known compound was obtained as a colorless oil (0.036 g, 0.097 mmol) per the procedure for Scheme 5.3. NMR ($CDCl_3$, δ in ppm): ^{1}H (300 MHz) 6.51 (br s, 1H, N**H**), 3.74 (s, 3H, COOC**H**$_3$), 2.82-1.86 (m, 6H, ring C**H**$_2$), 1.66-1.06 (m, 18H, C(C**H**$_3$)$_3$ and C'(C'**H**$_3$)$_3$); ^{13}C{^{1}H} (125 MHz), 205.6 (s, (**C**=O)CH$_2$), 168.6 (s, (**C**=O)OMe), 155.4 and 154.5 (2s, (**C**=O)O-*t*Bu and (**C**'=O')O'-*t*Bu'), 83.0 and 81.7 (2s, **C**(CH$_3$)$_3$ and **C**'(C'H$_3$)$_3$), 53.20, (s, O**C**H$_3$), 36.7 (s), 31.7 (s), 29.7 (s), 28.3 and 28.2 (2s, C(**C**H$_3$)$_3$ and C'(**C**'H$_3$)$_3$), 18.7 (s).

Enantiomeric excesses were determined by HPLC (see Figure A-16) with a Chiralpak AD column (96:4 v/v hexane/isopropanol, 1.0 mL/min, λ = 210 nm); for Δ-(*S*,*S*)-**1**$^{3+}$ 2Cl$^-$BAr$_{f20}$$^-$, t_R = 13.2 min (major), 19.5 min (minor).[8a,12]

***N,N'*-Bis(*t*-butoxycarbonyl)-1-hydrazino-2-oxocyclopentanecarboxylic acid ethyl ester (26b).**[8e] This known compound was obtained as a colorless oil (0.036 g, 0.092 mmol) per the procedure for Scheme 5.3. NMR ($CDCl_3$, δ in ppm): ^{1}H (500 MHz) 6.51 (br s, 1H, N**H**), 4.16 (br s, 2H, C**H**$_2$CH$_3$), 2.79-1.80 (m, 6H, 3 × ring C**H**$_2$), 1.60-1.28 (m, 18H, C(C**H**$_3$)$_3$ and C'(C'**H**$_3$)$_3$), 1.25-1.12 (m, 3H, CH$_2$C**H**$_3$); ^{13}C{^{1}H} (125

MHz), 205.6 (s, (**C**=O)CH_2), 167.8 (s, (**C**=O)OEt), 155.2 and 154.4 (2s, (**C**=O)O-*t*Bu and (**C**'=O')O'-*t*Bu'), 82.8 and 81.5 (2s, **C**$(CH_3)_3$ and **C**'$(C'H_3)_3$), 62.2 (s, **C**H_2CH_3), 35.9 (s), 32.0 (s), 29.7 (s), 28.2 and 28.1 (2s, C(**C**$H_3)_3$ and C'(**C**'$H_3)_3$), 18.6 (s), 14.1 (s, CH_2**C**H_3).

Enantiomeric excesses were determined by HPLC (see Figure A-17) with a Chiralpak AD column (96:4 v/v hexane/isopropanol, 1.0 mL/min, λ = 210 nm); for Δ-(*S*,*S*)-**1**$^{3+}$ 2Cl$^-$BAr$_{f20}^-$, t_R = 10.4 min (major), 15.5 min (minor).[8e,12]

***N,N'*-Bis(*t*-butoxycarbonyl)-1-hydrazino-2-oxocyclohexanecarboxylic acid ethyl ester (26c).**[8e] This known compound was obtained as a colorless oil (0.035 g, 0.088 mmol) per the procedure for Scheme 5.3. NMR ($CDCl_3$, δ in ppm): ^{1}H (500 MHz) 6.50 (br s, 1H, N**H**), 4.33-4.12 (m, 2H, C**H**$_2$CH$_3$), 2.92-1.81 (m, 8H, 4 × ring C**H**$_2$), 1.52-1.37 (m, 18H, C(C**H**$_3)_3$ and C'(C'**H**$_3)_3$), 1.28-1.22 (m, 3H, CH_2C**H**$_3$); ^{13}C{^{1}H} (CD_2Cl_2, 125 MHz) 202.2 (s, (**C**=O)CH_2), 169.1 (s, (**C**=O)OEt), 157.2 and 155.7 (2s, (**C**=O)O-*t*Bu and (**C**'=O')O'-*t*Bu'), 83.3, 81.5, and 78.6 (3s, **C**$(CH_3)_3$ and **C**'$(C'H_3)_3$),[13] 62.3 (s, **C**H_2CH_3), 40.3 (s), 35.3 (s), 30.1 (s), 29.4 (s), 28.2 and 28.1 (2s, C(**C**$H_3)_3$ and C'(**C**'$H_3)_3$), 21.0 (s), 20.4 (s), 14.3 (s, CH_2**C**H_3).

Enantiomeric excesses were determined by HPLC (see Figure A-18) with a Chiralpak AS-H column (99:1 v/v hexane/isopropanol, 1.0 mL/min, λ = 210 nm); for Δ-(*S*,*S*)-**1**$^{3+}$ 2Cl$^-$BAr$_{f20}^-$, t_R = 9.5 min (minor), 13.1 min (major).[8e,12]

***N,N'*-Bis(*t*-butoxycarbonyl)-1-hydrazino-1,2,3,4-tetrahydro-1-oxonaphthalene-2-carboxylic acid ester (26d).**[8e] This known compound was obtained as a colorless oil (0.042 g, 0.095 mmol) per the procedure for Scheme 5.3. NMR ($CDCl_3$, δ in ppm): ^{1}H (500 MHz) 8.10-7.75 (m, 1H, arom), 7.54-7.37 (m, 1H, arom), 7.35-7.10 (m, 2H, arom), 6.49-5.98 (m, 1H, N**H**), 4.46-4.10 (m, 2H, C**H**$_2$CH$_3$), 3.45-2.50 (m, 4H), 1.56-1.05 (m, 21H, C(C**H**$_3)_3$, C'(C'**H**$_3)_3$ and CH_2C**H**$_3$); ^{13}C{^{1}H} (125 MHz), 190.8 (s,

(**C**=O)CCOOEt), 169.7 (s, (**C**=O)OEt), 155.6 and 154.5 (2s, (**C**=O)O-*t*Bu and (**C**'=O')O'-*t*Bu'), 144.4 (s, arom), 133.6 (s, arom), 131.8 (s, arom), 128.7 (s, arom), 127.9 (s, arom), 126.6 (s, arom), 82.8, 81.3, 81.0, and 75.6 (4s, $\mathbf{C}(CH_3)_3$ and $\mathbf{C}'(C'H_3)_3$),[13] 62.4, 62.1 (2s, $\mathbf{C}H_2CH_3$), 36.8, 34.6, 31.3 and 29.8 (4s), 28.3, 28.2, 28.0 and 27.7 (4s, $C(\mathbf{C}H_3)_3$ and $C'(\mathbf{C}'H_3)_3$),[s7] 25.7 (s), 24.8 (s), 24.2 (s), 14.3 and 14.1 (2s, $CH_2\mathbf{C}H_3$).[13]

Enantiomeric excesses were determined by HPLC (see Figure A-19) with a Chiralpak AD-H column (80:20 v/v hexane/isopropanol, 1.0 mL/min, λ = 220 nm); for Δ-(*S*,*S*)-$\mathbf{1}^{3+}$ $2Cl^-BAr_{f20}^-$, t_R = 7.5 min (minor), 10.1 min (major).[8e,12]

***N,N'*-Bis(*t*-butoxycarbonyl)-2-hydrazino-2-methyl-3-oxobutyric acid ethyl ester (26e).**[8e] This known compound was obtained as a colorless oil (0.037 g, 0.098 mmol) per the procedure for Scheme 5.3. NMR ($CDCl_3$, δ in ppm): ^{1}H (500 MHz) 6.29-5.99 (br m, 1H, N**H**), 4.32-4.13 (m, 2H, $C\mathbf{H}_2CH_3$), 2.43-2.18 (3H, br m), 1.86-1.17 (m, 24H, $C(C\mathbf{H}_3)_3$, $C'(C'\mathbf{H}_3)_3$, $CC\mathbf{H_3}$ and $CH_2C\mathbf{H}_3$); $^{13}C\{^1H\}$ (125 MHz) 199.7 (s, (**C**=O)CH_3), 169.6 (s, (**C**=O)OEt), 156.5 and 155.7 (2s, (**C**=O)O-*t*Bu and (**C**'=O')O'-*t*Bu'), 85.0, 83.1, and 81.2 (3s, $\mathbf{C}(CH_3)_3$ and $\mathbf{C}'(C'H_3)_3$),[13] 62.2 (s, $\mathbf{C}H_2CH_3$), 29.8 (s), 28.3 and 28.1 (2s, $C(\mathbf{C}H_3)_3$ and $C'(\mathbf{C}'H_3)_3$), 24.5, 20.0, and 19.2 (3s),[13] 14.2 (s, $CH_2\mathbf{C}H_3$).

Enantiomeric excesses were determined by HPLC (see Figure A-20) with a Chiralpak AD-H column (95:5 v/v hexane/isopropanol, 1.0 mL/min, λ = 210 nm); for Δ-(*S*,*S*)-$\mathbf{1}^{3+}$ $2Cl^-BAr_{f20}^-$, t_R = 11.6 min (minor), 17.5 min (major); for Λ-(*S*,*S*)-$\mathbf{1}^{3+}$ $2Cl^-$ Bar_{f20}^-, t_R = 13.0 min (major), 18.4 min (minor); for Δ-(*S*,*S*)-$\mathbf{1}^{3+}$ $2Cl^-BAr_f^-$, t_R = 13.1 min (minor), 17.7 min (major).[8e,12]

Di-*t*-butyl-1-(1-cyano-2-oxocyclopentyl)hydrazine-1,2-dicarboxylate (26f).[8a] This known compound was obtained as a white flakes (0.031 g, 0.092 mmol) per the procedure for Scheme 5.3. NMR ($CDCl_3$, δ in ppm): ^{1}H (500 MHz) 6.84-6.24 (br s, 1H,

N**H**), 2.92-1.81 (m, 6H, 3 × ring C$\mathbf{H}_2$), 1.59-1.27 (m, 18H, C(C$\mathbf{H}_3$)$_3$ and C'(C'$\mathbf{H}_3$)$_3$); ^{13}C{^{1}H} (125 MHz) 202.5 (s, (**C**=O)CH_2), 155.3 and 153.1 (2s, (**C**=O)O-*t*Bu and (**C**'=O')O'-*t*Bu'), 115.2 (s, **C**N), 84.1 and 82.6 (2s, **C**$(CH_3)_3$ and **C**'(C'H_3)$_3$), 69.4 (s, **C**CN), 35.0 and 34.1 (2s, ring **C**H_2), 28.3 and 28.1 (2s, C(**C**H_3)$_3$ and C′(**C**′H_3)$_3$), 18.8 (s, ring **C**H_2).

Enantiomeric excesses were determined by HPLC (see Figure A-21) with a Chiralpak AD-H column (99:1 v/v, hexane/isopropanol, 1.0 mL/min, λ = 220 nm); for Δ-(*S*,*S*)-**1**$^{3+}$ 2Cl$^-$BAr$_{f20}^-$, t_R = 7.9 min (major), 10.8 min (minor).[8e,12]

***N,N'*-Bis(*t*-butoxycarbonyl)-2-hydrazino-2-acetylcyclopentanone (26g).** This new compound was obtained as a white flakes (0.037 g, 0.099 mmol) per the procedure for Scheme 5.3. NMR ($CDCl_3$, δ in ppm): ^{1}H (500 MHz) 6.30-5.79 (br m, 1H, N**H**), 3.25-1.58 (m, 11H), 1.52-1.24 (m, 18H, C(C$\mathbf{H}_3$)$_3$, and C'(C'$\mathbf{H}_3$)$_3$); ^{13}C{^{1}H} (125 MHz) 206.0 (s, (**C**=O)CH_2), 202.7 (s, (**C**=O)CH_3), 156.6 and 155.9 (2s, (**C**=O)O-*t*Bu and (**C**'=O')O'-*t*Bu'), 84.8, 83.1, 81.9, 81.5 (4s, **C**$(CH_3)_3$ and **C**'(C'H_3)$_3$),[s7] 41.8, 33.0 and 29.4 (3s), 28.3 and 28.1 (2s, C(**C**H_3)$_3$ and C′(**C**′H_3)$_3$), 27.3, 25.0, 20.7, and 20.2 (4s), mp 39-41 °C dec (open capillary). Anal. Calcd. for $C_{16}H_{32}O_5N_2$ (370.43): C 58.36, H 8.16, N 7.56; found C 58.47, H 8.03, N 7.41.

Enantiomeric excesses were determined by HPLC (see Figure A-22) with a Chiralpak AD-H column (95:5 v/v hexane/isopropanol, 1.0 mL/min, λ = 210 nm); for Δ-(*S*,*S*)-**1**$^{3+}$ 2Cl$^-$BAr$_{f20}^-$, t_R = 14.0 min (minor), 38.9 min (major); for Λ-(*S*,*S*)-**1**$^{3+}$ 2Cl$^-$ BAr$_{f20}^-$, t_R = 14.1 min (major), 42.8 min (minor); for Δ-(*S*,*S*)-**1**$^{3+}$ 2Cl$^-$BAr$_f^-$, t_R = 14.2 min (minor), 39.3 min (major).

***N,N'*-Bis(*t*-butoxycarbonyl)-1-hydrazino-2-oxocycloheptanecarboxylic acid methyl ester (26h).**[8a] This known compound was obtained as a white flakes (0.038 g, 0.094 mmol) per the procedure for Scheme 5.3. NMR ($CDCl_3$, δ in ppm): ^{1}H (500 MHz)

6.40-5.95 (br m, 1H, N**H**), 3.95-3.42 (s, 3H, COOC**H**$_3$), 3.25-0.66 (m, 28H, 5 × ring C**H**$_2$, C(C**H**$_3$)$_3$, and C'(C'**H**$_3$)$_3$); ^{13}C{^{1}H} (125 MHz) 204.5 and 201.9 (2s, (**C**=O)CH$_2$), 171.4 (s, (**C**=O)OMe), 156.0 and 155.6 (2s, (**C**=O)O-*t*Bu and (**C**'=O')O'-*t*Bu'), 83.2, 81.5, 80.1, and 78.9 (4s, **C**(CH$_3$)$_3$ and (**C**'C'H$_3$)$_3$),[13] 53.0 and 52.7 (2s, O**C**H$_3$),[13] 40.8, 39.7, 34.6, 33.1, 30.5, and 29.8 (6s),[13] 28.2 and 28.1 (2s, C(**C**H$_3$)$_3$ and C′(**C**′H$_3$)$_3$), 25.9 and 23.9 (2s).[13]

Enantiomeric excesses were determined by HPLC (see Figure A-23) with a Chiralpak OD-H column (97:7 v/v hexane/isopropanol, 1.0 mL/min, λ = 210 nm); for Δ-(*S*,*S*)-**1**$^{3+}$ 2Cl$^-$BAr$_{f20}$$^-$ t_R = 6.4 (minor), 8.7 min (major).[8a,12]

5.5. References

(1) (a) Dalko, P. I.; Moisan, L. *Angew. Chem., Int. Ed*. **2004**, *43*, 5138-5175; *Angew. Chem*. **2004**, *116*, 5248-5286. (b) Berkessel, A.; Groger, H. Asymmetric Organocatalysis: From Biomimetic Concepts to Application in Asymmetric Synthesis; Wiley-VCH: Weinheim, Germany, **2005**. (c) Takemoto, Y. *Org. Biomol. Chem*. **2005**, *3*, 4299-4306. (d) Taylor, M. S.; Jacobsen, E. N. *Angew. Chem., Int. Ed.* **2006**, *45*, 1520-1543; *Angew. Chem*. **2006**, *118*, 1550-1573. (e) Doyle, A. G.; Jacobsen, E. N. *Chem. Rev*. **2007**, *107*, 5713-5743. (f) Yu, X.; Wang, W. *Chem. Asian J*. **2008**, *3*, 516-532. (g) Zhang, Z.; Schreiner, P. R. *Chem. Soc. Rev*. **2009**, *38*, 1187-1198. (h) Piovesana, S.; Schietroma, D. M. S.; Bella, M. *Angew. Chem., Int. Ed*. **2011**, *50*, 6216-6232; *Angew. Chem*. **2011**, *123*, 6340-6357. (i) Phipps, R. J.; Hamilton, G. L.; Toste, F. D. *Nat. Chem*. **2012**, *4*, 603-614. (j) Brak, K.; Jacobsen, E. N. *Angew. Chem., Int. Ed*. **2013**, *52*, 534-561; *Angew. Chem.* **2013**, *125*, 558-588. (k) Held, F. E.; Tsogoeva, S. B. *Catal. Sci. Technol.* **2016**, DOI: 10.1039/C5CY01894C.

(2) (a) Delacroix, O.; Gladysz, J. A. *Chem. Commun.* **2003**, 665-675 (feature article). (b) Gong, L.; Chen, L.-A.; Meggers, E. *Angew. Chem. Int. Ed.* **2014**, *53*, 10868-10874; *Angew. Chem*. **2014**, *126*, 11046-11053.

(3) (a) Ganzmann, C.; Gladysz, J. A. *Chem*. *Eur*. *J*. **2008**, *14*, 5397-5400. (b) Lewis, K. G.; Ghosh, S. K.; Bhuvanesh, N.; and Gladysz, J. A. *ACS Cent. Sci.* **2015**, *1*, 50-56.

(4) (a) Scherer, A.; Mukherjee, T.; Hampel, F.; Gladysz, J. A. *Organometallics* **2014**, *33*, 6709-6722. (b) Mukherjee, T.; Ganzmann, C.; Bhuvanesh, N.; Gladysz, J. A. *Organometallics* **2014**, *33*, 6723-6737. (c) Thomas, C.; Gladysz, J. A. *ACS Catal.* **2014**, *4*, 1134-1138.

(5) (a) Chen, L.-A.; Xu, W.; Huang, B.; Ma, J.; Wang, L.; Xi, J.; Harms, K.;

Gong, L.; Meggers, E. *J. Am. Chem. Soc*. **2013**, *135*, 10598-10601. (b) Chen, L.-A.; Tang, X.; Xi, J.; Xu, W.; Gong, L.; Meggers, E. *Angew. Chem., Int. Ed*. **2013**, *52*, 14021-14025; *Angew. Chem*. **2013**, 12*5*, 14271-14275. (c) Ma, J.; Ding, X.; Hu, Y.; Huang, Y.; Gong, L.; Meggers, E. *Nat. Commun*. **2014**, *5*:4531 (d) Huo, H.; Fu, C.; Wang, C.; Harms, K.; Meggers, E. *Chem. Commun*. **2014**, *50*, 10409-10411.

(6) For relevant studies with achiral metal containing hydrogen bond donor catalysts, see (a) Nickerson, D. M.; Mattson, A. E. *Chem. Eur. J.* **2012**, *18*, 8310-8314. (b) Nickerson, D. M.; Angeles, V. V.; Auvil, T. J.; So, S. S.; Mattson, A. E. *Chem. Commun*. **2013**, *49*, 4289-4291.

(7) (a) Werner, A. *Chem. Ber.* **1911**, *44*, 3279-3284. (b) Werner, A. *Chem. Ber.* **1911**, *44*, 3272-3278. (c) Werner, A. *Chem. Ber.* **1911**, *44*, 2445-2455. (d) Werner, A. *Chem. Ber.* **1911**, *44*, 1887-1898. V. L. King is listed as an author for the experimental section. (e) Werner, A. *Chem. Ber.* **1912**, *45*, 121-130.

(8) (a) Saaby, S.; Bella, M.; Jørgensen, K. A. *J. Am. Chem. Soc*. **2004**, *126*, 8120-8121. (b) Pihko, P. M.; Pohjakallio, A. *Synlett 2004*, 2115-2118. (c) Liu, X.; Li, H.; Deng, L. *Org. Lett*. **2005**, *7*, 167-169. (d) Xu, X.; Yabuta, T.; Yuan, P.; Takemoto, Y. *Synlett* **2006**, 137-140. (e) Terada, M.; Nakano, M.; Ube, H. *J. Am. Chem. Soc.* **2006**, *128*, 16044-16045. (f) Jung, S. H.; Kim, D. Y. *Tetrahedron Lett*. **2008**, *49*, 5527-5530. (g) Konishi, H.; Lam, T. Y.; Malerich, J. P.; Rawal, V. H. *Org. Lett*. **2010**, *12*, 2028-2031. (h) Inokuma, T.; Furukawa, M.; Uno, T.; Suzuki, Y.; Yoshida, K.; Yano, Y.; Matsuzaki, K.; Takemoto, Y. *Chem. Eur. J*. **2011**, *17*, 10470-10477. (i) Xu, C.; Zhang, L.; Luo, S. *J. Org. Chem*. **2014**, *79*, 11517-11526.

(9) (a) Vogt, H.; Bräse, S. *Org. Biomol. Chem*. **2007**, *5*, 406-430. (b) Cativiela, C; Díaz-de-Villegas, M. D. *Tetrahedron: Asymmetry* **2007**, *18*, 569-623. (c) Cativiela, C.; Ordóñez, M. *Tetrahedron: Asymmetry* **2009**, *20*, 1-63.

(10) (a) Harper, K. C.; Sigman, M. S. *Proc. Natl. Acad. Sci. U.S.A* **2011**, *108*, 2179-2183. (b) Harper, K. C.; Bess, E. N.; Sigman, M. S. *Nat. Chem.* **2012**, *4*, 366-374. (c) Milo, A.; Neel, A. J.; Toste, F. D.; Sigman, M. S. *Science* **2015**, *347,* 737-743.

(11) Ghosh, S. K.; Ganzmann, C.; Bhuvanesh, N.; Gladysz, J. A. *Angew*. *Chem*., *Int*. *Ed*. **2016**, *55*, 4356-4360; *Angew*. *Chem*. **2016**, *128*, 4429-4433.

(12) The chiral HPLC column employed with **26a** featured the same stationary phase but a different particle size from that used earlier in the literature.[8a,e] It is presumed that the well separated enantiomers exhibit identical orders of elution. Configurations were assigned accordingly.

(13) In accord with previous reports,[8e,g] some ^{13}C NMR signals are doubled (unequal intensities) due to geometric isomerism about the carbamate carbon-nitrogen bonds (*Z*/*E* N–$^{+}$N(R)=C(O^{-})O-*t*Bu).

6. SYNTHESIS OF A SERIES OF ω-DIMETHYLAMINOALKYL SUBSTITUTED ETHYLENEDIAMINE LIGANDS FOR USE IN ENANTIOSELECTIVE CATALYSIS†

6.1. Introduction

Over the last fifteen years, a variety of small molecule hydrogen bond donor catalysts have been developed and found diverse applications in enantioselective syntheses.[1] Some of the most useful catalysts have been based upon urea and thiourea moieties.[2] These readily bind to a number of Lewis basic organic functional groups, as demonstrated by a series of crystal structures.[3] Importantly, some of the most effective urea and thiourea catalysts are bifunctional, incorporating an auxiliary tertiary amine group.[2b,4] This can serve as either a Lewis or Brønsted base during the catalytic cycle.

We have begun to study Werner complexes as possible NH hydrogen bond donor catalysts for enantioselective organic syntheses.[5,6] This includes the historically important chiral-at-metal tris(ethylenediamine) cobalt trication $[Co(en)_3]^{3+}$, which was among the first few inorganic species to be resolved into enantiomers,[7] as well as analogs with substituted diamines, such as 1,2-diphenylethylenediamine (dpen).[6] We have also developed cationic ruthenium complexes in which NH bonds remote from the metal effect catalysis.[8,9] Dramatic improvements in the performance of this catalyst family were realized when dimethylamino substituents were incorporated into the NH containing ligand.[8b] Closely related themes have also received attention in the Meggers group.[10]

†Reproduced from Ghosh, S. K.; Ganzmann, C.; Gladysz, J. A. *Tetrahedron: Asymmetry*. **2015**, *26*, 1273-1280, with permission from Elsevier.

In the first communication, which focused on additions of malonates to enones in organic media, we were only able to realize modest enantioselectivities using lipophilic salts of $[Co(en)_3]^{3+}$.[5] I speculated that adducts of ethylenediamine ligands containing an ω-dimethylaminoalkyl substituent might give improved results. Hence, I sought to synthesize a series of ligands $H_2NCH((CH_2)_nNMe_2)CH_2NH_2$ in enantiopure form, so that they could be incorporated into cobalt complexes such as $\mathbf{I}^{3+}$ (Figure 6.1) without increasing the numbers of diastereomers.

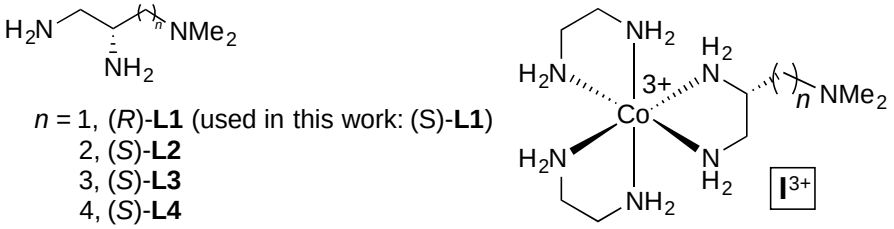

Figure 6.1. Target ligands and complexes.

Curiously, I could only locate one such triamine in the literature, that with n = 2.[11] The overall yield was modest, and only the ^{1}H NMR spectrum and optical rotation were reported. Hence, I set out to prepare the ligands with n = 1-4, termed **L1-L4** (Figure 6.1), and/or the functionally equivalent tris(hydrochloric acid) salts. In this section, I describe practical six to nine step syntheses for all of these species from inexpensive, commercially available enantiopure starting materials in 38-13% overall yields (average: 26%), and their detailed characterization. Some of the reactions involving **L1** were carried out by Dr. Carola Ganzmann. Applications of these ligands will be described separately in section 7.[12]

6.2. Results

6.2.1. L1

As shown in Scheme 6.1, commercial (*S*)-asparagine ((*L*)-asparagine or (*S*)-$\mathbf{1_{L1}}$, \$0.09/g for 100g)[13a] was elaborated in a series of five known steps.[14,15] The first involved treatment with CbzCl to give the Cbz protected amine (*S*)-$\mathbf{2_{L1}}$ (our yield/lit: 80/84%).[14a] A Hofmann type rearrangement was then effected with $PhI(OAc)_2$ to give

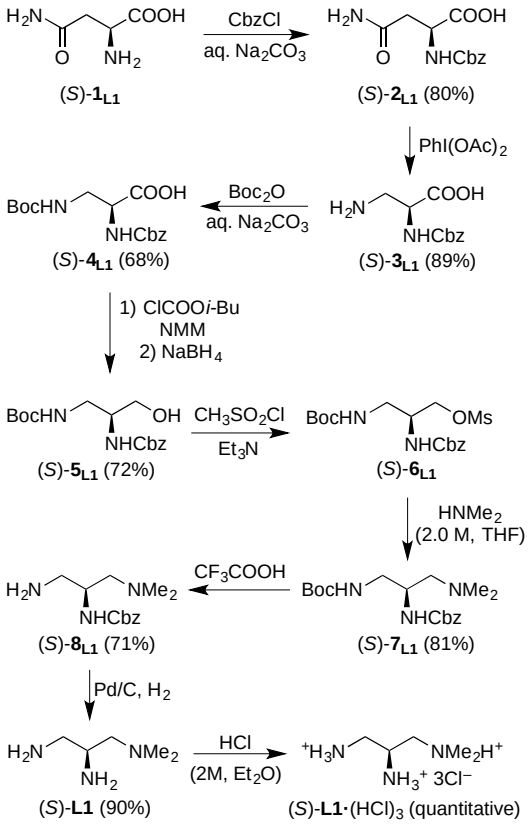

Scheme 6.1. Synthesis of the tris(hydrochloric acid) salt of (*S*)-**L1**.

the ß-amino acid (*S*)-$\mathbf{3_{L1}}$ (my yield/lit: 89/89%),[14b] which was protected with Boc to afford (S)-$\mathbf{4_{L1}}$ (my yield/lit: 68/91%).[14a,16] Following a patent procedure, the carboxylic

acid was activated with isobutyl chloroformate, and reaction with $NaBH_4$ gave the primary alcohol (*S*)-$\mathbf{5_{L1}}$ (my yield/lit: 72/55%).[15,16] Mesylation was effected to give (S)-$\mathbf{6_{L1}}$,[15] the last known compound in this sequence, which was employed in the following step assuming a quantitative yield.

In order to introduce the dimethylamino group, (*S*)-$\mathbf{6_{L1}}$ and a THF solution of $HNMe_2$ were refluxed (Scheme 6.1). Workup gave the protected triamine (*S*)-$\mathbf{7_{L1}}$ (81%, two steps). Addition of CF_3CO_2H removed the Boc protecting group, affording the diamine (*S*)-$\mathbf{8_{L1}}$ (71%). Hydrogenolysis then detached the Cbz group, giving the target triamine (*S*)-**L1** (90%) in 18% overall yield from (S)-$\mathbf{1_{L1}}$. For long term storage, this was converted to the tris(hydrochloric acid) salt (*S*)-$[H_3NCH((CH_2)NHMe_2)CH_2NH_3]^{3+}$ $3Cl^-$ ((*S*)-**L1**$\cdot(HCl)_3$) in 99% yield. This sequence has been repeated by several coworkers, sometimes with even higher yields than those indicated above and in the experimental section (maximum values for the first five yields in Scheme 6.1: 85%, 90%, 80%, 80%, 86%).

6.2.2. L2

As shown in Scheme 6.2, commercial (*S*)-5-hydroxymethyl-2-pyrrolidinone ((*S*)-$\mathbf{1_{L2}}$, $2.8/g for 100 g)[13b] was elaborated in a series of five known steps.[17] The first involved treatment with tosyl chloride to give the tosylate (*S*)-$\mathbf{2_{L2}}$ (my yield/lit: 84/93%).[17a] Subsequent reaction with NaN_3 afforded (*S*)-$\mathbf{3_{L2}}$ (my yield/lit: 90/99%).[17a] The azide was reduced to the primary amine (*S*)-$\mathbf{4_{L2}}$ with Pd/C and H_2 (my yield/lit: 91/99%).[17a] Hydrolysis (6 M HCl) then provided (*S*)-$\mathbf{5_{L2}}$ (my yield/lit: 97/83%).[17b] Both primary amine groups were protected using isobutyl chloroformate to give (*S*)-$\mathbf{6_{L2}}$ (my yield/lit: 88/88%).[17b]

It was next sought to remove a methylene group from the carboxylic acid chain. Thus, (*S*)-$\mathbf{6_{L2}}$ was first converted to the corresponding amide (*S*)-$\mathbf{7_{L2}}$ (85%), a new

compound. A modified Hofmann rearrangement was then carried out using $PhI(OAc)_2$. The resulting primary amine (*S*)-$\mathbf{8_{L2}}$ (57%) was a known compound.[17b] A reductive dimethylation (aqueous HCHO, Pd/C, H_2) yielded the new tertiary amine (*S*)-$\mathbf{9_{L2}}$ (50%). Refluxing aqueous HCl afforded the tris(hydrochloric acid) salt (*S*)-$[H_3NCH((CH_2)_2NHMe_2)CH_2NH_3]^{3+}$ $3Cl^-$ ((*S*)-**L2**·$(HCl)_3$) as a colorless sticky compound in 13% overall yield from (*S*)-$\mathbf{1_{L2}}$. As noted above, this compound has been previously synthesized, but in only 7% overall yield, although the sequence involved one fewer step.[11]

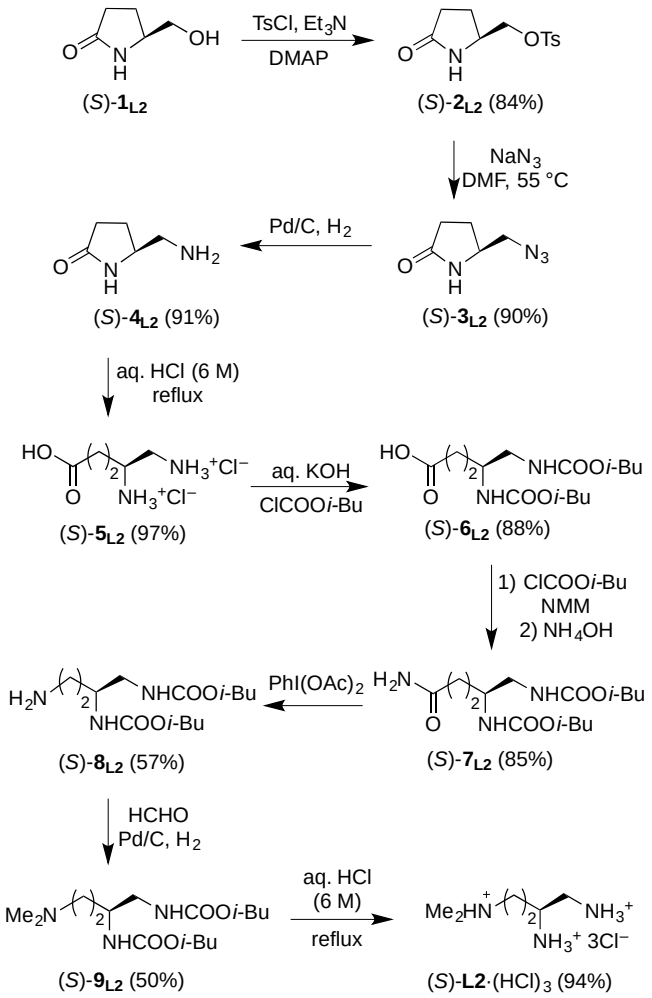

Scheme 6.2. Synthesis of the tris(hydrochloric acid) salt of (*S*)-**L2**.

6.2.3. L3

As shown in Scheme 6.3, **L3** can be accessed using (*S*)-$\mathbf{6_{L2}}$ from Scheme 6.2. The carboxylic acid was first activated with isobutyl chloroformate, and $NaBH_4$ reduction gave the new primary alcohol (*S*)-$\mathbf{1_{L3}}$ (82%). Mesylation was effected to give (*S*)-$\mathbf{2_{L3}}$. The crude mesylate was refluxed in a THF solution of $HNMe_2$, affording the corresponding dimethylamine (*S*)-$\mathbf{3_{L3}}$ (86%, two steps). The protecting groups were removed in refluxing aqueous HCl to give the new tris(hydrochloric acid) salt (*S*)-$[H_3NCH((CH_2)_3NHMe_2)CH_2NH_3]^{3+}$ $3Cl^-$ ((*S*)-**L3**·$(HCl)_3$) as a colorless sticky compound in 86% yield or 36% overall yield from the ultimate starting material in Scheme 6.2, (*S*)-$\mathbf{1_{L2}}$.

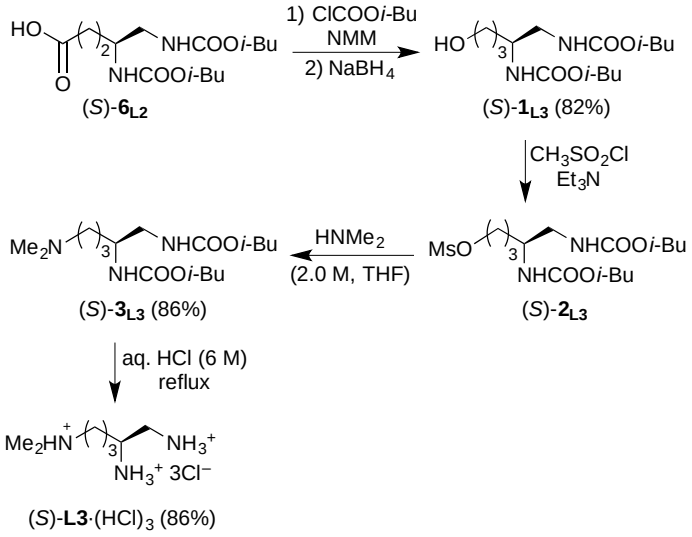

Scheme 6.3. Synthesis of the tris(hydrochloric acid) salt of (*S*)-**L3**.

6.2.4. L4

As shown in Scheme 6.4, commercial (*S*)-6-(((benzyloxy)carbonyl) amino)-2-((*tert*-butoxycarbonyl)amino)hexanoic acid ((*S*)-$\mathbf{1_{L4}}$, $0.96/g for 100 g)[13a] was elaborated in a

series of three known steps.[18] The carboxylic acid was first activated with isobutyl chloroformate, and $NaBH_4$ reduction yielded the primary alcohol (*S*)-$\mathbf{2_{L4}}$ (my yield/lit: 92/94%).[18a] Mesylation was effected to give (*S*)-$\mathbf{3_{L4}}$, which was treated with NaN_3 to give (*S*)-$\mathbf{4_{L4}}$ (my yield/lit: 80/86%).[18b] The azide was reduced to the primary amine using $NaBH_4$ in the presence of Pd/C. This was protected in situ with Boc to give (*S*)-$\mathbf{5_{L4}}$ (71%). During the preparation of the paper corresponding to this section,[19] an independent synthesis of (*S*)-$\mathbf{5_{L4}}$ was reported by Carell.[20] His route, which involves a starting material of similar cost, is slightly more efficient (five steps, 55% overall yield vs. four steps, 52% overall yield).

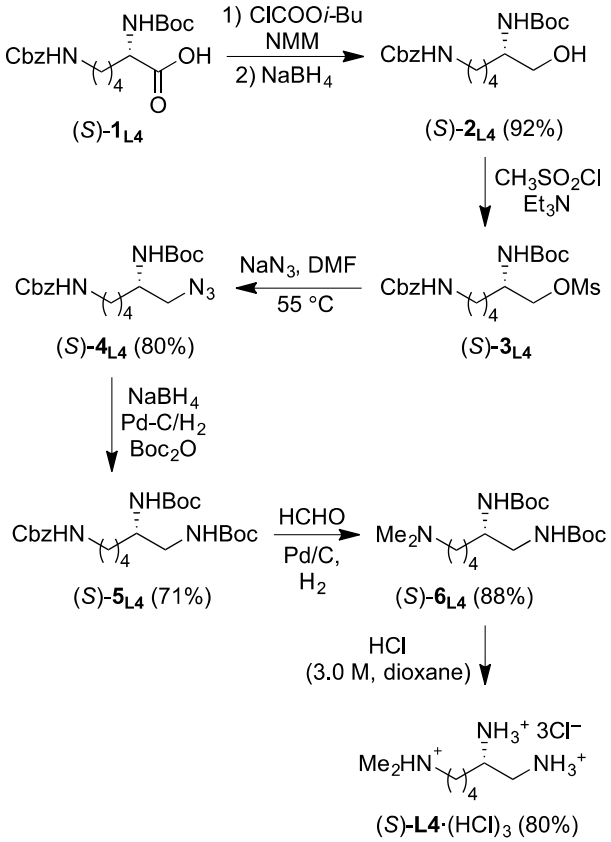

Scheme 6.4. Synthesis of the tris(hydrochloric acid) salt of (*S*)-**L4**.

Next, (*S*)-$\mathbf{5_{L4}}$ was treated with aqueous HCHO in presence of Pd/C and H_2. This removed the Cbz protecting group and delivered the new tertiary amine (*S*)-$\mathbf{6_{L4}}$ (88%). Finally, the Boc groups were removed using HCl in aqueous dioxane to give the new tris(hydrochloric acid) salt (*S*)-$[H_3NCH((CH_2)_4NHMe_2)CH_2NH_3]^{3+}$ $3Cl^-$ ((*S*)-**L4** $(HCl)_3$) as a colorless sticky compound in 80% yield or 38% overall yield from (*S*)-$\mathbf{1_{L4}}$.

All of the new compounds described above gave correct microanalyses. They were furthermore characterized by ^1H and ^{13}C NMR spectroscopy, as summarized in the experimental section.

6.3. Discussion

The syntheses in Schemes 6.1-6.4 represent highly optimized protocols leading to a novel family of enantiopure triamine ligands (**L1**-**L4**). One common feature is that the dimethylamino groups are introduced at late stages, either via reductive dimethylations or nucleophilic displacements involving mesylates and $HNMe_2$. A Hofmann type rearrangement allows **L2** and **L3** to be accessed from the same precursor, and **L1** to be prepared from a less costly precursor ((*S*)-$\mathbf{1_{L1}}$ vs. (*S*)-$\mathbf{3_{L1}}$).

To my knowledge, only one of the ligands and two late stage intermediates, (*S*)-**L2**·$(HCl)_3$),[11] (*S*)-$\mathbf{8_{L2}}$,[17b] and (*S*)-$\mathbf{5_{L4}}$,[20] have been independently synthesized. My route to (*S*)-**L2**·$(HCl)_3$ constitutes a distinct improvement. However, the literature preparation of (*S*)-$\mathbf{5_{L4}}$, which was only reported in 2015, is competitive with my methodology. Importantly, the enantiomers of the three starting materials used in Schemes 6.1-6.4 are commercially available, but at prices that are 3-4 times greater per mole.

In the planned applications with cobalt(III) complexes (e.g., $\mathbf{I}^{3+}$), the two primary amino groups of **L1**-**L4** are intended to serve as chelates. The tertiary dimethylamino groups are designed, by analogy to their roles in thiourea and urea catalysts,[2b,4] to aid the activation of substrates. However, other coordination modes and

roles can be envisioned, suggesting a class of compounds that may have a mechanistically diverse spectrum of applications in enantioselective synthesis. Also, although **L4** has not previously been synthesized, it has served as a linking unit in a series of cisplatin-N-mustard conjugates.[20]

In summary, a series of four homologous ω-dimethylaminoalkyl substituted ethylenediamine ligands (**L1**-**L4**) are now readily available in enantiopure form. In the following section 7, the cobalt(III) complexes that contain such ligands will be described.[12] Some of these will be highly enantioselective hydrogen bond donor catalysts, superior to those detailed previously.[6]

6.4. Experimental section

General Data: ^{1}H and $^{13}C\{^{1}H\}$ NMR spectra were recorded on standard 300-500 MHz spectrometers at ambient probe temperatures. Chemical shifts (δ in ppm) were referenced to residual solvent signals (^{1}H: $CHCl_3$, 7.26; DMSO-d_5, 2.49, HOD, 4.79 ppm; ^{13}C: $CDCl_3$, 77.2; DMSO-d_6, 39.5),[21] except for $^{13}C\{^{1}H\}$ spectra recorded in D_2O, which were referenced to internal dioxane (67.2).[21] IR spectra were recorded on ASI React IR®-1000 or Shimadzu IRAffinity-1 spectrometers. Microanalyses were conducted by Atlantic Microlab or in house using a Carlo Erba EA 1110 CHN instrument. Optical rotations were measured with a Perkin-Elmer model 431 polarimeter as described previously.[22]

Reactions were conducted under air unless noted. Chemicals were treated as follows: DMSO-d_6 and $CDCl_3$ (Cambridge Isotopes), stored over molecular sieves; CH_2Cl_2 (EMD Chemicals, ACS grade), CH_3OH (EMD, anhydrous, 99.8%), hexanes (Macron, ACS grade), Et_2O (Macron, ACS grade), EtOAc (Macron, ACS grade), THF (Macron, ACS grade), DMF (Mallinckrodt, ACS grade), EtOH (BDH, ACS grade), dioxane (Macron, ACS grade), 1,2-dimethoxyethane (Acros, 99+%), acetone (BDH, ACS grade), (L)-Asparagine (Aroz Technologies, LLC, 98%), (*S*)-5-Hydroxymethyl-2-pyrrolidinone (AK Scientific, Inc, 98%), (*S*)-6-(((Benzyloxy)carbonyl)amino)-2-((*tert*-butoxycarbonyl)amino)hexanoic acid (Aroz Technologies, LLC, 98%), citric acid (EMD, ACS grade), tosyl chloride (TsCl, Alfa Aesar, 98%), *N*-methyl morpholine (NMM, Acros, 99%), isobutyl chloroformate (ClCOO*i*-Bu, Alfa Aesar, 98%), iodosobenzenediacetate ($PhI(OAc)_2$, Alfa Aesar, 98+%), CbzCl (TCI, 30-35 weight% in toluene), Boc_2O (Chem-Impex International, Inc., 98%), Conc. NH_4OH (30%, EMD, ACS grade), aqueous HCHO (EMD, ACS grade), $NaBH_4$ (Aldrich, 98%), methanesulfonyl chloride (CH_3SO_2Cl, Acros, 99.5%), $HNMe_2$ (2.0 M in THF, Alfa

Aesar), Pd/C (10%, Aldrich), Pd/C (10%, "nominally 50% water wet", Alfa Aesar), NaOH (Macron, ACS grade), Et_3N (Alfa Aesar, 98%), NaN_3 (Alfa Aesar, 99%), $NaHCO_3$ (Alfa Aesar, 98%), CF_3COOH (99%, Acros), HCl (2.0 M in Et_2O, Acros), $KHSO_4$ (Alfa Aesar, 98%), Celite 545 (Aldrich), and Na_2SO_4 (EMD), used as received.

(*S*)-N^2-Benzyloxycarbonyl-N^3-*tert*-butyloxycarbonyl-2,3-diaminopropan-1-ol or (*S*)-((*t*-BuOC(O))NHCH$_2$CH(CH$_2$OH)NH(C(O)OCH$_2$Ph) ((*S*)-5$_{L1}$).[15,16] A round bottom flask was charged with (*S*)-**4$_{L1}$** (15.90 g, 47.0 mmol)[14a] and 1,2-dimethoxyethane (65 mL), and *N*-methyl morpholine (5.4 mL; 5.0 g, 49 mmol) was added with stirring. The solution was cooled to –25 °C, and isobutyl chloroformate (6.50 mL; 6.8 g, 50 mmol) was slowly added. The cold bath was removed. After 30 min, the precipitate was collected by filtration and washed with 1,2-dimethoxyethane (2 × 30 mL). The combined filtrate and washings were sparged with nitrogen and cooled to 0 °C. A solution of $NaBH_4$ (2.52 g, 66.5 mmol) in EtOH (150 mL) was added dropwise with stirring. After 1 h, H_2O (10 mL) was cautiously added. The cold bath was removed. After 12 h, the solvent was removed by rotary evaporation. The solid was dissolved in EtOAc (200 mL), and H_2O (200 mL) was added. The aqueous phase was extracted with EtOAc (2 × 50 mL) and the combined organic phases were dried ($MgSO_4$). The solvent was removed by rotary evaporation and the solid was chromatographed on a silica gel column (4 × 17 cm, 20:80 to 50:50 v/v EtOAc/hexane). The solvent was removed from the product containing fraction by rotary evaporation. The residue was dried by oil pump vacuum to give (*S*)-**5$_{L1}$** (11.0 g, 33.8 mmol, 72%) as a white solid.

NMR (DMSO-d_6, δ in ppm): ^{1}H (400 MHz)[16] 7.37-7.28 (m, 5H, **Ph**), 6.86 (d, $^3J_{HH}$ = 8.4 Hz, 1H, CHN**H**), 6.72 (t, $^3J_{HH}$ = 5.2 Hz, 1H, CH$_2$N**H**), 4.99 (m, 2H, OC**H**$_2$Ph), 4.61 (t, $^3J_{HH}$ = 5.6 Hz, 1H, O**H**), 3.52-3.48 (m, 1H, C**H**NHCbz), ca. 3.4 (C**H**$_2$OH, signal obscured by solvent impurity), 3.10-3.03 (m, 1H, C**H**H'NHBoc), 2.98-

2.93 (m, 1H, CH**H'**NHBoc), 1.35 (s, 9H, C(C**H**$_3$)$_3$); ^{13}C{^{1}H} ($CDCl_3$, 75.5 MHz) 157.6 and 156.3 (2 × s, (**C**=O)O from Boc and Cbz); **Ph** at 136.1 (s, *i*), 128.4 (s, *m*),[23] 128.0 (s, *p*), 127.9 (s, *o*); 80.1 (s, **C**(CH$_3$)$_3$), 66.7 (s, O**C**H$_2$Ph), 61.3 (s, **C**H$_2$OH), 52.8 (s, **C**HNHCbz), 40.1 (s, **C**H$_2$NHBoc), 28.2 (s, C(**C**H$_3$)$_3$).

(*S*)-*N*^{2}-Benzyloxycarbonyl-*N*^{3}-*tert*-butyloxycarbonyl-2,3-diaminopropyl methanesulfonate or (*S*)-((*t*-BuOC(O))NHCH$_2$CH(CH$_2$OSO$_2$Me)NH(C(O)OCH$_2$Ph) ((*S*)-6$_{L1}$).[15] A Schlenk flask was charged with (*S*)-**5$_{L1}$** (10.4 g, 32.1 mmol), CH_2Cl_2 (150 mL), and Et_3N (10.7 mL, 7.77 g, 76.9 mmol), and cooled to –78 °C. Methanesulfonyl chloride (4.7 mL, 7.0 g, 61 mmol) was added dropwise with stirring. The cold bath was allowed to warm to 0 °C over the course of 3 h. Aqueous citric acid (20% w/v, 200 mL) and CH_2Cl_2 (100 mL) were added. The organic phase was separated, washed with saturated $NaHCO_3$ (200 mL) and brine (200 mL), and dried ($MgSO_4$). The solvent was removed by oil pump vacuum to give (*S*)-**6$_{L1}$** as a white solid. This material was used without further purification.

NMR (DMSO-d$_6$, δ in ppm): ^{1}H (500 MHz): 7.36-7.28 (m, 5H, **Ph**), 5.73 (br d, $^3J_{HH}$ = 5.2 Hz, 1H, CHN**H**), 5.07 (s, C**H**$_2$OPh), 4.94 (br t, $^3J_{HH}$ = 6 Hz, 1H, CH$_2$N**H**), 4.27-4.21 (m, 2H, C**H**$_2$OS), 3.98-3.93 (m, 1H, C**H**NHCbz), 3.36-3.30 (m, 2H, C**H**$_2$NHBoc), 2.98 (s, 3H, SC**H**$_3$), 1.40 (s, 9H, C(C**H**$_3$)$_3$).

(*S*)-*N*^{1},*N*^{1}-dimethyl-*N*^{2}-Benzyloxycarbonyl-*N*^{3}-*tert*-butyloxycarbonyl-*N*^{1},*N*^{1}-dimethylpropane-1,2,3-triamine or (*S*)-((*t*-BuOC(O))NHCH$_2$CH(CH$_2$NMe$_2$)NH(C(O)OCH$_2$Ph) ((*S*)-7$_{L1}$). A round bottom flask was charged with the crude (*S*)-**6$_{L1}$** from the preceding synthesis and $HNMe_2$ (2.0 M in THF; 80 mL, 160 mmol), and fitted with a condenser cooled to –55 °C (using a cold fluid recirculating bath) to return the $HNMe_2$ to the flask. The flask was placed in a 80 °C oil bath. After 9 h, the bath was allowed to cool to rt and the solvent was removed by rotary evaporation. The residue was dissolved

in CH_2Cl_2 (200 mL), washed with saturated $NaHCO_3$ (200 mL) and brine (200 mL), and dried ($MgSO_4$). The solvent was removed by rotary evaporation and the oily yellow residue was chromatographed on a silica gel column (3 × 30 cm, 10:1 v/v CH_2Cl_2/CH_3OH). The solvent was removed from the product containing fractions by rotary evaporation to give (*S*)-$\mathbf{7_{L1}}$ as a white solid (9.08 g, 25.8 mmol, 81% for two steps), mp 88 °C (open capillary). Anal. Calcd. for $C_{18}H_{29}N_3O_4$ (351.44): C 61.52, H 8.32, N 11.96; found C 61.50, H 8.29, N 11.74. $[\alpha]_{24}^{589} = -2.6 \pm 0.2°$ (1.25 mg mL^{-1}, CH_3OH).

NMR ($CDCl_3$, δ in ppm): ^1H (400 MHz) 7.34-7.28 (m, 5H, **Ph**), 5.43 (br s, 1H, CHN**H**Boc), 5.16 (br s, 1H, CH_2N**H**Boc), 5.07 (m, 2H, OC**H**$_2$Ph), 3.68-3.66 (m, 1H, C**H**NHCbz), 3.41-3.35 (m, 1H, C**H**H'NHBoc), 3.22-3.17 (m, 1H, CH**H'**NHBoc), 2.35 (dd, $^2J_{HH}$ = 12.2 Hz, $^3J_{HH}$ = 8.0 Hz, 1H, C**H**H'N$(CH_3)_2$), 2.24 (dd, $^2J_{HH}$ = 12.6 Hz, $^3J_{HH}$ = 7.0 Hz, 1H, CH**H'**N$(CH_3)_2$), 2.19 (s, 6H, N(C**H**$_3)_2$), 1.41 (s, 9H, C(C**H**$_3)_3$); $^{13}C\{^1H\}$ (100.6 MHz) 156.7 and 156.6 (2 × s, (**C**=O)O from Boc and Cbz); **Ph** at 136.4 (s, *i*), 128.4 (s, *m*),[23] 128.03 (s, *p*), 127.97 (s, *o*); 79.4 (s, **C**$(CH_3)_3$), 66.7 (s, O**C**H_2Ph), 60.6 (s, **C**H_2N$(CH_3)_2$), 50.7 (s, **C**HNHCbz), 45.6 (s, N(**C**$H_3)_2$), 43.2 (s, **C**H_2NHBoc), 28.3 (s, C(**C**$H_3)_3$). IR (powder film, cm^{-1}): 3358 (m, ν_{NH}), 1677 (vs, $\nu_{C=O}$), 1522 (vs, δ_{NH}); MS:[24] 352 (100) $[\mathbf{7_{L1}}+H]^+$, 296 (100) $[\mathbf{7_{L1}}+2H\text{-}C(CH_3)_3]^+$.

(*S*)-*N*^{2}-Benzyloxycarbonyl-*N*^{1},*N*^{1}-dimethylpropane-1,2,3-triamine or (*S*)-$NH_2CH_2CH(CH_2NMe_2)NH(C(O)OCH_2Ph)$ ((*S*)-$\mathbf{8_{L1}}$). A round bottom flask was charged with (*S*)-$\mathbf{7_{L1}}$ (9.08 g, 25.8 mmol) and CH_2Cl_2 (150 mL). Then CF_3COOH (40.0 mL, 61.9 g, 540 mmol) was added in one portion with stirring. After 14 h, aqueous NaOH (10%, 200 mL) was added and the phases were separated. The aqueous phase was extracted with CH_2Cl_2 (2 × 150 mL) and the combined organic phases were dried (Na_2SO_4). The solvent was removed by rotary evaporation and the clear oil was

chromatographed on a silica gel column (3 × 15 cm, 1:1 v/v CH_2Cl_2/CH_3OH). The solvent was removed from the product containing fractions (R_f = 0.09, TLC) by rotary evaporation to give (*S*)-**8$_{L1}$** as a waxy solid (5.08 g, 18.18 mmol, 71%). Anal. Calcd. for $C_{13}H_{21}N_3O_2 \cdot 0.33CH_2Cl_2$ (279.35): C 57.31, H 7.82, N 15.04; found C 57.00, H 7.44, N 14.97. $[\alpha]_{24}^{589} = -5.3 \pm 0.2°$ (11.5 mg mL^{-1}, CH_3OH).

NMR ($CDCl_3$, δ in ppm): ^{1}H (400 MHz): 7.32-7.25 (m, 5H, **Ph**), 5.34 (br s, 1H, N**H**), 5.06 (m, 2H, OC**H**$_2$Ph), 3.65-3.64 (m, 1H, C**H**NHCbz), 2.83 (dd, $^2J_{HH}$ = 13.2 Hz, $^3J_{HH}$ = 4.4 Hz, 1H, C**H**H'NH_2), 2.73 (dd, $^2J_{HH}$ = 13.2 Hz, $^3J_{HH}$ = 4.4 Hz, 1H, CH**H'**NH_2), 2.33 (dd, $^2J_{HH}$ = 11.8 Hz, $^3J_{HH}$ = 8.2 Hz, 1H, C**H**H'N$(CH_3)_2$), 2.22 (dd, $^2J_{HH}$ = 12.2 Hz, $^3J_{HH}$ = 6.6 Hz, 1H, CH**H'**N$(CH_3)_2$), 2.18 (s, 6H, N(C**H**$_3)_2$), 1.37 (br s, 2H, NH_2); $^{13}C\{^1H\}$ (100.6 MHz) 156.2 (s, (**C**=O)O), **Ph** at 136.2 (s, *i*), 128.0 (s, *m*),[23] 127.6 (s, *p*), 127.5 (s, *o*); 66.1 (s, O**C**H_2Ph), 60.3 (s, **C**H_2N$(CH_3)_2$), 53.1 (s, CH_2Cl_2), 50.8 (s, **C**HNHCbz), 45.3 (s, N(**C**$H_3)_2$), 43.8 (s, **C**H_2NH_2). IR ((powder film, cm^{-1}): 3358 (m, ν_{NH}), 2995, 2822, and 2771 (3 × m, ν_{CH}), 1693 (vs, $\nu_{C=O}$), 1531 (s, δ_{NH}), 1247 (vs, $\nu_{(C=O)OC}$); MS:[24] 252 (95) [**8$_{L1}$**+H]$^+$, 180 (100) [**8$_{L1}$**+H–$C_3H_8N_2$]$^+$.

(*S*)-*N*^{1},*N*^{1}-dimethylpropane-1,2,3-triamine or (*S*)-$NH_2CH_2CH(CH_2NMe_2)$-NH_2 ((*S*)-L1) A Schlenk flask was charged with (*S*)-**8$_{L1}$** (5.08 g, 18.18 mmol), CH_3OH (60 mL), and Pd/C (10%, 0.795 g). The solution was sparged with H_2 and stirred under a H_2 atmosphere (balloon). After 14 h, the mixture was filtered through a plug of Celite and the solvent was removed under reduced pressure (17 mbar) at 0 °C to give (*S*)-**L1** as a colorless oil (1.90 g, 16.3 mmol, 90%). $[\alpha]_{24}^{589} = -9.3 \pm 0.1°$ (1.08 mg mL^{-1}, CH_3OH).

NMR ($CDCl_3$, δ in ppm): ^{1}H (400 MHz): 2.90-2.85 (m, 1H, C**H**NH_2), 2.72 (dd, $^2J_{HH}$ = 12.4 Hz, $^3J_{HH}$ = 4.0 Hz, 1H, C**H**H'NH_2), 2.52 (dd, $^2J_{HH}$ = 12.6 Hz, $^3J_{HH}$ = 7.0 Hz, 1H, C**H**H'N$(CH_3)_2$), 2.21 (s, 6H, N(C**H**$_3)_2$, partly overlapped by CH**H'**N$(CH_3)_2$),

2.16 (m, 1H, CH**H'**N$(CH_3)_2$, partly overlapped by N$(CH_3)_2$), 2.10 (dd, $^2J_{HH}$ = 12.0 Hz, $^3J_{HH}$ = 4.4 Hz, 1H, CH**H'**NH_2); $^{13}C\{^1H\}$ (75.5 MHz) 64.1 (s, **C**$H_2N(CH_3)_2$), 50.1 (s, **C**HNH_2), 46.1 (s, **C**H_2NH_2), 45.5 (s, N(**C**$H_3)_2$). IR (powder film, cm^{-1}): 3280 (m, ν_{NH}), 2949 and 2831 (2 × m, ν_{CH}), 1571 (s, δ_{NH}), 1461 (s, δ_{CH_2}); MS:[25] 118 (100) [**L1**+H]$^+$.

Tris(hydrochloric acid) salt of (*S*)-*N*^{1},*N*^{1}-dimethylpropane-1,2,3-triamine or (*S*)-$H_3NCH_2CH(CH_2NMe_2H)NH_3]^{3+}$ 3Cl$^-$ ((*S*)-L1·$(HCl)_3$). A Schlenk flask was charged with (*S*)-**L1** (1.90 g, 16.3 mmol) and CH_3OH (10 mL). A solution of HCl in Et_2O (2.0 M, 12 mL) was added dropwise. A precipitate formed. The supernatant was decanted and the precipitate was washed with Et_2O (2 × 10 mL) and dried by oil pump vacuum to give (*S*)-**L1**·$(HCl)_3$·H_2O as a white powder (3.95 g, 16.1 mmol, 99%), dec pt 213 °C (capillary). Anal. Calcd. for $C_5H_{18}Cl_3N_3$·H_2O (244.59): C 24.55, H 8.24, N 17.18; found C 24.58, H 8.00, N 16.96. $[\alpha]_{24}^{589}$ = –8.7 ± 0.4° (1.16 mg mL^{-1}, H_2O).

NMR (D_2O, δ in ppm): ^1H (400 MHz): 4.20-4.13 (m, 1H, C**H**NH_3), C**H**$_2N(CH_3)_2H$ and C**H**$_2NH_3$ at 3.68-3.57 (m, 2H) and 3.54-3.42 (m, 2H), 3.06 (s, 6H, N(C**H**$_3)_2H^+$); $^{13}C\{^1H\}$ (100.6 MHz) 59.4 (s, **C**$H_2N(CH_3)_2H$), 47.7 (s, N(**C**$H_3)_2H$), 46.6 (s, **C**HNH_3), 42.4 (s, **C**H_2NH_3). IR (powder film, cm^{-1}): 3479 and 3424 (2 × m, ν_{OH}), 2902 and 2816 (2 × s, ν_{CH}), 2708 and 2627 (2 × s, $\nu_{NH_3^+}$), 1625 (w, δ_{NH}), 1481 (vs, δ_{CH_2}).

(*S*)-*N*^{4},*N*^{5}-Di-*i*-butoxycarbonyl-4,5-diaminopentamide or (*S*)-(*i*-BuOC(O))-NHCH$(CH_2CH_2CONH_2)CH_2$NH(C(O)O*i*-Bu) ((*S*)-7_{L2}). A round bottom flask was charged with ((*S*)-$\mathbf{6_{L2}}$ (4.010 g, 12.078 mmol)[17b] and THF (130 mL). Then *N*-methyl morpholine (1.70 mL, 1.565 g, 15.49 mmol) was added with stirring and the solution was cooled to –20 °C. Isobutyl chloroformate (2.0 mL, 2.091 g, 15.30 mmol) was slowly added. After 0.5 h, aqueous NH_4OH (30%, 8.8 mL) was added. The cold bath was allowed to warm to 0 °C over the course of 6 h. The solvent was removed by rotary

evaporation and the residue was chromatographed on a silica gel column (3 × 14 cm, 93:7 v/v CH_2Cl_2/(85:15 v/v CH_3OH/30% aqueous NH_4OH)). The solvent was removed from the product containing fractions by rotary evaporation. The residue was dried by oil pump vacuum to give (*S*)-**7$_{L2}$** (3.42 g, 10.2 mmol, 85%) as a white solid, mp 126-129 °C (open capillary). Anal. Calcd. for $C_{15}H_{29}N_3O_5$ (331.41): C 54.36, H 8.82, N 12.68; found C 54.33, H 8.71, N 12.54.

NMR (DMSO-d_6, δ in ppm): ^{1}H (500 MHz) 7.21 (br s, 1H, CHN**H**), 7.04 (t, $^3J_{HH}$ = 5.5 Hz, 1H, CON**H**H'), 6.83 (m, 1H, CONH**H**'), 6.68 (br s, 1H, CH_2N**H**), 3.70 (d, $^3J_{HH}$ = 7.0 Hz, 4H, 2 × OC**H**$_2$CH(CH_3)$_2$), 3.44 (br s, 1H, C**H**NH), 2.98 (t, $^3J_{HH}$ = 6.0 Hz, 2H, C**H**$_2$NH), 2.09-1.93 (m, 2H, C**H**$_2$CONH$_2$), 1.87-1.73 (m, 2H, 2 × C**H**(CH_3)$_2$), 1.69-1.57 (m, 1H, CHC**H**H'CH_2), 1.50-1.37 (m, 1H, CHCH**H**'CH_2), 0.94-0.77 (m, 12H, 2 × CH(C**H**$_3$)$_2$); ^{13}C{^{1}H} (125 MHz) 174.0 (s, **C**ONH$_2$), 157.6 and 156.2 (2 × s, 2 × (**C**=O)O), 69.7 and 69.6 (2 × s, 2 × O**C**H$_2$CH(CH_3)$_2$), 50.6 (s, **C**HNH), 44.2 (s, **C**H$_2$NH), 31.7 (s, **C**H$_2$CONH$_2$), 27.68 and 27.65 (2 × s, 2 × **C**H(CH_3)$_2$), 27.5 (s, CH**C**HH'CH_2), 19.0 and 18.9 (2 × s, 2 × CH(**C**H$_3$)$_2$). IR (powder film, cm^{-1}): 3414 (m, ν_{NH}), 3352 and 3312 (m, ν_{NH}), 2959 and 2876 (2 × m, ν_{CH}), 1690, 1678, and 1663 (3 × vs, 3 × $\nu_{C=O}$), 1539 (s, δ_{NH}).

(*S*)-*N*^{1},*N*^{2}-Di-*i*-butoxycarbonyl-1,2,4,-triaminobutane or (*S*)-(*i*-BuOC(O))-NHCH(CH$_2$CH$_2$NH$_2$)CH$_2$NH(C(O)O*i*-Bu) ((*S*)-8$_{L2}$). A round bottom flask was charged with (*S*)-**7$_{L2}$** (3.0 g, 8.96 mmol), CH_3CN (25 mL), EtOAc (25 mL), H_2O (12 mL), and PhI(OAc)$_2$ (4.2 g, 13 mmol) with stirring. After 15 h, the solvents were removed by rotary evaporation. The residue was chromatographed on a silica gel column (3 × 8 cm, 100:0 to 80:20 v/v CH_2Cl_2/CH_3OH). The solvent was removed from the product containing fractions to give (*S*)-**8$_{L2}$** (1.55 g, 5.05 mmol, 57%)[17b] as a colorless sticky liquid.

NMR ($CDCl_3$, δ in ppm): ^{1}H (500 MHz) 5.57 (br s, 1H, CHN**H**), 5.43 (br s, 1H, CH_2N**H**), 3.89-3.70 (m, 5H, 2 × OC**H**$_2$CH$(CH_3)_2$ and C**H**NH), 3.26 (br s, 2H, C**H**$_2$NH), 2.81 (t, $^3J_{HH}$ = 5 Hz, 2H, C**H**$_2$$NH_2$), 2.36 (br s, 2H, N**H**$_2$), 1.94-1.79 (m, 2H, 2 × C**H**$(CH_3)_2$), 1.73-1.63 (m, 1H, CHC**H**H'CH_2), 1.60-1.47 (m, 1H, CHCH**H**'CH_2), 0.89 (d, $^3J_{HH}$ = 5 Hz, 12H, 2 × CH(C**H**$_3)_2$); ^{13}C{^{1}H} (125 MHz) 157.6 and 157.4 (2 × s, 2 × (**C**=O)O), 71.1 and 71.0 (2 × s, 2 × O**C**H_2CH$(CH_3)_2$), 49.9 (s, **C**HNH), 45.1 (s, **C**H_2NH), 38.2 (s, **C**$H_2$$NH_2$), 35.1 (s, CH**C**HH'$CH_2$), 28.0 (s, 2 × **C**H$(CH_3)_2$), 19.0 (s, 2 × CH(**C**$H_3)_2$).

(*S*)-*N*^{1},*N*^{2}-Di-*i*-butoxycarbonyl-*N*^{4},*N*^{4}-dimethyl-1,2,4-triaminobutane or (*S*)-(*i*-BuOC(O))NHCH($CH_2CH_2NMe_2$)CH_2NH(C(O)O*i*-Bu) ((*S*)-$\mathbf{9_{L2}}$). A Fisher Porter bottle was charged with (*S*)-$\mathbf{8_{L2}}$ (1.80 g, 5.863 mmol), CH_3OH (50 mL), distilled H_2O (15 mL), and 37% aqueous HCHO (1.6 mL). The mixture was stirred for 1 h. Then 10% Pd/C (1.2 g, "nominally 50% water wet") was added, and 50 psig of H_2 was introduced. After 24 h, the mixture was filtered through a plug of Celite and washed with CH_3OH/distilled H_2O (1:1 v/v). The solvent was removed by rotary evaporation and the residue was chromatographed on a silica gel column (3 × 8 cm, 100:0 to 80:20 v/v CH_2Cl_2/CH_3OH). The solvent was removed from the product containing fractions by rotary evaporation and oil pump vacuum to give (*S*)-$\mathbf{9_{L2}}$ (1.02 g, 2.87 mmol, 50%) as colorless oil that often solidified upon storage, mp 47-50 °C (open capillary). Anal. Calcd. for $C_{16}H_{33}N_3O_4$·0.75CH_3OH, (355.48): C 56.59, H 10.21, N 11.82; Calcd. for $C_{16}H_{33}N_3O_4$·0.33CH_3OH, (342.02, corresponding to ^{1}H NMR integration): C 57.35, H 10.11, N 12.29; found C 56.26, H 9.95, N 12.22.

NMR ($CDCl_3$, δ in ppm): ^{1}H (500 MHz) 5.98 (br s, 1H, CHN**H**), 5.53 (br s, 1H, CH_2N**H**), 3.87-3.78 (m, 4H, 2 × OC**H**$_2$CH$(CH_3)_2$), 3.77-3.70 (m, 1H, C**H**NH), 3.47 (s, 1H, C**H**$_3$OH), 3.37-3.30 (m, 1H, CH**H**'NH), 3.29-3.19 (m, 1H, C**H**H'NH), 2.57-2.39 (m,

2H, C**H**$_2$N(CH$_3$)$_2$), 2.30 (s, 6H, N(C**H**$_3$)$_2$), 1.96-1.82 (m, 2H, 2 × C**H**(CH$_3$)$_2$), 1.82-1.72 (m, 1H, CHC**H**H'CH$_2$), 1.71-1.57 (m, 1H, CHCH**H**'CH$_2$), 1.02-0.83 (m, 12H, 2 × CH(C**H**$_3$)$_2$); ^{13}C{^{1}H} (125 MHz) 157.5 and 157.2 (2 × s, 2 × (**C**=O)O), 71.1 and 71.0 (2 × s, 2 × O**C**H$_2$CH(CH$_3$)$_2$), 56.0 (s, **C**H$_2$N(CH$_3$)$_2$), 51.0 (s, **C**HNH), 45.1 and 45.0 (2 × s, **C**H$_2$NH and N(**C**H$_3$)$_2$), 29.2 (s, 2 × CH**C**HH'CH$_2$), 28.0 (s, 2 × **C**H(CH$_3$)$_2$), 19.0 (s, 2 × CH(**C**H$_3$)$_2$). IR (powder film, cm^{-1}): 3325 (m, ν_{NH}), 2959, 2874, and 2762 (m and 2 × w, ν_{CH}), 1684 (vs, $\nu_{C=O}$), 1533 (s, δ_{NH}).

Tris(hydrochloric acid) salt of (*S*)-*N*^{4}, *N*^{4}-dimethylbutane-1,2,4-triamine or (*S*)-H$_3$NCH(CH$_2$CH$_2$NMe$_2$H)CH$_2$NH$_3$]$^{3+}$ 3Cl$^-$ ((*S*)-L2·(HCl)$_3$). A round bottom flask was charged with (*S*)-**9**$_{\mathbf{L2}}$ (0.9 g, 2.7 mmol) and aqueous HCl (6.0 M, 50 mL) with stirring and fitted with a condenser. The solution was refluxed. After 50 h, the solvent was removed by rotary evaporation (using a base trap to protect the pump). The residue was dissolved in H_2O and the solution was washed with CH_2Cl_2. The solvent was removed from the aqueous phase by rotary evaporation and the residue was dried by oil pump vacuum to give the ((*S*)-**L2**·(HCl)$_3$ (0.607 g, 2.53 mmol, 94%)[11] as sticky solid.

NMR (D_2O, δ in ppm): ^{1}H (500 MHz) 3.88-3.72 (m, 1H, C**H**NH$_3$), 3.51-3.32 (m, 4H, C**H**$_2$NH(CH$_3$)$_2$ and C**H**$_2$NH$_3$), 2.96 (s, 6H, NH(C**H**$_3$)$_2$), 2.40-2.19 (m, 2H, CHC**H**H'CH$_2$); ^{13}C{^{1}H} (125 MHz) 53.9 (s, **C**H$_2$NH(CH$_3$)$_2$), 47.9 (s, **C**HNH$_3$), 43.7 (s, NH(**C**H$_3$)$_2$), 41.3 (s, **C**H$_2$NH$_3$), 26.4 (s, CH**C**HH'CH$_2$).

(*S*)-*N*^{4},*N*^{5}-Di-*i*-butoxycarbonyl-4,5-diaminopentane-1-ol or (*S*)-((*i*-BuOC-(O))NHCH(CH$_2$CH$_2$CH$_2$OH)CH$_2$NH(C(O)O*i*-Bu) ((*S*)-1$_{\mathbf{L3}}$).** A round bottom flask was charged with (*S*)-**6**$_{\mathbf{L2}}$ (14.220 g, 42.831 mmol)[17b] and 1,2-dimethoxyethane (70 mL), and *N*-methyl morpholine (5.24 mL; 4.821 g, 47.73 mmol) was added with stirring. The solution was cooled to –25 °C, and isobutyl chloroformate (6.80 mL; 7.11 g, 52.03 mmol) was slowly added. The cold bath was removed. After 30 min, the precipitate was

collected by filtration and washed with 1,2-dimethoxyethane (2 × 30 mL). The combined filtrate/washings were sparged with nitrogen and cooled to 0 °C. A solution of $NaBH_4$ (2.43 g, 64.3 mmol) in EtOH (150 mL) was added dropwise with stiring. After 2 h, H_2O (10 mL) was cautiously added. The cold bath was removed. After 12 h, the solvent was removed by rotary evaporation. The solid was dissolved in EtOAc (300 mL), and H_2O (200 mL) was added. The aqueous phase was extracted with EtOAc (2 × 100 mL) and the combined extracts were dried (Na_2SO_4). The solvent was removed by rotary evaporation. The solid was chromatographed on a silica gel column (4 × 17 cm, 20:80 to 50:50 v/v EtOAc/hexane). The solvent was removed from the product containing fractions by rotary evaporation. The residue was dried by oil pump vacuum to give (*S*)-**1_{L3}** (11.137 g, 35.022 mmol, 82%) as a white solid, mp 87-90 °C (open capillary). Anal. Calcd. for $C_{15}H_{30}N_2O_5$ (318.41): C 56.58, H 9.50, N 8.80; found C 56.30, H 9.67, N 8.73.

NMR ($CDCl_3$, δ in ppm): ^{1}H (500 MHz) 5.17 (br s, 1H, CHN**H**), 5.08 (d, $^3J_{HH}$ = 10 Hz, 1H, CH_2N**H**), 3.90-3.76 (m, 4H, 2 × OC**H**$_2$CH(CH_3)$_2$), 3.72 (br s, 1H, C**H**NH), 3.68-3.60 (m, 2H, C**H**$_2$OH), 3.26 (d, $^3J_{HH}$ = 5 Hz, 2H, C**H**$_2$NH), 1.97-1.81 (m, 2H, 2 × C**H**(CH_3)$_2$), 1.69-1.56 (m, 3H, CHC**H**H'C**H**$_2$), 1.55-1.44 (m, 1H, CHCH**H'**CH_2), 0.97-0.86 (m, 12H, 2 × CH(C**H**$_3$)$_2$); ^{13}C{^{1}H} (125 MHz) 157.6 and 157.3 (2 × s, (**C**=O)O), 71.2 and 71.1 (2 × O**C**H_2CH(CH_3)$_2$), 62.2 (s, **C**H_2OH), 51.7 (s, **C**HNH), 45.1 (s, **C**H_2NH), 29.2 and 28.6 (2 × s, CH**C**HH'**C**H_2), 28.0 (s, 2 × **C**H(CH_3)$_2$), 19.0 (s, 2 × CH(**C**H_3)$_2$). IR (powder film, cm^{-1}): 3323 (m, ν_{OH}), 2957 and 2860 (2 × w, ν_{CH}), 1684 (vs, $\nu_{C=O}$), 1541 (s, δ_{NH}).

(*S*)-N^4,N^5-Di-*i*-butoxycarbonyl-4,5-diaminopentyl methanesulfonate or (*S*)-(*i*-BuOC(O))NHCH($CH_2CH_2CH_2OSO_2CH_3$)CH_2NH(C(O)O*i*-Bu) ((*S*)-2_{L3}). A round bottom flask was charged with (*S*)-**1_{L3}** (5.032 g, 15.82 mmol), CH_2Cl_2 (80 mL),

and Et_3N (5.30 mL; 3.843 g, 38.04 mmol), and cooled to –78 °C. Methanesulfonyl chloride (2.30 mL; 3.404 g, 29.71 mmol) was added dropwise with stirring. The cold bath was allowed to warm to 0 °C over the course of 5 h. Aqueous citric acid (20% w/v, 140 mL) and CH_2Cl_2 (150 mL) were added and the phases were separated. The organic phase was washed with saturated aqueous $NaHCO_3$ and dried (Na_2SO_4). The solvent was removed by rotary evaporation. The residue was dried by oil pump vacuum to give crude (*S*)-**2$_{L3}$** (6.227 g, 15.72 mmol) as a yellowish white solid. This material was used without further purification.

NMR ($CDCl_3$, δ in ppm): ^{1}H (500 MHz) 5.11 (br s, 1H, CHN**H**), 5.01 (br s, 1H, CH_2N**H**), 4.23 (t, $^3J_{HH}$ = 6 Hz, 2H, C**H**$_2$OS), 3.80 (br s, 4H, 2 × OC**H**$_2$CH(CH$_3$)$_2$), 3.71 (br s, 1H, C**H**NH), 3.25 (br s, 2H, C**H**$_2$NH), 3.00 (s, 3H, SC**H**$_3$), 1.96-1.73 (m, 4H, 2 × C**H**(CH$_3$)$_2$ and CHCHH'C**H**$_2$), 1.69-1.58 (m, 1H, CHCH**H'**CH$_2$), 1.55-1.43 (m, 1H, CHC**H**H'CH$_2$), 0.89 (d, $^3J_{HH}$ = 7 Hz, 12H, 2 × CH(C**H**$_3$)$_2$); ^{13}C{^{1}H} (125 MHz) 157.4 and 157.0 (2 × s, (**C**=O)O), 71.2 and 71.1 (2 × O**C**H$_2$CH(CH$_3$)$_2$), 69.5 (s, **C**H$_2$OS), 51.3 (s, **C**HNH), 44.9 (s, **C**H$_2$NH), 37.3 (s, S**C**H$_3$) 28.7 and 25.6 (2 × s, CH**C**HH'**C**H$_2$), 27.9 (s, 2 × **C**H(CH$_3$)$_2$), 19.0 (s, 2 × CH(**C**H$_3$)$_2$).

(*S*)-*N*^{1},*N*^{2}-Di-*i*-butoxycarbonyl-*N*^{5},*N*^{5}-dimethyl-1,2,5-triaminopentane or (*S*)-(*i*-BuOC(O))NHCH(CH$_2$CH$_2$CH$_2$NMe$_2$)CH$_2$NH(C(O)O*i*-Bu) ((*S*)-3$_{L3}$). A sealable tube (180 mL, threaded cap) was charged with crude (*S*)-**2$_{L3}$** (6.227 g, 15.72 mmol) and $HNMe_2$ (2.0 M in THF; 80 mL, 160 mmol). The cap was tightened, and the bottom half of the tube was placed in an 80 °C oil bath. After 15 h, the bath was removed. After 2 h, the tube was vented and the solvent was removed by rotary evaporation. The residue was dissolved in CH_2Cl_2 (200 mL), washed with saturated aqueous $NaHCO_3$ (150 mL) and brine (100 mL), and dried (Na_2SO_4). The solvent was removed by rotary evaporation. The residue was chromatographed on a silica gel column

(3 × 16 cm, 100:0 to 85:15 v/v CH_2Cl_2/CH_3OH). The solvent was removed from the product containing fractions to give (*S*)-**3$_{L3}$** (4.664 g, 13.52 mmol, 86% from (*S*)-**1$_{L3}$**) as a yellow oil that often solidified upon storage, mp 68-71 °C (open capillary). Anal. Calcd. for $C_{17}H_{35}N_3O_4$ (345.48): C 59.10, H 10.21, N 12.16; found C 58.41, H 10.09, N 11.92.

NMR ($CDCl_3$, δ in ppm): ^{1}H (500 MHz) 5.73 (d, $^3J_{HH}$ = 7 Hz, 1H, CHN**H**), 5.25 (br s, 1H, CH_2N**H**), 3.80 (d, $^3J_{HH}$ = 6 Hz, 4H, 2 × OC**H**$_2$CH$(CH_3)_2$), 3.69-3.60 (m, 1H, C**H**NH), 3.39-3.14 (m, 2H, C**H**$_2$NH), 2.26 (br s, 2H, C**H**$_2$N$(CH_3)_2$), 2.20 (s, 6H, N(C**H**$_3)_2$), 1.98-1.78 (m, 2H, 2 × C**H**$(CH_3)_2$), 1.62-1.36 (m, 4H, CHC**HH'**C**H**$_2$), 0.98-0.82 (m, 12H, 2 × CH(C**H**$_3)_2$); ^{13}C{^{1}H} (125 MHz) 157.4 and 157.3 (2 × s, (**C**=O)O), 71.1 and 70.9 (2 × O**C**H_2CH$(CH_3)_2$), 59.1 (s, **C**H_2N$(CH_3)_2$), 51.5 (s, **C**HNH), 45.4 (s, **C**H_2NH), 45.1 (s, N(**C**$H_3)_2$), 30.4 and 23.6 (2 × s, CH**C**HH'**C**H_2), 28.0 (s, 2 × **C**H$(CH_3)_2$), 19.0 (s, 2 × CH(**C**$H_3)_2$). IR (powder film, cm^{-1}): 3329 (m, ν_{NH}), 2961 and 2943 (2 × m, ν_{CH}), 1697 and 1683 (s and vs, $\nu_{C=O}$), 1537 (s, δ_{NH}).

Tris(hydrochloric acid) salt of (*S*)-*N*^{5},*N*^{5}-dimethylpentane-1,2,5-triamine or (*S*)-$H_3NCH(CH_2CH_2CH_2NMe_2H)CH_2NH_3]^{3+}$ 3Cl$^-$ ((*S*)-L3·(HCl)$_3$). A round bottom flask was charged with (*S*)-**3$_{L3}$** (4.212 g, 12.21 mmol) and aqueous HCl (6.0 M, 250 mL) and fitted with a condenser. The solution was refluxed. After 36 h, the solvent was removed by rotary evaporation (using a base trap to protect the pump). The residue was dissolved in H_2O and the solution was washed with CH_2Cl_2. The solvent was removed from the aqueous phase by rotary evaporation. The residue was washed with Et_2O and CH_3OH, and dried by oil pump vacuum. This gave the solvate ((*S*)-**L3**·$(HCl)_3$·CH_3OH (2.994 g, 10.44 mmol, 86%) as a colorless sticky hygroscopic solid. Anal. Calcd. for $C_7H_{22}Cl_3N_3$·CH_3OH (286.67):[26] C 33.52, H 9.14, N 14.66; Calcd. for $C_7H_{22}Cl_3N_3$·0.33CH_3OH (265.2, corresponding to ^{1}H NMR integration): C 33.20, H 8.86, N

15.84; found C 33.31, H 8.81, N 14.85.

NMR (D_2O, δ in ppm): ^1H (500 MHz) 3.77-3.66 (m, 1H, C**H**NH_3), 3.42-3.37 (m, 2H, C**H**$_2NH_3$), 3.34 (s, 1H, C**H**$_3OH$), 3.26-3.18 (m, 2H, C**H**$_2NH(CH_3)_2$), 2.91 (s, 6H, NH(C**H**$_3)_2$), 2.01-1.74 (m, 4H, CHC**HH'**C**H**$_2$); $^{13}C\{^1H\}$ (125 MHz) 57.2 (s, **C**HNH_3), 49.6 (s, **C**$H_2N(CH_3)_2$), 43.4 (s, **C**H_2NH_3), 41.2 (s, NH(**C**$H_3)_2$), 27.7 and 20.7 (2 × s, CH**C**HH'**C**H_2).

(2*S*)-N^6-benzyloxycarbonyl-N^1,N^2-di-*tert*-butoxycarbonyl-1,2,6-triaminohexane or (*S*)-(*t*-BuOC(O))NHCH($CH_2CH_2CH_2CH_2$NH(C(O)OCH_2Ph))CH_2NH(C(O)O*t*-Bu) ((*S*)-$\mathbf{5_{L4}}$). A round bottom flask was charged with 10% Pd/C (0.16 g, "nominally 50% water wet") and H_2O (8 mL) and flushed with N_2. After 10 min, a solution of $NaBH_4$ (0.284g, 7.50 mmol) in H_2O (8 mL) was added with stirring, followed by solid Boc_2O (0.82 g, 3.75 mmol) and then a solution of (*S*)-$\mathbf{4_{L4}}$ (0.98 g, 2.5 mmol)[18b] in CH_3OH (22 mL). After 1 h, the mixture was filtered through celite. The filtrate was neutralized with $KHSO_4$, and the solvent was removed by rotary evaporation. Then H_2O (50 mL) was added and the mixture was extracted with EtOAc (2 × 70 mL). The combined extracts were dried (Na_2SO_4). The solvent was removed by rotary evaporation and the solid was chromatographed on a silica gel column (3 × 8 cm, 20:80 to 50:50 v/v EtOAc/hexane). The solvent was removed from the product containing fractions by rotary evaporation. The residue was dried by oil pump vacuum to give (*S*)-$\mathbf{5_{L4}}$ (0.823 g, 1.77 mmol, 71%)[20] as a white solid.

NMR ($CDCl_3$, δ in ppm):[20] ^1H (500 MHz) 7.39-7.27 (m, 4H, **Ph**),[27] 5.07 (br s, 2H, OC**H**$_2$Ph), 4.96 (br s, 1H, N**H**(C=O)O), 4.85-4.61 (br m, 2H, 2 × N**H**(C=O)O), 3.57 (br s, 1H, C**H**NH(Boc)), 3.22-3.03 (m, 4H, C**H**$_2$NH(Boc) and C**H**$_2$NH(Cbz)), 1.52-1.32 (m, 24H, 3 × C**H**$_2$, 2 × OC(C**H**$_3)_3$); $^{13}C\{^1H\}$ (125 MHz) 156.6, 156.5, and 156.2 (3 × s, 3 × (**C**=O)O); **Ph** at 136.6 (s, *i*), 128.4 (s, *o*), 128.0 (s, *p*), 127.9 (s, *m*);[23] 79.3 (s, 2 ×

O**C**$(CH_3)_3$), 66.5 (s, O**C**H_2Ph), 51.1 (s, **C**HNH(Boc)), 44.5 (s, **C**H_2NH(Boc)), 40.4 (s, **C**H_2NH(Cbz)), 32.2 (s, **C**H_2), 29.5 (s, **C**H_2), 28.4 (s, 2 × C(**C**$H_3)_3$), 22.7 (s, **C**H_2). IR (powder film, cm^{-1}): 3352 (m, ν_{NH}), 2982 and 2932 (2 × w, ν_{CH}), 1682 (vs, $\nu_{C=O}$), 1530 (s, δ_{NH}).

(*S*)-*N*^{1},*N*^{2}-di-*tert*-butoxycarbonyl-*N*^{6},*N*^{6}-dimethyl-1,2,6-triaminohexane or (*S*)-(*t*-BuOC(O))NHCH($CH_2CH_2CH_2CH_2NMe_2$)CH_2NH(C(O)O*t*-Bu) ((*S*)-$\mathbf{6_{L4}}$). A Fisher Porter bottle was charged with (*S*)-$\mathbf{5_{L4}}$ (5.72 g, 12.3 mmol), CH_3OH (100 mL), distilled H_2O (30 mL), and 37% aqueous HCHO (2.6 mL). The mixture was stirred for 1 h. Then 10% Pd/C (3.0 g, "nominally 50% water wet") was added, and H_2 was introduced (50 psig). After 24 h, the mixture was filtered through a plug of Celite and washed with CH_3OH/distilled H_2O (1:1 v/v). The solvent was removed by rotary evaporation. The residue was chromatographed on a silica gel column (3 × 14 cm, 100:0 to 85:15 v/v CH_2Cl_2/CH_3OH). The solvent was removed from the product containing fractions by rotary evaporation and oil pump vacuum to give (*S*)-$\mathbf{6_{L4}}$ (4.07 g, 10.8 mmol, 88%) as a colorless sticky solid. Anal. Calcd. for $C_{18}H_{37}N_3O_4 \cdot H_2O$ (377.51): C 57.27, H 10.41, N 11.13; found C 57.22, H 10.03, N 10.58.[28]

NMR ($CDCl_3$, δ in ppm): ^{1}H (500 MHz) 4.96 (br s, 1H, N**H**(C=O)O), 4.74 (br s, 1H, N**H**(C=O)O), 3.57 (br s, 1H, C**H**NH(Boc)), 3.22-3.03 (br s, 2H, C**H**$_2$NH(Boc)), 2.26 (t, $^3J_{HH}$ = 7.5 Hz, 2H, C**H**$_2$N$(CH_3)_2$), 2.21 (s, 6H, N(C**H**$_3)_2$), 1.52-1.31 (m, 26H, 3 × C**H**$_2$, 2 × C(C**H**$_3)_3$, and **H**$_2$O); ^{13}C{^{1}H} (125 MHz) 156.5, and 156.2 (2 × s, 2 × (**C**=O)O), 79.2 (s, 2 × O**C**$(CH_3)_3$), 59.3 (s, **C**H_2N$(CH_3)_2$), 51.2 (s, **C**HNH(Boc)), 45.2 (s, CH_2N(**C**$H_3)_2$), 44.8 (s, **C**H_2NH(Boc)), 32.5 (s, **C**H_2), 28.3 (s, **C**H_2), 27.1 (s, 2 × C(**C**$H_3)_3$), 23.5 (s, **C**H_2). IR (powder film, cm^{-1}): 3346 (m, ν_{NH}), 2976 and 2932 (2 × m, ν_{CH}), 1682 (vs, $\nu_{C=O}$), 1526 (s, δ_{NH}).

Tris(hydrochloric acid) salt of (*S*)-*N*^{6},*N*^{6}-dimethylhexane-1,2,6-triamine or (*S*)-$H_3NCH(CH_2CH_2CH_2CH_2NMe_2H)CH_2NH_3]^{3+}$ $3Cl^-$ ((*S*)-L4·$(HCl)_3$). A round bottom flask was charged with (*S*)-$\mathbf{6_{L4}}$ (3.61 g, 10.0 mmol) and 12.0 M HCl/dioxane (25:75 v/v; 150 mL) with stirring. After 12 h, the solvent was removed by rotary evaporation (using a base trap to protect the pump). The residue was dissolved in H_2O and the solution was washed with CH_2Cl_2. The solvent was removed from the aqueous phase by rotary evaporation. The residue was washed with Et_2O and CH_3OH, and dried by oil pump vacuum to give (*S*)-**L4**·$(HCl)_3$·CH_3OH (2.40 g, 7.98 mmol, 80%) as a colorless sticky hygroscopic solid. Anal. Calcd. for $C_8H_{24}Cl_3N_3$·CH_3OH (300.67):[26] C 35.95, H 9.39, N 13.97; Calcd. for $C_8H_{24}Cl_3N_3$·0.33CH_3OH (279.23, corresponding to ^{1}H NMR integration): C 35.83, H 9.14, N 15.05; found C 35.97, H 9.16, N 13.81.

NMR (D_2O, δ in ppm): ^{1}H (500 MHz) 3.75-3.69 (m, 1H, C**H**NH_3), 3.42-3.37 (m, 2H, C**H**$_2NH_3$), 3.36 (s, 1H, C**H**$_3OH$), 3.26-3.17 (m, 2H, C**H**$_2NH(CH_3)_2$), 2.91 (s, 6H, $NH(CH_3)_2$), 1.94-1.78 (m, 4H, CHC**HH**'CH_2C**H**$_2$), 1.62-1.50 (m, 2H, CHCHH'C**H**$_2CH_2$); ^{13}C{^{1}H} (125 MHz) 57.8 (s, **C**$H_2NH(CH_3)_2$), 49.9 (s, **C**HNH_3), 49.8 (s, **C**H_3OH), 43.4 (s, $NH(\mathbf{C}H_3)_2$), 41.4 (s, **C**H_2NH_3), 30.2, 24.3, and 22.0 (3 × s, CH**C**HH'**C**H_2**C**H_2).

6.5. References

(1) Reviews: (a) Doyle, A. G.; Jacobsen, E. N. *Chem*. *Rev*. **2007**, *107*, 5713-5743. (b) Yu, X.; Wang, W. *Chem*. *Asian J*. **2008**, *3*, 516-532.

(2) Reviews: (a) Brak, K.; Jacobsen, E. N. *Angew. Chem., Int. Ed.* **2013**, *52*, 534-561; *Angew. Chem.* **2013**, *125*, 558-588. (b) Tsakos, M.; Kokotos, C. G. *Tetrahedron* **2013**, *69*, 10199-10222. (c) Zhang, Z.; Schreiner, P. R. *Chem*. *Soc*. *Rev*. **2009**, *38*, 1187-1198.

(3) (a) Etter, M. C.; Urbañczyk-Lipkowska, Z.; Zia-Ebrahimi, M.; Panunto, T. W. *J*. *Am*. *Chem*. *Soc*. **1990**, *112*, 8415-8426. (b) Etter, M. C. *Acc*. *Chem*. *Res*. **1990**, *23*, 120-126.

(4) (a) Okino, T.; Hoashi, Y.; Takemoto, Y. *J*. *Am*. *Chem*. *Soc*. **2003**, *125*, 12672-12673. (b) Takemoto, Y. *Chem. Pharm. Bull.* **2010**, *58*, 593-601.

(5) Ganzmann, C.; Gladysz, J. A. *Chem*. *Eur*. *J*. **2008**, *14*, 5397-5400.

(6) Lewis, K. G.; Ghosh, S. K.; Bhuvanesh, N.; Gladysz, J. A. *ACS Cent. Sci.* **2015**, *1*, 50-56.

(7) (a) Werner, A. *Chem*. *Ber*. **1911**, *44*, 1887-1898. (b) Werner, A. *Chem*. *Ber*. **1912**, *45*, 121-130.

(8) (a) Scherer, A.; Mukherjee, T.; Hampel, F.; Gladysz, J. A. *Organometallics* **2014**, *33*, 6709-6722. (b) Mukherjee, T.; Ganzmann, C.; Bhuvanesh, N.; Gladysz, J. A. *Organometallics* **2014**, *33*, 6723-6737.

(9) Thomas, C.; Gladysz, J. A. *ACS Catalysis* **2014**, *4*, 1134-1138.

(10) (a) Ma, J.; Ding, X.; Hu, Y.; Huang, Y.; Gong, L.; Meggers, E. *Nat. Commun*. **2014**, *5*, 4531. (b) Chen, L.-A.; Xu, W.; Huang, B.; Ma, J.; Wang, L.; Xi, J.; Harms, K.; Gong, L.; Meggers, E. *J. Am. Chem. Soc.* **2013**, *135*, 10598-10601.

(11) (a) Treder, A. P.; Andruszkiewicz, R.; Zgoda, W.; Ford, C.; Hudson, A. L.

Bioorg. Med. Chem. Lett. **2009**, *19*, 1009-1011. (b) The synthesis of (*S*)-**L2**·$(HCl)_3$ reported in the preceding paper used precursors from this work: Treder, A. P.; Walkowiak, A.; Zgoda, W.; Andruszkiewicz, R. *Synthesis* **2005**, 2281-2283.

(12) Ghosh, S. K.; Ganzmann, C.; Bhuvanesh, N.; Gladysz, J. A. *Angew. Chem., Int. Ed.* **2016**, *55*, 4356-4360; *Angew. Chem.* **2016**, *128*, 4429-4433.

(13) Prices were obtained as follows: (a) Aroz Technologies, LLC, http://www.aroztech. com/, accessed 14 July 2015. (b) AK Scientific, http://www.aksci.com, accessed 14 July 2015.

(14) (a) Zhang, Z.; Van Aerschot, A.; Hendrix, C.; Busson, R.; David, F.; Sandra, P.; Herdewijn, P. *Tetrahedron* **2000**, *56*, 2513-2522. (b) Chhabra, S. R.; Mahajan, A.; Chan, W. C. *J. Org. Chem.* **2002**, *67*, 4017-4029.

(15) Nakamoto, Y.; Yoshino, T.; Naito, H.; Nagata, T.; Yoshikawa, K.; Suzuki, M. WO 2004058728; *Chem. Abstr.* **2004**, *141*, 123611.

(16) For a similar conversion of (*S*)-$\mathbf{3_{L1}}$ to (*S*)-$\mathbf{4_{L1}}$ (90%), and subsequent esterification/reduction to (*S*)-$\mathbf{5_{L1}}$ (96%), see Webber, S. E.; Okano, K.; Little, T. L.; Reich S. H.; Xin, Y.; Fuhrman, S. A.; Matthews, D. A.; Love, R. A.; Hendrickson, T. F.; Patick, A. K.; Meador, III, J. W.; Ferre, R. A.; Brown, E. L.; Ford, C. E.; Binford, S. L.; Worland, S. T. *J. Med. Chem.* **1998**, *41*, 2786-2805.

(17) (a) Ghosh, A. K.; Leshchenko-Yashchuk, S.; Anderson, D. D.; Baldridge, A.; Noetzel, M.; Miller, H. B.; Tie, Y; Wang, Y. -F.; Koh, Y.; Weber, I. T.; Mitsuya, H. *J. Med. Chem.* **2009**, *52*, 3902-3914. (b) Altman, J.; Ben-Ishai, D. *Tetrahedron: Asymmetry* **1993**, *4*, 91-100.

(18) (a) Rodriguez, M.; Linares, M.; Doulut, S.; Heitz, A.; Martinez, J. *Tetrahedron Lett.* **1991**, *32*, 923-926. (b) Kokotos, G.; Markidis, T.; Constantinou-Kokotou, V. *Synthesis* **1996**, 1223-1226.

(19) Ghosh, S. K.; Ganzmann, C.; Gladysz, J. A. *Tetrahedron: Asymmetry* **2015**, *26*, 1273-1280.

(20) Schiesser, S.; Hackner, B.; Vrabel, M.; Beck, W.; Carell, T. *Eur. J. Org. Chem.* **2015**, 2654-2660.

(21) Fulmer, G. R.; Miller, A. J. M.; Sherden, N. H.; Gottlieb, H. E.; Nudelman, A.; Stoltz, B. M.; Bercaw, J. E.; Goldberg, K. I. *Organometallics* **2010**, *29*, 2176-2179.

(22) Dewey, M. A.; Gladysz, J. A. *Organometallics* **1993**, *12*, 2390-2392.

(23) The $^{13}C\{^{1}H\}$ signal with the chemical shift closest to benzene was assigned to the *meta* carbon atom: Mann, B. E. *J. Chem. Soc. Perkin Trans. 2* **1972**, 30-34.

(24) MALDI TOF, without matrix, m/z (%); the peaks correspond to the most intense signal of the isotope envelope.

(25) FAB, 3-NBA (3-NBA = 3-nitrobenzyl alcohol), m/z (%); the peaks correspond to the most intense signal of the isotope envelope.

(26).The ^{1}H NMR data for this salt suggest the presence of $0.33CH_3OH$, but the fit to the microanalytical data is better for $1.00CH_3OH$.

(27) This signal integrates to four protons rather than the expected five.

(28) The value for nitrogen is slightly outside the range associated with analytical purity, but is reported nonetheless to accurately reflect the composition of the sample.

7. WERNER COMPLEXES WITH ω-DIMETHYLAMINOALKYL SUBSTITUTED ETHYLENEDIAMINE LIGANDS: BIFUNCTIONAL HYDROGEN BOND DONOR CATALYSTS FOR HIGHLY ENANTIOSELECTIVE MICHAEL ADDITIONS†

7.1. Introduction

During the past two decades, numerous types of small molecule hydrogen bond donor catalysts have been developed, almost always under the umbrella of "organocatalysis".[1,2] These have included many chiral, enantiopure species, and applications to a variety of enantioselective organic reactions.[2] I, together with others in the Gladysz group, have sought to broaden this field to include inorganic and organometallic hydrogen bond donors that feature earth abundant metals and chirality motifs not normally achievable in organic architectures.[3-5] Allied themes have been studied by Meggers and others.[6-8]

Importantly, the performances of hydrogen bond donor catalysts are often markedly improved when they are rendered bifunctional.[5b,9-11] For example, thioureas constitute a widely applied class of two fold NH bond donors,[2,10,12] and the incorporation of tertiary amines can give catalysts that afford superior rates, yields, and enantioselectivities in addition reactions.[10] Figure 7.1 shows the examples of mono-functional and bifunctional thiourea catalysts which were used in the Michael reaction of diethyl malonate (**22b**) to *trans*-ß-nitrostyrene (**21a**). The monofunctional catalyst gave the addition product with 57% yield (24 h) in presence of an external base (Et_3N),

†Reproduced in part with permission from Ghosh, S. K.; Ganzmann, C.; Gladysz, J. A. *Angew. Chem. Int. Ed.* **2016**, *55*, 4356-4360. Coyright 2016 WILEY-VCH Verlag GmbH & Co. KGaA, Weinheim.

whereas the bifunctional catalyst gave an 86% yield with 93% enantioselectivity within same time.[10a] The external base was not required in case of bifunctional catalyst as the base is incorporated within the catalyst (see Figure 7.1)

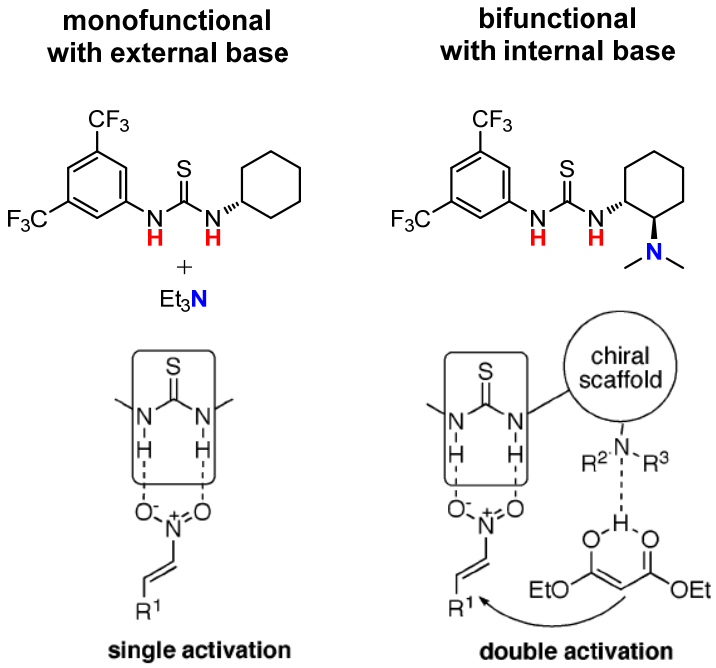

Figure 7.1. Monofunctional and bifunctional thiourea catalysts and their possible activation modes.

From past research in Gladysz group, attention has been drawn to Werner complexes of cobalt(III) and 1,2-diamines.[3] These represent textbook examples of substitution inert low spin d^6 complexes, and are therefore incapable of traditional metal based substrate activation. However, the coordinated NH groups are superb hydrogen bond donors.[3] Furthermore, salts of the helically chiral ethylenediamine substituted cations $[Co(en)_2(A)(A')]^{n+}$ and $[Co(en)_3]^{3+}$ represent the first inorganic molecules to be separated into enantiomers.[13] The mirror images of the trication $[Co(en)_3]^{3+}$ are

depicted in Scheme 7.1, together with the Λ/Δ descriptors employed to distinguish the cobalt configurations. By using lipophilic anions such as BAr_f^- ($B(3,5\text{-}C_6H_3(CF_3)_2)_4^-$), this species could be solubilized in nonpolar solvents that do not compete with substrates for the hydrogen bonding sites.[3a] However, while Λ- or Δ-$[Co(en)_3]^{3+}$ $3BAr_f^-$ proved to be competent catalysts, enantioselectivities have been modest in all reactions assayed to date (≤33% ee).

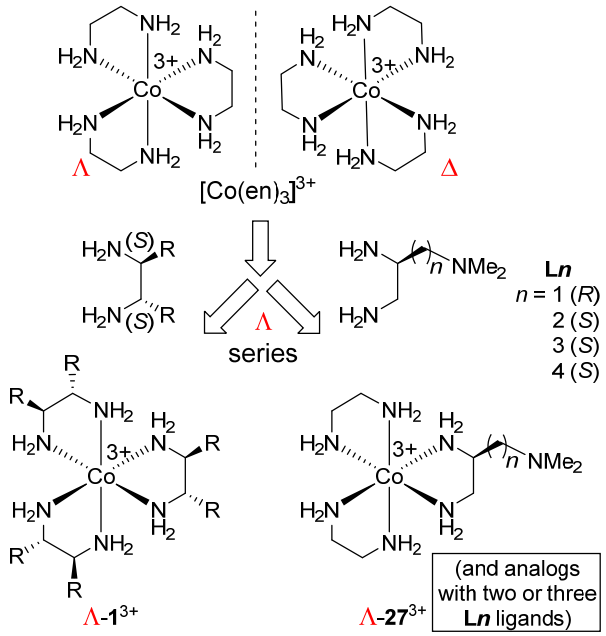

Scheme 7.1. Design of families of cobalt(III) hydrogen bond donor catalysts.

Hence, two related families of catalysts were targeted. As shown in Scheme 7.1, one involved analogs with 1,2-disubstituted diamines. As described in section 4, those with aryl substituents have afforded greatly improved enantioselectivities.[3b] The other involved the exchange of one or more of the 1,2-ethylenediamine ligands by analogs with ω-dimethylaminoalkyl substituents, $H_2NCH((CH_2)_nNMe_2)CH_2NH_2$ (*n* = **a**, 1; **b**, 2; **c**, 3; **d**, 4; **L1**-**L4**, respectively).[14] In this section, it is shown that when a single

ethylenediamine ligand in $[Co(en)_3]^{3+}$ is replaced by **L*n*** with a suitable methylene spacer length (*n*), exceptional catalysts are obtained that match or exceed the highest enantioselectivities realized with hydrogen bond donors to date. Some of the reactions involving the poor catalyst **27a**$^{3+}$ 3BAr$_f^-$ were done by Dr. Carola Ganzmann.

7.2. Results

7.2.1. Syntheses of the catalysts

As depicted in Scheme 7.2, the triply protonated triamine ligands (*S*)-**L*n***·(HCl)$_3$ (*n* = 1-4, 0.92-0.83 equiv)[14] and the racemic carbonate

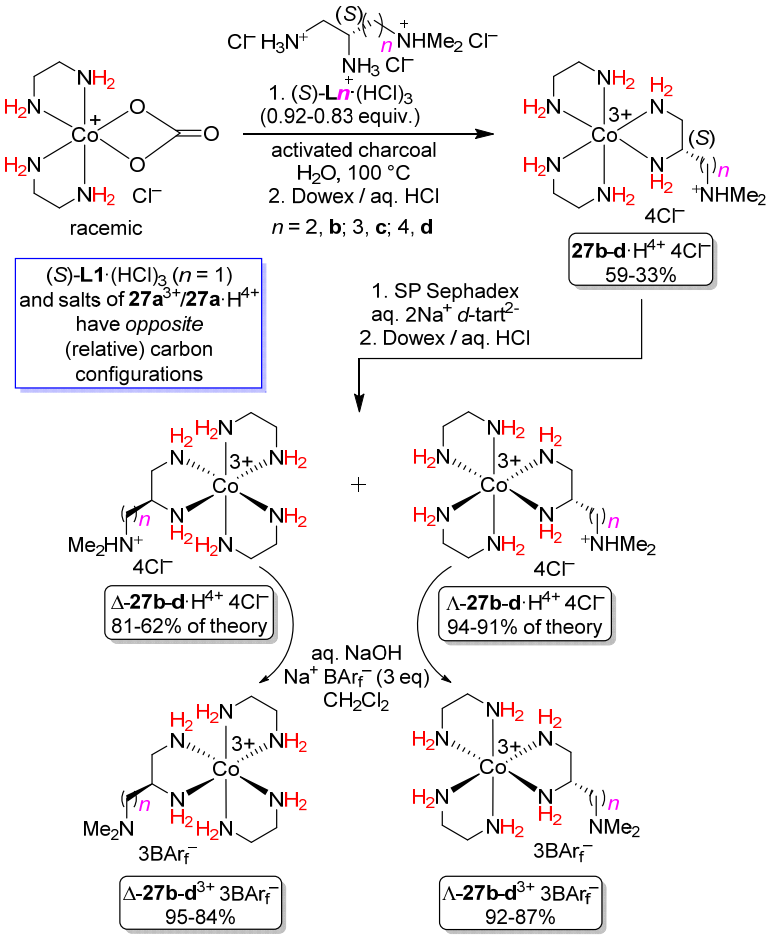

Scheme 7.2. Syntheses of bifunctional catalysts **27a-d**$^{3+}$ 3BAr$_f^-$ from (*S*)-**L*n***·(HCl)$_3$ (*n* = 1-4).

complex $[Co(en)_2O_2CO]^+$ Cl^-[15] were combined in water in the presence of activated charcoal and heated to 100 °C. In this process, the charcoal labilizes the normally substitution inert cobalt(III) educt,[16] and the carbonate ligand that is displaced acts as a dibase, deprotonating the two $-NH_3^+$ moieties of (*S*)-**L*n***·$(HCl)_3$. The resulting tetra-cation salts $[Co(en)_2((S)\text{-}H_2NCH((CH_2)_nNMe_2H)CH_2NH_2)]^{4+}$ $4Cl^-$ (**27a-d**·H^{4+} $4Cl^-$) were separated from redistribution products using a DOWEX 50WX2 ion exchange

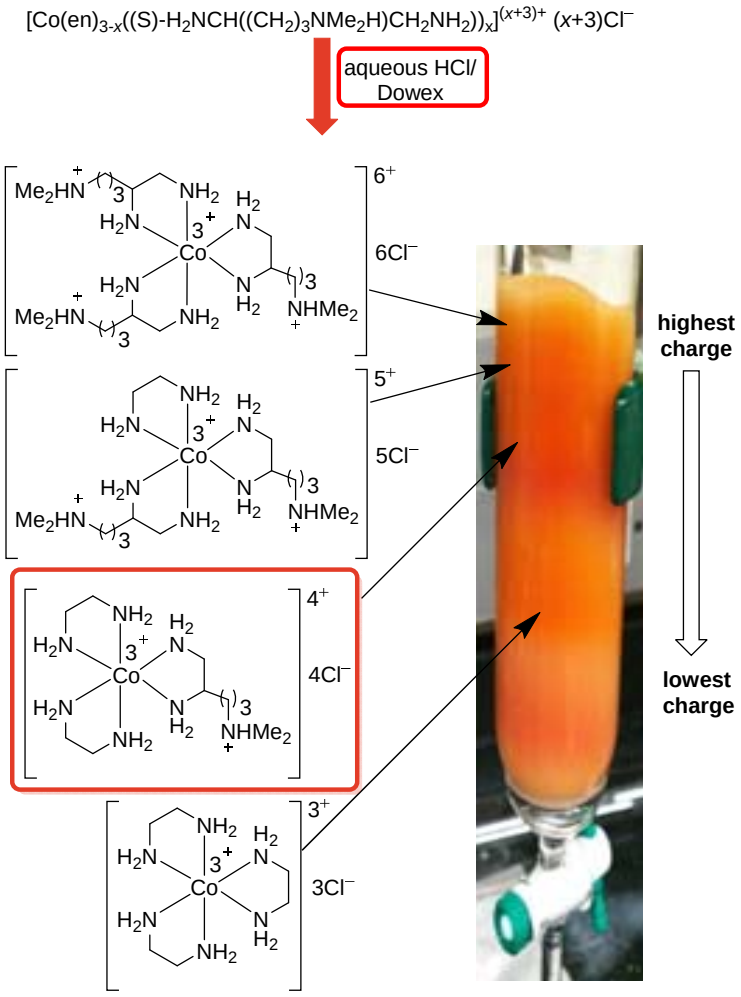

Figure 7.2. Separation of the tetracation **27c**·H^{4+} $4Cl^-$ from redistribution products.

resin column as illustrated for $n = 3$ in Figure 7.2. This gave hydrates of **27a-d**·H^{4+} $4Cl^{-}$ as orange powders in 59-33% yields (based upon the limiting triamine) as mixtures of Λ/Δ diastereomers (**a**, 30:70; **b-d**, 70-72:30-28), consistent with the use of a racemic cobalt carbonate precursor.

The reusable chiral support Sephadex has often been employed to separate enantiomeric and diastereomeric cobalt(III) diamine complexes.[17] When **27a-d**·H^{4+} $4Cl^{-}$ were eluted from SP-Sephadex columns with tartrate gradients, $2Na^{+}$ *d*-$tart^{2-}$, two well resolved bands were obtained. A representative separation for the diastereomers of **27c**·H^{4+} $4Cl^{-}$ is shown in Figure 7.3, together with the structure of SP-Sephadex.[17c]

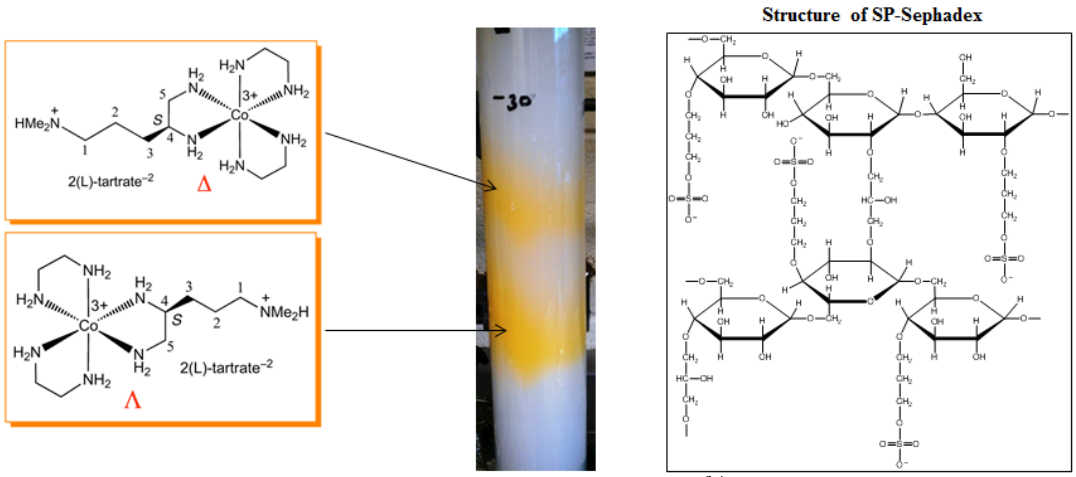

Figure 7.3. Separation of the diastereomers of **27c**·H^{4+} $4Cl^{-}$ and structure of SP-Sephadex.

Each band was collected, concentrated, and eluted through DOWEX columns to exchange the tartrate anions back to chloride anions. The resulting Λ- and Δ-**27a-d**·H^{4+} $4Cl^{-}$ were characterized by NMR ($^{1}H/^{13}C\{^{1}H\}$, D_2O) and elemental analyses as summarized in the experimental section. The cobalt configurations of Λ- and Δ-**27a-d**·H^{4+} $4Cl^{-}$ were assigned by CD spectroscopy and by comparison with the known CD

spectra of Λ- and Δ-$[Co(en)_3]^{3+}$ $3I^-$ as illustrated in Figure 7.4. In addition, that of Δ-**27a**·H^{4+} $4Cl^-$ was confirmed by the crystal structure shown in Figure 7.5.

In the crystal, the octahedral cobalt(III) tetracation of Δ-**27a**·H^{4+} $4Cl^-$ is surrounded by four chloride ions and three water molecules. The chloride anions and water molecules form hydrogen bonds with the amino groups of the ligands (NH···O and NH···Cl^-) and between each other (O-H···Cl^- and O-H···O). Thus, the tetracation units are linked together in a network. The cobalt configuration was confirmed to be Δ. Among the three chelate rings, one is parallel to the C_3 axis, occupying the Δ(*lel*) or Δ(λ) conformation, and other two are perpendicular to the C_3 axis, occupying Δ(*ob*) or Δ(δ) conformations. The overall designation for Δ-**27a**·H^{4+} $4Cl^-$·$3H_2O$ is Δ-*lelob*$_2$.

It was next sought to solubilize deprotonated analogs of the diastereomerically pure cations in organic media. Thus, Λ- and Δ-**27a-d**·H^{4+} $4Cl^-$ were treated with aqueous NaOH (1.0 equiv) and then CH_2Cl_2 solutions of Na^+ BAr_f^- (Scheme 7.3). Workups gave Λ- and Δ-$[Co(en)_2((S)\text{-}H_2NCH((CH_2)_nNMe_2)CH_2NH_2)]^{3+}$ $3BAr_f^-$·xH_2O (**27a-d**$^{3+}$ $3BAr_f^-$·xH_2O; x = 9-12) as orange solids in 92-87% and 95-84% yields, respectively (51-25% overall from **L*n***). Attempts to more rigorously dry cobalt(III) BAr_f^- salts can be problematic. For example, when the solvent is removed from CH_2Cl_2 solutions of the bifunctional catalyst Λ-**27d**$^{3+}$ $3BAr_f^-$ at 40 °C by rotary evaporation and/or oil pump vacuum, a violet residue results and considerable decomposition is evident by ^{13}C NMR. However, Λ-$[Co(en)_3]^{3+}$ $3BAr_f^-$ persists under these conditions, although about half the water molecules are removed. When Λ-$[Co(en)_3]^{3+}$ $3BAr_f^-$ is

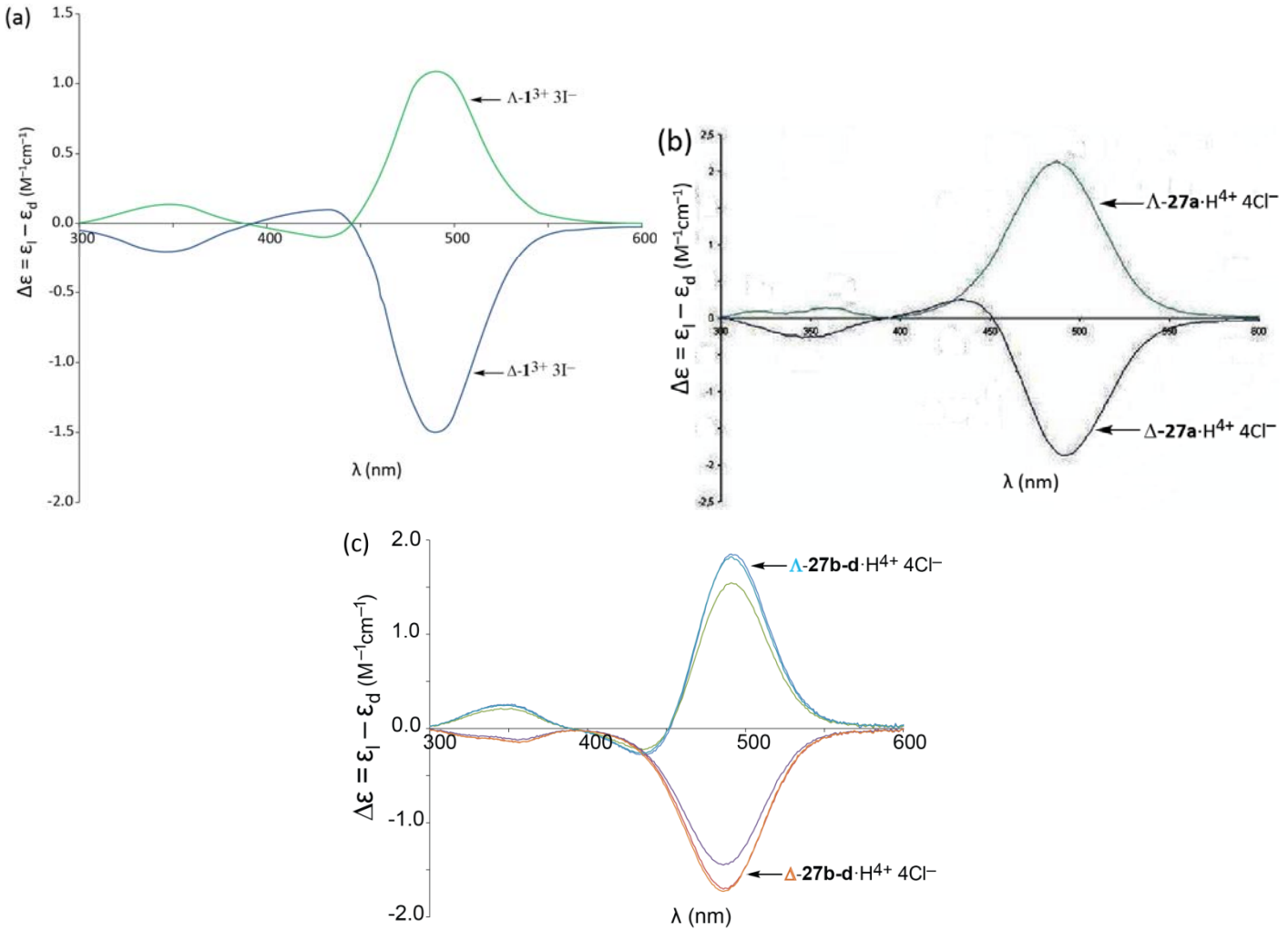

Figure 7.4. Circular dichroism spectra of (a) Δ- and Λ-$[Co(en)_3]^{3+}$ $3I^-$, (b) Δ- and Λ-**27a**·H^{4+} $4Cl^-$, and (c) Δ- and Λ-**27b-d**·H^{4+} $4Cl^-$.

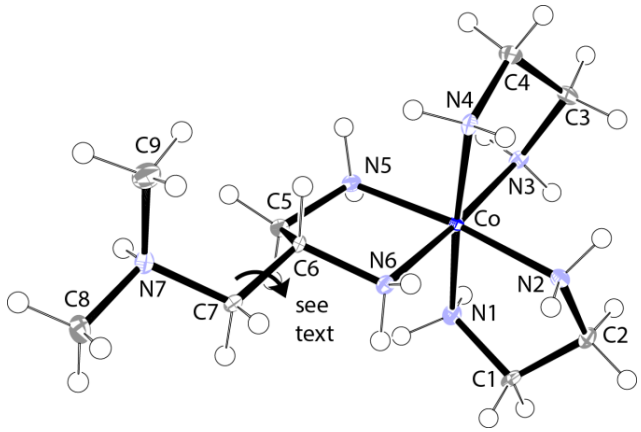

Figure 7.5. The crystal structure of the tetracation of Δ-**27a**·H^{4+} $4Cl^{-}$·$3H_2O$ with thermal ellipsoids at the 50% probability level (the anions and water molecules are not shown). Key bond lengths (Å) and angles (°): Co-N1 1.9692(18), Co-N2 1.9703(19), Co-N3 1.9634(18), Co-N4 1.9627(18), Co-N5 1.9685(19), Co-N6 1.9710(18), C1-N1 1.489(3), C2-N2 1.488(3), C3-N3 1.489(3), C4-N4 1.494(3), C5-N5 1.495(3), C6-N6 1.483(3), C7-N7 1.488(3), C8-N7 1.490(3), C9-N7 1.492(3), C1-C2 1.504(3), C3-C4 1.510(3), C5-C6 1.517(3), C6-C7 1.532(3), N1-Co-N2 85.06(8), N1-Co-N3 91.57(8), N4-Co-N1 175.52(8), N1-Co-N5 90.82(8), N1-Co-N6 92.60(8), N3-Co-N6 175.39(8), N5-Co-N2 173.98(7), N4-Co-N3 84.58(8), N4-Co-N6 91.33(8), N4-Co-N5 91.70(8), N4-Co-N2 92.71(8).

kept under oil pump vacuum at 80 °C, all of the water molecules are removed but appreciable decomposition occurs, as assayed by ^{1}H NMR (some decomposition of the anion is also evident by ^{19}F NMR). One can speculate that, as is often seen with certain fluoride salts, the anion becomes activated in the absence of a minimum level of hydration.

7.2.2. Enantioselective catalysis

The diastereomerically pure BAr_f^- salts were screened as catalysts (10 mol%) for additions of dimethyl malonate (**22c**, 1.2 equiv) to *trans*-ß-nitrostyrene (**21a**) at room temperature. This transformation has been effected by other hydrogen bond donor catalysts, always in conjunction with an external or internal base,[3b,5,18] as well as transition metal catalysts.[19] In accord with the oxidative and hydrolytic stabilities of

cobalt(III) diamine complexes, reactions were carried out in air. Conversions to the addition product **23a<u>c</u>** were assayed by ^{1}H NMR in the presence of an internal standard. Key data are summarized in Scheme 7.3.

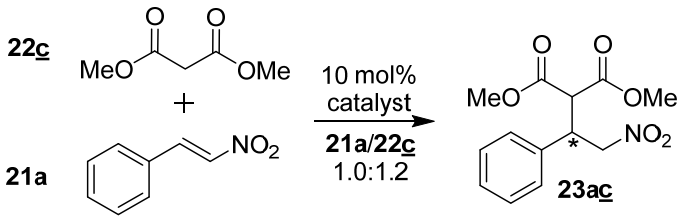

entry	solvent	catalyst	temp	conversion (%) (time)[a]	ee (%) (config)[a]
1	CD_2Cl_2	Λ-**27a**$^{3+}$ 3BAr$_f^-$	rt	20 (48 h)	21 (*S*)[b]
2	CD_2Cl_2	Δ-**27a**$^{3+}$ 3BAr$_f^-$	rt	33 (48 h)	11 (*S*)[b]
3	CD_2Cl_2	Λ-**27b**$^{3+}$ 3BAr$_f^-$	rt	85 (24 h)	75 (*R*)
4	CD_2Cl_2	Δ-**27b**$^{3+}$ 3BAr$_f^-$	rt	42 (45 h)	9 (*R*)
5	CD_2Cl_2	Λ-**27c**$^{3+}$ 3BAr$_f^-$	rt	99 (2 h)	86 (*R*)
6	CD_2Cl_2	Δ-**27c**$^{3+}$ 3BAr$_f^-$	rt	99 (4 h)	5 (*R*)
7	CD_2Cl_2	Λ-**27d**$^{3+}$ 3BAr$_f^-$	rt	85 (6 h)	48 (*R*)
8	CD_2Cl_2	Δ-**27d**$^{3+}$ 3BAr$_f^-$	rt	70 (3 h)	33 (*R*)
9	CD_3CN	Λ-**27c**$^{3+}$ 3BAr$_f^-$	rt	80 (24 h)	31 (*R*)
10	acetone-d_6	Λ-**27c**$^{3+}$ 3BAr$_f^-$	rt	79 (4 h)	46 (*R*)
11	CD_2Cl_2	Λ-**27c**$^{3+}$ 3BAr$_f^-$	0 °C	99 (6 h)	86 (*R*)
12	CD_2Cl_2	Λ-**27b**$^{3+}$ 3BAr$_f^-$	–35 °C	35 (48 h)	73 (*R*)
13	CD_2Cl_2	Λ-**27c**$^{3+}$ 3BAr$_f^-$	–35 °C	97 (15 h)	97 (*R*)
14	CD_2Cl_2	Λ-**27d**$^{3+}$ 3BAr$_f^-$	–35 °C	75 (48 h)	62 (*R*)

[a] For experimental details see the experimental section. [b] The *relative* configuration of the carbon stereocenter in this catalyst is opposite to the others.

Scheme 7.3. Optimization of conditions for catalysis.

When either diastereomer of **27a**$^{3+}$ 3BAr$_f^-$ was employed in CD_2Cl_2, reactions were sluggish at room temperature and **23a<u>c</u>** was obtained in only 21-11% ee (entries 1,2). However, Λ-**27b**$^{3+}$ 3BAr$_f^-$ was a much more effective catalyst (entry 3), affording 85% conversion to **23a<u>c</u>** of 75% ee (*R* major) after 24 h. In contrast, the diastereomer Δ-**27b**$^{3+}$ 3BAr$_f^-$ was a sluggish catalyst (entry 4), and gave **23a<u>c</u>** of only 9% ee (*R* major). When the methylene tether was further lengthened to give Λ- and Δ-**27c**$^{3+}$ 3BAr$_f^-$, both diastereomers exhibited much faster rates (≥99% conversions, 2-4 h; entries 5-6).

However, the Λ diastereomer again afforded a much more enantioselective reaction (86% vs. 5% ee). Finally, Λ- and Δ-**27d**$^{3+}$ 3BAr$_f^-$ gave somewhat slower rates, with more comparable enantioselectivities (48% vs. 33% ee; entries 7-8). In efforts to date, the analog of Λ-**27c**$^{3+}$ 3BAr$_f^-$ in which the dimethylamino group is replaced by a pyrrolidinyl group has given comparable enantioselectivities. The preparation of this molecule is provided in a separate research report. Interestingly, in every case the dominant product configuration was controlled by the ligand based carbon stereocenter.

The most enantioselective catalysts, Λ-**27b-d**$^{3+}$ 3BAr$_f^-$, were further studied. With Λ-**27c**$^{3+}$ 3BAr$_f^-$, the ee values decreased when reactions were conducted in CD_3CN or acetone (entries 9, 10 vs. 5). However, Λ-**27c**,**d**$^{3+}$ 3BAr$_f^-$ afforded much higher enantioselectivities when reactions were conducted at –35 °C (entries 13,14), with the former giving 97% conversion to **23a<u>c</u>** of 97% ee after 15 h. Accordingly, these conditions were applied to a variety of other substrates per Scheme 7.4. The yield data are for isolated products.

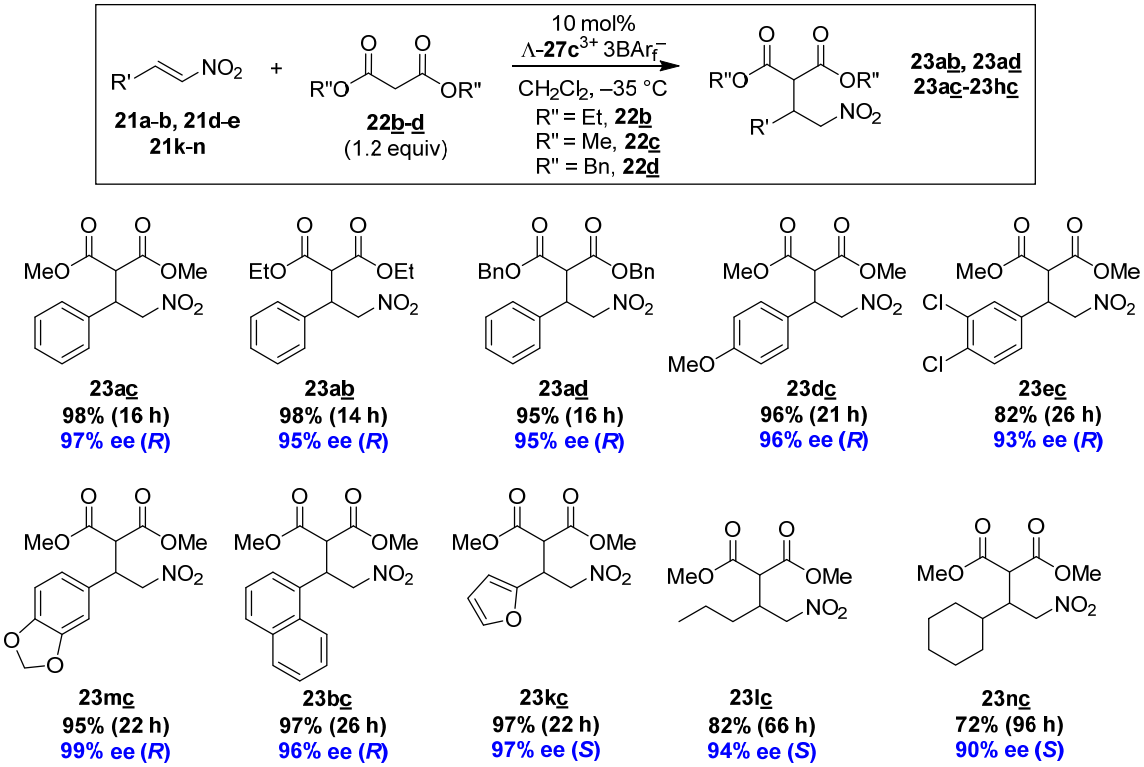

Scheme 7.4. Scope of additions under optimum conditions.

As shown in Scheme 7.4, enantioselectivities decreased only slightly when dimethyl malonate was replaced by the diethyl or dibenzyl esters (from 97% to 95% ee). When electron donating or withdrawing substituents were introduced on the phenyl ring of **21a**, the ee values remained high (99-93% ee). Similar values were obtained with other aryl moieties such as 1-naphthyl and 2-furyl (97-96% ee). However, particularly noteworthy were analogous additions to ß-alkylnitroethenes. These afforded adducts of 94-90% ee, a rarely seen level of asymmetric induction, as further analyzed in the discussion section.

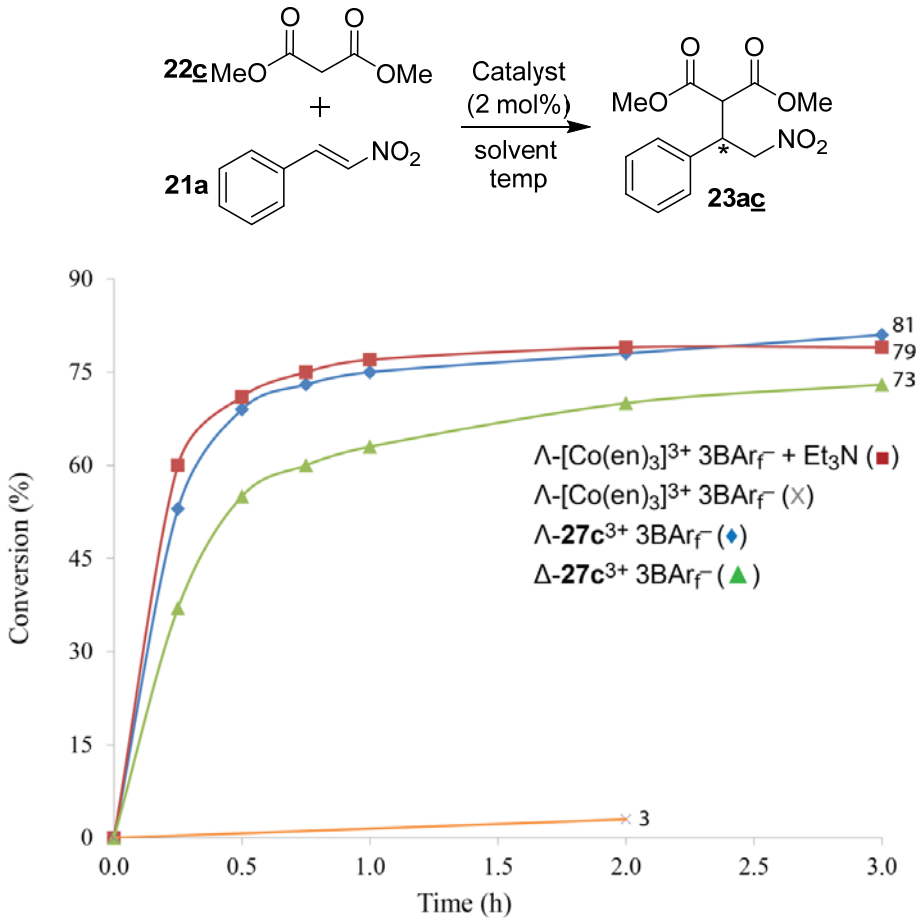

Figure 7.6. Rates of reaction of *trans*-ß-nitrostyrene (**21a**) and dimethyl malonate (**22c**, 1.2 equiv) in CD_2Cl_2 in the presence of an internal standard and catalyst (2 mol%; see experimental section): (■) Λ-$[Co(en)_3]^{3+}$ $3BAr_f^-$/Et_3N, (♦) Λ-**27c**$^{3+}$ $3BAr_f^-$, (▲) Δ-**27c**$^{3+}$ $3BAr_f^-$, Λ-$[Co(en)_3]^{3+}$ $3BAr_f^-$.

In view of these excellent results in Scheme 7.4, the rates of several catalytic systems were monitored by ^1H NMR using 2% loadings in CD_2Cl_2 at ambient temperature. As shown in Figure 7.6, when the monofunctional complex Λ-$[Co(en)_3]^{3+}$ $3BAr_f^-$ (Scheme 7.1), augmented by an equimolar quantity of Et_3N, was compared to bifunctional Λ-**27c**$^{3+}$ $3BAr_f^-$, nearly equal rates were found. However, the former system gave only a 9% ee, as opposed to 81% for the latter. The less enantioselective diastereomeric catalyst Δ-**27c**$^{3+}$ $3BAr_f^-$ gave a slower rate. Importantly, when Λ-

$[Co(en)_3]^{3+}$ $3BAr_f^-$ was employed in the absence of an external base, there was no detectable conversion after 2 h (<3%).

7.3. Discussion

The trends in Scheme 7.3 raise a number of issues. Efficacies in enantioselective catalysis are normally analyzed in the context of a $\Delta\Delta G^{\ddagger}$ value for two competing diastereomeric transition states. Given the lower symmetries of Λ-**27b-d**$^{3+}$ $3BAr_f^-$ (C_1) compared to the trication $[Co(en)_3]^{3+}$ or substituted analogs **1**$^{3+}$ (Scheme 7.1; both D_3), a much wider range of ternary assemblies are possible.

Since the carbon configurations of the catalysts set the dominant product configurations, it might be suggested that the malonate esters simultaneously interact with the dimethylamino groups and the proximal NH donor sites, and that this somehow fixes the nitroethene C=C enantioface that is predominantly attacked.[10a,20] For the system in Figure 7.5 (protonated form of a poor catalyst), this would correspond to N7 (after rotation about C6-C7) and the nearest hydrogen atoms on N1, N5, or N6. In any event, Scheme 7.3 establishes a "sweet spot" with respect to both rate and enantioselectivity with three methylene groups and Λ/*S* cobalt/carbon configurations.[21]

The data from Figure 7.6 show that the internal trialkylamine base in Λ-**27c**$^{3+}$ $3BAr_f^-$ does not lead to a rate acceleration versus an external triethylamine base. This is in contrast to the results in Figure 7.1, for which an internal base improves the rate of a thiourea catalyst versus one used with external base. However, the enantioselectivity is much higher with the bifunctional catalyst Λ-**27c**$^{3+}$ $3BAr_f^-$ (81% versus 9%; Figure 7.6). Both the rate and enantioselectivity of Δ-**27c**$^{3+}$ $3BAr_f^-$ are poorer than other two catalysts in Figure 7.6.

It is difficult to compare enantioselective catalysts in an even handed manner. However, while some of the ee values in Scheme 7.4 have been matched by other

hydrogen bond donor catalysts (Figure 7.7), I am unaware of a system with comparable overall effectiveness. For example, **23a<u>c</u>** has been accessed in 93-96% ee via recipes that use 2-3 equiv of **22<u>c</u>** and require 36-24 h (10 mol% catalyst),[18a-c] and in 99% ee via a protocol that uses 5 equiv of **22<u>c</u>** and requires 144 h.[18d] Similarly, **23a<u>b</u>** has been accessed in 92-95% ee over 44-48 h,[18b,c,e] **23d<u>c</u>** in 92-97% ee over 30-72 h,[18a-c] **23b<u>c</u>** in 98% ee over 36 h,[18a] and **23k<u>c</u>** in 98-93% ee over 30-36 h (all 10 mol% catalyst).[18a,b,d] Enantioselectivities of >85% with ß-alkylnitroethenes are especially rare; I am aware of

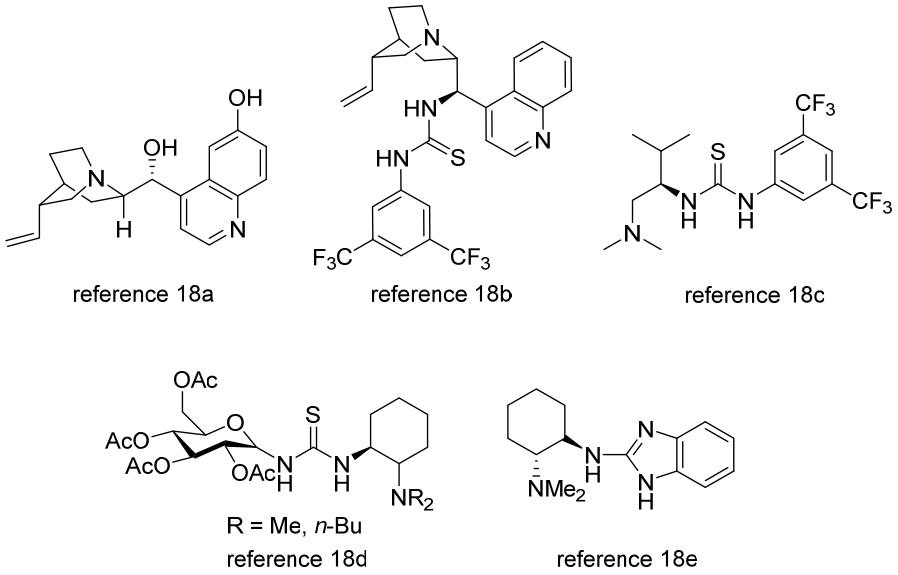

Figure 7.7. Hydrogen bond donor catalysts that have been reported to give high ee values for some of the products in Scheme 7.4.

only a single example with **23l<u>c</u>** (90% ee over 36 h; 10 mol%[18d]) and **23n<u>c</u>** (94% ee over 108 h, 20 mol%[18a]). For **23a<u>c</u>**, two transition metal catalysts have been reported that are effective at 2 mol% loadings (94-95% ee, 48-4 h).[19a,b] All data in Scheme 7.4 are superior to those reported for the monofunctional cobalt(III) catalysts Λ-$\mathbf{1}^{3+}$ $3X^-$ (Scheme 7.1, R = Ph).[3b] in section 4.

In conclusion, I have shown that the performance of hydrogen bond donor catalysts based upon the "second coordination sphere" of Werner cobalt(III) diamine complexes can be dramatically enhanced by incorporating additional functionality. Such cobalt systems represent exciting new additions to the pool of chiral building blocks for enantioselective catalysts. Since many more NH bonds are available to simultaneously participate in transition state assemblies than with thioureas or related NH bond donors, these species should also give rise to new chemistries not realizable with established catalysts. Finally, it is worth noting that little of the organocatalysis review literature[1,2] attempts to treat related systems with "spectator" metal fragments that do not directly participate in bond breaking or making. This unfortunate emphasis on pedigree over functionality only serves to obscure logical mechanism based connections and impede the discovery of new classes of catalysts. Indeed, given the countless numbers of classical coordination compounds featuring NH donor ligands, it is highly probable that many additional families of metal containing hydrogen bond donor catalysts have been in existence for some time.

7.4. Experimental section

General Data: NMR spectra were recorded on standard 400-500 MHz spectrometers at ambient probe temperatures. ^{1}H chemical shifts (δ in ppm) were referenced to residual solvent signals ($CHCl_3$, 7.26; $CDHCl_2$, 5.32; acetone-d_5, 2.05; CD_2HCN, 1.95; HDO, 4.79). ^{13}C chemical shifts (δ in ppm) were referenced to internal dioxane (67.2; spectra in D_2O) or solvent signals ($CDCl_3$, 77.2; CD_3CN, 1.3).[21] Melting points were determined in open capillaries using an OptiMelt MPA 100 instrument. Circular dichroism spectra were obtained with a Chirascan CD Spectrometer (Applied Photophysics). C/H/N analyses were carried out by Atlantic Microlab or in house; sodium was assayed by instrumental neutron activation analysis (INAA). HPLC analyses were carried out with a Shimadzu instrument package (pump/autosampler/detector LC-20AD/SIL-20A/SPD-M20A).

$CDCl_3$, CD_2Cl_2, acetone-d_6, and acetonitrile-d_3 (Cambridge Isotopes) were stored over molecular sieves. HPLC grade solvents (hexanes, Fischer; isopropanol, JT Baker) were degassed before use. Hexanes (Macron, ACS grade), CH_2Cl_2 (EMD, ACS grade), EtOAc (Macron, ACS grade), and dioxane (Macron, ACS grade) were used as received. The Na^+ BAr_f^- was prepared by a literature procedure.[22]

The *trans*-β-nitrostyrene (**21a**, Alfa Aesar, 98%) was column chromatographed (silica gel, 9:1 v/v hexanes/EtOAc) prior to use. The *trans*-4-methoxy-β-nitrostyrene (**21d**), 3,4-dichloro-β-nitrostyrene (**21e**), 3,4-methylenedioxy-β-nitrostyrene (**21m**), and 1-(2-furyl)-2-nitroethylene (**21k**) were used as received from Alfa Aesar (NMR spectra verified that **21e,k,m** were >98% *trans*). The *trans*-1-(naphth-1-yl)-2-nitroethylene (**21b**), *trans*-1-nitro-1-pentene (**21l**), and *trans*-1-cyclohexyl-2-nitroethylene (**21n**) were prepared by literature procedures.[23]

Dimethyl malonate (**22c**, Alfa Aesar, 98%), diethyl malonate (**22b**, Alfa Aesar,

99%), dibenzyl malonate (**22d**, TCI, 99%), $2Na^+$ *d*-$tart^{2-}\cdot 2H_2O$ (Alfa Aesar, 99%), Ph_2SiMe_2 (Aldrich, 97%), Et_3N (Alfa Aesar, 98%), NaOH (Macron, ACS grade), HCl (Macron, ACS grade), Na_2SO_4 (EMD), SP-Sephadex C25 (Aldrich), activated charcoal (Acros, Norit SX 4), DOWEX 50WX2 (200-400 mesh, Aldrich), and silica gel (Silicycle SiliaFlash® F60) were used as received.

Λ-$[Co(en)_3]^{3+}$ $3BAr_f^-$. This synthesis mirrors that reported previously for the enantiomer.[3a] A round bottom flask was charged with a solution of Na^+ BAr_f^- (0.498 g, 0.561 mmol) in CH_2Cl_2 (20 mL). A solution of Λ-$[Co(en)_3]^{3+}$ $3I^-\cdot H_2O$ (0.120 g, 0.187 mmol)[24] in water (20 mL) was added with stirring. After 15 min, the biphasic mixture was allowed to stand. The lower orange CH_2Cl_2 phase was separated. This solution was allowed to evaporate to give Λ-$[Co(en)_3]^{3+}$ $3BAr_f^-\cdot 14H_2O$ as an orange solid (0.505 g, 0.164 mmol, 88%),[26] which continuously darkened with heating and liquefied at 136-141 °C. Anal. Calcd. for $C_{102}H_{60}B_3CoF_{72}N_6\cdot 14H_2O$ (3081.07): C 39.76, H 2.88, N 2.73; found: C 39.95, H 2.89, N 2.69.

NMR (CD_2Cl_2, δ in ppm): ^{1}H (500 MHz) BAr_f^- at 7.72 (t, $^3J_{HH}$ = 2.5 Hz, 24H, *o*), 7.58 (s, 12H, *p*); N**H**$_2$ at 4.81-4.60 (br m, 12H); 2.98 (br s, 6H, 3C**H**H'C**H**H'), 2.73 (s, 29H, **H**$_2$O), 2.65 (s, 6H, 3CH**H'**CH**H'**); ^{13}C{^{1}H} NMR (125 MHz) BAr_f^- at 162.1 (q, $^1J_{BC}$ = 49.6 Hz, *i*), 135.2 (m, *o*), 129.5 (qm, $^2J_{CF}$ = 31.5 Hz, *m*), 125.0 (q, $^1J_{CF}$ = 271.0 Hz, **C**F$_3$), 117.9 (m, *p*); 45.8 (s, 3**C**H$_2$**C**H$_2$).

Λ- and Δ-$[Co(en)_2((S)\text{-}H_2NCH(CH_2NMe_2H)CH_2NH_2)]^{4+}$ $4Cl^-$ (Λ- and Δ-27a·H^{4+} $4Cl^-$). A. A round bottom flask was charged with $[Co(en)_2O_2CO]^+$ Cl^- (0.606 g, 2.21 mmol),[15] activated charcoal (0.440 g), and H_2O (20 mL), and fitted with a condenser. The mixture was heated to 40 °C and a solution of the tris(hydrochloric acid) salt of (*S*)-$H_2NCH(CH_2NMe_2H)CH_2NH_2$ ((*S*)-**L1**·$(HCl)_3$; 0.500 g, 2.04 mmol; 0.92 equiv)[14a] in H_2O (5 mL) was added in one portion with stirring. The temperature was

raised to 100 °C. After 0.75 h, the mixture was filtered. The solvent was removed from the red filtrate by rotary evaporation. The deep red solid was dissolved in HCl (0.50 M, 50 mL). The solution was added to a Dowex column (50WX2, hydrogen form; 3 × 20 cm; packed in water), which was eluted with HCl (1.0 M, 250 mL; 2.0 M, until the second orange band began to elute; then 3.0 M). The solvent was removed from the second orange band by rotary evaporation to give crude **27a**·H^{4+} $4Cl^-$ as an orange solid (0.410 g. 0.934 mmol, 45%) and a 30:70 mixture of Λ/Δ isomers, as assayed by $^{13}C\{^1H\}$ NMR (δ, D_2O, 58.1/ 57.8 ppm).[25] NMR (D_2O, δ in ppm): ^1H (400 MHz) N**H**$_2$ at 5.62-4.84 (br m, 11H), 4.73-4.65 (br m, 1H); 2C**H**$_2$C**H**$_2$, C**H**$_2$C**H**C**H**$_2$N**Me**$_2$H$^+$ at 3.84-3.59 (m, 3H), 3.31-3.15 (m, 1H), 3.13-2.73 (m, 15H); $^{13}C\{^1H\}$ (125 MHz) 58.1/57.8 (s, **C**H_2NHMe_2^+), 53.5/52.5 (s, **C**HNH_2), 48.2/47.3 (s, CH**C**$H_2$$NH_2$), 45.82, 45.77, 45.6, 45.41, 45.36, 45.3, 45.2, 45.0, 44.7, 44.6 (10 × s, 2**C**H_2**C**H_2, NH**Me**$_2^+$).

B. A solution of **27a**·H^{4+} $4Cl^-$ from A (0.201 g, 0.455 mmol) in H_2O (20 mL) was added to a SP Sephadex column (C-25; 6.0 × 50 cm). Elution with 0.10 M (250 mL), 0.15 M (250 mL), 0.20 M (500 mL) and 0.25 M aqueous $2Na^+$ *d*-$tart^{2-}$·$2H_2O$ gave two bands. The first was concentrated to 150 mL. This was added to a Dowex column (3.3 × 25 cm), which was eluted with aqueous HCl (gradient, 1.0 M to 3.0 M). The orange band was collected (yellow eluent) and the solvent was removed by rotary evaporation and oil pump vacuum. This gave Δ-**27a**·H^{4+} $4Cl^-$·$3H_2O$ as an orange solid (0.129 g, 0.262 mmol, 58% or 82% of theory from the 30:70 mixture),[26] which turned green at ca. 220 °C and liquefied at 239 °C. Anal. Calcd. for $C_9H_{32}Cl_4CoN_7$·$3H_2O$ (493.19): C 21.92, H 7.77, N 19.88; found: C 22.14, H 7.40, N 19.46.

NMR (D_2O, δ in ppm): ^1H (400 MHz) N**H**$_2$ at 5.51 (br s, 1H), 5.38 (br s, 1H), 5.27-5.12 (br m, 5H), 5.11-4.8 (br m, 5H); 2C**H**$_2$C**H**$_2$, C**H**$_2$C**H**C**H**$_2$N**Me**$_2$H$^+$ at 3.80-3.69 (m, 1H), 3.68-3.55 (m, 2H), 3.20 (br d, 1H), 3.04 (s, 6H), 3.03-2.92 (m, 3H), 2.91-

2.70 (m, 7H); $^{13}C\{^{1}H\}$ (100.6 MHz) 57.9 (s, **C**$H_2NMe_2H^+$), 53.4 (s, **C**HNH_2), 48.1 (s, CH**C**H_2NH_2), 45.8, 45.6, 45.4, 45.3 (4 × s, 2**C**H_2**C**H_2), 44.7 (s/double intensity, N**Me**$_2H^+$).

The second band from the Sephadex column was concentrated to 100 mL. This was added to a Dowex column (3.0 × 12 cm), which was eluted with aqueous HCl (gradient, 1.0 M to 3.0 M). The orange band was collected (yellow eluent) and the solvent was removed by rotary evaporation and oil pump vacuum. This gave Λ-**27a**·H^{4+} $4Cl^-$·$4H_2O$ as an orange solid (0.055 g, 0.125 mmol, 28% or 93% of theory from the 30:70 mixture),[26] which turned green around 220 °C and liquefied at 239 °C. Anal. Calcd. for $C_9H_{32}Cl_4CoN_7$·$4H_2O$ (511.2): C 21.15, H 7.89, N 19.18; found: C 21.51, H 7.43, N 18.84.

NMR (D_2O, δ in ppm): ^{1}H (400 MHz) N**H**$_2$ at 5.49-5.40 (br m, 2H), 5.37-5.14 (br m, 4H), 5.07 (br s, 1H), 5.00-4.86 (br m, 4H), 4.73-4.65 (br m, 1H); 2C**H**$_2$C**H**$_2$, C**H**$_2$C**H**C**H**$_2$N**Me**$_2H^+$ at 3.73-3.64 (m, 2H), 3.62-3.54 (m, 1H), 3.15 (br d, 1H), 3.04 (s, 6H), 3.01-2.73 (m, 10H); $^{13}C\{^{1}H\}$ (100.6 MHz) 58.1 (s, **C**$H_2NMe_2H^+$), 52.4 (s, **C**HNH_2), 47.1 (s, CH**C**H_2NH_2), 45.8, 45.7 (2 × s, N**Me**$_2H^+$), 45.3, 45.1, 45.0, 44.7 (4 × s, 2**C**H_2**C**H_2).

Λ-27a^{3+} 3BAr$_f^-$. A beaker was charged with Λ-**27a**·H^{4+} $4Cl^-$·$4H_2O$ (0.051 g, 0.10 mmol), H_2O (20 mL), and aqueous NaOH (0.10 M; 1.0 mL, 0.10 mmol). A solution of Na^+ BAr_f^- (0.266 g, 0.300 mmol) in CH_2Cl_2 (20 mL) was added with stirring. After 15 min, the biphasic mixture was allowed to stand. The lower orange CH_2Cl_2 phase was separated. This solution was allowed to evaporate to give Λ-**27a**$^{3+}$ $3BAr_f^-$·$10H_2O$ as an orange solid (0.28 g, 0.092 mmol, 92%; from **L1**: 24% or 34% of theory),[26] which continuously darkened with heating and liquefied at 157-162 °C. Anal. Calcd. for C_{105}-

$H_{67}B_3CoF_{72}N_7 \cdot 10H_2O$ (3066.1): C 41.13, H 2.86, N 3.20; found: C 41.33, H 2.66, N 2.13.[27]

^{1}H NMR (500 MHz, CD_3CN, δ in ppm): BAr_f^- at 7.71 (s, 24H, *o*), 7.68 (s, 12H, *p*); N**H**$_2$ at 4.35-3.64 (br overlapping m, 11H), 3.54 (br s, 1H); C**H**$_2$N**Me**$_2$, C**H**C**H**$_2$NH$_2$, 2C**H**$_2$C**H**$_2$, and **H**$_2$O at 3.05-2.59 (br m, 10H), 2.55-2.40 (m, 3H), 2.36-2.10 (m, 27H); ^{13}C{^{1}H} (125 MHz, CD_2Cl_2, δ in ppm): BAr_f^- at 162.1 (q, $^1J_{BC}$ = 50.0 Hz, *i*), 135.2 (s, *o*), 129.2 (qm, $^2J_{CF}$ = 31.3 Hz, *m*), 125.0 (q, $^1J_{CF}$ = 271.0 Hz, **C**F$_3$), 117.9 (s, *p*); 59.4 (s, **C**H$_2$NMe$_2$), 58.3 (s, **C**HNH$_2$), 48.2 (s, CH**C**H$_2$NH$_2$), 46.9 (s/double intensity, N**Me**$_2$), 46.1, 46.02, 45.98 (s, s, s/double intensity, 2**C**H$_2$**C**H$_2$).

Δ-27a^{3+} 3BAr$_f^-$. A beaker was charged with Δ-**27a**·H^{4+} 4Cl$^-$·3H$_2$O (0.050 g, 0.101 mmol), H_2O (10 mL), and aqueous NaOH (0.10 M; 1.0 mL, 0.10 mmol). A solution of Na^+ BAr_f^- (0.269 g, 0.303 mmol) in CH_2Cl_2 (20 mL) was added with stirring. After 15 min, the biphasic mixture was allowed to stand. The lower orange CH_2Cl_2 phase was separated. This solution was allowed to evaporate to give Δ-**27a**$^{3+}$ 3BAr_f^-·12H_2O as an orange solid (0.263 g, 0.0850 mmol, 84%; from **L1**: 22% or 31% of theory),[26] which continuously darkened with heating and liquefied at 116-119 °C. Anal. Calcd. for $C_{105}H_{67}B_3CoF_{72}N_7 \cdot 12H_2O$ (3102.14): C 40.65, H 2.96, N 3.16; found: C 40.77, H 2.88, N 3.09.

NMR (CD_3CN, δ in ppm): ^{1}H (400 MHz) BAr_f^- at 7.77 (m, 24H, *o*), 7.66 (s, 12H, *p*); N**H**$_2$ at 5.51-3.82 (7 br overlapping m, 9H), 3.71 (br s, 2H), 3.49 (br s, 1H); C**H**$_2$N**Me**$_2$, C**H**C**H**$_2$NH$_2$, 2C**H**$_2$C**H**$_2$, and **H**$_2$O at 2.99-2.60 (br m, 10H), 2.57-2.33 (m, 4H), 2.25 (br s, 28H); ^{13}C{^{1}H} (100.6 MHz) BAr_f^- at 162.6 (q, $^1J_{BC}$ = 49.7 Hz, *i*), 135.7 (s, *o*), 129.9 (q, $^2J_{CF}$ = 31.6 Hz, *m*), 126.0 (q, $^1J_{CF}$ = 271.7 Hz, **C**F$_3$), 118.7 (s, *p*); 60.5 (s, **C**H$_2$NMe$_2$), 57.5 (s, **C**HNH$_2$), 48.5 (s, CH**C**H$_2$NH$_2$), 46.2 (s/double intensity, N**Me**$_2$), 45.7, 45.6, 45.4, 45.3 (4 × s, 2**C**H$_2$**C**H$_2$).

Λ- and Δ-[Co(en)$_2$((*S*)-H$_2$NCH((CH$_2$)$_2$NMe$_2$H)CH$_2$NH$_2$)]$^{4+}$ 4Cl$^-$ (Λ- and Δ-27b·H^{4+} 4Cl$^-$). A. A round bottom flask was charged with [Co(en)$_2$O$_2$CO]$^+$ Cl$^-$ (0.768, 2.80 mmol),[15] activated charcoal (0.450 g), and H$_2$O (20 mL), and fitted with a condenser. The mixture was heated to 40 °C and a solution of the tris(hydrochloric acid) salt of (*S*)-H$_2$NCH((CH$_2$)$_2$NMe$_2$H)CH$_2$NH$_2$ ((*S*)-**L2**·(HCl)$_3$, 0.561 g, 2.34 mmol; 0.83 equiv)[14a] in H$_2$O (5 mL) was added in one portion with stirring. The temperature was raised to 100 °C. After 0.75 h, the mixture was filtered. The solvent was removed from the red filtrate by rotary evaporation. The deep red solid was dissolved in HCl (0.50 M, 100 mL). The solution was added to a Dowex column (50WX2 hydrogen form; 4.5 × 30 cm; packed in water), which was eluted with HCl (1.0 M, 500 mL; 1.5 M, 500 mL; 2.0 M, until the second orange band began to elute; then 3.0 M). The solvent was removed from the second orange band by rotary evaporation to give crude **27b**·H^{4+} 4Cl$^-$ as an orange solid (0.349 g. 0.770 mmol, 33%) and a 72:28 mixture of Λ/Δ isomers, as assayed by ^{13}C{^{1}H} NMR (δ, D$_2$O, 55.9/54.7 ppm).[25] NMR (D$_2$O, δ in ppm): ^{1}H (500 MHz) N**H**$_2$ at 5.53-4.87 (br m, 9H), 4.50 (br s, 1H);[28] 3.45-3.37 (m, 1H, CHC**H**H'NH$_2$), 3.35-3.25 (m, 1H, CHCH**H**'NH$_2$), 3.23-2.54 (m, 17H, C**H**$_2$NH**Me**$_2^+$, C**H**NH$_2$, and 2C**H**$_2$C**H**$_2$), 2.29-2.19 (m, 2H, CHC**H**$_2$CH$_2$); ^{13}C{^{1}H} (125 MHz) 55.9/54.7 (s, **C**HNH$_2$), 55.1 (s, **C**H$_2$NHMe$_2^+$), 49.4/48.5 (s, CH**C**H$_2$NH$_2$), 45.8, 45.7, 45.6, 45.5, 45.4, 45.3, 45.2, 45.1 (8 × s, 2**C**H$_2$**C**H$_2$), 43.6, 43.4 (2 × s, NH**Me**$_2^+$), 27.4 (s, CH**C**H$_2$CH$_2$).

B. A solution of **27b**·H^{4+} 4Cl$^-$ from A (0.274 g, 0.605 mmol) in H$_2$O (40 mL) was added to a SP Sephadex column (C-25; 6.0 × 40 cm). Elution with 0.10 M (250 mL), 0.15 M (250 mL), 0.20 M (500 mL) and 0.25 M aqueous 2Na$^+$ *d*-tart^{2-}·2H$_2$O gave two bands. The first was concentrated to 100 mL. This was added to a Dowex column (3.3 × 25 cm), which was eluted with aqueous HCl (gradient, 1.0 M to 3.0 M). The

orange band was collected (yellow eluent) and the solvent was removed by rotary evaporation and oil pump vacuum. This gave Λ-**27b**·H^{4+} $4Cl^{-}$·0.6 NaCl·H_2O as an orange solid (0.198 g, 0.391 mmol, 65% or 91% of theory from the 72:28 mixture),[26] dec pt 181-214 °C.[29] Anal. Calcd. for $C_{10}H_{34}Cl_4CoN_7$·0.6NaCl·H_2O (506.25):[30,31] C 23.72, H 7.17, N 19.37, Na 2.72; found: C 23.87, H 6.81, N 19.07, Na 2.33.

NMR (D_2O, δ in ppm): ^{1}H (500 MHz) N**H**$_2$ at 5.45 (br s, 1H), 5.30-4.83 (br m, 11H); 3.46-3.35 (m, 1H, CHC**H**H'NH_2), 3.34-3.25 (m, 1H, CHCH**H**'NH_2), 3.19-2.54 (m, 17H, C**H**$_2$NH**Me**$_2^+$, C**H**NH_2, 2C**H**$_2$C**H**$_2$), 2.29-2.18 (m, 2H, CHC**H**$_2$$CH_2$); ^{13}C{^{1}H} (125 MHz) 56.1 (s, **C**HNH_2), 55.0 (s, **C**H_2NHMe$_2^+$), 49.6 (s, CH**C**$H_2$$NH_2$), 45.6, 45.4, 45.34, 45.27 (4 × s, 2**C**H_2**C**H_2), 43.6, 43.4 (2 × s, NH**Me**$_2^+$), 27.3 (s, CH**C**$H_2$$CH_2$).

The second band from the Sephadex column was concentrated to 100 mL. This was added to a Dowex column (3.0 × 12 cm), which was eluted with aqueous HCl (gradient, 1.0 M to 3.0 M). The orange band was collected (yellow eluent) and the solvent was removed by rotary evaporation and oil pump vacuum. This gave Δ-**27b**·H^{4+} $4Cl^{-}$·1.5NaCl·$2H_2O$ as an orange solid (0.078 g, 0.136 mmol, 22% or 80% of theory from the 72:28 mixture),[26] dec pt 66-87 °C.[29] Anal. Calcd. for $C_{12}H_{38}Cl_4CoN_7$·1.5NaCl·$2.0H_2O$ (576.86):[30,31] C 20.82, H 6.64, N 17.00; found: C 21.13, H 6.37, N 16.74.

NMR (D_2O, δ in ppm): ^{1}H (500 MHz) N**H**$_2$ at 5.38 (br s, 1H), 5.25-5.00 (br m, 5H), 4.72-4.60 (br m, 2H), 4.48 (br s, 1H);[28] 3.43-3.34 (m, 1H, CHC**H**H'NH_2), 3.33-3.26 (m, 1H, CHCH**H**'NH_2), 3.25-3.10 (m, 2H, C**H**$_2$$NHMe_2^+$), 3.08-2.53 (m, 15H, CH_2NH**Me**$_2^+$, C**H**NH_2, 2C**H**$_2$C**H**$_2$), 2.28-2.16 (m, 2H, CHC**HH**'CH_2); ^{13}C{^{1}H} (125 MHz) 55.0 (s, **C**$H_2$$NHMe_2^+$), 54.7 (s, **C**H$NH_2$), 48.6 (s, CH**C**$H_2$$NH_2$), 45.71, 45.65, 45.1, 45.0 (4 × s, 2**C**H_2**C**H_2), 43.5, 43.4 (2 × s, NH**Me**$_2^+$), 27.4 (s, CH**C**$H_2$$CH_2$).

Λ-27b^{3+} 3BAr$_f^-$. A beaker was charged with Λ-**27b**·H^{4+} 4Cl$^-$·0.6NaCl·H$_2$O (0.0510 g, 0.101 mmol), H$_2$O (15 mL), and aqueous NaOH (0.10 M; 1.05 mL, 0.105 mmol). A solution of Na$^+$ BAr$_f^-$ (0.269 g, 0.303 mmol) in CH_2Cl_2 (15 mL) was added with stirring. After 15 min, the biphasic mixture was allowed to stand. The lower orange CH_2Cl_2 phase was separated. This solution was allowed to evaporate to give Λ-**27b**$^{3+}$ 3BAr$_f^-$·11H$_2$O as an orange solid (0.282 g, 0.091 mmol, 91%; from **L2**: 19% or 27% of theory),[26] which upon warming continually darkened and liquefied at 124 °C. Anal. Calcd. for $C_{106}H_{69}B_3CoF_{72}N_7$·11H$_2$O (3098.14): C 41.09, H 2.96, N 3.16; found: C 41.05, H 2.91, N 3.12.

NMR (CD_3CN, δ in ppm): ^{1}H (500 MHz) BAr$_f^-$ at 7.70 (s, 24H, *o*), 7.66 (s, 12H, *p*); N**H**$_2$ at 4.67-3.48 (br m, 12H); C**H**$_2$N**Me**$_2$, C**H**NH$_2$, CHC**H**$_2$NH$_2$, 2C**H**$_2$C**H**$_2$, and **H**$_2$O at 3.05-2.60 (br m, 10H), 2.58-2.47 (m, 2H), 2.38-2.16 (m, 33H); 1.94-1.87 (m, 1H, CHC**H**H'CH$_2$), 1.76-1.68 (m, 1H, CHCH**H**'CH$_2$); ^{13}C{^{1}H} (125 MHz) BAr$_f^-$ at 162.6 (q, $^1J_{BC}$ = 50.0 Hz, *i*), 135.7 (s, *o*), 130.0 (qm, $^2J_{CF}$ = 31.3 Hz, *m*), 125.5 (q, $^1J_{CF}$ = 270.0 Hz, **C**F$_3$), 118.6 (m, *p*); 58.8 (s, **C**HNH$_2$), 56.6 (s, CH**C**H$_2$NH$_2$), 49.4 (s, **C**H$_2$NMe$_2$), 45.7, 45.6, 45.30, 45.26 (s, s, s/triple intensity, s, 2**C**H$_2$**C**H$_2$, N**Me**$_2$), 28.2 (s, CH**C**H$_2$CH$_2$).

Δ-27b^{3+} 3BAr$_f^-$. A beaker was charged with Δ-**27b**·H^{4+} 4Cl$^-$·1.5NaCl·2H$_2$O (0.034 g, 0.0581 mmol), H$_2$O (15 mL), and aqueous NaOH (0.10 M; 0.60 mL, 0.060 mmol). A solution of Na$^+$ BAr$_f^-$ (0.154 g, 0.174 mmol) in CH_2Cl_2 (15 mL) was added with stirring. After 15 min, the biphasic mixture was allowed to stand. The lower orange CH_2Cl_2 phase was separated. This solution was allowed to evaporate to give Δ-**27b**$^{3+}$ 3BAr$_f^-$·11H$_2$O as an orange solid (0.170 g, 0.055 mmol, 95%; from **L2**: 7% or 25% of theory),[26] which upon warming continually darkened and liquefied at 127 °C. Anal.

Calcd. for $C_{106}H_{69}B_3CoF_{72}N_7 \cdot 11H_2O$ (3098.14): C 41.09, H 2.96, N 3.16; found: C 41.03, H 3.00, N 3.07.

NMR (CD_3CN, δ in ppm): ^1H (500 MHz) BAr_f^- at 7.71 (s, 24H, *o*), 7.68 (s, 12H, *p*); N**H**$_2$ at 4.88 (br s, 1H), 4.56-3.64 (m, 10H), 3.50 (br s, 1H); C**H**$_2$N**Me**$_2$, C**H**NH_2, CHC**H**$_2NH_2$, 2C**H**$_2$C**H**$_2$, and **H**$_2$O at 3.01 (br s, 1H), 2.89-2.46 (br m, 9H), 2.40-2.16 (m, 33H); 1.93-1.87 (m, 1H, CHC**H**H'CH_2), 1.78-1.66 (m, 1H, CHCH**H**'CH_2); $^{13}C\{^1H\}$ (125 MHz) BAr_f^- at 162.6 (q, $^1J_{BC}$ = 50.0 Hz, *i*), 135.7 (s, *o*), 129.9 (qm, $^2J_{CF}$ = 31.3 Hz, *m*), 125.5 (q, $^1J_{CF}$ = 271.3 Hz, **C**F_3), 118.7 (m, *p*); 57.3 (s, **C**HNH_2), 56.3 (s, CH-**C**H_2NH_2), 48.6 (s, **C**H_2NMe_2), 46.1, 46.0 (2 × s, N**Me**$_2$), 45.34, 45.30, 45.25 (s/double intensity, s, s, 2**C**H_2**C**H_2), 27.8 (s, CH**C**H_2CH_2).

Λ- and Δ-[Co(en)$_2$((*S*)-H$_2$NCH((CH$_2$)$_3$NMe$_2$H)CH$_2$NH$_2$)]$^{4+}$ 4Cl$^-$ (Λ- and Δ-27c·H^{4+} 4Cl$^-$). A. A round bottom flask was charged with $[Co(en)_2O_2CO]^+$ Cl^- (1.075 g, 3.916 mmol),[15] activated charcoal (0.450 g), and H_2O (20 mL), and fitted with a condenser. The mixture was heated to 40 °C and a solution of the tris(hydrochloric acid) salt of (*S*)-$H_2NCH((CH_2)_3NMe_2H)CH_2NH_2$ ((*S*)-**L3**·$(HCl)_3$, 0.921 g, 3.23 mmol; 0.83 equiv)[14a] in H_2O (5 mL) was added in one portion with stirring. The temperature was raised to 100 °C. After 0.75 h, the mixture was filtered. The solvent was removed from the red filtrate by rotary evaporation. The deep red solid was dissolved in HCl (0.50 M, 100 mL). The solution was added to a Dowex column (50WX2 hydrogen form; 4.5 × 37 cm; packed in water), which was eluted with HCl (1.0 M, 500 mL; 1.5 M, 500 mL; 2.0 M, until the second orange band began to elute; then 3.0 M). The solvent was removed from the second orange band by rotary evaporation to give crude **27c**·H^{4+} $4Cl^-$ as an orange solid (0.706 g. 1.512 mmol, 47%) and a 70:30 mixture of Λ/Δ isomers, as assayed by $^{13}C\{^1H\}$ NMR (δ, D_2O, 58.5/57.1 ppm).[25] NMR (D_2O, δ in ppm): ^1H (500 MHz) N**H**$_2$ at 5.40-4.85 (br m, 10H), 4.64-4.37 (br m, 2H); C**H**$_2$NH**Me**$_2^+$, C**H**NH_2,

CHC**H**$_2$NH$_2$, CHC**H**$_2$C**H**$_2$, and 2C**H**$_2$C**H**$_2$ at 3.27-3.13 (m, 2H), 3.12-2.69 (m, 16H), 2.66-2.59 (br s, 1H), 2.01-1.72 (br m, 4H); ^{13}C{^{1}H} (125 MHz) 58.5/57.1 (s, **C**HNH$_2$), 57.7 (s, **C**H$_2$NHMe$_2^+$), 49.7/48.8 (s, CH**C**H$_2$NH$_2$), 45.7, 45.6, 45.5, 45.4, 45.34, 45.27, 45.1, 45.0 (8 × s, 2**C**H$_2$**C**H$_2$), 43.4, 43.3 (2 × s, NH**Me**$_2^+$), 29.2, 29.1, 22.1 (3 × s, CH**C**H$_2$**C**H$_2$).

B. A solution of **27c**·H^{4+} 4Cl$^-$ from A (0.648 g, 1.387 mmol) in H$_2$O (40 mL) was added to a SP Sephadex column (C-25; 6.0 × 60 cm). Elution with 0.10 M (250 mL), 0.15 M (250 mL), 0.20 M (500 mL) and 0.25 M aqueous 2Na$^+$ *d*-tart^{2-}·2H$_2$O gave two bands. The first was collected and concentrated to 150 mL. This was added to a Dowex column (3.3 × 25 cm), which was eluted with aqueous HCl (gradient, 1.0 M to 3.0 M). The orange band was collected (yellow eluent) and the solvent was removed by rotary evaporation and oil pump vacuum. This gave Λ-**27c**·H^{4+} 4Cl$^-$·0.4NaCl·0.5H$_2$O as an orange solid (0.442 g, 0.885 mmol, 64% or 91% of theory from the 70:30 mixture),[26] dec pt 177-213 °C.[29] Anal. Calcd. for C$_{11}$H$_{36}$Cl$_4$CoN$_7$·0.4NaCl· 0.5H$_2$O (499.58):[30,31] C 26.45, H 7.46, N 19.63, Na 1.84; found: C 26.74, H 7.15, N 19.41, Na 1.60.

NMR (D$_2$O, δ in ppm): ^{1}H (500 MHz) N**H**$_2$ at 5.40 (br s, 1H), 5.23-4.86 (m, 9H), 4.69-4.41 (m, 2H); C**H**$_2$NH**Me**$_2^+$, C**H**NH$_2$, CHC**H**$_2$NH$_2$, and 2C**H**$_2$C**H**$_2$ at 3.31-3.12 (m, 2H), 3.11-2.44 (m, 18H); 2.01-1.71 (m, 4H, CHC**H**$_2$C**H**$_2$); ^{13}C{^{1}H} (125 MHz) 58.4 (s, **C**HNH$_2$), 57.6 (s, **C**H$_2$NHMe$_2^+$), 49.7 (s, CH**C**H$_2$NH$_2$), 45.5, 45.4, 45.34, 45.27 (4 × s, 2**C**H$_2$**C**H$_2$), 43.38, 43.33 (2 × s, NH**Me**$_2^+$), 29.1, 22.1 (2 × s, CH**C**H$_2$**C**H$_2$).

The second band from the Sephadex column was concentrated to 100 mL. This was added to a Dowex column (3.0 × 12 cm), which was eluted with aqueous HCl (gradient, 1.0 M to 3.0 M). The orange band was collected (yellow eluent) and the solvent was removed by rotary evaporation and oil pump vacuum. This gave Δ-**27c**·H^{4+}

$4Cl^{-}\cdot 0.5NaCl\cdot H_2O$ as an orange solid (0.172 g, 0.334 mmol, 24% or 80% of theory from the 70:30 mixture),[26] dec pt 165-213 °C.[29] Anal. Calcd. for $C_{11}H_{36}Cl_4CoN_7\cdot 0.5NaCl\cdot H_2O$ (514.43):[30,31] C 25.68, H 7.45, N 19.06; found: C 26.02, H 6.99, N 18.75.

NMR (D_2O, δ in ppm): ^{1}H (500 MHz) N**H**$_2$ at 5.31 (br s, 1H), 5.13 (br s, 3H), 5.03 (br s, 2H), 4.57 (br s, 1H), 4.43 (br s, 1H);[28] 3.27-3.09 (m, 3H, C**H**$_2$NHMe$_2^+$, C**H**NH$_2$), 3.07-2.57 (m, 16H, CH$_2$NH**Me**$_2^+$, CHC**H**$_2$NH$_2$, 2C**H**$_2$C**H**$_2$), 1.98-1.73 (m, 4H, CHC**H**$_2$C**H**$_2$); ^{13}C{^{1}H} (125 MHz) 57.7 (s, **C**H$_2$NHMe$_2^+$), 57.1 (s, **C**HNH$_2$), 48.7 (s, **C**H$_2$NH$_2$), 45.7, 45.6, 45.1, 45.0 (4 × s, 2**C**H$_2$**C**H$_2$), 43.4 (s/double intensity, NH**Me**$_2^+$), 29.2, 22.1 (2 × s, CH**C**H$_2$**C**H$_2$).

Λ-27c^{3+} 3BAr$_f^-$. A beaker was charged with Λ-**27c**$\cdot H^{4+}$ $4Cl^{-}\cdot 0.4NaCl\cdot 0.5H_2O$ (0.141 g, 0.282 mmol), H_2O (30 mL), and aqueous NaOH (0.10 M; 2.82 mL, 0.282 mmol). Then a solution of Na^+ BAr_f^- (0.750 g, 0.846 mmol) in CH_2Cl_2 (30 mL) was added with stirring. After 15 min, the biphasic mixture was allowed to stand. The lower orange CH_2Cl_2 phase was separated. This solution was allowed to evaporate to give Λ-**27c**$^{3+}$ $3BAr_f^-\cdot 11H_2O$ as an orange solid (0.764 g, 0.246 mmol, 87%; from **L3**: 26% or 37% of theory),[26] which upon warming continually darkened and liquefied at 133 °C. Anal. Calcd. for $C_{107}H_{71}B_3CoF_{72}N_7\cdot 11H_2O$ (3112.17): C 41.29, H 3.01, N 3.15; found: C 41.23, H 2.98, N 3.17.

NMR (CD_3CN, δ in ppm): ^{1}H (500 MHz) BAr_f^- at 7.70 (s, 24H, *o*), 7.66 (s, 12H, *p*); N**H**$_2$ at 4.62 (br s, 1H), 4.37-3.61 (m, 10H), 3.48 (br s, 1H); C**H**$_2$N**Me**$_2$, C**H**NH$_2$, CHC**H**$_2$NH$_2$, 2C**H**$_2$C**H**$_2$, and **H**$_2$O at 2.98-2.57 (br m, 11H), 2.49-2.23 (br m, 24H), 2.20 (br s, 6H); CHC**H**$_2$C**H**$_2$ at 1.78-1.48 (m, 4H); ^{13}C{^{1}H} (125 MHz) BAr_f^- at 162.6 (q, $^1J_{BC}$ = 50.0 Hz, *i*), 135.7 (s, *o*), 129.9 (qm, $^2J_{CF}$ = 31.3 Hz, *m*), 125.5 (q, $^1J_{CF}$ = 270.0 Hz, **C**F$_3$), 118.7 (m, *p*); 59.4, 59.3 (2 × s, **C**HNH$_2$, CH**C**H$_2$NH$_2$), 50.1 (s, **C**H$_2$NMe$_2$),

45.8, 45.6, 45.5, 45.4, 45.3 (s, s, s/double intensity, s, s, 2**C**H_2**C**H_2, N**Me**$_2$), 30.4, 24.8 (2 × s, CH**C**H_2**C**H_2).

Δ-27c^{3+} 3BAr$_f^-$. A beaker was charged with Δ-**27c**·H^{4+} 4Cl^-·0.5NaCl·H_2O (0.144 g, 0.280 mmol), H_2O (30 mL), and aqueous NaOH (0.10 M; 2.80 mL, 0.28 mmol). Then a solution of Na^+ BAr_f^- (0.745 g, 0.840 mmol) in CH_2Cl_2 (30 mL) was added with stirring. After 15 min, the biphasic mixture was allowed to stand. The lower orange CH_2Cl_2 phase was separated. This solution was allowed to evaporate to give Δ-**27c**$^{3+}$ 3BAr_f^-·9H_2O as an orange solid (0.767 g, 0.249 mmol, 89%; from **L3**: 10% or 36% of theory),[26] which upon warming continually darkened and liquefied at 131 °C. Anal. Calcd. for $C_{107}H_{71}B_3CoF_{72}N_7$·9$H_2O$ (3076.14): C 41.78, H 2.92, N 3.19; found: C 41.74, H 3.10, N 3.19.

NMR (CD_3CN, δ in ppm): ^{1}H (500 MHz) BAr_f^- at 7.71 (s, 24H, *o*), 7.68 (s, 12H, *p*); N**H**$_2$ at 4.43-3.60 (m, 11H), 3.48 (br s, 1H); C**H**$_2$N**Me**$_2$, C**H**NH_2, CHC**H**$_2$$NH_2$, 2C**H**$_2$C**H**$_2$, and **H**$_2$O at 2.92-2.58 (br m, 10H), 2.39-2.11 (m, 33H); CHC**H**$_2$C**H**$_2$ at 1.79-1.66 (m, 2H), 1.63-1.51 (m, 2H); ^{13}C{^{1}H} (125 MHz) BAr_f^- at 162.6 (q, $^1J_{BC}$ = 50.0 Hz, *i*), 135.7 (s, *o*), 129.9 (qm, $^2J_{CF}$ = 31.3 Hz, *m*), 125.5 (q, $^1J_{CF}$ = 270.0 Hz, **C**F_3), 118.7 (m, *p*); 59.5, 58.0 (2 × s, **C**H**C**$H_2$$NH_2$), 49.0 (s, **C**$H_2$$NMe_2$), 46.01, 45.96 (2 × s, N**Me**$_2$), 45.5, 45.4, 45.34, 45.26 (4 × s, 2**C**H_2**C**H_2), 30.5, 24.6 (2 × s, CH**C**H_2**C**H_2).

Λ- and Δ-[Co(en)$_2$((*S*)-H_2NCH((CH$_2$)$_4$NMe$_2$H)CH$_2$NH$_2$)]$^{4+}$ 4Cl$^-$ (Λ- and Δ-27d·H^{4+} 4Cl$^-$). A. A round bottom flask was charged with $[Co(en)_2O_2CO]^+$ Cl^- (0.754 g, 2.752 mmol),[15] activated charcoal (0.550 g), and H_2O (30 mL), and fitted with a condenser. The mixture was heated to 40 °C. Then a solution of the tris(hydrochloric acid) salt of (*S*)-H_2NCH((CH$_2$)$_4$NMe$_2$H)CH$_2$$NH_2$ ((*S*)-**L4**·(HCl)$_3$, 0.690 g, 2.29 mmol; 0.83 equiv)[14a] in H_2O (5 mL) was added in one portion with stirring. The temperature was raised to 100 °C. After 0.75 h, the mixture was filtered. The solvent was removed

from the red filtrate by rotary evaporation. The deep red solid was dissolved in HCl (0.50 M, 100 mL). The solution was added to a Dowex column (50WX2 hydrogen form; 4.5 × 30 cm; packed in water), which was eluted with HCl (1.0 M, 500 mL; 1.5 M, 500 mL; 2.0 M, until the second orange band began to elute; then 3.0 M). The solvent was removed from the second orange band by rotary evaporation to give crude **27d**·H^{4+} $4Cl^{-}$ as an orange solid (0.652 g. 1.36 mmol, 59%) and a 72:28 mixture of Λ/Δ isomers, as assayed by ^{13}C {^{1}H} NMR (δ, D_2O, 58.8/57.5 ppm).[25] NMR (D_2O, δ in ppm): ^{1}H (500 MHz) N**H**$_2$ at 5.32 (br s, 2H), 5.21-4.84 (br m, 8H), 4.50 (br m, 2H); 3.16 (t, $^{3}J_{HH}$ = 8.0 Hz, 2H, C**H**$_2$NHMe$_2^+$), 3.11-2.66 (m, 16H, CH_2NH**Me**$_2^+$, C**H**NH_2, CHC**H**H'NH_2, 2C**H**$_2$C**H**$_2$), 2.62-2.49 (m, 1H, CHCH**H**'NH_2), 1.84-1.70 (m, 4H, $CHCH_2$C**H**$_2$C**H**$_2$), 1.61-1.40 (m, 2H, CHC**H**$_2CH_2CH_2$); $^{13}C\{^{1}H\}$ (125 MHz) 58.8/57.5 (s, **C**HNH_2), 58.0 (s, **C**H_2NHMe$_2^+$), 49.8/48.8 (2 × s, CH**C**H_2NH_2), 45.69, 45.65, 45.5, 45.38, 45.36, 45.3, 45.1, 45.0 (8 × s, 2**C**H_2**C**H_2), 43.3 (s/double intensity, NH**Me**$_2^+$), 32.1/31.8, 24.5/24.4, 23.6/23.5 (6 × s, CH**C**H_2**C**H_2**C**H_2).

B. A solution of **27d**·H^{4+} $4Cl^{-}$ from A (0.582 g, 1.212 mmol) in H_2O (40 mL) was added to a SP Sephadex column (C-25; 6.0 × 60 cm). Elution with 0.10 M (250 mL), 0.15 M (250 mL), 0.20 M (500 mL) and 0.25 M aqueous $2Na^+$ *d*-tart^{2-}·$2H_2O$ gave two bands. The first was collected and concentrated to 150 mL. This was added to a Dowex column (3.3 × 25 cm), which was eluted with aqueous HCl (gradient, 1.0 M to 3.0 M). The orange band was collected (yellow eluent) and the solvent was removed by rotary evaporation and oil pump vacuum. This gave Λ-**27d**·H^{4+} $4Cl^{-}$·NaCl·$1.2H_2O$ as an orange solid (0.461 g, 0.821 mmol, 68% or 94% of theory from the 72:28 mixture),[26] dec pt 160-209 °C.[29] Anal. Calcd. for $C_{12}H_{38}Cl_4CoN_7$·NaCl·$1.2H_2O$ (561.28): C 25.68, H 7.25, N 17.47, Na 4.10; found: C 25.92, H 6.94, N 17.11, Na 2.63.[30,31]

NMR (D_2O, δ in ppm): ^1H (500 MHz) N**H**$_2$ at 5.34 (br s, 1H), 5.22-4.86 (br m, 9H), 4.49 (br s, 2H); 3.16 (br s, 2H, C**H**$_2$NHMe$_2^+$), 3.10-2.64 (m, 16H, CH_2NH**Me**$_2^+$, C**H**NH_2, $CHCHH'NH_2$, 2C**H**$_2$C**H**$_2$), 2.58 (br s, 1H, $CHCH$**H**'NH_2), 1.78 (br s, 4H, $CHCH_2$C**H**$_2$C**H**$_2$), 1.61-1.40 (m, 2H, CHC**H**$_2CH_2CH_2$); $^{13}C\{^1H\}$ (125 MHz) 58.8 (s, **C**HNH_2), 58.0 (s, **C**H_2NHMe$_2^+$), 49.8 (s, CH**C**H_2NH_2), 45.5, 45.32, 45.25, 45.1 (4 × s, 2**C**H_2**C**H_2), 43.3 (s/double intensity, NH**Me**$_2^+$), 31.9, 24.4, 23.5 (3 × s, CH**C**H_2**C**H_2**C**H_2).

The second band from the Sephadex column was collected and concentrated to 100 mL. This was added to a Dowex column (3.0 × 12 cm), which was eluted with aqueous HCl (gradient, 1.0 M to 3.0 M). The orange band was collected (yellow eluent) and the solvent was removed by rotary evaporation and oil pump vacuum. This gave Δ-**27d**·H^{4+} $4Cl^-$·1.5NaCl·H_2O as an orange solid (0.121 g, 0.206 mmol, 17% or 61% of theory from the 72:28 mixture),[26] dec pt 180-209 °C.[29] Anal. Calcd. for $C_{12}H_{38}Cl_4CoN_7$·1.5NaCl·H_2O (586.90):[30,31] C 24.56, H 6.87, N 16.71; found: C 24.92, H 6.56, N 16.19.

NMR (D_2O, δ in ppm): ^1H (500 MHz) N**H**$_2$ at 5.29 (br s, 2H), 5.22-4.87 (br m, 6H), 4.58-4.34 (m, 3H);[28] 3.19-3.13 (m, 2H, C**H**$_2$NHMe$_2^+$), 3.12-2.68 (m, 15H, CH_2NH**Me**$_2^+$, C**H**NH_2, 2C**H**$_2$C**H**$_2$), 2.64-2.51 (m, 2H, CHC**H**$_2NH_2$), 1.86-1.71 (m, 4H, $CHCH_2$C**H**$_2$C**H**$_2$), 1.58-1.42 (m, 2H, CHC**H**$_2CH_2CH_2$); $^{13}C\{^1H\}$ (125 MHz) 57.9 (s, **C**H_2NHMe$_2^+$), 57.5 (s, **C**HNH_2), 48.8 (s, CH**C**H_2NH_2), 45.64, 45.61, 45.04, 44.97 (4 × s, 2**C**H_2**C**H_2), 43.3 (s/double intensity, NH**Me**$_2^+$), 32.1, 24.5, 23.7 (3 × s, CH**C**H_2**C**H_2**C**H_2).

Λ-27d^{3+} 3BAr$_f^-$. A beaker was charged with Λ-**27d**·H^{4+} $4Cl^-$·NaCl·1.2H_2O (0.120 g, 0.215 mmol), H_2O (30 mL), and aqueous NaOH (0.10 M; 2.25 mL, 0.225 mmol). A solution of Na^+ BAr_f^- (0.572 g, 0.645 mmol) in CH_2Cl_2 (30 mL) was added

with stirring. After 15 min, the biphasic mixture was allowed to stand. The lower orange CH_2Cl_2 phase was separated. This solution was allowed to evaporate to give Λ-**27d**$^{3+}$ 3BAr_f^-·9H_2O as an orange solid (0.611 g, 0.198 mmol, 92%; from **L4**: 37% or 51% of theory),[26] which upon warming continually darkened and liquefied at 110 °C. Anal. Calcd. for $C_{108}H_{73}B_3CoF_{72}N_7$·9$H_2O$ (3090.17): C 41.98, H 2.97, N 3.17; found: C 42.23, H 2.79, N 2.62.

NMR (CD_3CN, δ in ppm): ^{1}H (500 MHz) BAr_f^- at 7.71 (s, 24H, *o*), 7.67 (s, 12H, *p*); N**H**$_2$ at 4.51-3.96 (br m, 8H), 3.92-3.70 (m, 3H), 3.53 (br s, 1H); C**H**$_2$N**Me**$_2$, C**H**NH_2, CHC**H**$_2NH_2$, 2C**H**$_2$C**H**$_2$, and **H**$_2$O at 2.90-2.64 (br m, 9H), 2.58-2.12 (m, 32H); 1.74-1.35 (m, 6H, CHC**H**$_2$C**H**$_2$C**H**$_2$); ^{13}C{^{1}H} (125 MHz) BAr_f^- at 162.6 (q, $^1J_{BC}$ = 50.0 Hz, *i*), 135.7 (s, *o*), 129.9 (qm, $^2J_{CF}$ = 31.3 Hz, *m*), 125.1 (q, $^1J_{CF}$ = 270.0 Hz, **C**F_3), 118.6 (m, *p*); 59.3, 59.2 (2 × s, **C**HNH_2, CH**C**H_2NH_2), 50.1, 45.8, 45.6, 45.4, 45.3, 45.0 (s, s, s, s, s, s/broad, 2**C**H_2**C**H_2, N**Me**$_2$, **C**H_2NMe_2), 32.2, 26.7, 24.4 (3 × s, CH**C**H_2**C**H_2**C**H_2).

Δ-27d^{3+} 3BAr$_f^-$. A beaker was charged with Δ-**27d**·H^{4+} 4Cl^-·1.5NaCl·H_2O (0.060 g, 0.102 mmol), H_2O (15 mL), and aqueous NaOH (0.10 M; 1.05 mL, 0.105 mmol). A solution of Na^+ BAr_f^- (0.271 g, 0.306 mmol) in CH_2Cl_2 (15 mL) was added with stirring. After 15 min, the biphasic mixture was allowed to stand. The lower orange CH_2Cl_2 phase was separated. This solution was allowed to evaporate to give Δ-**27d**$^{3+}$ 3BAr_f^-·10H_2O as an orange solid (0.285 g, 0.092 mmol, 90%; from **L4**: 9% or 32% of theory),[26] which upon warming continually darkened and liquefied at 100 °C. Anal. Calcd. for $C_{108}H_{73}B_3CoF_{72}N_7$·10$H_2O$ (3108.18): C 41.73, H 3.02, N 3.15; found: C 41.60, H 3.13, N 3.13.

NMR (CD_3CN, δ in ppm): ^{1}H (500 MHz) BAr_f^- at 7.71 (s, 24H, *o*), 7.68 (s, 12H, *p*); N**H**$_2$ at 4.66-3.48 (m, 12H); C**H**$_2$N**Me**$_2$, C**H**NH_2, CHC**H**$_2NH_2$, 2C**H**$_2$C**H**$_2$, and **H**$_2$O

at 3.03-2.19 (br m, 37H); 1.75-1.22 (m, 6H, CHC**H**$_2$C**H**$_2$C**H**$_2$); ^{13}C{^{1}H} (125 MHz) BAr$_f^-$ at 162.6 (q, $^1J_{BC}$ = 50.0 Hz, *i*), 135.7 (s, *o*), 130.0 (qm, $^2J_{CF}$ = 31.3 Hz, *m*), 125.5 (q, $^1J_{CF}$ = 270.0 Hz, **C**F$_3$), 118.7 (m, *p*); 59.3, 58.1 (2 × s, **C**HNH$_2$, CH**C**H$_2$NH$_2$), 49.0, 46.04, 45.97, 45.4, 45.3, 45.1 (s, s, s, s, s, s/broad, 2**C**H$_2$**C**H$_2$, N**Me**$_2$, **C**H$_2$NMe$_2$), 32.4, 26.8, 24.7 (3 × s, CH**C**H$_2$**C**H$_2$**C**H$_2$).

Experiments in Scheme 7.3. A 5 mm NMR tube was charged with a solution of **21a** (0.0075 g, 0.050 mmol, 1.0 equiv), catalyst (0.0050 mmol, 0.10 equiv), and Ph_2SiMe_2 (0.0020 mL, internal standard) in a deuterated solvent (0.50 mL). A ^{1}H NMR spectrum was recorded to measure the initial ratio of **21a** to the standard. Then **22c** (0.0068 mL, 0.060 mmol, 1.2 equiv) was added at the specified temperature. The conversions were monitored by ^{1}H NMR and TLC. After the specified time, the mixture was loaded onto a plug of silica gel, which was eluted with hexanes/EtOAc (1:1 v/v, 50 mL). The solvent was removed by rotary evaporation to give **23ac**, and the enantiomeric purity was assayed by chiral HPLC.[32]

Experiments in Scheme 7.4. A 1.5 mL vial was charged with a solution of nitroolefin (**21-**R, 0.10 mmol, 1.0 equiv) and Λ-**27c**$^{3+}$ 3BAr$_f^-$·11H$_2$O (0.031 g, 0.010 mmol, 0.10 equiv) in CH_2Cl_2 (0.70 mL). The sample was cooled to –35 °C, and dialkyl malonate (**22-**R″, 0.120 mmol, 1.20 equiv) was added. The conversion was monitored by TLC. After the specified time, the mixture was chromatographed on a silica gel column (1.9 × 14 cm, 9:1 v/v hexanes/EtOAc). The solvent was removed from the product containing fractions by rotary evaporation. The product was dried by oil pump vacuum at room temperature (yields: Scheme 7.4) and the enantiomeric purities were assayed by chiral HPLC.[32]

Experiments in Figure 7.6 (Rate Profiles). A (monofunctional catalyst)**.** A 5 mm NMR tube was charged with a solution of **21a** (0.0150 g, 0.101 mmol), dimethyl

malonate (**22c**, 0.0138 mL, 0.121 mmol, 1.20 equiv), Λ-$[Co(en)_3]^{3+}$ $3BAr_f^-\cdot 14H_2O$ (0.006 g, 0.0020 mmol, 0.020 equiv), and Ph_2SiMe_2 (0.0020 mL, internal standard) in CD_2Cl_2 (1.0 mL). A ^1H NMR spectrum was recorded to measure the initial ratio of **21a** to the standard. Then a solution of Et_3N in CD_2Cl_2 (0.20 M, 0.010 mL, 0.0020 mmol, 0.020 equiv) was added and the conversion to **23ac** was periodically assayed by ^1H NMR. After 3 h, the mixture was loaded directly onto a plug of silica gel, which was eluted with hexanes/EtOAc (1:1 v/v, 50 mL). The solvent was removed from the eluent by rotary evaporation. The enantiomeric purity of **23ac** was assayed by chiral HPLC (9% ee, *R* dominant).[32,33] **B** (bifunctional catalyst)**.** A 5 mm NMR tube was charged with a solution of **21a** (0.0150 g, 0.101 mmol), Λ- or Δ-**27c**$^{3+}$ $3BAr_f^-$ (0.0062, 0.0020 mmol, 0.020 equiv), and Ph_2SiMe_2 (0.0020 mL, internal standard) in CD_2Cl_2 (1.0 mL). A ^1H NMR spectrum was recorded to measure the initial ratio of **21a** to the standard. Then **22c** (0.0138 mL, 0.121 mmol, 1.20 equiv) was added and the reaction carried out and analyzed as in A.

Dimethyl 2-(2-nitro-1-phenylethyl)malonate (23ac).[3b,18c,d,19] This known compound was isolated as a white solid per the general procedure for Scheme 7.4. The ^1H and $^{13}C\{^1H\}$ NMR spectra were identical with those reported earlier. Chiral HPLC (see Figure A-4): Chiralpak AS-H column (90:10 v/v hexane/isopropanol, 1.0 mL/min, λ = 220 nm); t_R = 17.3 min (minor), 19.6 min (major).[32]

Diethyl 2-(2-nitro-1-phenylethyl)malonate (23ab).[3b,18c,d,19] This known compound was isolated as a colorless oil per the general procedure for Scheme 7.4. The ^1H and $^{13}C\{^1H\}$ NMR spectra were identical with those reported earlier. Chiral HPLC (see Figure A-3): Chiralpak AS-H column (90:10 v/v hexane/isopropanol, 1.0 mL/min, λ = 220 nm); t_R = 11.4 min (minor), 12.8 min (major).[32]

Dibenzyl 2-(2-nitro-1-phenylethyl)malonate (23ad).[19b] This known compound was isolated as a colorless oil per the general procedure for Scheme 7.4. NMR ($CDCl_3$, δ in ppm):[34] ^1H (500 MHz) 7.35-7.25 (m, 11H), 7.18-7.16 (m, 2H), 7.09-7.07 (m, 2H), 5.18 (d, $^2J_{HH}$ = 12.0 Hz, 1H, C**H**H'Ph), 5.15 (d, $^2J_{HH}$ = 12.5 Hz, 1H, CH**H**'Ph), 4.96 (d, $^2J_{HH}$ = 12.0 Hz, 1H, C'**H**H'Ph), 4.93 (d, $^2J_{HH}$ = 12.0 Hz, 1H, C'H**H**'Ph), 4.86-4.84 (m, 2H, C**H**$_2$NO$_2$), 4.26 (td, $^3J_{HH}$ = 8.5 Hz, $^3J_{HH}$ = 5.5 Hz, 1H, C**H**CH$_2$NO$_2$), 3.94 (d, $^3J_{HH}$ = 9.0 Hz, 1H, C**H**(CO$_2$Bn)$_2$); $^{13}C\{^1H\}$ (125 MHz) 167.1 (s, **C**O$_2$Bn), 166.5 (s, **C**'O$_2$Bn), 135.9 (s, *i*-Ph), 134.7 (s, *i*-Bn), 134.6 (s, *i*-Bn'), 129.0, 128.62, 128.61, 128.5, 128.44, 128.35, 128.3, 128.2, 127.9 (s/double intensity, s/double intensity, s, s/double intensity, s, s, s/double intensity, s/double intensity, s/double intensity, o/m/p Ph, Bn, Bn'), 77.4 (s, **C**H$_2$NO$_2$), 67.8 (s, **C**H$_2$Ph), 67.6 (s, **C'**H$_2$Ph), 54.9 (s, **C**H(CO$_2$Bn)$_2$), 42.9 (s, **C**HCH$_2$NO$_2$). Chiral HPLC (see Figure A-24): Chiralcel AS-H column (90:10 v/v hexane/isopropanol, 1.0 mL/min, λ = 220 nm); t_R = 18.5 min (minor), 21.7 min (major).

Dimethyl 2-(2-nitro-1-(4-methoxyphenyl)ethyl)malonate (23dc).[3b,18d] This known compound was isolated as a colorless oil per the general procedure for Scheme 7.4. The ^1H and $^{13}C\{^1H\}$ NMR spectra were identical with those reported earlier. Chiral HPLC (see Figure A-7): Chiralpak AD column (80:20 v/v hexane/isopropanol, 1.0 mL/min, λ = 220 nm); t_R = 11.7 min (major), 18.2 min (minor).[32]

Dimethyl 2-(2-nitro-1-(3,4-dichlorophenyl)ethyl)malonate (23ec).[3b,18d] This known compound was isolated as a white solid per the general procedure for Scheme 7.4. The ^1H and $^{13}C\{^1H\}$ NMR spectra were identical with those reported earlier. Chiral HPLC (see Figure A-8): Chiralpak AS-H column (90:10 v/v hexane/isopropanol, 1.0 mL/min, λ = 220 nm); t_R = 20.8 min (minor), 22.9 min (major).[32]

Dimethyl 2-(2-nitro-1-(3,4-dioxolophenyl)ethyl)malonate (23mc).[19a] This known compound was isolated as a colorless oil per the general procedure for Scheme

7.4. NMR ($CDCl_3$, δ in ppm):[34] ^1H (500 MHz) 6.74-6.67 (m, 3H, $C_6\mathbf{H}_3$), 5.95 (s, 2H, $OC\mathbf{H}_2O$), 4.87 (dd, $^2J_{HH}$ = 13.0 Hz, $^3J_{HH}$ = 8.0 Hz, 1H, $C\mathbf{H}H'NO_2$), 4.80 (dd, $^2J_{HH}$ = 13.0 Hz, $^3J_{HH}$ = 9.5 Hz, 1H, $CH\mathbf{H}'NO_2$), 4.16 (td, $^3J_{HH}$ = 9.0 Hz, $^3J_{HH}$ = 5.0 Hz, 1H, $C\mathbf{H}CH_2NO_2$), 4.79 (dd, $^3J_{HH}$ = 9.0 Hz, 1H, $C\mathbf{H}(CO_2Me)_2$), 3.76 (s, 3H, $C\mathbf{H}_3$), 3.61 (s, 3H, $C'\mathbf{H}_3$); $^{13}C\{^1H\}$ (125 MHz) 167.9 (s, $\mathbf{C}O_2Me$), 167.3 (s, $\mathbf{C}'O_2Me$), 148.2, 147.7, 129.7, 121.5, 108.8, 108.3, 101.5 (7 × s, $\mathbf{C}_6H_3$, $O\mathbf{C}H_2O$), 77.7 (s, $\mathbf{C}H_2NO_2$), 55.0 (s, $\mathbf{C}H(CO_2Me)_2$), 53.2 (s, $\mathbf{C}H_3$), 53.1 (s, $\mathbf{C}'H_3$), 42.8 (s, $\mathbf{C}HCH_2NO_2$). Chiral HPLC (see Figure A-25): Chiralcel AS-H (90:10 v/v hexane/isopropanol, 1.0 mL/min, λ = 220 nm); t_R = 49.8 min (major), 58.2 min (minor).[32]

Dimethyl 2-(2-nitro-1-α-naphthylethyl)malonate (23bc).[3b,18d] This known compound was isolated as a colorless oil per the general procedure for Scheme 7.4. The ^1H and $^{13}C\{^1H\}$ NMR spectra were identical with those reported earlier. Chiral HPLC (see Figure A-5): Chiralpak AD column (90:10 v/v hexane/isopropanol, 1.0 mL/min, λ = 254 nm); t_R = 13.6 min (major), 19.1 min (minor).[32]

Dimethyl 2-(2-nitro-1-furylethyl)malonate (23kc).[3b,18d] This known compound was isolated as a yellowish oil per the general procedure for Scheme 7.4. The ^1H and $^{13}C\{^1H\}$ NMR spectra were identical with those reported earlier. Chiral HPLC (see Figure A-14): Chiralcel OD column (90:10 v/v hexane/isopropanol, 1.0 mL/min, λ = 220 nm); t_R = 12.6 min (minor), 28.4 min (major).[32]

Dimethyl 2-(2-nitro-1-propylethyl)malonate (23lc).[3b,18d] This known compound was isolated as a colorless oil per the general procedure for Scheme 7.4. The ^1H and $^{13}C\{^1H\}$ NMR spectra were identical with those reported earlier. Chiral HPLC (see Figure A-15): Chiralcel OD column (97.5:2.5 v/v hexane/isopropanol, 1.0 mL/min, λ = 220 nm); t_R = 9.2 min (minor), 16.4 min (major).[32]

Dimethyl 2-(2-nitro-1-cyclohexylethyl)malonate (23nc).[18a,b] This known compound was isolated as a colorless oil per the general procedure for Scheme 7.4. NMR ($CDCl_3$, δ in ppm):[34] ^1H (500 MHz) 4.72 (dd, $^2J_{HH}$ = 15.0 Hz, $^3J_{HH}$ = 5.0 Hz, 1H, C**H**H'NO_2), 4.61 (dd, $^2J_{HH}$ = 13.5 Hz, $^3J_{HH}$ = 6.5 Hz, 1H, CH**H**'NO_2), 3.76 (s, 3H, OC**H**$_3$), 3.75 (d, $^3J_{HH}$ = 5.0 Hz, 1H, C**H**$(CO_2Me)_2$), 3.74 (s, 3H, OC'**H**$_3$), 2.90 (m, 1H, C**H**CH_2NO_2), 1.79-1.64 (m, 4H, ring C**H**$_2$/C**H**), 1.49-1.39 (m, 1H, ring C**H**$_2$/C**H**), 1.28-1.06 (m, 4H, ring C**H**$_2$/C**H**), 1.04-0.93 (m, 2H, ring C**H**$_2$/C**H**); $^{13}C\{^1H\}$ (125 MHz) 168.9 (s, **C**O_2Me), 168.6 (s, **C**'O_2Me), 75.4 (s, **C**H_2NO_2), 52.9 (s, O**C**H_3), 52.7 (s, O**C**'H_3), 51.0 (s, **C**$H(CO_2Me)_2$), 42.1 (s, **C**HCH_2NO_2), 39.6, 30.2, 29.8, 26.22, 26.17, 26.0 (6 × s, ring **C**H_2/**C**H). Chiral HPLC (see Figure A-26): Chiralcel OD column (90:10 v/v hexane/ isopropanol, 0.5 mL/ min, λ = 220 nm); t_R = 12.1 min (minor), 25.7 min (major).[32]

7.5. Crystallography.

One drop of conc. HCl was added to a solution of Δ-**27a**·H^{4+} $4Cl^-$·$3H_2O$ (0.020 g) in six drops of distilled water. After several days at room temperature, orange crystals had formed and were analyzed as outlined in Table 7.1. Cell parameters were obtained from 180 frames using a 0.5° scan.[35] Integrated intensity information for each reflection was obtained by reduction of the data frames with the program APEX2.[36] Data were corrected for Lorentz and polarization factors, as well as for crystal decay effects. SADABS[37] was employed to correct the data for absorption effects. The space group was determined from systematic reflection conditions and statistical tests. The structure was solved by direct methods using SHELXTL (SHELXS),[38] and revealed the same number of water molecules as in the starting material. The hydrogen atoms were fixed in idealized positions using a riding model. Non-hydrogen atoms were refined with anisotropic thermal parameters. The parameters were refined by weighted least squares

refinement on F^2 to convergence.[38,39] The absolute structure parameter was estimated as 0.006(3) (Table 7.1).[40]

CCDC 1439942 contains the supplementary crystallographic data which can be obtained from www.ccdc.cam.ac.uk/data_request/cif.

Table 7.1. Crystallographic data for Δ-**27a**·H^{4+} $4Cl^{-}$·$3H_2O$

Empirical formula	$C_9H_{38}Cl_4CoN_7O_3$
Formula weight	493.19
Temperature	110(2) K
Wavelength	1.54178 Å
Crystal system	Orthorhombic
Space group	P2(1)2(1)2(1)
Unit cell dimensions	
a	7.4152(4) Å
b	14.4006(6) Å
c	20.3682(9) Å
α	90°
β	90°
γ	90°
V	2174.98(18) $Å^3$
Z	4
Density (calculated)	1.506 Mg/m^3
Absorption coefficient	10.909 mm^{-1}
F(000)	1040
Crystal size	0.08 × 0.07 × 0.02 mm^3
Theta range for data collection	4.34 to 60.00°.
Index ranges	$-8 \le h \le 8$, $-16 \le k \le 16$, $-21 \le l \le 22$
Reflections collected	36509
Independent reflections	3167 [R(int) = 0.0583]
Completeness to theta = 60.00°	99.5%
Absorption correction	Semi-empirical from equivalents
Max. / min. transmission	0.8113 / 0.4757
Refinement method	Full-matrix least-squares on F^2
Data / restraints / parameters	3167 / 0 / 230
Goodness-of-fit on F^2	0.995
Final R indices [I>2σ(I)]	*R*1 = 0.0215, *w*R2 = 0.0411
R indices (all data)	*R*1 = 0.0234, *w*R2 = 0.0414
Absolute structure parameter	–0.006(3)
Largest diff. peak and hole	0.161 and –0.195 e·$Å^{-3}$

7.6. References

(1) (a) Dalko, P. I.; Moisan, L. *Angew. Chem., Int. Ed*. **2004**, *43*, 5138-5175; *Angew. Chem.* **2004**, *116*, 5248-5286. (b) Berkessel, A.; Gröger, H. *Asymmetric Organocatalysis: From Biomimetic Concepts to Application in Asymmetric Synthesis*; Wiley-VCH: Weinheim, Germany, 2005. (c) *Asymmetric Organocatalysis*; List, B., Ed; Topics in Current Chemistry *291*; Springer, Berlin, **2009**. (d) Scheffler, U.; Mahrwald, R. *Chem. Eur. J.* **2013**, *19*, 14346-14396. (e) Volla, C. M. R.; Atodiresei, I.; Rueping, M. *Chem. Rev.* **2014**, *114*, 2390-2431.

(2) (a) Taylor, M. S.; Jacobsen, E. N. *Angew. Chem., Int. Ed.* **2006**, *45*, 1520-1543; *Angew. Chem*. **2006**, *118*, 1550-1573. (b) Doyle, A. G.; Jacobsen, E. N. *Chem. Rev.* **2007**, *107*, 5713-5743. (c) Yu, X.; Wang, W. *Chem. Asian J.* **2008**, *3*, 516-532.

(3) (a) Ganzmann, C.; Gladysz, J. A. *Chem. Eur. J.* **2008**, *14*, 5397-5400. (b) Lewis, K. G.; Ghosh, S. K.; Bhuvanesh, N.; Gladysz, J. A. *ACS Cent. Sci.* **2015**, *1*, 50-56.

(4) Thomas, C.; Gladysz, J. A. *ACS Catal*. **2014**, *4*, 1134-1138.

(5) (a) Scherer, A.; Mukherjee, T.; Hampel, F.; Gladysz, J. A. *Organometallics* **2014**, *33*, 6709-6722. (b) Mukherjee, T.; Ganzmann, C.; Bhuvanesh, N.; Gladysz, J. A. *Organometallics* **2014**, *33*, 6723-6737.

(6) (a) Chen, L.-A.; Xu, W.; Huang, B.; Ma, J.; Wang, L.; Xi, J.; Harms, K.; Meggers, E. *J. Am. Chem. Soc*. **2013**, *135*, 10598-10601. (b) Chen, L.-A.; Tang, X.; Xi, J.; Xu, W.; Gong, L.; Meggers, E. *Angew. Chem., Int. Ed*. **2013**, *52*, 14021-14025; *Angew. Chem*. **2013**, 12*5*, 14271-14275. (c) Ma, J.; Ding, X.; Hu, Y.; Huang, Y.; Gong, L.; Meggers, E. *Nat. Commun*. **2014**, *5*:4531. (d) Huo, H.; Fu, C.; Wang, C.; Harms, K.; Meggers, E. *Chem. Commun*. **2014**, *50*, 10409-10411. (e) Hu, Y.; Zijun, Z.; Gong, L.; Meggers, E. *Tetrahedron Lett*. **2015**, *56*, 4653-4656. (f) Hu, Y.; Zijun, Z.; Gong, L.;

Meggers, E. *Org. Chem. Front.* **2015**, *2*, 968-972.

(7) Maleev, V. I.; North, M.; Larionov, V. A.; Fedyanin, I. V.; Savel´yeva, T. F.; Moscalenko, M. A.; Smolyakov, A. F.; Belokon, Y. N. *Adv. Synth. Catal.* **2014**, *356*, 1803-1810.

(8) For relevant studies with achiral metal containing hydrogen bond donor catalysts, see (a) Nickerson, D. M.; Mattson, A. E. *Chem. Eur. J.* **2012**, *18*, 8310-8314. (b) Nickerson, D. M.; Angeles, V. V.; Auvil, T. J.; So, S. S.; Mattson, A. E. *Chem. Commun*. **2013**, *49*, 4289-4291.

(9) Hiemstra, H.; Wynberg, H. *J. Am. Chem. Soc.* **1981**, *103*, 417-430.

(10) (a) Okino, T.; Hoashi, Y.; Furukawa, T.; Xu, X.; Takemoto, Y. *J. Am. Chem. Soc*. **2005**, *127*, 119-125. (b) Miyabe, H.; Takemoto, Y. *Bull. Chem. Soc. Jpn.* **2008**, *81*, 785-795. (c) Siau, W.-Y.; Wang, J. *Catal. Sci. Technol.* **2011**, *1*, 1298-1310. (d) Serdyuk, O. V.; Heckel, C. M.; Tsogoeva, S. B. *Org. Biomol. Chem*. **2013**, *11*, 7051-7071. (e) Held, F. E.; Tsogoeva, S. B. *Catal. Sci. Technol.* **2016**, *6*, 645-667.

(11) For the related concept of organomulticatalysis, see (a) Piovesana, S.; Schietroma, D. M. S.; Bella, M. *Angew. Chem., Int. Ed*. **2011**, *50*, 6216-6232; *Angew. Chem.* **2011**, *123*, 6340-6357. (b) Wende, R. C.; Schreiner, P. R. *Green Chem.* **2012**, *14*, 1821-1849.

(12) Zhang, Z.; Schreiner, P. R. *Chem. Soc. Rev.* **2009**, *38*, 1187-1198.

(13) (a) Werner, A. *Chem. Ber.* **1911**, *44*, 1887-1898. V. L. King is listed as an author for the experimental section. (b) Werner, A. *Chem. Ber.* **1911**, *44*, 2445-2455. (c) Werner, A. *Chem. Ber.* **1911**, *44*, 3272-3278. (d) Werner, A. *Chem. Ber.* **1911**, *44*, 3279-3284. (e) Werner, A. *Chem. Ber.* **1912**, *45*, 121-130.

(14) (a) Ghosh, S. K.; Ganzmann, C.; Gladysz, J. A. *Tetrahedron: Asymmetry* **2015**, *26*, 1273-1280. (b) As illustrated in Scheme 7.1, (*S*)-**L1** and (*S*)-**L2-4** have

opposite *relative* configurations at carbon.

(15) Springbørg, J.; Schäffer, C. E. *Inorg. Synth.* **1973**, *14*, 63-68.

(16) (a) Douglas, B. E. *J. Am. Chem. Soc.* **1954**, *76*, 1020-1021. (b) Sen, D.; Fernelius, W. C. *J. Inorg. Nucl. Chem.* **1959**, *10*, 269-274. (c) Bianchi, A, Bencini, A. Synthesis and Spectroscopy of Transition Metal Complexes. In *Inorganic and Bio-Inorganic Chemistry*, vol. II, part of Encyclopedia of Life Support Systems (EOLSS), Bertini, I., Ed.; EOLSS Publishers Co. Ltd., Oxford, 2009, pp 150-256.

(17) (a) Yoshikawa, Y.; Yamasaki, K. *Coord. Chem. Rev.* **1979**, *28*, 205-229. (b) Yoneda, H. *J. Chromatogr.* **1985**, *313*, 59-91. (c) In SP-Sephadex, the sulfopropyl groups replaced the sulfoethyl groups in SE-Sephadex: see 17a.

(18) (a) Li, H.; Wang, Y.; Tang, L.; Deng, L. *J. Am. Chem. Soc.* **2004**, *126*, 9906-9907. (b) Ye, J.; Dixon, D. J.; Hynes, P. S. *Chem. Commun.* **2005**, 4481-4483. (c) Andrés, J. M.; Manzano, R.; Pedrosa, R. *Chem. Eur. J.* **2008**, *14*, 5116-5119. (d) Li, X.-J.; Liu, K.; Ma, H.; Nie, J.; Ma, J.-A. *Synlett* **2008**, *20*, 3242-3246. (e) Almaşi, D.; Alfonso, D. A.; Gómez-Bengoa, E.; Nájera, C. *J. Org. Chem.* **2009**, *74*, 6163-6168.

(19) (a) Watanabe, M.; Ikagawa, A.; Wang, H.; Murata, K.; Ikariya, T. *J. Am. Chem. Soc.* **2004**, *126*, 11148-11149. (b) Evans, D. A.; Mito, S.; Seidel, D. *J. Am. Chem. Soc.* **2007**, *129*, 11583-11592.

(20) It has also been proposed that tertiary amine groups in bifunctional thiourea catalysts interact with ß-arylnitroethene substrates: Hamza, A.; Schubert, G.; Soós, T.; Pápai, I. *J. Am. Chem. Soc.* **2006**, *128*, 13151-13160.

(21) Fulmer, G. R.; Miller, A. J. M.; Sherden, N. H.; Gottlieb, H. E.; Nudelman, A.; Stoltz, B. M.; Bercaw, J. E.; Goldberg, K. I. *Organometallics* **2010**, *29*, 2176-2179.

(22) (a) Brookhart, M.; Grant, B.; Volpe, Jr., A. F. *Organometallics* **1992**, *11*, 3920-3922. (b) For hazardous aspects of this synthesis, consult Yakelis, N. A.; Bergman,

R. G. *Organometallics* **2005**, *24*, 3579-3581.

(23) (a) Xia, X.-F.; Shu, X.-Z.; Ji, K.-G.; Yang, Y.-F.; Shaukat, A.; Liu, X.-Y.; Liang, Y.-M. *J. Org. Chem.* **2010**, *75*, 2893-2902. (b) Lucet, D.; Sabelle, S.; Kostelitz, O.; Gall, T. L.; Mioskowski, C. *Eur. J. Org. Chem.* **1999**, 2583-2591.

(24) Broomhead, J. A.; Dwyer, F. P.; Hogarth, J. W. *Inorg. Synth.* **1960**, *6*, 183-186.

(25) No attempts were made to characterize the degree of hydration of salts that were mixtures of diastereomers.

(26) Given the baseline separation of the Λ and Δ diastereomers on Sephadex columns, this salt is presumed to be diasteromerically pure. However, distinctive ^{1}H NMR signals are lacking. The ^{13}C NMR spectrum indicates a minimum diastereomeric purity of >95:<5 (due to a number of factors, only moderate signal/noise levels could be realized).

(27) Since the nitrogen microanalysis is low, this complex cannot be represented as analytically pure. Nonetheless, the data are reported to illustrate the best values obtained to date.

(28) Some of the NH_2 protons are overlapped by residual HDO.

(29) It deserves emphasis that for **27b-d**·H^{4+} $4Cl^{-}$, the Λ diasteromers elute (as *d*-$tart^{2-}$ salts) from the Sephadex column before the Δ diastereomers. However, with **27a**·H^{4+} $4Cl^{-}$ the Δ diastereomer elutes first (as a *d*-$tart^{2-}$ salt). These assignments are based upon the CD spectra in Figures 7.4 and the crystal structure of Δ-**27a**·H^{4+} $4Cl^{-}$ ·$3H_2O$ (Figure 7.5). For the most relevant reference CD spectra (Λ- or Δ-$[Co(en)_3]^{3+}$ $3X^{-}$), see: (a) Gillard, R. D. *Nature* **1964**, *201*, 989-991. (b) Saito, Y. *Coord. Chem. Rev.* **1974**, *13*, 305-337. (c) Nakashima, T.; Mishiro, J.; Ito, M.; Kura, G.; Ikuta, Y.; Matsumoto, N.; Nakajima, K.; Kojima, M. *Inorg. Chem.* **2003**, *42*, 2323-2330.

The order of elution is more completely analyzed as follows. Due to the arbitrary nature of the Cahn-Ingold-Prelog sequence rules, (*R*)-**L1** has the same *relative* configuration as (*S*)-**L2-4**. However, *S* enantiomers ((*S*)-**L1-4**) were used for all experiments. Hence, when comparing (1) **27b-d**·H^{4+} $4Cl^{-}$, Λ/*S* before Δ/*S*, and (2) **27a**·H^{4+} $4Cl^{-}$, Δ/*S* before Λ/*S*, the latter is equivalent, in a *relative* sense, to Δ/*R* before Λ/*R* for **27b-d**·H^{4+} $4Cl^{-}$.

(30) There have been several reports of the cocrystallization of $[Co(en)_3]^{3+}$ $3Cl^{-}$, H_2O, and NaCl: (a) Nakatsu, K.; Shiro, M.; Saito, Y.; Kuroya, H. *Bull. Chem. Soc. Japan* **1957**, *30*, 158-164. (b) Farrugia, L. J.; Peacock, R. D.; Stewart, B. *Acta Cryst.* **2000**, *C56*, 149-151.

(31) The sodium cations associated with **27b-d**·H^{4+} $4Cl^{-}$ originate from the aqueous sodium tartrate gradient employed with the Sephadex column. The chloride anions originate from the aqueous HCl gradient employed with the Dowex column. Due to the large amount of sample required for instrumental neutron activation analyses, sodium was only determined for the Λ diastereomers. Since the ^1H NMR spectra were recorded in D_2O, the hydration levels could not be independently verified. Thus, the calculated microanalysis values represent a fit of the hydration levels to the C/H/N/Na values found. Some ^1H NMR spectra were also recorded in non-dried DMF-d_7. These exhibited broad hydroxyl peaks at ca. δ 3.7 ppm that integrated to 2-3 water molecules, but this solvent was too expensive for routine use. In any case, the exact compositions of these tetrachloride salts are in one sense only bookkeeping details, as the NaCl is removed during subsequent anion metatheses that afford the BAr_f^{-} salts used as catalysts. Since **27a-d**$^{3+}$ $3BAr_f^{-}$ are soluble in CD_3CN, the degrees of hydration can be independently assayed by integrating ^1H NMR spectra. Finally, with the Δ diastereomers of **27b-d**·H^{4+} $4Cl^{-}$, the sodium values and hydration levels were varied to give the best

fit to the C/H/N values.

(32) The dominant configurations of **23a<u>c</u>**, **23a<u>b</u>**, and **23a<u>d</u>** (all *R*) were assigned by chiral HPLC using conditions similar to those in the literature.[3b,18c,d,19] The dominant configurations of **23b<u>c</u>**, **23d<u>c</u>-e<u>c</u>**, **23k<u>c</u>-n<u>c</u>** were assigned assuming analogous relative retention times.

(33) This reaction was also carried out on an identical scale in CH_2Cl_2 but using 10 mol% Λ-$[Co(en)_3]^{3+}$ $3BAr_f^-\cdot 14H_2O$. This gave **23a<u>c</u>** of 7% ee (*R* dominant).

(34) The NMR signals of this addition product were assigned by analogy to those of **23a<u>c</u>**: see 18e.

(35) Sheldrick, G. M. "Cell_Now: Program for Obtaining Unit Cell Constants from Single Crystal Data" (version 2008/1), University of Göttingen, Germany.

(36) APEX2 "Program for Data Collection and Integration on Area Detectors", BRUKER AXS Inc., 5465 East Cheryl Parkway, Madison, WI 53711-5373, USA.

(37) Sheldrick, G.M. "SADABS: Program for Absorption Correction for Data from Area Detector Frames" (version 2008/1), University of Göttingen, 2008.

(38) Sheldrick, G.M. *Acta Cryst*. **2008**, *A64*, 112-122.

(39) Dolomanov, O. V, Bourhis, L. J., Gildea, R. J., Howard, J. A. K., Puschmann, H. *J. Appl. Cryst*. **2009**, *42*, 339-341.

(40) Flack, H. D.; Bernardinelli, G.; Clemente, D. A.; Linden, A.; Spek, A. L. *Acta Cryst.* **2006**, *B62*, 695–701.

8. NEW MEDIA FOR CLASSICAL COORDINATION CHEMISTRY: PHASE TRANSFER OF WERNER AND RELATED POLYCATIONS INTO HIGHLY NONPOLAR FLUOROUS SOLVENTS†

8.1. Introduction

The chiral octahedral tris(ethylenediamine) cobalt trication $[Co(en)_3]^{3+}$, and related Werner systems, represent important milestones in the development of inorganic chemistry and stereochemistry.[1-3] As Werner reported in 1912,[2b] the two enantiomers of $[Co(en)_3]^{3+}$ can be separated by crystallization of the diastereomeric tartrate salts. As depicted in Scheme 8.1, the configurations of the cobalt stereocenters are denoted Λ and Δ. Separation is commonly followed by halide anion exchange. Despite the simplicity of this procedure, applications of Werner salts in enantioselective organic reactions have only been developed during the past 5 years.[4]

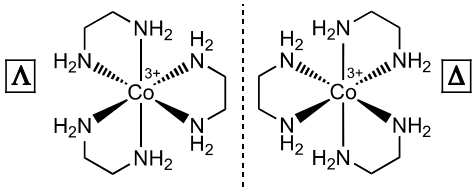

Scheme 8.1. Enantiomers of the trication of $[Co(en)_3]^{3+}$ $3Cl^-$.

One factor inhibiting progress has been the lack of solubility in organic solvents. The racemic tetraphenylborate salt $[Co(en)_3]^{3+}$ $3BPh_4^-$ has been reported, and is only

†Reproduced with permission from Ghosh, S. K.; Sullivan, A. R.; Leas, J. G.; Bhuvanesh, N.; Gladysz, J. A. *Inorg. Chem.* **2013**, *52*, 9369-9378. Copyright 2013 American Chemical Society.

soluble in methanol and THF.[5,6] We recently found that the more lipophilic B(3,5-$C_6H_3(CF_3)_2)_4$ or "barf" (BAr_f) salt could easily be prepared by adding a CH_2Cl_2 solution of Na^+ BAr_f^- to an aqueous solution of enantiopure Δ-$[Co(en)_3]^{3+}$ $3I^-$.[4a,7] The trication rapidly transferred into the organic phase, and solvent removal afforded the hydrate $[Co(en)_3]^{3+}$ $3BAr_f^-\cdot 14H_2O$. This substance was soluble in a wide range of organic solvents, and the water is believed to be associated with a "second" or "outer" coordination sphere involving hydrogen bonding with the NH protons.

Ongoing work in our laboratory has demonstrated the extraordinary utility of such BAr_f salts in enantioselective catalysis.[4] Accordingly, I became curious about the possibility of extending this chemistry to fluorous analogs and media.[8] Fluorous catalysts, which often feature ponytails of the formula $(CF_2)_{n-1}CF_3$ (R_{fn}), are easily separated from organic products and recycled by a number of protocols.[9] Furthermore, the "fluorous BAr_f" salt Na^+ B(3,5-$C_6H_3(R_{f6})_2)_4^-$ (**28**, Na^+ BAr_{f6}^-) had previously been reported.[10-12] Hence, I wondered whether it would be possible to render such polycations highly fluorophilic and readily soluble in perfluoroalkanes, which are some of the least polar solvents known.

In this section, I describe the facile solubilization of tricationic Werner salts in fluorous media. Since some difficulties were encountered in the synthesis of Na^+ BAr_{f6}^-, optimized procedures that have been repeated by several coworkers are provided. In order to confirm that this concept may be extended beyond cobalt hexaamine complexes, the synthesis of a fluorophilic salt of the extensively studied ruthenium dication $[Ru(bipy)_3]^{2+}$ is also detailed.[13] During the course of these efforts, the crystal structure of a fluorous arene could be determined, and was found to exhibit several unusual features.

8.2. Results

8.2.1. Synthesis of Na^+ BAr_{f6}^- (28)

The van Koten/Deelman and Bühlmann research groups have reported syntheses of Na^+ BAr_{f6}^-,[10,11] and each requires the fluorous bromoarene precursor Br(3,5-$C_6H_3(R_{f6})_2$) (**29**). One route to the latter involves the selective disubstitution of 1,3,5-tribromobenzene using perfluorohexyliodide ($R_{f6}I$) and copper.[11,14,15] However, several coworkers have had difficulty stopping this reaction at the optimum stage, and with the separation of monosubstitution or trisubstitution byproducts. Thus, I have synthesized **28** by modifying the sequence of van Koten and Deelman,[10] which is summarized in Scheme 8.2.

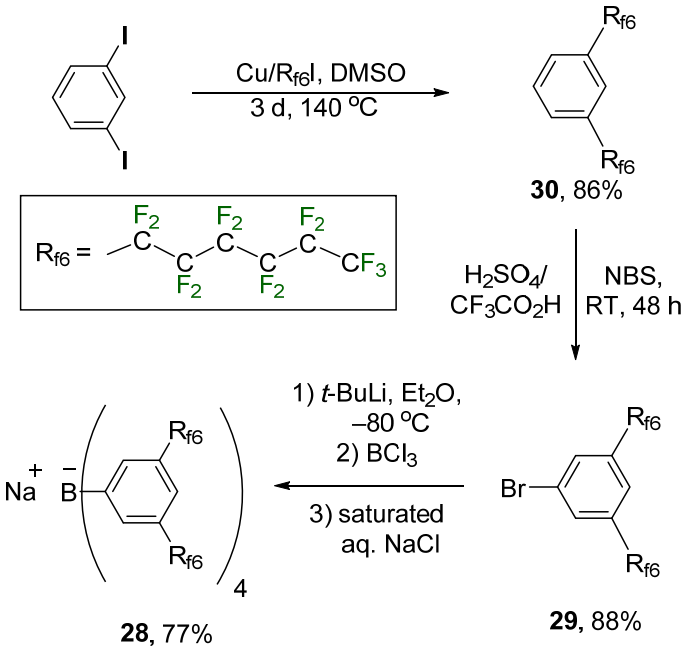

Scheme 8.2. Modified syntheses of Na^+ BAr_{f6}^- (**28**).

First, the copper mediated cross coupling of 1,3-diiodobenzene and a slight excess of $R_{f6}I$ was carried out at 140 °C. Only DMSO was used as the solvent, as opposed to DMSO/C_6F_6 as employed earlier.[10] The co-catalyst 2,2'-bipyridine was also omitted, necessitating a higher temperature. Workup after 3 d gave 1,3-di(perfluorohexyl)benzene or 1,3-$C_6H_4(R_{f6})_2$ (**30**) in 86-70% yields.

Next, **30** was brominated using a procedure developed by Dolbier for the analogous reaction of 1,3-di(trifluoromethyl)benzene.[16] Thus, **30** was dissolved in 29:71 (v/v) H_2SO_4/CF_3CO_2H and NBS was added in portions over the course of 6 h. Workup after 2 d gave the aryl bromide Br(3,5-$C_6H_3(R_{f6})_2$ **(29**) as a spectroscopically pure white solid in 88-75% yields. The literature procedure used a 41:59 (v/v) H_2SO_4/CF_3CO_2H mixture, with a charge of NBS added every two days over the course of seven days.[10] I repeatedly verified that these seemingly minor differences afforded, as reported, a ca. 6:1 **29**/**30** mixture in only 54% yield.

Fluorous molecules often resist crystallization, but colorless crystals of **29** were obtained from an acetone-d_6 solution. X-ray data were collected and the structure was determined as summarized in Table 8.1 and the experimental section. Two views of the molecular structure, and key bond lengths and angles, are provided in Figure 8.1.[17]

The perfluorohexyl groups adopt conformations that project "upwards" from the plane of the arene ring, as reflected by C2-C3-C7-C8, C4-C3-C7-C8, C4-C5-C13-C14, and C6-C5-C13-C1 torsion angles of 97.6° to 83.1° (Figure 8.1, bottom). Despite initial appearances, there is no mirror plane containing the carbon-bromine bond and the *para* carbon atom (Br1, C1, C4). Powder X-ray diffraction data obtained with samples of **29** prior to crystallization agreed well with the single crystal data. There are several interesting aspects of this crystal structure, but further analyses are deferred to the discussion section.

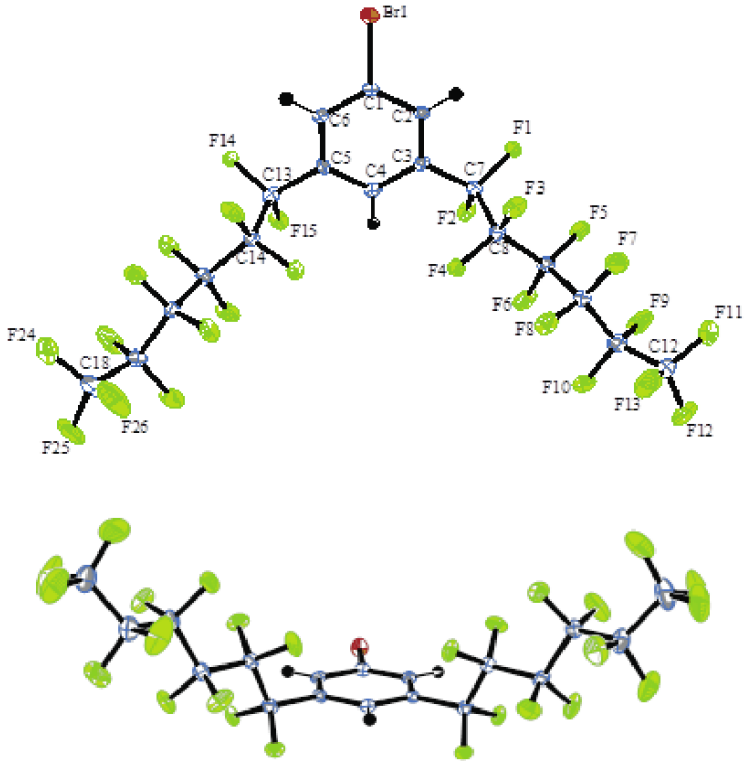

Figure 8.1. Two views of the molecular structure of **29** with thermal ellipsoids at the 50% probability level. Key bond lengths (Å) and angles (°): C1-Br 1.899(2), C1-C2 1.385(3), C2-C3 1.391(3), C4-C5 1.394(3), C5-C6 1.391(3), C6-C1 1.383(3), C3-C7 1.507(3), C5-C13 1.506(3), average of ten CF-CF 1.544(5), Br-C1-C2 119.14(17), C1-C2-C3 118.7(2), C2-C3-C4 120.7(2), C3-C4-C5 119.3(2), C4-C5-C6 120.8(2), C5-C6-C1 118.5(2), C6-C1-C2 121.9(2), C6-C1-Br 118.93(17), C2-C3-C7 120.3(2), C4-C3-C7 119.0(2), C4-C5-C13 119.2(2), C6-C5-C13 120.0(2), average of eight CF-CF-CF 115.0(8).

Table 8.1. Crystallographic data for **29**.

empirical formula	$C_{18}H_3BrF_{26}$
formula weight	793.11
temperature of collection [K]	110(2)
wavelength [Å]	1.54178
crystal system	tetragonal
space group	*I*4
unit cell dimensions	
a [Å]	29.5335(13)
b [Å]	29.5335(13)
c [Å]	5.5624(3)
α [°]	90
β [°]	90
γ [°]	90
V [Å^3]	4851.7(4)
Z	8
ρ_{calc} [Mg/m^3]	2.172
μ [mm^{-1}]	4.348
F(000) 3040	
crystal dimension [mm^3]	0.45 × 0.04 × 0.04
Θ [°]	2.12 to 59.92
range/indeces (*h, k, l*)	–33,33; –33,33; –6,5
reflections collected	56681
independent reflections	3534 [R(int) = 0.0559]
completeness to Θ = 59.92°	98.9%
absorption correction	semi-empirical from equivalents
max. and min. transmission	0.8453 and 0.2451
refinement method	full-matrix least-squares on F^2
data/restraints/parameters	3534/1/407
goodness-of-fit on F^2	1.051
final R indices [I>2σ(I)]	R_1 = 0.0190, wR_2 = 0.0466
R indices (all data)	R_1 = 0.0198, wR_2 = 0.0470
absolute structure parameter	0.00(9)
largest diff. peak/hole [e Å^{-3}]	0.187/–0.316

The "fluorous BAr_f" salt **28** was synthesized according to the literature recipe in Scheme 8.2,[10] but with a chromatographic workup (silica gel, ether and then CH_2Cl_2/CH_3OH) that avoided persistent acetone solvates encountered with the reported purification. White needles were obtained from perfluoro(2-butyltetrahydrofuran) (FC-75) in 77-70% yields. As summarized in Table 8.2, **28** was soluble in all fluorous solvents investigated, as well as the hybrid solvent $C_6H_5CF_3$[18] and a number of organic solvents. It was insoluble in benzene, toluene, and hexanes. The NMR properties of **28**-**30** closely agreed with those previously reported. In the case of **28**, a $^{13}C\{^1H,^{19}F\}$NMR spectrum was recorded, which showed a quartet for the *ipso* carbon at 161.8 ppm due to ^{11}B-^{13}C coupling (J = 50.0 Hz), and singlets as opposed to multiplets for the CF_2 groups.

Table 8.2. Solubility data (24 °C).

Solvent	Compound		
	28	**31**[a]	**32**[b]
FC-72[c]	Soluble	Soluble	Soluble
FC-75[d]	Soluble	Soluble	Soluble
PFMC[e]	Soluble	Soluble	Soluble
$C_6H_5CF_3$	Soluble	Soluble	Soluble
Acetone	Soluble	Soluble	Soluble
Et_2O	Soluble	Soluble	Soluble
CH_3OH	Soluble	Soluble	Soluble
CH_2Cl_2	Soluble	Soluble	Soluble
CD_3CN	Soluble	Sp. soluble	Insoluble
Ethyl acetate	Soluble	Soluble	Sp. soluble
Benzene	Insoluble	Insoluble	Insoluble
Toluene	Insoluble	Insoluble	Insoluble
Hexanes	Insoluble	Insoluble	Insoluble
FC-72[c]	Soluble	Soluble	Soluble

[a] $\cdot x H_2O$, x = 14-15; [b] $x H_2O$, x = 4-8; [c] Perfluorohexanes. [d] Perfluoro-(2-butyltetrahydrofuran); [e] Perfluoro(methylcyclohexane)

8.2.2. Syntheses of BAr_{f6} Salts of Werner Complexes

As shown in Scheme 8.3 (top) and the photographs in Figure 8.2, a yellow aqueous solution of the racemic trichloride salt Δ-$[Co(en)_3]^{3+}$ $3Cl^-{\cdot}2.5H_2O$[19] and a colorless perfluoro(methylcyclohexane) (PFMC) solution of Na^+ BAr_{f6}^- (**28**) were combined (1:3 mol ratio) and stirred. The lower PFMC phase turned yellow, and the upper aqueous phase decolorized. This suggested the complete transfer of the trication $[Co(en)_3]^{3+}$ into the fluorous phase. The phases were separated and the PFMC was removed. This gave the new, anion exchanged salt $[Co(en)_3]^{3+}$ $3BAr_{f6}^-{\cdot}xH_2O$ (**31**$\cdot xH_2O$) as an orange oil in 96% yield, which was characterized by NMR (^1H, ^{13}C) and elemental analysis (experimental section). In multiple runs, **31** was reproducibly isolated with 14-15 (x) water molecules of hydration, as assayed by ^1H NMR integrals and supported by microanalyses. In other studies,[4,20] such tris(diamine) trications have been shown to be superb hydrogen bond donors.

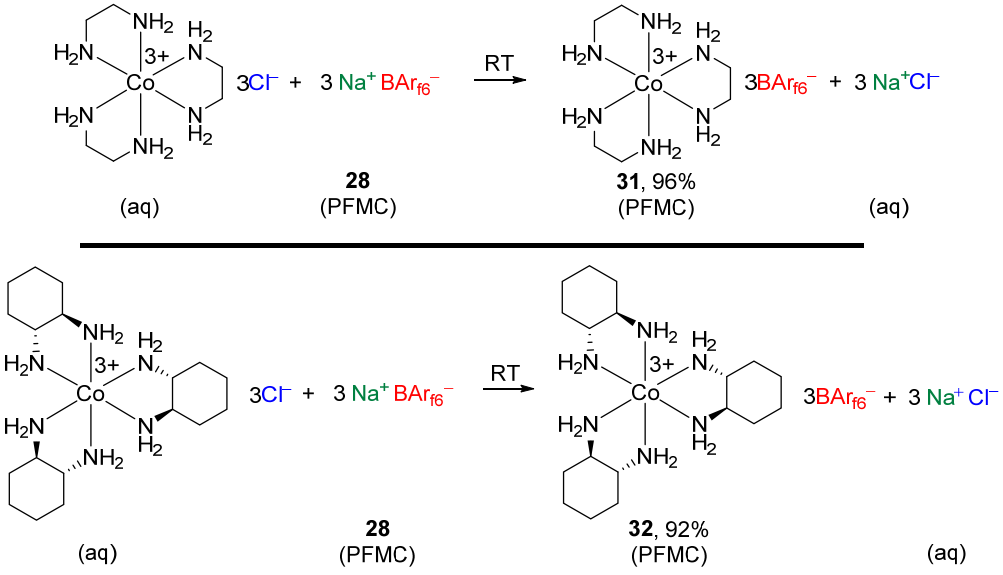

Scheme 8.3. Syntheses of fluorous BAr_{f6} salts of Werner trications.

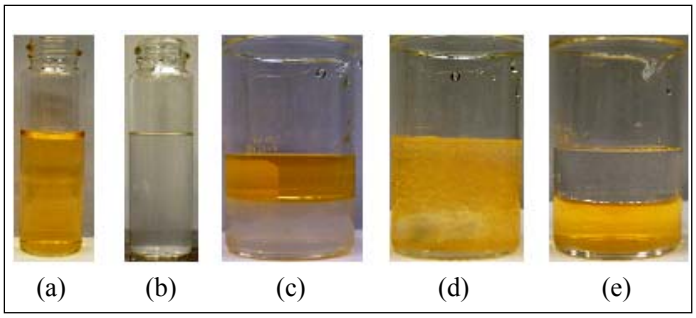

Figure 8.2. (a) 2.1×10^{-3} M aqueous solution of $[Co(en)_3]^{3+}$ $3Cl^-$ (10 mL). (b) 6.3×10^{-3} M Na^+ BAr_{f6}^- solution in PFMC (10 mL). (c) Biphasic mixture after gentle addition of (b) to (a). (d) The sample from (c) was stirred (10 min). (e) The sample from (d) after stirring was halted.

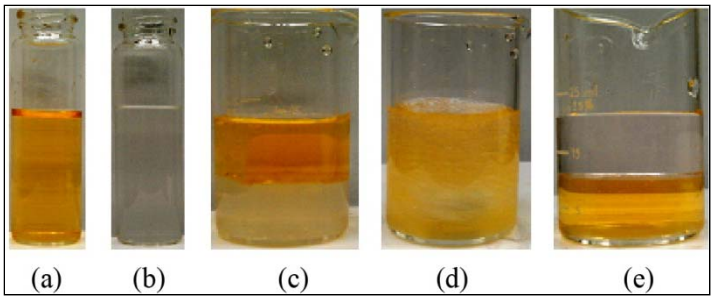

Figure 8.3. (a) 2.1×10^{-3} M aqueous solution of $[Co(R,R\text{-chxn})_3]^{3+}$ $3Cl^-$ (10 mL). (b) 6.3×10^{-3} M Na^+ BAr_{f6}^- solution in PFMC (10 mL). (c) Biphasic mixture after gentle addition of (b) to (a). (d) The sample from (c) was stirred (10 min). (e) The sample from (d) after stirring was halted.

This protocol was extended to a related cobalt complex with somewhat more lipophilic and enantiopure *trans*-1,2-cyclohexanediamine or *R,R*-chxn ligands. As shown in Scheme 8.3 (bottom) and the photographs in Figure 8.3, an aqueous solution of the previously reported salt $[Co(R,R\text{-chxn})_3]^{3+}$ $3Cl^- \cdot 4H_2O$[21] was treated with a PFMC solution of Na^+ BAr_{f6}^- The aqueous phase decolorized and the cobalt trication transferred to the fluorous phase. An identical workup gave $[Co(R,R\text{-chxn})_3]^{3+}$ $3BAr_{f6}^- \cdot xH_2O$ **(32**$\cdot xH_2O$**)** in 92% yield, which in multiple runs was isolated as a tetrahydrate to octahydrate (x = 4-8). It was observed that both the starting material and product exhibit

three chxn ^{13}C NMR signals, strongly suggestive of a single diastereomer (chirality at cobalt). In previous work (lacking ^{13}C NMR data), the Δ or Δ-*lel*$_3$ isomer has been shown to be considerably more stable.[21b]

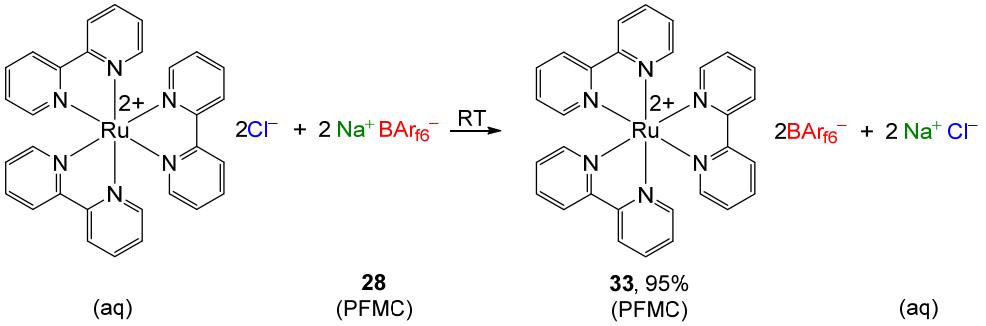

Scheme 8.4. Synthesis of a fluorous BAr$_{f6}$ salt of the dication [Ru(bipy)$_3$]$^{2+}$.

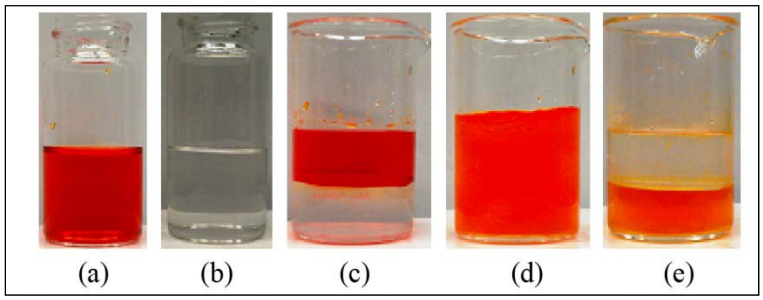

Figure 8.4. (a) 2.1 × 10^{-3} M aqueous solution of [Ru(bipy)$_3$]$^{2+}$ 2Cl$^-$·6H$_2$O (10 mL). (b) 4.20 × 10^{-3} M Na$^+$ BAr$_{f6}$$^-$ solution in PFMC (10 mL). (c) Biphasic mixture after gentle addition of (b) to (a). (d) The sample from (c) was stirred (10 min). (e) The sample from (d) after stirring was halted.

Finally, to confirm the generality of these phase transfer phenomena, a comparable protocol was applied to the classic ruthenium dication, [Ru(bipy)$_3$]$^{2+}$.[13] As shown in Scheme 8.4 and the photographs in Figure 8.4, an aqueous solution of racemic [Ru(bipy)$_3$]$^{2+}$ 2Cl$^-$·6H$_2$O[22] was treated with a PFMC solution of Na$^+$ BAr$_{f6}$$^-$ (1:2 mol ratio). The lower PFMC phase turned red, and the upper aqueous phase decolorized. An identical workup gave [Ru(bipy)$_3$]$^{2+}$ 2BAr$_{f6}$$^-$·*x*H$_2$O (**33**·*x*H$_2$O) as a sticky red oil in

95% yield, which was characterized by NMR (^{1}H, ^{13}C) and elemental analysis (experimental section). The latter was best fit by a hemihydrate (x = 0.5), in agreement with the ^{1}H NMR integral.

8.2.3. Additional Physical Characterization of Werner Complexes

The fluorophilicities of substances can be quantified by partition coefficients.[23] These are frequently determined using the biphasic system toluene/PFMC. For example, the lipophilic alkanes *n*-decane through *n*-hexadecane exhibit partition coefficients of 94.6:5.4 to 98.9:1.1.[23] For this study, data for water/PFMC mixtures were also sought, given the solvents employed in Schemes 8.3-8.4 and Figures 8.2-8.4. Partition coefficients were assayed by ^{19}F NMR and UV-vis spectroscopy, as described in the experimental section. The ^{19}F NMR data are summarized in Table 8.3, and the UV/vis data were in good agreement.

Table 8.3. Partition coefficients measured by ^{19}F NMR (24 °C).

Compound	Biphasic System	Partition Coefficients
Na^+ BAr_{f6}^- (**28**)[a]	Water/PFMC	0.2:99.8
	Toluene/PFMC	1:99
Na^+ BAr_{f6}^-[b]	CH_2Cl_2/PFMC	>99.9:<0.1
31[c]	Water/PFMC	<1:>99
	Toluene/PFMC	<0.1:>99.9
$[Co(en)_3]^{3+}$ $3BAr_{f6}^-$[d]	CH_2Cl_2/PFMC	>99.9:<0.1
32[e]	Water/PFMC	<1:>99
	Toluene/PFMC	<0.1:>99.9
33[f]	Water/PFMC	1:99
	Toluene/PFMC	1:99

[a] $2.5H_2O$; [b] $2H_2O$; [c] xH_2O, x = 14-15; [d] $7H_2O$; [e] xH_2O, x = 4-8; [f] xH_2O, x = 0.5-2.0.

The toluene/PFMC partition coefficients of the precursor salt Na^+ BAr_{f6}^- (**28**) and the tricationic cobalt salt $[Co(en)_3]^{3+}$ $3BAr_{f6}^-$ (**31**) were 1:99 and <0.1:>99.9, respectively. The 1,2-cyclohexanediamine analog **32** exhibited a comparable fluorophilicity, at least within the limits of the assay method. The dicationic ruthenium salt **33** appeared to be slightly less fluorophilic than the cobalt complexes (1:99). In a control experiment, it was verified that the non-fluorous analog of **28**, Na^+ BAr_f^-, exhibited a CH_2Cl_2/PFMC partition coefficient of >99.9:<0.1. The non-fluorous analog of **31**, $[Co(en)_3]^{3+}$ $3BAr_f^-$, behaved similarly (neither of these salts are soluble in toluene). None of the salts exhibited an appreciable absolute solubility in water, although from a partitioning standpoint water seemed to be a slightly better solvent than toluene.

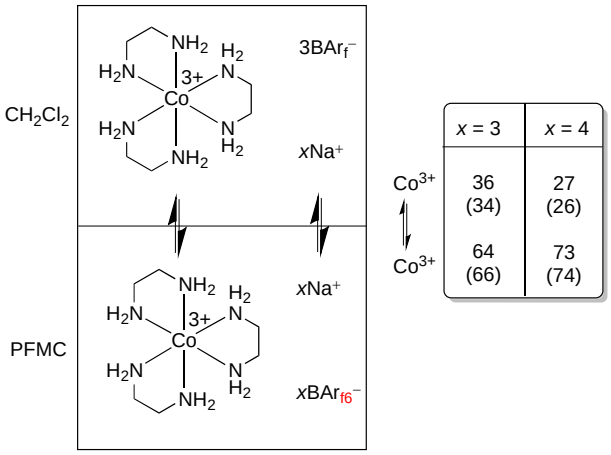

Scheme 8.5. Partitioning of $[Co(en)_3]^{3+}$ between a CH_2Cl_2 solution of $3BAr_f^-$ and a PFMC solution of $xBAr_{f6}^-$ in the presence of xNa^+ (x = 3, 4) as determined by ^1H NMR and UV-vis spectroscopy (unbracketed and bracketed values).

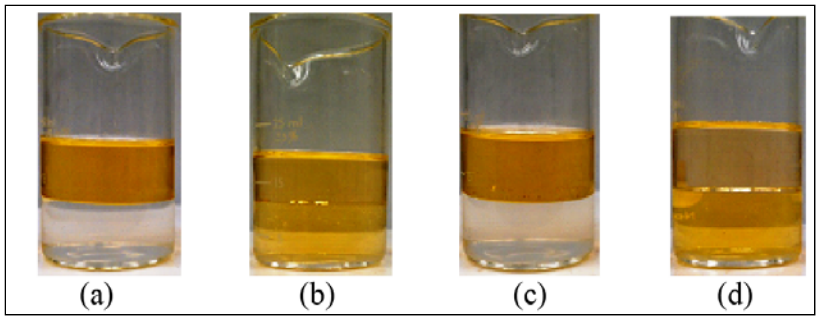

Figure 8.5. (a) Biphasic mixture after gentle addition of a 1.74×10^{-3} M CH_2Cl_2 solution of $[Co(en)_3]^{3+}$ $3BAr_f^-$ (10 mL, upper layer) to a 5.22×10^{-3} M PFMC solution of Na^+ BAr_{f6}^- (10 mL, bottom layer). (b) The sample from (a) after stirring was halted. (c) Biphasic mixture after gentle addition of a 1.74×10^{-3} M CH_2Cl_2 solution of $[Co(en)_3]^{3+}$ $3BAr_f^-$ (10 mL, upper layer) to a 6.96×10^{-3} M PFMC solution of Na^+ BAr_{f6}^- (10 mL, bottom layer). (d) The sample from (c) after stirring was halted.

A final question involves how the cobalt trication $[Co(en)_3]^{3+}$ would partition between organic and fluorous phases in the presence of both the non-fluorous and fluorous anions BAr_f^- and BAr_{f6}^-. In other words, would this species prefer fluorous or non-fluorous environs? Of course, a second cation is required to set up the equilibrium. Hence, the result will reflect the weighted partitioning preference of both species. As shown in Scheme 8.5 and Figure 8.5, equal volumes of CH_2Cl_2 and PFMC were charged with the non-fluorous salt $[Co(en)_3]^{3+}$ $3BAr_f^-$ and 3.0 equiv of the fluorous sodium salt Na^+ BAr_{f6}^-, respectively. The trication $[Co(en)_3]^{3+}$ partitioned predominantly into the fluorous phase (64:36), as assayed by ^1H NMR. By inference, the sodium monocation partitioned predominantly into the more polar organic phase. When an analogous experiment was carried out with 4.0 equiv of Na^+ BAr_{f6}^-, the $[Co(en)_3]^{3+}$ concentration ratio increased to 73:27. Similar data were obtained by UV-vis spectroscopy.

Given the great interest in the photophysical properties of the ruthenium dication $[Ru(bipy)_3]^{2+}$,[13] the UV-vis spectrum of **33** was measured in PFMC. A strong UV absorption tailed into the visible region, which exhibited a characteristic band at 446 nm

(ε 15310 $M^{-1}cm^{-1}$). This λ_{max} is slightly lower than that that found for other salts of $[Ru(bipy)_3]^{2+}$ in aqueous and organic solutions (average ca. 450 nm),[13a] as well as another fluorous salt described in the discussion section.[24] When the PFMC solution of **33** was irradiated at 446 nm, the fluorescence spectrum exhibited a λ_{max} at 594 nm. This Stokes shift (148 nm) is to my knowledge the largest observed for a $[Ru(bipy)_3]^{2+}$ salt to date,[13a,24] and is consistent with the non-polar fluorous medium destabilizing the more polar excited state to a greater extent than the less polar ground state.

8.3. Discussion

The preceding results, together with other recently reported data,[6] establish that it is possible to selectively solubilize tris(1,2-diamine) cobalt trications in aqueous, organic, and fluorous solvents depending upon the counteranion selected. Similar results can be expected with a variety of other tris(diamine) Werner complexes, which are generally di- to tetracations derived from middle to late transition metals.[25] Thus, chemistry that has been largely limited to aqueous solutions for over a century can now be explored in less polar media that allow a much broader range of solutes.

For example, Table 8.2 shows that the fluorous Werner salts **31** and **32** are soluble in the usual fluorous (FC-72, FC-75, PFMC) and hybrid ($C_6H_5CF_3$) solvents, as well as a range of more polar organic solvents (acetone, Et_2O, CH_3OH, CH_2Cl_2, ethyl acetate). Thus, it is now possible to employ them as homogeneous catalysts in organic and fluorous media. Furthermore, Table 8.3 establishes that these salts markedly prefer to partition into fluorous over organic solvents (PFMC vs. toluene). Hence, it should prove possible to extract, recover, and recycle such salts using fluorous solvents or supports.

In this context, it has been found that the non-fluorous Werner salt $[Co(en)_3]^{3+}$ $3BAr_f^-$ catalyzes the Michael additions of malonates to enones in the presence of tertiary

amines.[4a,7] The trication is believed to function as a "second" coordination sphere chiral hydrogen bond donor towards the enone, activating it towards addition. Although enantioselectivities are modest (up to 33% ee), two classes of newer generation catalysts have recently been developed that afford Michael adducts with 80-95% ee.[4b-e] Obviously, fluorous analogs could have attractive features, and catalysis data will be reported in due course.

Important related work of Vincent deserves emphasis.[24] He first prepared a salt of the ruthenium dication $[Ru(bipy)_3]^{2+}$ with fluorous carboxylate anions, $[Ru(bipy)_3](O_2CCF(CF_3)(OCF_2CF(CF_3))_3OCF_2CF_2CF_3)_2$ (**34**). When taken up in CH_2Cl_2/perfluorodecalin mixtures, **34** partitioned exclusively into the organic phase. However, when two equivalents of the carboxylic acid $HO_2CCF(CF_3)(OCF_2CF(CF_3))_3OCF_2CF_2CF_3)_2$ were added, the ruthenium was found exclusively in the fluorous phase. This was attributed to the generation of the salt **35** (Figure 8.6), which features

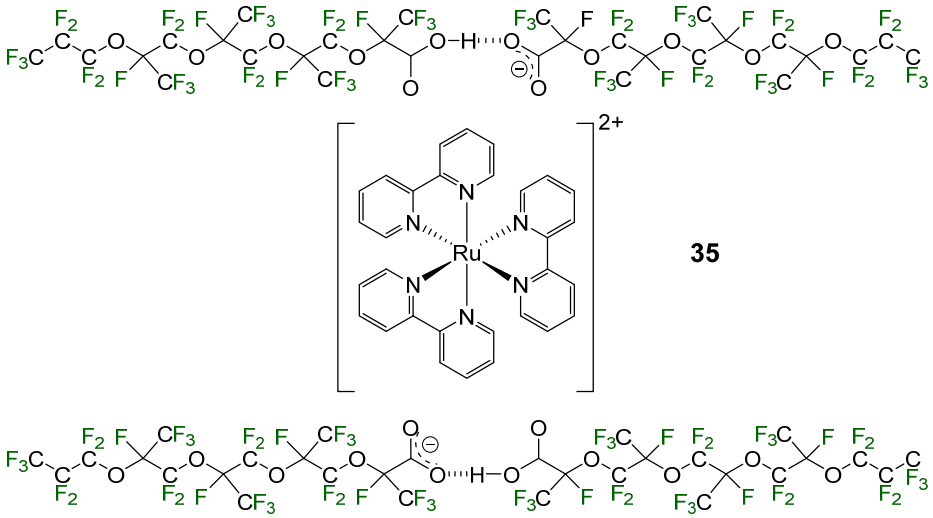

Figure 8.6. A fluorophilic salt of $[Ru(bipy)_3]^{2+}$ prepared by Vincent.

two much more fluorophilic monoanions derived from hydrogen bonded carboxylate ions and carboxylic acids. It should be noted in passing that it is also possible to solubilize poly*anions* – even dodecaanions – in fluorous media with suitable fluorous *cations*.[26]

The UV-vis spectrum of **35** exhibited a band at 450 nm (perfluorodecalin; ε 14100 M^{-1} cm^{-1}), a very slightly longer wavelength than my fluorophilic analog **33** (Scheme 8.4; 446 nm and ε 15300). In contrast, the λ_{max} in the fluorescence spectrum of **35** was at a somewhat shorter wavelength (585 vs. 594 nm), making for a slightly reduced Stokes shift (135 vs. 148 nm), suggestive of a marginally more polar environment. Salts of $[Ru(bipy)_3]^{2+}$ mediate a number of photochemically triggered processes with a range of substrates.[13,27] There would seem to be possibilities for new selectivities or chemistries in fluorous media, for example due to the much higher solubilities of small gaseous molecules as compared to aqueous media.[28] Vincent established that **35** is an efficient photosensitizer for singlet oxygen, and observed enhanced $^1O_2$ lifetimes.

Additional features of the crystal structure of bromoarene **29** (Figure 8.1) merit analysis. First, as noted in Table 8.1, **29** crystallizes in a chiral, polar space group (*I*4) as a tetragonal crystal system with α, ß, and γ equal to 90°. As represented in Figure 8.7 (top), the unit cell dimensions are markedly skewed, with *a* and *b* equal to 29.5335(13) Å and *c* being >80% less at 5.5624(3) Å. The perfluorohexyl groups associated with the eight molecules in the unit cell lie *roughly* in a plane defined by the *a*/*b* axes. They exhibit C-C-C-C and F-C-C-F torsion angles characteristic of perfluoroalkyl groups, with the values for *anti* segments distinctly less than 180° (165.8(3.4)° and 164.3(1.8)°, respectiveely).[29] They also segregate, as found for most fluorous molecules, into fluorous domains.[29]

Consider next the eight aryl rings. Figure 8.7 shows that (1) they are oriented distinctly out of the plane defined by the *a*/*b* axes, with plane/plane angles of 48.1°, and (2) all of the bromine atoms are found on the same "side" or *a*/*b* face of the unit cell.

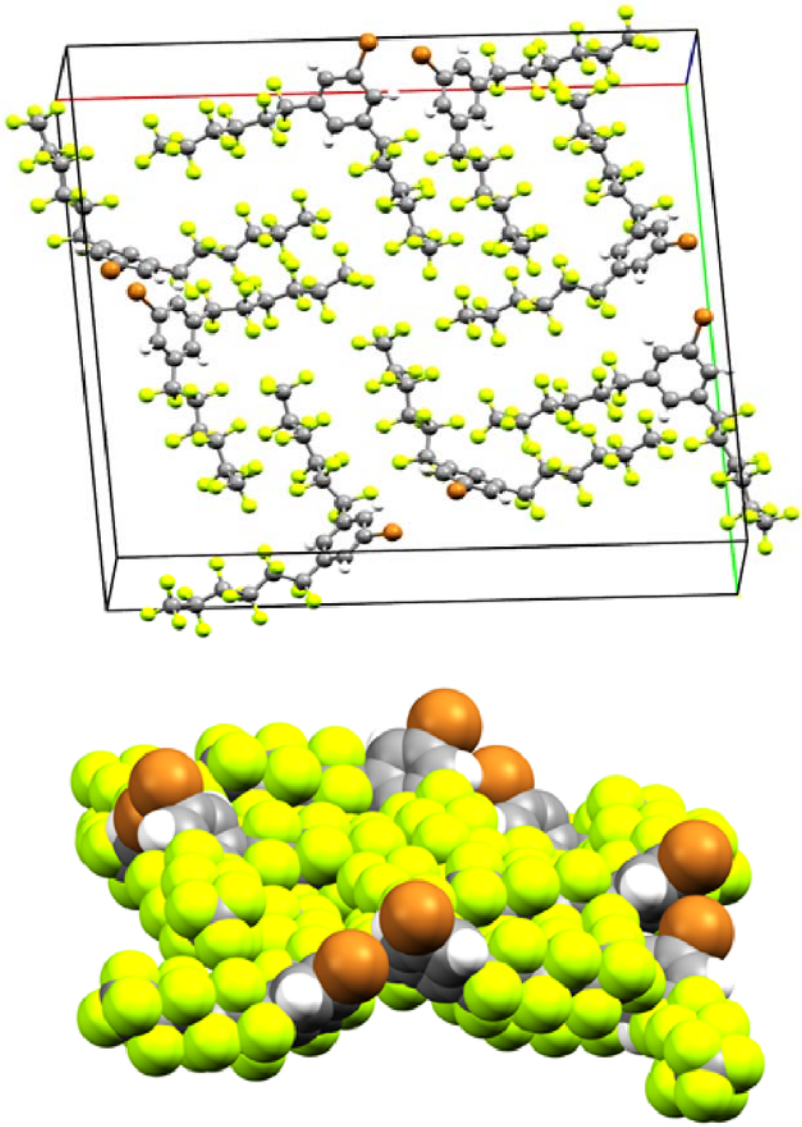

Figure 8.7. Packing of **29** in the unit cell (Z = 8). Top: ball and stick representation; bottom: space filling representation.

The bromine atoms from one unit cell nest approximately into the centroids of the arene rings of the adjacent unit cell (*c* direction), with bromine-centroid and centroid-centroid distances of 3.850 Å and 5.562 Å, respectively. The planes of the nesting rings are parallel, with separations of 3.71 Å.

The features in the preceding paragraph are manifestations of the polar nature of the crystal. Such crystals are sometimes observed to give non-linear optical phenomena such as frequency doubling.[30,31] However, when a powdered sample of **29** is irradiated with a Nd:YAG laser (1064 nm; "Kurtz test"[32]), no detectable visible light is scattered. Crystals of **29** are highly piezoelectric (qualitative plastic comb test), and the space group (*I*4) is one of ten that can exhibit spontaneous polarization without mechanical stress.[31]

8.4. Summary

In summary, this study has extended previous efforts in bringing the chemistry of Werner cations from aqueous solutions into the full spectrum of modern liquid phases. Towards this end, an improved, scalable synthesis of Na^+ BAr_{f6}^- (**28**), a sodium salt of a highly fluorophilic anion, has been developed. Based upon the successful demonstration with the salts **31**-**33**, it can be anticipated that metal polycations can generally be solubilized in fluorous phases with the anion BAr_{f6}^-. The toluene/PFMC partition coefficients establish very high fluorophilicities ($\leq$1:$\geq$99) and provide a valuable foundation for the design of future applications. Finally, an intermediate in the synthesis of **28**, the fluorous bromoarene **29**, crystallizes in an uncommon polar space group and exhibits a range of interesting properties.

8.5. Experimental section

General data: NMR spectra were recorded on a Varian 500 MHz spectrometer at ambient probe temperatures and referenced as follows: ^{1}H: residual internal $CHCl_3$ (δ, 7.26 ppm), acetone-d_5 (2.05 ppm), or CHD_2CN (1.94 ppm); ^{13}C: internal acetone-d_6 (29.8 ppm), $CDCl_3$ (77.0 ppm), or CD_3CN (1.3 ppm). UV-visible spectra were recorded on a Shimadzu UV-1800 spectrometer. Emission spectra were recorded on a PTI QuantaMaster spectrofluorimeter. Microanalyses were conducted by Atlantic Microlab.

All reactions were carried out under air unless noted. All workups were carried out in air. Chemicals were treated as follows: Et_2O (Fisher Scientific), dried and degassed using a Glass Contour solvent purification system; copper (100 mesh 99.5%, Alfa Aesar), perfluorohexyliodide ($R_{f6}I$; SynQuest Labs, 98%), C_6F_6 (TCI, 99%), 1,3-diiodobenzene (Alfa Aesar, 98%), NBS (Alfa Aesar, 99%), H_2SO_4 (EDM, 95%), CF_3CO_2H (Alfa Aesar, 99.5%), *t*-BuLi (Alfa Aesar, 1.70 M in pentane), BCl_3 (Acros, 1.00 M in hexane), NaCl (EDM, 98%), NaOH (Mallinckrodt), FC-75 (perfluoro(2-butyltetrahydrofuran); Alfa Aeser, 99%), FC-72 (perfluorohexanes; Apollo Scientific, 98%), PFMC (perfluoro(methylcyclohexane); Alfa Aesar, 94%), $CDCl_3$, CD_3CN, and acetone-d_6 (3 × Cambridge Isotope Laboratories), CF_3CH_2OH (Sigma-Aldrich, ≥99%), $C_6H_5CF_3$ (Acros, 99%), silica (Acros, 60 Å), CH_2Cl_2 (EMD Chemicals), hexanes (Macron Chemicals), cyclohexane (Fisher Scientific, 99.4%), CH_3OH, benzene (2 × BDH, 99.8%), DMSO (Fisher Scientific, 99.9%), ethyl acetate (Macron Chemicals, 99.5%), and toluene (Mallinckrodt, 98%), used as received.

1,3-$C_6H_4(R_{f6})_2$ (30).[10] An oven dried Schlenk tube was charged with copper (7.02 g, 110 mmol), 1,3-diiodobenzene (7.09 g, 21.5 mmol), and DMSO (60 mL) with stirring under N_2. Then perfluorohexyliodide ($R_{f6}I$; 10.2 mL, 47.1 mmol) was added dropwise over 5 min. The tube was sealed and kept at 140 °C (with stirring). After 3 d,

the mixture was cooled to room temperature, and water (100 mL) was added. Some solid precipitated. The mixture was transferred to a separatory funnel and extracted with CH_2Cl_2 (3 × 150 mL; most of the solid was retained on the sides of the funnel). The combined extracts were filtered, washed with water (100 mL) and then brine (100 mL), and dried (Na_2SO_4). The solvent was removed by rotary evaporation. The yellow oil was dissolved in FC-72 (15 mL), which was washed with acetone (2 × 20 mL; separatory funnel). The solvent was removed from the fluorous phase by rotary evaporation to give **30** as a light yellow oil (13.27 g, 18.58 mmol, 86%), the properties of which agreed with those previously reported.[10] ^{1}H NMR (δ (ppm), 500 MHz, $CDCl_3$ or $C_6F_6/CDCl_3$ mixture): 7.83 or 7.89 (s, 1H, doubly *o* to R_{f6}), 7.82 or 7.88 (s, 2H, singly *o* to R_{f6}), 7.69 or 7.78 (m, 1H, doubly *m* to R_{f6}).

Br(3,5-$C_6H_3(R_{f6})_2$) (29).[10,14] A round-bottomed flask was charged with **30** (11.4 g, 16.0 mmol). A mixture of H_2SO_4 (13.0 mL) and CF_3CO_2H (34.0 mL) was added with stirring. Then solid NBS (4.42 g, 24.8 mmol) was added over the course of 6 h (one portion/h). After an additional 48 h (with stirring), the mixture was poured into a beaker of ice (300 g). Aqueous NaOH was added dropwise until a pH of 7-9 was reached. The mixture was extracted with CH_2Cl_2 (3 × 200 mL; separatory funnel). The combined extracts were dried (Na_2SO_4). The solvent was removed by rotary evaporation to give **29** as a white solid (11.23 g, 14.14 mmol, 88%), mp 44-42 °C, which was pure by GLC (Shimadzu SHRXI-5MS column) and which had previously been characterized as a mixture by a related route[10] and a pure compound by a different route.[14] ^{1}H NMR (δ (ppm), 500 MHz, $CDCl_3$ or $C_6F_6/CDCl_3$ mixture): 7.96 or 8.02 (s, 2H, *o*-BrC_6H_3), 7.74 or 7.84 (s, 1H, *p*-BrC_6H_3). $^{13}C\{^1H,^{19}F\}$ NMR (δ (ppm), 125 MHz, $CDCl_3$): 133.6 (s), 131.7 (s), 124.3 (s), 123.4 (s), 117.1 (s), 114.6 (s), 111.1 (s), 110.5 (s), 110.2 (s), 108.4 (s). UV-vis (nm, 1.94×10^{-3} M in PFMC (ε, $M^{-1}cm^{-1}$)): 274 (995), 281 (969).

Na^+ $B(3,5\text{-}C_6H_3(R_{f6})_2)_4^-$ (28; **Na^+ BAr_{f6}^-**).[10,11] A Schlenk flask was charged with **29** (3.70 g, 4.64 mmol) and Et_2O (170 mL) under a positive N_2 pressure and transferred to a –78 °C cold bath. After 20 min, *t*-BuLi (1.70 M in pentane; 6.00 mL, 10.2 mmol) was added dropwise over 10 min with stirring. After an additional hour, BCl_3 (1.00 M in hexane, 1.00 mL, 1.00 mmol) was added. After an additional 2 h, the cold bath was removed. After 2-3 h, the solution was poured into water (200 mL), which was saturated with NaCl with stirring. The mixture was extracted with Et_2O (3 × 150 mL). The combined extracts were dried ($MgSO_4$). The solvent was removed by rotary evaporation. The brown oil was chromatographed on a silica gel column (3 × 16 cm) packed in hexanes. The column was eluted with Et_2O, and a brown band was collected. The column was then eluted with CH_2Cl_2/CH_3OH (98:2 to 80:20 v/v). The fractions were monitored by tlc. The product containing fractions were combined and the solvent was removed by rotary evaporation. The off white solid was recrystallized from FC-75 and the white solid was dried by oil pump vacuum to give **28**·$2.5H_2O$ as a white solid (2.26 g, 0.771 mmol, 76%), mp 89-86 °C, the properties of which agreed with those previously reported.[10,11] ^1H NMR (δ (ppm), 500 MHz, acetone-d_6): 7.71 (s, 8H, *o*-BC_6H_3), 7.58 (s, 4H, *p*-BC_6H_3), 2.86-2.82 (m, 5H, H_2O). $^{13}C\{^1H,^{19}F\}$ NMR (δ (ppm), 125 MHz, acetone-d_6):[33] 161.8 (q, $^1J_{BC}$ = 50.0 Hz, *i*-BC_6H_3), 137.5 (s, *o*-BC_6H_3), 128.2 (s, *m*-BC_6H_3), 121.4 (s, *p*-BC_6H_3), 118.1 (s, CF_3), 116.8 (s, BCC$\underline{C}F_2$), 112.1 (s, CF_2), 111.8 (s, CF_2), 111.2 (s, CF_2), 109.3 (s, CF_2). Anal. Calcd for $C_{72}H_{12}BF_{104}Na$·$2.5H_2O$: C, 29.50; H, 0.58; F, 67.40. Found: C, 29.23; H, 0.49; F, 67.50.

$[Co(en)_3]^{3+}$ $3BAr_{f6}^-$ (31). A beaker was charged with a solution of **28**·$2.5H_2O$ in PFMC (0.0063 M; 10.0 mL, 0.0630 mmol). An aqueous solution of $[Co(en)_3]^{3+}$ $3Cl^-$ ·$2.5H_2O$ (0.0021 M; 10.0 mL, 0.0210 mmol)[19] was added. The biphasic mixture was vigorously stirred for 10 min. Stirring was halted, and the lower fluorous phase was

separated and dried ($MgSO_4$). The solvent was removed by rotary evaporation and oil pump vacuum to give **31**·$x$$H_2O$ (x = 14-15**)** as an orange oil (0.0183 g, 0.020 mmol, 96%). ^{1}H NMR (δ (ppm), 500 MHz, acetone-d_6): 7.71 (s, 24H, o-BC_6H_3), 7.58 (s, 12H, p-BC_6H_3), 5.70 (br s, 6H,[34] N*H*H'), 5.29 (br s, 6H,[34] NH*H*'), 3.31 (br s, 12H, CH_2), 2.83 (s, 28-30H, H_2O). ^{13}C{^{1}H,^{19}F} NMR (δ (ppm), 125 MHz, acetone-d_6):[33] 161.9 (q, $^1J_{BC}$ = 50.0 Hz, i-BC_6H_3), 137.5 (s, o-BC_6H_3), 128.3 (s, m-BC_6H_3), 121.4 (s, p-BC_6H_3), 118.1 (s, CF_3), 116.8 (s, BCC*C*F_2), 112.1 (s, CF_2), 111.8 (s, CF_2), 111.2 (s, CF_2), 109.3 (s, CF_2), 46.2 (s, CH_2). Anal. Calcd for $C_{222}H_{60}CoB_3F_{312}N_6$·$14.5H_2O$: C, 29.33; H, 0.99; N, 0.92; F, 65.20. Found: C, 29.43; H, 0.91; N, 0.88; F, 64.63.[35]

[Co(*R,R*-chxn)$_3$]$^{3+}$ 3BAr$_{f6}^-$ (32). A beaker was charged with a solution of **28** in PFMC (0.0063 M; 10.0 mL, 0.0630 mmol). Then an aqueous solution of [Co(*R,R*-chxn)$_3$]$^{3+}$ $3Cl^-$·$4H_2O$ (0.0021 M; 10.0 mL, 0.0210 mmol)[6,21] was added. The biphasic mixture was vigorously stirred for 10 min. Stirring was halted, and the lower fluorous phase was separated and dried ($MgSO_4$). The solvent was removed by rotary evaporation and oil pump vacuum to give **32**·$x$$H_2O$ (x = 4-8) as an orange oil (0.175 g, 0.019 mmol, 92%). ^{1}H NMR (δ (ppm), 500 MHz, acetone-d_6): 7.70 (s, 24H, o-BC_6H_3), 7.57 (s, 12H, p-BC_6H_3), 5.53 (br s, 4H,[34] N*H*H'), 5.16 (br s, 4H, NH*H*'), 3.00 (br s, 6H, CHN), 2.84 (s, 8-16H, H_2O), 2.35 (m, 6H of $(CH_2)_4$), 1.74 (m, 6H of $(CH_2)_4$), 1.62 (m, 6H of $(CH_2)_4$), 1.22 (m, 6H of $(CH_2)_4$). ^{13}C{^{1}H,^{19}F} NMR (δ (ppm), 125 MHz, acetone-d_6):[33] 161.8 (q, $^1J_{BC}$ = 50 Hz, i-BC_6H_3), 137.5 (s, o-BC_6H_3), 128.3 (s, m-BC_6H_3), 121.4 (s, p-BC_6H_3), 118.1 (s, CF_3), 116.8 (s, BCC*C*F_2), 112.1 (s, CF_2), 111.8 (s, CF_2), 111.2 (s, CF_2), 109.3 (s, CF_2), 61.5 (s, C*H*NH_2), 33.6 (s, CH_2), 24.6 (s, CH_2). Anal. Calcd for $C_{234}H_{78}CoB_3F_{312}N_6$· $4H_2O$: C, 31.01; H, 0.96; N, 0.93; F, 65.40. Found: C, 31.05; H, 0.86; N, 0.95; F, 63.97.[35]

[Ru(bipy)$_3$]$^{2+}$ 2BAr$_{f6}^-$ (33). A beaker was charged with a solution of **28** in

PFMC (0.0130 M; 10.0 mL, 0.13 mmol). Then an aqueous solution of $[Ru(bipy)_3]^{2+}$ $2Cl^{-}\cdot 6H_2O$ (0.00650 M, 10.0 mL, 0.065 mmol)[21] was added. The biphasic mixture was vigorously stirred for 10 min. Stirring was halted, and the lower fluorous phase was separated and dried ($MgSO_4$). The solvent was removed by rotary evaporation and oil pump vacuum to give **33**$\cdot x H_2O$ (x = 0.5-2.0) as a sticky red oil (0.391 g, 0.062 mmol, 95%). ^{1}H NMR (δ (ppm), 500 MHz, acetone-d_6): 8.86 (d, J = 10.0 Hz, 6H of 3bipy), 8.24 (t, J = 7.50 Hz, 6H of 3bipy), 8.10 (d, J = 5.00 Hz, 6H of 3bipy), 7.72 (s, 16H, o-BC_6H_3), 7.61 (m, 6H of 3bipy), 7.58 (s, 8H, p-BC_6H_3), 2.81 (m, 1-4H, H_2O). $^{13}C\{^1H,^{19}F\}$ NMR (δ (ppm), 125 MHz, acetone-d_6): 161.5 (q, $^1J_{BC}$ = 50 Hz, i-BC_6H_3)), 158.2 (s), 152.7 (s), 139.0 (s), 137.5 (s), 128.8 (s), 128.2 (s), 125.3 (s), 121.4 (s), 118.1 (s, CF_3), 116.8 (s), 112.0 (s), 111.8 (s), 111.2 (s), 109.3 (s). UV-vis (nm, 6.77×10^{-5} M in PFMC (ε, $M^{-1}cm^{-1}$)): 446 (15300). Fluorescence (nm, 3.05×10^{-6} M in PFMC, λ_{ex} = 446 nm): 594. Anal. Calcd for $C_{174}H_{48}RuB_2F_{208}N_6\cdot 0.5H_2O$: C, 33.14; H, 0.78; N, 1.33; F, 62.66. Found: C, 33.08; H, 0.68; N, 1.42; F, 59.80.[35]

$[Co(en)_3]^{3+}$ $3BAr_f^-$.[36] A beaker was charged with a solution of Na^+ BAr_f^- $\cdot 2H_2O$ (0.510 g, 0.557 mmol)[37] in CH_2Cl_2 (20 mL). Then a solution of racemic $[Co(en)_3]^{3+}$ $3Cl^-$ $\cdot 2.5H_2O$ (0.073 g, 0.186 mmol)[19] in water (20 mL) was added. The heterogeneous mixture was vigorously stirred for 15 min. The orange CH_2Cl_2 phase was separated from the colorless aqueous phase. The CH_2Cl_2 was allowed to evaporate in a fume hood overnight to give $[Co(en)_3]^{3+}$ $3BAr_f^-\cdot 7H_2O$ as an orange powder (0.514 g, 0.173 mmol, 93%).[38] ^{1}H NMR (δ (ppm), 500 MHz, CD_3CN): 7.70 (m,[39] 24H, o-BC_6H_3), 7.67 (s, 12H, p-BC_6H_3), 4.20 (br s, 6H, N*H*H'), 3.76 (br s, 4H, NH*H'*), 2.75 (br s, 6H, C*H*H'), 2.70 (br s, 6H, CH*H'*), 2.27 (s, 14H, H_2O). $^{13}C\{^1H\}$ NMR (δ (ppm), 125 MHz, CD_3CN):[40] 162.6 (q, $^1J_{BC}$ = 50.0 Hz, i-BC_6H_3), 135.7 (s, o-BC_6H_3), 130.1 (q, $^2J_{CF}$ = 31.3 Hz, *C*CF_3), 125.5 (q, $^1J_{CF}$ = 270 Hz, CF_3), 118.7 (t, $^3J_{CF}$ = 3.8 Hz, p-

BC_6H_3), 45.6 (s, CNH_2). Anal. Calcd. for $C_{102}H_{60}B_3CoF_{72}N_6 \cdot 7H_2O$: C, 41.46; H, 2.52; N, 2.84. Found: C, 41.45; H, 2.54; N, 2.76.

Partition Coefficients. The following are representative. **A** (UV-vis). A standard solution of **28**·$2.5H_2O$ (0.0591 g, 0.0200 mmol) in PFMC (20.00 mL volumetric flask) was prepared (1.00×10^{-3} M). This was diluted in a series of volumetric flasks to give 6.25×10^{-5} M, 1.25×10^{-4} M, and 2.50×10^{-4} M solutions. The three solutions gave UV-vis absorbances (A, 271 nm) of 0.33450, 0.60840, and 1.2424, indicating good agreement with Beer's law and an extinction coefficient (ε) of 4968 $M^{-1}cm^{-1}$ (R = 0.999). **B**. A standard solution of $[Co(en)_3]^{3+}$ $3BAr_f^-\cdot 7H_2O$ (0.0503 g, 0.0170 mmol) in CH_2Cl_2 (10.00 mL volumetric flask) was prepared (1.70×10^{-3} M). This was diluted in a series of volumetric flasks to give 8.0×10^{-4} M, 1.2×10^{-3} M, and 1.70×10^{-3} M solutions. The three solutions gave UV-vis absorbances (A, 468 nm) of 0.0643, 0.1026, and 0.1423, indicating good agreement with Beer's law and an extinction coefficient (ε) of 82.99 $M^{-1}cm^{-1}$ (R = 0.998). **C** (partitioning, UV-vis). Water (4.0 mL) and a 1.00×10^{-3} M PFMC solution of **28**·$2.5H_2O$ (4.0 mL) were combined in a vial (20 mL) at room temperature (24 °C) and vigorously stirred (10 min). Stirring was halted. After 15 min, an aliquot (3.0 mL) was removed from the aqueous phase. An aliquot (0.50 mL) was removed from the PFMC phase and diluted to 2.0 mL. Aliquots were assayed by UV-vis, and the absorbances (0.02160 and 1.1735) indicated 4.30×10^{-6} M and 2.36×10^{-4} M concentrations, respectively (see data from **A**). This corresponds to a concentration ratio of $4.30 \times 10^{-6}/9.45 \times 10^{-4}$ (1.72×10^{-5} mmol of **28** in the aqueous phase and 3.8×10^{-3} mmol of **28** in the fluorous phase), or ca. 1:99 (Table 8.3). **D** (partitioning, NMR). A 20 mL vial was charged with a PFMC solution of **28**·$2.5H_2O$ (5.0×10^{-4} M, 4.0 mL) and toluene (4.0 mL), capped, and vigorously stirred. After 10 min at room temperature (24 °C), aliquots were removed from the fluorous (2.0 mL) and organic (2.0 mL) phases.

The solvent was evaporated from each, and the residues were dried under vacuum. A solution of $C_6H_5CF_3$ (internal standard; 0.020 mL) in acetone-d_6 (5.0 mL) was prepared. Each residue was dissolved in this solution and ^{19}F NMR spectra were recorded. The relative peak integrations gave the ratios in Table 8.3. For non-fluorous BAr_f, CF_3CH_2OH was used as the internal standard. **E**. A 30 mL beaker was charged with a PFMC solution of **28**·2.5H_2O (5.22×10^{-3} M, 10.0 mL, 0.0522 mmol) and a CH_2Cl_2 solution of $[Co(en)_3]^{3+}$ $3BAr_f^-\cdot 7H_2O$ (1.74×10^{-3} M, 10.0 mL, 0.0174 mmol). The mixture was vigorously stirred. After 10 min at room temperature (24 °C), aliquots were removed from the fluorous (7.0 mL) and organic (7.0 mL) phases. The solvent was evaporated from each, and the residues were dried by oil pump vacuum. A solution of cyclohexane (internal standard; 0.020 mL) in acetone-d_6/$C_6H_5CF_3$ (5.0 mL, 4:1 v/v) was prepared. Each residue was dissolved in this solution and ^1H NMR spectra were recorded. The relative peak integrations gave the ratios in Scheme 8.5. **F** (UV-vis). A beaker was charged with a solution of **28**·2.5 H_2O in PFMC (5.7×10^{-3} M; 6.0 mL, 0.0342 mmol) and a solution of $[Co(en)_3]^{3+}$ $3BAr_f^-\cdot 7H_2O$ (1.9×10^{-3} M, 6.0 mL, 0.0114 mmol) in CH_2Cl_2. The mixture was vigorously stirred. After 10 min at room temperature (24 °C), aliquots were removed from the organic (3.0 mL) and fluorous (3.0 mL) phases. These were assayed by UV-vis, and the absorbances (0.0520 and 0.1314) indicated 6.3×10^{-4} M (see data from **B**) and 1.21×10^{-3} M (see data from **A**) concentrations, respectively. This corresponds to a concentration ratio of $6.3 \times 10^{-4}/1.21 \times 10^{-3}$ (0.0038 mmol of $[Co(en)_3]^+$ in the CH_2Cl_2 phase and 0.0073 mmol of $[Co(en)_3]^+$ in the fluorous phase).

8.6. Crystallography.

A small vial was charged with **29** (0.025 g) and acetone-d_6 (0.15 mL), and the solution was kept at room temperature. After few days, colorless crystals had formed and

were analyzed as outlined in Table 8.1. Cell parameters were obtained from 180 data frames using a 0.5° scan.[41] No super-cell or erroneous reflections were observed. Integrated intensity information for each reflection was obtained by reduction of the data frames with the program APEX2.[42] Data were corrected for Lorentz and polarization factors, as well as for crystal decay and (using SADABS)[43] absorption effects. The space group was determined from systematic reflection conditions and statistical tests. The structure was solved by direct methods using SHELXTL (SHELXS).[44] The absence of additional symmetry was verified using PLATON (ADDSYM).[45] The hydrogen atoms were fixed in idealized positions using a riding model. Non-hydrogen atoms were refined with anisotropic thermal parameters. The parameters were refined by weighted least squares refinement on F^2 to convergence.[44,46] The absolute structure parameter was estimated as 0.00(9) (Table 8.1).[47]

CCDC 968151 contains the supplementary crystallographic data for this section. These data can be obtained free of charge from the Cambridge Crystallographic Data Centre via www.ccdc.cam.ac.uk/data_request/cif.

8.7. References

(1) Kauffman, G. B. *Coord. Chem. Rev.* **1974**, *12*, 105–149.

(2) (a) For the first enantiopure cobalt complex, see Werner, A. *Chem. Ber.* **1911**, *44*, 1887–1898. (b) For the first enantiopure $[Co(en)_3]^{3+}$ species, see Werner, A. *Chem. Ber.* **1912**, *45*, 121–130.

(3) Saito, Y. *Inorganic Molecular Dissymmetry*; Springer-Verlag: Berlin, 1979, Ch. IV.

(4) (a) Ganzmann, C.; Gladysz, J. A. *Chem. Eur. J.* **2008**, *14*, 5397–5400. (b) Lewis, K. G.; Ghosh, S. K.; Bhuvanesh, N.; Gladysz, J. A. *ACS Cent. Sci*. **2015**, *1*, 50-56. (c) Ghosh, S. K.; Ganzmann, C.; Bhuvanesh, N.; Gladysz, J. A. *Angew. Chem., Int. Ed*. **2016**, *55*, 4356-4360; *Angew. Chem*. **2016**, *128*, 4429-4433. (d) Kumar, A.; Ghosh, S. K.; Gladysz, J. A. *Org. Lett*. **2016**, *18*, 760-763. (e) Joshi, H.; Ghosh, S. K.; Gladysz, J. A. *Synthesis* **2017** (in press).

(5) (a) Gillard, R. D.; Vaughan, D. H. *Transition Met. Chem.* **1978**, 3, 44–48. (b) Wang, Z.; Kutal, C. *Inorg. Chim. Acta* **1994**, *226*, 285–291. (c) Davies, J. D.; Daly, W. H.; Wang, Z.; Kutal, C. *Chem. Mater.* **1996**, *8*, 850–855.

(6) See also Nakayama, N.; Miura, A.; Komamura, T. Japanese Patent 7, 234, 475, **1995**; *Chem. Abs.* **1995**, *124*, 131660.

(7) Although this compound contains twenty-four sp^3 carbon-fluorine bonds, significantly fluorophilic molecules that feature only isolated trifluoromethyl groups (as opposed to compact arrays such as $OC(CF_3)_3$) are rare. Given the >99.9:<0.1 CH_2Cl_2/PFMC partition coefficients for Na^+ BAr_f^- and $[Co(en)_3]^{3+}$ $3BAr_f^-$ in Table 8.3, we hesitate to even refer to such salts as "light fluorous".

(8) *Handbook of Fluorous Chemistry*, Gladysz, J. A.; Curran, D. P.; Horváth, I. T., Eds.; Wiley/VCH: Weinheim, 2004.

(9) "Strategies for the Recovery of Fluorous Catalysts and Reagents: Design and Evaluation", Gladysz, J. A.; Corrêa da Costa, R. In *Handbook of Fluorous Chemistry*, Gladysz, J. A., Curran, D. P., Horváth, I. T., Eds.; Wiley/VCH: Weinheim, 2004, p. 24–40.

(10) van den Broeke, J.; Deelman, J. B.; van Koten, G. *Tetrahedron Lett.* **2001**, *42*, 8085–8087.

(11) Boswell, P.; Bühlmann, P. *J. Am. Chem. Soc.* **2005**, *127*, 8958–8959.

(12) Given the representation of **28** as Na^+ BAr_{f6}^-, one could employ Na^+ BAr_{fl}^- as an alternative representation for Na^+ BAr_f^-. Based upon the extensively established use of the latter in the literature, we have elected to retain the traditional designation.

(13) (a) Juris, A.; Balzani, V. *Coord. Chem. Rev.* **1988**, *84*, 85–277 (see Table 7.1 for relevant UV-vis and fluorescence data). (b) Kalyanasundaram, K. *Coord. Chem. Rev.* **1982**, *46*, 159–244.

(14) Adams, D. J.; Bennett, J. A.; Cole-Hamilton, D. J.; Hope, E. G.; Hopewell, J.; Kight, J.; Pogorzelec, P.; Stuart, A. M. *Dalton Trans.* **2005**, 3862–3867.

(15) See also Cavazzini, M.; Manfredi, A.; Montanari, F.; Quici, S.; Pozzi, G. *Eur. J. Org. Chem.* **2001**, 4639–4649.

(16) Duan, J.; Zhang, L. H.; Dolbier, W. *Synlett* **1999**, *8*, 1245–1246.

(17) I and my collaborators have been informed of an independently determined, unpublished crystal structure of **29**: Hope, Eric, G.; Stuart, A. M. University of Leicester, private communication. However, as of June 2017 it has not been deposited in the Cambridge Crystallographic Data Centre.

(18) (a) "Catalysis Involving Fluorous Phases: Fundamentals and Directions for Greener Methodologies", Gladysz, J. A. in *Handbook of Green Chemistry*, Anastas, P.,

Ed; Volume 1: *Homogeneous Catalysis*; Crabtree, R. H. Volume Ed; Wiley/VCH, Weinheim, **2009**, 17–38. (b) Matsubara, H.; Ryu, I. *Topics in Current Chemistry* **2012**, *308*, 135–152.

(19) (a) Work, J. B. *Inorg. Synth.* **1946**, *2*, 221–222. (b) This paper establishes that the crystals obtained in reference 19a contain 2.8-3.0 molecules of water per cobalt atom: Whuler, A.; Brouty, C.; Spinat, P.; Herpin, P. *Acta Cryst.* **1975**, *B31*, 2069–2076. (c) See also Nakatsu, K.; Saito, Y.; Kuroya, H. *Bull. Chem. Soc. Jpn*. **1956**, *29*, 428–434. (d) The hydration level assigned to the starting material (2.5 molecules per cobalt) was based upon microanalysis.

(20) Ghosh, S. K.; Lewis, K. G.; Kumar, A.; Gladysz, J. A. *Inorg. Chem.* **2017**, 56, 2304-2320.

(21) (a) Jaeger, F. M.; Bijkerk, L. *Z. Anorg. Allg. Chem.* **1937**, *233*, 97–139. (b) Harung, S. E.; Sørensen, B. S.; Creaser, I.; Maegaard, H.; Pfenniger, U. *Inorg. Chem.* **1976**, *15*, 2123–2126. (c) McCann, M.; Townsend, S.; Devereux, M.; McKee, V.; Walker, B. *Polyhedron*, **2001**, *20*, 2799–2806. (d) The sample employed was prepared by a procedure analogous to that with the racemic ligand in reference 21c, and a microanalysis verified the hydration level reported for the complex with the enantiopure ligand in reference 21a. Anal. Calcd. for $C_{18}H_{50}Cl_3CoN_6O_4$ (579.92) C, 37.28; H, 8.69; N, 14.49. Found: C, 36.86; H, 8.74; N, 14.44; $[\alpha]^{25}_{589}$ = 81.4° (*c* = 5.00 mg·mL^{-1}, H_2O).

(22) Broomhead, J. A.; Young, C. G. *Inorg. Synth*. **1990**, *28*, 338–340.

(23) "Partition Coefficients involving Fluorous Solvents", Gladysz, J. A.; Emnet, C.; Rábai, J. in *Handbook of Fluorous Chemistry*, Gladysz, J. A.; Curran, D. P.; Horváth, I. T. Eds.; Wiley/VCH, Weinheim, 2004, pp. 56–100.

(24) Corrêa da Costa, R.; Buffeteau, T.; Guerzo, A. D.; McClenagham. N. D.;

Vincent, J. M. *Chem. Commun.* **2011**, *47*, 8250–8252.

(25) (a) Rollinson, C. L.; Bailar, J. C. Jr. *Inorg. Synth.* **1946**, *2*, 196–200. (b) Giedt, D. C.; Nyman, C. J. *Inorg. Synth.* **1966**, *8*, 239–241. (c) Galsbøl, F. *Inorg. Synth.* **1970**, *12*, 269–280. (d) Galsbøl, F.; Rasmussen. B. S. *Acta Chem. Scand. A* **1982**, *36*, 83–87. (e) Srinivasan, B. R.; Naik, A. R.; Näther, C.; Pausch, H.; Bensch, W. *J. Coord. Chem.* **2009**, *62*, 3583–3591.

(26) Maayan, G.; Fish, R. H.; Neumann, R. *Org. Lett.* **2003**, *5,* 3547–3550.

(27) (a) Pham, P. V.; Nagib, D. A.; MacMillan, D. W. C. *Angew. Chem. Int. Ed*. **2011**, *50*, 6119–6122; *Angew. Chem*. **2011**, *123*, 6243–6246 and references therein. (b) Narayanam, J. M. R.; Stephenson, C. R. J. *Chem. Soc. Rev.* **2011**, *40*, 102–113.

(28) "Fluorous Solvents and Related Media", Gladysz, J. A.; Emnet, C. in *Handbook of Fluorous Chemistry*, Gladysz, J. A.; Curran, D. P.; Horváth, I. T. Eds.; Wiley/VCH, Weinheim, 2004, pp. 11–23.

(29) Tuba, R.; Brothers, E. N.; Reibenspies, J. H.; Bazzi, H. S.; Gladysz, J. A. *Inorg. Chem.* **2012**, *51*, 9943–9949.

(30) Wampler, R. D.; Begue, N. J.; Simpson, G. J. *Cryst. Growth & Design* **2008**, *8*, 2589–2594.

(31) Halasyamani, P. S.; Poeppelmeier, K. R. *Chem. Mater.* **1998**, *10*, 2753–2769.

(32) (a) Marder, S. R.; Perry, J. W.; Tiemann, B. G.; Schaefer, W. P. *Organometallics* **1991**, *10*, 1896–1901. (b) Whittall, I. R.; McDonagh, A. M.; Humphrey, M. G.; Samoc, M. *Adv. Organomet. Chem.* **1998**, *42*, 291–362.

(33) The signal assignments are based upon fluorine couplings observed in the $^{13}C\{^{1}H\}$ NMR spectrum of **28**.

(34) This corresponds to the theoretical number of protons for this signal. In

practice, the observed integration was 1-2 protons less, and this is provisionally attributed to H/D exchange. See also reference 20.

(35) The fluorine analysis does not closely correspond to the calculated value, but in view of the excellent C/H/N agreement is believed to result from an analytical artifact.

(36) This racemic complex has been previously reported in enantiopure form in reference 4a,c.

(37) (a) Brookhart, M.; Grant, B.; Volpe, A. F. *Organometallics* **1992**, *11*, 3920–3922. (b) Yakelis, N. A.; Bergman, R. G. *Organometallics* **2005**, *24*, 3579–3581. (c) Nishida, H.; Takada, N.; Yoshimura, M.; Sonoda, T.; Kobayashi, H. *Bull. Chem. Soc. Jpn*. **1984**, *57*, 2600–2604.

(38) When one attempts to dry this complex or the enantiopure analog (reference 4a) by oil pump vacuum (room temperature to 50 °C), or over P_2O_5 or molecular sieves in solution, additional ^{1}H NMR signals appear in the aromatic region, indicating some type of decomposition.

(39) This multiplet exhibits a triplet fine structure, J = 2.5 Hz.

(40) The aryl carbon assignments follow those given in references 10 and 37a.

(41) Sheldrick, G. M. "Cell_Now (version 2008/1): Program for Obtaining Unit Cell Constants from Single Crystal Data": University of Göttingen, Germany.

(42) APEX2 "Program for Data Collection and Integration on Area Detectors" BRUKER AXS Inc., 5465 East Cheryl Parkway, Madison, WI 53711-5373 USA.

(43) Sheldrick, G. M. "SADABS (version 2008/1): Program for Absorption Correction for Data from Area Detector Frames", University of Göttingen, Germany.

(44) Sheldrick, G. M. *Acta Cryst*. **2008**, *A64*, 112–122.

(45) Spek, A. L. *J. Appl. Cryst.* **2003**, *36,* 7–13.

(46) Dolomanov, O. V, Bourhis, L. J., Gildea, R. J., Howard, J. A. K., Puschmann, H. *J. Appl. Cryst*. **2009**, *42*, 339–341.

(47) Flack, H. D.; Bernardinelli, G.; Clemente, D. A.; Linden, A.; Spek, A. L. *Acta Cryst.* **2006**, *B62*, 695–701.

9. SUMMARY AND CONCLUSION

This thesis has described the development of highly effective, chiral-at-metal monofunctional and bifunctional hydrogen bond donor catalysts based on cobalt (III) Werner complexes (Figure 9.1) and their applications in enantioselective catalysis. Since cobalt (III) Werner cations are substitution inert, substrate activation and asymmetric induction must take place via second-coordination sphere mechanisms involving hydrogen bonding to the NH_2 moieties of the diamine ligands.

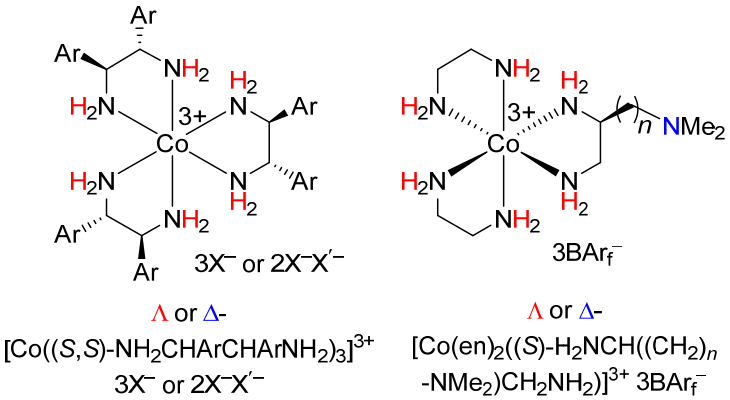

Figure 9.1. Chiral-at-metal hydrogen bond donor catalysts based on cobalt (III) Werner complexes.

Thirteen bulky monofunctional complexes of the formula Δ- or Λ-$[Co((S,S)\text{-}NH_2CHArCHArNH_2)_3]^{3+}$ $2Cl^-B(aryl)_4^-$ (BAr_f^-: aryl = 3,5-$C_6H_3(CF_3)_2$; BAr_{f20}^-: aryl = C_6F_5; Ar = C_6H_5, 4-C_6H_4*n*-Bu, 4-C_6H_4Cl, 4-$C_6H_4CF_3$, 4-$C_6H_4OCH_3$, α-naphthyl, ß-naphthyl, 2-C_6H_4OBn) were synthesized in a highly stereoselective pathway and chromatographed on silica gel columns. Anion metatheses of Δ- or Λ-$[Co((S,S)\text{-}NH_2CHArCHArNH_2)_3]^{3+}$ $2Cl^-BAr_f^-$ afforded the corresponding $2BF_4^-BAr_f^-$ and $2PF_6^-BAr_f^-$ salts. The complexes Δ- or Λ-$[Co((S,S)\text{-dpen})_3]^{3+}$ $3B(aryl)_4^-$ (dpen = 1,2-

diphenylethylenediamine), Λ-$[Co((S,S)\text{-dpen})_3]^{3+}$ $3BF_4^-$, and Λ-$[Co((S,S)\text{-dpen})_3]^{3+}$ $3PF_6^-$ were also synthesized. These complexes were used in the Michael additions of dialkyl malonates to nitroalkenes and α-aminations of 1,3-dicarbonyl compounds. In both cases, the reactions were highly enantioselective (up to 98% and 99% ee) and the chirality of the products were controlled by the cobalt configurations of the catalysts.

To synthesize the bifunctional catalysts, first the tris(hydrochloric acid) salts of the chiral triamine ligands $H_2NCH((CH_2)_nNMe_2)CH_2NH_2$ (n = 1-4) were synthesized in enantiopure form (section 6). These salts were reacted with the racemic carbonate complex $[Co(en)_2O_2CO]^+$ Cl^- (en = ethylenediamine) and the reaction mixtures were chromatographed on Dowex cation exchange resin columns to give $[Co(en)_2((S)\text{-}H_2NCH((CH_2)_nNHMe_2)CH_2NH_2)]^{4+}$ $4Cl^-$ (Figure 7.2). The Δ and Λ diastereomers of the complexes were separated using Sephadex columns (Figure 7.3). The cobalt configurations of Λ- and Δ-$[Co(en)_2((S)\text{-}H_2NCH((CH_2)_nNHMe_2)CH_2NH_2)]^{4+}$ $4Cl^-$ were assigned by comparison of their CD spectra with the known CD spectra of Λ- and Δ-$[Co(en)_3]^{3+}$ $3I^-$ (Figure 7.4). Anion metatheses with Na^+ BAr_f^- gave Λ- and Δ-$[Co(en)_2((S)\text{-}H_2NCH((CH_2)_nNHMe_2)CH_2NH_2)]^{3+}$ $3BAr_f^-$. These salts were screened as catalysts for additions of dimethyl malonate to *trans*-ß-nitrostyrene (Scheme 7.3). The diastereomer Λ-$[Co(en)_2((S)\text{-}H_2NCH((CH_2)_3NHMe_2)CH_2NH_2)]^{3+}$ $3BAr_f^-$ was found to be the best catalyst with excellent yields and enantioselectivities (up to 98% yield and 99% ee).

To extend this chemistry into the fluorous media, the highly "fluorous BAr_f" salt Na^+ BAr_{f6}^- (BAr_{f6}^- = $B(3,5\text{-}C_6H_3((CF_2)_5CF_3)_2)_4^-$) was synthesized by an optimized procedure (77-70%, section 8). To show its effectiveness in the transportation of Werner cations and other polycations into fluorous media, the salts $[Co(en)_3]^{3+}$ $3BAr_{f6}^-$, $[Co(R,R\text{-chxn})_3]^{3+}$ $3BAr_{f6}^-$ (chxn = *trans*-1,2-cyclohexanediamine), and $[Ru(bipy)_3]^{2+}$

$2BAr_{f6}^-$ (bipy = 2,2′-bipyridine) were synthesized in excellent yields. All of these salts exhibit toluene/PFMC (PFMC = perfluoromethylcyclohexane) partition coefficients of $\leq$1:$\geq$99 (Table 8.3), establishing that the anion BAr_{f6}^- can efficiently transport polar polycations into highly nonpolar fluorous phases.

These catalysts enable the syntheses of highly functionalized and synthetically useful building blocks that are very important for agricultural, pharmaceutical industries. In addition, the simple operational procedure and the use of air stable, inexpensive catalysts make this a highly attractive and effective approach.

APPENDIX A

Table A-1. Crystal structures containing the $[Co(en)_3]^{3+}$ trication in the Cambridge Structural Database (CSD) minus duplicates.[a]

entry/ reference	CSD Refcode	*ob*/*lel* orientation	cobalt configuration	space group	name as represented in CSD
1	ABIXIT	$oblel_2$	Λ,Δ	*P*-31*c*	bis(tris(Ethylenediamine)-cobalt) piperazinium bis(bis(μ_5-hydrogen phosphato)-pentakis(μ_2-oxo)-decaoxo-penta-molybdenum(vi)) hexahydrate
2	ACUBAB	ob_3	Λ,Δ	*P*-31*c*	catena-(tris(ethylenediamine)-cobalt(iii) hexakis(μ_5-phosphato)-(μ_2-chloro)-octa-zinc dihydrate)
3	ARILES	lel_3	Λ,Δ	*C*2/*c*	is(tris(Ethylenediamine)-cobalt(iii)) (μ_3-borotriphosphato)-tris((μ_2-oxo)-oxo-vanadium(v)) dihydrogen phosphate tetrahydrate
4	BESFAG	lel_3	Λ,Δ	*P*-1	tris(Ethylenediamine)-cobalt(iii) dihydrogen tetrahydrofuran-tetracarboxylate trihydrogen tetrahydrofuran-tetracarboxylate hydrate
5	BIRSUO[b]	lel_3	Λ,Δ	*P*-3	tris(Ethylenediamine)-cobalt(iii) arsenate trihydrate
6	BIWLIC	lel_3	Λ,Δ	*I*-42*d*	catena-[bis(λ,δ-tris(1,2-Diaminoethane)-cobalt) bis(bis(μ_2-phosphato)-di-aluminium) dodecahydrate]
7	CASTAS	lel_3	Λ	$I2_12_12_1$	catena-(bis(d-tris(Ethylenediamine)-cobalt) tetrakis(μ_2-phosphato)-di-aluminium tridecahydrate)
8	COCRCL	lel_3	Λ	*P*321	tris(Ethylenediamine)-cobalt(iii) tris(ethylenediamine)-chromium(iii) chloride hydrate
9	COCREN	lel_3	Λ	$P112_1$	(+)-tris(Ethylenediamine) cobalt(iii)(-)-tris(ethylenediamine) chromium(iii) thiocyanate hydrate
10	COENCF	$oblel_2$	Λ,Δ	$P2_1/n$	tris(Ethylenediamine) cobalt(iii) hexacyanoferrate(iii) dihydrate
11	COENCH[b]	lel_3	Λ	$P4_32_12$	(+)D-tris(Ethylenediamine)-cobalt(iii) chloride monohydrate
12	COENCL	lel_3	Λ	*P*321	(+)-tris(Ethylenediamine)-cobalt(iii) (-)-tris(ethylenediamine)-chromium(iii) chloride hydrate
13	COENSI	lel_3	Λ,Δ	$P2_1/n$	tris(Ethylenediamine)-cobalt(iii) hydrogen silicate hydrate
14	COENTC[b]	lel_3	Λ,Δ	*Pbca*	(+-)-tris(Ethylenediamine)-cobalt(iii) tris(thiocyanate)
15	COENTD[c]	lel_3	Λ	*c*	(+)-tris(Ethylenediamine)-cobalt(iii) (-)-tris(ethylenediamine)-chromium(iii) hexakis(thiocyanate)
16	COTENC[b]	lel_3	Λ,Δ	*P*-3*c*1	(+-)-tris(Ethylenediamine)-cobalt(iii) trichloride hydrate

17	CUDGEN	ob_3	Λ,Δ	$P6/mcc$	tris(Ethylenediamine)-cobalt(iii) hydroxonium hexakis(μ_4-oxo)-dodecakis(μ_2-oxo)-dodecaoxo-hexa-arsenic(iii)-cobalt(ii)-hexa-molybdenum(vi) dihydrate
18	DUCYIL[b]	$oblel_2$	Λ,Δ	P-1	tris(ethane-1,2-diamine)-cobalt(iii) hexahydroxyoctaborate tetrahydroxypentaborate pentahydrate
19	EDANEC[b]	$oblel_2$	Λ	$P2_12_12_1$	Λ-$(+)_{589}$-tris(Ethylenediamine)-cobalt(iii) tris(iodide) monohydrate
20	EDCOBR[b]	lel_3	Λ	$P4_32_12$	D-tris(Ethylenediamine)-cobalt(iii) tribromide monohydrate
21	EGOXII	$oblel_2$	Λ,Δ	$P2_1/c$	catena-(tris(1,2-ethanediamine)-cobalt(iii) tetrakis(μ_3-hydrogen phosphito)-(μ_2-hydrogen phosphito)-(μ_2-dihydrogen phosphito)-tetra-zinc(ii))
22	ENCCUC10[d]	$lelob_2$	Λ,Δ	$Pbca$	bis(tris(Ethylenediamine)-cobalt(iii)) bis(μ-chloro)-hexachloro-di-copper(ii) dichloride dihydrat
23	ENCOCD	lel_3	Λ,Δ	$P2_1/c$	bis(tris(Ethylenediamine)-cobalt(iii)) hexachloro-cadmium(ii) dichloride dihydrate
24	ENCOCT[b]	lel_3	Λ	$P1$	tris(Ethylenediamine)-cobalt(iii) chloride (+)-tartrate pentahydrate
25	ENCOFD[c]	*c*	*c*	*c*	(+-)-tris(Ethylenediamine)-cobalt(iii) trifluoride
26	ENCOIH	$lelob_2$	Λ, Δ	$Pbca$	(+-)-tris(Ethylenediamine)-cobalt(iii) iodide monohydrate
27	ENCOPB	lel_3+ $oblel_2$[e]	Λ, Δ[e]	$P2_1$	bis(tris(Ethylenediamine)-cobalt(iii)) catena(bis(μ_2-chloro)-heptachloro-di-lead(ii)) chloride trihydrate
28	ENCOPC	$lelob_2$	Λ, Δ	$P2_1/c$	tris(Ethylenediamine) cobalt pentacyano-nitrosyl-chromate dihydrate
29	ENCOPN[b]	lel_3	Λ, Δ	$Pnma$	bis(tris(Ethylenediamine)-cobalt(iii)) tris(monohydrogen-phosphate) nonahydrate
30	ENCOSN	$oblel_2$	Λ, Δ	$Pbca$	tris(Ethylenediamine) cobalt(iii) trichlorotin(ii) dichloride
31	ENCOTT[c]	*c*	*c*	$P2_1$	$(+)_{589}$-Hydrogen tris(ethylenediamine) cobalt(iii) D-tartrate trihydrate
32	ENCTAR[c]	*c*	*c*	$P1$	tris(Ethylenediamine) cobalt(iii) D-tartrate bromide pentahydrate
33	ENICON	$oblel_2$	Δ	$P2_12_12_1$	tris(Ethylenediamine) cobalt(iii) tetrakis(isothiocyanato) cobalt(ii) nitrate
34	EPAXOJ	lel_3	Λ, Δ	$C2/c$	tris(1,2-Diaminoethane)cobalt(iii) bis(tetrabromo-gold(iii)) bromide
35	EXOVAO	lel_3+ $oblel_2$	Λ, Δ	P-1	bis(tris(Ethylenediamine-N,N')-cobalt(iii)) bis(μ_2-(1-hydroxyethylidene)diphosphonato)-dichloro-di-ruthenium(ii,iii) chloride trihydrate
36	FAHHIH	lel_3	Λ, Δ	P-1	bis[tris(ethylenediamine-N,N')-cobalt(iii)] tris(oxalate) hydrate
37	FAHHON	$oblel_2$	Λ, Δ	$C2/c$	bis[tris(ethylenediamine-N,N')-cobalt(iii)] tris(oxalate) heptahydrate
38	FASHUE	lel_3	Λ, Δ	$P2_1/c$	bis(tris(Ethylenediamine)-cobalt(iii)) hexabromo-cadmium(ii) dibromide dihydrate
39	FASJAM	lel_3	Λ, Δ	$P2_1/c$	bis(tris(Ethylenediamine)-cobalt(iii)) trans-tetrabromo-dichloro-cadmium(ii) dibromide dihydrate
40	FAXMEX[b]	lel_3	Λ, Δ	$P6_322$	tris(Ethylenediamine-N,N')-cobalt(iii) chloride di-iodide monohydrate clathrate
41	FIRQIH[b]	lel_3	Λ	$P6_322$	tris(Ethylendiamine-N,N')-cobalt(iii) hexafluoro-gallate

42	GAPHUA	lel_3	Λ, Δ	$P2_12_12_1$	tris(Ethylenediamine-N,N')-cobalt(iii) iodide oxalate sesquihydrate
43	GAXKIB[b]	$lelob_2$	Λ, Δ	$C2/c$	tris(ethane-1,2-diamine)-cobalt(iii) sesquikis(3,4,5-trioxocyclopent-1-ene-1,2-diolate) trihydrate
44	GEPGEO[b]	$oblel_2$	Λ, Δ	$P4_2bc$	Tris(ethylenediamine)-cobalt(iii) tetrathioarsenate(v)
45	GINLUK[b]	lel_3	Λ	$P2_12_12_1$	Λ-bis(tris(Ethylenediamine-N,N)-cobalt) tris(d-tartrate) nonadecahydrate
46	GINMAR[b]	lel_3	Δ	$P1$	Delta-bis(tris(Ethylenediamine-N,N)-cobalt) tris(d-tartrate) hydrate
47	GIXRIP	lel_3	Λ,Δ	P-$3c1$	tris(Ethylenediamine-N,N')-cobalt(iii) trichloride argon clathrate
48	GIXROV	lel_3	Λ,Δ	P-$3c1$	tris(Ethylenediamine-N,N')-cobalt(iii) trichloride xenon clathrate
49	GIXRUB	lel_3	Λ,Δ	P-$3c1$	tris(Ethylenediamine-N,N')-cobalt(iii) trichloride dioxygen clathrate
50	GIXSAI	lel_3	Λ,Δ	P-$3c1$	tris(Ethylenediamine-N,N')-cobalt(iii) trichloride methane clathrate
51	GIXSEM	lel_3	Λ,Δ	P-$3c1$	tris(Ethylenediamine-N,N')-cobalt(iii) trichloride carbon tetrachloride clathrate
52	GIZLIL	lel_3	Λ,Δ	P-$3c1$	tris(Ethylenediamine-N,N')-cobalt(iii) trichloride tetrahydrate clathrate
53	GIZLOR	lel_3	Λ,Δ	P-$3c1$	tris(Ethylenediamine-N,N')-cobalt(iii) trichloride ethanol clathrate
54	GIZLUX	lel_3	Λ,Δ	P-$3c1$	tris(Ethylenediamine-N,N')-cobalt(iii) trichloride benzene clathrate
55	GULNEH	$lelob_2$	Λ,Δ	$C2/m$	bis(tris(Ethylenediamine)-cobalt(iii)) (μ_2-oxalato-O,O',O",O'")-tetrakis(oxalato-O,O')-di-manganese(ii) hexahydrate
56	GUZNIY[b]	lel_3	Λ,Δ	$P2_1/n$	rac-tris(Ethylenediamine-N,N')-cobalt(iii) cyclotriphosphate dihydrate
57	GUZNOE[b]	lel_3	Λ	$P2_1$	Λ-tris(Ethylenediamine-N,N')-cobalt(iii) cyclotriphosphate dihydrate
58	HAJCOM	lel_3	Λ,Δ	P-1	bis[tris(ethylenediamine)-cobalt(iii)] (μ_2-oxalato)-tetrakis(oxalato)-di-cobalt(ii) tetrahydrate
59	HEQWIL	$oblel_2$	Λ,Δ	$C2/c$	tris(ethane-1,2-diamine)-cobalt(iii) chloride ethanedioate trihydrate
60	HEYVAJ	$oblel_2$	Λ,Δ	$Pn2_1a$	bis(tris(Ethylenediamine)-cobalt(iii)) (μ_2-chloro)-aqua-pentachloro-di-mercurate(ii) tetrachloride
61	HEYVEN	lel_3	Λ,Δ	$C2/c$	tris(Ethylenediamine)-cobalt(iii) bis(tetrachloro-gold(iii)) chloride
62	IGOZEK	lel_3	Λ,Δ	$P2_1/c$	bis(tris(Ethylene-1,2-diamine)-cobalt) hexakis(μ_2-fluoro)-diaqua-hexadecafluoro-tetra-zirconium
63	IRIRAC[b]	lel_3	Λ,Δ	P-$3c1$	(+-)-tris(Ethylenediamine)-cobalt(iii) trichloride
64	IYIBIC	$lelob_2$	Δ	$P2_12_12_1$	bis(tris(D-Penicillaminato-N,O,S,S)-tri-palladium(ii)) Δ-tris(ethylenediamine)-cobalt(iii) triperchlorate decahydrate
65	IYIBOI	$lelob_2$	Λ	$P2_12_12_1$	bis(tris(D-Penicillaminato-N,O,S,S)-tri-palladium(ii)) Λ-tris(ethylenediamine)-cobalt(iii) triperchlorate hydrate
66	IZEQUZ[c]	*c*	*c*	$C2/c$	tris(Ethylenediamine)-cobalt diaqua-bis(ethylenediamine)-cobalt (μ_8-arsenato)-

					hexadecakis(μ_3-oxo)-octakis(μ_2-oxo)-hexadecaoxo-octa-molybdenum(v,vi)-octa-vanadium(iv)
67	JIMRUT	*lel*$_3$	Λ,Δ	*Pnna*	catena-(tris(Ethylene-1,2-diamine)-cobalt tetrakis(μ_3-phosphato)-tri-gallium pentahydrate)
68	LALDUZ	*oblel*$_2$	Λ,Δ	*P*-1	catena-(tris(Ethylenediamine)-cobalt(iii) hemikis(pentakis(μ_2-oxalato)-bis(oxalato)-tetra-zinc) pentahydrate)
69	LITSOW	*oblel*$_2$	Λ	$P2_12_12_1$	tris(Ethylenediamine)-cobalt(iii) (μ_2-iodo)-hexachloro-di-mercury(ii)
70	LIYMUB	*lel*$_3$	Λ,Δ	$P2_1/n$	tris(Ethylenediamine-N,N')-cobalt(iii) oxalate perchlorate dihydrate
71	MARGAP	*oblel*$_2$	Λ,Δ	*P*-1	bis(tris(ethane-1,2-diamine)-cobalt(iii)) tris(5,5'-azotetrazolate) trihydrate
72	MOMWOB	*lel*$_3$	Λ,Δ	*P*-1	tris(ethylenediamine)-cobalt(iii) tetraiodo-tellurium(ii) iodide
73	MOMWUH	*lelob*$_2$	Λ,Δ	$P2_1/n$	tris(ethylenediamine)-cobalt(iii) hexaaiodo-tellurium(iv) iodide
74	MOTXID	*oblel*$_2$	Λ,Δ	$Cmc2_1$	tetrakis(tris(1,2-diaminoethane)-cobalt(iii)) tris(hexacyano-iron(ii)) hydrate
75	MOTXOJ	*lel*$_3$	Λ,Δ	$P2_1/c$	bis(tris(1,2-diaminoethane)-cobalt(iii)) hexacyano-iron(ii) dichloride dihydrate
76	MUTWUU	*oblel*$_2$	Λ,Δ	*C*2/*c*	bis(tris(Ethylenediamine)-cobalt) tris(bis(pyridine-2,6-dicarboxylato)-cobalt) hexadecahydrate
77	NAXTUC	*oblel*$_2$	*f*	$P2_1/c$	tris(Ethylenediamine)-cobalt(iii) 4,4'-diazido-2,2'-stilbenedisulfonate perchlorate monohydrate
78	NAZZEU	*lel*$_3$	Λ,Δ	*C*2/*c*	bis(tris(Ethylenediamine-N,N')-cobalt) bis(μ_2-fluoro)-decafluoro-di-zirconium hexafluoro-silicate tetrahydrate
79	NEJDEM[b]	*oblel*$_2$	Λ,Δ	*Pnma*	tris(ethylenediamine-N,N')-cobalt(iii) sesquikis(squarate) hydrate
80	NEKHUG	*lelob*$_2$	Λ,Δ	*Pmna*	tris(Ethylenediamine)-cobalt tris(μ_2-chloro)-aqua-octabromo-tri-rhenium bromide
81	NIHNEZ	*oblel*$_2$	Λ,Δ	$Pna2_1$	tris(ethylenediamine)-cobalt(iii) tetrathioantimonate(v)
82	NONKAC	*lel*$_3$	Λ	$C222_1$	catena(d-tris(1,2-Diaminoethane)-cobalt(iii) trialumino-tetraphosphate trihydrate)
83	NOYQOH	*oblel*$_2$	Λ,Δ	$Pca2_1$	(+-)-tris(Ethylenediamine)-cobalt(iii) nitrate
84	OBIWAZ	*oblel*$_2$	Λ,Δ	*Pnma*	bis[tris(ethylenediamine)-cobalt(iii)] (μ_{12}-silicato)-octakis(μ_3-oxo)-hexadecakis(μ_2-oxo)-tetradecaoxo-octa-molybdenum(vi)-hexa-vanadium hexahydrate
85	OKOQOW	*oblel*$_2$	Λ,Δ	$P2_1/n$	catena-[bis(tris(ethane-1,2-diamine)-cobalt) heptakis(μ-heptanedioato)-bis(μ-oxido)-octakis(μ-hydroxy)-tetrakis(μ-oxido)-tetracosa(oxido)-dodeca-uranium acetonitrile solvate trihydrate]
86	OLANOE	*oblel*$_2$	Λ,Δ	$P2_1/n$	bis(tris(Ethylene-1,2-diamine)-cobalt) bis(iodide) hexacyanoferrate(ii) hydrate
87	PEFPUM	*lel*$_3$+ *lelob*$_2$	Λ,Δ	*P*-1	bis(tris(Ethylenediamine)-cobalt(iii)) bis(μ_5-phosphato)-pentakis(μ_2-oxo)-decaoxo-penta-molybdenum hydrate
88	PEJGAO	*lel*$_3$	Λ	$P2_1$	Λ-tris(ethane-1,2-diamine)-cobalt sesquikis(fumaric acid) hydrate

89	PEJGES[b]	lel_3	Λ	$P1$	Λ-tris-1,2-(ethylenediamino)-cobalt(iii) sesquikis(terephthalate) decahydrate
90	PEJGIW	$oblel_2$	Λ,Δ	$P\text{-}1$	tris(ethane-1,2-diamine)-cobalt(iii) sesquikis(acetylenedicarboxylate) tetrahydrate
91	PEJGOC[b]	$oblel_2$	Λ,Δ	$P2_1/c$	tris(ethane-1,2-diamine)cobalt benzene-1,3,5-tricarboxylate hydrate
92	PEJGUI	lel_3	Δ	$C2$	Δ-tris-1,2-(ethylenediamino)-cobalt(iii) fumarate nitrate dihydrate
93	PERHIE	$oblel_2$	Λ,Δ	$P2_1/c$	tris(1,2-diaminoethane)-cobalt(iii) hexacyano-iron(iii) monohydrate
94	PESVEP	$oblel_2$	Λ,Δ	$P2_1/c$	tris(1,2-diaminoethane)-cobalt(iii) hexacyano-iron(iii)
95	PEVXAP	lel_3+ $oblel_2$	Δ	$P1$	bis(tris(Ethylenediamine-N,N')-cobalt) divanadate(v) hydrogen-vanadate(v) hexahydrate
96	PIBFEL	lel_3	Λ	$P2_1$	tris(Ethylendiamine)-cobalt bis(oxalato)-ethylenediamine-cobalt di-iodide trihydrate
97	PIBFIP	lel_3	Δ	$P2_12_12_1$	tris(Ethylenediamine)-cobalt bis(oxalato)-ethylenediamine-cobalt di-iodide monohydrate
98	PIBFOV	lel_3	Λ	$P2_12_12_1$	tris(Ethylenediamine)-cobalt tris(oxalato)-(glycinato-O,N)-cobalt iodide monohydrate
99	PIMXIS	$lelob_2$	Λ	$R3$	tris(1,2-Diaminoethane-N,N')-cobalt(iii) hexachloro-iron hexachloride monohydrate
100	POVPEV	lel_3	Λ,Δ	$P2_1/c$	bis(tris(1,2-bis(Diamino)ethane)-cobalt) tetraiodide oxalate deuteruim oxide solvate
101	QATWIT	$lelob_2$	Δ	$P2_12_12_1$	tris(ethylenediamine)-cobalt (benzoato)-tetrabromo-cadmium(ii) monohydrate
102	QORFIM	lel_3	Λ,Δ	$C2/c$	catena-(tris(1,2-Diaminoethane-N,N')-cobalt(iii) (dihydrogen diborate-triphosphate))
103	REGSIG	lel_3+ $oblel_2$	Λ,Δ	$P2/a$	hexakis(tris(Ethylenediamine)-cobalt(iii)) bis(nitrato-O)-tris(nitrato-O,O')-diaqua-lead(ii) pentadecakis(nitrate) dihydrate
104	RUBDEY	lel_3	Λ,Δ	$C2/c$	bis(tris(ethylenendiamine)-cobalt(iii)) (trihydrogen diphosphato)-bis(dihydrogen phosphato)-bis(hydrogen phosphato)-aluminium phosphoric acid
105	SADQUL	$lelob_2$	Λ,Δ	$Pbca$	catena-(tris(Ethylene-1,2-diamine)-cobalt (μ_3-sulfido)-tetrakis(μ_2-sulfido)-thio-di-antimony-germanium)
106	SAETCO	lel_3	Λ	$P3$	Sodium D-tris(ethylenediamine)-cobalt(iii) heptachloride hexahydrate
107	SAFFIQ	$oblel_2$	Λ,Δ	$P\text{-}1$	tris(ethane-1,2-diamine)-cobalt(iii) aqua-(tris(ethanedioato))-indium(iii)
108	SATKEE	lel_3	Λ,Δ	$Cmc2_1$	tris(Ethylenediamine)-cobalt(iii) tris(μ_2-iodo)-hexaiodo-di-bismuth
109	SAYKUY	$lelob_2$	Λ,Δ	$P2_1/a$	rac-tris(Ethylenediamine-N,N')-cobalt trichloro-iodo-mercury(ii) chloride
110	SINQUB	lel_3	Λ	$I2$	catena-(d-tris(Ethylenediamine)-cobalt tris(μ_2-hydrogen phosphato)-(μ_2-phosphato)-di-gallium)
111	SINRIQ	lel_3	Λ	$I2$	catena-(d-tris(Ethylenediamine)-cobalt tris(μ_2-hydrogen phosphato)-(μ_2-phosphato)-aluminium-gallium)
112	SOZFIW[b]	lel_3	Λ	$R3$	Λ-tris(Ethylenediamine-N,N')-cobalt(iii) Λ-tris(oxalato-O,O')-rhodium(iii)

113	SOZFOC[b]	lel_3	Λ	$P2_1$	tris(Ethylenediamine-N,N')-cobalt(iii) Δ-tris(oxalato-O,O')-rhodium(iii)
114	SUYFIC[b]	$oblel_2$	Λ,Δ	$Pna2_1$	tris(Ethane-1,2-diamine)-cobalt(iii) carbonate iodide tetrahydrate
115	TAKHOD	lel_3	Λ,Δ	$P2_1/c$	tris(Ethylenediamine)-cobalt(iii) trichloro-fluoro-tin(ii) chloride
116	TEDDOV	lel_3	Λ,Δ	$Pb3$	tris(Ethylenediamine)-cobalt(iii) hexanitro-rhodium(iii) trihydrate
117	TENCON[b]	lel_3	Λ	$P2_12_12_1$	(+-)-tris(Ethylenediamine)-cobalt(iii) nitrate
118	TIFDOC	$oblel_2$	Λ,Δ	$C2/c$	rac-tris(Ethylenediamine-N,N')-cobalt(iii) rac-tris(pyridine-2,6-dicarboxylato-N,O,O')-terbium(iii) hydrate
119	TIFDUI	$oblel_2$+ $lelob_2$	Δ	$P2_1$	Δ-tris(Ethylenediamine-N,N')-cobalt(iii) cdelta/Λ-tris(pyridine-2,6-dicarboxylato-N,O,O')-terbium(iii) hydrate
120	TUZGEA	lel_3	Δ	$P2_12_12_1$	catena-(α-(+)-tris(Ethylenediamine)-cobalt tris((μ2-oxo)-dioxo-vanadium) monohydrate)
121	UNAVIP	lel_3	Λ	$P2_12_12_1$	tris(ethylenediamine)-cobalt(iii) (μ12-phosphato)-tetracosakis(μ2-oxo)-dodecaoxo-dodeca-molybdenum N,N-diethylformamide solvate
122	UNAVOV	lel_3+ $oblel_2$	Λ,Δ	P-1	tris(ethylenediamine)-cobalt(iii) (μ12-phosphato)-tetracosakis(μ2-oxo)-dodecaoxo-dodeca-molybdenum N,N-dimethylformamide solvate
123	UNAVUB	ob_3	Λ,Δ	P-1	tris(ethylenediamine)-cobalt(iii) bis(hydroxonium) bis(μ5-oxo)-tetrakis(μ3-oxo)-hexakis(μ2-oxo)-tetradecaoxo-octa-molybdenum chloride N,N-dimethylformamide solvate
124	UNAWAI	lel_3	Λ	$P2_12_12_1$	tris(ethylenediamine)-cobalt(iii) (μ12-phosphato)-tetracosakis(μ2-oxo)-dodecaoxo-dodeca-tungsten N,N-diethylformamide solvate
125	UNAWEM	lel_3	Λ,Δ	$P2_1/c$	tris(ethylenediamine)-cobalt(iii) (μ12-phosphato)-tetracosakis(μ2-oxo)-dodecaoxo-dodeca-tungsten N,N-dimethylformamide solvate
126	UNAWIQ	lel_3	Λ,Δ	$P2_1/n$	bis(tris(ethylenediamine)-cobalt(iii)) sesquikis((μ12-silicato)-tetracosakis(μ2-oxo)-dodecaoxo-dodeca-tungsten) N,N-diethylformamide methanol solvate hemihydrate
127	UNAWOW	lel_3+ $oblel_2$	Λ,Δ	P-1	sesquikis(tris(ethylenediamine)-cobalt(iii)) (μ12-silicato)-tetracosakis(μ2-oxo)-dodecaoxo-dodeca-tungsten hemichloride N,N-dimethylformamide solvate sesquihydrate
128	UQUNIE	$oblel_2$	Λ,Δ	P-1	tris(ethylenediamine)-cobalt(iii) diformato-dioxalato-indium(iii) dihydrate
129	VISHOW	lel_3	Λ,Δ	$C2/c$	bis(tris(ethane-1,2-diamine)-cobalt(iii)) bis(μ4-oxo)-bis(μ3-oxo)-octakis(μ2-oxo)-dodecaoxo-hepta-tungsten hexahydrate
130	WACMIX	lel_3	Λ,Δ	$P2_1/c$	tris(ethylenediamine)-cobalt(iii) ethylenediammonium polyoxoborotrivanada(v)triphosphate hydrate
131	WESRER	ob_3	Λ	$P2_12_12$	tris(Ethylenediamine-N,N')-cobalt(iii) bis((ethylenediaminetetra-acetato-O,O',O",O"',N,N')-cobalt(iii)) chloride decahydrate

132	WILREP	lel_3	Λ,Δ	$C2/c$	bis(rac-tris(Ethylenediamine)-cobalt(iii)) bis(μ$_2$-hydrogen phosphato-O,O')-bis(μ$_2$-dihydrogen phosphato-O,O')-octachloro-tetra-zinc(ii)
133	WILRIT	$oblel_2$	Λ,Δ	$P2_1/c$	catena-(rac-tris(Ethylenediamine)-cobalt(iii) bis(μ$_2$-hydrogen phosphato-O,O')-(μ$_2$-dihydrogen phosphato-O,O')-dichloro-di-zinc(ii))
134	WIMJEI	lel_3	Δ	$P3_2$	tris(Ethylenediamine-N,N')-cobalt(iii) (2(R)-((4,4-diphenylcyclohexyl)phosphono-oxymethyl)diethylenetriaminepenta-acetato)-aqua-gadolinium(iii) hydrate
135	WIPBUT	lel_3	Λ,Δ	$C2$	bis(d-tris(Ethylenediamine)-cobalt(iii)) bis(μ$_2$-hydrogen phosphato-O,O')-bis(μ$_2$-dihydrogen phosphato-O,O')-octachloro-tetra-zinc(ii)
136	WOQDUC[b]	$oblel_2$	Λ,Δ	$C2/c$	hexakis(cyano)-cobalt tris(1,2-ethanediamine)-cobalt pentahydrate
137	WOQFAK	lel_3	Λ,Δ	$P2_1/c$	hexakis(cyano)-chromium tris(1,2-ethanediamine)-cobalt dihydrate
138	WUQKEZ	lel_3	Λ	$P1$	tris(1,2-diaminoethane)-cobalt(iii) sesquikis(carbonate) α-cyclodextrin tridecahydrate
139	WUQKID	lel_3	Λ	$P1$	tris(1,2-diaminoethane)-cobalt(iii) sesquikis(carbonate) α-cyclodextrin ethanol solvate tetradecahydrate
140	WUQKOJ	lel_3+ $oblel_2$	Δ	$P1$	tris(1,2-diaminoethane)-cobalt(iii) sesquikis(carbonate) α-cyclodextrin hydrate
141	XAGWEI[f]	*f*	*f*	$P2_1/m$	catena-(tris(ethylenediamine)-cobalt bis(μ$_3$-hydrogen phosphato)-(μ$_2$-hydrogen phosphato)-tetrakis(μ$_2$-dihydrogen phosphato)-bis(dihydrogen phosphato)-tri-indium monohydrate)
142	XEMSEP[b]	$oblel_2$	Δ	$P1$	tris(Ethane-1,2-diamine)-cobalt(iii) tris(perrhenate)
143	XONLIV	lel_3+ $lelob_2$	Λ,Δ	$P2_1/c$	tetrakis(tris(Ethylenediamine)-cobalt(iii)) tris(hexacyanoruthenate(ii)) decahydrate
144	YEMFOM	$lelob_2$	Λ	$P6_522$	catena-[tris(Ethylenediamine)-cobalt(iii) (μ$_6$-hydrogen diphosphato)-bis(μ$_3$-hydrogen phosphato)-tri-zinc]
145	YIVHIU	lel_3	Λ,Δ	$Pna2_1$	catena(tris(Ethylenediamine-N,N')-cobalt(iii) tetrakis(phosphato)-tri-aluminium trihydrate)
146	YURJOL	lel_3	Λ,Δ	$Pna2_1$	tris(ethane-1,2-diamine)-cobalt(iii) 1,3,5,7-tetrahydroxy-1,3,5,7-tetrabora-2,4,6,8,10-pentaoxabicyclo(3.3.1)decane chloride trihydrate
147	YUXPOW	lel_3	Λ,Δ	$P2_1/c$	tris(Ethylenediamine)-cobalt(iii) pentafluoro-di-tin(ii) dichlorofluoro-tin(ii) chloride
148	ZZZAZY	lel_3	Λ,Δ	$P2_1/n$	DL-tris(Ethylenediamine)-cobalt(iii) DL-tartrate decahydrate
149	ZZZUZM[c]	*c*	*c*	$P4_132$	L-tris(Ethylenediamine)-cobalt (iii) tribromide monohydrate
150	ZZZVXG[c]	*c*	Λ,Δ	$P\text{-}3c1$	rac-tris(Ethylenediamine)-cobalt(iii) tribromide trihydrate

[a] Dications (cobalt(II)) have been excluded. [b] This salt is analyzed in the main text. [c] The atomic coordinates for this salt are not available in the CSD, precluding certain assignments. [d] For duplicate structures in the CSD, an Arabic numeral is generally appended to the refcode. For this salt (refcode ENCCUC10), there is no corresponding structure that lacks the "10". Hence, it is included in the table of unique structures. In a private communication, a CSD representative confirmed this, but also indicated that there are plans to reinstate some structures with lower numerals that were deleted earlier. [e]

This crystal contains both orientations (*oblel*$_2$ for the Λ enantiomer, *lel*$_3$ for the Δ enantiomer).[f] The high degree of disorder in this structure precludes certain assignments.

Table A-2. Duplicate crystal structures containing the $[Co(en)_3]^{3+}$ trication in the Cambridge Structural Database (CSD).

entry/ reference	CSD Refcode	*ob*/*lel* orientation	cobalt configuration	space group	name as represented in CSD
151	ACUBAB01[a]	*a*	*a*	*P*-31*c*	catena-[tris(Ethylenediamine)-cobalt(iii) hexakis(μ_5-phosphato)-(μ_2-chloro)-octa-zinc dihydrate]
152	ACUBAB02[a]	*a*	*a*	*P*-31*c*	catena-(tris(Ethylenediamine)-cobalt(iii) hexakis(μ_5-phosphato)-(μ_2-chloro)-octa-zinc dihydrate)
153	COCREN01	lel_3	Λ	$P112_1$	(+)-tris(Ethylenediamine) cobalt(iii)(-)-tris(ethylenediamine) chromium(iii) thiocyanate hydrate
154	COENTC01[a]	*a*	Λ,Δ	*a*	(+-)-tris(Ethylenediamine)-cobalt(iii) thiocyanate
155	COENTD01[a]	*a*	Λ	*a*	(+)-tris(Ethylenediamine)-cobalt(iii) (-)-tris(ethylenediamine)-chromium(iii) hexakis(thiocyanate)
156	COENTD10	lel_3	Λ	$P2_12_12_1$	(+)-tris(Ethylenediamine)-cobalt(iii) (-)-tris(ethylenediamine)-chromium(iii)
157	COTENC01	lel_3	Λ,Δ	*P*-3*c*1	D,L-tris(Ethylenediamine)-cobalt(iii) trichloride trihydrate
158	ENCOCT01	lel_3	Λ	*P*1	tris(Ethylenediamine)-cobalt(iii) $(+)_{589}$-(R,R)-tartrate chloride pentahydrate
159	ENCOFD01[a]	*a*	*a*	*a*	(+-)tris-(Ethylenediamine)-cobalt(iii) trifluoride
160	ENCOFD02[a]	*a*	*a*	$P2_1/n$	(+-)tris-(Ethylenediamine)-cobalt(iii) trifluoride
161	ENCOPB01	lel_3+ $oblel_2$[b]	Λ,Δ[b]	$P2_1$	catena-(bis(tris(Ethylenediamine)-cobalt(iii)) bis(μ_2-chloro)-heptachloro-di-lead(ii) chloride
162	GIZLIL01	lel_3	Λ,Δ	*P*-3*c*1	tris(Ethylenediamine-N,N')-cobalt(iii) trichloride tetrahydrate clathrate
163	IRIRAC01	lel_3	Λ,Δ	*P*-3*c*1	tris(Ethylenediamine-N,N')-cobalt(iii) trichloride
164	NIHNEZ01	$oblel_2$	Λ,Δ	$P4_2bc$	tris(ethylenediamine)-cobalt(iii) tetrathioantimonate(v)
165	PIMXIS01	$lelob_2$	Λ	*R*32	tris(1,2-Diaminoethane-N,N')-cobalt(iii) hexachloro-iron hexachloride monohydrate
166	SAETCO01	lel_3	Λ	*P*3	bis[tris(Ethylenediammine)-cobalt(iii) trichloride] sodium chloride hexahydrate
167	TUZGEA01	lel_3	Δ	$P2_12_12_1$	catena-(Δ-tris(Ethylenediamine)-cobalt(iii) tris((μ_2-oxo)-dioxo-vanadium(v)) clathrate
168	TUZGEA02	lel_3	Δ	$P2_12_12_1$	catena-(tris(1,2-Ethylenediamine)-cobalt tris(μ_2-oxo)-hexaoxo-tri-vanadium monohydrate)
169	ZZZAZY10	lel_3	Λ,Δ	$P2_1/n$	Delta,Lambda-bis(tris(Ethylenediamine-N,N)-cobalt) tris(d,l-tartrate) decahydrate

[a] The atomic coordinates for this salt are not available in the CSD, precluding certain assignments. [b] This crystal contained both orientations ($oblel_2$ for the Λ enantiomer, lel_3 for the Δ enantiomer

Table A-3. Dependence of the chemical shifts of the diastereotopic NHH' protons of Λ-(*S*,*S*)-**1**$^{3+}$ 2X^{-}BAr$_f^{-}$ on concentration.

Λ-(*S*,*S*)-**1**$^{3+}$ 2Cl^{-}BAr$_f^{-}$			Λ-(*S*,*S*)-**1**$^{3+}$ 2BF$_4^{-}$BAr$_f^{-}$			Λ-(*S*,*S*)-**1**$^{3+}$ 3BAr$_f^{-}$		
con (M)	δ-NH/C$_3$ (ppm)	δ-NH'/C$_2$ (ppm)	con (M)	δ-NH/C$_3$ (ppm)	δ-NH'/C$_2$ (ppm)	con (M)	δ-NH/C$_3$ (ppm)	δ-NH'/C$_2$ (ppm)
0.00429	8.34	3.77	0.008	6.02	4.20	0.00416	5.54	4.7
0.00857	8.23	3.83	0.016	5.98	4.26	0.00833	5.57	4.73
0.01710	8.07	3.92	0.024	5.93	4.31	0.01250	5.58	4.75
0.02570	7.97	3.99	0.032	5.92	4.36	0.01670	5.60	4.77
0.03430	7.86	4.06	0.048	5.87	4.37	0.02080	5.61	4.77
0.04290	7.79	4.12				0.0250	5.61	4.78
0.05140	7.72	4.15				0.0290	5.62	4.79

Table A-4. Dependence of the chemical shifts of the diastereotopic NHH' protons of Λ-(*S*,*S*)-**1**$^{3+}$ 2Cl^{-}BAr$_f^{-}$ on temperature.

Temperature (° C)	δ-NH/C$_3$ (ppm)	δ-NH'/C$_2$(ppm)
–75	7.37	4.60
–60	7.43	4.58
–45	7.58	4.48
–30	7.75	4.27
–15	7.92	4.10
0	8.08	3.95
23	8.27	3.75
35	8.37	3.65

Table A-5. Summary of crystallographic data for solvates of stereoisomers of $\mathbf{1}^{3+}$ $3Cl^{-}$.

Complex	Λ-(*S*,*S*)-$\mathbf{1}^{3+}$ $3Cl^{-}\cdot 2H_2O$ $\cdot 2CH_3OH$	Δ-(*R*,*R*)-$\mathbf{1}^{3+}$ $3Cl^{-}\cdot H_2O$ $\cdot 3CH_3OH$[a]	Δ-(*S*,*S*)-$\mathbf{1}^{3+}$ $3Cl^{-}$ $\cdot 12.5H_2O$
empirical formula	$C_{44}H_{60}Cl_3CoN_6O_4$	$C_{44.88}H_{61.54}Cl_3CoN_6O_{3.88}$[a]	$C_{84}H_{146}Cl_6Co_2N_{12}O_{25}$[b]
formula weight	902.26	912.60	2054.69[b]
temperature of collection [K]	110(2)	110(2)	110(2)
diffractometer	Bruker APEX 2	Bruker GADDS	Bruker GADDS
wavelength [Å]	0.71073	1.54178	1.54178
crystal system	tetragonal	tetragonal	monoclinic
space group	P4(3)	P4(1)	P2(1)
unit cell dimensions:			
a [Å]	13.839(4)	13.8725(7)	12.0877(6)
b [Å]	13.839(4)	13.8725(7)	25.0985(14)
c [Å]	24.216(9)	24.3173(13)	16.8235(8)
α [deg]	90	90	90
β [deg]	90	90	90.887(3)
γ [deg]	90	90	90
V [$Å^3$]	4638(2)	4679.8(4)	5103.4(5)
Z	4	4	2[b]
ρ_{calc} [Mg/m^3]	1.292	1.295	1.337
Absorption coefficient [mm^{-1}]	0.590	4.822	4.607
F(000)	1904	1928	2180
crystal size [mm^3]	0.60 × 0.10 × 0.10	0.12 × 0.08 × 0.04	0.16 × 0.15 × 0.07
Θ [deg]	2.23 to 27.49	3.19 to 60.00	2.63 to 60.00
range / indices (*h*, *k*, *l*)	–17,17; –17,17; –31,31	–15,15; –15,15; –25,26	–13,13; –28,27; –18,18

reflections collected	70126	65183	112447
independent reflections	10535 [R(int) = 0.0425]	6282 [R(int) = 0.0647]	14790 [R(int) = 0.0916]
completeness to Θ = 27.49°	99.7%	98.5%	99.9%
absorption correction	semiempirical from equivalents	semiempirical from equivalents	semiempirical from equivalents
max. and min. transmission	0.9434 and 0.7187	0.8305 and 0.5953	0.7386 and 0.5260
refinement method	full-matrix least-squares on F^2	full-matrix least-squares on F^2	full-matrix least-squares on F^2
data / restraints / parameters	10535 / 7 / 525	6282 / 21 / 546	14790 / 265 / 1105
goodness-of-fit on F^2	1.059	1.071	1.149
final R indices [I>2σ(I)]	$R1$ = 0.0442, w$R2$ = 0.1171	$R1$ = 0.0407, w$R2$ = 0.0841	$R1$ = 0.0746, w$R2$ = 0.1791
R indices (all data)	$R1$ = 0.0501, w$R2$ = 0.1220	$R1$ = 0.0510, w$R2$ = 0.0871	$R1$ = 0.0807, w$R2$ = 0.1830
absolute structure parameter	0.000(12)	0.012(4)	0.069(5)
largest diff. peak and hole [e Å^{-3}]	0.945 / –0.255	0.362 / –0.622	0.972 / –0.698

[a]This salt is presented, for simplicity, as a tris(CH_3OH) solvate; however, as detailed in the experimental section, one CH_3OH molecule refined to an occupancy of 0.88. [b]For the asymmetric unit; see experimental section.

Table A-6. Key interatomic distances (Å) and angles (°) in crystallographically characterrized complexes.[a]

atoms	Λ-(*S*,*S*)-**1**$^{3+}$ 3Cl$^-$ ·2H_2O·2CH_3OH	trication A[b]	trication B[b]	Δ-(*R*,*R*)-**1**$^{3+}$ 3Cl$^-$ ·H_2O·3CH_3OH
Co1-N1	1.910(2)	1.967(6)	1.976(5)	1.962(3)
Co1-N2	1.975(3)	1.961(6)	1.959(6)	1.989(3)
Co1-N3	1.985(2)	1.954(5)	1.955(6)	1.957(3)
Co1-N4	1.963(2)	1.958(6)	1.950(6)	1.967(3)
Co1-N5	1.963(3)	1.963(6)	1.973(7)	1.989(3)
Co1-N6	1.949(3)	1.949(5)	1.963(6)	1.970(3)
N1-C1	1.492(4)	1.488(9)	1.501(9)	1.484(5)
N2-C8	1.511(4)	1.489(9)	1.505(9)	1.483(5)
N3-C15	1.509(3)	1.475(9)	1.486(9)	1.506(5)
N4-C22	1.502(4)	1.502(9)	1.495(9)	1.511(5)
N5-C29	1.498(4)	1.494(9)	1.491(10)	1.504(5)
N6-C36	1.506(4)	1.508(9)	1.489(10)	1.504(5)
N1···Cl1	3.194(3)	3.3604(1)	-	3.279(3)
N3···Cl1	3.428(3)	3.2343(2)	-	3.194(3)
N5···Cl1	3.269(3)	3.2762(1)	-	3.445(3)
N2···Cl3	3.259(3)	3.2403(1)	3.3656(1)	3.208(3)
N4···Cl3	3.198(3)	3.2363(1)	3.2062(2)	3.265(3)
N6···Cl3	3.195(3)	3.3277(2)	3.2268(1)	3.220(3)
N5···Cl2	3.231(3)	4.2407(2)	-	3.327(4)
N4···Cl2	3.266(3)	3.2458(2)	-	3.202(3)
N1H···Cl1	2.313	2.6254		2.437
N3H···Cl1	2.606	2.5448		2.346
N5H···Cl1	2.436	2.5689		2.634
N2H···Cl3	2.379	2.5258	2.6708	2.324
N4H···Cl3	2.376	2.4211	2.5065	2.379
N6H···Cl3	2.364	2.6166	2.4632	2.398
N5H···Cl2	2.386	3.8632	-	2.498
N4H···Cl2	2.387	2.4074	-	2.356
N3-Co1-N6	172.7(1)	175.2(2)	174.7(3)	172.66(14)

N1-Co1-N4	172.7(1)	175.5(2)	175.1(3)	171.66(13)
N2-Co1-N5	171.9(1)	175.3(2)	175.4(3)	171.62(14)
N3-Co1-N1	90.9(1)	92.3(2)	91.8(2)	90.95(14)
N3-Co1-N2	96.3(1)	91.4(2)	90.8(3)	94.98(14)
N3-Co1-N4	84.4(1)	84.4(2)	84.4(2)	84.56(13)
N3-Co1-N5	90.5(1)	92.7(2)	92.2(2)	91.07(13)
N6-Co1-N1	94.7(1)	92.1(2)	92.3(2)	94.39(14)
N6-Co1-N2	89.0(1)	91.0(2)	92.8(2)	90.60(14)
N6-Co1-N4	90.5(1)	91.3(2)	91.7(2)	90.74(13)
N6-Co1-N5	84.6(1)	85.1(2)	84.5(3)	83.87(12)
N1-Co1-N2	84.3(1)	84.7(2)	84.8(2)	83.76(14)
N2-Co1-N4	90.7(1)	92.3(2)	92.2(2)	89.62(14)
N4-Co1-N5	94.3(1)	90.5(2)	91.5(2)	96.72(14)
N5-Co1-N1	91.3(1)	92.7(2)	91.6(2)	90.37(14)
N1–H···Cl1	165.5	137.35		155.7
N3–H···Cl1	152.4	132.09		156.9
N5–H···Cl1	154.0	134.07		150.5
N2–H···Cl3	165.8	134.78	132.9	161.2
N4–H···Cl3	152.2	147.71	133.1	168.2
N6–H···Cl3	153.6	134.60	140.5	151.9
N5–H···Cl2	156.3	108.14	-	153.2
N4–H···Cl2	165.5	151.51	-	156.6

[a] The atoms are numbered such that for each salt, N1, N3, and N5 define one of the C_3 NH faces to which a chloride anion is hydrogen bonded, and N2, N4, and N6 the other. [b] These values are for one of the two independent trications of Δ-(*S*,*S*)-$\mathbf{1}^{3+}$ $3Cl^-$ in the unit cell. These are distinguished by a different H_2O hydrogen bonding pattern.

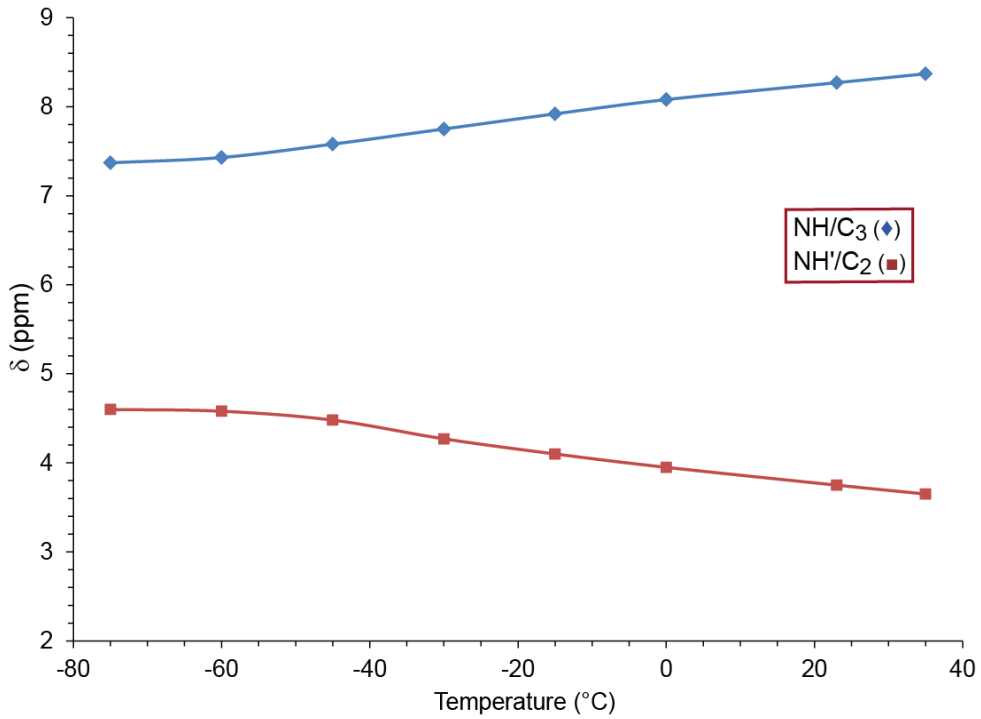

Figure A-1. Dependence of the chemical shifts of the diastereotopic NHH' protons of Λ-(*S*,*S*)-**1**$^{3+}$ 2Cl^{-}BAr$_f^{-}$ on temperature.

(a)

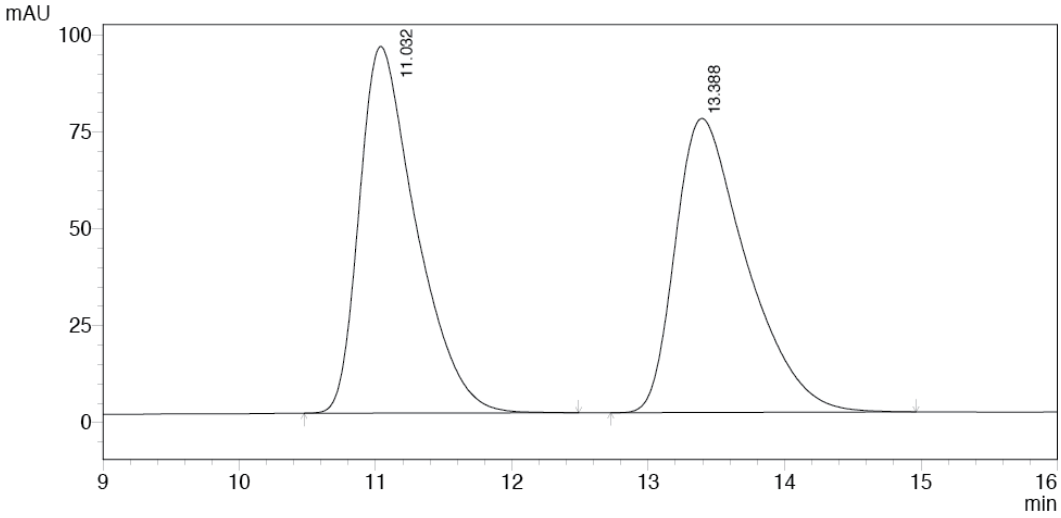

PDA 220nm

Peak#	Ret. Time	Area	Height	Area %	Height %
1	11.032	2745001	94604	49.931	55.488
2	13.388	2752610	75890	50.069	44.512
Total		5497611	170494	100.000	100.000

(b)

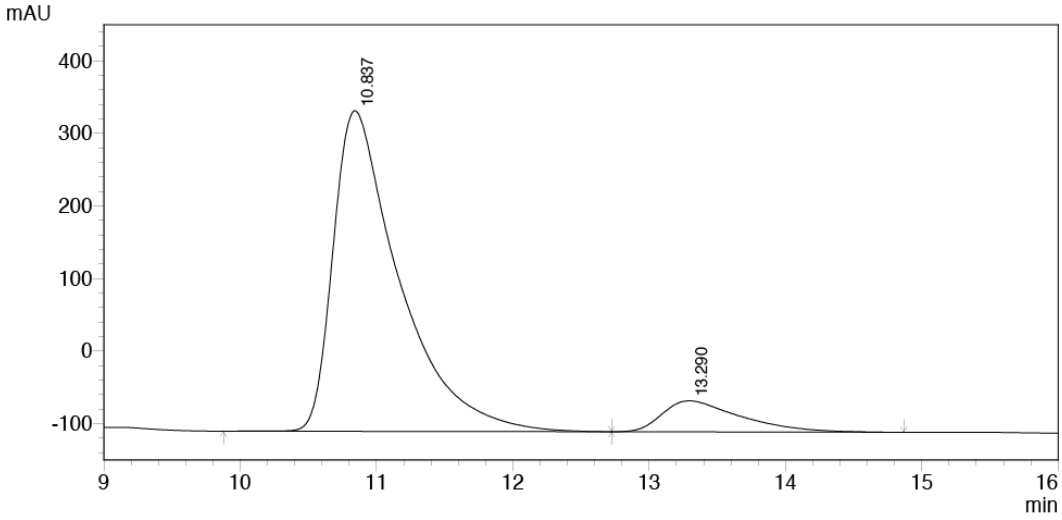

PDA 220nm

Peak#	Ret. Time	Area	Height	Area %	Height %
1	10.837	14897274	441745	89.745	91.162
2	13.290	1702201	42826	10.255	8.838
Total		16599476	484571	100.000	100.000

Figure A-2. HPLC traces of **23a<u>a</u>** (Scheme 4.3, entry 1): (a) racemic sample; (b) catalyzed by Λ-(*S*,*S*)-$\mathbf{1}^{3+}$ $2Cl^{-}BAr_f^{-}$.

(a)

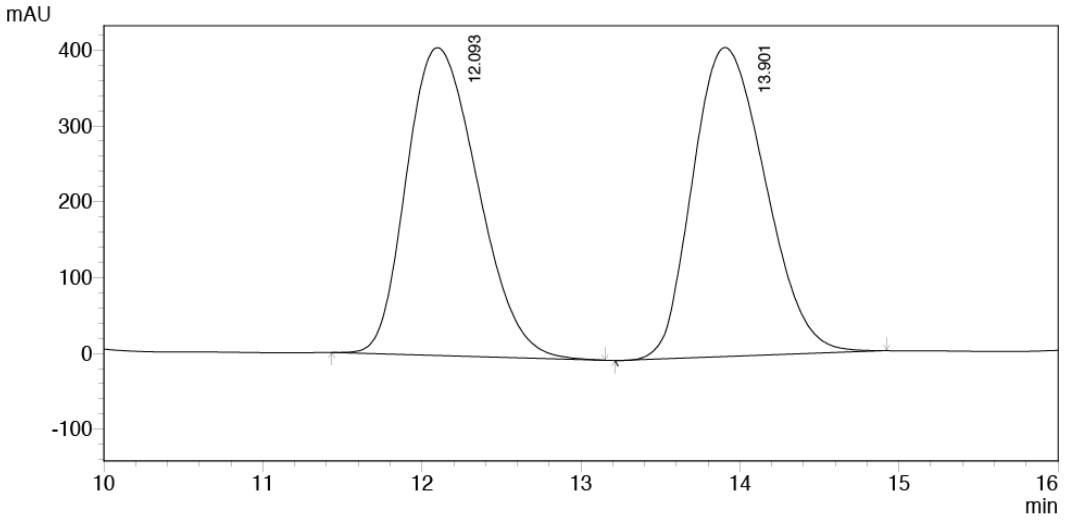

PDA 220nm

Peak#	Ret. Time	Area	Height	Area %	Height %
1	12.093	12661766	405824	49.414	49.903
2	13.901	12962212	407395	50.586	50.097
Total		25623977	813219	100.000	100.000

(b)

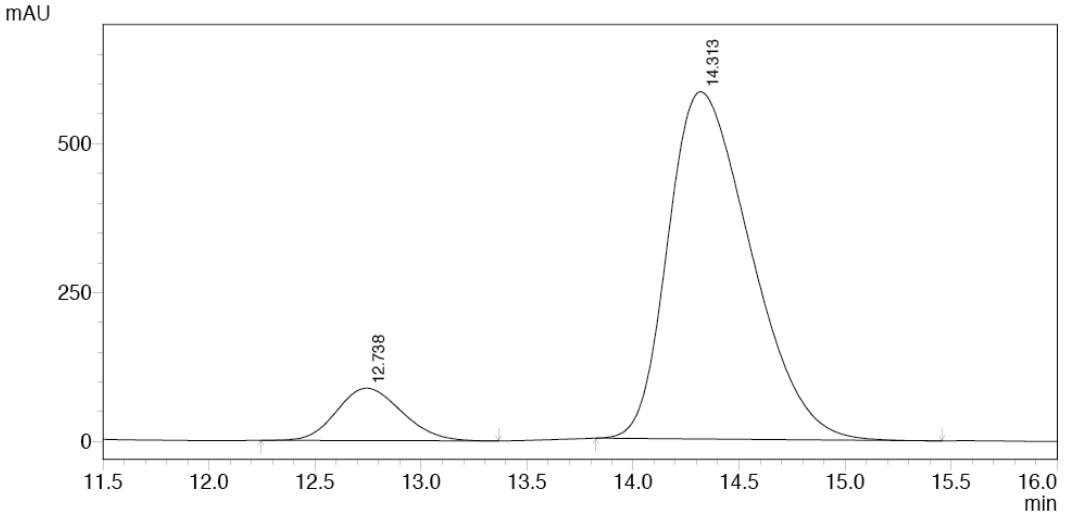

PDA 220nm

Peak#	Ret. Time	Area	Height	Area %	Height %
1	12.738	1877941	87934	10.619	13.108
2	14.313	15806284	582897	89.381	86.892
Total		17684225	670831	100.000	100.000

(c)

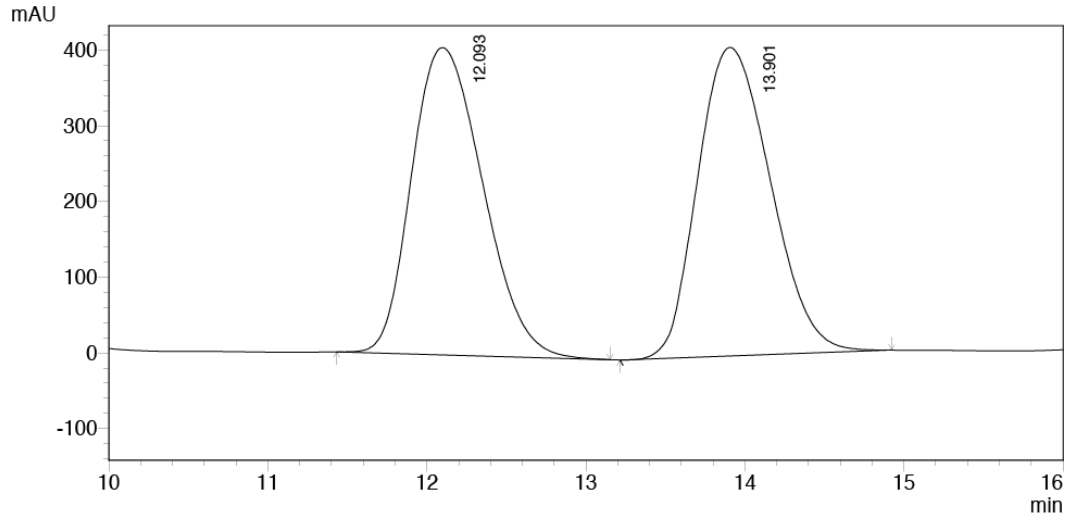

PDA 220nm

Peak#	Ret. Time	Area	Height	Area %	Height %
1	12.093	12661766	405824	49.414	49.903
2	13.901	12962212	407395	50.586	50.097
Total		25623977	813219	100.000	100.000

(d)

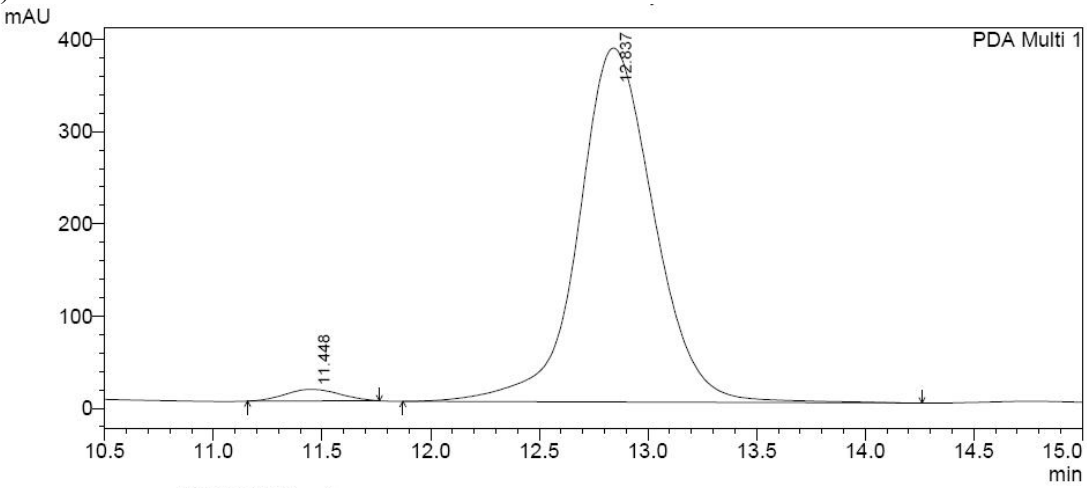

PDA Ch1 220nm 4nm

Peak#	Ret. Time	Area	Height	Area %	Height %
1	11.448	220671	12690	2.312	3.197
2	12.837	9325694	384240	97.688	96.803
Total		9546365	396930	100.000	100.000

Figure A-3. HPLC traces of **23ab** (Scheme 4.3, entry 3): (a) racemic sample; (b) catalyzed by Λ-(*S*,*S*)-$\mathbf{1}^{3+}$ $2Cl^{-}BAr_f^{-}$. For Scheme 7.4 (c) racemic sample; (d) catalyzed by Λ-$\mathbf{27c}^{3+}$ $3BAr_f^{-}$.

(a)

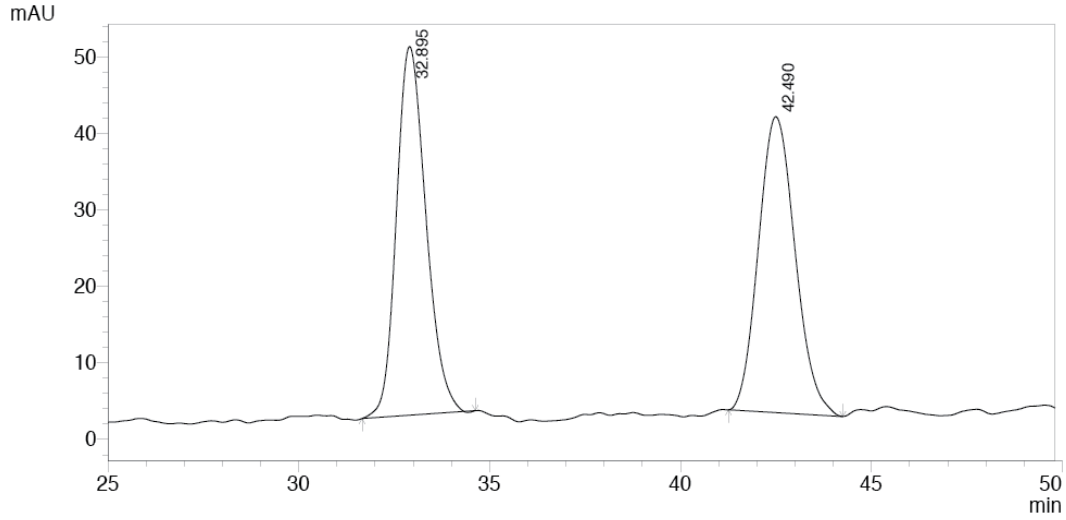

PDA 220nm

Peak#	Ret. Time	Area	Height	Area %	Height %
1	32.895	2592054	48187	49.983	55.472
2	42.490	2593793	38681	50.017	44.528
Total		5185847	86867	100.000	100.000

(b)

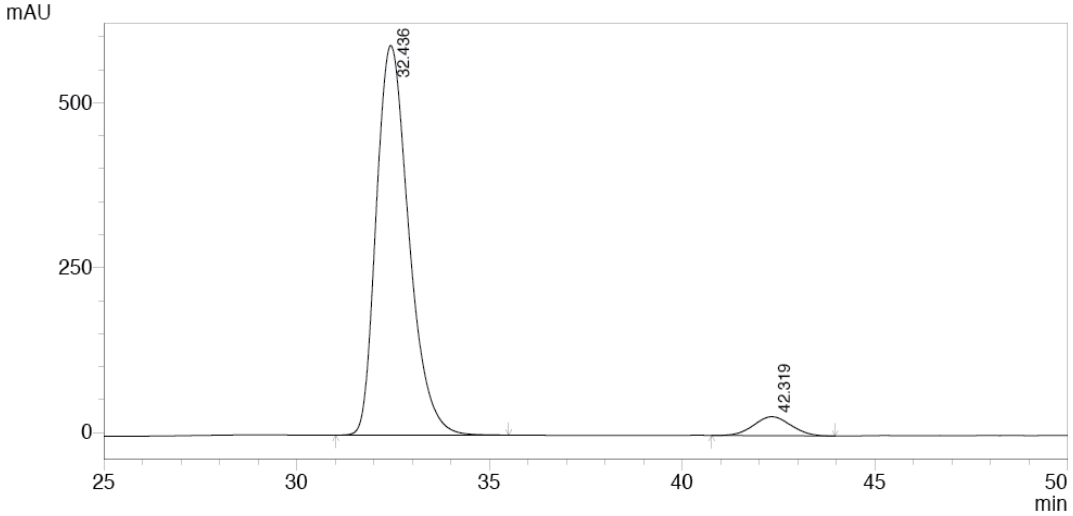

PDA 220nm

Peak#	Ret. Time	Area	Height	Area %	Height %
1	32.436	34674163	590859	94.706	95.343
2	42.319	1938180	28862	5.294	4.657
Total		36612343	619722	100.000	100.000

(c)

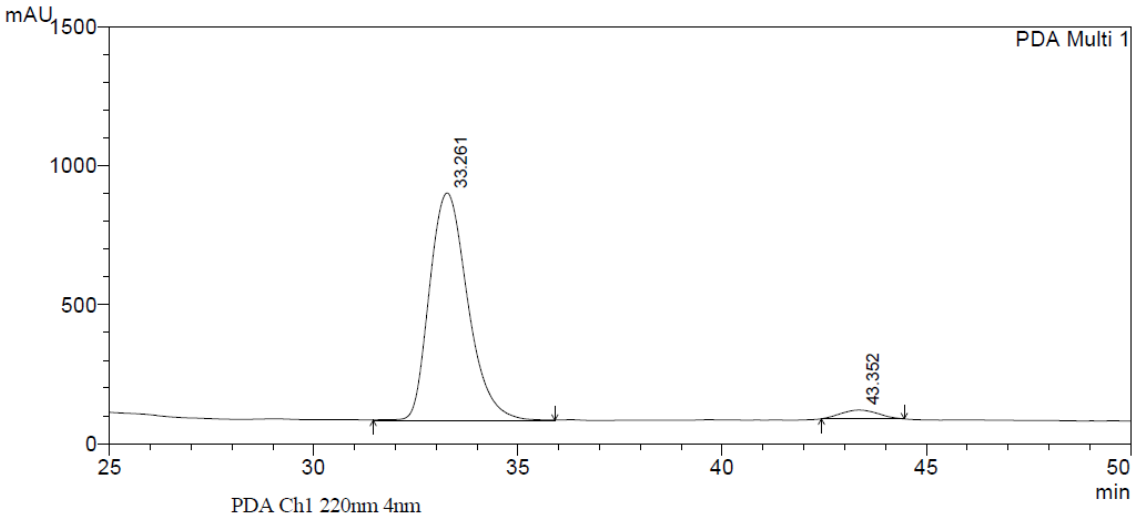

PDA Ch1 220nm 4nm

Peak#	Ret. Time	Area	Height	Area %	Height %
1	33.261	53520336	818591	96.395	96.248
2	43.352	2001490	31911	3.605	3.752
Total		55521826	850502	100.000	100.000

(d)

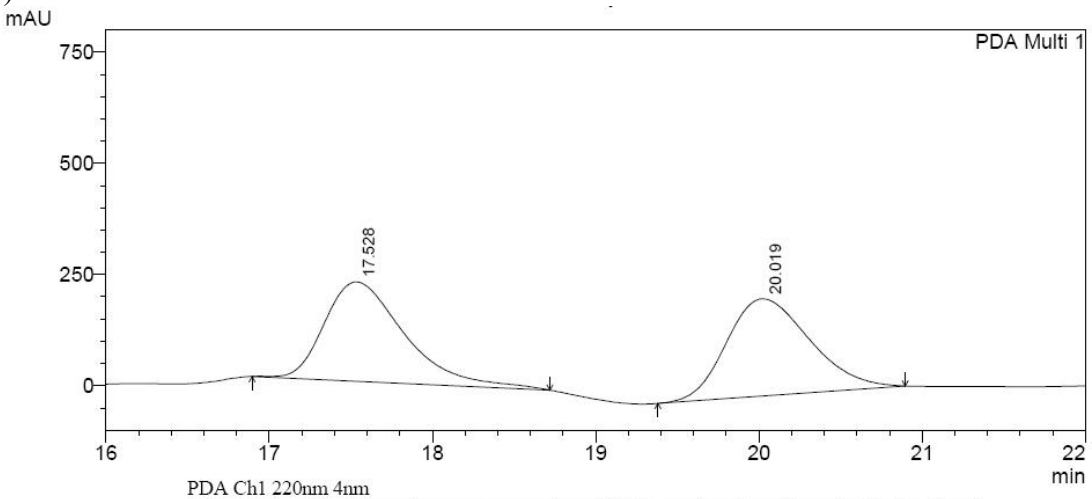

PDA Ch1 220nm 4nm

Peak#	Ret. Time	Area	Height	Area %	Height %
1	17.528	7605900	223271	49.450	50.511
2	20.019	7775022	218750	50.550	49.489
Total		15380922	442021	100.000	100.000

(e)

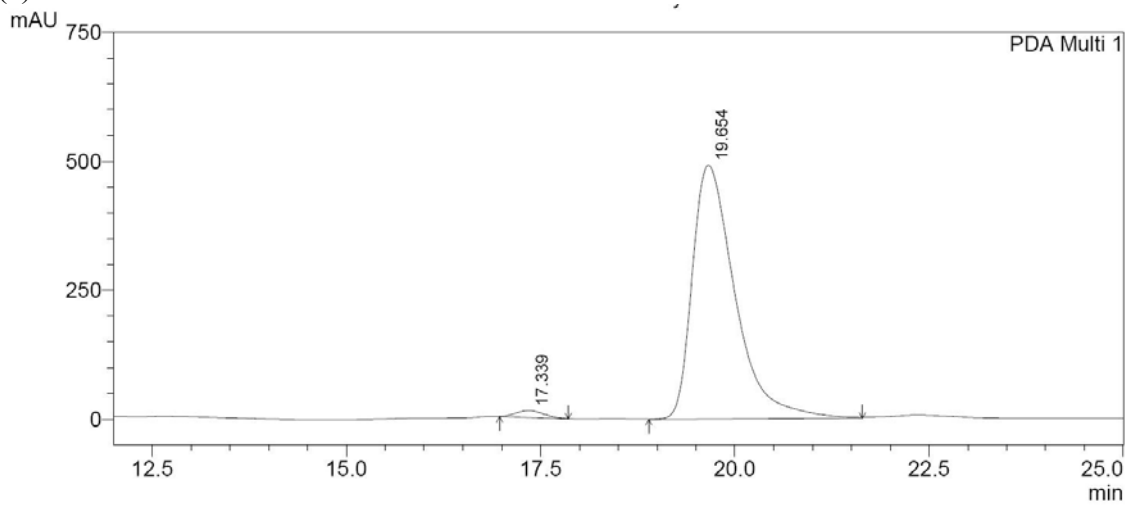

PDA Ch1 220nm 4nm

Peak#	Ret. Time	Area	Height	Area %	Height %
1	17.339	327538	13281	1.705	2.626
2	19.654	18884533	492519	98.295	97.374
Total		19212071	505800	100.000	100.000

Figure A-4. HPLC traces of **23ac** (Scheme 4.4, entry 1, Chiralcel OD column): (a) racemic sample; (b) catalyzed by Λ-(*S*,*S*)-$\mathbf{1}^{3+}$ $2BF_4^-BAr_f^-$; (c) catalyzed by Λ-(*S*,*S*)-$\mathbf{1}^{3+}3BF_4^-$; (d) racemic sample (Chiralpak AS-H column); (e) catalyzed by Λ-$\mathbf{27c}^{3+}$ $3BAr_f^-$ (Scheme 7.4, Chiralpak AS-H column).

(a)

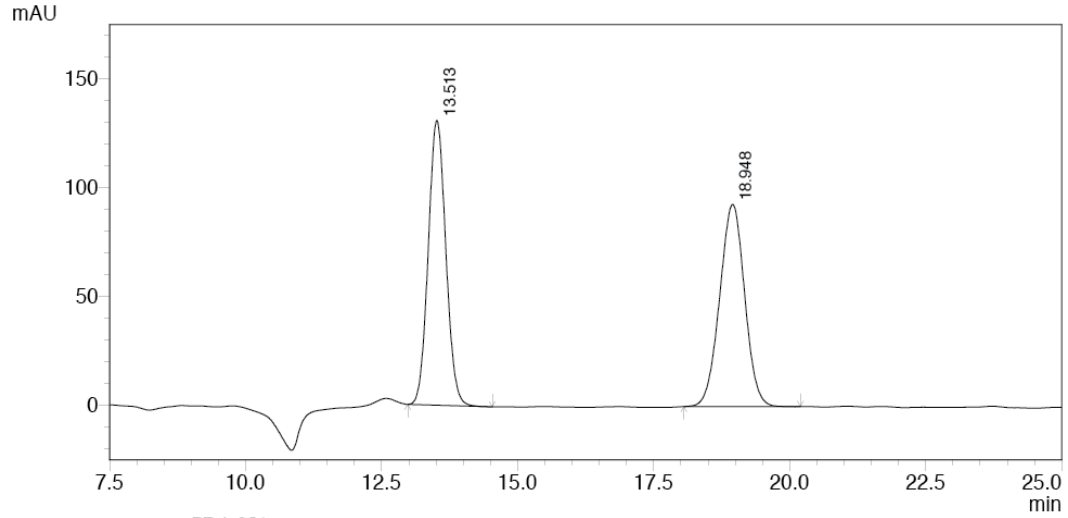

PDA 254nm

Peak#	Ret. Time	Area	Height	Area %	Height %
1	13.513	2941994	130912	49.780	58.498
2	18.948	2967956	92876	50.220	41.502
Total		5909950	223789	100.000	100.000

(b)

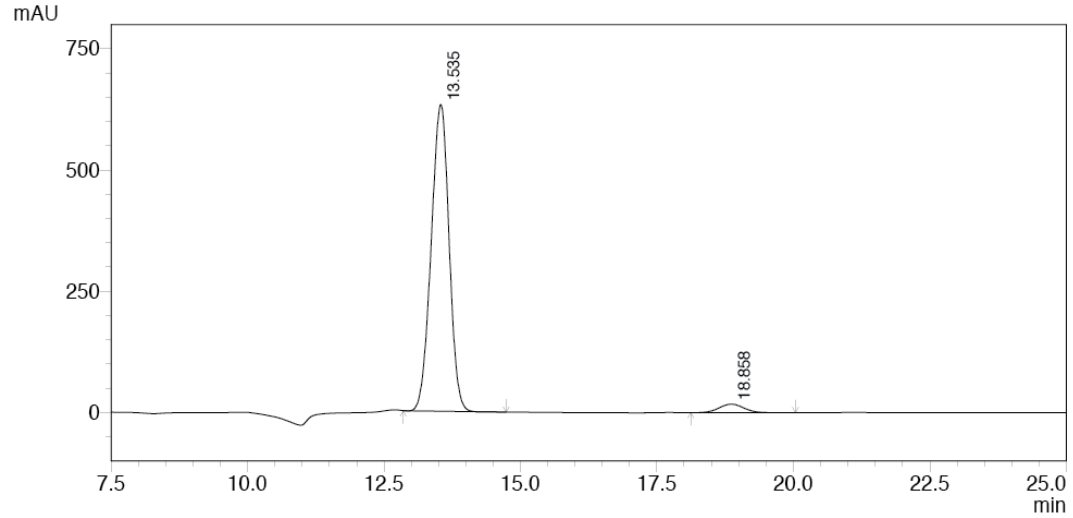

PDA 254nm

Peak#	Ret. Time	Area	Height	Area %	Height %
1	13.535	14427103	632667	96.261	97.288
2	18.858	560393	17639	3.739	2.712
Total		14987496	650305	100.000	100.000

(c)

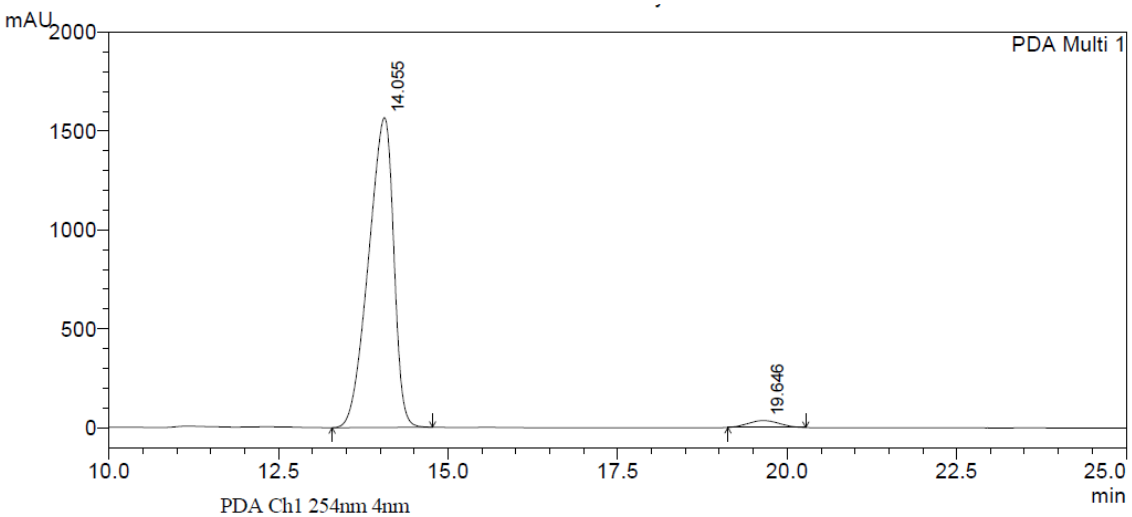

PDA Ch1 254nm 4nm

Peak#	Ret. Time	Area	Height	Area %	Height %
1	14.055	40487308	1566198	97.320	97.810
2	19.646	1114899	35065	2.680	2.190
Total		41602207	1601263	100.000	100.000

(d)

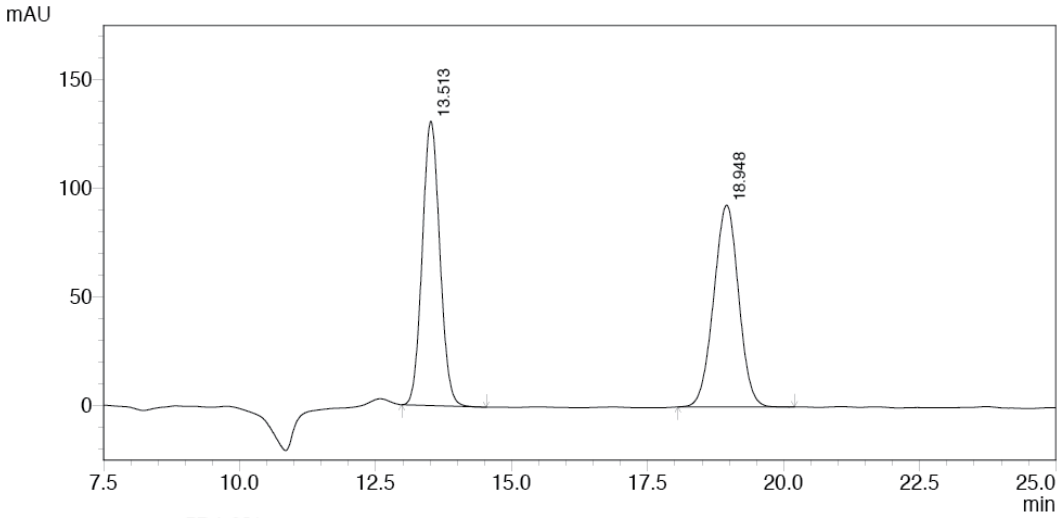

PDA 254nm

Peak#	Ret. Time	Area	Height	Area %	Height %
1	13.513	2941994	130912	49.780	58.498
2	18.948	2967956	92876	50.220	41.502
Total		5909950	223789	100.000	100.000

(e)

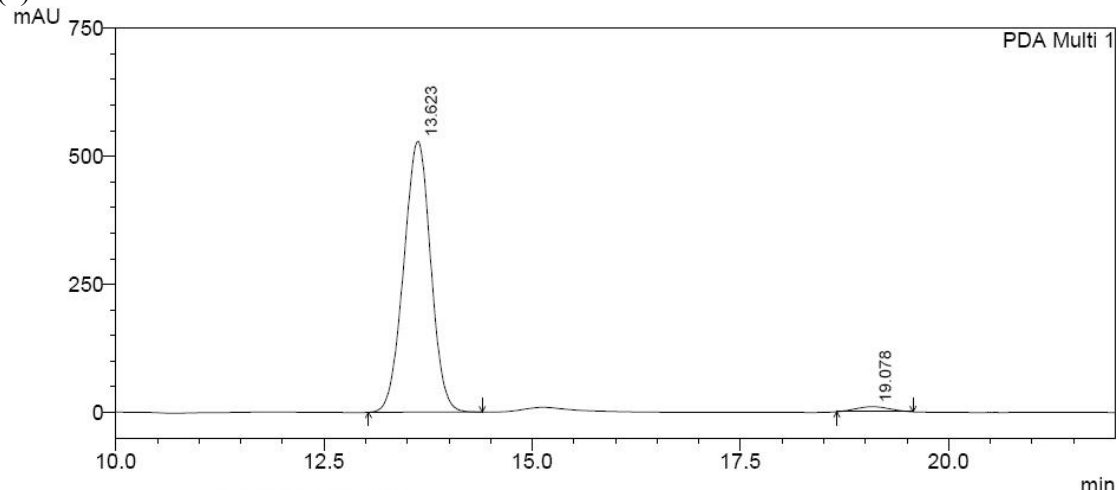

PDA Ch1 254nm 4nm

Peak#	Ret. Time	Area	Height	Area %	Height %
1	13.623	11935915	528561	97.757	98.195
2	19.078	273876	9715	2.243	1.805
Total		12209791	538276	100.000	100.000

Figure A-5. HPLC traces of **23bc** (Scheme 4.4, entry 2): (a) racemic sample; (b) catalyzed by Λ-(*S*,*S*)-**1**$^{3+}$ 2$BF_4^-$$BAr_f^-$; (c) catalyzed by Λ-(*S*,*S*)-**1**$^{3+}$3BF_4^-. For Scheme 7.4 (d) racemic sample; (e) catalyzed by Λ-**27c**$^{3+}$ 3BAr_f^-.

(a)

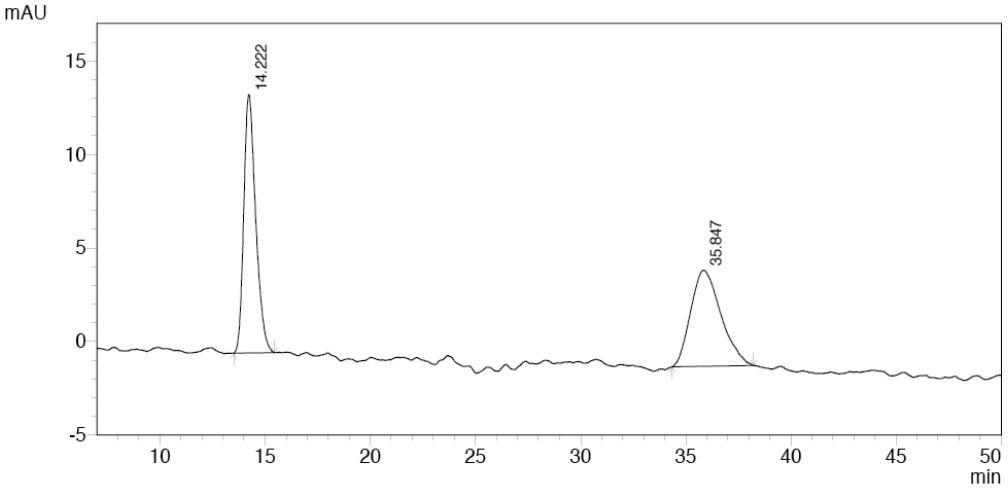

PDA 254nm

Peak#	Ret. Time	Area	Height	Area %	Height %
1	14.222	545650	13812	51.472	72.833
2	35.847	514433	5152	48.528	27.167
Total		1060083	18965	100.000	100.000

(b)

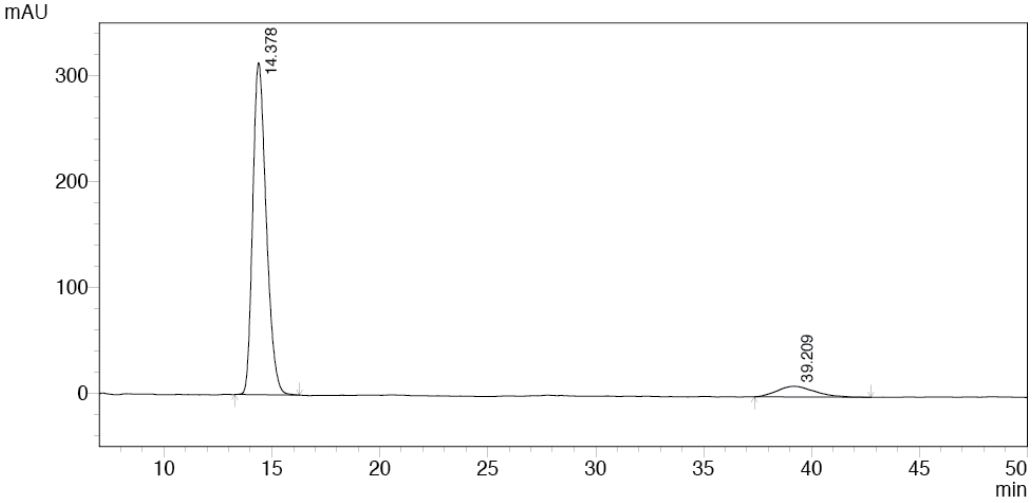

PDA 254nm

Peak#	Ret. Time	Area	Height	Area %	Height %
1	14.378	13650190	313478	91.924	96.896
2	39.209	1199200	10041	8.076	3.104
Total		14849390	323518	100.000	100.000

(c)

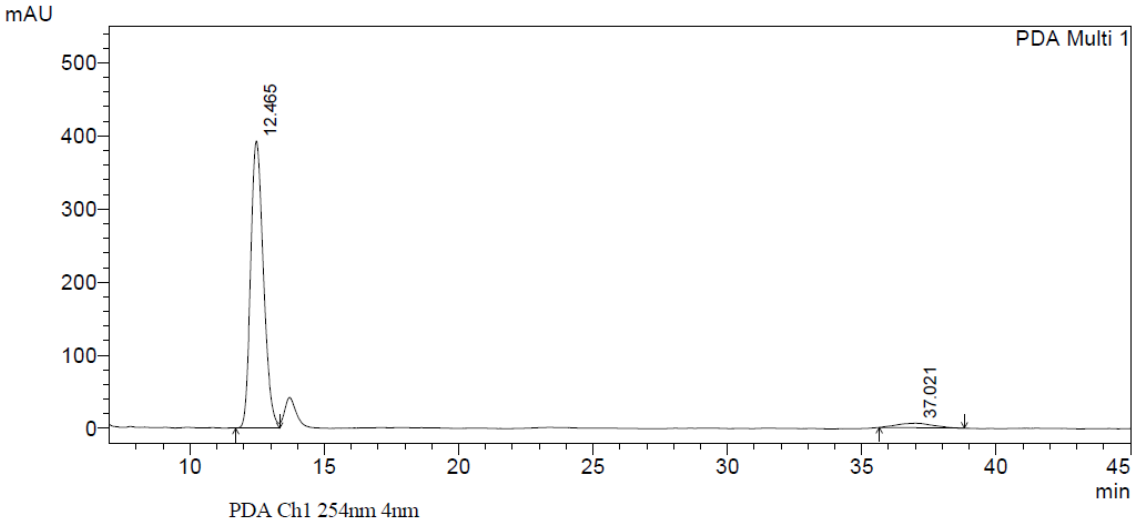

PDA Ch1 254nm 4nm

Peak#	Ret. Time	Area	Height	Area %	Height %
1	12.465	13013612	393149	95.892	98.467
2	37.021	557439	6123	4.108	1.533
Total		13571051	399272	100.000	100.000

Figure A-6. HPLC traces of **23cc** (Scheme 4.4, entry 3): (a) racemic sample; (b) catalyzed by Λ-(*S*,*S*)-$\mathbf{1}^{3+}$ $2BF_4^-BAr_f^-$; (c) catalyzed by Λ-(*S*,*S*)-$\mathbf{1}^{3+}$ $3BF_4^-$ (older column).

(a)

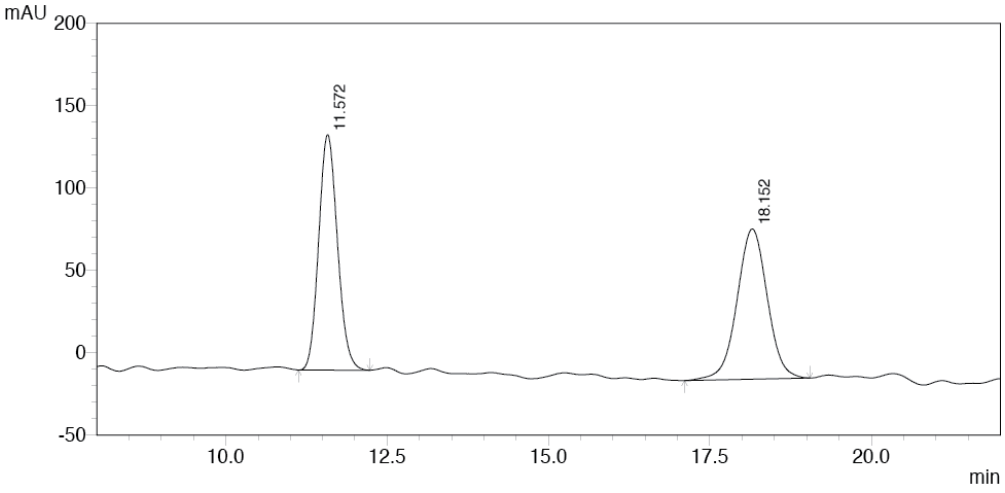

PDA 220nm

Peak#	Ret. Time	Area	Height	Area %	Height %
1	11.572	2892734	142917	49.286	61.046
2	18.152	2976564	91196	50.714	38.954
Total		5869298	234114	100.000	100.000

(b)

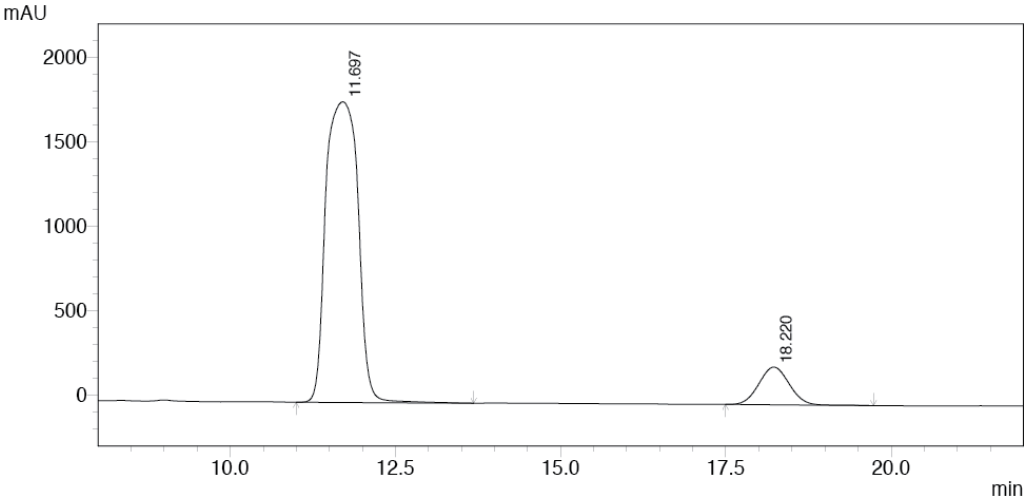

PDA 220nm

Peak#	Ret. Time	Area	Height	Area %	Height %
1	11.697	60314078	1781389	89.351	88.845
2	18.220	7188616	223672	10.649	11.155
Total		67502694	2005061	100.000	100.000

(c)

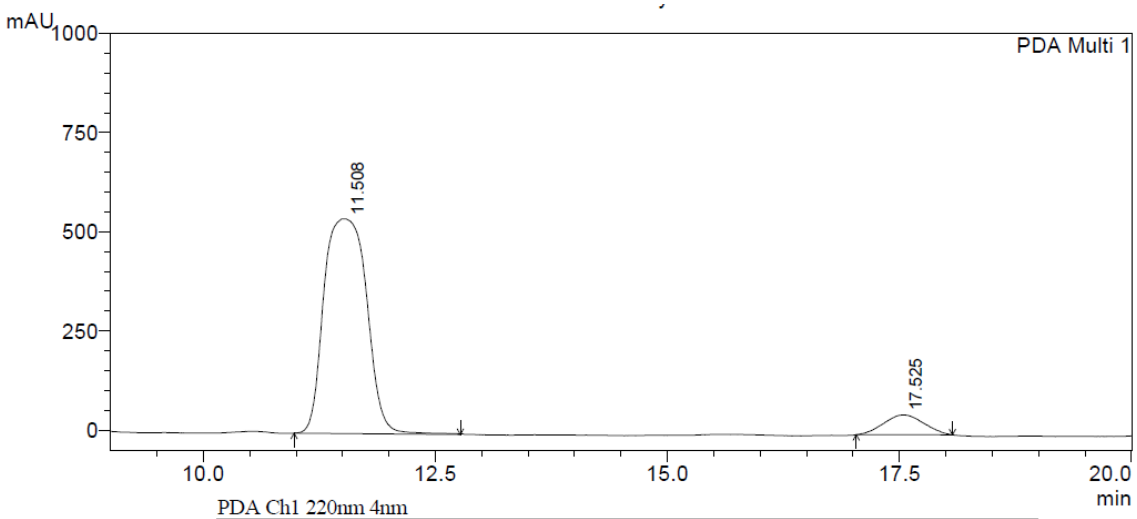

PDA Ch1 220nm 4nm

Peak#	Ret. Time	Area	Height	Area %	Height %
1	11.508	17303657	540750	92.054	91.598
2	17.525	1493635	49601	7.946	8.402
Total		18797292	590351	100.000	100.000

(d)

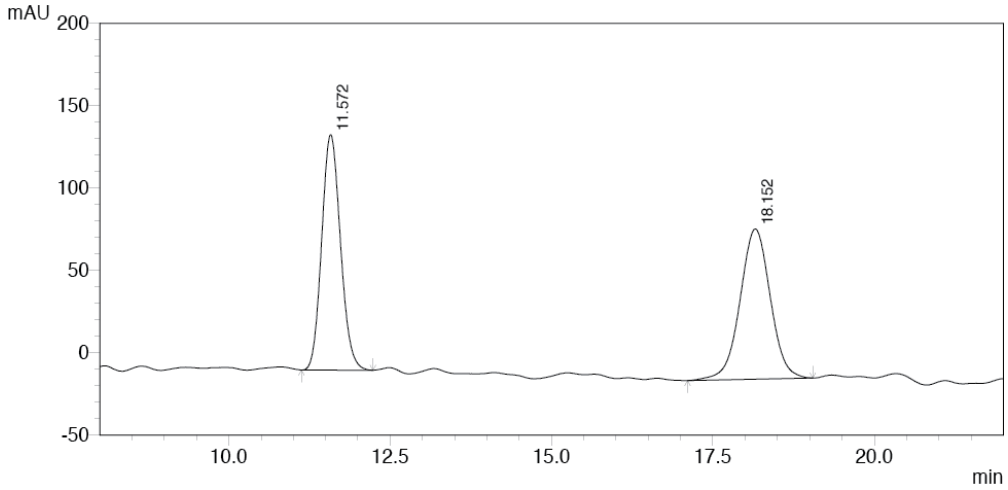

PDA 220nm

Peak#	Ret. Time	Area	Height	Area %	Height %
1	11.572	2892734	142917	49.286	61.046
2	18.152	2976564	91196	50.714	38.954
Total		5869298	234114	100.000	100.000

(e)

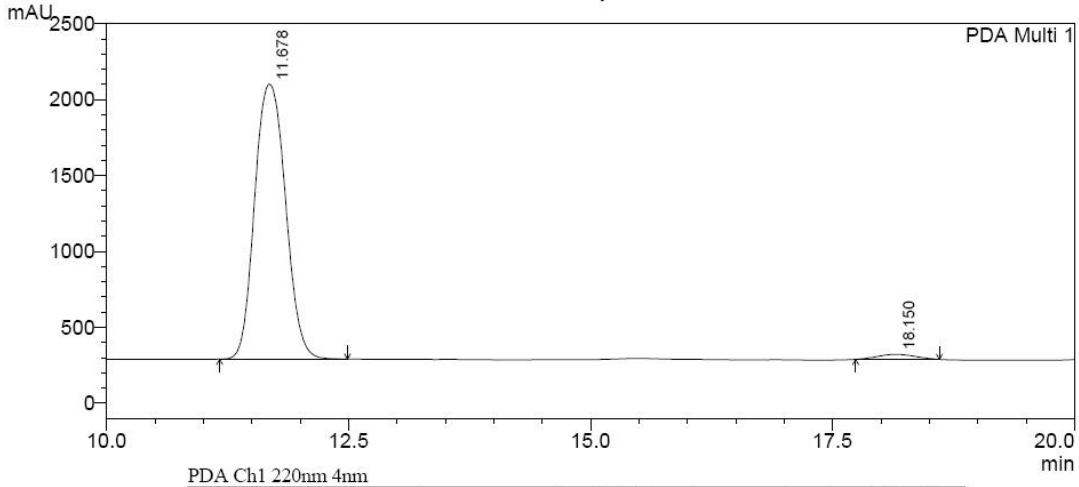

PDA Ch1 220nm 4nm

Peak#	Ret. Time	Area	Height	Area %	Height %
1	11.678	40220611	1810836	97.815	98.197
2	18.150	898357	33258	2.185	1.803
Total		41118968	1844093	100.000	100.000

Figure A-7. HPLC traces of **23dc** (Scheme 4.4, entry 4): (a) racemic sample; (b) catalyzed by Λ-(*S*,*S*)-$\mathbf{1}^{3+}$ $2BF_4^-BAr_f^-$; (c) catalyzed by Λ-(*S*,*S*)-$\mathbf{1}^{3+}$ $3BF_4^-$. For Scheme 7.4 (d) racemic sample; (e) catalyzed by Λ-$\mathbf{27c}^{3+}$ $3BAr_f^-$.

(a)

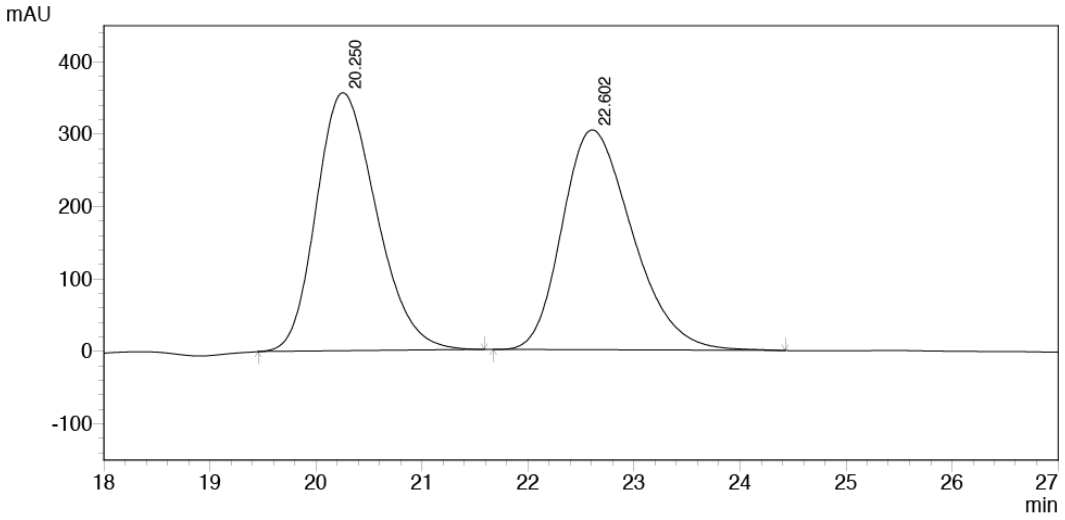

PDA 220nm

Peak#	Ret. Time	Area	Height	Area %	Height %
1	20.250	14034598	356495	50.085	53.998
2	22.602	13986920	303708	49.915	46.002
Total		28021519	660203	100.000	100.000

(b)

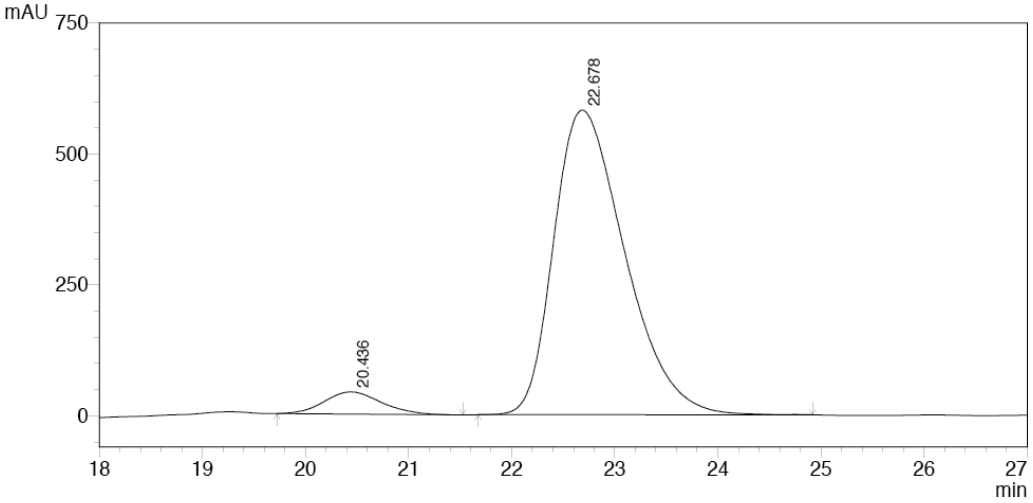

PDA 220nm

Peak#	Ret. Time	Area	Height	Area %	Height %
1	20.436	1637581	42354	5.544	6.785
2	22.678	27899733	581886	94.456	93.215
Total		29537314	624240	100.000	100.000

(c)

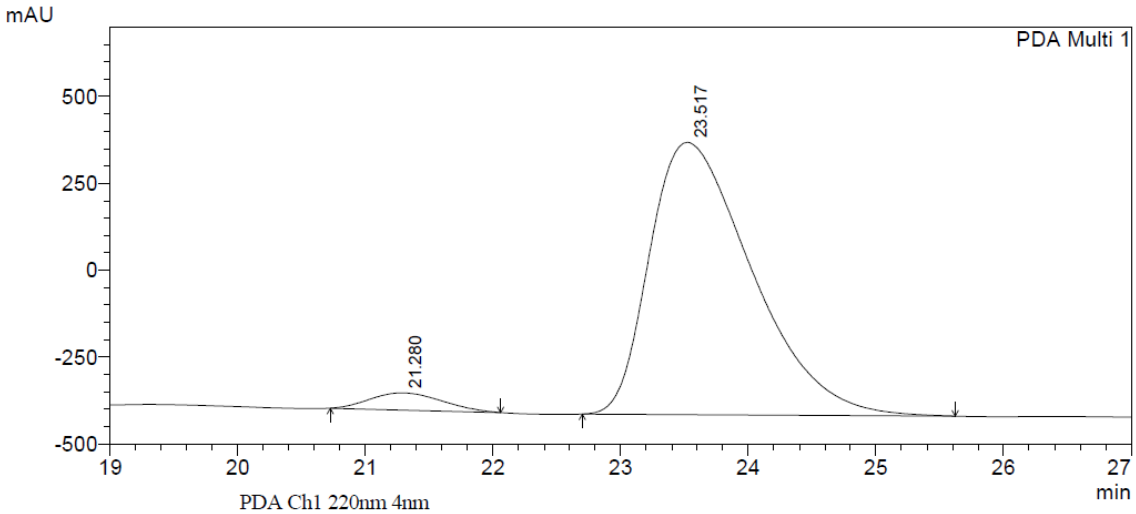

PDA Ch1 220nm 4nm

Peak#	Ret. Time	Area	Height	Area %	Height %
1	21.280	1936609	49425	4.245	5.932
2	23.517	43682241	783840	95.755	94.068
Total		45618850	833265	100.000	100.000

(d)

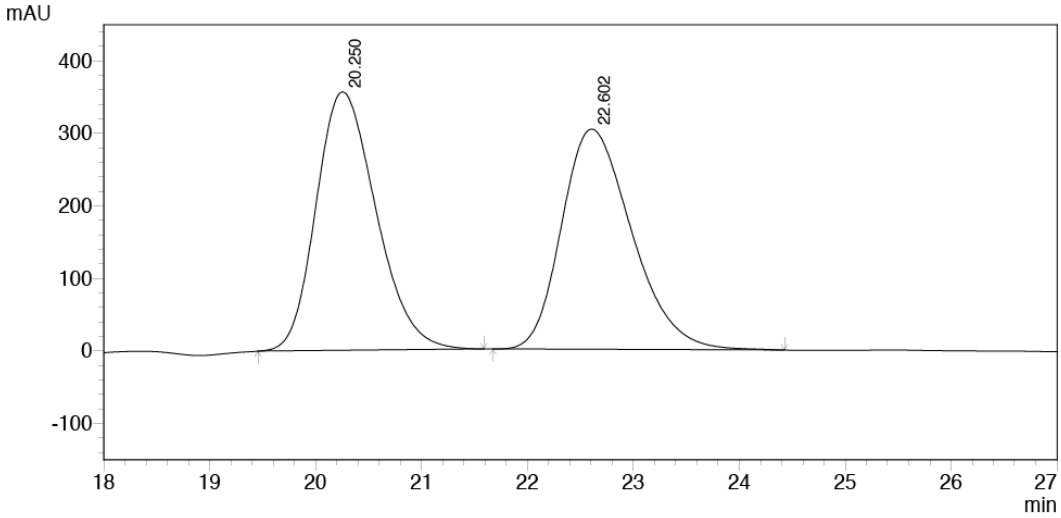

PDA 220nm

Peak#	Ret. Time	Area	Height	Area %	Height %
1	20.250	14034598	356495	50.085	53.998
2	22.602	13986920	303708	49.915	46.002
Total		28021519	660203	100.000	100.000

(e)

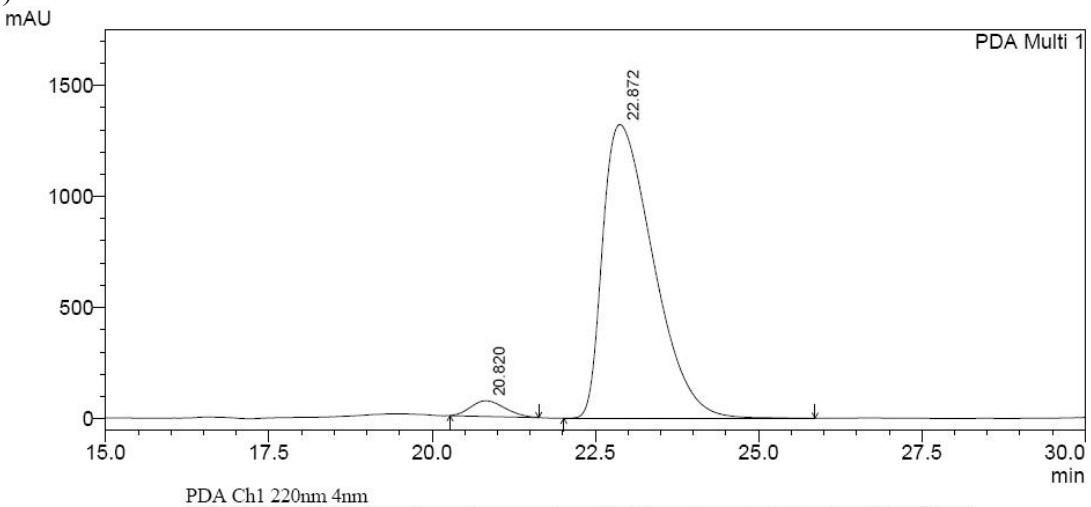

PDA Ch1 220nm 4nm

Peak#	Ret. Time	Area	Height	Area %	Height %
1	20.820	2553734	70202	3.458	5.044
2	22.872	71288723	1321676	96.542	94.956
Total		73842457	1391878	100.000	100.000

Figure A-8. HPLC traces of **23ec** (Scheme 4.4, entry 5): (a) racemic sample; (b) catalyzed by Λ-(*S*,*S*)-$\mathbf{1}^{3+}$ $2BF_4^-BAr_f^-$; (c) catalyzed by Λ-(*S*,*S*)-$\mathbf{1}^{3+}$ $3BF_4^-$. For Scheme 7.4 (d) racemic sample; (e) catalyzed by Λ-$\mathbf{27c}^{3+}$ $3BAr_f^-$.

(a)

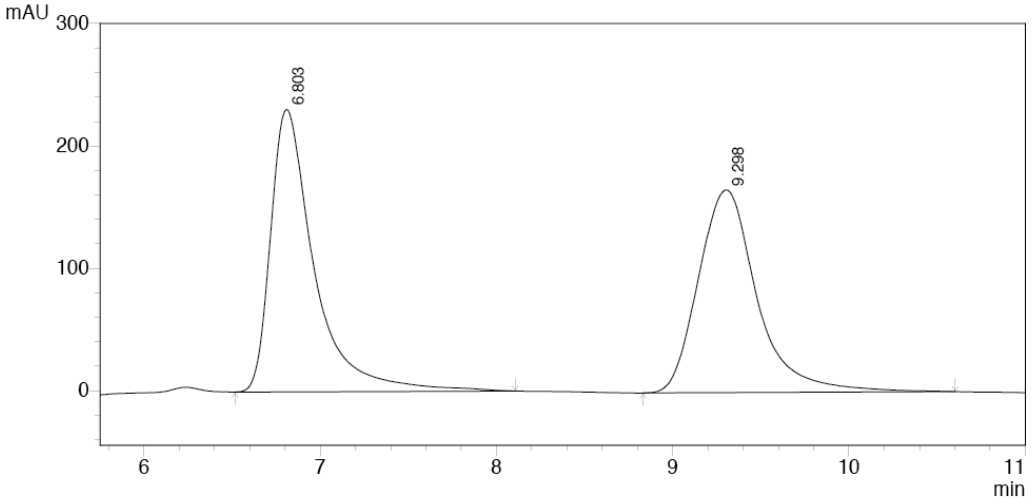

PDA 220nm

Peak#	Ret. Time	Area	Height	Area %	Height %
1	6.803	3983767	230889	50.865	58.208
2	9.298	3848303	165770	49.135	41.792
Total		7832070	396659	100.000	100.000

(b)

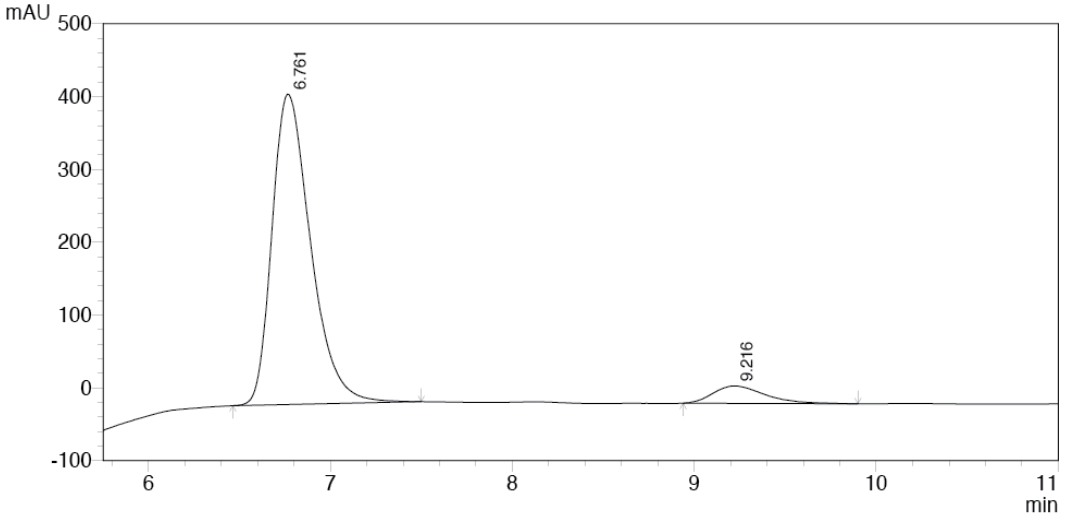

PDA 220nm

Peak#	Ret. Time	Area	Height	Area %	Height %
1	6.761	6296885	426260	93.049	94.722
2	9.216	470397	23751	6.951	5.278
Total		6767282	450011	100.000	100.000

Figure A-9. HPLC traces of **23fc** (Scheme 4.4, entry 6): (a) racemic sample; (b) catalyzed by Λ-(*S*,*S*)-$\mathbf{1}^{3+}$ $2BF_4^-BAr_f^-$.

(a)

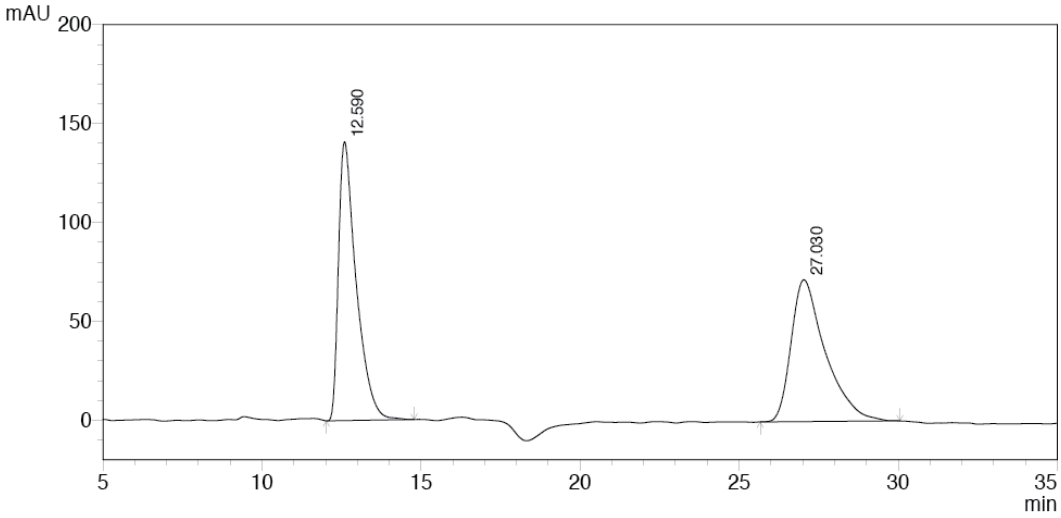

PDA 220nm

Peak#	Ret. Time	Area	Height	Area %	Height %
1	12.590	5460013	141005	50.419	66.304
2	27.030	5369188	71660	49.581	33.696
Total		10829201	212664	100.000	100.000

(b)

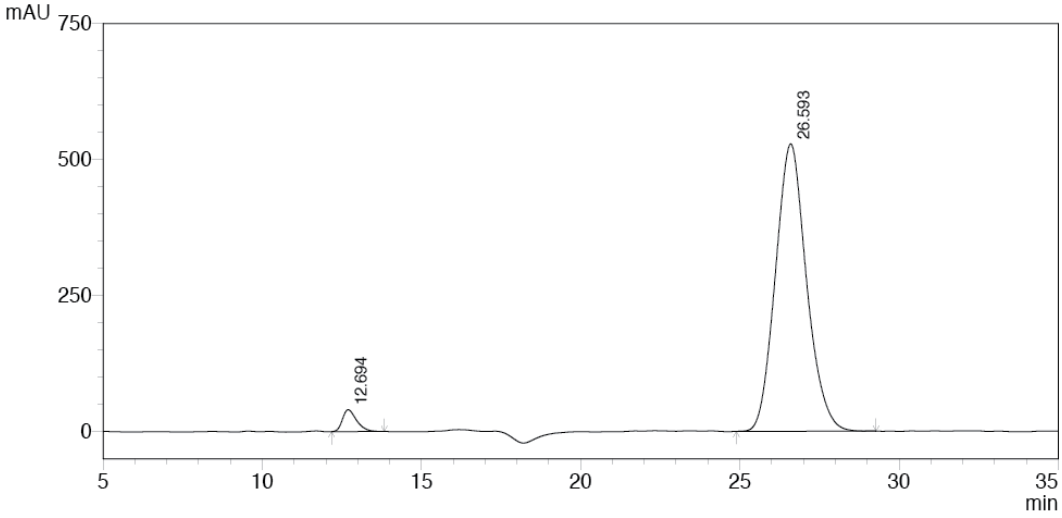

PDA 220nm

Peak#	Ret. Time	Area	Height	Area %	Height %
1	12.694	1238157	40259	3.339	7.083
2	26.593	35848703	528088	96.661	92.917
Total		37086861	568347	100.000	100.000

(c)

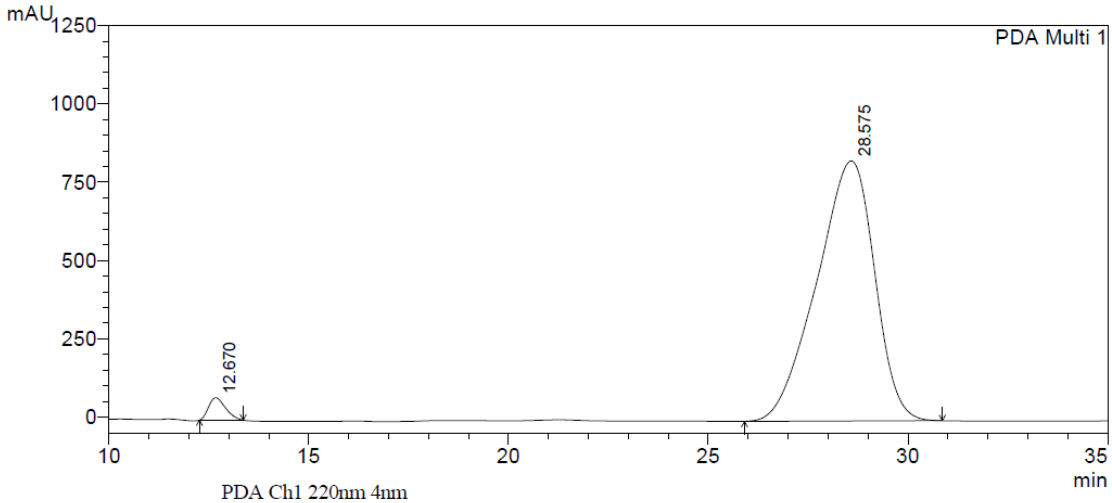

PDA Ch1 220nm 4nm

Peak#	Ret. Time	Area	Height	Area %	Height %
1	12.670	2106599	71450	2.458	7.929
2	28.575	83582140	829703	97.542	92.071
Total		85688739	901153	100.000	100.000

Figure A-10. HPLC traces of **23gc** (Scheme 4.4, entry 7): (a) racemic sample; (b) catalyzed by Λ-(*S*,*S*)-$\mathbf{1}^{3+}$ $2BF_4^-BAr_f^-$; (c) catalyzed by Λ-(*S*,*S*)-$\mathbf{1}^{3+}$ $3BF_4^-$.

(a)

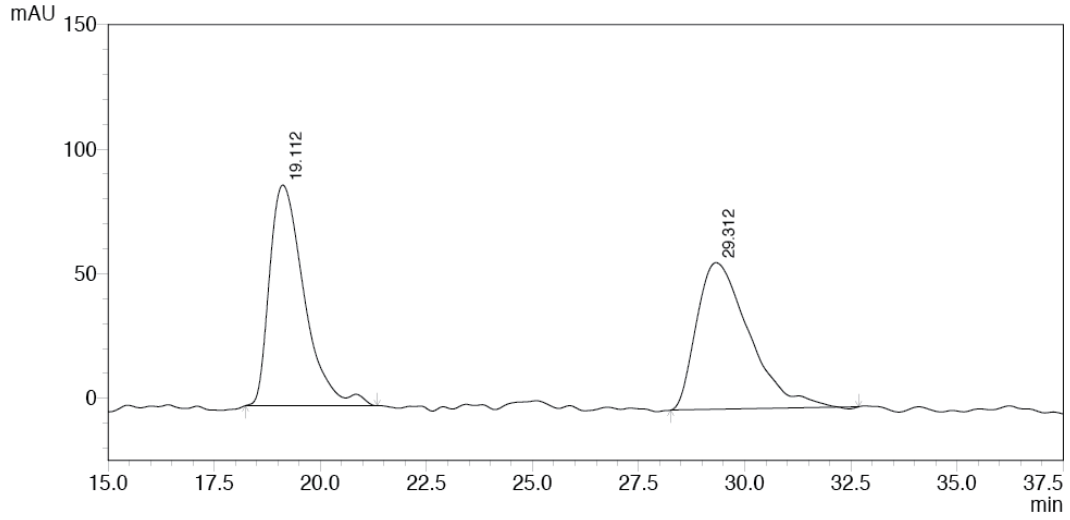

PDA 220nm

Peak#	Ret. Time	Area	Height	Area %	Height %
1	19.112	5040868	88545	49.885	60.058
2	29.312	5064198	58886	50.115	39.942
Total		10105066	147431	100.000	100.000

(b)

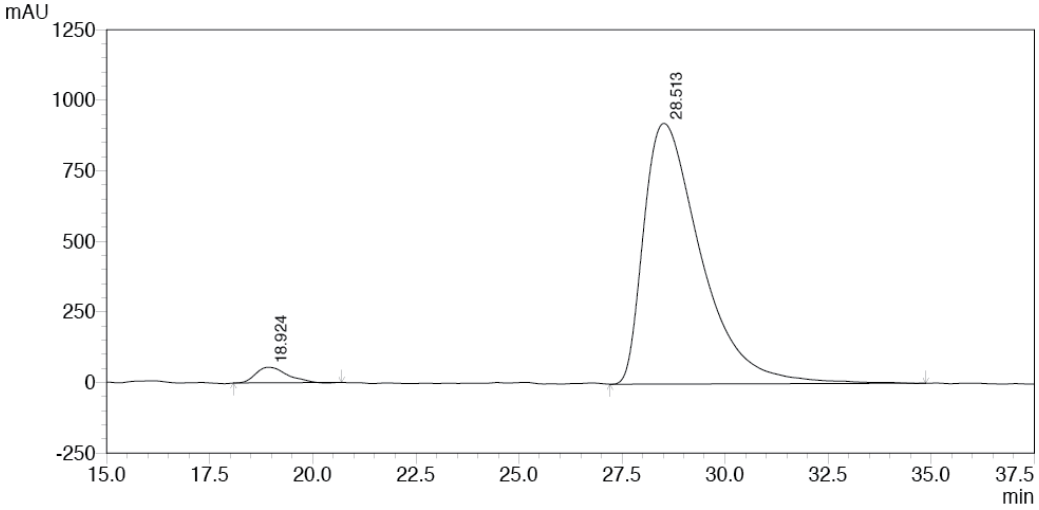

PDA 220nm

Peak#	Ret. Time	Area	Height	Area %	Height %
1	18.924	2878634	55143	3.121	5.635
2	28.513	89360381	923530	96.879	94.365
Total		92239015	978673	100.000	100.000

(c)

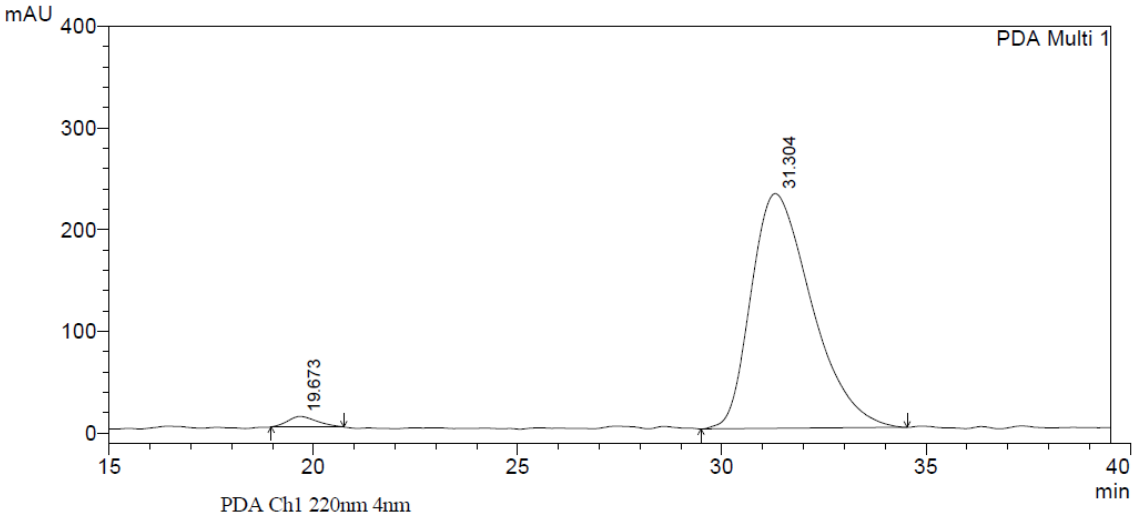

PDA Ch1 220nm 4nm

Peak#	Ret. Time	Area	Height	Area %	Height %
1	19.673	516825	10453	2.121	4.329
2	31.304	23852738	231012	97.879	95.671
Total		24369562	241465	100.000	100.000

Figure A-11. HPLC traces of **23hc** (Scheme 4.4, entry 8): (a) racemic sample; (b) catalyzed by Λ-(*S*,*S*)-$\mathbf{1}^{3+}$ $2BF_4^-BAr_f^-$; (c) catalyzed by Λ-(*S*,*S*)-$\mathbf{1}^{3+}$ $3BF_4^-$.

(a)

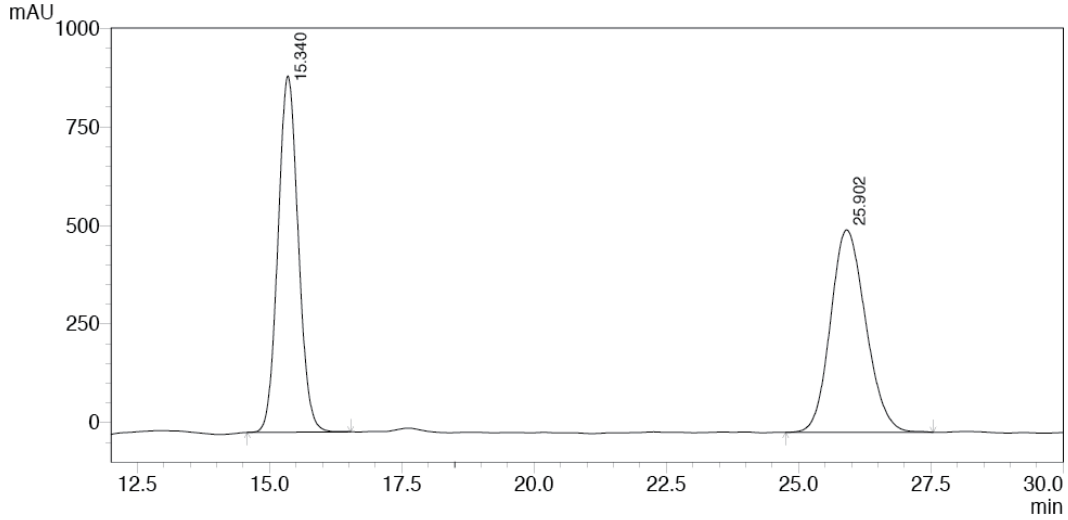

PDA220nm

Peak#	Ret. Time	Area	Height	Area %	Height %
1	15.340	24105156	903431	50.293	63.762
2	25.902	23824081	513442	49.707	36.238
Total		47929237	1416873	100.000	100.000

(b)

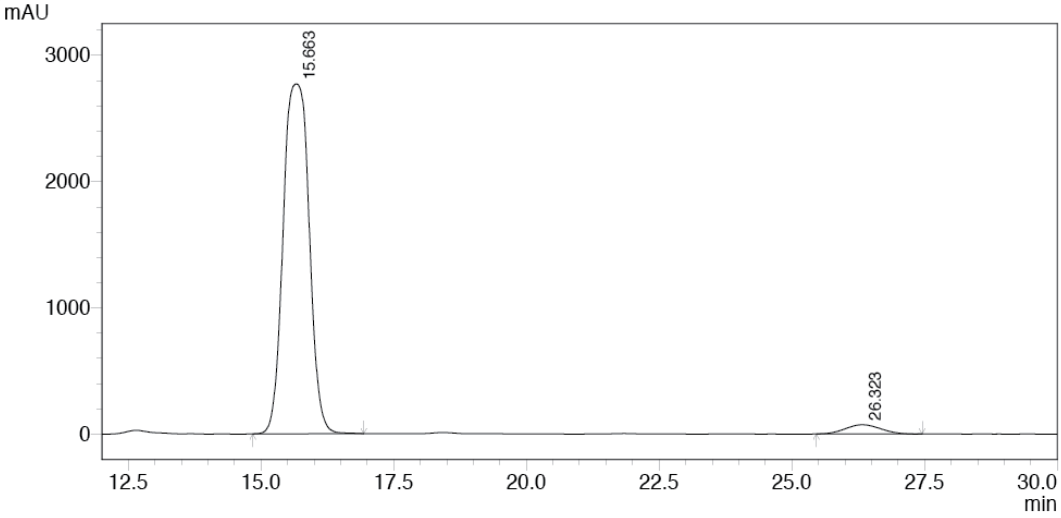

PDA 220nm

Peak#	Ret. Time	Area	Height	Area %	Height %
1	15.663	94240443	2770460	96.556	97.428
2	26.323	3360915	73149	3.444	2.572
Total		97601359	2843609	100.000	100.000

(c)

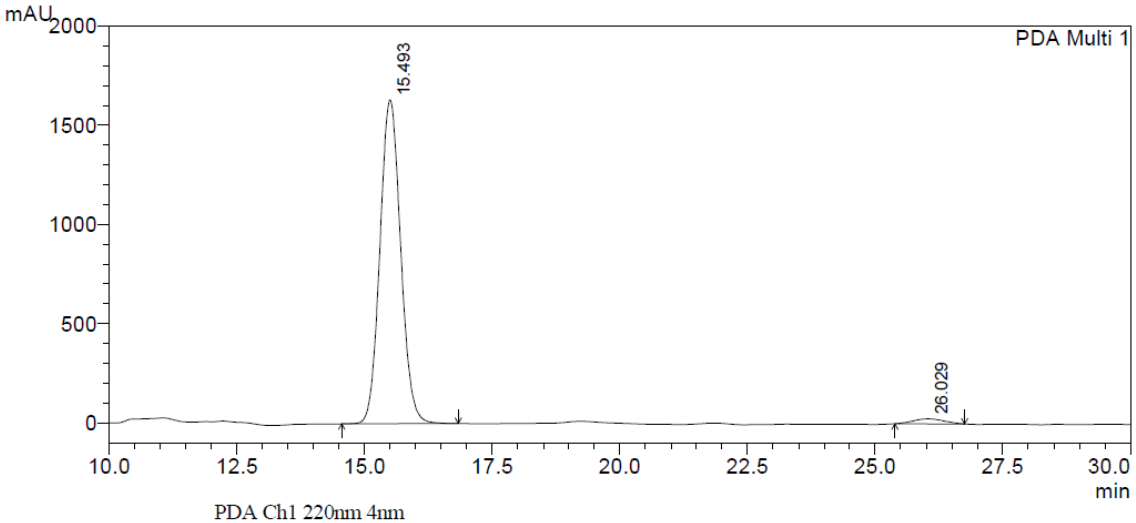

PDA Ch1 220nm 4nm

Peak#	Ret. Time	Area	Height	Area %	Height %
1	15.493	46134869	1632201	97.791	98.512
2	26.029	1042135	24649	2.209	1.488
Total		47177003	1656850	100.000	100.000

Figure A-12. HPLC traces of **23ic** (Scheme 4.4, entry 9): (a) racemic sample; (b) catalyzed by Λ-(*S*,*S*)-$\mathbf{1}^{3+}$ $2BF_4^-BAr_f^-$; (c) catalyzed by Λ-(*S*,*S*)-$\mathbf{1}^{3+}$ $3BF_4^-$.

(a)

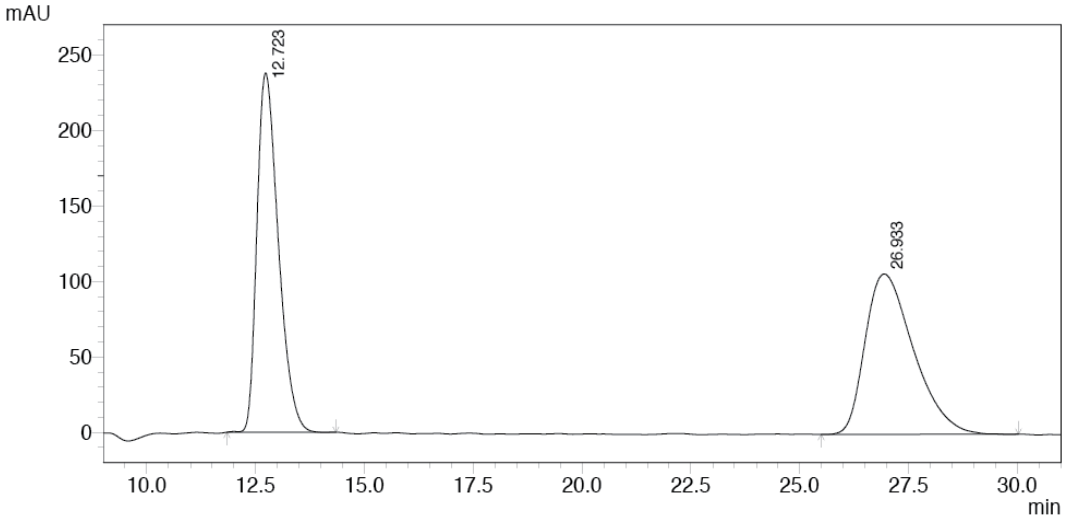

PDA 220nm

Peak#	Ret. Time	Area	Height	Area %	Height %
1	12.723	8141200	238008	49.819	69.153
2	26.933	8200292	106170	50.181	30.847
Total		16341493	344178	100.000	100.000

(b)

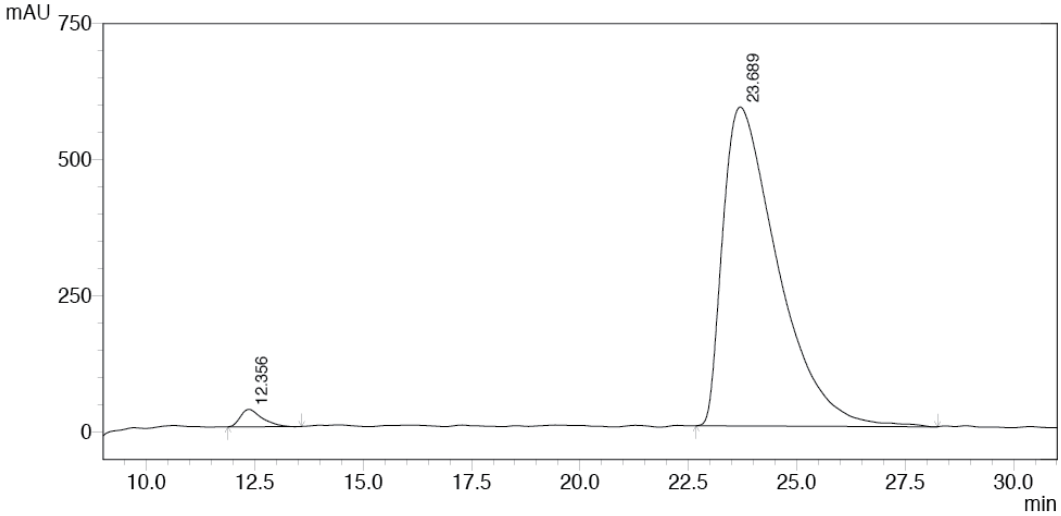

PDA 220nm

Peak#	Ret. Time	Area	Height	Area %	Height %
1	12.356	1090049	31778	2.068	5.151
2	23.689	51627061	585142	97.932	94.849
Total		52717109	616920	100.000	100.000

(c)

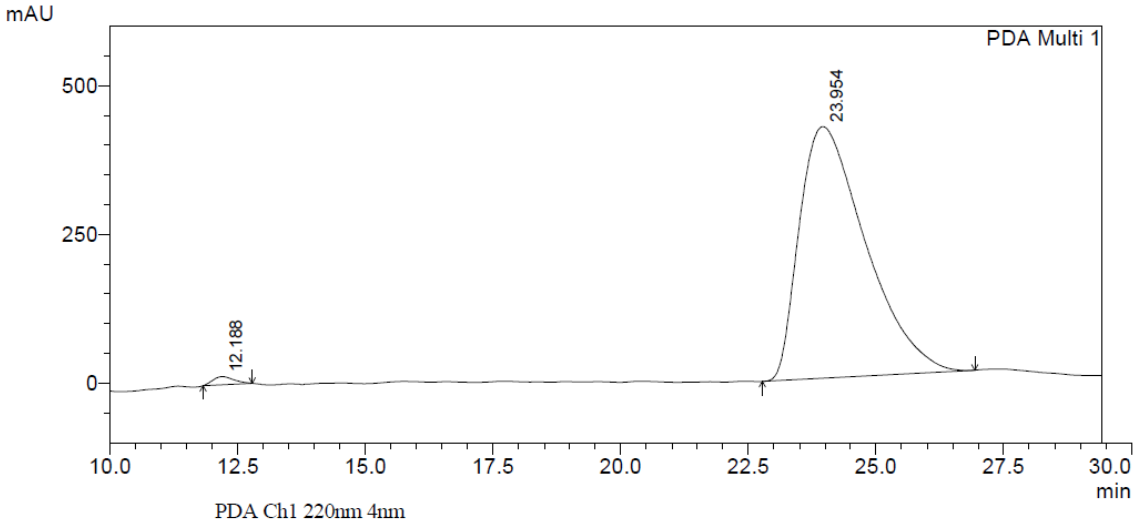

PDA Ch1 220nm 4nm

Peak#	Ret. Time	Area	Height	Area %	Height %
1	12.188	394877	13671	1.023	3.133
2	23.954	38205544	422701	98.977	96.867
Total		38600420	436372	100.000	100.000

Figure A-13. HPLC traces of **23jc** (Scheme 4.4, entry 10): (a) racemic sample; (b) catalyzed by Λ-(*S*,*S*)-$\mathbf{1}^{3+}$ $2BF_4^-BAr_f^-$; (c) catalyzed by Λ-(*S*,*S*)-$\mathbf{1}^{3+}$ $3BF_4^-$.

(a)

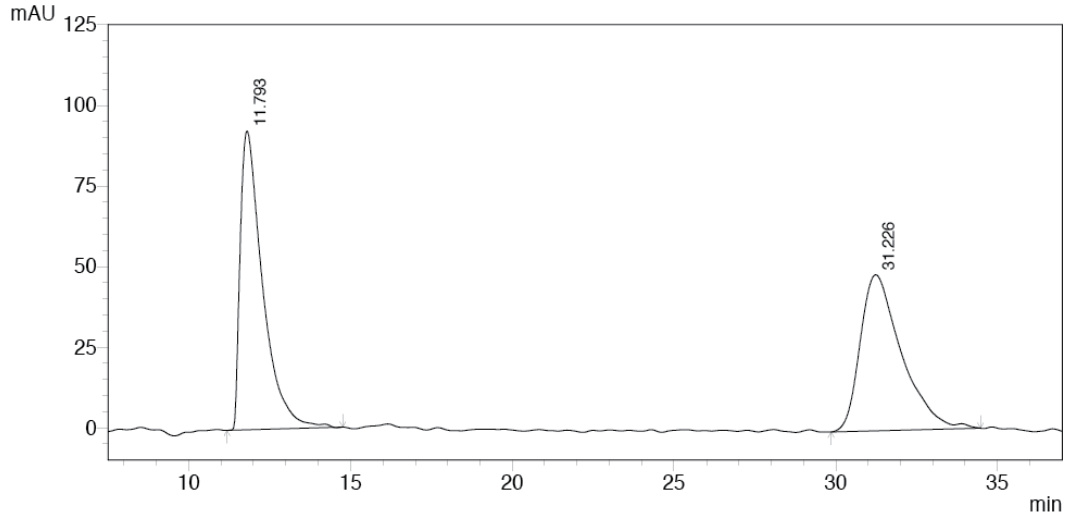

PDA 220nm

Peak#	Ret. Time	Area	Height	Area %	Height %
1	11.793	4468208	92606	51.035	65.690
2	31.226	4287008	48367	48.965	34.310
Total		8755216	140974	100.000	100.000

(b)

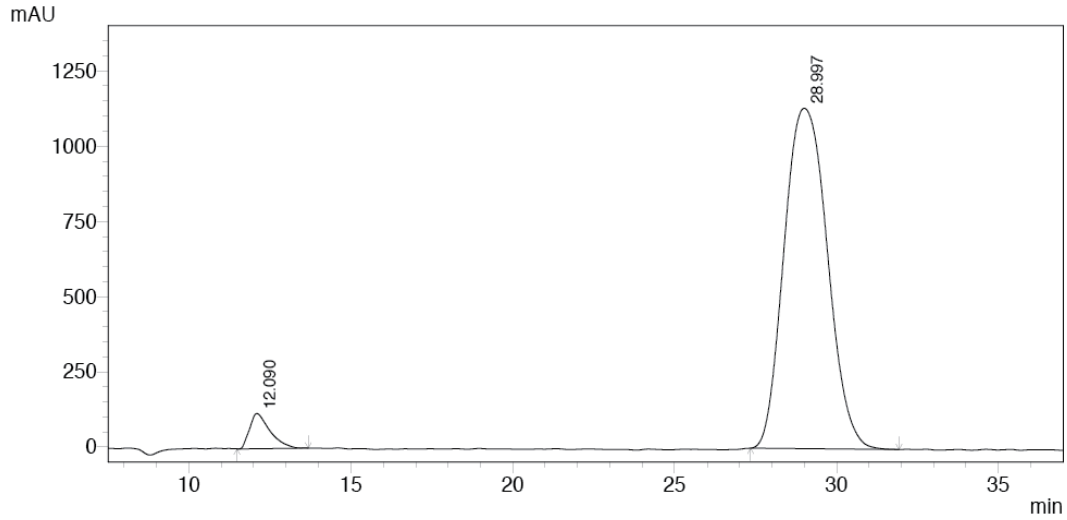

PDA 220nm

Peak#	Ret. Time	Area	Height	Area %	Height %
1	12.090	5063370	116519	4.580	9.340
2	28.997	105482048	1131049	95.420	90.660
Total		110545419	1247568	100.000	100.000

(c)

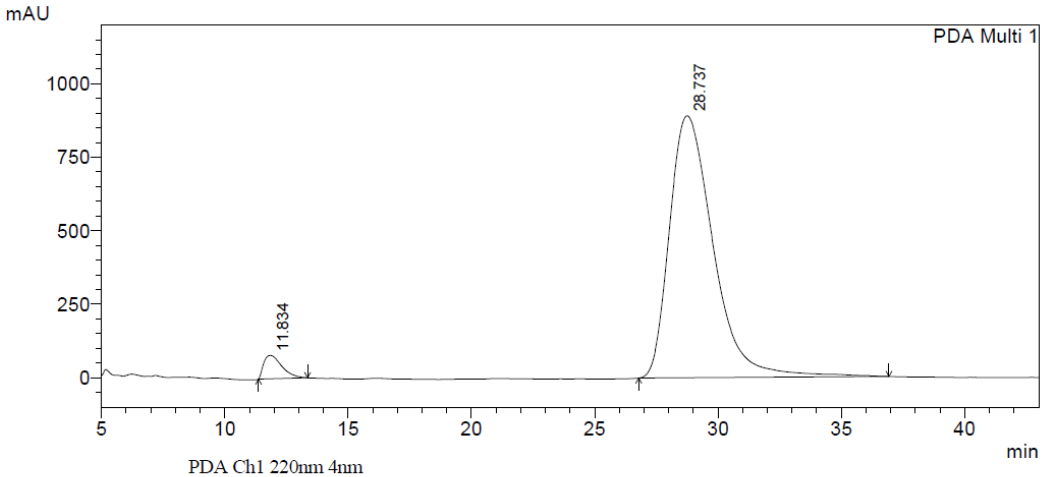

PDA Ch1 220nm 4nm

Peak#	Ret. Time	Area	Height	Area %	Height %
1	11.834	4048469	79205	3.554	8.165
2	28.737	109879149	890798	96.446	91.835
Total		113927618	970003	100.000	100.000

(d)

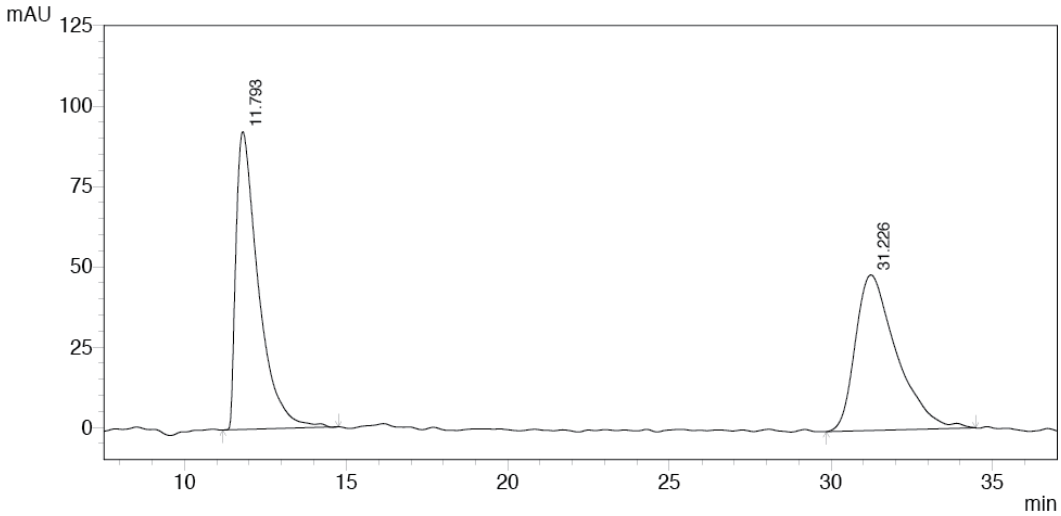

PDA 220nm

Peak#	Ret. Time	Area	Height	Area %	Height %
1	11.793	4468208	92606	51.035	65.690
2	31.226	4287008	48367	48.965	34.310
Total		8755216	140974	100.000	100.000

(e)

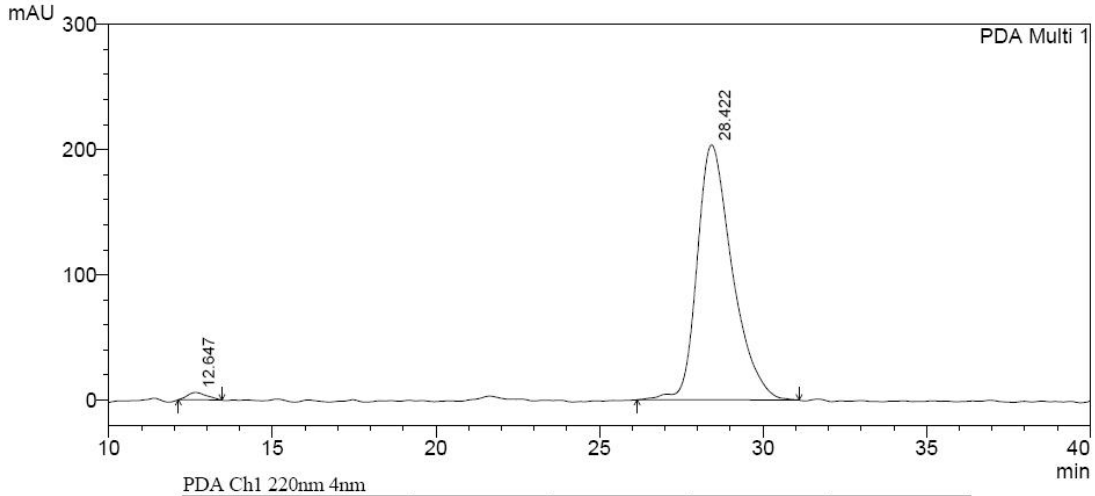

PDA Ch1 220nm 4nm

Peak#	Ret. Time	Area	Height	Area %	Height %
1	12.647	243332	5915	1.569	2.824
2	28.422	15260843	203525	98.431	97.176
Total		15504175	209440	100.000	100.000

Figure A-14. HPLC traces of **23kc** (Scheme 4.4, entry 11): (a) racemic sample; (b) catalyzed by Λ-(*S*,*S*)-**1**$^{3+}$ 2$BF_4^-$$BAr_f^-$; (c) catalyzed by Λ-(*S*,*S*)-**1**$^{3+}$ 3BF_4^-. For Scheme 7.4 (d) racemic sample; (e) catalyzed by Λ-**27c**$^{3+}$ 3BAr_f^-.

(a)

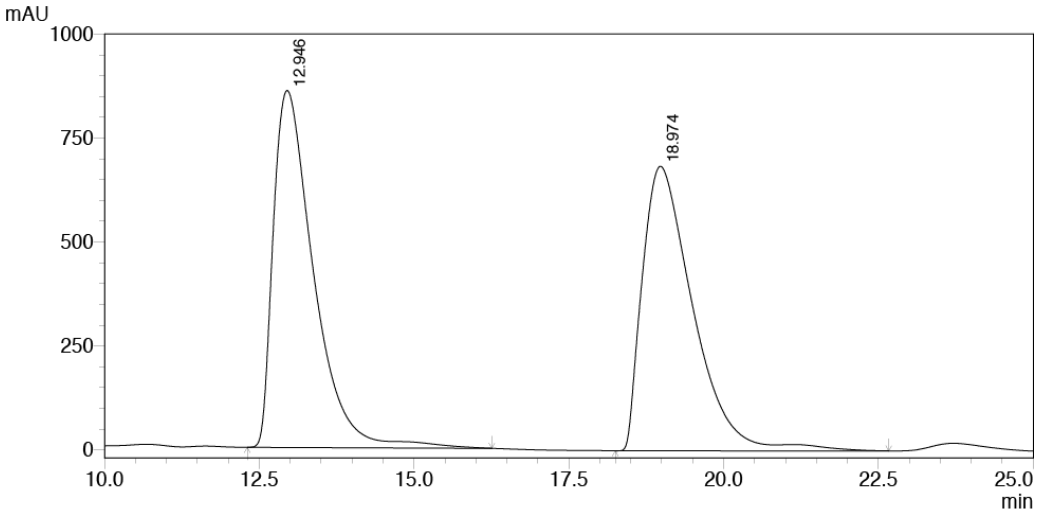

PDA 220nm

Peak#	Ret. Time	Area	Height	Area %	Height %
1	12.946	38973226	858914	49.978	55.647
2	18.974	39007602	684601	50.022	44.353
Total		77980828	1543515	100.000	100.000

(b)

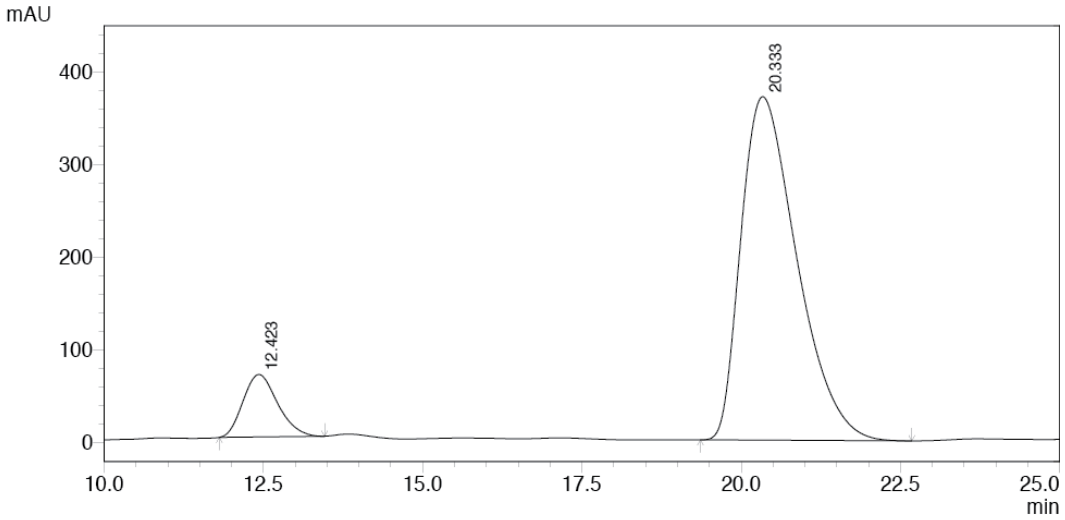

PDA 220nm

Peak#	Ret. Time	Area	Height	Area %	Height %
1	12.423	2538858	67307	10.100	15.379
2	20.333	22598513	370346	89.900	84.621
Total		25137371	437652	100.000	100.000

(c)

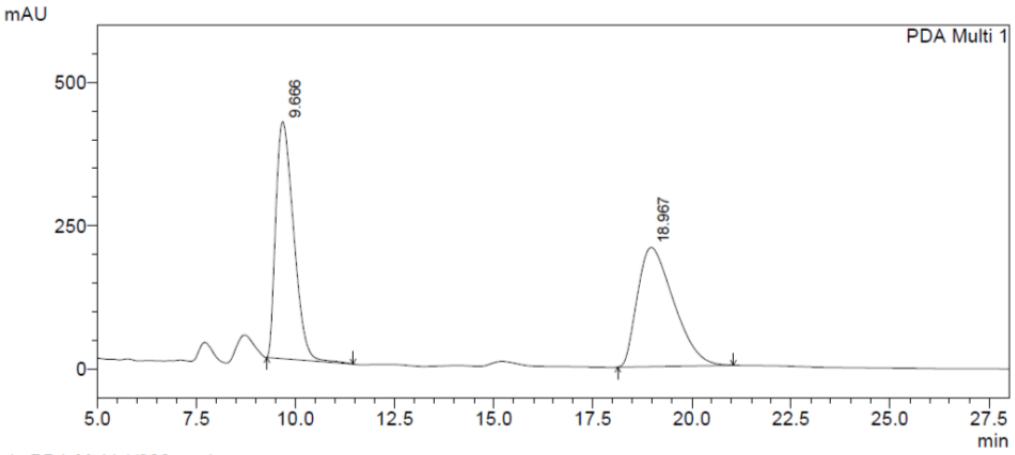

1 PDA Multi 1/220nm 4nm

PeakTable

PDA Ch1 220nm 4nm

Peak#	Ret. Time	Area	Height	Area %	Height %
1	9.666	12941031	413408	49.424	66.552
2	18.967	13242511	207771	50.576	33.448
Total		26183542	621179	100.000	100.000

(d)

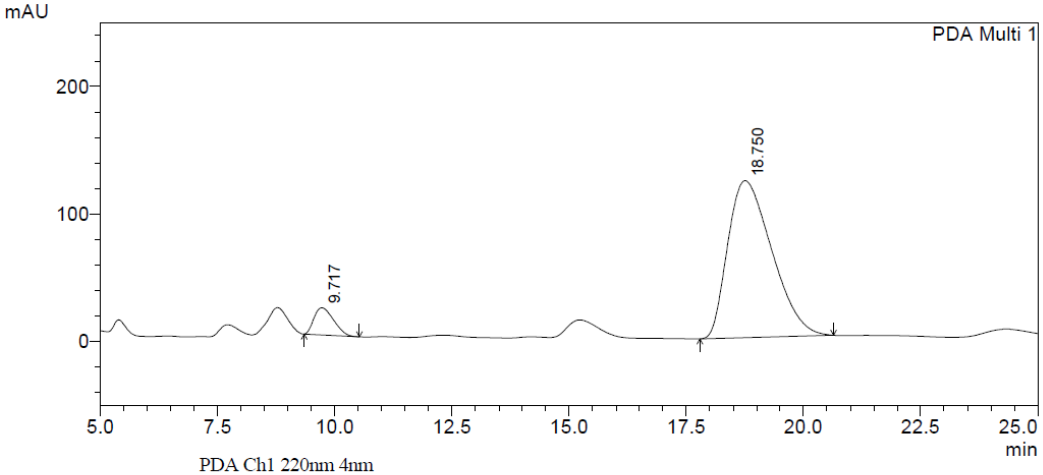

PDA Ch1 220nm 4nm

Peak#	Ret. Time	Area	Height	Area %	Height %
1	9.717	622512	21401	7.162	14.797
2	18.750	8069654	123232	92.838	85.203
Total		8692166	144634	100.000	100.000

(e)

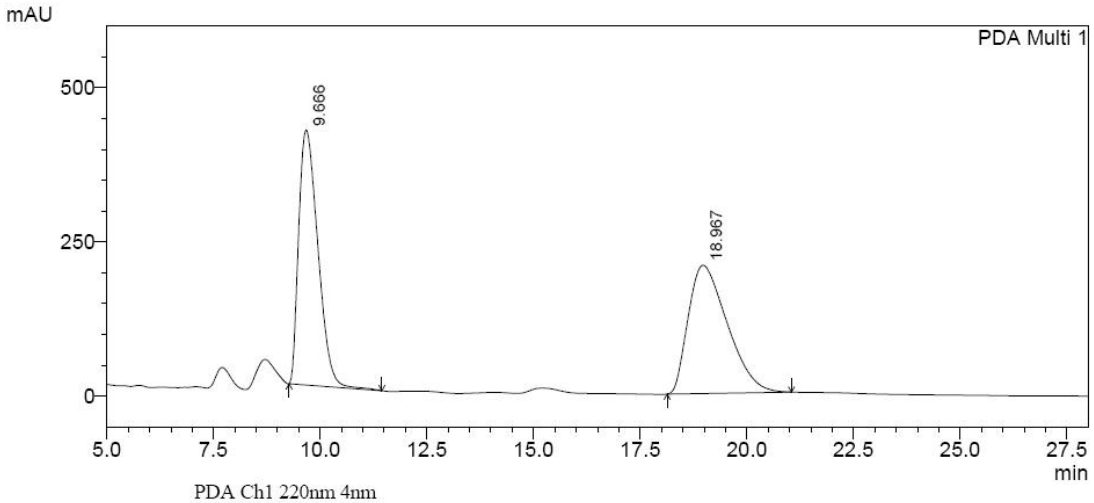

PDA Ch1 220nm 4nm

Peak#	Ret. Time	Area	Height	Area %	Height %
1	9.666	12941031	413408	49.424	66.552
2	18.967	13242511	207771	50.576	33.448
Total		26183542	621179	100.000	100.000

(f)

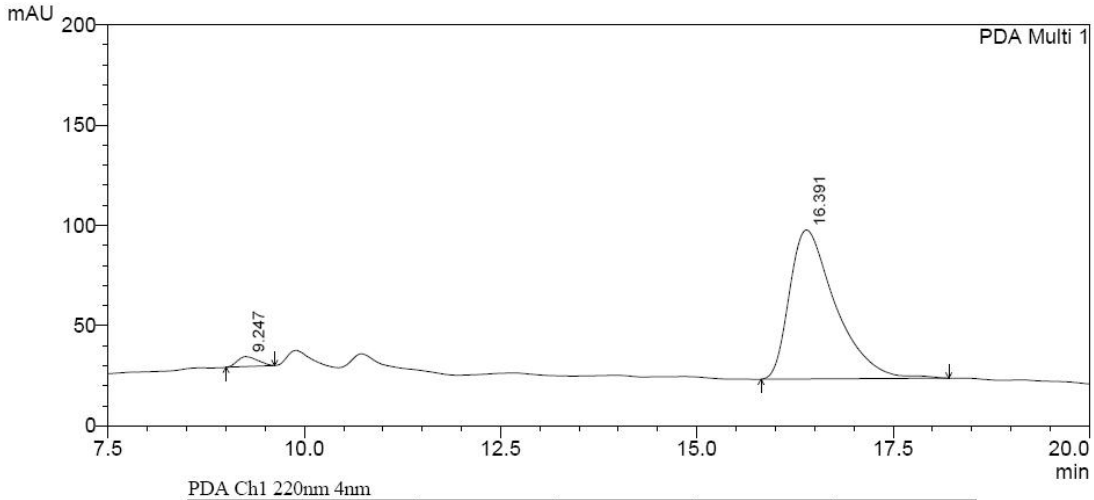

PDA Ch1 220nm 4nm

Peak#	Ret. Time	Area	Height	Area %	Height %
1	9.247	90392	4965	2.896	6.268
2	16.391	3030909	74252	97.104	93.732
Total		3121301	79217	100.000	100.000

Figure A-15. HPLC traces of **23lc** (Scheme 4.4, entry 12): (a) racemic sample; (b) catalyzed by Λ-(*S*,*S*)-$\mathbf{1}^{3+}$ $2BF_4^-BAr_f^-$ and analyzed per a; (c) racemic sample six months later (older column); (d) catalyzed by Λ-(*S*,*S*)-$\mathbf{1}^{3+}$ $3BF_4^-$ and analyzed per c. For Scheme 7.4 (e) racemic sample; (f) catalyzed by Λ-$\mathbf{27c}^{3+}$ $3BAr_f^-$.

(a)

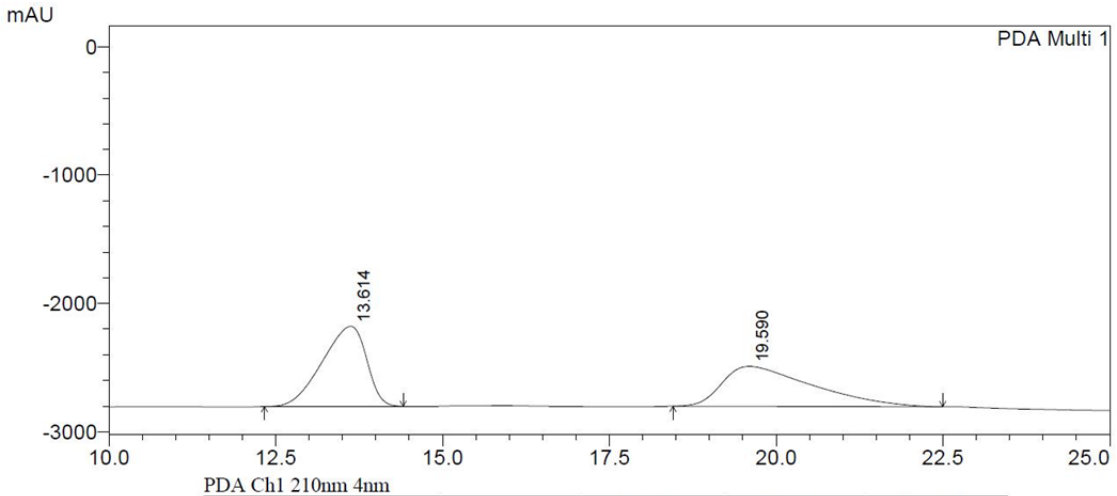

PDA Ch1 210nm 4nm

Peak#	Ret. Time	Area	Height	Area %	Height %
1	13.614	28867701	624847	49.677	66.716
2	19.590	29242982	311735	50.323	33.284
Total		58110683	936582	100.000	100.000

(b)

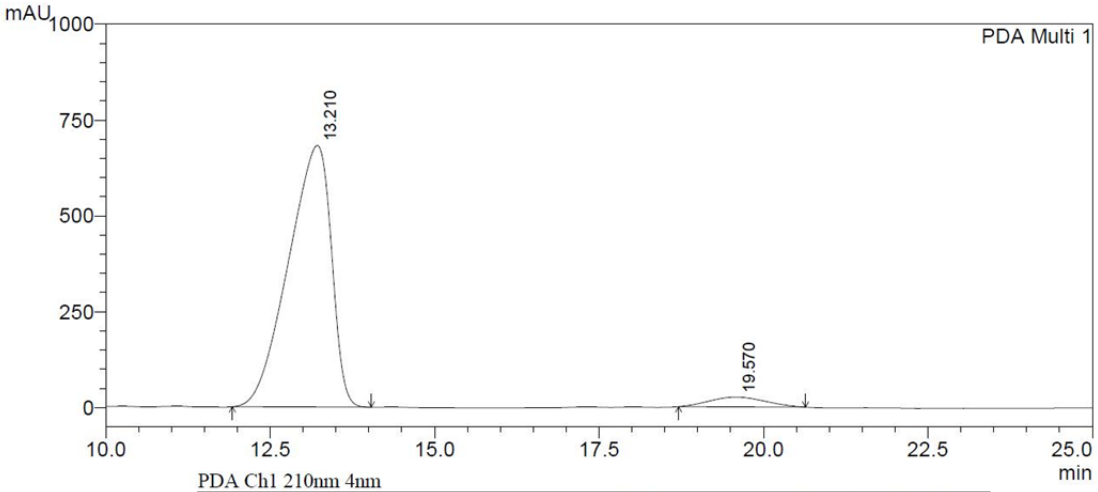

PDA Ch1 210nm 4nm

Peak#	Ret. Time	Area	Height	Area %	Height %
1	13.210	31007029	682784	95.407	96.408
2	19.570	1492803	25440	4.593	3.592
Total		32499831	708224	100.000	100.000

Figure A-16. HPLC traces of **26a** (Scheme 5.3): (a) racemic sample; (b) catalyzed by Δ-(*S*,*S*)-**2**$^{3+}$ 2Cl^{-}BAr$_{f20}$$^{-}$.

(a)

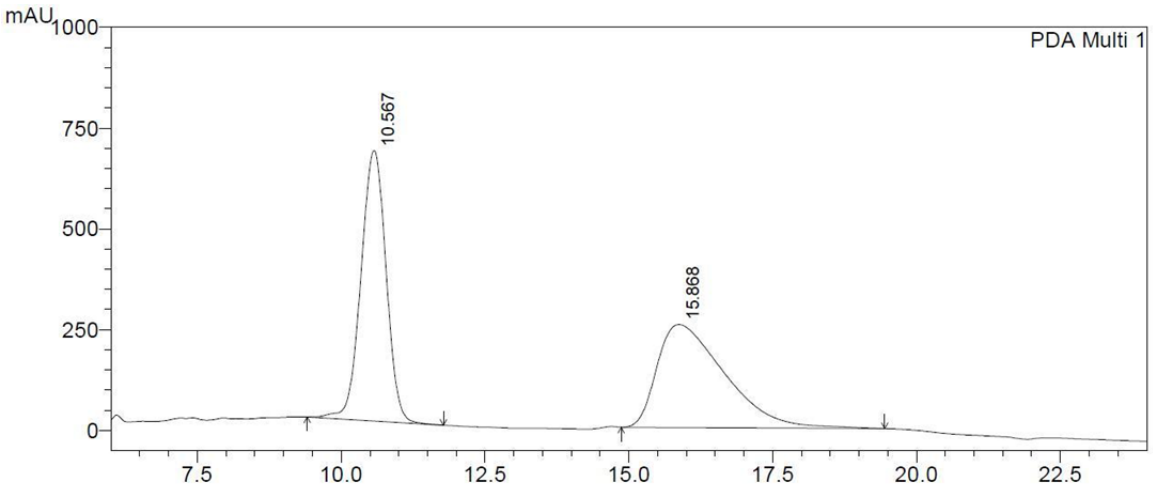

PDA Ch1 210nm 4nm

Peak#	Ret. Time	Area	Height	Area %	Height %
1	10.567	20407922	671133	49.435	72.401
2	15.868	20874427	255836	50.565	27.599
Total		41282348	926970	100.000	100.000

(b)

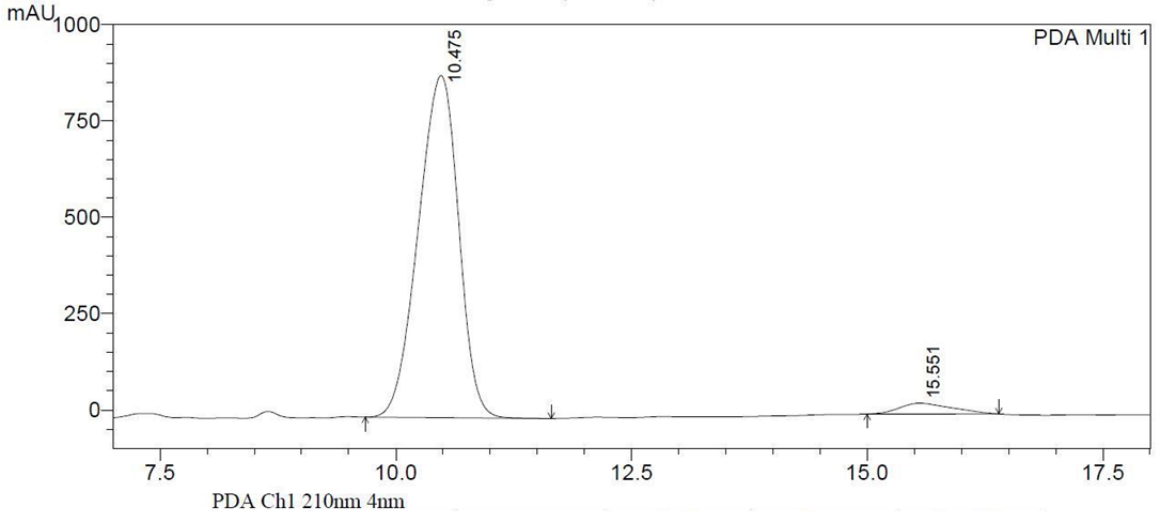

PDA Ch1 210nm 4nm

Peak#	Ret. Time	Area	Height	Area %	Height %
1	10.475	26391931	888032	96.031	96.934
2	15.551	1090761	28089	3.969	3.066
Total		27482693	916122	100.000	100.000

Figure A-17. HPLC traces of **26b** (Scheme 5.3): (a) racemic sample; (b) catalyzed by Δ-(*S*,*S*)-**1**$^{3+}$ 2Cl^{-}BAr$_{f20}$$^{-}$.

(a)

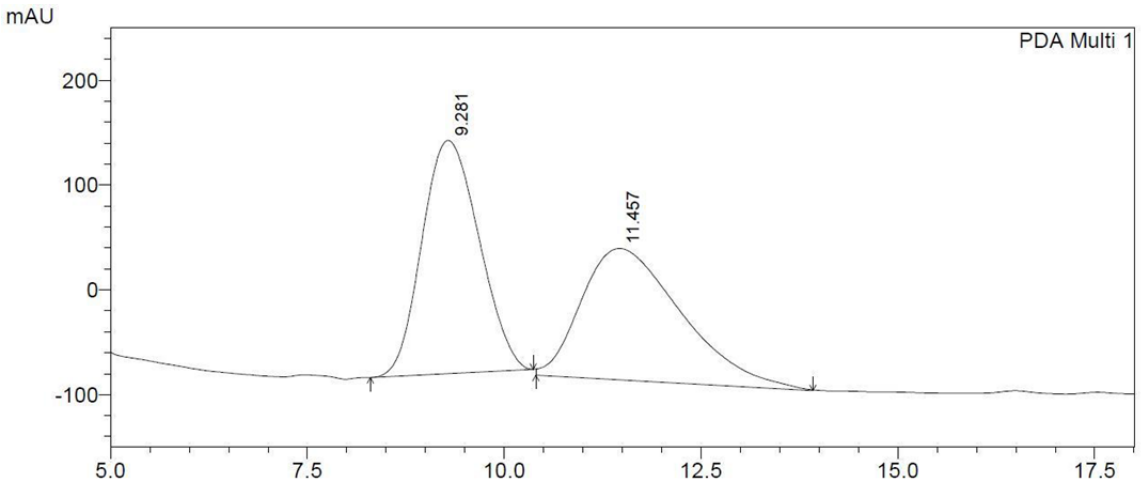

PDA Ch1 210nm 4nm

Peak#	Ret. Time	Area	Height	Area %	Height %
1	9.281	11226181	222795	50.279	63.974
2	11.457	11101394	125466	49.721	36.026
Total		22327575	348261	100.000	100.000

(b)

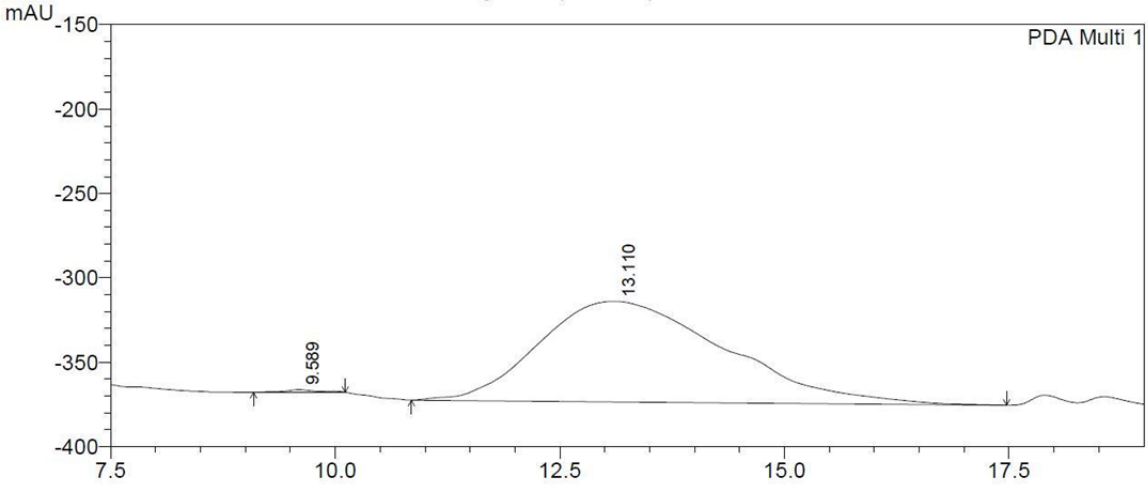

PDA Ch1 210nm 4nm

Peak#	Ret. Time	Area	Height	Area %	Height %
1	9.589	41593	1543	0.482	2.524
2	13.110	8586118	59581	99.518	97.476
Total		8627712	61124	100.000	100.000

Figure A-18. HPLC traces of **26c** (Scheme 5.3): (a) racemic sample; (b) catalyzed by Δ-(*S*,*S*)-$\mathbf{1}^{3+}$ $2Cl^{-}BAr_{f20}{}^{-}$.

(a)

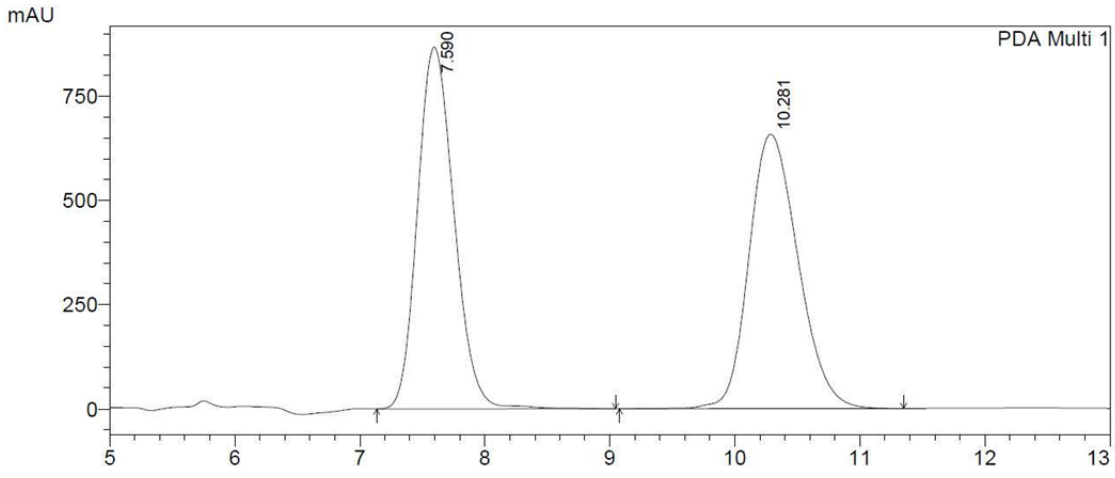

PDA Ch1 220nm 4nm

Peak#	Ret. Time	Area	Height	Area %	Height %
1	7.590	17637206	868310	49.488	56.875
2	10.281	18002230	658393	50.512	43.125
Total		35639437	1526703	100.000	100.000

(b)

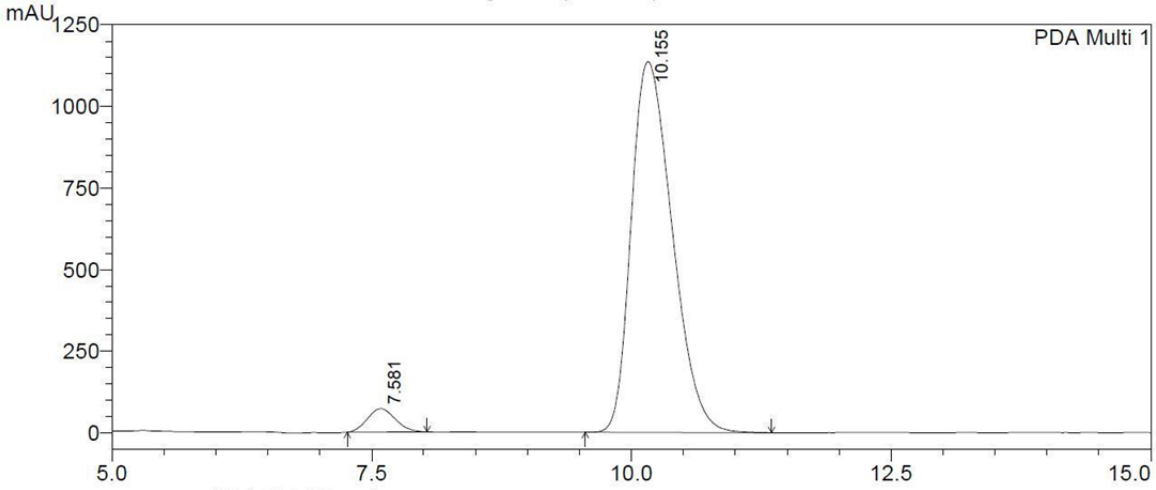

PDA Ch1 220nm 4nm

Peak#	Ret. Time	Area	Height	Area %	Height %
1	7.581	1342127	71767	4.126	5.943
2	10.155	31189712	1135834	95.874	94.057
Total		32531838	1207601	100.000	100.000

Figure A-19. HPLC traces of **26d** (Scheme 5.3): (a) racemic sample; (b) catalyzed by Δ-(*S*,*S*)-**1**$^{3+}$ 2Cl^{-}BAr$_{f20}$$^{-}$.

(a)

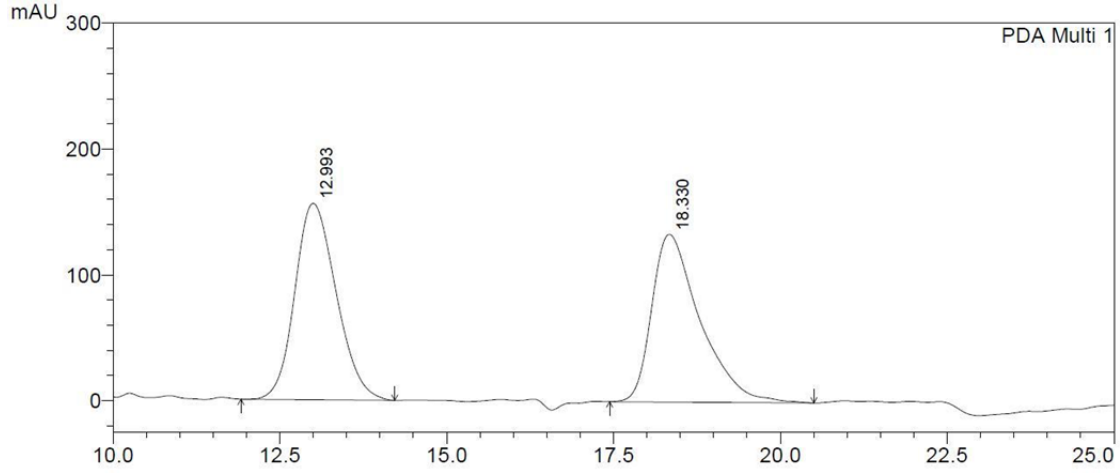

PDA Ch1 210nm 4nm

Peak#	Ret. Time	Area	Height	Area %	Height %
1	12.993	6742894	156218	50.131	53.946
2	18.330	6707674	133365	49.869	46.054
Total		13450568	289583	100.000	100.000

(b)

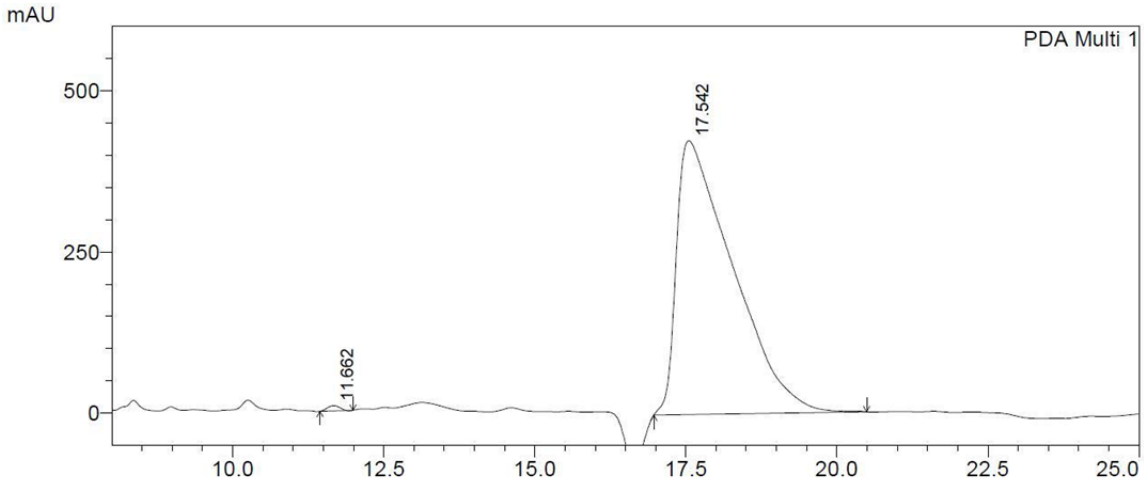

PDA Ch1 210nm 4nm

Peak#	Ret. Time	Area	Height	Area %	Height %
1	11.662	113331	8102	0.409	1.870
2	17.542	27619178	425105	99.591	98.130
Total		27732509	433207	100.000	100.000

(c)

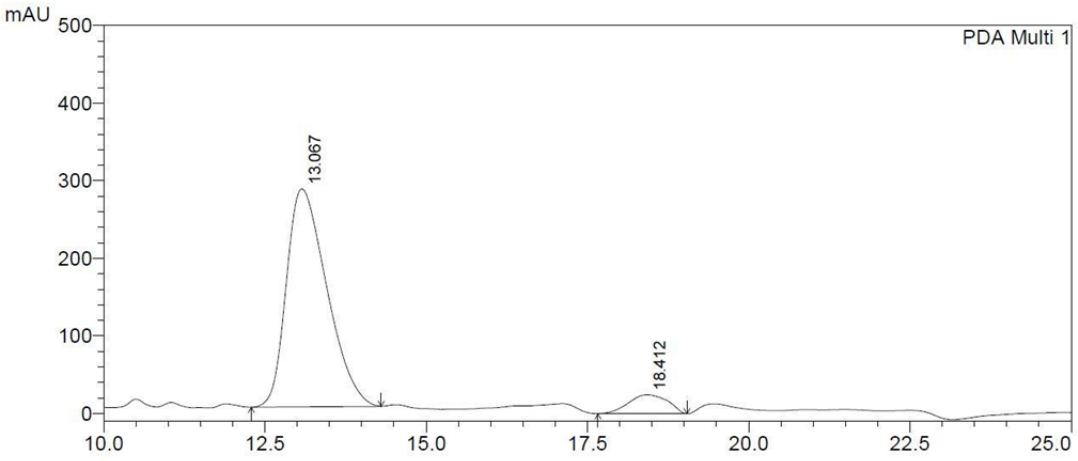

PDA Ch1 210nm 4nm

Peak#	Ret. Time	Area	Height	Area %	Height %
1	13.067	12256259	281152	92.206	91.991
2	18.412	1036038	24478	7.794	8.009
Total		13292297	305631	100.000	100.000

(d)

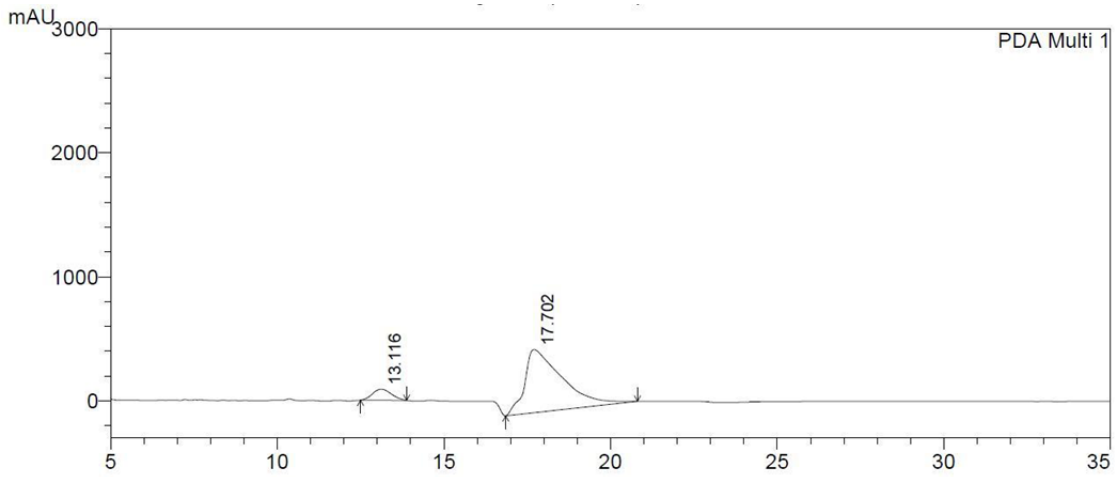

PDA Ch1 210nm 4nm

Peak#	Ret. Time	Area	Height	Area %	Height %
1	13.116	3528111	89685	8.121	14.952
2	17.702	39917264	510128	91.879	85.048
Total		43445375	599813	100.000	100.000

Figure A-20. HPLC traces of **26e** (Scheme 5.3): (a) racemic sample; (b) catalyzed by Δ-(*S*,*S*)-**1**$^{3+}$ 2Cl^{-}BAr$_{f20}$$^{-}$; (c) catalyzed by Λ-(*S*,*S*)-**1**$^{3+}$ 2Cl^{-}BAr$_{f20}$$^{-}$; (d) catalyzed by Δ-(*S*,*S*)-**1**$^{3+}$ 2Cl^{-}BAr$_{f}$$^{-}$.

(a)

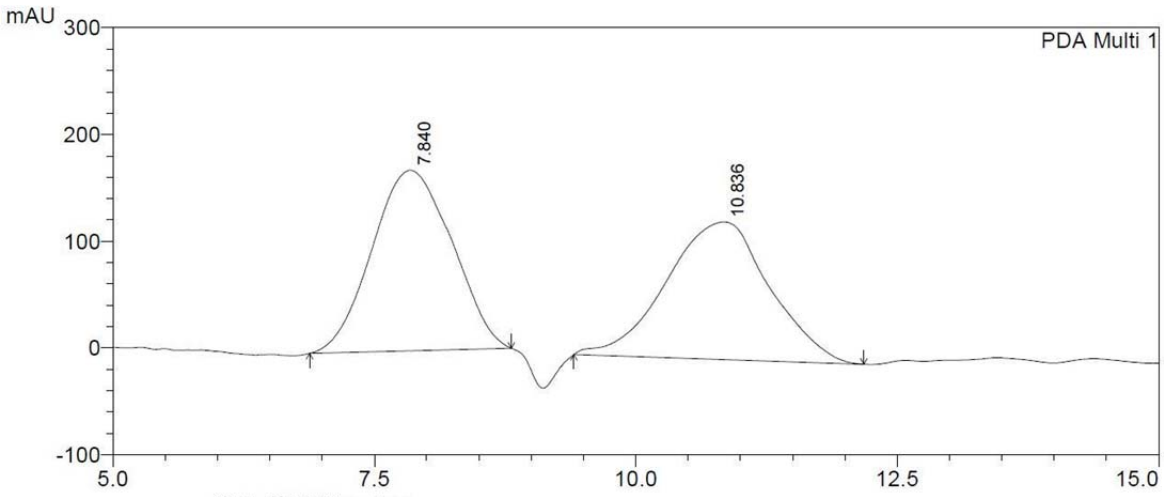

PDA Ch1 210nm 4nm

Peak#	Ret. Time	Area	Height	Area %	Height %
1	7.840	9014007	169267	50.432	56.757
2	10.836	8859668	128966	49.568	43.243
Total		17873675	298233	100.000	100.000

(b)

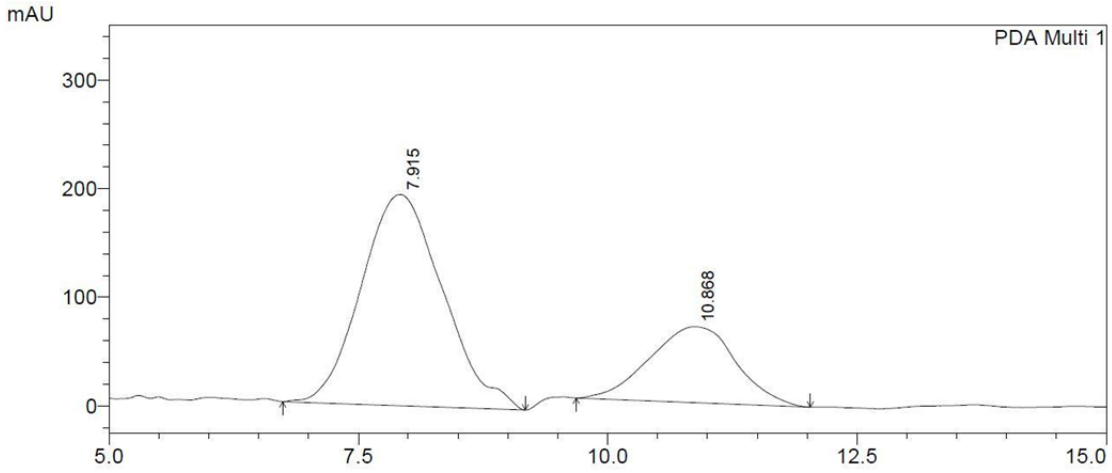

PDA Ch1 220nm 4nm

Peak#	Ret. Time	Area	Height	Area %	Height %
1	7.915	11064043	194419	72.435	73.564
2	10.868	4210357	69866	27.565	26.436
Total		15274400	264285	100.000	100.000

Figure A-21. HPLC traces of **26f** (Scheme 5.3): (a) racemic sample; (b) catalyzed by Δ-(*S*,*S*)-**1**$^{3+}$ 2Cl^{-}BAr$_{f20}$$^{-}$.

(a)

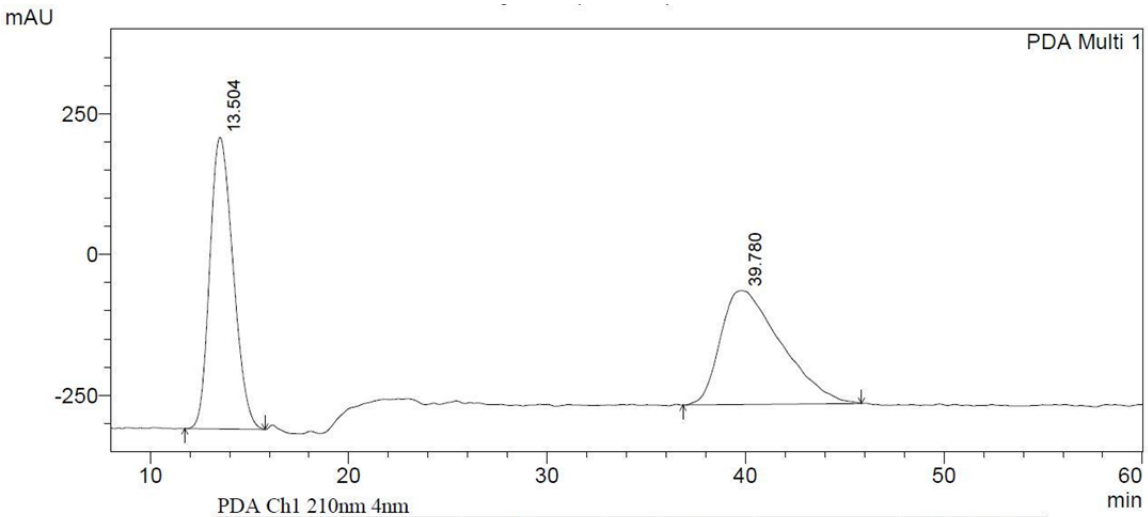

PDA Ch1 210nm 4nm

Peak#	Ret. Time	Area	Height	Area %	Height %
1	13.504	42441422	517451	49.740	71.908
2	39.780	42884772	202154	50.260	28.092
Total		85326194	719605	100.000	100.000

(b)

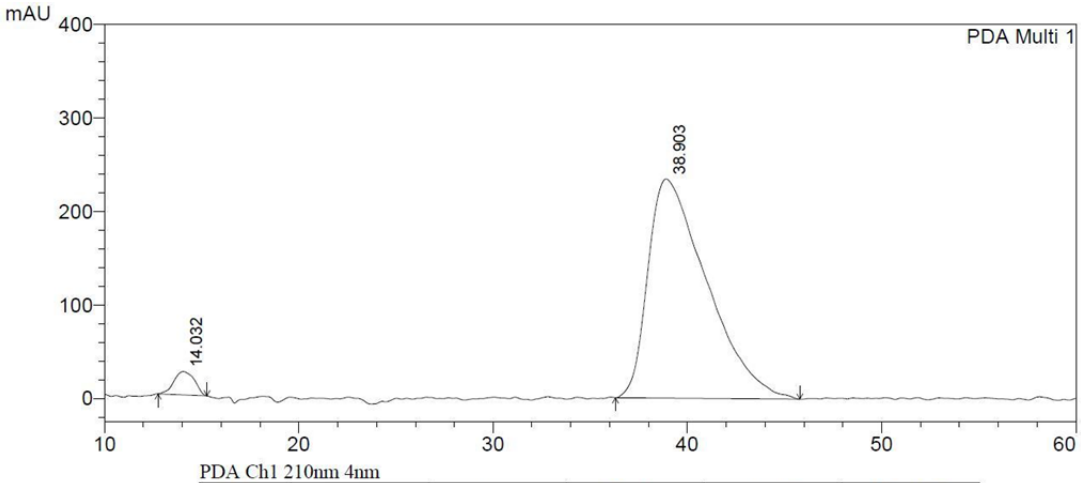

PDA Ch1 210nm 4nm

Peak#	Ret. Time	Area	Height	Area %	Height %
1	14.032	1827668	24905	3.568	9.596
2	38.903	49391197	234622	96.432	90.404
Total		51218865	259527	100.000	100.000

(c)

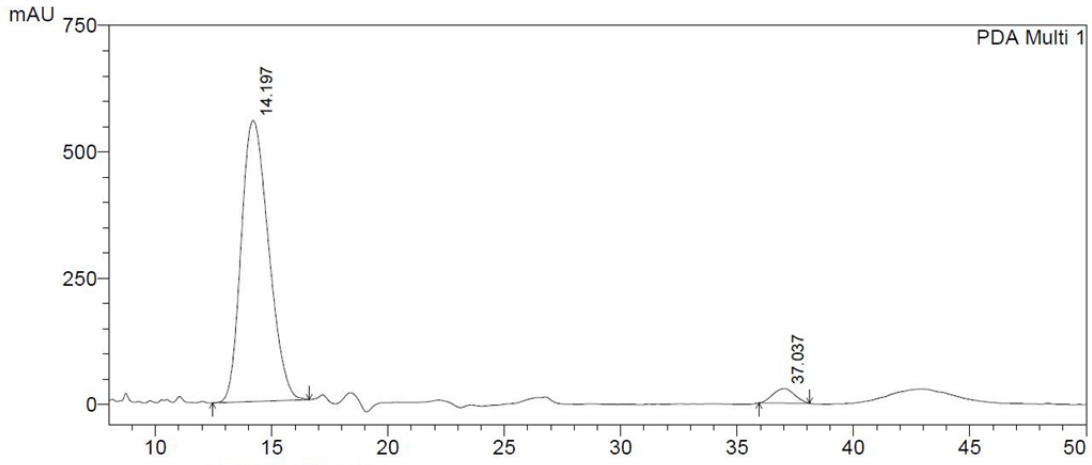

PDA Ch1 210nm 4nm

Peak#	Ret. Time	Area	Height	Area %	Height %
1	14.197	45599748	555890	96.078	95.103
2	37.037	1861244	28622	3.922	4.897
Total		47460992	584512	100.000	100.000

(d)

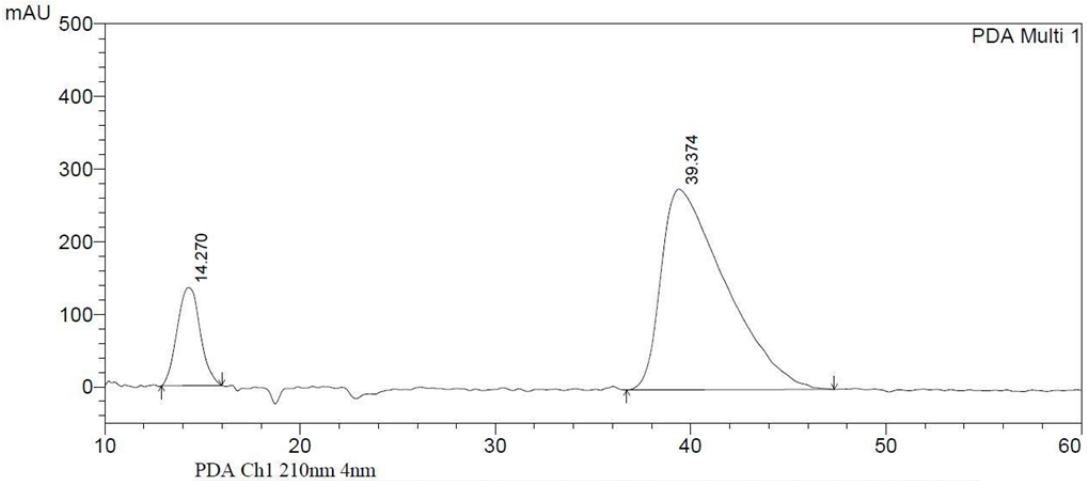

PDA Ch1 210nm 4nm

Peak#	Ret. Time	Area	Height	Area %	Height %
1	14.270	11105744	135430	14.902	32.877
2	39.374	63419273	276503	85.098	67.123
Total		74525018	411933	100.000	100.000

Figure A-22. HPLC traces of **26g** (Scheme 5.3): (a) racemic sample; (b) catalyzed by Δ-(*S*,*S*)-$\mathbf{1}^{3+}$ $2Cl^{-}BAr_{f20}^{-}$; (c) catalyzed by Λ-(*S*,*S*)-$\mathbf{1}^{3+}$ $2Cl^{-}BAr_{f20}^{-}$; (d) catalyzed by Δ-(*S*,*S*)-$\mathbf{1}^{3+}$ $2Cl^{-}BAr_{f}^{-}$.

(a)

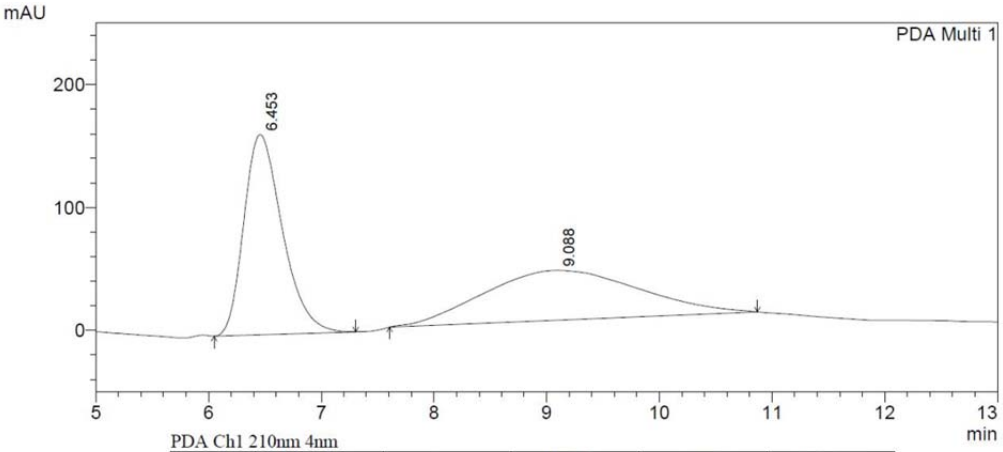

PDA Ch1 210nm 4nm

Peak#	Ret. Time	Area	Height	Area %	Height %
1	6.453	3872918	162873	49.970	80.056
2	9.088	3877530	40577	50.030	19.944
Total		7750448	203450	100.000	100.000

(b)

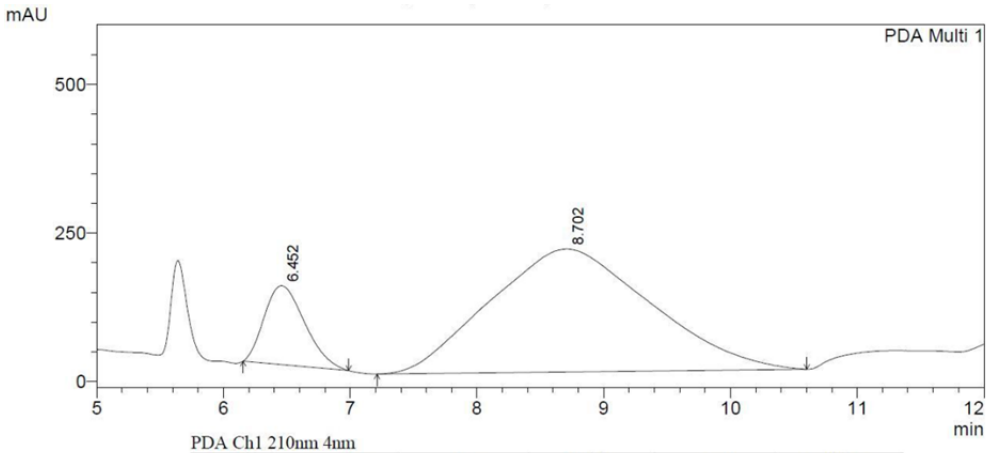

PDA Ch1 210nm 4nm

Peak#	Ret. Time	Area	Height	Area %	Height %
1	6.452	2950859	132448	13.960	39.038
2	8.702	18186903	206836	86.040	60.962
Total		21137762	339285	100.000	100.000

Figure A-23. HPLC traces of **26h** (Scheme 5.3): (a) racemic sample; (b) catalyzed by Δ-(*S*,*S*)-**1**$^{3+}$ 2Cl^{-}BAr$_{f20}$$^{-}$.

(a)

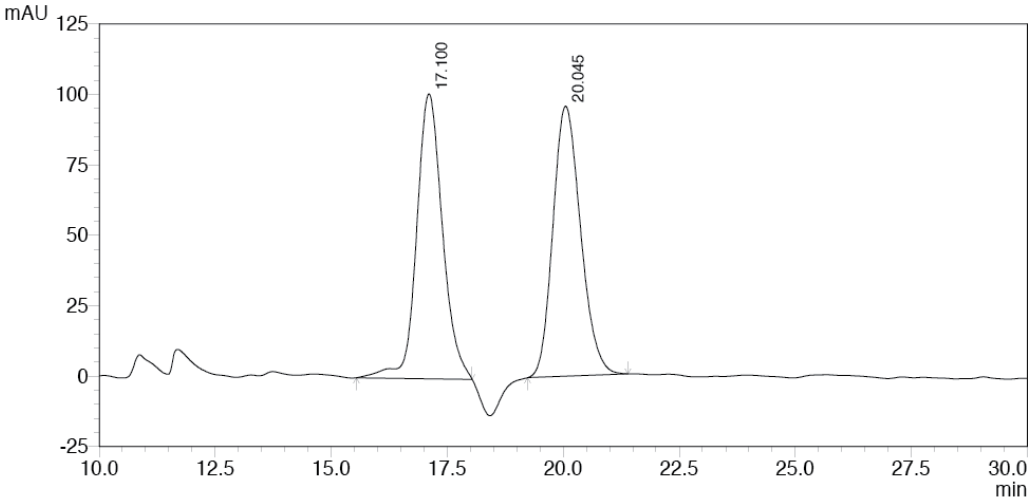

PDA 220nm

Peak#	Ret. Time	Area	Height	Area %	Height %
1	17.100	3930096	101137	49.659	51.334
2	20.045	3984017	95881	50.341	48.666
Total		7914113	197019	100.000	100.000

(b)

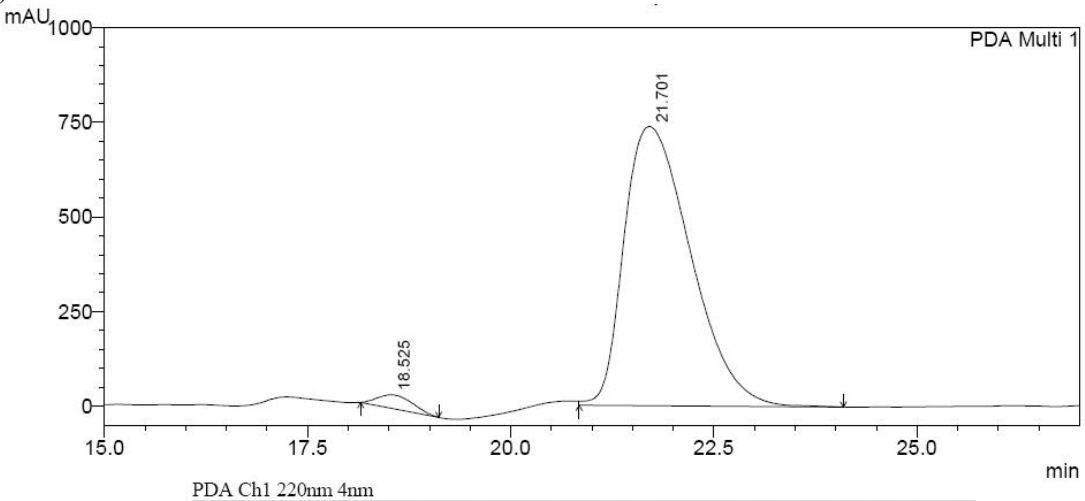

PDA Ch1 220nm 4nm

Peak#	Ret. Time	Area	Height	Area %	Height %
1	18.525	1083941	35019	2.505	4.532
2	21.701	42192240	737671	97.495	95.468
Total		43276182	772691	100.000	100.000

Figure A-24. HPLC traces of **23ad** (Scheme 7.4): (a) racemic sample; (b) catalyzed by Λ-**27c**$^{3+}$ 3BAr$_f^-$.

(a)

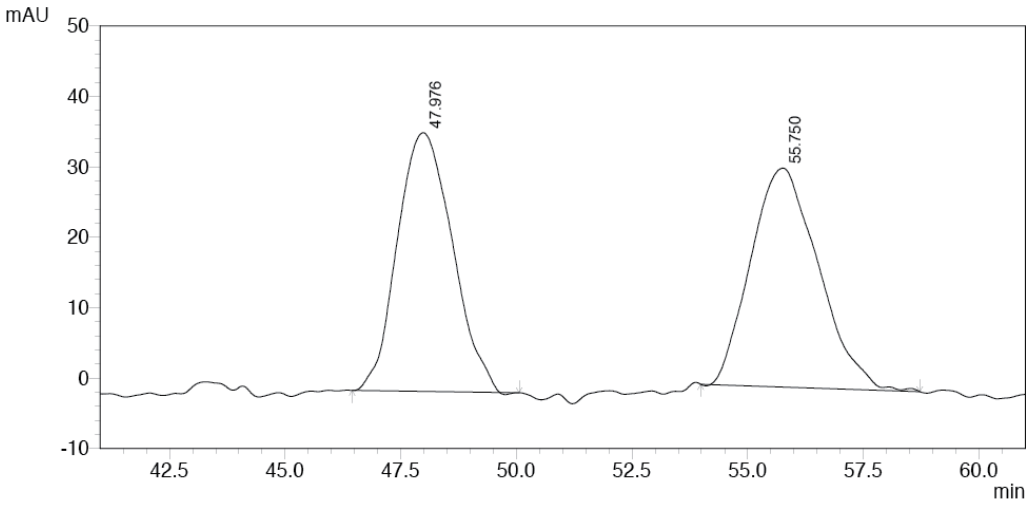

PDA 220nm

Peak#	Ret. Time	Area	Height	Area %	Height %
1	47.976	3039461	36726	48.983	54.165
2	55.750	3165671	31078	51.017	45.835
Total		6205132	67804	100.000	100.000

(b)

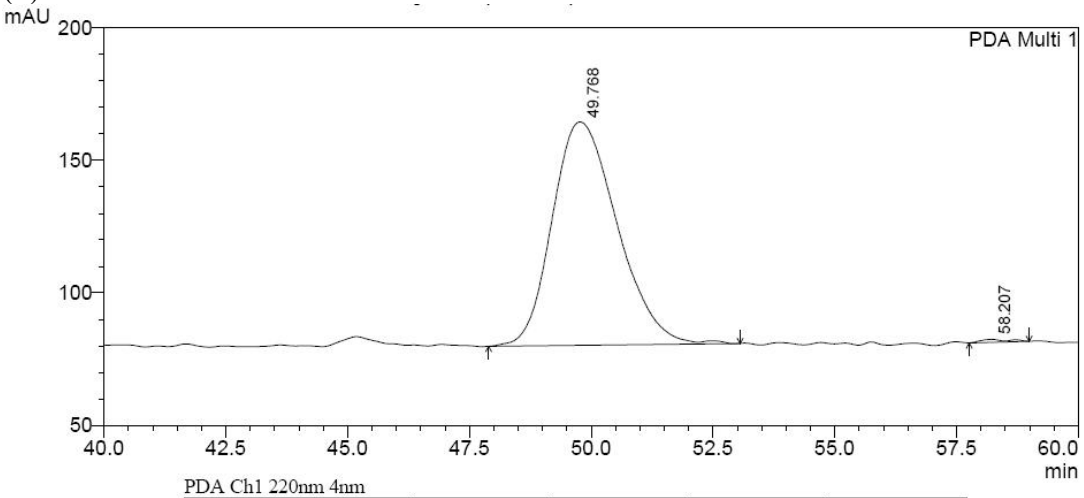

PDA Ch1 220nm 4nm

Peak#	Ret. Time	Area	Height	Area %	Height %
1	49.768	7819949	84231	99.451	98.650
2	58.207	43203	1153	0.549	1.350
Total		7863152	85384	100.000	100.000

Figure A-25. HPLC traces of **23mc** (Scheme 7.4): (a) racemic sample; (b) catalyzed by Λ-**27c**$^{3+}$ 3BAr$_f^-$.

(a)

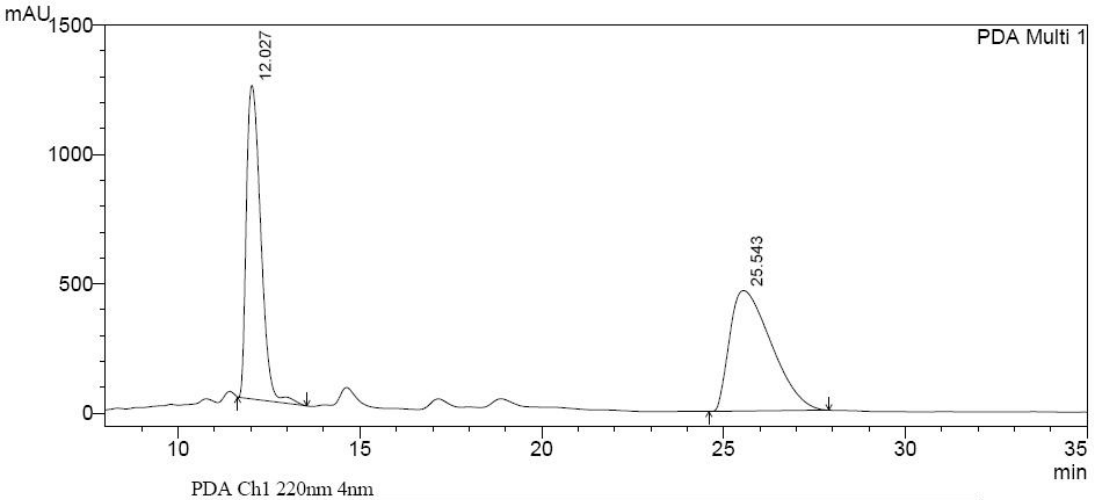

PDA Ch1 220nm 4nm

Peak#	Ret. Time	Area	Height	Area %	Height %
1	12.027	33430366	1212132	47.315	72.234
2	25.543	37224641	465942	52.685	27.766
Total		70655007	1678074	100.000	100.000

(b)

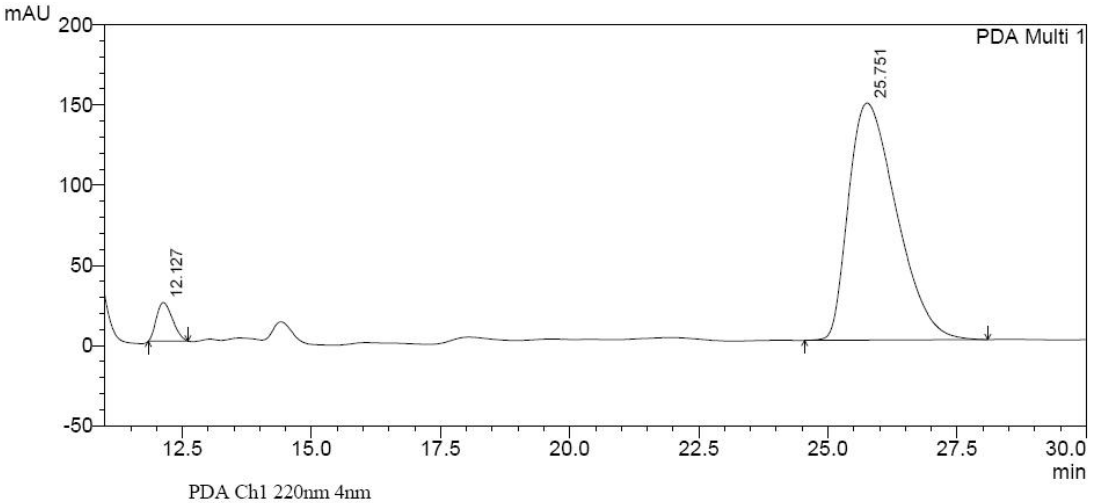

PDA Ch1 220nm 4nm

Peak#	Ret. Time	Area	Height	Area %	Height %
1	12.127	522185	24081	5.184	14.015
2	25.751	9550714	147748	94.816	85.985
Total		10072899	171829	100.000	100.000

Figure A-26. HPLC traces of **23nc** (Scheme 7.4): (a) racemic sample; (b) catalyzed by Λ-**27c**$^{3+}$ 3BAr$_f^-$.

APPENDIX B

Additional Syntheses and Data From Section 3.

Δ-(*R*,*R*)-1^{3+} $2Cl^-BAr_f^-$. This compound was prepared analogously to the enantiomer. The NMR spectra were similar.

Λ-(*R*,*R*)-1^{3+} $2Cl^-BAr_f^-$. This complex was prepared analogously to the enantiomer. Anal. Calcd. for $C_{74}H_{60}BCl_2CoF_{24}N_6$ (1629.92): C 54.53, H 3.71, N 5.16; found C 54.44, H 4.08, N 5.15. The NMR spectra were similar.

***trans*-[Co((*S*,*S*)-dpen)$_2$(Cl)$_2$]$^+$ Cl$^-$**. A round bottom flask was charged with a solution of $CoCl_2{\cdot}6H_2O$ (3.02 g, 12.5 mmol) in ethanol (25 mL). Then a solution (*S*,*S*)-dpen (5.04 g, 23.5 mmol) in ethanol (30 mL) was added with stirring. The solution was cooled to 15 °C, and aqueous HCl (2.5 mL, 4.0 M) and H_2O_2 (3.0 mL, 15%) were added with stirring. After 6 h, aqueous HCl (3.0 mL, 12.0 M) was added and the mixture was concentrated to ca. one third of the original volume by heating at 100 °C (oil bath). The sample was cooled to –8 °C (ice/salt bath) and filtered. The filter cake was washed with H_2O (30 mL) and diethyl ether (2 × 15 mL) and dried by oil pump vacuum (6 h) to give *trans*-[Co((*S*,*S*)-dpen)$_2$(Cl)$_2$]$^+$ Cl$^-$ as green powder (4.47 g, 7.57 mmol, 64% based upon (*S*,*S*)-dpen).

NMR (CD_3OD, δ in ppm): ^{1}H (500 MHz) 7.43-7.22 (m, 20H, Ph), 6.61 (d, $^3J_{HH}$ = 10 Hz, 4H, N**H**H'), 5.16 (br, 4H, NH**H'**), 4.87 (br s, CD_3O**H**/**H**$_2$O, 5H), 4.67 (s, 4H, C**H**NH_2); $^{13}C\{^1H\}$ (125 MHz) 138.8 (s, *i*), 130.2 (s, *o*), 129.9 (s, *p*), 128.7 (s, *m*), 66.8 (s, **C**HNH_2).

Comproportionation, Λ-[Co((*S*,*S*)-1^{3+} $3BAr_f^-$ and Λ-[Co((*S*,*S*)-1^{3+} $3Cl^-$ (Scheme 3.7**).** An experiment analogous to that in the main text was conducted with Λ-(*S*,*S*)-**1**$^{3+}$ $3BAr_f^-{\cdot}8H_2O$ (0.035 g, 0.0102 mmol), CH_2Cl_2 (8 mL), and Λ-(*S*,*S*)-**1**$^{3+}$ $3Cl^-$

·3H_2O (0.0175 g, 0.0204 mmol, 2.0 equiv). The solvent was removed by rotary evaporation and oil pump vacuum (8 h) to give Λ-(*S*,*S*)-**1**$^{3+}$ 2$Cl^-BAr_f^-$·2H_2O as an orange solid (0.048 g, 0.029 mmol, 95%). ^{1}H NMR (CD_2Cl_2, δ in ppm, 500 MHz, key data): 8.07 (br s, 6H, N**H**H'), 4.46 (s, 6H, C**H**NH_2), 3.95 (br s, 6H, NH**H'**); $^{13}C\{^1H\}$ (CD_2Cl_2, δ in ppm, 125 MHz, key data): 63.3 (s, **C**HNH_2).

Additional NMR Data (alternative solvents, concentrations, etc.)

Δ-(*S*,*S*)-1^{3+} 2$Cl^-BAr_f^-$. ^{1}H NMR (500 MHz, acetone-d_6, δ in ppm): BAr_f^- at 7.79 (s, 8H, *o*), 7.67 (s, 4H, *p*); (*S*,*S*)-dpen ligand at 7.45-7.40 (m, 12H, Ph), 7.33-7.26 (m, 18H, Ph), 7.13 (br s, 6H, N**H**H'), 6.16 (d, 6H, $^3J_{HH}$ = 10 Hz, NH**H'**), 5.11-5.05 (m, 6H, C**H**NH_2), 2.83 (br s, 8H, **H**$_2$O).

Λ-(*S*,*S*)-1^{3+} 3PF_6^-. ^{1}H NMR (500 MHz, 10:1 v/v DMSO-d_6/CH_3OH, δ in ppm): 7.47 (d, $^3J_{CH}$ = 7.5 Hz, 12H, *o*-Ph), 7.39 (t, $^3J_{CH}$ = 7.5 Hz, 12H, *m*-Ph), 7.33 (d, 6H, *p*-Ph), 5.55 (br s, 6H, N**H**H'), 5.37 (br s, 6H, NH**H'**), 4.83 (s, 6H, C**H**NH_2), 3.36 (s, 8H, **H**$_2$O).

Λ-(*S*,*S*)-15^{3+} 3Cl^- (intermediate in the synthesis of Λ-(*S*,*S*)-**15**$^{3+}$ 2$Cl^-BAr_f^-$). NMR (DMSO-d_6, δ in ppm): ^{1}H (500 MHz) 7.78 (br s, 24H, Ar), 7.04 (br s, 6H, N**H**H'), 5.89 (br s, 6H, NH**H'**), 5.21 (s, 6H, C**H**NH_2), 3.63 (br s, 8H, **H**$_2$O); $^{13}C\{^1H\}$ (125 MHz) 140.8 (s, *i*-Ar), 129.8 (s, Ar), 129.4 (s, Ar), 125.0 (s, Ar), 123.9 (q, $^1J_{CF}$ = 270.9 Hz, **C**F_3), 61.0 (s, **C**HNH_2).